SOURCE ROCK EVALUATION OF MIDDLE - LATE MIOCENE SEQUENCES, NORTH SABAH BASIN, MALAYSIA

by

Azlina Anuar

A Dissertation Submitted for the Degree of Doctor of Philosophy in the University of London and for the Diploma of Membership of Imperial College of Science, Technology and Medicine.

Petroleum Geology Group

Department of Geology, Royal School of Mines

Imperial College, Prince Consort Road

London SW7 2BP

February, 1994

BIBL LONDON UNIV

Dedicated with love to Mak and Ayah

ABSTRACT

This thesis presents the results of an organic geochemical investigation performed on 318 core, side-wall core and ditch-cutting samples collected from seven exploration wells in the northern part of Sabah Basin, Malaysia. The principal aims of the study are to identify the possible source rocks for the hydrocarbons in Sabah Basin, to correlate oils to their sources, to determine the timing of hydrocarbon generation and to elucidate the factors controlling organic matter deposition and preservation in the study area. Identifying and mapping source rock horizons have always been problematic in the thick Tertiary basins of NW Borneo despite the presence of many large hydrocarbon accumulations, for example, the highly petroliferous Baram Delta offshore Brunei and Sarawak, and the giant Samarang Field offshore Sabah.

Oils of the region are reported to have the characteristic fingerprint of higher land plants Type III kerogen, being waxy with low sulphur contents and generally high API gravities. Results from this study concur with the terrigenous origin of the hydrocarbons. There is no evidence for marine organic matter even in sediments deposited in marine palaeoenvironments. This absence of marine organic matter is attributed to the oxic conditions of Sabah Basin which prevailed throughout the Neogene. Coastal plain sediments represent the main source rocks for the Sabah Basin hydrocarbons. In general, they are only of poor to marginal quality but this is compensated by approximately 2000m thick of low-yield source rocks present with effective migration and drainage being provided by numerous interbedded sandstones, and possible rapid hydrocarbon generation due to high sediment burial rates resulting from both sedimentary and tectonic loading. Deep marine sediments containing terrigenous organic matter represent likely sources for hydrocarbons in the distal parts of the basin. There is some evidence of preferential transportation of the more resistant exinitic matter into deeper water areas leading to their enrichment in marine sediments. The consistently similar mass fragmentograms suggest that the oils and sediment extracts originated either from the same source rock or, more likely, from different source rocks with similar chemical compositions.

As none of the analysed samples have entered the hydrocarbon generation window, the source rocks have been traced using seismic sections into areas where they have been sufficiently buried to began generating hydrocarbons. The oil window occurs between 4000m - 5000m depth, with hydrocarbon generation commencing around 8 Ma in the proximal area and around 6 Ma in the more distal areas. Biomarker thermal maturity parameters are shown to fluctuate irregularly with an overall pattern of decreasing with depth, contradicting normal diagenetic evolution. Their variations

resemble those of the Production Index, indicating the influence of migrated hydrocarbons on the biomarkers. Finally, it is concluded that despite the generally oxic depositional environment, source rocks were successfully preserved in Sabah Basin due to high primary terrigenous productivity supplying the basin with higher plant waxes, cuticles and resins, which are by nature resistant to degradation, coinciding with extremely rapid sediment accumulation rate that assisted organic matter preservation. Information from this study helps in the understanding of hydrocarbon occurrences in this highly petroliferous region, where no rich source rock horizons are mappable and where the hydrocarbons originate from the least oil prone Type III kerogen.

Acknowledgements

I wish to express my thanks to PETRONAS, especially to Dr. Khalid Ngah, Deputy Director of PETRONAS Petroleum Research & Scientific Services, Kuala Lumpur for the support and funding of this study. The guidance and supervision given by Dr. Robert Kinghorn and Dr. Mokhlesur Rahman throughout the duration of this research are gratefully appreciated. I also wish to acknowledge Dr. Paul Grant for his assistance in using the BasinMod programme, Dr. Peter Bush for the useful comments he gave after reading my transfer report, and Prof. Howard Johnson for reviewing some of the chapters; his comments and suggestions are much appreciated. Special thanks are due to Mr. Michael Cocksedge, Dr. Andrew Carr, Dr. Philip Highton and Dr. Gavin Law of British Gas London Research Station for their help in the GC-MS studies and vitrinite reflectance measurements. Dr. Olav H. J. Christie of Rogaland Research, Stavanger, Norway is gratefully acknowledge for his advice on multivariate analysis.

The assistance provided by Dr. Peter Nagtegaal, and the staff at the Sarawak Shell, Miri core warehouse during sample collection are gratefully acknowledged. Appreciation is extended to Encik Abdul Jalil Muhamad, Puan Mona Liza Anwar and the staff of the Organic Geochemistry Section in PETRONAS Petroleum Research & Scientific Services, Kuala Lumpur. Encik Tan Ee Kim and the staff at PETRONAS Petroleum Research & Scientific Services core warehouse are also thanked for their help in sample collection. I also give my thanks to Fawzia, Lynn, Ella, Gill and Alban for their friendship and general assistance during my stay in Imperial College.

Finally, I wish to extend my utmost gratitude to my husband, Azim for the many helpful discussions, guidance and constructive criticisms during the course of this project. His patience, love and understanding are monumental.

TABLE OF CONTENTS

	Page
Abstract	iii
Acknowledgements	iv
Table of contents	v
List of tables	ix
List of illustrations	xii
CHAPTER 1. INTRODUCTION	
1.1 Regional background	1
1.2 Aims and organisation of dissertation	7
CHAPTER 2. GEOLOGY OF SABAH BASIN	
2.1 Structural development	9
2.2 Stratigraphic framework	12
2.3 Description of Stage IV sequences	20
2.3.1 Stage IVA	20
2.3.2 Stage IVB	23
2.3.3 Stage IVC	23
2.3.4 Stage IVD	23
2.3.5 Stage IVE	25
2.3.6 Stages IVF and IVG	25
2.4 Hydrocarbon occurrences	25
2.5 The study area	25
2.5.1 Introduction	25
2.5.2 Geological setting of the study area	27
2.5.2a South Furious Field	27
2.5.2b Tembungo Field	27
2.5.2c Rusa Timur	30
2.5.2d Gajah Hitam	32
CHAPTER 3. RESEARCH STRATEGY	
3.1 Sampling programme	33
3.2 Sample selection	33
3.3 Final sample set collected for analyses	35
3.3.1 Well : South Furious-2	35
3.3.2 Well : South Furious-3	37
3.3.3 Well : Tembungo-1	37
3.3.4 Well : Tembungo-2	37
3.3.5 Well : Tembungo-6	37
3.3.6 Well : Rusa Timur-1	37
3.3.7 Well : Gajah Hitam-1	37
3.4 Analytical programme : organic geochemical analyses	44
CHAPTER 4. REVIEW OF ORGANIC GEOCHEMICAL TECHNIQUES	
4.1 Sample preparation	47
4.2 Whole rock analyses	47

4.2.1 Determination of organic carbon content . . . 47
4.2.2 Rock-Eval pyrolysis 48
4.3 Solvent extraction 51
4.4 Extractable organic matter analyses 52
4.4.1 Gas chromatography 52
4.4.2 Gas chromatography - mass spectrometry . . . 54
4.4.3 Tandem gas chromatography - mass spectrometry . . 55
4.4.4 Stable carbon isotope, $\delta^{13}C_{extracts}$ 56
4.5 Kerogen isolation. 56
4.6 Isolated kerogen analyses 58
4.6.1 Density separation 58
4.6.2 Elemental analysis 58
4.6.3 Visual examination 60
4.6.3a Kerogen typing 60
4.6.3b Vitrinite reflectance measurement . . . 60
4.6.4 Stable carbon isotope, $\delta^{13}C_{kerogen}$ 60

CHAPTER 5. RESULTS FROM SAMPLE SCREENING AND KEROGEN ANALYSES

5.1 General characteristics of dispersed organic matter : quantity, quality and maturity 62
5.1.1 Stage III. 62
5.1.1a Organic matter content 62
5.1.1b Organic matter type and quality . . . 63
5.1.1c Organic matter maturity 68
5.1.2 Stage IVA 68
5.1.2a Organic matter content 69
5.1.2b Organic matter type and quality . . . 69
5.1.2c Organic matter maturity 82
5.1.3 Stage IVB 83
5.1.3a Organic matter content 83
5.1.3b Organic matter type and quality . . . 84
5.1.3c Organic matter maturity 87
5.1.4 Stage IVC 89
5.1.4a Organic matter content 89
5.1.4b Organic matter type and quality . . . 90
5.1.4c Organic matter maturity 98
5.1.5 Stage IVD 100
5.1.5a Organic matter content 100
5.1.5b Organic matter type and quality . . . 104
5.1.5c Organic matter maturity 114
5.2 Extractable organic matter 115
5.3 Stable carbon isotope ratios, $\delta^{13}C$ 116
5.4 Source rock considerations 117
5.5 Summary 122

CHAPTER 6. BIOLOGICAL MARKER ANALYSIS

6.1 Introduction 123
6.2 Triterpane fingerprints of sediment extracts and oils . . . 125
6.2.1 Results : Sediment extracts of Stage III . . . 125

6.2.2 Results : Sediment extracts of Sub-Stage IVA . . 128
6.2.3 Results : Sediment extracts of Sub-Stage IVB . . 136
6.2.4 Results : Sediment extracts of Sub-Stage IVC . . 136
6.2.5 Results : Sediment extracts of Sub-Stage IVD . . 140
6.2.6 Results : Oil samples 140
6.3 Sterane fingerprints of sediment extracts and oils . . . 140
6.3.1 Results : Sediment extracts of Stage III . . . 140
6.3.2 Results : Sediment extracts of Sub-Stage IVA . . 149
6.3.3 Results : Sediment extracts of Sub-Stage IVB . . 149
6.3.4 Results : Sediment extracts of Sub-Stage IVC . . 149
6.3.5 Results : Sediment extracts of Sub-Stage IVD . . 149
6.3.6 Results : Oil samples 161
6.4 Organic facies as indicated by biological markers . . . 161
6.4.1 Introduction 161
6.4.2 Results : Sediment extracts of South Furious-2 and South Furious-3 . . 166
6.4.3 Results : Sediment extracts of Tembungo-1, Tembungo-2 and Tembungo-6 167
6.4.4 Results : Sediment extracts of Rusa Timur-1 and Gajah Hitam-1 167
6.4.5 Results : Oil samples 168
6.5 Biomarkers as thermal maturity indicators 172
6.5.1 Introduction 172
6.5.1a Steranes 172
6.5.1b Triterpanes 172
6.5.2 Results : Sediment extracts 174
6.5.3 Results : Oil samples 179
6.6 Pattern recognition within a multivariate data set : Principal components analysis . . 184
6.6.1 Introduction 184
6.6.2 Input data 186
6.6.3 Results : Principal component analysis of oil and extract samples 186
6.6.4 Results : Principal component analysis of oil samples . 193
6.7 Summary 196

CHAPTER 7. THERMAL MATURATION OF SEDIMENTARY ORGANIC MATTER

7.1 Introduction 198
7.2 Burial history 201
7.2.1 Input data 201
7.3 Timing of hydrocarbon generation 207
7.3.1 TTI - Lopatin's method 207
7.3.1a Well results 208
7.3.1b Hydrocarbon Kitchen 1 : Pritchard Syncline . 216
7.3.1c Hydrocarbon Kitchen 2 : Furious Syncline . 218
7.3.1d Hydrocarbon Kitchen 3 : The Graben . . 220
7.3.2 Arrhenius - based TTI method 222
7.3.2a Well results 225
7.3.2b Hydrocarbon Kitchen 1 : Pritchard Syncline . 225
7.3.2c Hydrocarbon Kitchen 2 : Furious Syncline . 226
7.3.2d Hydrocarbon Kitchen 3 : The Graben . . 226

7.3.3 BasinMod kinetic modelling 227
7.3.3a Well results 227
7.3.3b Hydrocarbon Kitchen 1 : Pritchard Syncline . 227
7.3.3c Hydrocarbon Kitchen 2 : Furious Syncline . 227
7.3.3d Hydrocarbon Kitchen 3 : The Graben . . 230
7.4 Discussion 230
7.5 Summary 233

CHAPTER 8. ORGANIC MATTER DEPOSITION AND PRESERVATION
8.1 Introduction 236
8.2 Climate and vegetation 236
8.3 Neogene sedimentation 237
8.4 Organic matter production and preservation 240
8.4.1 Organic matter production in Sabah Basin . . . 240
8.4.2 Organic matter preservation conditions in general . . 240
8.4.3 Organic matter preservation in Sabah Basin . . . 242
8.5 Variation in organic matter quality and quantity . . . 249
8.5.1 Organic matter variation pattern with environmental depth zones 249
8.5.2 Origin of variation 252
8.5.3 Implications for source rock distribution . . . 252
8.6 Summary 255

CHAPTER 9. CONCLUSIONS AND FUTURE WORK. . . 257

REFERENCES 260

APPENDIX I. Detailed description of organic geochemical techniques employed in the study 271
APPENDIX II: Photographs of isolated kerogen . . . 281
APPENDIX III: Abstracts of presented work . . . 291

LIST OF TABLES

Table 1.1 Key to the basins shown in Figure 1.1 (from Hutchison, 1989).

Table 1.2 Estimated ultimate recoverable reserves of Sabah, Sarawak and Brunei.

Table 3.1 Wells and Stages investigated in the study of Sabah Basin source rocks.

Table 3.2 The number of samples collected from Stages III and IV of the seven wells.

Table 3.3 Organic geochemical analyses performed.

Table 4.1 Comparison between the use of platinum and nickel boats when analysing elemental compositions.

Table 5.1 Screening results for Stage III sediments (South Furious area only).

Table 5.2 Elemental analysis results : Stage III (South Furious area only).

Table 5.3 Visual analysis and density separation of kerogen concentrates : Stage III (South Furious area only).

Table 5.4 Isoprenoid ratios for Stage III sediments (South Furious area only).

Table 5.5 Vitrinite reflectance : Stage III (South Furious area only).

Table 5.6 TOC and Pyrolysis results : Stage IVA.

Table 5.7 Elemental analysis results : Stage IVA.

Table 5.8 Visual analysis and density separation of kerogen concentrates : Stage IVA.

Table 5.9 Isoprenoid ratios for Stage IVA.

Table 5.10 Vitrinite reflectance values : Stage IVA.

Table 5.11 TOC and Pyrolysis results : Stage IVB.

Table 5.12 Elemental analysis results : Stage IVB.

Table 5.13 Visual analysis and density separation of kerogen concentrates : Stage IVB.

Table 5.14 Isoprenoid ratios for Stage IVB.

Table 5.15 Vitrinite reflectance values : Stage IVB.

Table 5.16 TOC and Pyrolysis results : Stage IVC.

Table 5.17 Elemental analysis results : Stage IVC.

Table 5.18 Visual analysis and density separation of kerogen concentrates : Stage IVC.

Table 5.19 Isoprenoid ratios for Stage IVC.

Table 5.20 Vitrinite reflectance values : Stage IVC.

Table 5.21 Depositional environment variations.

Table 5.22 TOC and Pyrolysis results : Stage IVD (coastal to inner neritic sediments).

Table 5.23 TOC and Pyrolysis results : Stage IVD (middle neritic sediments).

Table 5.24 TOC and Pyrolysis results : Stage IVD (outer neritic sediments).

Table 5.25 TOC and Pyrolysis results : Stage IVD (bathyal sediments).

Table 5.26 Elemental analysis results : Stage IVD.

Table 5.27 Visual analysis and density separation of kerogen concentrates : Stage IVD.

Table 5.28 Isoprenoid ratios for Stage IVD.

Table 5.29 Vitrinite reflectance values : Stage IVD.

Table 5.30 Stable carbon isotope ratios.

Table 5.31 Average screening results.

Table 6.1 Key to peak identities for triterpane (m/z 191) and sterane (m/z 217) mass fragmentograms shown in this study.

Table 6.2 Key to Figure 6.4.

Table 6.3 Results from the thermal maturity parameters for the sediment extract samples of (a) South Furious-2, (b) South Furious-3, (c) Tembungo-1, (d) Tembungo-2, (e) Rusa Timur-1 and (f) Gajah Hitam-1 wells.

Table 6.4 Results from the thermal maturity parameters for the seven oil samples.

Table 6.5 The raw biomarker peak height data of South Furious-2 samples used in the multivariate analyses of the 17 sediment extract and 7 oil samples.

Table 6.6 The raw biomarker peak height data of Rusa Timur-1 and Gajah Hitam-1 used in the multivariate analyses of the 17 sediment extract and 7 oil samples.

Table 6.7 The raw biomarker peak height data of the seven oil samples used in the multivariate analyses of the 17 sediment extract and 7 oil samples.

Table 7.1 Arrhenius kinetic parameters used by Hunt & Hennet (1992) for the construction of the TTI graphs for each kerogen type. Note the degree of variations within kerogen Types I and II.

Table 7.2 South Furious-2 : Input data for burial history and thermal maturation modelling.

Table 7.3 South Furious-3 : Input data for burial history and thermal maturation modelling.

Table 7.4 Tembungo-1 : Input data for burial history and thermal maturation modelling.

Table 7.5 Tembungo-2 : Input data for burial history and thermal maturation modelling.

Table 7.6 Tembungo-6 : Input data for burial history and thermal maturation modelling.

Table 7.7 Rusa Timur-1 : Input data for burial history and thermal maturation modelling.

Table 7.8 Gajah Hitam-1 : Input data for burial history and thermal maturation modelling.

Table 7.9 Pritchard Syncline : Input data for burial history and thermal maturation modelling.

Table 7.10 Furious Syncline : Input data for burial history and thermal maturation modelling.

Table 7.11 Graben between Rusa Timur-1 and Belangkas : Input data for burial history and thermal maturation modelling.

Table 7.12 Relation between sediment temperature, the index value, n, and the temperature factor, γ (from Waples, 1985).

Table 7.13 Summary of Lopatin TTI calculations for sediments in South Furious-2.

Table 7.14 Summary of Lopatin TTI calculations for sediments in South Furious-3.

Table 7.15 Summary of Lopatin TTI calculations for sediments in Tembungo-1.

Table 7.16 Summary of Lopatin TTI calculations for sediments in Tembungo-2.

Table 7.17 Summary of Lopatin TTI calculations for sediments in Tembungo-6.

Table 7.18 Summary of Lopatin TTI calculations for sediments in Rusa Timur-1.

Table 7.19 Summary of Lopatin TTI calculations for sediments in Gajah Hitam-1.

Table 7.20 Summary of Lopatin TTI calculations for sediments in the Pritchard Syncline.

Table 7.21 Summary of Lopatin TTI calculations for sediments in the Furious Syncline.

Table 7.22 Summary of Lopatin TTI calculations for sediments in the graben located between Rusa Timur-1 and Belangkas.

Table 7.23 Arrhenius TTI values for oil and gas generation in the Pritchard Syncline using kerogen Type III and oil to gas kinetics.

Table 7.24 Arrhenius TTI values for oil and gas generation in the Furious Syncline using kerogen Type III and oil to gas kinetics.

Table 7.25 Arrhenius TTI values for oil and gas generation in the graben between Rusa Timur-1 and Belangkas using kerogen Type III and oil to gas kinetics.

Table 7.26 Summary of thermal modelling results from Lopatin TTI, Arrhenius-based TTI and BasinMod kinetic modelling for a) the Pritchard Syncline, b) the Furious Syncline and c) The Graben.

Table 7.27 Timing of hydrocarbon generation in the three kitchen areas determined from TTI_{LOP}, TTI_{ARR} and BasinMod.

LIST OF ILLUSTRATIONS

Figure 1.1 The Tertiary basins of South East Asia. See Table 1.1 for basin names, classification and average geothermal gradients (after Hutchison, 1989). Highlighted are the basins located around the periphery of Borneo.

Figure 1.2 Exploration well density and major discoveries in Brunei (from Ellenor, 1984).

Figure 1.3 Location of oil discoveries and major gas fields in East Malaysia (from Scherer, 1980).

Figure 1.4 Location of the Central Luconia Province and the D18 field, offshore Sarawak (from Almond *et. al.*, 1990).

Figure 1.5 Location map of wells included in this study - South Furious-2, South Furious-3, Tembungo-1, Tembungo-2, Tembungo-6, Rusa Timur-1 and Gajah Hitam-1.

Figure 2.1 Tectonic elements of South East Asia (after James, 1984, based on Hamilton, 1979 and Holloway, 1982).

Figure 2.2 Sabah Basin location map (after Letouzey *et. al.*, 1988).

Figure 2.3 NW-SE section across Sabah Trough - Sabah Basin - Mt. Kinabalu (modified after Bol & van Hoorn, 1980 and ASCOPE, 1980).

Figure 2.4 Structural sketch map of Bol & van Hoorn (1980) showing the timing of deformational phases in offshore Sabah Basin.

Figure 2.5 Migrated seismic section of the 'Sabah Ridges' (Bol & van Hoorn, 1980). For the location of the section, please refer to **Figure 2.4.**

Figure 2.6 Migrated seismic section of the Ketam structure (Bol & van Hoorn, 1980). For the location of the section, please refer to **Figure 2.4.**

Figure 2.7 Migrated seismic section of the Bunbury - St. Joseph High (Bol & van Hoorn, 1980). For the location of the section, please refer to **Figure 2.4.**

Figure 2.8 Migrated seismic section of the South Furious - St. Joseph trend (Bol & van Hoorn, 1980). For the location of the section, please refer to **Figure 2.4.**

Figure 2.9 Migrated seismic section of the Mantanani - Barton trend (Bol & van Hoorn, 1980). For the location of the section, please refer to **Figure 2.4.**

Figure 2.10 Migrated seismic sections of the (a) Bonanza and (b) Samarang structures (Bol & van Hoorn, 1980). For the location of the section, please refer to **Figure 2.4.**

Figure 2.11 Chronostratigraphic framework of the Sabah Basin (after Johnson & Huong, 1991).

Figure 2.12 Schematic outline of NW Borneo palaeoenvironmental units (Ho Kiam Fui, 1978).

Figure 2.13 Palaeoenvironmental map at the top of sub-Stage IVA.

Figure 2.14 Palaeoenvironmental map at the top of sub-Stage IVB.

Figure 2.15 Palaeoenvironmental map at the top of sub-Stage IVC.

Figure 2.16 Palaeoenvironmental map at the top of sub-Stage IVD.

Figure 2.17 Location of the study area with respect to the tectonic provinces of Bol & van Hoorn (1980).

Figure 2.18 Well correlation : South Furious Field.

Figure 2.19 Well correlation : Tembungo Field.

Figure 2.20 Well correlation : Rusa Timur- Gajah Hitam area.

Figure 3.1 An example of Gamma Ray, Resistivity, Sonic and Density log responses for an organic carbon-rich interval in the South Furious-3 well.

Figure 3.2. South Furious-2 : sampling locations and sample types. Also indicated are the palaeoenvironments and sedimentary Stages/sub-Stages.

Figure 3.3 South Furious-3 : sampling locations and sample types. Also indicated are the palaeoenvironments and sedimentary Stages/sub-Stages.

Figure 3.4 Tembungo-1 : sampling locations and sample types. Also indicated are the palaeoenvironments and sedimentary Stages/sub-Stages.

Figure 3.5 Tembungo-2 : sampling locations and sample types. Also indicated are the palaeoenvironments and sedimentary Stages/sub-Stages.

Figure 3.6 Tembungo-6 : sampling locations and sample types. Also indicated are the palaeoenvironments and sedimentary Stages/sub-Stages.

Figure 3.7 Rusa Timur-1 : sampling locations and sample types. Also indicated are the palaeoenvironments and sedimentary Stages/sub-Stages.

Figure 3.8 Gajah Hitam-1 : sampling locations and sample types. Also indicated are the palaeoenvironments and sedimentary Stages/sub-Stages.

Figure 3.9 Flow diagram of the analytical procedures undertaken.

Figure 4.1 A general schematic diagram showing the release of hydrocarbons and CO_2 during pyrolysis, with time increasing from left to right. The primary parameters measured by the pyrolysis instrument are S1, S2, S3 and Tmax. The secondary parameters of Hydrogen Index (HI) and Production Index (PI) are calculated from the equation shown (from Peters, 1986).

Figure 4.2 Plotting the Hydrogen Index (HI, mg HC/g TOC) against pyrolysis Tmax (° C) can be used as one method of determining kerogen type (from Parnell & Rahman, 1990).

Figure 4.3 Analysis of bitumen and crude samples.

Figure 4.4 Approximate ranges of the sterane 20S/(20S+20R) and hopane 22S/(22S+22R), and other molecular ratios in relation to vitrinite reflectance values and yields of extractable hydrocarbon extracts (from Mackenzie & Maxwell, 1981).

Figure 4.5 Analyses performed on isolated kerogen samples.

Figure 4.6 (a) Simplified diagram of combustion train and analytical system for Carbon, Hydrogen and Nitrogen (CHN) analysis, (b) details of the combustion train, and (c) the detector flow diagram (Perkin-Elmer Handbook, 1986).

Figure 4.7 The combustion train used for oxygen analysis (Perkin-Elmer Handbook, 1986).

Figure 5.1 Hydrogen Index vs Tmax cross-plot (from Parnell & Rahman, 1990) for Stage III sediments.

Figure 5.2 Elemental compositions of Stage III kerogens plotted on the van Krevelen diagram (from Durand, 1980).

Figure 5.3 The variations in kerogen composition of South Furious-2 and South Furious-3 Stage III sediments from (a) organic petrography and (b).density separation. Also shown are the corresponding (c) Hydrogen Index and (d) Total Organic Carbon contents.

Figure 5.4 Gas chromatogram of Stage III South Furious-2 saturate fraction 1871m/6138ft.

Figure 5.5 Gas chromatogram of Stage III South Furious-2 saturate fraction 1921m/6302ft.

Figure 5.6 Gas chromatogram of Stage III South Furious-2 saturate fraction 1979m/6493ft.

Figure 5.7 Hydrogen Index vs Tmax cross-plot (from Parnell & Rahman, 1990) for Stage IVA sediments.

Figure 5.8 Elemental compositions of Stage IVA kerogens plotted on the van Krevelen diagram (from Durand, 1980).

Figure 5.9 The variations in kerogen composition of South Furious-2, South Furious-3 and Rusa Timur-1 Stage IVA sediments from (a) organic petrography and (b) density separation. Also shown are the corresponding (c) Hydrogen Index and (d) Total Organic Carbon contents.

Figure 5.10 Gas chromatogram of Stage IVA South Furious-2 saturate fraction 446m/1463ft.

Figure 5.11 Gas chromatogram of Stage IVA South Furious-2 saturate raction 1006m/3301ft.

Figure 5.12 Gas chromatogram of Stage IVA South Furious-2 saturate raction 1293m/4242ft.

Figure 5.13 Gas chromatogram of Stage IVA South Furious-2 saturate fraction 1606m/5269ft.

Figure 5.14 Gas chromatogram of Stage IVA South Furious-2 saturate fraction 1738m/5702ft.

Figure 5.15 Gas chromatogram of Stage III South Furious-2 saturate fraction 1779m/5837ft.

Figure 5.16 Gas chromatogram of Stage IVA Rusa Timur-1 saturate fraction 2040m/6693ft.

Figure 5.17 Hydrogen Index vs Tmax cross-plot (from Parnell & Rahman, 1990) for Stage IVB sediments.

Figure 5.18 Elemental compositions of Stage IVB kerogens plotted on the van Krevelen diagram (from Durand, 1980).

Figure 5.19 The variations in kerogen composition of Rusa Timur-1 Stage IVB ediments from (a) organic petrography and (b).density separation. Also shown are he corresponding (c) Hydrogen Index and (d) Total Organic Carbon contents.

Figure 5.20 Gas chromatogram of Stage IVB Rusa Timur-1 saturate fraction 1814m/5951ft.

Figure 5.21 Hydrogen Index vs Tmax cross-plot (from Parnell & Rahman, 1990) for sub-Stage IVC sediments.

Figure 5.22 Elemental compositions of Stage IVC kerogens plotted on the van Krevelen diagram (from Durand, 1980).

Figure 5.23 The variations in kerogen composition of Tembungo-1, Tembungo-2, Tembungo-6, Rusa Timur-1 and Gajah Hitam-1 Stage IVC sediments from (a) organic petrography and (b).density separation. Also shown are the corresponding (c) Hydrogen Index and (d) Total Organic Carbon contents.

Figure 5.24 Gas chromatogram of Stage IVC Tembungo-6 saturate fraction 1901m/6237ft.

Figure 5.25 Gas chromatogram of Stage IVC Rusa Timur-1 saturate fraction 1619m/5312ft.

Figure 5.26 Gas chromatogram of Stage IVC Gajah Hitam-1 saturate fraction 2117m/6946ft.

Figure 5.27 Gas chromatogram of Stage IVC Gajah Hitam-1 saturate fraction 2401m/7877ft.

Figure 5. 28 Hydrogen Index vs Tmax cross-plot (from Parnell & Rahman, 1990) for Stage IVD sediments according to palaeoenvironments : (a) coastal-inner neritic, (b) middle neritic, (c) outer neritic and (d) bathyal.

Figure 5.29 Elemental compositions of Stage IVD kerogens plotted on the van Krevelen diagram (from Durand, 1980).

Figure 5.30 The variations in kerogen composition of Tembungo-1, Tembungo-2, Tembungo-6, Rusa Timur-1 and Gajah Hitam-1 Stage IVD sediments from (a) organic petrography and (b).density separation. Also shown are the corresponding (c) Hydrogen Index and (d) Total Organic Carbon contents.

Figure 5.31 Gas chromatogram of Stage IVD Tembungo-1 saturate fraction 1809m/5935ft.

Figure 5.32 Gas chromatogram of Stage IVD Tembungo-2 saturate fraction 1994m/6542ft.

Figure 5.33 Gas chromatogram of Stage IVD Rusa Timur-1 saturate fraction 772m/2533ft.

Figure 5.34 Gas chromatogram of Stage IVD Rusa Timur-1 saturate fraction 1406m/4613ft.

Figure 5.35 Isotope type-curves (Stahl, 1978) for South Furious and Rusa Timur oils, and kerogens from (a) Stage III, (b) Stage IVA and (c) Stage IVB sediments.

Figure 5.36 Δ_K values of Stage III (South Furious area), Stage IVA (South Furious area) and Stage IVB (Rusa Timur area) kerogens.

Figure 5.37 (a) $\Delta_{K\text{-}SAT}$ and (b) $\Delta_{K\text{-}ARO}$ values of Stage III (South Furious area), Stage IVA (South Furious area) and Stage IVB (Rusa Timur area) kerogens and hydrocarbon fractions.

Figure 6.1 Well and oil sample locations, Sabah Basin, Malaysia.

Figure 6.2 Triterpane (m/z 191) distributions of Stage III sediment extract samples obtained from South Furious-2 well, **(a)** 1871m/6138ft, **(b)** 1921m/6302ft and **(c)** 1979m/6493ft.

Figure 6.3 Triterpane (m/z 91) distributions of Stage IVA sediment extract samples obtained from **(1)** South Furious-2 well (a to g), **(2)** South Furious-3 well (a to f) and **(3)** Rusa Timur-1 well (a).

Figure 6.4 Comparison between the resulting partial mass chromatograms of m/z 151 and 207, indicating seco-bicadinanes, m/z 369 and 412, indicating bicadinanes and m/z 383 and 426, indicating homobicadinanes of **(a)** South Furious-2 Stage IVA extract sample 1002m/3287ft from this study and **(b)** the published data of van Aarssen *et. al.* (1992).

Figure Triterpane (m/z 191) distribution of a Stage IVB sediment extract sample obtained from Rusa Timur-1 well.

Figure 6.6 Triterpane (m/z 191) distributions of Stage IVC sediment extract samples obtained from **(1)** Rusa Timur-1 well (a) and **(2)** Gajah Hitam-1 well (a to b).

Figure 6.7 Triterpane (m/z 191) distributions of Stage IVD sediment extract samples obtained from **(1)** Tembungo-1 well (a), **(2)** Tembungo-2 well (a) and **(3)** Rusa Timur-1 well (a to b).

Figure 6.8 Triterpane (m/z 191) distributions of the seven oil samples collected from different locations in the Sabah Basin. Refer to **Figure 6.1** for locations.

Figure 6.9 Sterane (m/z 217) distributions for Stage III sediment extract samples obtained from South Furious-2 well **(a)** 1871m/6138ft, **(b)** 1921m/6302ft and **(c)** 1979m/6493ft.

Figure 6.10 Sterane (m/z 217) distributions of Stage IVA sediment extract samples obtained from **(1)** South Furious-2 well (a to g), **(2)** South Furious-3 well (a to f) and **(3)** Rusa Timur-1 well F (a).

Figure 6.11 Sterane (m/z 217) distribution of a Stage IVB sediment extract sample obtained from Rusa Timur-1 well.

Figure 6.12 Sterane (m/z 217) distributions of Stage IVC sediment extract samples obtained from **(1)** Rusa Timur-1 well (a) and **(2)** Gajah Hitam-1 well (a to b).

Figure 6.13 Sterane (m/z 217) distributions of Stage IVD sediment extract samples obtained from **(1)** Tembungo-1 well (a), **(2)** Tembungo-2 well (a) and **(3)** Rusa Timur-1 well (a to b).

Figure 6.14 Sterane (m/z 217) distributions of the seven oil samples collected from different locations in the Sabah Basin. Refer to **Figure 6.1** for locations.

Figure 6.15 The dividing line between the 'inner' and 'outer' oils based on the relative abundance of C_{30} regular steranes and triterpane/sterane ratios. Oil 1 (Rusa Timur) and Oil 2 (Tembungo) are deduced to have been generated by land-derived organic matter deposited in deep-marine environments while the other oils were sourced by terrestrial organic matter deposited in deltaic-lower coastal plain environments.

Figure 6.16 Comparative chart of hopane/sterane ratios in oils sourced from marine, paralic and lacustrine/terrigenous kerogens (modified from Genik, 1993).

Figure 6.17 The transformation of sterane 20R to the 20S configuration (from Mackenzie & McKenzie, 1983).

Figure 6.18 The transformation of triterpane 22R to the 22S configuration (from Mackenzie & McKenzie, 1983).

Figure 6.19 Comparison between the sterane 20S/(20S+20R) and triterpane 22S/(22S+22R) biomarker maturity ratios with the production index values for **(a)** South Furious-2, **(b)** South Furious-3, **(c)** Rusa Timur-1 and **(d)** Gajah Hitam-1.

Figure 6.20 Results from the 18α(H)/18β(H)-oleanane biomarker ratio and the Oleanane Parameter from **(a)** South Furious-2 and the Oleanane Parameter determined from **(b)** South Furious-3, Rusa Timur-1 and Gajah Hitam-1.

Figure 6.21 The moretane/C_{30}-hopane and Tm/Ts biomarker ratios for **(a)** South Furious-2, **(b)** South Furious-3, **(c)** Tembungo-1 and **(d)** Gajah Hitam-1.

Figure 6.22 The decomposition of the original data matrix, **A**, into the score, **S** and loading, **L** matrices. **E** is the residual matrix (Christie, pers. comm.).

Figure 6.23 The average distribution of the 29 normalised biomarker peak heights for the 17 sediment extract and 7 oil samples included in the multivariate analysis.

Figure 6.24 Loading plots for the first three principal components versus biomarker variables **(a)** PC 1, 36.0% **(b)** PC 2, 13.5% and **(c)** PC 3, 9.4%, accounting for 58.9% of the total information within the data set. Refer to **Table 6.1** for key to biomarker variables.

Figure 6.25 Sample score plots : **(a)** the scores of PC 1 versus PC 2 and **(b)** the scores of PC 1 versus PC 3.

Figure 6.26 The average distribution of the 29 normalised biomarker peak heights for the multivariate analysis of the 7 oil samples.

Figure 6.27 Loading plots for the first two principal components versus biomarker variables **(a)** PC 1, 60.4% and **(b)** PC 2, 24.2%, accounting for 84.6% of the total variation within the data set. Refer to **Table 6.1** for key to biomarker variables.

Figure 6.28 The sample scores of PC 1 versus PC 2.

Figure 7.1 Well locations and three data points taken in the hydrocarbon kitchens.

Figure 7.2 Measured vitrinite reflectance versus depth profiles for **(a)** South Furious-2, **(b)** South Furious-3, **(c)** Tembungo-1, **(d)** Tembungo-2, **(e)** Tembungo-6, **(f)** Rusa Timur-1 and **(g)** Gajah Hitam-1.

Figure 7.3 The burial history curves for the sedimentary sequences in **(a)** South Furious-2, **(b)** South Furious-3, **(c)** Tembungo-1, **(d)** Tembungo-2, **(e)** Tembungo-6, **(f)** Rusa Timur-1 and **(g)** Gajah Hitam-1.

Figure 7.4 Hydrocarbon generation window in the Pritchard Syncline determined from Lopatin's TTI method.

Figure 7.5 Hydrocarbon generation window in the Furious Syncline determined from Lopatin's TTI method.

Figure 7.6 Hydrocarbon generation window in The Graben located between Rusa Timur-1 and Belangkas area determined from Lopatin's TTI method.

Figure 7.7 Graph showing relationship between time, temperature and TTI_{ARR} for kerogen Type III kinetics as represented by the Tent Island Formation of the Beaufort-Mackenzie Basin of Canada (from Hunt & Hennet, 1992).

Figure 7.8 Graph showing relationship between time, temperature and TTI_{ARR} for the conversion of oil to gas (E = 230 kJ/mol and A = 3.17 x 10^{21} my) (from Hunt & Hennet, 1992).

Figure 7.9 Graph showing the relationship between TTI_{ARR} and percent of hydrocarbon generated (from Hunt & Hennet, 1992).

FIGURE 7.10 Hydrocarbon generation window in the Pritchard Syncline determined from the Arrhenius-based TTI method.

FIGURE 7.11 Hydrocarbon generation window in the Furious Syncline determined from the Arrhenius-based TTI method.

FIGURE 7.12 Hydrocarbon generation window in the graben located between Rusa Timur-1 and Belangkas area determined from the Arrhenius-based TTI method.

Figure 7.13 Hydrocarbon generation window in the Pritchard Syncline determined by BasinMod kinetic modelling.

Figure 7.14 Hydrocarbon generation window in the Furious Syncline determined by BasinMod kinetic modelling.

Figure 7.15 Hydrocarbon generation window in The Graben determined by BasinMod kinetic modelling.

Figure 7.16 Comparisons between the location of the oil window in the Pritchard Syncline determined by the different methods used.

Figure 7.17 Comparisons between the location of the oil window in the Furious Syncline determined by the different methods used.

Figure 7.18 Comparisons between the location of the oil window in The Graben determined by the different methods used.

Figure 8.1 Palaeoenvironmental changes throughout the deposition of the Middle - Upper Miocene sediments in the Sabah Basin. The palaeoenvironments shown are for the top of each sedimentary Stage, and the palaeoenvironmental interpretations were based upon PETRONAS in-house biostratigraphic reports.

Figure 8. 2 (a) Bathymetric chart of Kuehl *et al.*'s (1993) study area. Of interest here are the sample locations of box cores No. 6 and No. 7 whose results will have some significance for the Sabah Basin. (b) Temperature and dissolved oxygen distributions across the Palawan sill with depth distribution of the box cores. (From Kuehl *et al.*, 1993).

Figure 8.3 Depth distribution and interactions of decomposition processes in buried sediments (from Jones, 1985).

Figure 8.4 Average sediment accumulation rates in Sabah Basin throughout the Neogene (Azim-Ibrahim, 1994).

Figure 8.5 Organic carbon accumulation rates are higher by 2-3 times in the Sulu Sea compared to the South China Sea (From Kuehl *et al.*, 1993).

Figure 8.6 Increasing sedimentation rate results in the better preservation of organic matter by the rapid passage through the near-surface zone of microbial degradation. (From Ibach, 1982). However, organic matter productivity must be simultaneously high to counterbalance the effect of sediment volume and thus avoid dilution.

Figure 8.7 Variations in (a) average TOC (wt%), (b) average Hydrogen Index, HI (mgHC/gTOC) and (c) average organic matter compositions with palaeo-depositional environments of Hedgpeth (1957a) (From Anuar *et. al.*, 1993).

Figure 8.8 Simplified source rock distribution map for (a) Stage IVA and (b) Stage IVB.

CHAPTER ONE

INTRODUCTION

1.1 Regional background

The Sabah Basin is one of several petroliferous Tertiary basins located around the periphery of Borneo (**Figure 1.1, Table 1.1**). Hydrocarbon exploration activities in Tertiary sediments along the NW margin of Borneo started with the discovery of the Miri Field (onshore Sarawak) in 1910. Following that, exploration in Brunei began in 1913, resulting in the 1929 discovery of Seria Field in the Baram Delta (Ellenor, 1984). By the end of 1983, 10 commercially exploitable oil and gas fields including major accumulations of Seria, SW Ampa and Champion (**Figure 1.2**) were discovered. Estimated ultimate recovery for discovered reserves, both proven and probable, in Brunei's Baram Delta range between 2000-3500 million barrels of oil and 7.7-10.0 trillion cubic feet of gas (1283-1667 million barrels of oil equivalent, where 6000 cubic feet = 1 barrel of oil), making the total oil and gas reserves 3283-5167 million barrels of oil (ASCOPE, 1981).

In neighbouring Sarawak, the Baram Delta is estimated to have 600 million barrels of total oil reserves from nine commercial oil fields, the first of which (Baram-1; Rijks, 1981) was discovered in 1963. The largest of these, the Baronia Field discovered in 1967 (**Figure 1.3**), qualifies as a giant field according to AAPG classification with 185 million barrels of oil and 1.26 trillion cubic feet of gas of reserves (Scherer, 1980). Other hydrocarbon occurrences in Sarawak include the Central Luconia gas fields with 15 trillion cubic feet of total gas reserves (2500 million barrels of oil equivalent) and the more recently discovered D18 Field in the Balingian Province (**Figure 1.4**) reported to have significant amounts of hydrocarbon reserves (Almond *et. al.*, 1990).

Exploration activities in Sabah increased after the discoveries of the Tembungo and Erb West fields in 1971. The Tembungo Field is unique compared to others because it is the only one producing from turbidite sandstones (Whittle & Short, 1978), with 15 million barrels of oil reserves (ASCOPE, 1981). Other oil fields in Sabah Basin include South Furious (1974), St. Joseph (1975), Barton (1971), Kinabalu (1989) and the giant Samarang Field (1973 - 230 million barrels of recoverable oil reserves; Scherer, 1980). Cumulative total hydrocarbon reserves of Sabah, Sarawak and Brunei is conservatively estimated to range between 6.6-8.5 billion barrels (**Table 1.2**).

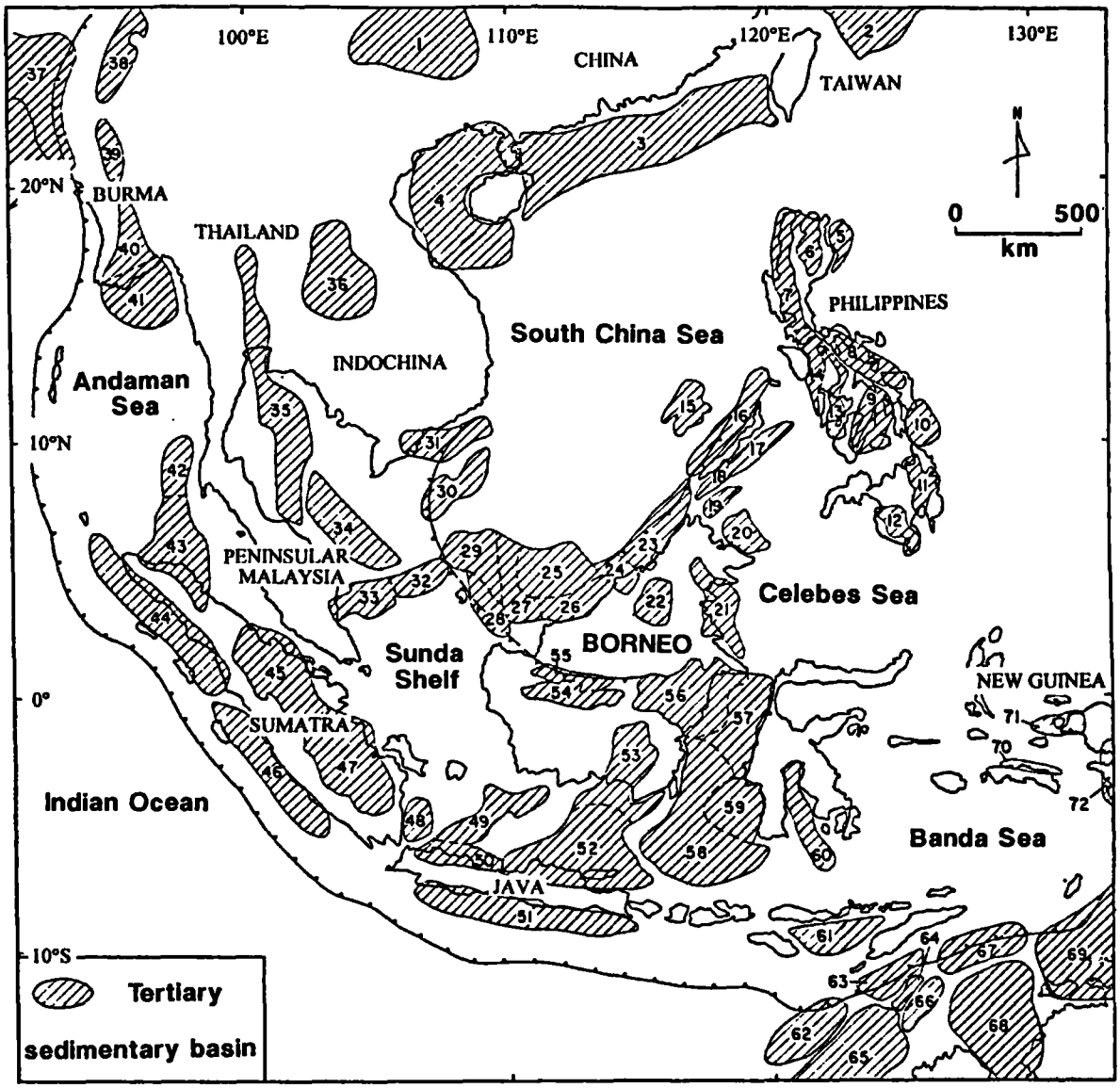


FIGURE 1.1 The Tertiary basins of South East Asia. See **Table 1.1** for basin names, classification and average geothermal gradients (after Hutchison, 1989). Highlighted are the basins located around the periphery of Borneo.

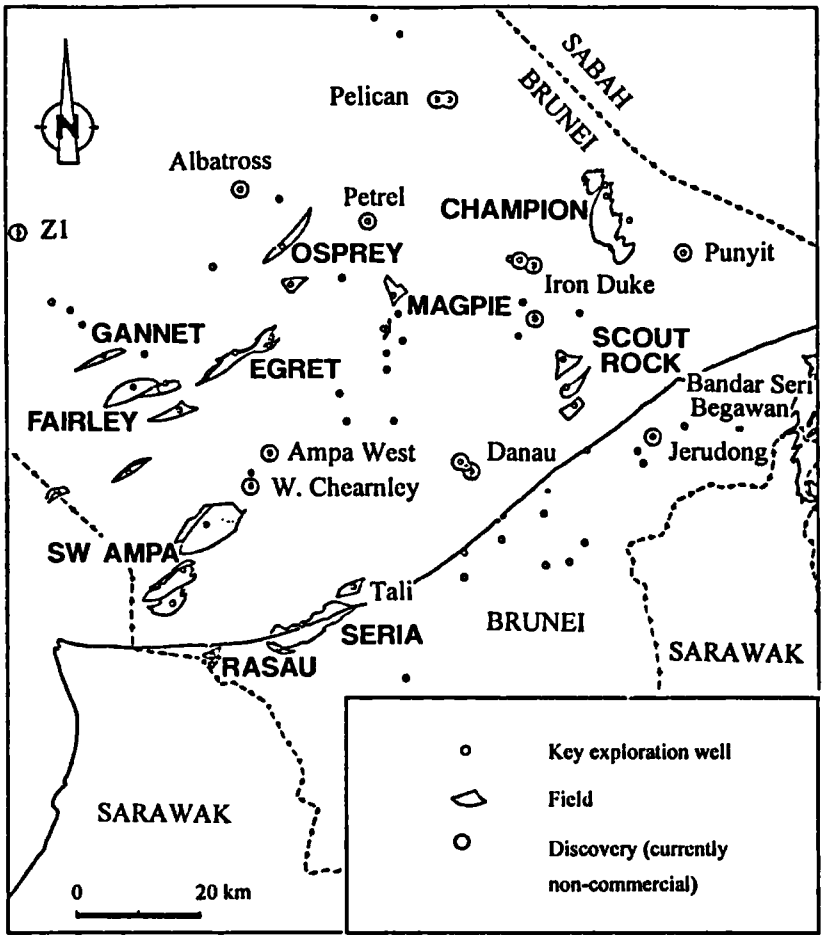


FIGURE 1.2 Exploration well density and major discoveries in Brunei (from Ellenor, 1984).

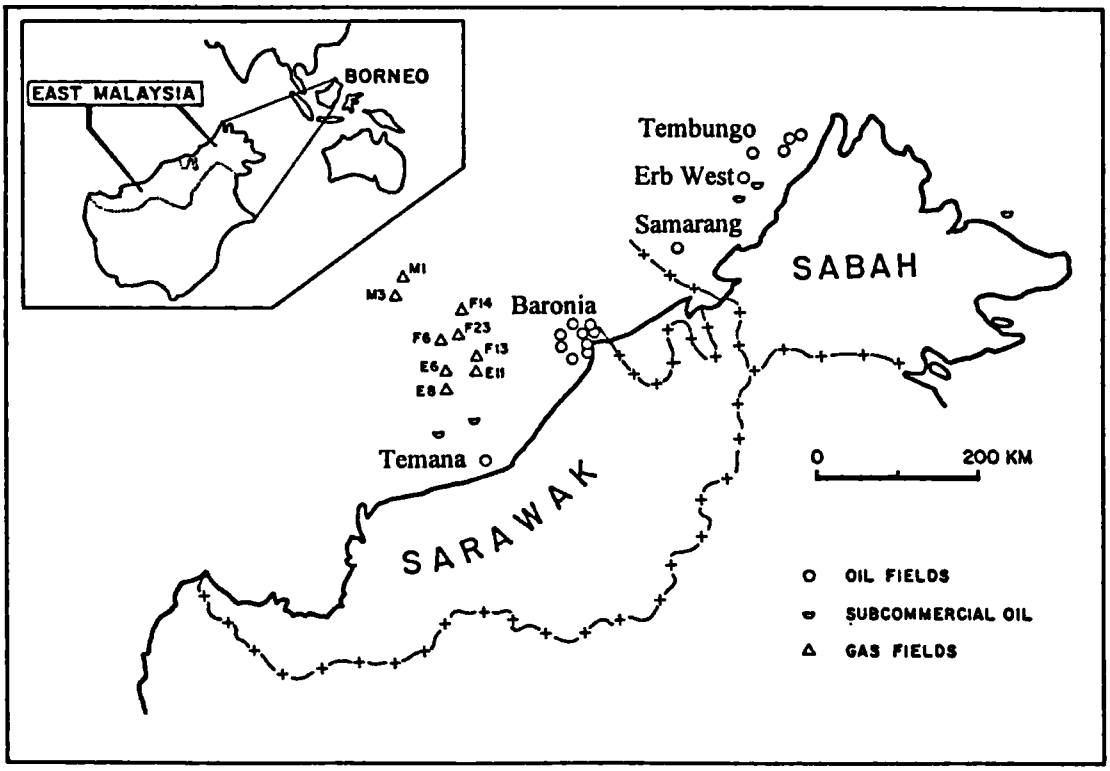


FIGURE 1.3 Location of oil discoveries and major gas fields in East Malaysia (from Scherer, 1980).

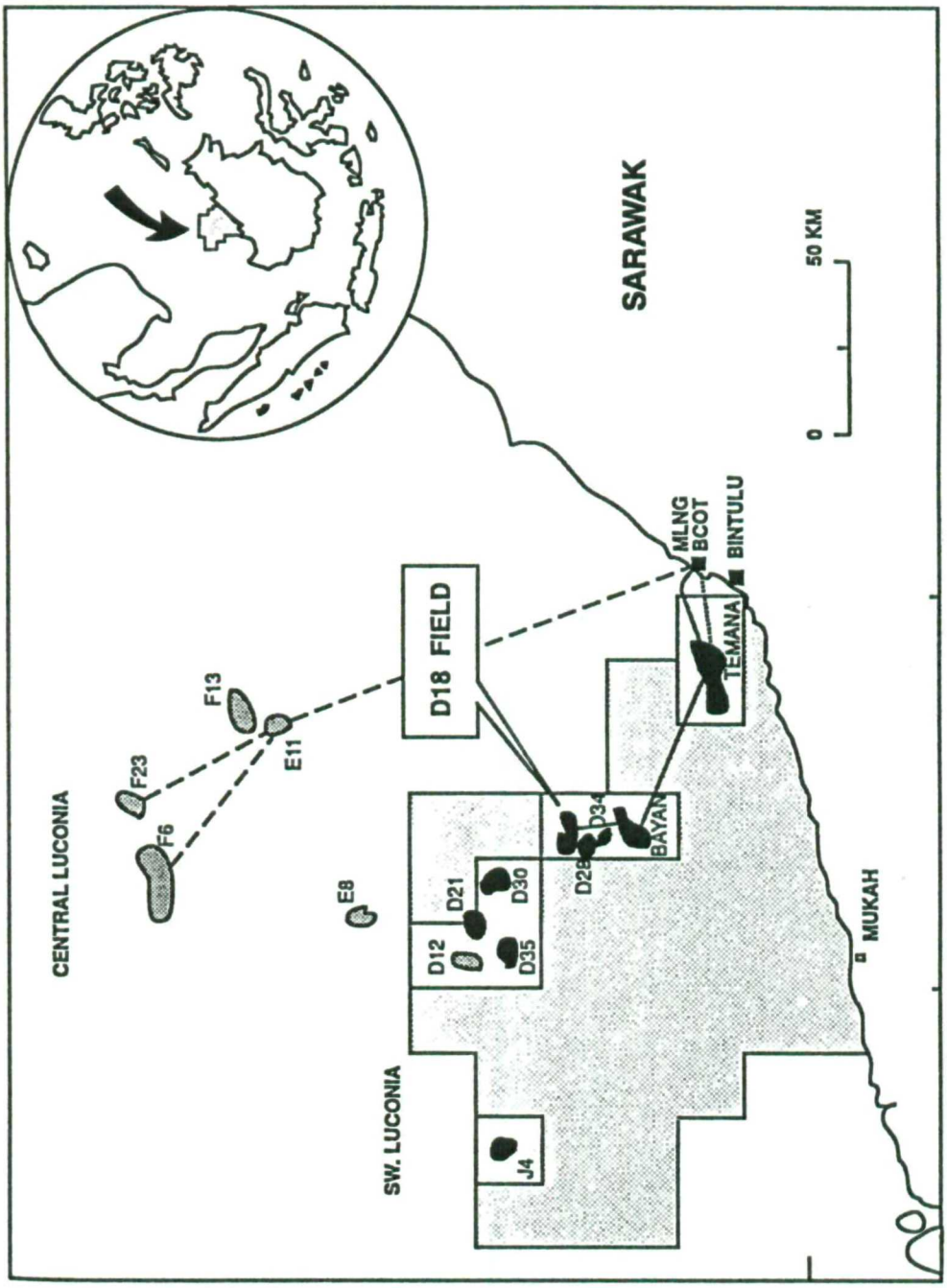


FIGURE 1.4 Location of the Central Luconia Province and the D18 field, offshore Sarawak (from Almond *et. al.*, 1990).

Table 1.1 Key to the basins shown in Figure 1.1 (from Hutchison, 1989).

No.	Basin Name	Class	Av. G.	No.	Basin Name	Class	Av. G.
1	SW China	C	27	36	Khorat-Vientiane	C	
2.	East China Sea	B		37	Bengal	B/E	
3	South China Shelf	B	33-48	38	Upper Chindwin	F/E	
4	Gulf of Bacbo (Tonkin)	A	40	39	Central Basin	F/E	
5	Sierra Madre	F		40	Lower Irrawady	I	
6	Cagayan Valley	G	22	41	Gulf of Martaban	I	
7	Luzon Central Valley	F	24	42	South Andaman	H	33
8	Ragay-Samar	G	41	43	North Sumatra	I	47
9	Visayan	G	31	44	Sibolga	F	24
10	Leyte	F	41	45	Central Sumatra	I	61
11	Davao-Agusan	G		46	Bengkulu	F	24
12	Cotabato	F	18	47	South Sumatra	I	49
13	Iloilo	F	29	48	Sunda	I	46
14	South Mindoro	G	29	49	Billiton sub-basin	I	32
15	Reed Bank	J		50	North-west Java	I	46
16	West Palawan	D/J	27	51	South Java	F	
17	East Palawan	F	22	52	East Java	I	39
18	Balabac	H		53✓	Barito	I	36
19✓	Bancauam	H		54	Melawi	F	
20✓	Sandakan	F	28	55	Ketungau	F	
21✓	Tarakan	A	38	56✓	Kutei	A	32
22	Kelabit-Long Bawan	J		57	North Makassar	A	
23✓	Sabah	D/F	28	58	Paternoster Platform	J	
24✓	Baram Delta	J	28	59	South Makassar	A	25
25✓	Central Luconia	J	43	60	Bone	A	8
26✓	Balingian	J	41	61	Savu	F	
27	West Luconia	J		62	Scott Plateau	B	
28	Sokong sub-basin	J	56	63	Ashmore Block	B	23
29	Northeast Natuna	J	34	64	Vulcan sub-basin	B	26
30	Saigon	A		65	Browse Basin	B	27
31	Vung Tau	A		66	Londonderry High	B	37
32	West Natuna	A	38	67	Sahul Ridge	B	47
33	Penyu	A	38	68	Bonaparte Gulf	A	
34	Malay	K	45	69	Money Shoals	B	
35	Gulf of Thailand	K	50	70	Bula	F	17
	(Chao-Phraya,			71	Salawati	B	36
	Phitsanulok)			72	Bintuni	B	30

Av. G. = average geothermal gradient in °C/km.

Basin classification : **A** = aulacogen rifts in continental lithosphere (ref. 1), continental interior fracture (Ref. 2); **B** = Atlantic-type miogeoclinal margin (Ref. 1), continental margin sag (Ref. 2); **C** = cratonic basin (Ref. 1), continental interior sag (Ref. 2); **D** = trench (Ref. 1), oceanic trench (Ref. 2); **E** = foredeep or collision zone (Ref. 1), continental margin sag affected on one side by a foldbelt (Ref. 2);**F** = fore-arc basin (Ref. 1), trench-associated basin (Ref. 2); **G** = intra-arc basin (Ref. 3), trench-associated basin (Ref. 2); **H** = marginal sea basin (Ref. 1); **I** = continental wrench or shear basin (Ref. 2); **J** = basin on and peripheral to continental fragments (Ref. 3), various classifications but mainly a combination of continental margin sag and foldbelt (Ref. 2); **K** = Pannonian-type back-arc basin (Ref. 1), continental wrench or shear basin (Ref. 2).

References : **1** = Bally & Snelson (1980), **2** = Kingston *et. al.* (1983), **3** = Hutchison (1984).

Other Tertiary hydrocarbon-bearing basins with Type III organic matter reported as source material in the Borneo area include the Handil, Badak, Nilam and Bekapai fields of Kutei Basin, where the Mahakam Delta is situated (**Figure 1.1**).

Table 1.2 Estimated ultimate recoverable reserves of Sabah, Sarawak and Brunei.

Area	Oil (million bbls)	Gas (trillion cu. ft.)	Gas (million bbls. oil equiv.)	Total oil & gas (million bbls.)
Sabah	> 250			> 250
Luconia Province-Balingian Province		15 unpublished	2500	2500
Baram Delta :				
1. Sarawak	600	-	600	600
2. Brunei	2000-3500	7.7-10	1283-1667	3283-5167
			Cumulative total :	6583-8467

Oils encountered in these basins are generally light (API gravity : 25-45°) and waxy with low sulphur contents. The occasional occurrence of heavy, non-waxy hydrocarbons are related to shallow reservoirs where bacterial degradation had resulted in the removal and subsequent loss of wax contents (Scherer, 1980). The characteristics of the crude oils concur with land derived organic matter as the source material (Scherer, 1980; Rijks, 1981; Ellenor, 1984). No marine source rocks have been detected (Rijks, 1981). The ability of land plant material to generate liquid hydrocarbons is generally accepted based upon the many reported occurrences in Australian basins (Thomas, 1982; Thompson *et. al.*, 1985; Shanmugam, 1985; Philp & Gilbert, 1986; Powell *et. al.*, 1991), in Indonesia (Noble *et. al.*, 1991; Robinson, 1987) and the Mahakam Delta, Kalimantan (Combaz & de Matharel, 1978; Hoffman *et. al.*, 1984).

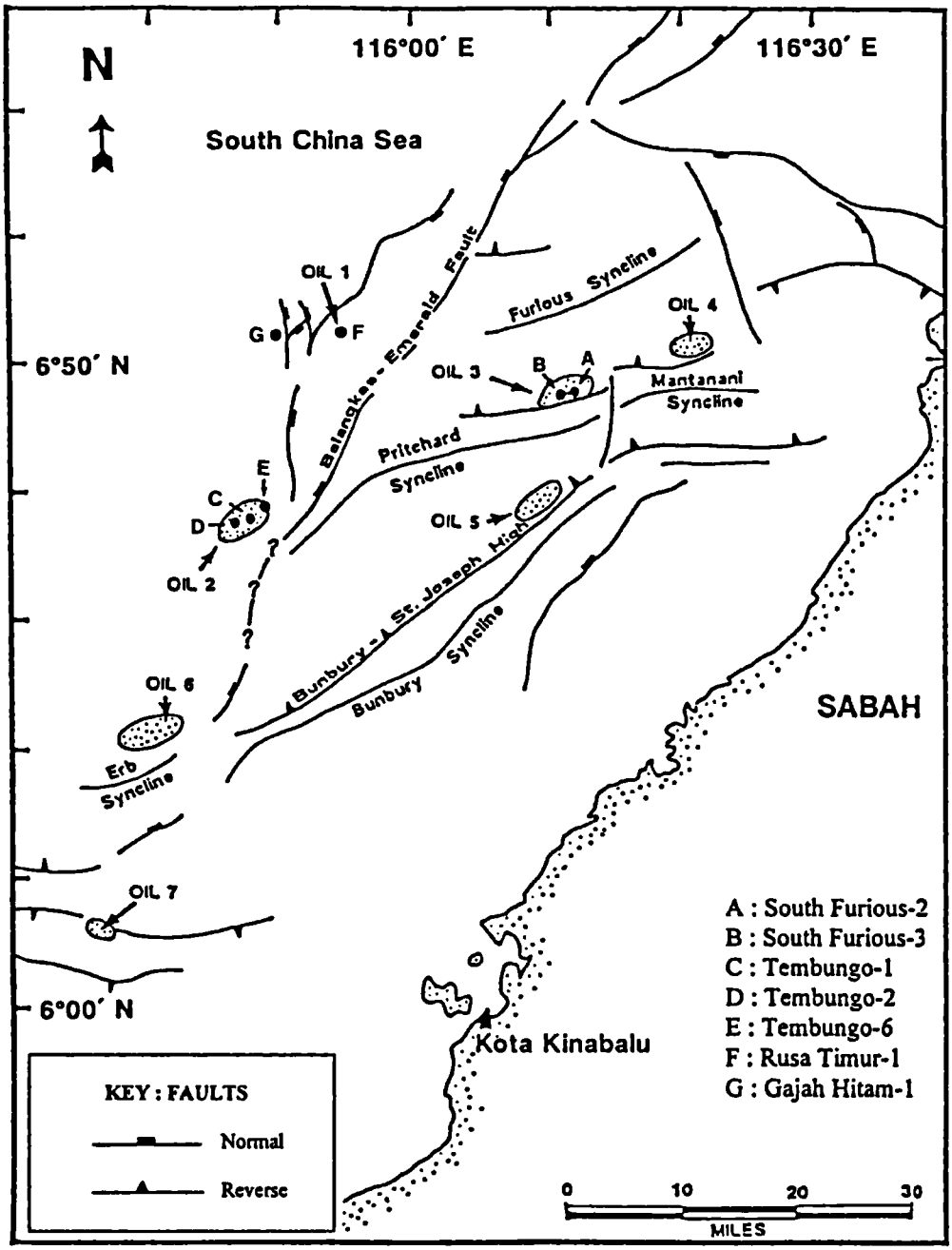
However, the very large hydrocarbon reserves in the Sarawak-Brunei-Sabah area raises the question - how can such large reserves be produced from the least oil-prone, Type III land-derived organic matter? Ellenor (1984) reported that no discrete rich source rock layers of mappable extent have been identified in Brunei, and such is the present case for Sarawak and Sabah Basins. Despite active exploration, uncertainty still surrounds the identity of the source rocks responsible for generating the oil and gas. The timing of hydrocarbon generation and migration with respect to trap formation is also still uncertain.

1.2 Aims and organisation of dissertation

This project was undertaken as part of a larger joint source rock study with British Gas (Malaysia) involving several fields in Sabah Basin with the objective of identifying the source rocks responsible for the hydrocarbons present in the basin. For this study, a total of 318 core, sidewall core and ditch-cutting samples were collected from seven wells : South Furious-1, South Furious-2, Tembungo-1, Tembungo-2, Tembungo-6, Rusa Timur-1 and Gajah Hitam-1 (**Figure 1.5**). These areas are located along the general depositional dip, with South Furious in the shallowest and Rusa Timur/Gajah Hitam in the deepest regions. They were chosen so that organic matter distribution and variations along the depositional dip can be studied. South Furious and Tembungo are hydrocarbon-producing fields, Rusa Timur-1 had oil and gas shows and Gajah Hitam-1 was a dry-hole. The two latter wells were included in the study because they are the only wells, at present, located in the deep water area of Sabah Basin. Information from them will be useful for organic matter distribution studies as well as providing the opportunity to investigate the presence or absence of marine source rocks.

Chapter 2 provides the geological background of Sabah Basin and the study area following a more regional outlook in **Chapter 1**. Details on sampling horizons and number of samples are outlined in **Chapter 3**, along with a list of organic geochemical analyses performed on the samples. In **Chapter 4**, the organic geochemical techniques used in this study are briefly reviewed so as to provide a general guide to result interpretations. Analytical results from TOC determination, pyrolysis, solvent extraction, gas chromatography, kerogen density separation, optical petrography, elemental analysis, vitrinite reflectance measurements and stable carbon isotope data are presented in **Chapter 5**. Based on cumulative results, the most plausible source rocks are identified. The following **Chapter 6** discusses results from biological markers observed in gas chromatography - mass spectrometry fragmentograms of triterpane m/z 191 and sterane m/z 217 with respect to organic matter source type, palaeodepositional environments as well as thermal maturity indicators. Principal components analysis was performed on biomarker data to aid information extraction.

In **Chapter 7**, burial histories of individual wells and sediments in the hydrocarbon kitchens are reconstructed using the Platte River Associates' modelling package, BasinMod. Thermal maturity level from vitrinite reflection measurements were compared with BasinMod's calculated values. Timing of hydrocarbon generation in the kitchen areas determined from three methods - Lopatin's TTI, Hunt & Hennet's Arrhenius-based TTI_{ARR} and BasinMod - is also discussed. Factors controlling organic matter deposition and preservation are investigated in **Chapter 8** to elucidate the possible reasons for the success of Type III source rocks in generating the large hydrocarbon accumulations in the Sabah Basin. The conclusions to this study are presented in **Chapter 9**.



KEY : OIL 1 = Rusa Timur
OIL 2 = Tembungo
OIL 3 = South Furious
OIL 4 = Barton
OIL 5 = St. Joseph
OIL 6 = Erb West
OIL 7 = Ketam

FIGURE 1.5 Location map of wells included in this study - South Furious-2, South Furious-3, Tembungo-1, Tembungo-2, Tembungo-6, Rusa Timur-1 and Gajah Hitam-1.

CHAPTER TWO

GEOLOGY OF SABAH BASIN

2.1 Structural development

South East Asia lies at the junction of three major tectonic plates : the Asian, Pacific and Indo-Australian Plates (**Figure 2.1**). The Sabah Basin (**Figure 2.2**) is a 350 km long and 140 km wide trench-associated Tertiary basin (Kingston *et. al.*, 1983) situated offshore Sabah. It elongates in a northeast-southwest direction and contains approximately 12km of predominantly siliciclastic sediments (Levell, 1987). It is situated on what is interpreted to be an accretionary prism which formed as a result of the opening of the South China Sea (Taylor & Hayes, 1980; Holloway, 1981; Ru & Pigott, 1986; Pautot *et. al.*, 1986). From their analysis of magnetic anomaly data, Taylor and Hayes (1980) concluded that sea-floor spreading of the South China Sea occurred between 17-32 Ma, from Middle Oligocene through to Early Miocene. The opening of the South China Sea has been genetically linked to the Oligocene-Miocene left-lateral strike-slip motion on the Red River Fault (China), resulting from escape tectonics following the Eocene collision of India with Eurasia (Tapponier *et. al.*, 1986).

Due to the opening of South China Sea, the south China micro-continental crust eventually collided with Borneo in Early Miocene, forming a collision zone along Borneo's north-western margin. The resulting deformation and uplift of the Eocene-Oligocene Crocker Formation (**Figure 2.3**) rejuvenated the Sabah landmass and formed an eroding provenance which provided the source of clastic infill for the offshore Sabah Basin during the Neogene. Four major tectonic provinces aligned parallel to each other (**Figure 2.3**) were identified by Bol & van Hoorn (1980) :

1. Palaeogene Foldbelt Zone : An inner province of Palaeogene deep water sediments deposited in the north-south trending NW Borneo geosyncline which were deformed mainly during Early Miocene. The rugged and mountainous Crocker Range was formed by Pleistocene epeirogenic movements (vertical uplift).
2. Basement Faulting Zone : A province of Lower-Middle Miocene deep marine to continental sediments which were folded into tight, narrow and partly up-thrusted trends during the early Late Miocene and Early Pliocene, possibly due to deep-seated basement faulting.

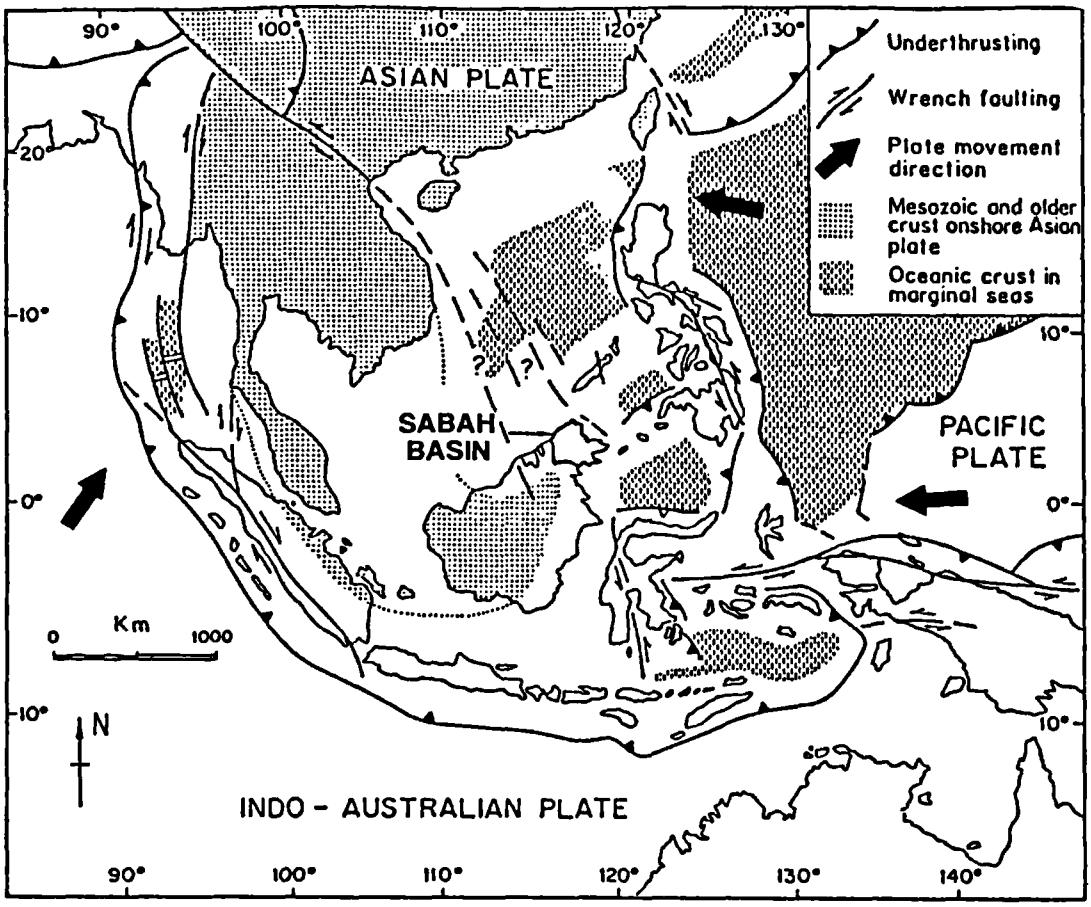


FIGURE 2.1 Tectonic elements of South East Asia (after James, 1984, based on Hamilton, 1979 and Holloway, 1982).

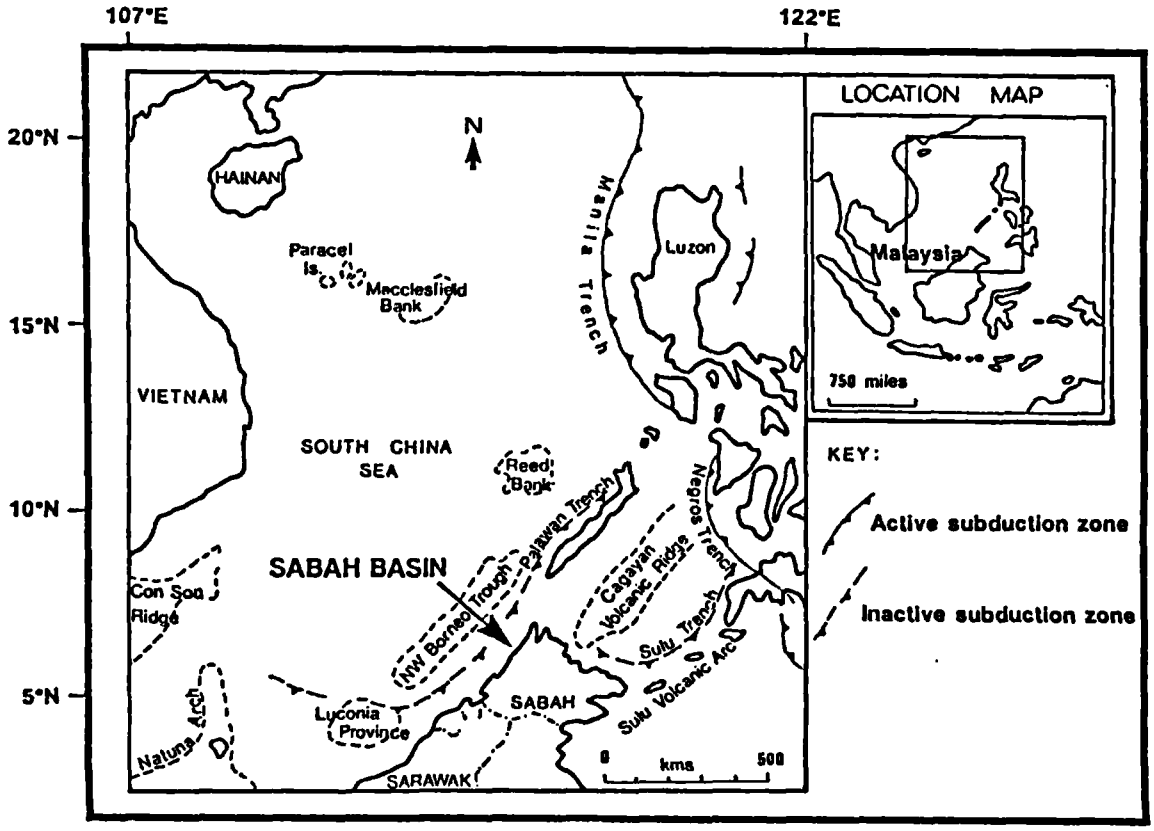


FIGURE 2.2 Sabah Basin location map **(after Letouzey et. al., 1988)**

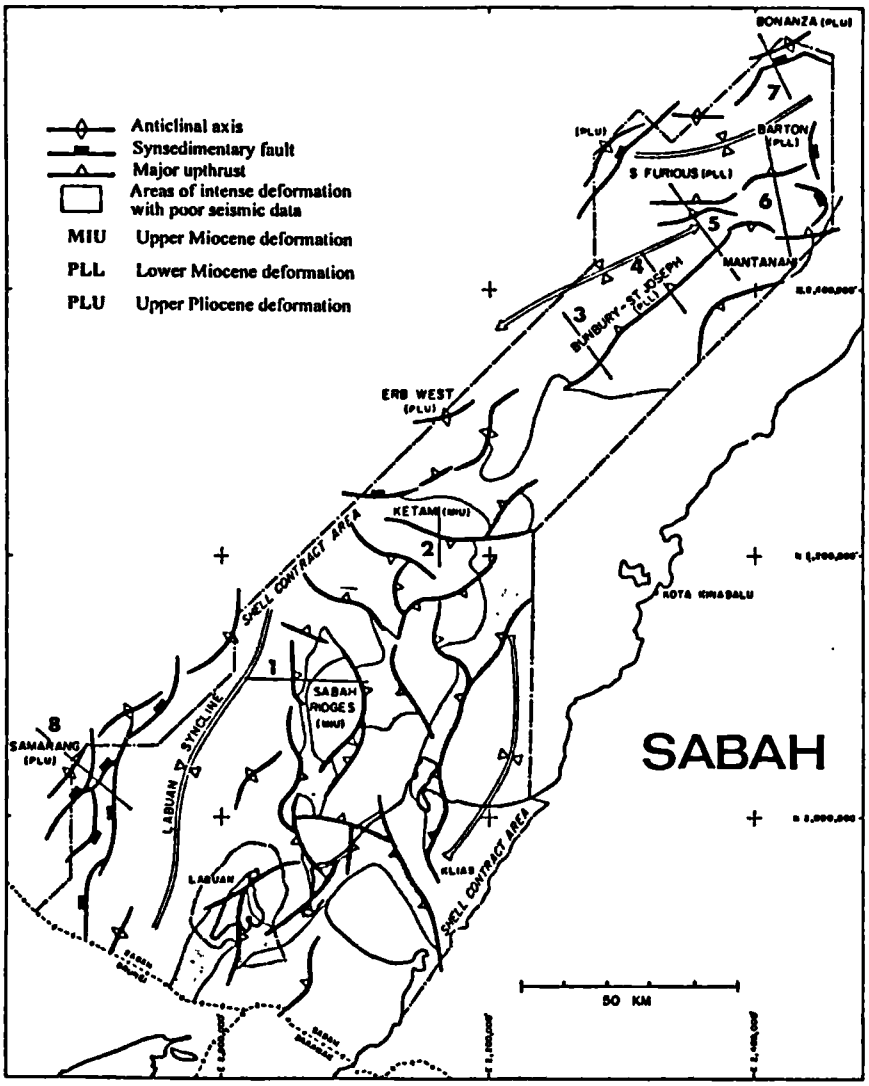


FIGURE 2.4 Structural sketch map of Bol & van Hoorn (1980) showing the timing of deformational phases in offshore Sabah Basin.

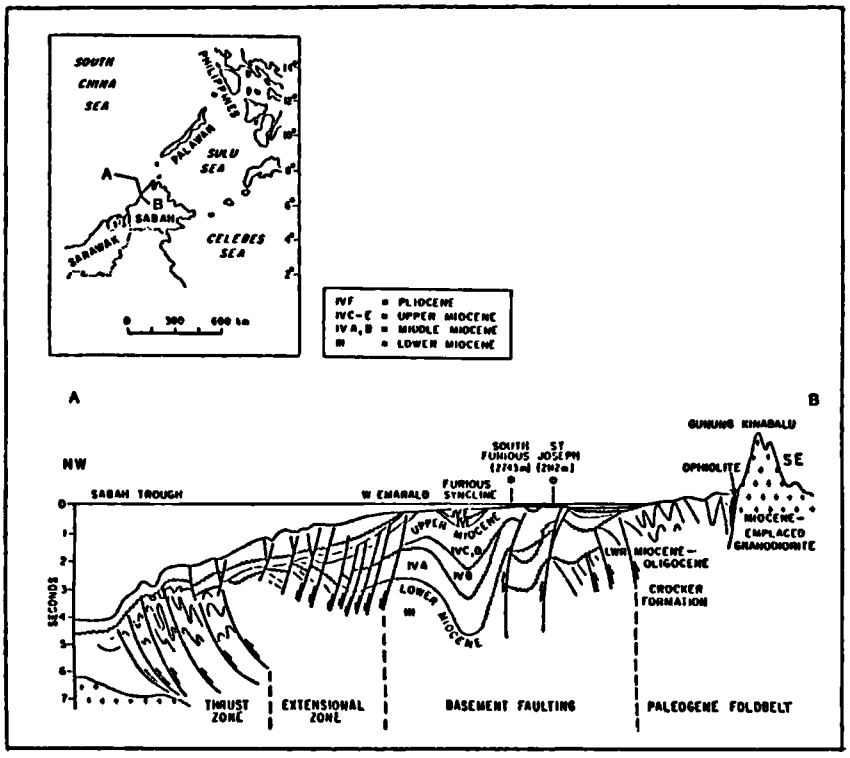


FIGURE 2.3 NW-SE section across Sabah Trough - Sabah Basin - Mt. Kinabalu (modified after Bol & van Hoorn, 1980 and ASCOPE, 1980).

3. Extensional Zone : A province of extensional and partly syn-sedimentary faulting. The thick succession of Upper Miocene-Lower Pliocene deltaic to shallow marine sediments were mildly affected by Late Pliocene compressional movements.
4. Thrust Zone : An outer province of intensely folded, over-thrusted and imbricated Neogene deep water sediments, deformed during the Pliocene.

Bol & van Hoorn (1980) recognised three separate phases of structural deformation: (i) a Late Miocene phase in central and south Sabah, (ii) an Early Pliocene folding in north-northeast Sabah and (iii) a Late Pliocene phase along the western-most margin of Sabah Basin (**Figure 2.4**). Recent structural movements are suggested by the presence of faults propagating through to the present sea-bed (Azim-Ibrahim, 1994). The over-printing of several episodes of structural events resulted in complex fault patterns in Sabah Basin.

The Late Miocene deformation which affected south and central Sabah is characterised by thrust-bounded steep anticlines separated by broad, deep and gently folded synclines. Poor or incoherent seismic reflections are associated with the crestal part of these narrow highs (**Figure 2.5**) which are also referred to as the 'Sabah Ridges' (Bol & van Hoorn, 1980). Towards central Sabah, the tight and asymmetric Ketam anticline (**Figure 2.4**) represents the continuation of the ridges (**Figure 2.6**). The Early Pliocene deformational phase primarily affected the north-eastern parts of the basin, resulting in two major structural trends : the Bunbury-St. Joseph High (**Figure 2.7**), and the South Furious-St. Joseph and Mantanani-Barton structures (**Figures 2.8 & 2.9**). Finally, the Late Pliocene tectonic phase mostly affected the western margins of Sabah Basin (**Figure 2.4**), an area characterised by extensional and syn-sedimentary faulting. These extensional zones were inverted by the Late Pliocene mild compressional movements, forming a series of NE-SW trending, gentle anticlines with numerous crestal faults (Bol & van Hoorn, 1980). Examples of these anticlines are the densely faulted Bonanza structure and the oil-bearing Samarang structure (**Figure 2.10**).

2.2 Stratigraphic framework

The stratigraphic framework of Sabah Basin is defined by four major Tertiary sedimentary units informally known as Stages I, II, III and IV (**Figure 2.11**). These units are seismically-defined by the correlation of nine regional unconformities and their correlative conformities (Bol & van Hoorn, 1980). The sedimentary sequences were deposited during two main phases of basin development (Levell, 1987) :

1. A pre-Middle Miocene phase of deep marine sedimentation constituting sediments of Stages I, II and III. These were subjected to strong compressional forces related to the subduction of the south China rifted margin beneath Sabah, forming an imbricate wedge. Stage III is currently regarded as the economic basement for hydrocarbon exploration.

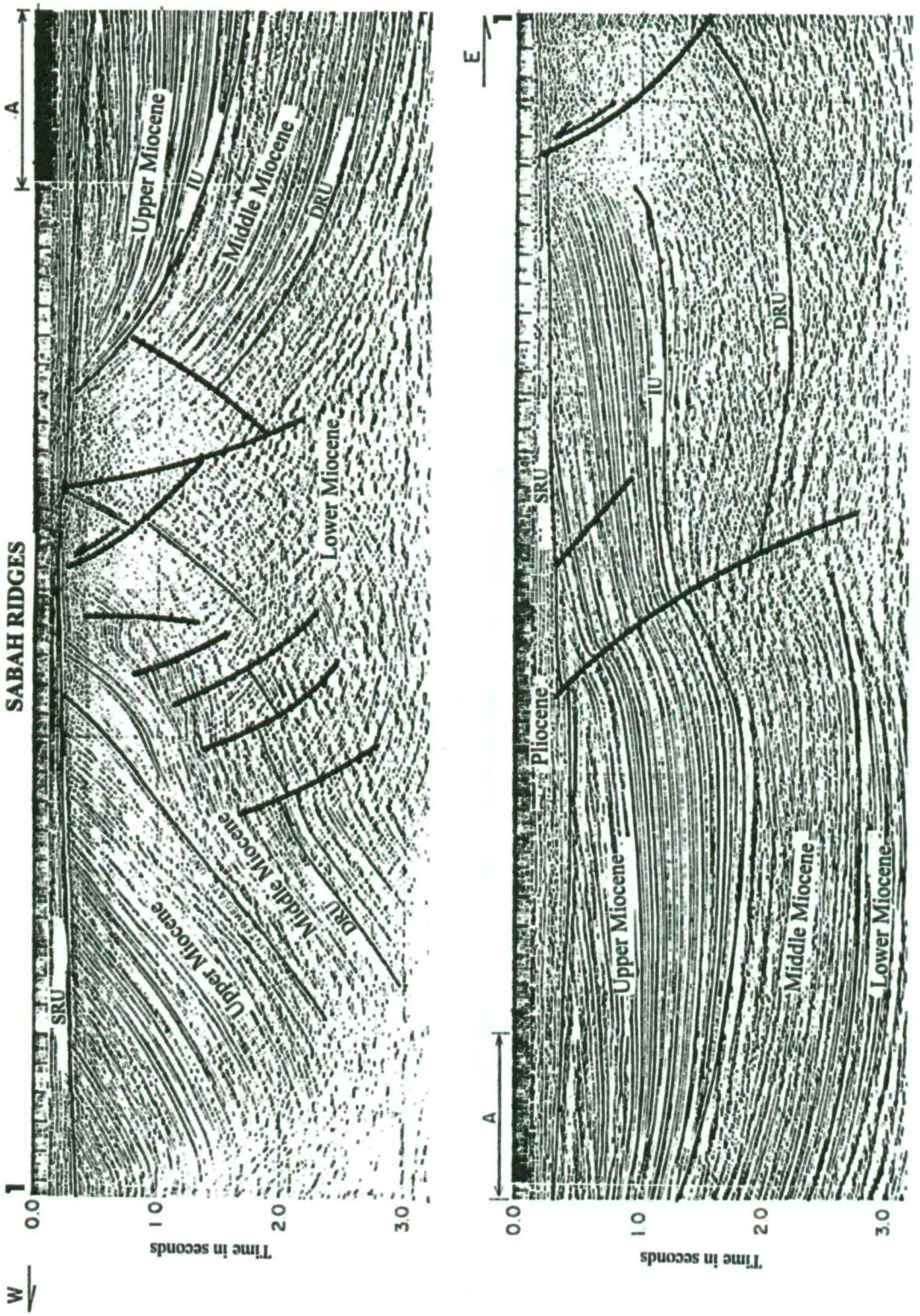


FIGURE 2.5 Migrated seismic section of the 'Sabah Ridges' (Bol & van Hoorn, 1980). For the location of the section, please refer to **FIGURE 2.4.**

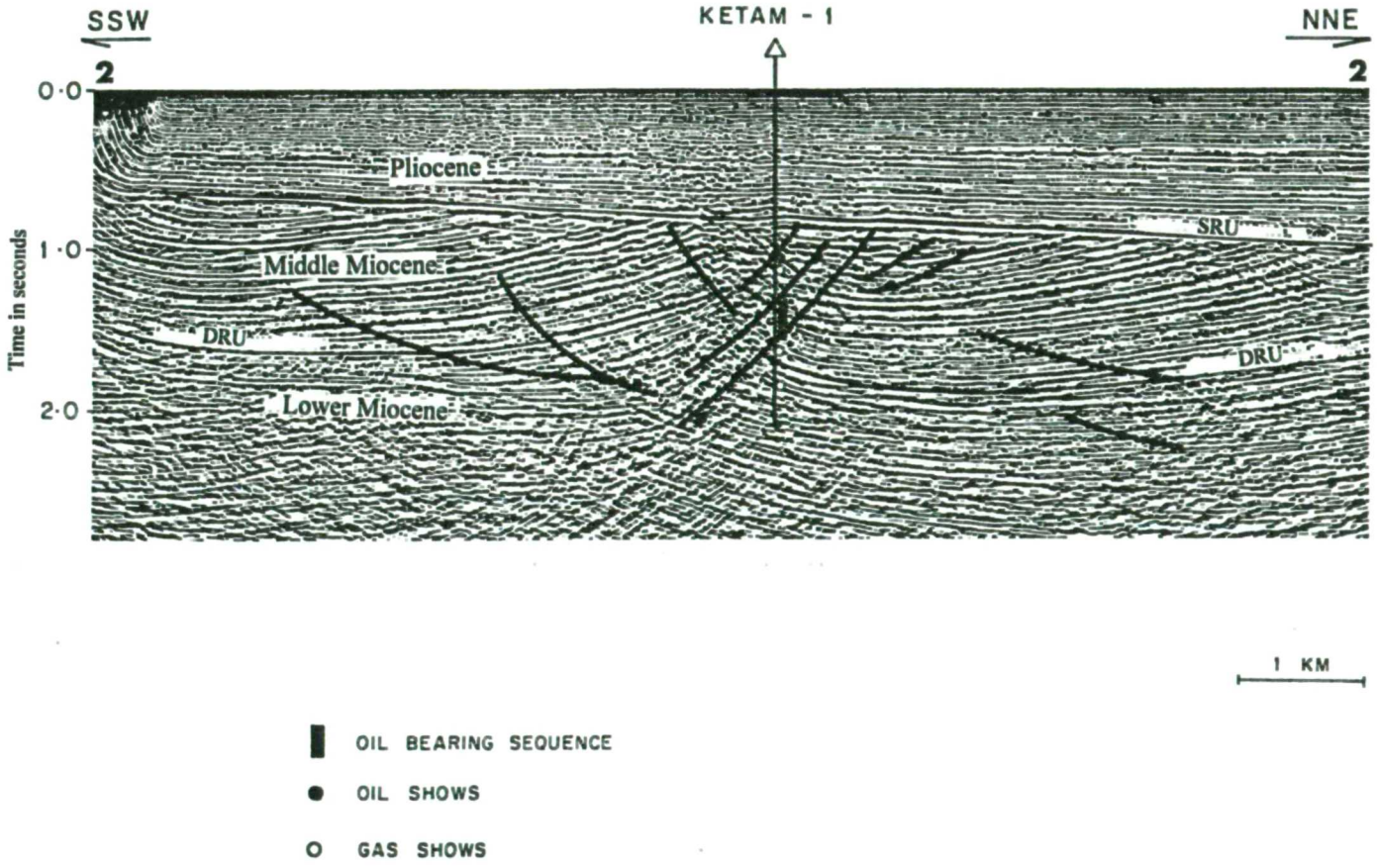


FIGURE 2.6 Migrated seismic section of the Ketam structure (Bol & van Hoorn, 1980). For the location of the section, please refer to **FIGURE 2.4**.

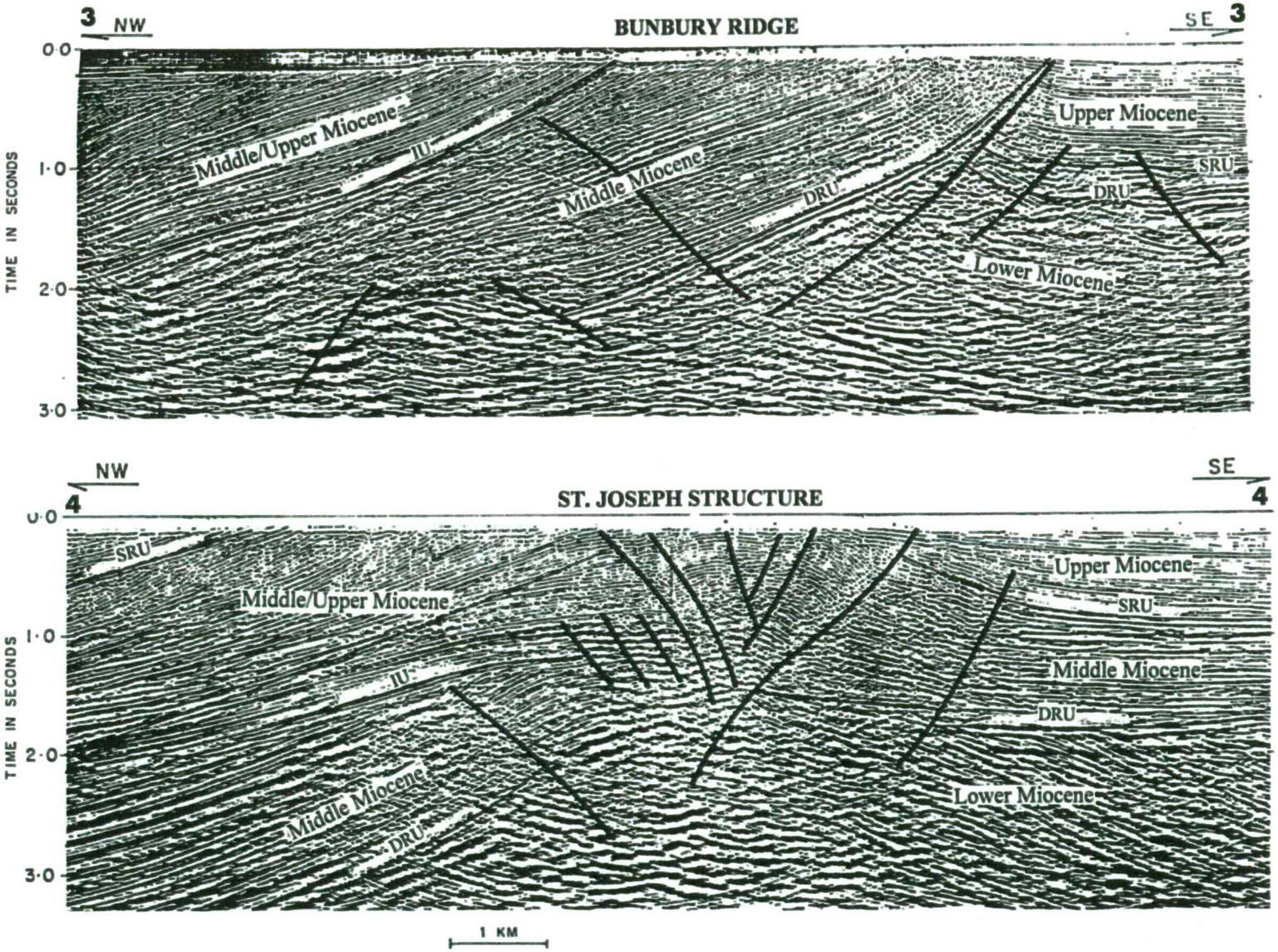


FIGURE 2.7 Migrated seismic section of the Bunbury - St. Joseph High (Bol & van Hoorn, 1980). For the location of the section, please refer to **FIGURE 2.4**.

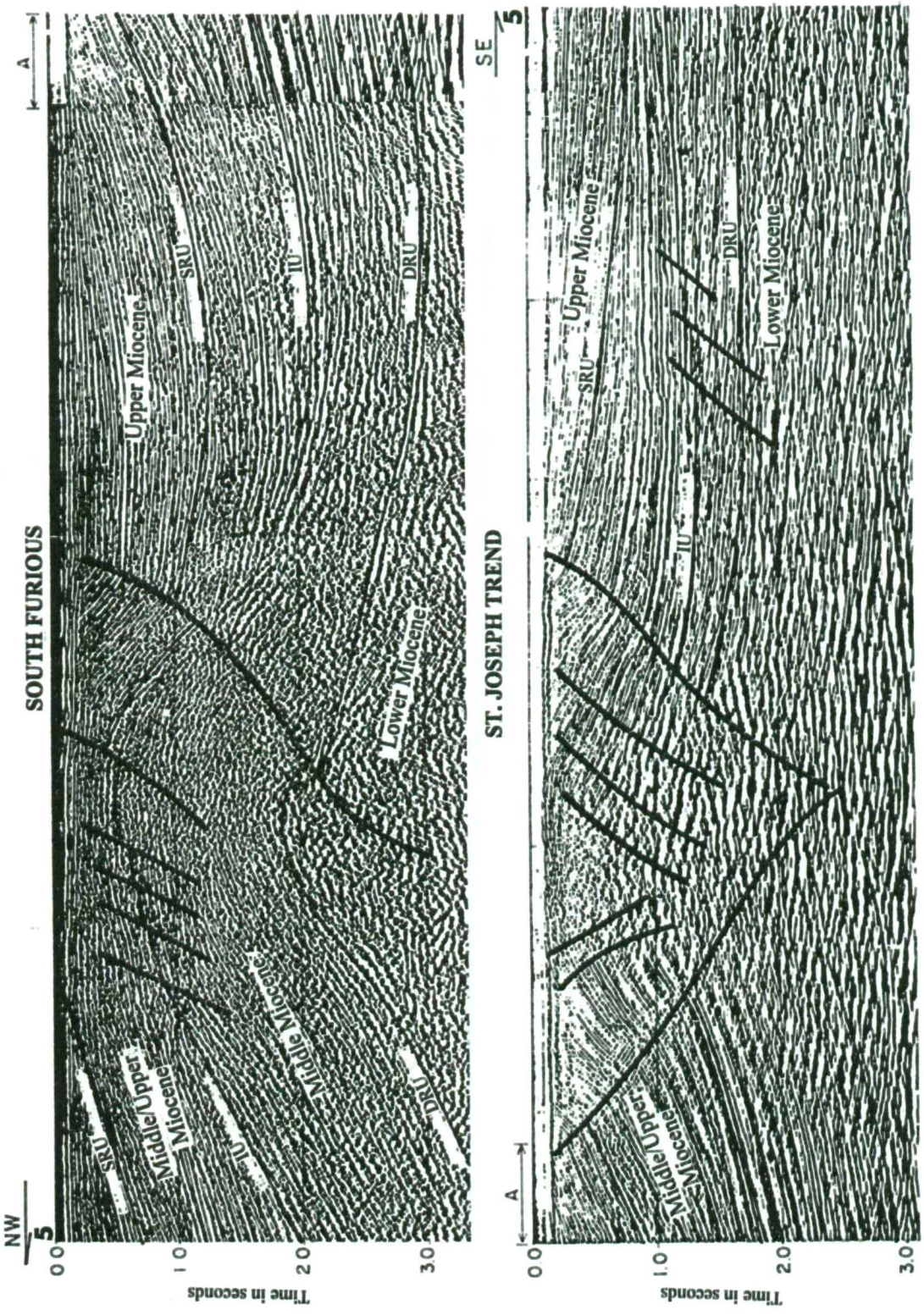


FIGURE 2.8 Migrated seismic section of the South Furious - St. Joseph trend (Bol & van Hoorn, 1980). For the location of the section, please refer to **FIGURE 2.4**.

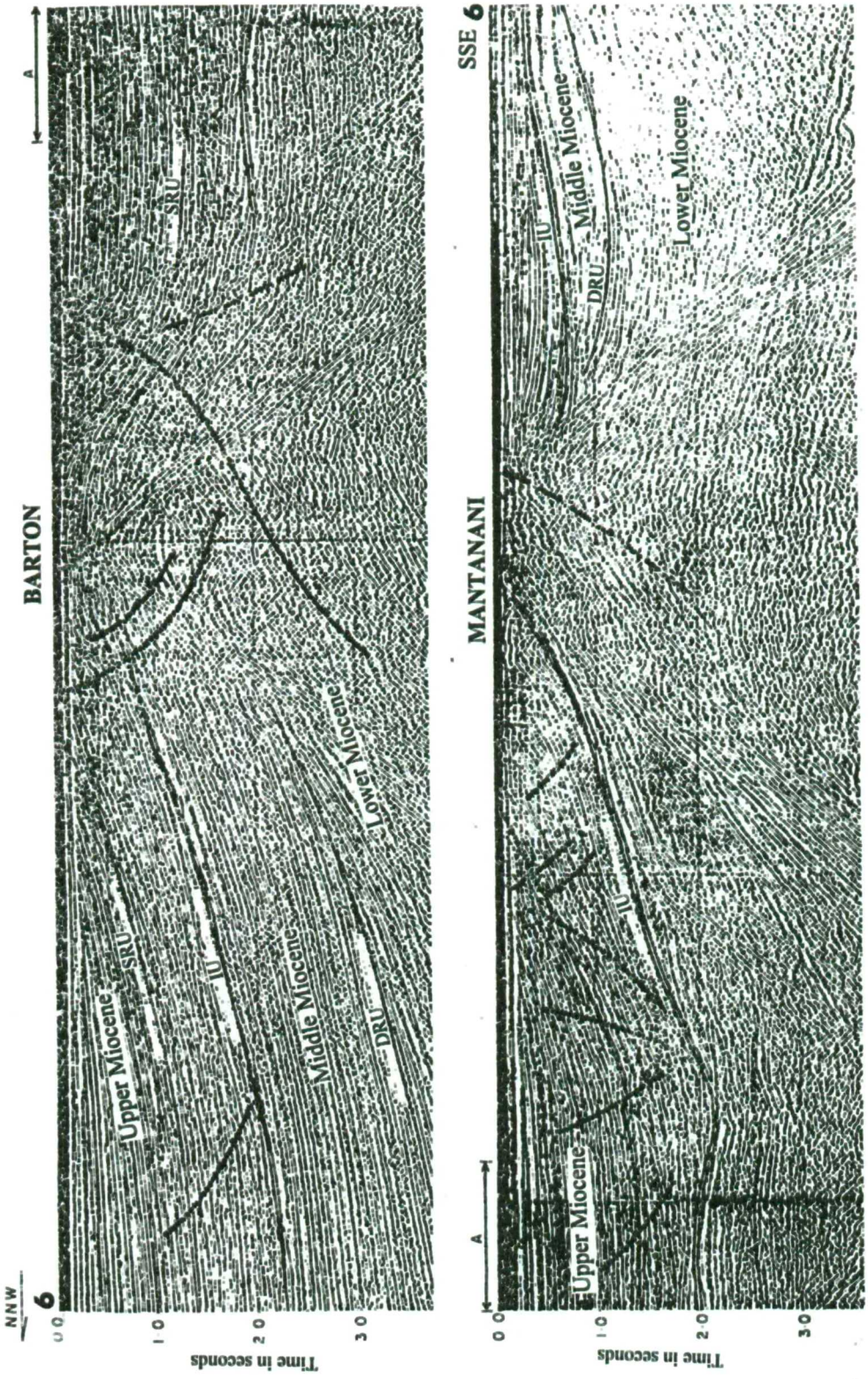


FIGURE 2.9 Migrated seismic section of the Mantanani - Barton trend (Bol & van Hoorn, 1980). For the location of the section, please refer to **FIGURE 2.4**.

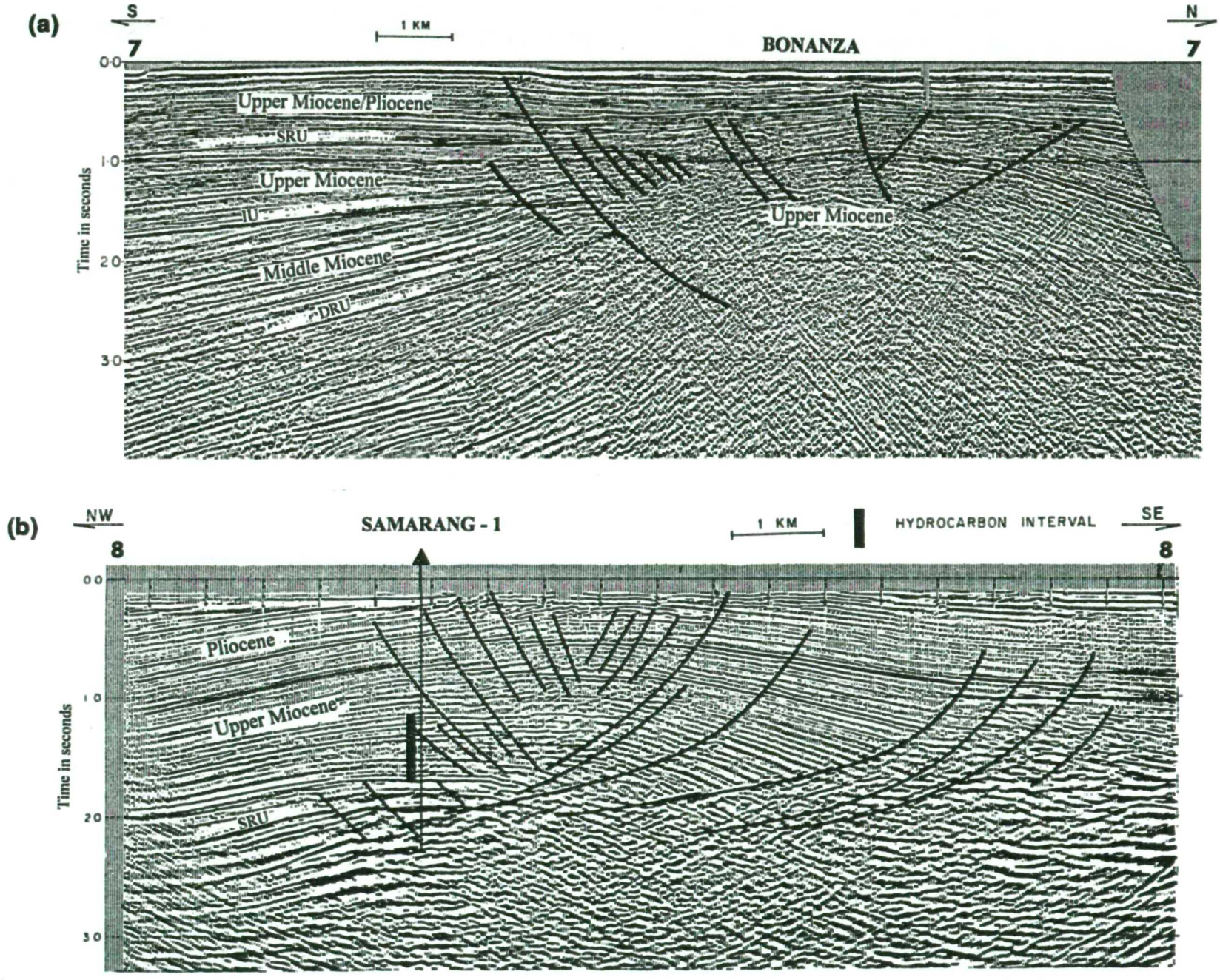


FIGURE 2.10 Migrated seismic sections of the (a) Bonanza and (b) Samarang structures (Bol & van Hoorn, 1980). For the location of the section, please refer to FIGURE 2.4

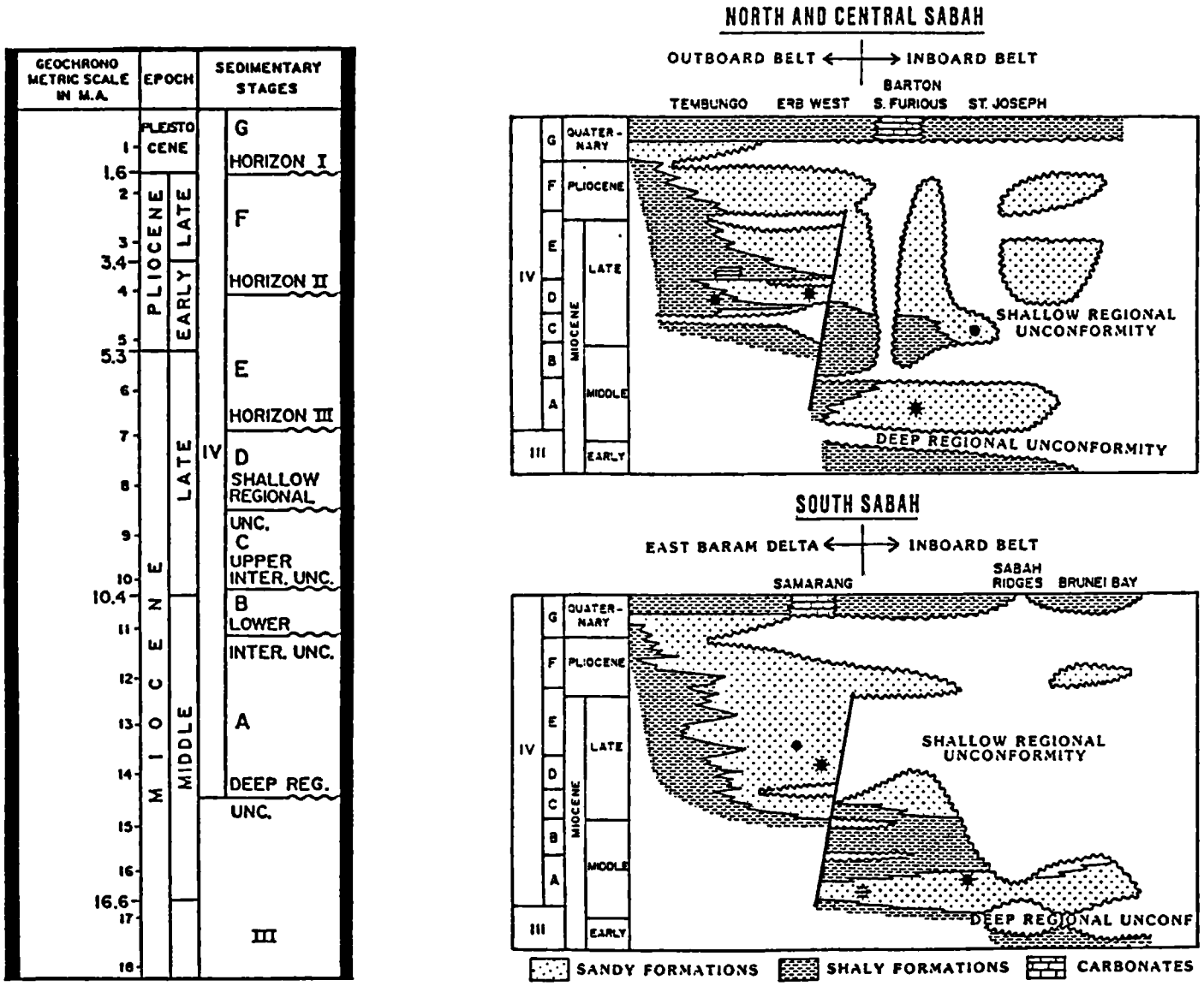


FIGURE 2.11 Chronostratigraphic framework of the Sabah Basin (after Johnson & Huong, 1991).

2. A Middle Miocene and later phase of lower coastal plain to deep marine sedimentation, representing Stage IV sediments.

The above units are separated by a major regional unconformity called the **Deep Regional Unconformity** (**DRU**) (Levell, 1987). All commercial accumulations discovered to date are in the Middle Miocene and younger deposits of the Stage IV mega-sequence (**Figure 2.11**). Only a few hydrocarbon occurrences have been discovered in pre-Middle Miocene deep-water deposits.

The prospective Stage IV mega-sequence has been further divided into seven sub-Stages (IVA-IVG) separated by seismically-defined unconformities and their correlative conformities in the deeper parts of the basin. These unconformities, which formed as the result of several episodes of both local structural deformation and a regional tilting towards the north-west, provide the correlation framework for Sabah Basin. The unconformities are referred to as : the **Lower** and **Upper Intermediate Unconformities** (**LIU** and **UIU**) in late Middle Miocene, the **Shallow Regional Unconformity** (**SRU**) in middle Late Miocene, **Horizon III** in late Late Miocene and **Horizons II** and **I** in Pliocene and Pleistocene, respectively. They can be easily mapped on seismic sections in the inner part of the basin but become difficult to map in the outer part, especially in rapidly subsiding synclinal areas where subsidence rates of more than 500-1000m/Ma are common (Azim-Ibrahim, 1994).

2.3 Description of Stage IV sequences

As this study is largely concerned with analysing the source rock potential of Stage IV sediments, a brief description of the sub-Stages IVA-IVG is provided below. A schematic palaeoenvironmental model based on the Baram Delta depositional system, which was first published by Ho Kiam Fui (1978) and used later by several other workers (Rijks, 1981; Rice-Oxley, 1991), is also adopted for this study (**Figure 2.12**).

2.3.1 Sub-Stage IVA

Uplift of the pre-Middle Miocene deep marine sequences resulted in the formation of the **Deep Regional Unconformity** (**DRU**), marking the base of sub-Stage IVA. Large volumes of sediments were eroded and transported from uplifted areas into the basin. The sequence represents a period of significant deltaic deposition offshore Sabah, reaching close to 2000m (approximately 6560 feet) in thickness. Well-developed lower coastal plain and upper coastal plain sandstone reservoirs were encountered in the inner parts of the basin, transitional into a regular alternation of estuarine/tidal channels and lagoonal clays in the South Furious and Barton areas. The vertical stacking of each environmental unit throughout sub-Stage IVA, coupled with the absence of seismic foresetting, suggest that sedimentation kept pace with subsidence (Levell, 1987). The end of sub-Stage IVA deposition (**Figure 2.13**) is represented by a marine onlap

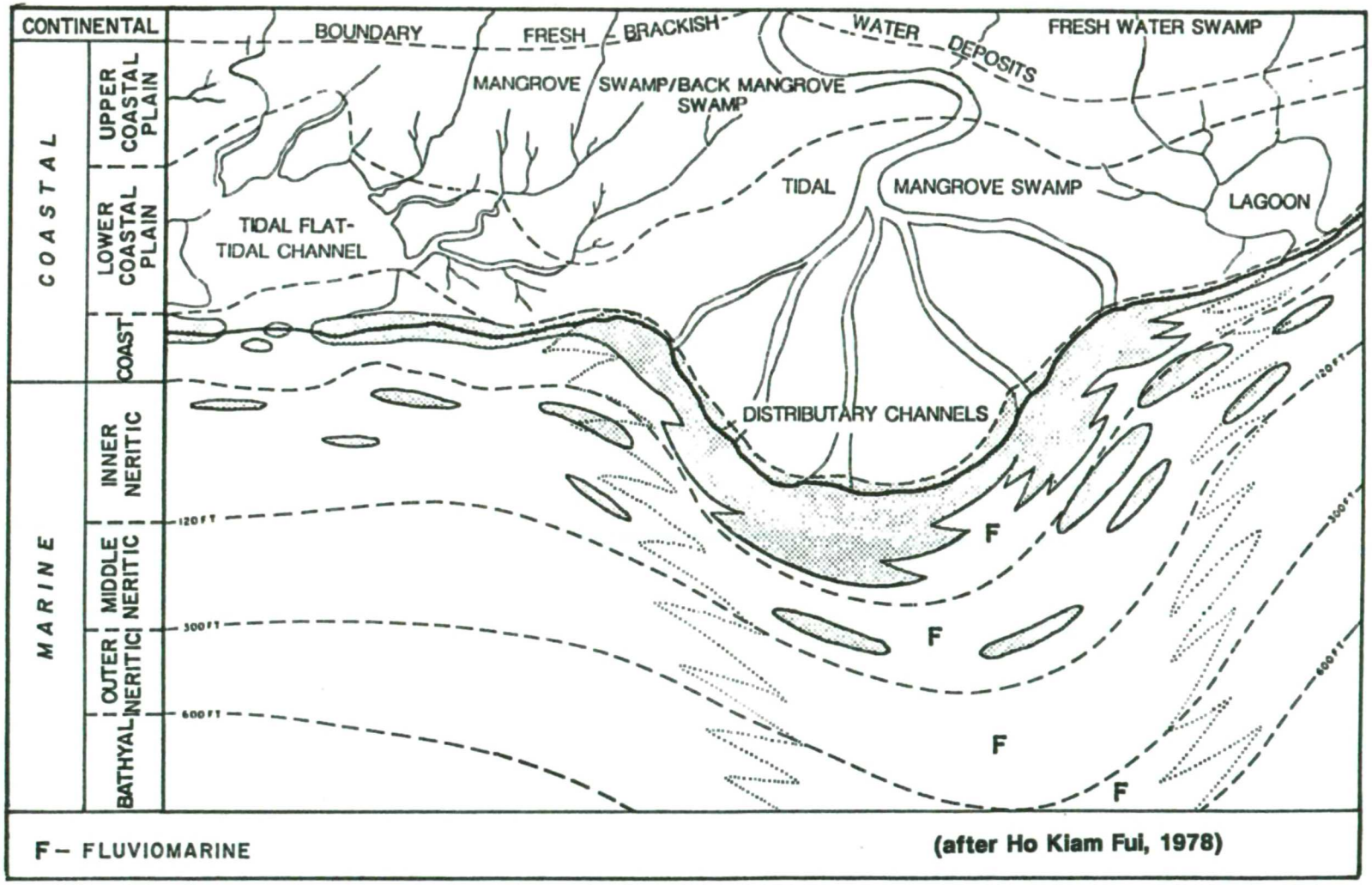


FIGURE 2.12 Schematic outline of NW Borneo palaeoenvironmental units (Ho Kiam Fui, 1978).

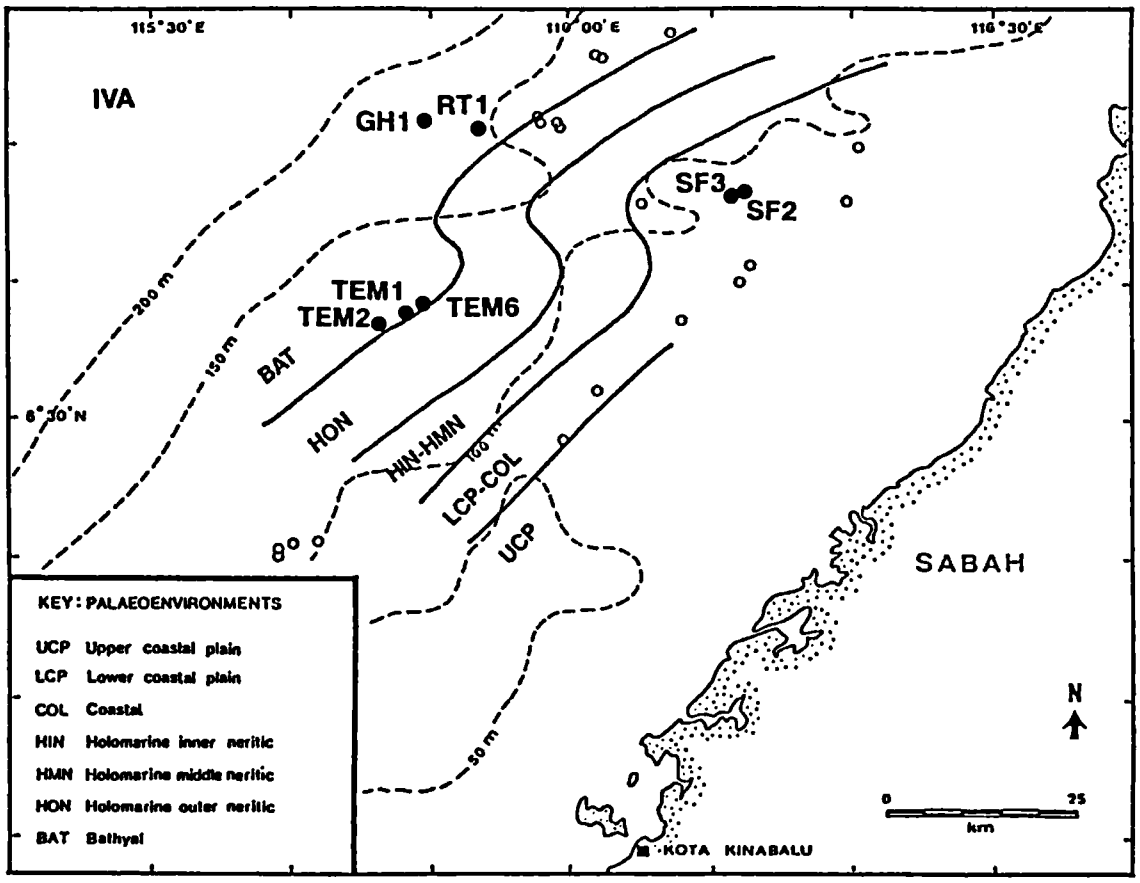


FIGURE 2.13 Palaeoenvironmental map at the top of sub-Stage IVA.

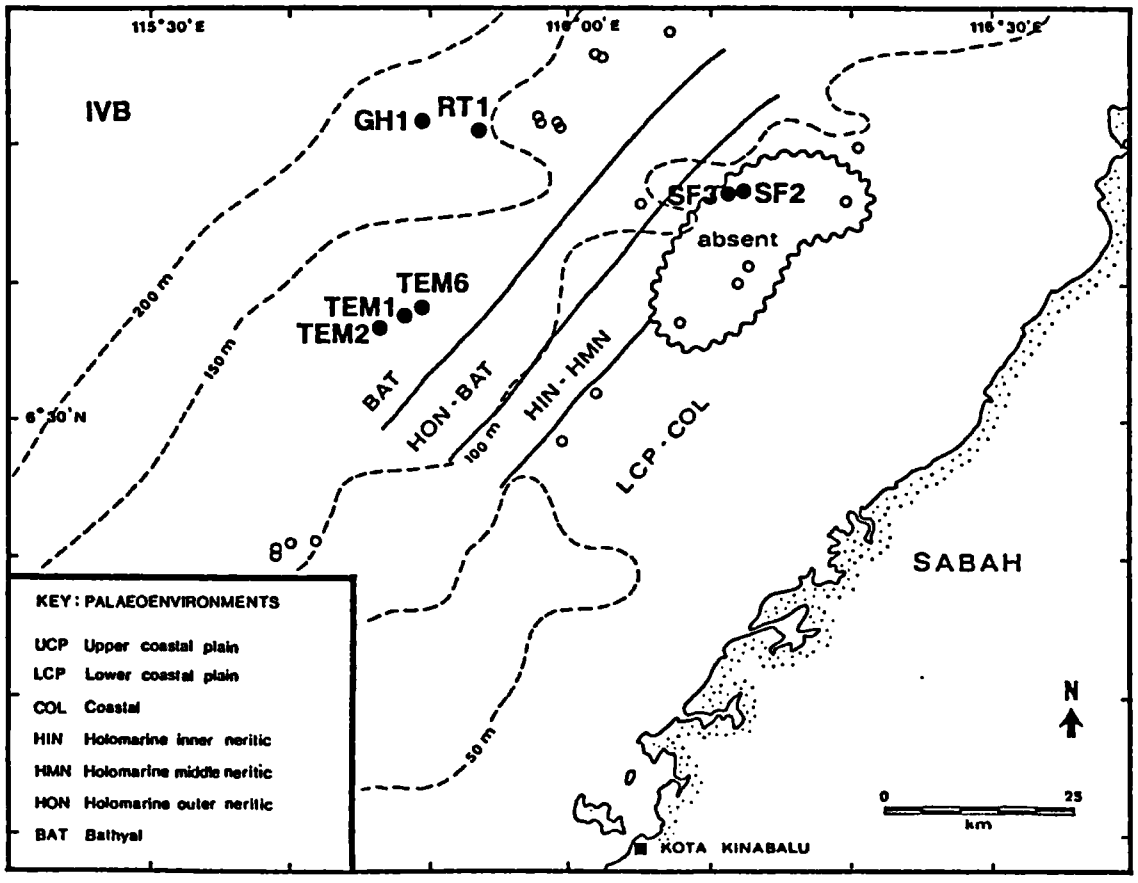


FIGURE 2.14 Palaeoenvironmental map at the top of sub-Stage IVB.

unconformity, known as the **Lower Intermediate Unconformity (LIU)**, caused by the increased rate of relative sea-level rise in Middle Miocene (Azim-Ibrahim, 1994).

2.3.2 Sub-Stage IVB

Sub-Stage IVB sediments mainly comprises a marine transgressive sequence. Exploration wells, supported by seismic evidence (e.g. hummocky seismic facies), indicate that the sediments consist of deep-marine shales and slope turbidites (Azim-Ibrahim, 1994). Shallow marine to lower coastal plain sediments of sub-Stage IVB may be present in the inboard area along the Bunbury-St. Joseph High but they cannot be distinguished from the sub-Stage IVA sequence due to the general absence of foraminifera and nannofossils. A marine erosional unconformity known as the **Upper Intermediate Unconformity (UIU)** marks the top of sub-Stage IVB. The submarine erosion of this unconformity was partly caused by the incision of submarine slump scars (Levell & Kasumajaya, 1985). The palaeoenvironmental map at the top of sub-Stage IVB shows non-deposition in the South Furious-Barton-Bambazon areas (**Figure 2.14**). No hydrocarbon accumulations have been encountered in this sub-Stage by any of the wells drilled between 1954-1984 (Sabah : well penetration chart 1954-1984, PETRONAS).

2.3.3 Sub-Stage IVC

Sub-Stage IVC represents the beginning of a Late Miocene regressive phase. During this regression, significant shelf edge slumping occurred along the Bunbury-St Joseph High and created basin-slope and basin-floor turbidites in the offshore basin. Deltaic build-up was best developed in the south and became less pronounced towards the north (**Figure 2.15**). The regressive phase of sub-Stage IVC was punctuated by the Late Miocene tectonic event which uplifted the inboard area. This formed an angular unconformity called the **Shallow Regional Unconformity (SRU)**, marking the top of sub-Stage IVC. This event further accentuated the Late Miocene regression, shedding large volumes of sediment into rapidly subsiding synclines.

2.3.4 Sub-Stage IVD

Sub-Stage IVD is recognisable on seismic sections by its well-developed foresetted sequence (Azim-Ibrahim, 1994). The presence of fluvio-marine intercalations in a much thicker section in the SW Emerald area and seismic foresetting suggest an actively out-building delta system. The base of the prograding lower part of sub-Stage IVD has been shown to consist of middle to outer neritic and deep-water sandstones, some with excellent reservoir characteristics such as those in Tembungo-2 well (Whittle & Short, 1978). A major transgressive event during the Late Miocene, particularly pronounced in the central and northern parts of Sabah Basin, terminated the sub-Stage IVD regressive phase. The palaeo-environmental map of the top of sub-Stage IVD shows the

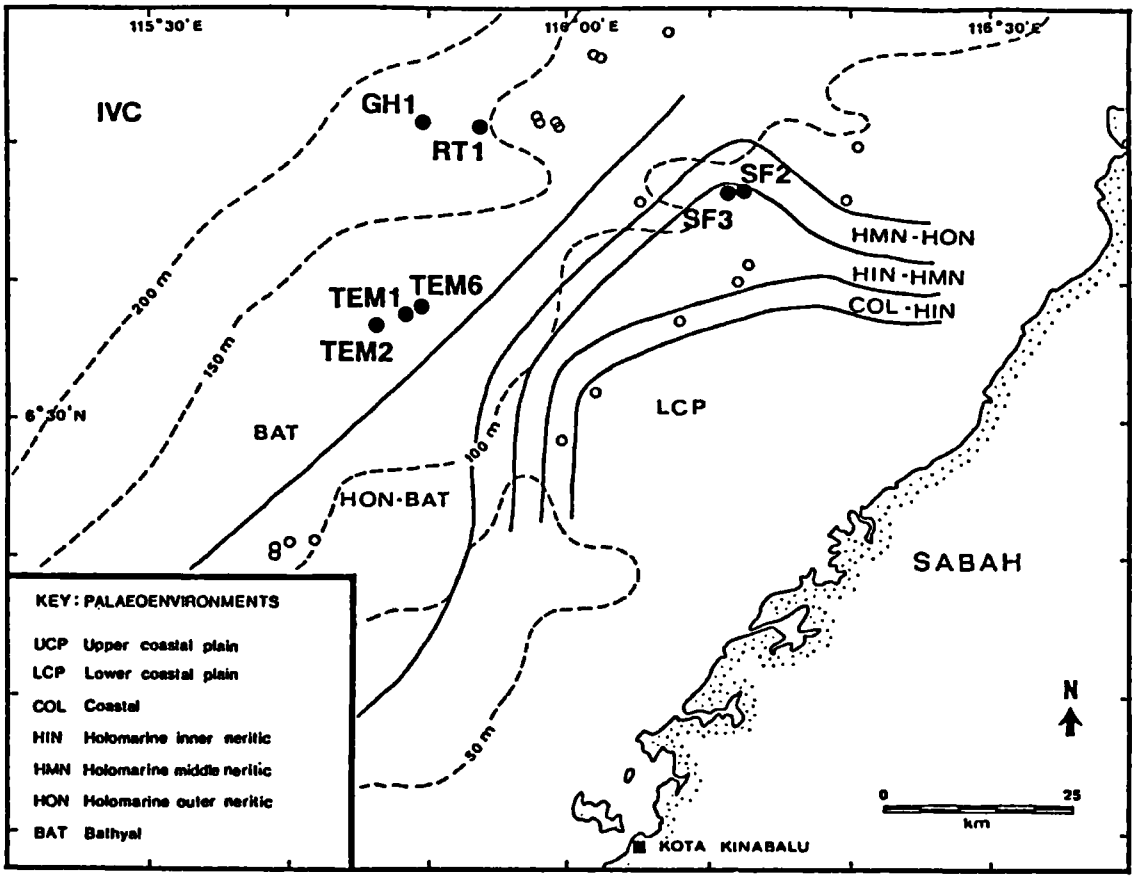


FIGURE 2.15 Palaeoenvironmental map at the top of sub-Stage IVC.

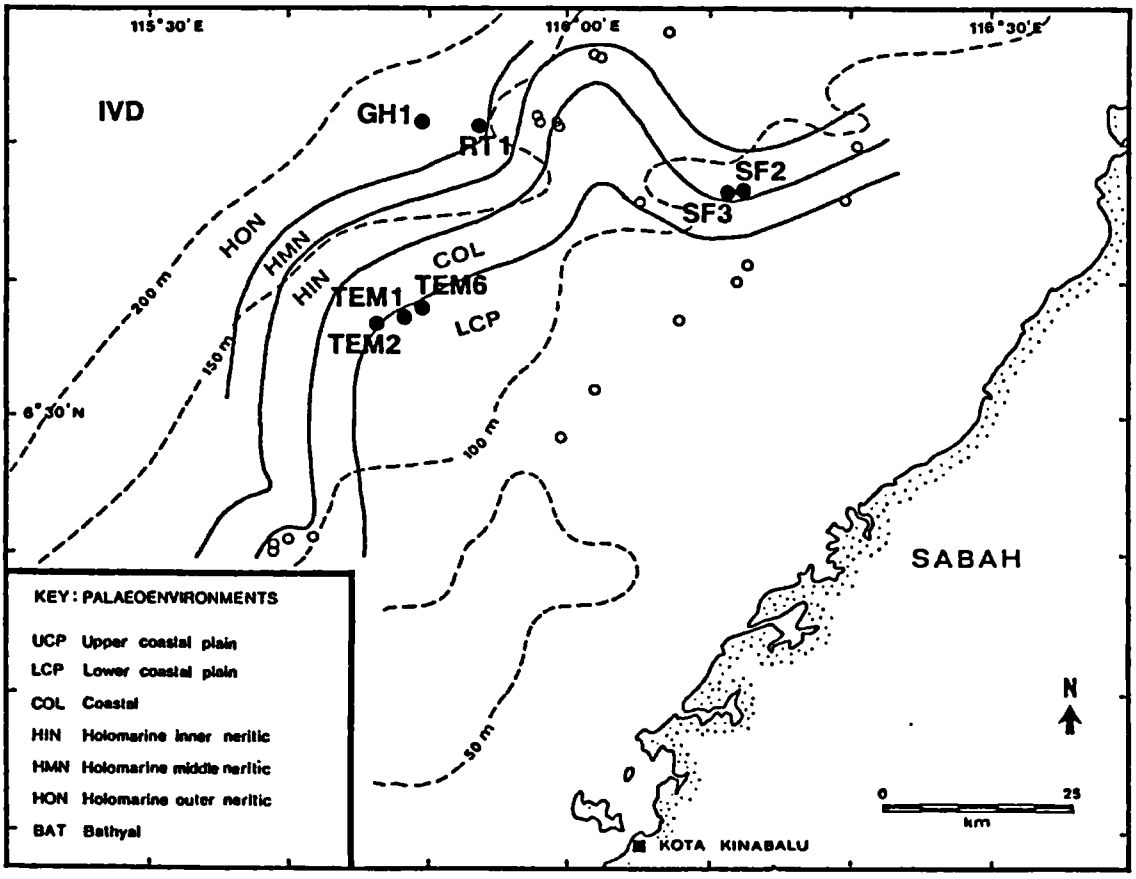


FIGURE 2.16 Palaeoenvironmental map at the top of sub-Stage IVD.

final extent of the progradational wedge (**Figure 2.16**). The top of this sub-Stage is marked by **'Horizon III'**.

2.3.5 Sub-Stage IVE

The transgression occurring during this sub-Stage is contemporaneous with subsiding movements along the Belangkas-Emerald Fault and with the beginning of growth of the Tembungo structure (Azim-Ibrahim, 1994). Minor deltaic deposition persisted off southern and central Sabah while reef build-ups were widespread in the northern areas. The top of Stage IVE is marked by **Horizon II**, a mild onlap unconformity associated with the formation of generally NW-SE oriented open anticlines and synclines.

2.3.6 Sub-Stages IVF and IVG

Sub-Stages IVF and IVG sediments represent continued deltaic progradation in the south. Shelf conditions existed in most of the northern areas with reefs growing on structural highs. The top of sub-Stage IVF is a Pliocene erosional unconformity referred to as **'Horizon I'**, while the top of sub-Stage IVG is the present sea-bed. No hydrocarbon accumulations have been encountered in these shallow sediments.

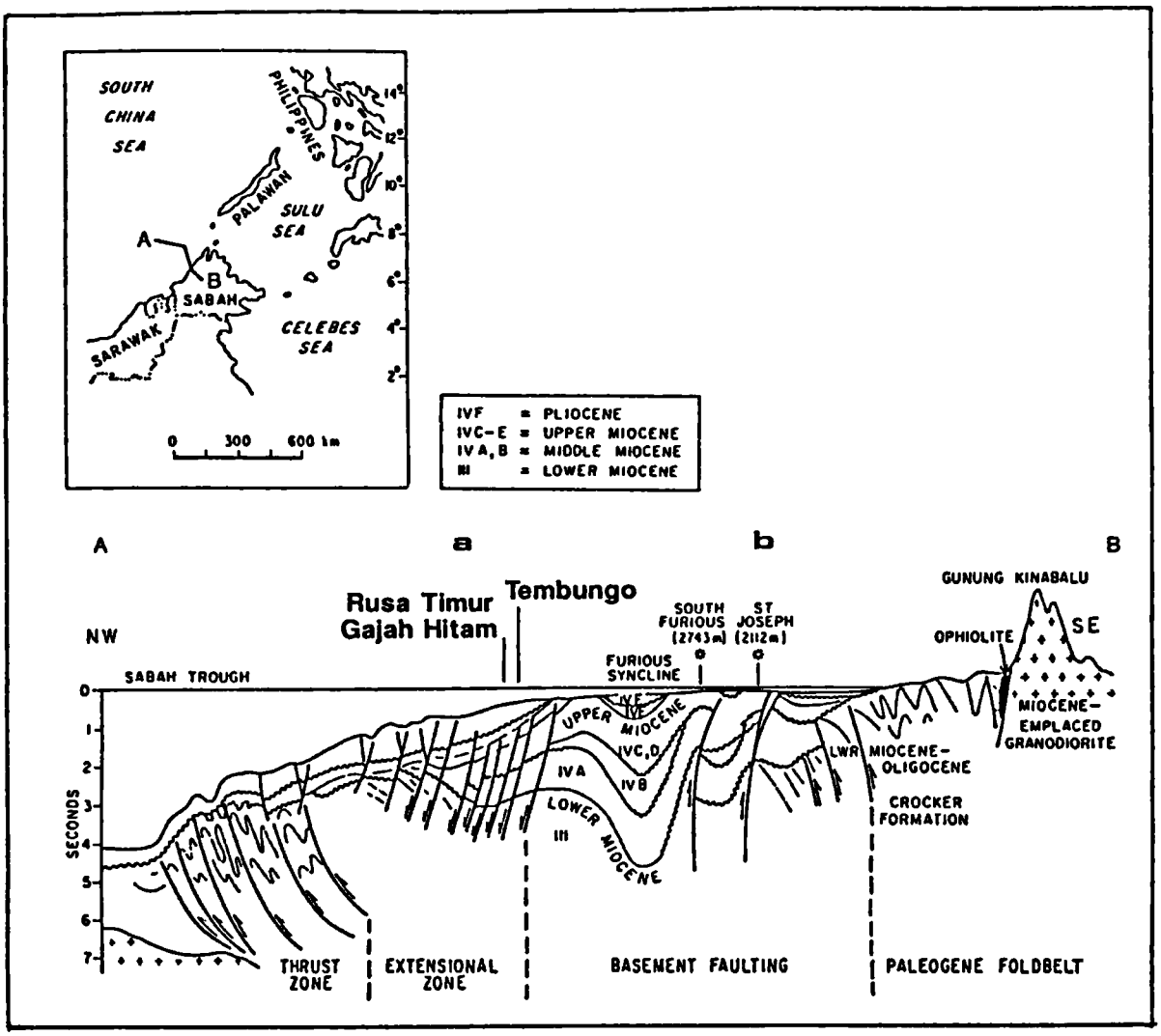
2.4 Hydrocarbon occurrences

In the inner part of Sabah Basin, the main hydrocarbon accumulations are found primarily in lower coastal plain to fluvio-marine sands of sub-Stages IVA and IVC. The main hydrocarbon reservoirs in the outer part of the basin are in sub-Stage IVD coastal to shallow marine and turbidite sands and the shallow-marine sands of sub-Stages IVC, IVE and IVF (**Figure 2.11**). In general, Sabah crudes are waxy and sulphur-free with API gravities ranging between 20° and 44° (Jamil *et. al.*, 1991). The average geothermal gradient for Sabah Basin is reported to be 28°C/km by Hutchison (1989)(**Table 1.1**).

2.5 The study area

2.5.1 Introduction

The seven wells included in this study are South Furious-2, South Furious-3, Tembungo-1, Tembungo-2, Tembungo-3, Rusa Timur-1 and Gajah Hitam-1 (**Figure 1.5**). In relation to the four tectonic provinces identified by Bol & van Hoorn (1980), the South Furious wells are located in the Basement Faulting Zone while the Tembungo wells, as well as Rusa Timur-1 and Gajah Hitam-1, are in the Extensional Zone (**Figure 2.17**). Sampling was done in sediments of Stages III and IV (sub-Stages IVA, IVB, IVC and IVD). Details on well sampling horizons and total sample numbers are outlined in **Chapter 3.**



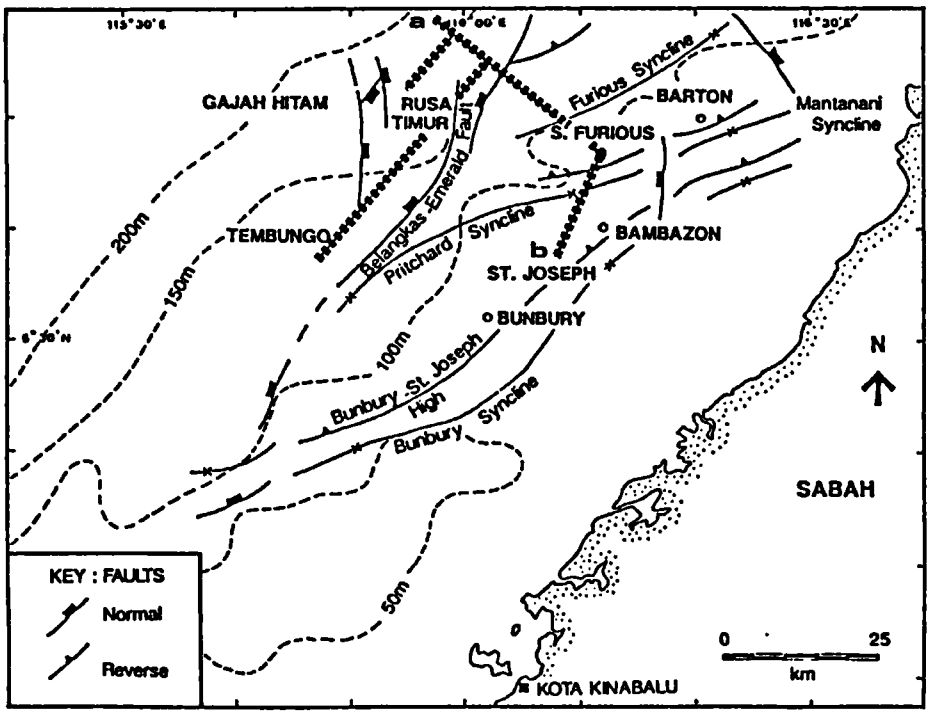


FIGURE 2.17 Location of the study area with respect to the tectonic provinces of Bol & van Hoorn (1980).

2.5.2 Geological Setting Of The Study Area

2.5.2a South Furious Field

South Furious is a large reverse-faulted anticline of considerable structural complexity elongated in a general east-west direction. It is flanked by two broad synclines, the Furious Syncline to its north, and the Pritchard Syncline to its south (**Figure 1.5**). Located to its east is the Mantanani Syncline. The stratigraphic sequence in the South Furious Field is made up of three major clastic units deposited from Early to Late Miocene (Stages III-IV) unconformably overlain by a thin veneer of about 170m (500 feet) of Quaternary calcareous sands, clays and reef deposits (**Figure 2.18**).

Below the **Deep Regional Unconformity (DRU)**, a continuous sequence of Early to Middle Miocene deep-marine shales (Stage III) was penetrated. Overlying the **DRU**, sediments of Middle Miocene age (sub-Stage IVA) were laid down in coastal plain environments. The transgressive unit of marine shales (sub-Stage IVB), which disconformably overlies the sub-Stage IVA sediments, was truncated by the **Upper Intermediate Unconformity (UIU)**. This unconformity is in turn overlain by Late Miocene deep-marine clastics (sub-Stage IVC). The prospective sequence consists of coastal plain sands between the DRU and the UIU. South Furious oils are waxy with the API gravity ranging between 26°-35°.

2.5.2b Tembungo Field

The Tembungo field, discovered in 1971, is located about 75km (47 miles) offshore Sabah north-west of Kota Kinabalu (**Figure 1.5**). It is a NW-SE trending wrench-initiated and shale-supported anticline 17 km long (11 miles) and 8 km (5 miles) wide, with a large number of tensional crestal faults resulting from rapid uplift of over 610m (2000 feet) within the last one million years (Whittle & Short, 1978). These tensional faults act as barriers to fluid migration with each fault block having its own separate fluid system. The Tembungo structure is bounded on the east by the regional Belangkas-Emerald west-dipping normal fault. Slightly further eastwards lies the Pritchard Syncline. The section penetrated at Tembungo ranges from Recent-Middle Miocene (**Figure 2.19**).

The Middle Miocene sediments consist of shallow-water claystones, shales, silts and very poorly-developed sandstones. The lack of inter-communication between sands combined with an extremely rapid rate of deposition (Azim-Ibrahim, 1994) has led to the entrapment of pore fluid in the sediments which resulted in abnormal pore pressures within the sediments. The top boundary of the Middle Miocene sequence, marked by the **Shallow Regional Unconformity (SRU)**, forms the base of a major Upper Miocene/Lower Pliocene progradational sedimentary wedge. The sequence consists of a typical regressive cycle with bathyal shales and sands of turbiditic origin overlain by slope shales and finally by shallow-water regressive sandstones. The

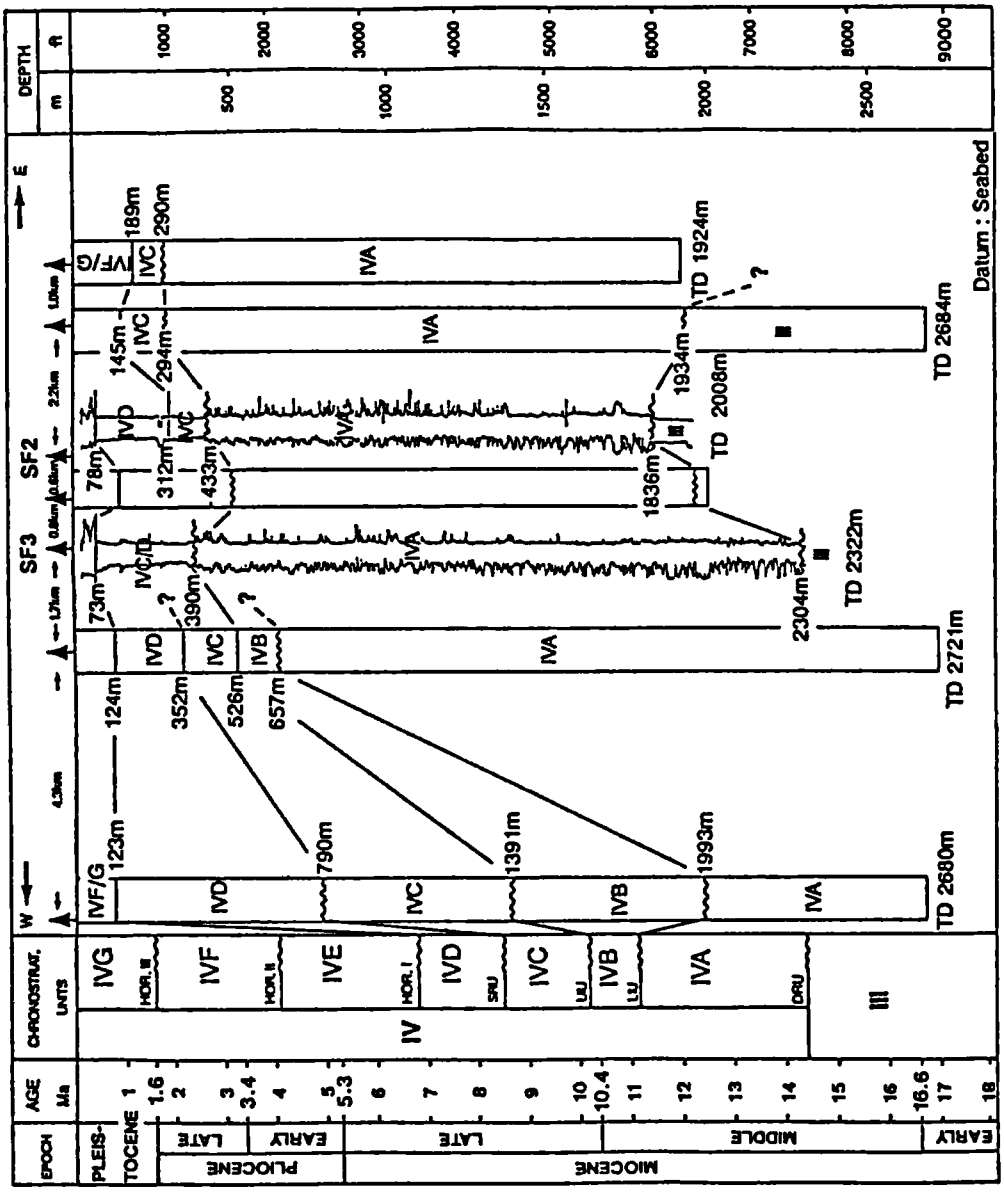


FIGURE 2.18 Well correlation : South Furious Field.

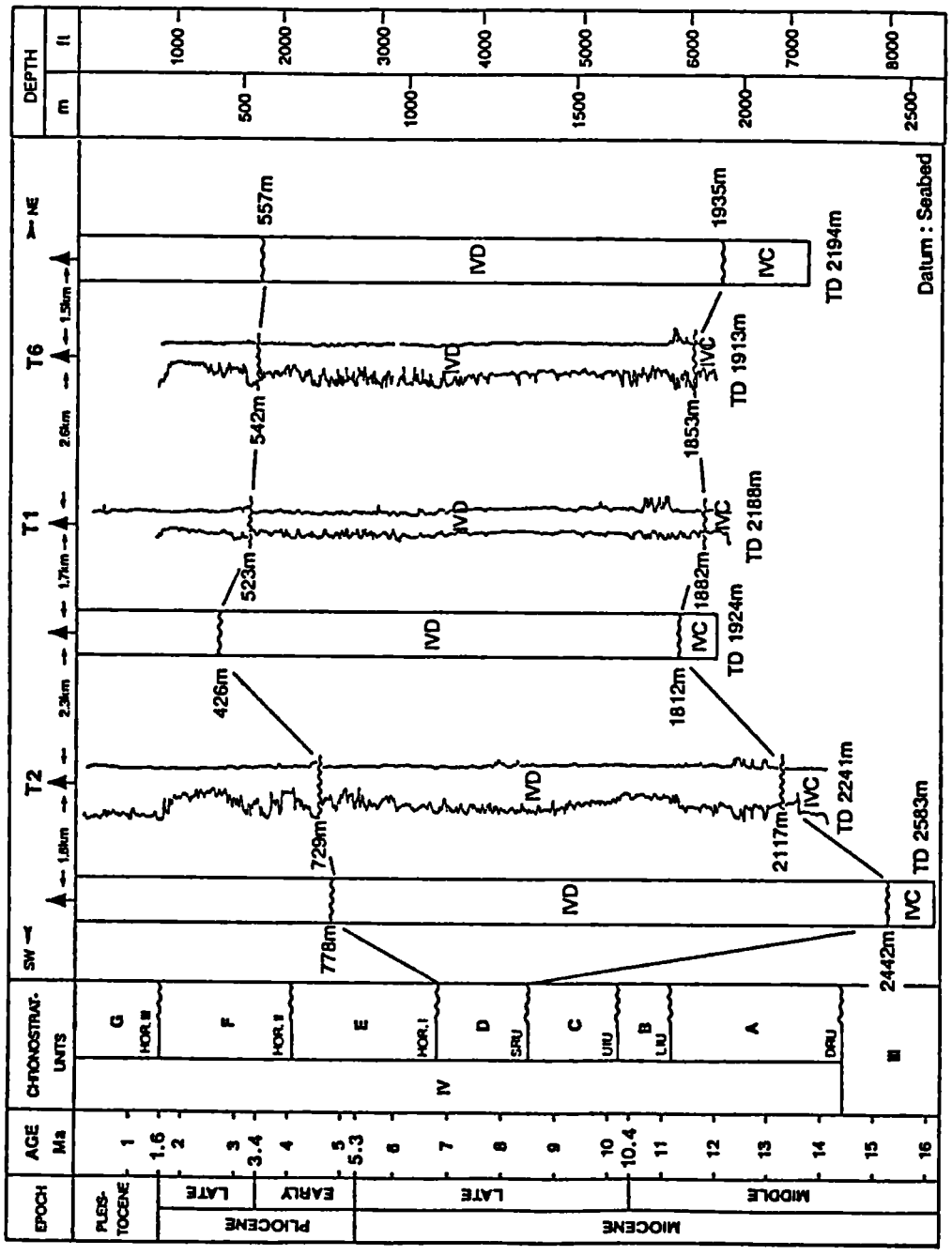


FIGURE 2.19 Well correlation : Tembungo Field.

neritic section contains good quality sandstones with minor amounts of claystones and limestones.

The productive reservoir section of Tembungo is the Upper Miocene deep-water turbidite sandstones. Individual sand units are up to 30m (100 feet) thick and are generally massive (Whittle & Short, 1978; Azim-Ibrahim, 1994). The reason for the absence of grading is that the sediments are thought to reflect the depositional process of grain-size sorting during transportation. A major world-wide sea-level fall at the end of Middle Miocene (Haq *et. al.*, 1987)) accompanied by local events of deformation exposed large areas of neritic sediments which were consequently eroded and dumped over the shelf-edge as low stand basin-slope and basin-floor turbidites. Tembungo oils are sulphur-free, waxy with API gravities ranging between 38°-40° (Whittle & Short, 1978; Jamil *et. al.*, 1991). Some hydrocarbons have been found in the neritic section; however, none proved to be commercial. The oil has probably migrated from the main reservoir along the many faults present in the structure.

2.5.2c Rusa Timur

The Rusa Timur structure lies in a graben bounded to its west by an east-dipping normal fault, and by the west-dipping Belangkas-Emerald Fault on its east (**Figure 1.5**). It penetrated Middle Miocene-Pleistocene sedimentary sequence with sub-Stage IVA sediments being the lowermost stratigraphic unit (**Figure 2.20**). The Pliocene-Pleistocene sections overlying the Rusa Timur structure largely comprise marine shales acting as seal to the underlying sandstones. Oil and gas were encountered in the sub-Stage IVD sandstones. The oil had an API gravity of 31.5°.

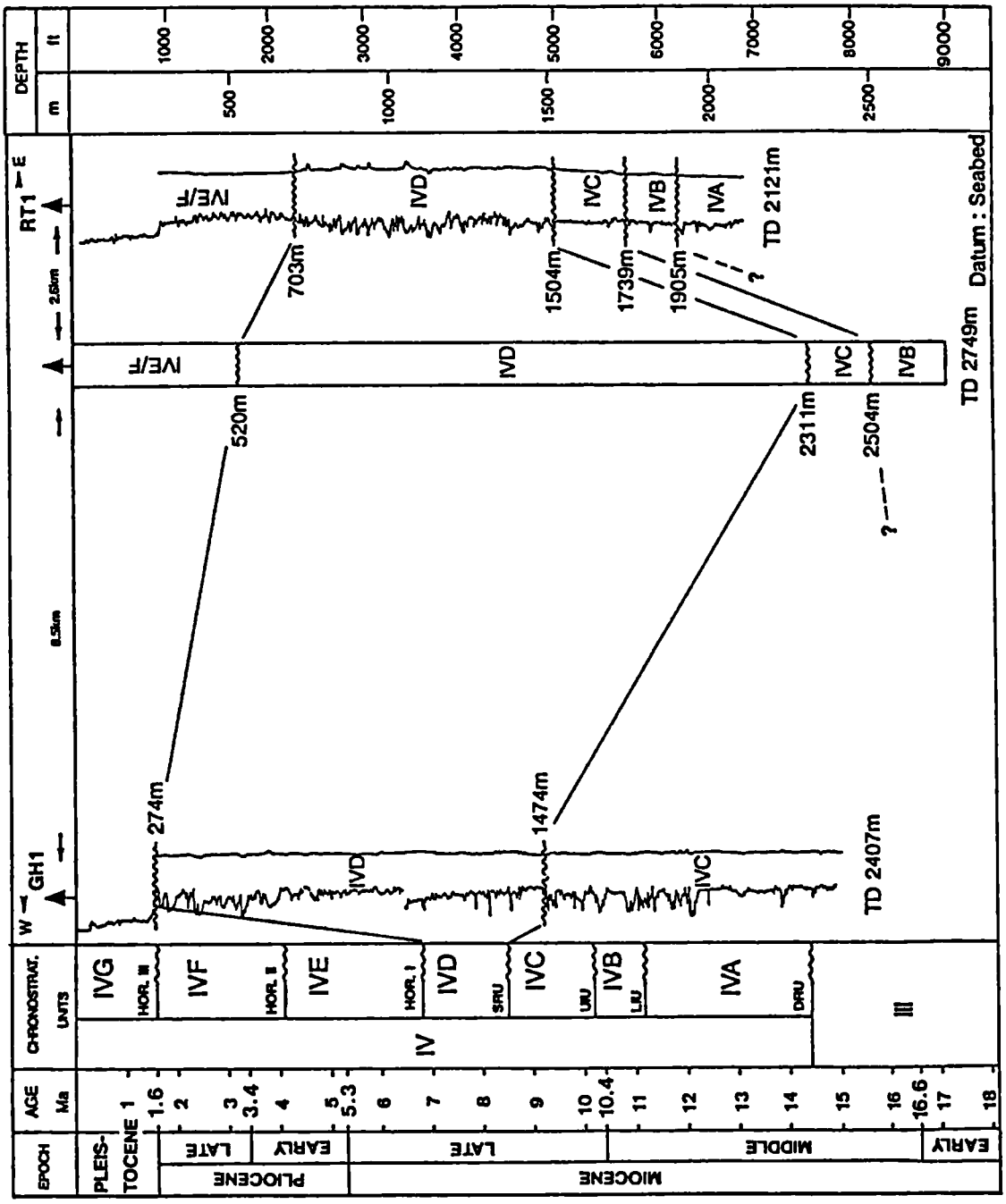


FIGURE 2.20 Well correlation : Rusa Timur- Gajah Hitam area.

2.5.2d Gajah Hitam

The Gajah Hitam structure lies 25km north of the Tembungo field (**Figure 1.5**). It is bounded to the east and west by N-S trending faults and appears as a horst in E-W cross-section. The main uplift of the Gajah Hitam structure occurred during the Pliocene and it remained high from the end of Pliocene to the present day, resulting in substantially less than 350m (1000 feet) of crestal Miocene sediments. The lowermost sediments penetrated in the Gajah Hitam area are Middle Miocene bathyal shales of sub-Stage IVC (**Figure 2.20**). The overlying sub-Stage IVD sediments comprise monotonous deep-marine shale with local development of turbiditic reservoir sandstones. Progradation began near the base of sub-Stage IVD which is marked by the **Shallow Regional Unconformity** (**SRU**), and built progressively to the north-west. This prograding unit exhibits a gradual transition from outer to inner neritic environments. The overlying Pliocene to Pleistocene sections are predominantly marine shales. Gajah Hitam-1 failed to encounter any significant hydrocarbons, with only minor gas shows in the sub-Stage IVD sandstones.

CHAPTER THREE

RESEARCH STRATEGY

3.1 Sampling programme

Initial preparation for the sampling programme involved the study of well logs from twenty exploration wells. Only shale/shaly samples from Stages III-IV were considered for organic geochemical investigation as most wells rarely penetrated sediments older than Stage III. Sediments younger than sub-Stage IVD are excluded from the study because they are generally of insufficient maturity to generate hydrocarbons.

Preliminary identification of sampling horizons based on wireline log responses were calibrated with lithological descriptions of cores, side-wall cores and ditch-cuttings from well completion reports and sample inspection. Gamma Ray, Resistivity, Sonic and Density logs were utilised for this purpose based on the fact that the amount of organic matter present in sediments affects the responses of these logs (Meyer & Nederlof, 1984; Herron, 1991). As a general rule, sediments with high organic carbon contents will have relatively higher Gamma Ray and Resistivity log responses accompanied by relatively lower Sonic velocity (i.e. higher transit time) and Density log responses compared to sediments with low organic carbon contents (**Figure 3.1**).

3.2 Sample selection

Sampling was done in July 1991 at the core ware-houses of PETRONAS Petroleum Research & Scientific Services in Kuala Lumpur and Sarawak Shell in Lutong, Sarawak. Core samples were given the highest priority, followed by side-wall cores and ditch-cuttings for sample reliability. Ditch-cuttings are least favourable due to the higher possibilities of sample contamination through cavings or sloughing. However, ideal situations where continuous core samples are available are extremely rare. Save for a number of side-wall plugs, which are of very limited amounts and are usually taken in reservoir sections anyway, the most abundant samples are ditch-cuttings.

The availability and condition of samples from the previously identified horizons influenced the final set of samples selected for this study. Some samples may have been used up by previous researchers for various analyses, while others were too contaminated by drilling mud that separating them would have yielded an actual sample amount too small to allow extensive geochemical analyses. As a result of these

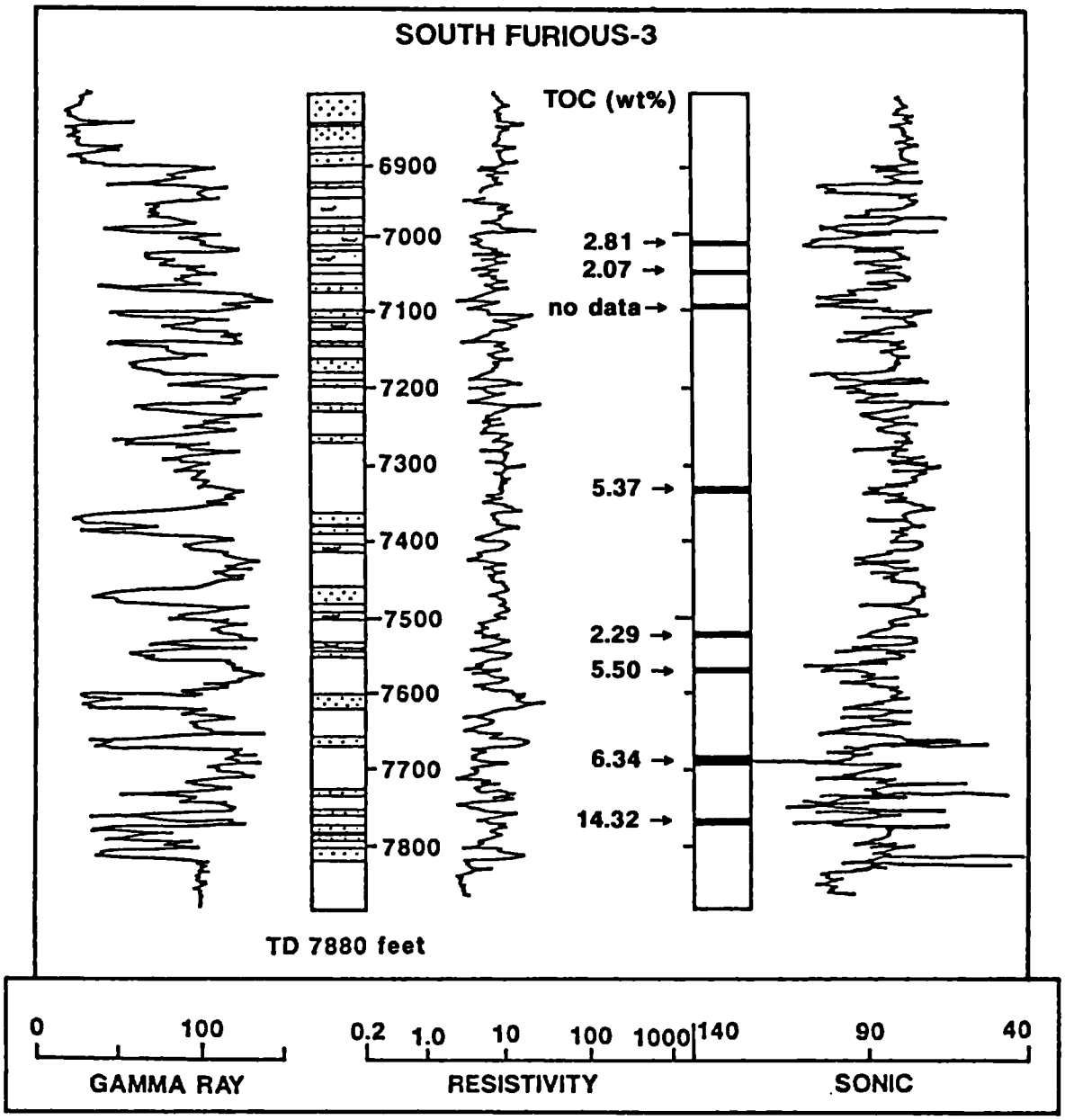


FIGURE 3.1 An example of gamma ray, resistivity and sonic log responses for an organic carbon-rich interval in the South Furious-3 well.

problems, samples from only seven out of the twenty wells were available for the study. The well locations are shown in **Figure 1.5.**

3.3 Final sample set collected for analyses

Information for the wells and sedimentary Stages/sub-Stages included in this study are listed in **Table 3.1.** for reference.

Table 3.1 Wells and Stages investigated in the study of Sabah Basin source rocks.

WELL	TOTAL DEPTH (m)	STAGE	DEPTH INTERVAL * (m)
South Furious-2	2008	IVA	433 - 1836
		III	1836 - 2008 (TD)
South Furious-3	2322	IVA	390 - 2304
		III	2304 - 2322 (TD)
Tembungo-1	2188	IVD	523 - 1882
		IVC	1882 - 2188 (TD)
Tembungo-2	2241	IVD	729 - 2117
		IVC	2117 - 2241 (TD)
Tembungo-6	1913	IVD	542 - 1853
		IVC	1853 - 1913 (TD)
Rusa Timur-1	2121	IVD	703 - 1504
		IVC	1504 - 1739
		IVB	1739 - 1905
		IVA	1905 - 2121 (TD)
Gajah Hitam-1	2407	IVD	274 - 1474
		IVC	1474 - 2407 (TD)

* All depths are calculated from the sea-bed [i.e. log depth - (kelly bushing + water depth)]

The final sample set chosen for organic geochemical analyses are as follows :

3.3.1 Well : South Furious-2

Sample no. : 14 core samples
18 side-wall cores
27 ditch-cuttings
Total: 59 samples

Figure 3.2 shows the location of samples selected for screening analyses from South Furious-2.

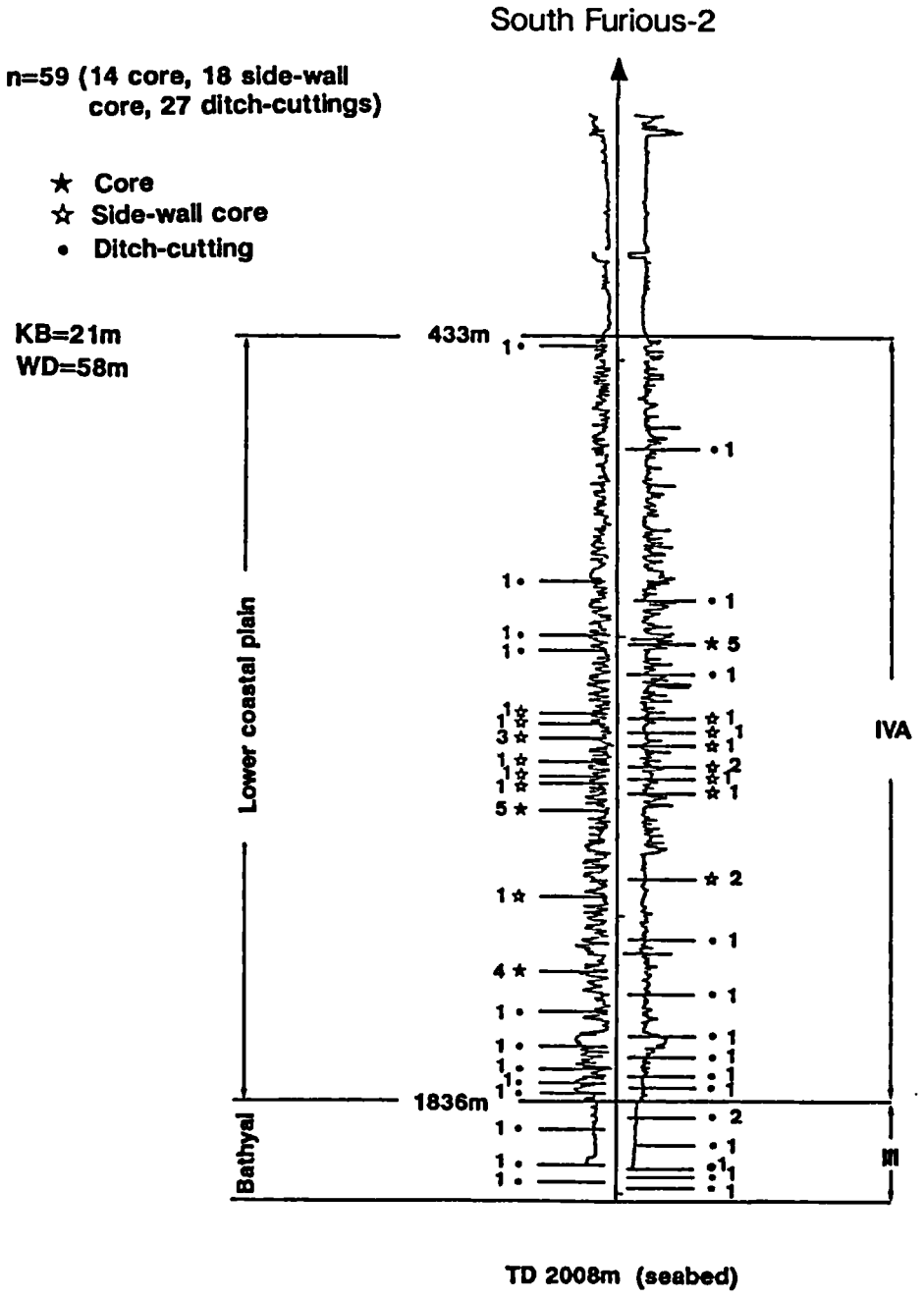


FIGURE 3.2. South Furious-2 : sampling locations and sample types. Also indicated are the palaeoenvironments and sedimentary Stages/sub-Stages.

3.3.2 Well : South Furious-3

Sample no. : 8 core samples
45 ditch-cuttings
Total: 63 samples

Figure 3.3 shows the sampling locations for South Furious-3.

3.3.3 Well : Tembungo-1

Sample no. : 4 core samples
57 ditch-cuttings
Total: 61 samples

Figure 3.4 shows the sampling location for Tembungo-1.

3.3.4 Well : Tembungo-2

Sample no. : 11 core samples
29 ditch-cuttings
Total: 40 samples

Figure 3.5 shows the sampling interval for Tembungo-2.

3.3.5. Well : Tembungo-6

Sample no. : 42 ditch-cuttings
Total: 42 samples

Figure 3.6 shows the sampling intervals for Tembungo-6.

3.3.6. Well : Rusa Timur-1

Sample no. : 6 core samples
22 ditch-cuttings
Total: 28 samples

Figure 3.7 shows the sampling locations for Rusa Timur-1.

3.3.7. Well : Gajah Hitam-1

Sample no. : 12 core samples
13 ditch-cuttings
Total: 25 samples

Figure 3.8 shows the sampling intervals for Gajah Hitam-1.

Thus, a total of 318 shale/shaly samples made up of 65 core samples, 18 side-wall core samples and 235 ditch-cutting samples from Stage III to sub-Stage IVD (**Table 3.2**). were collected from seven wells and prepared for preliminary organic geochemical screening.

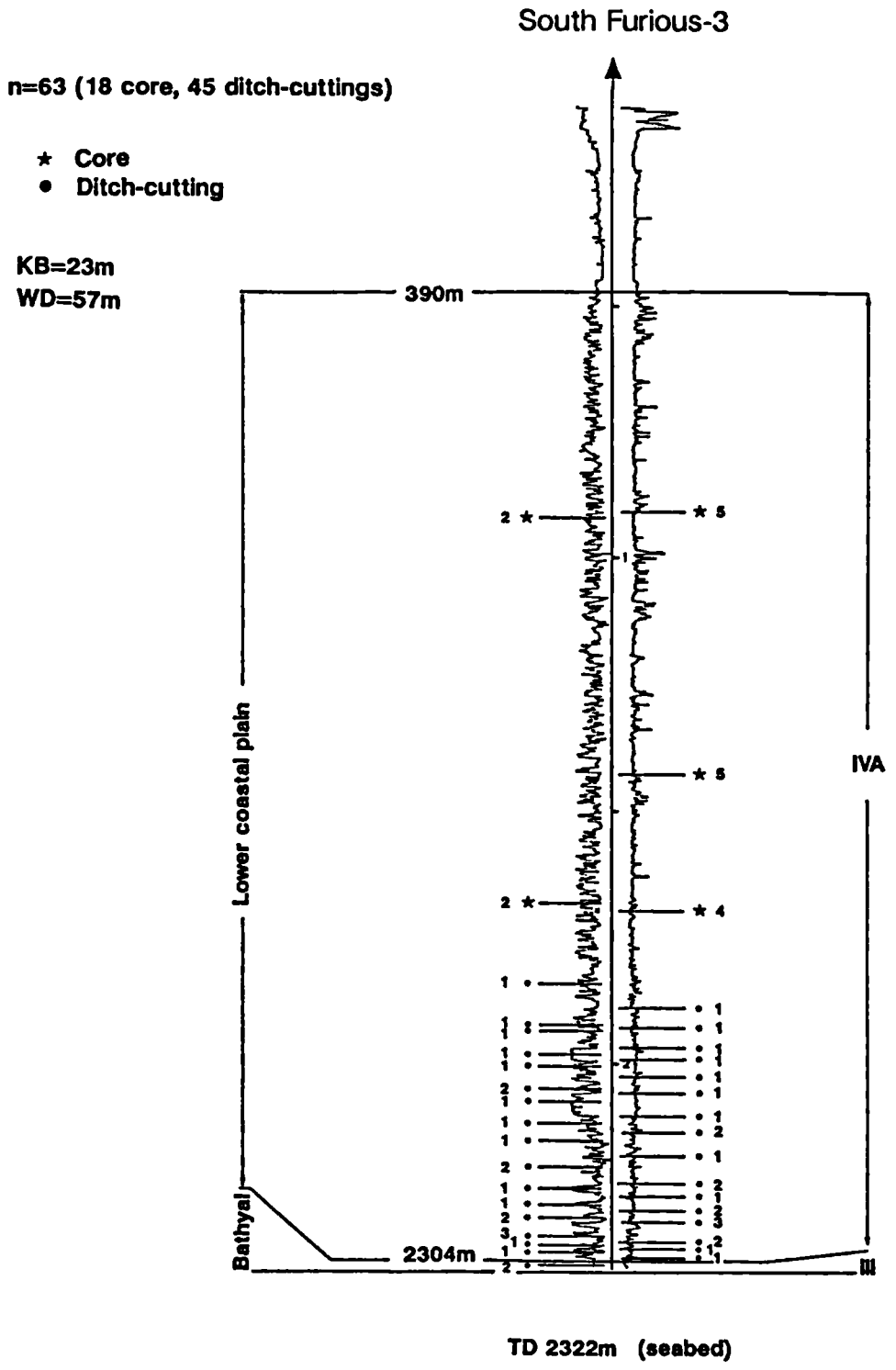


FIGURE 3.3 South Furious-3 : sampling locations and sample types. Also indicated are the palaeoenvironments and sedimentary Stages/sub-Stages.

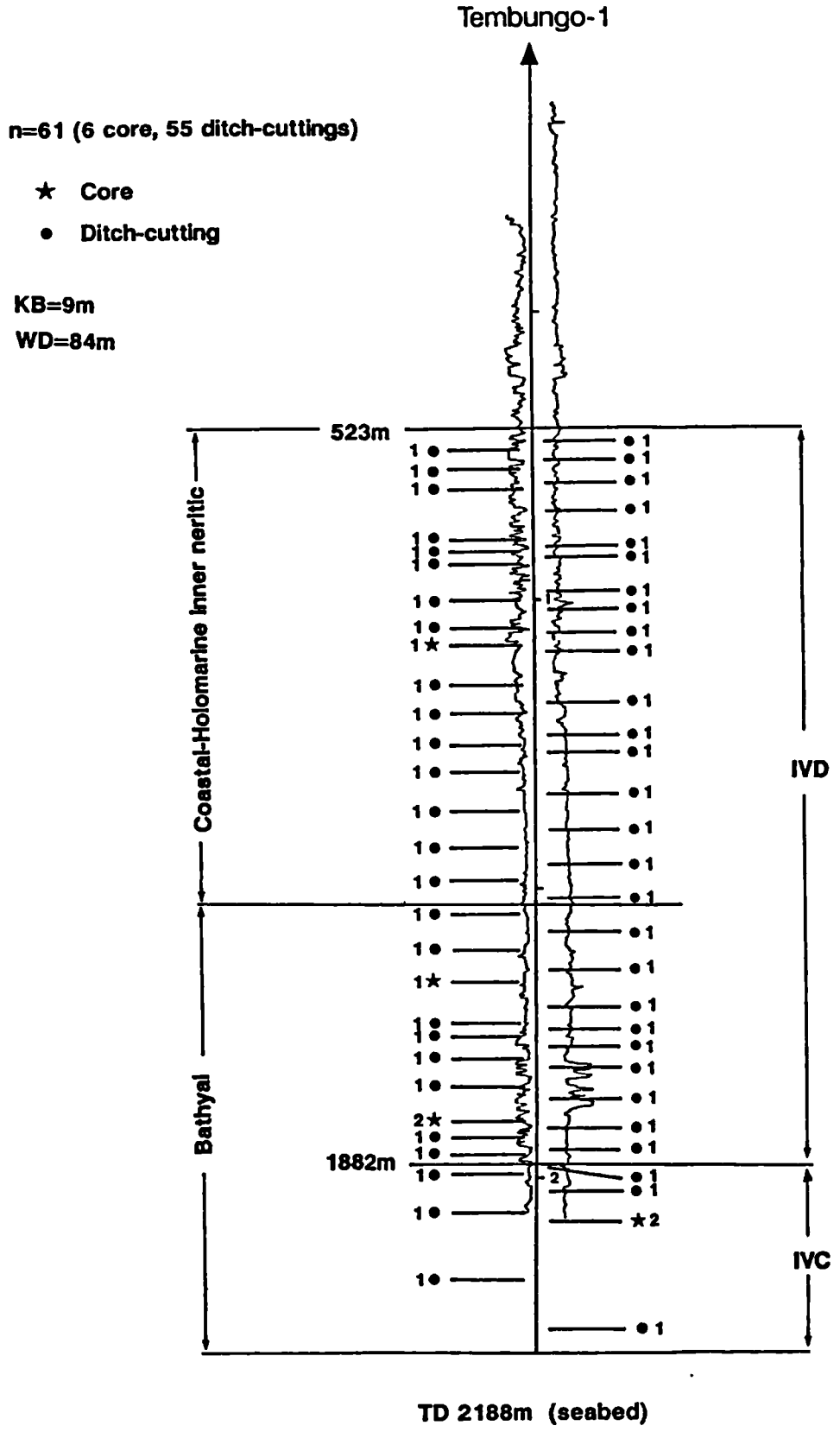


FIGURE 3.4 Tembungo-1 : sampling locations and sample types. Also indicated are the palaeoenvironments and sedimentary Stages/sub-Stages.

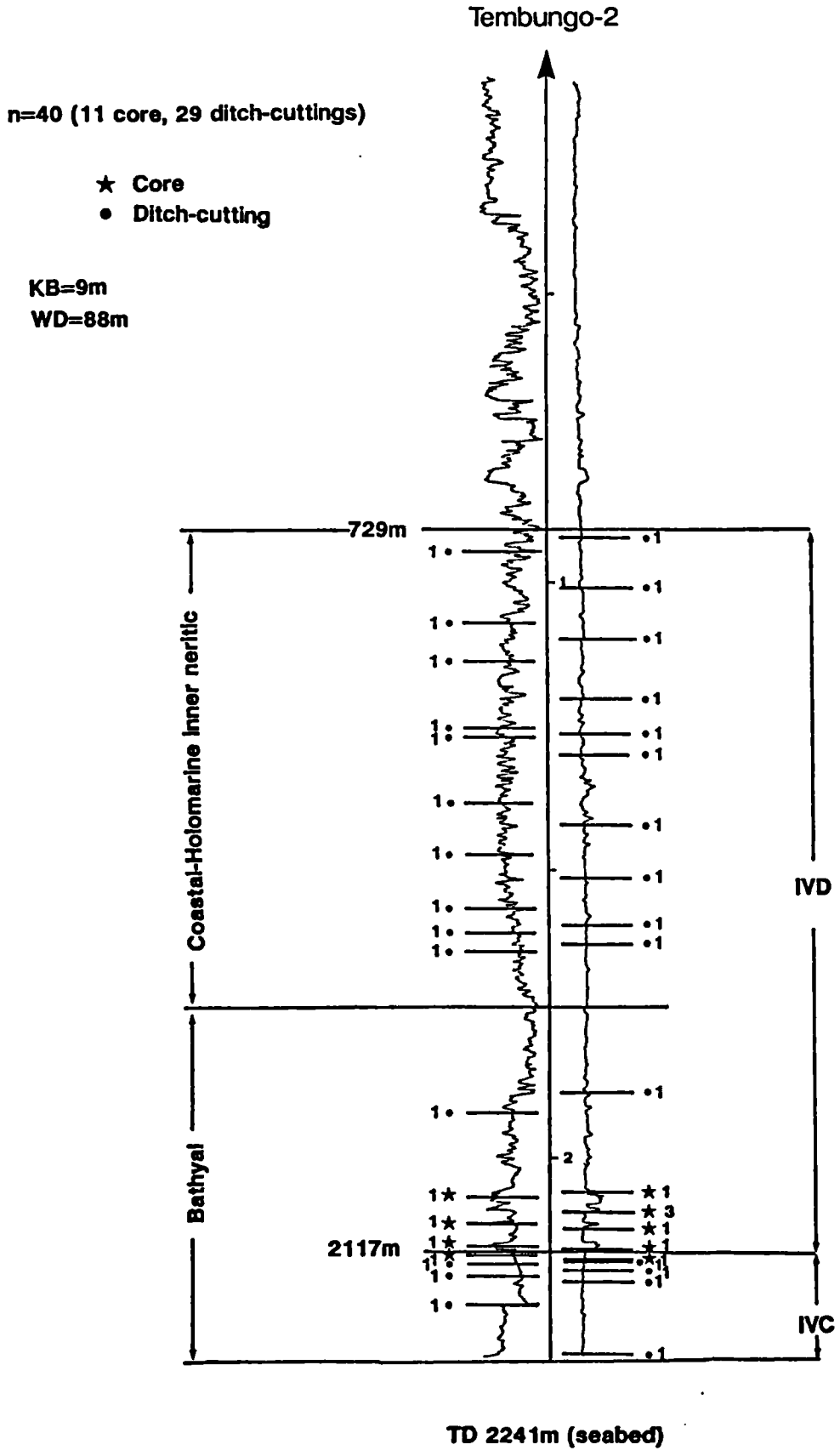


FIGURE 3.5 Tembungo-2 : sampling locations and sample types. Also indicated are the palaeoenvironments and sedimentary Stages/sub-Stages.

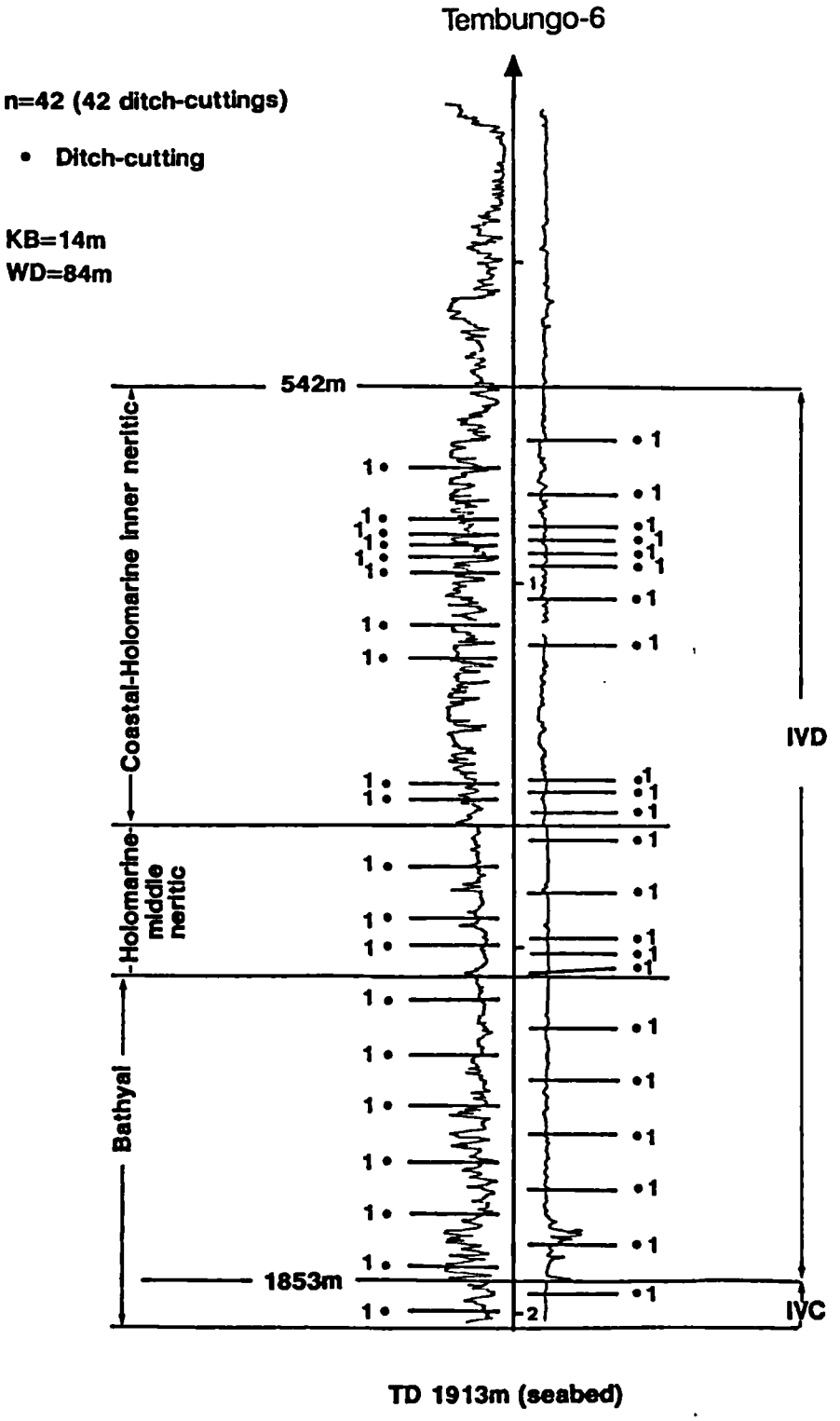


FIGURE 3.6 Tembungo-6 : sampling locations and sample types. Also indicated are the palaeoenvironments and sedimentary Stages/sub-Stages.

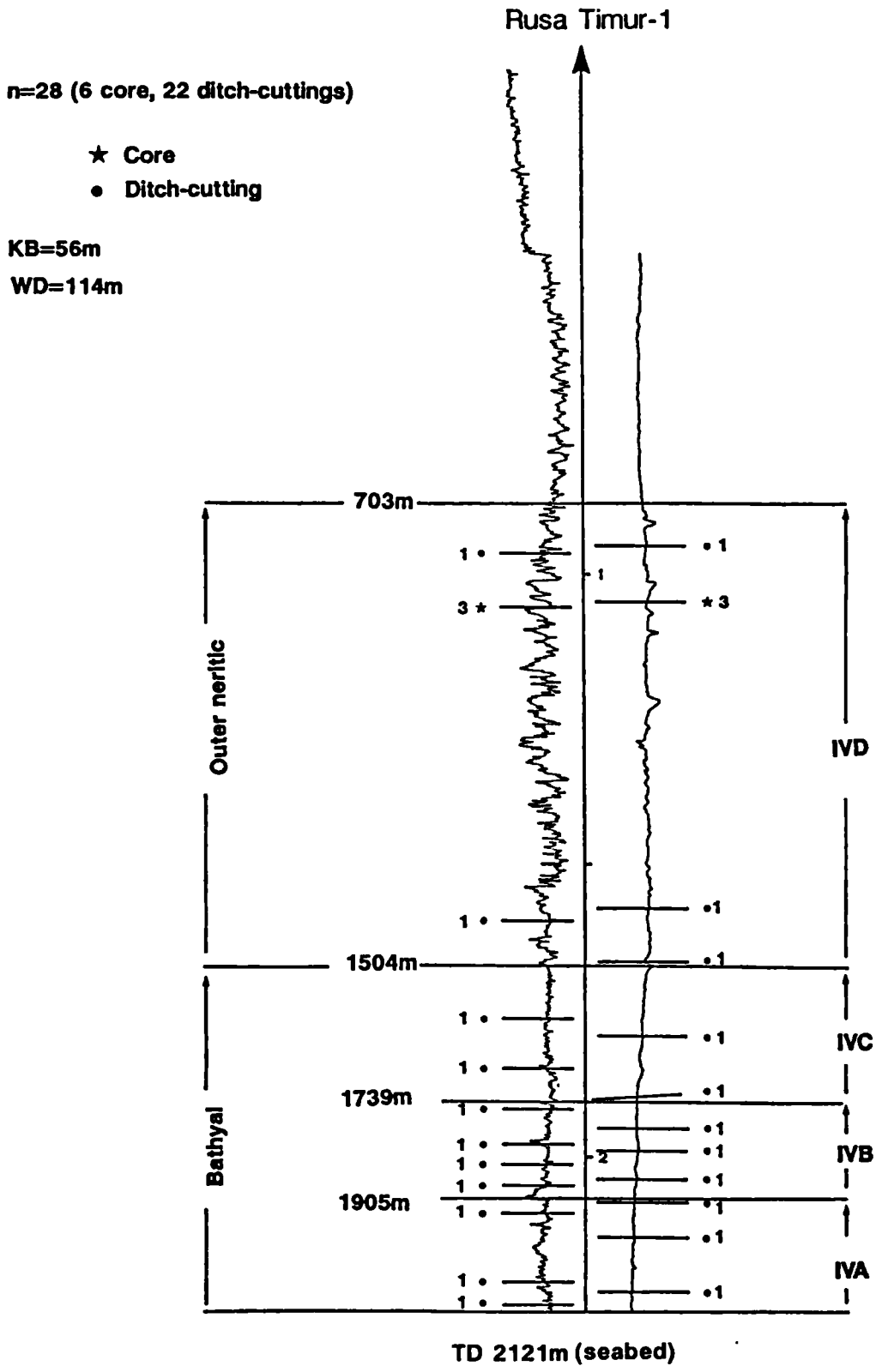


FIGURE 3.7 Rusa Timur-1 : sampling locations and sample types. Also indicated are the palaeoenvironments and sedimentary Stages/sub-Stages.

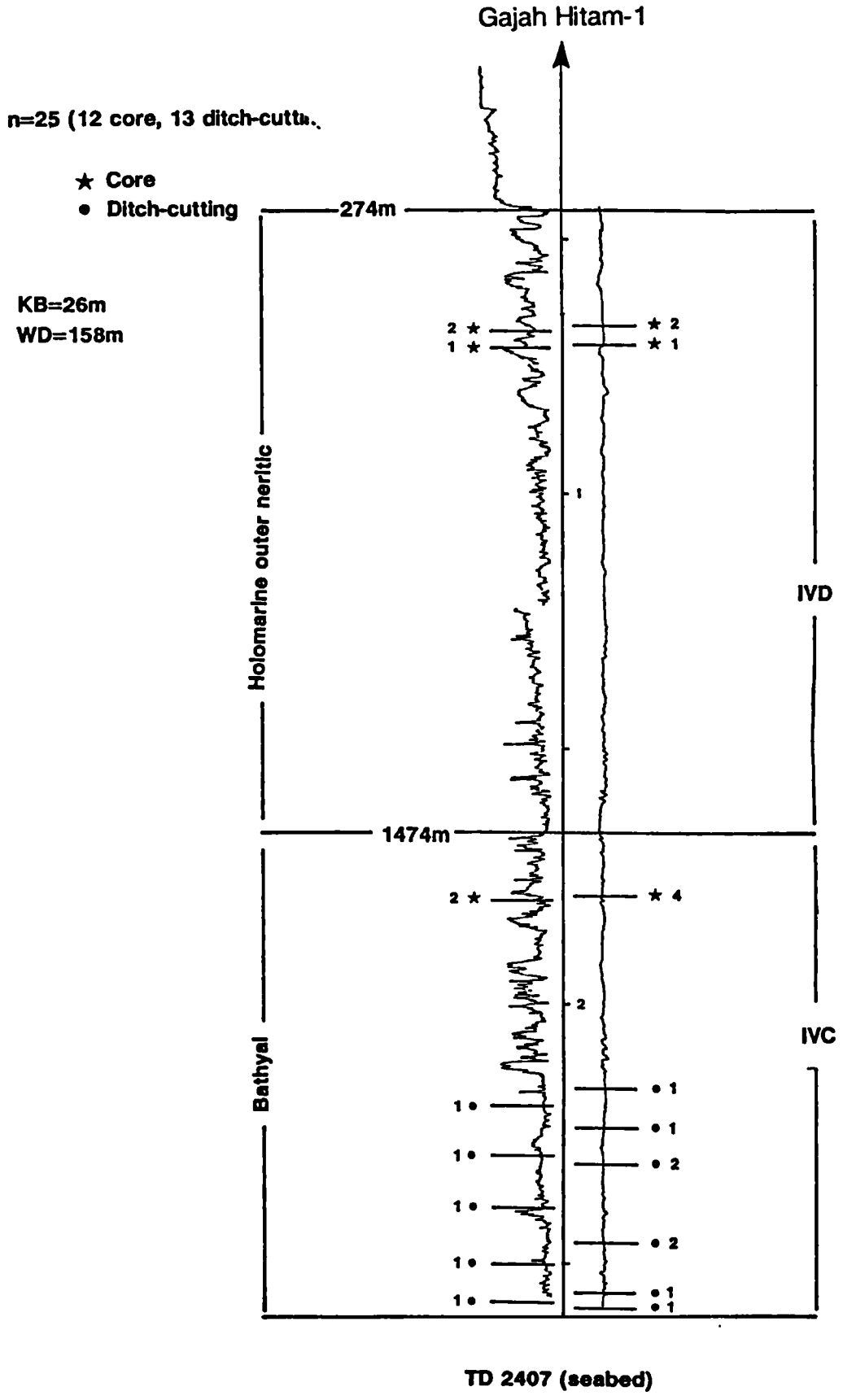


FIGURE 3.8 Gajah Hitam-1 : sampling locations and sample types. Also indicated are the palaeoenvironments and sedimentary Stages/sub-Stages.

Table 3.2 The number of samples collected from Stages III and IV of the seven wells.

Stages	Sub-Stages	Wells						
		SF2	SF3	T1	T2	T6	RT1	GH1
	IVD	-	-	33	20	40	11	6
IV	IVC	-	-	28	20	2	4	19
	IVB	n.d.e.*	n.d.e.	n.p.•	n.p.	n.p.	7	n.p.
	IVA	50	61	n.p.	n.p.	n.p.	6	n.p.
III		9	2	n.p.	n.p.	n.p.	n.p.	n.p.
Sub-total :		59	63	61	40	42	28	25
Cumulative total :		318 samples						

KEY :

SF2 = South Furious-2 **T1** = Tembungo-1 **RT1** = Rusa Timur-1

SF3 = South Furious-3 **T2** = Tembungo-2 **GH1** = Gajah Hitam-1

T6 = Tembungo-6

* n.d.e = not deposited or eroded • n.p. = not penetrated

3.4 Analytical programme : Organic geochemical analyses

Table 3.3 lists the analyses performed in this study, the type of samples used and the information obtained from these analyses. The flow diagram **(Figure 3.9)** charts the steps taken, starting from the sample screening stage to the eventual correlation of the Sabah oil samples to their most likely source rocks.

Table 3.3 Organic geochemical analyses performed

Analysis	Sample Type	Information Retrieved	Samples analysed
Total Organic Carbon	Whole rock	Sediment richness Quantity of organic carbon	318
Rock-Eval pyrolysis	Whole rock	Organic matter type, quality and maturity	318
Density separation	Kerogen	Organic matter type, maturity	74
Elemental analysis	Kerogen	Organic matter type, maturity	74
Organic petrography	Kerogen	Organic matter type	74
Vitrinite reflectance	Kerogen	Organic matter type, maturity	46
Solvent extraction	Whole rock	Extractable organic matter quantity, sediment potential	26

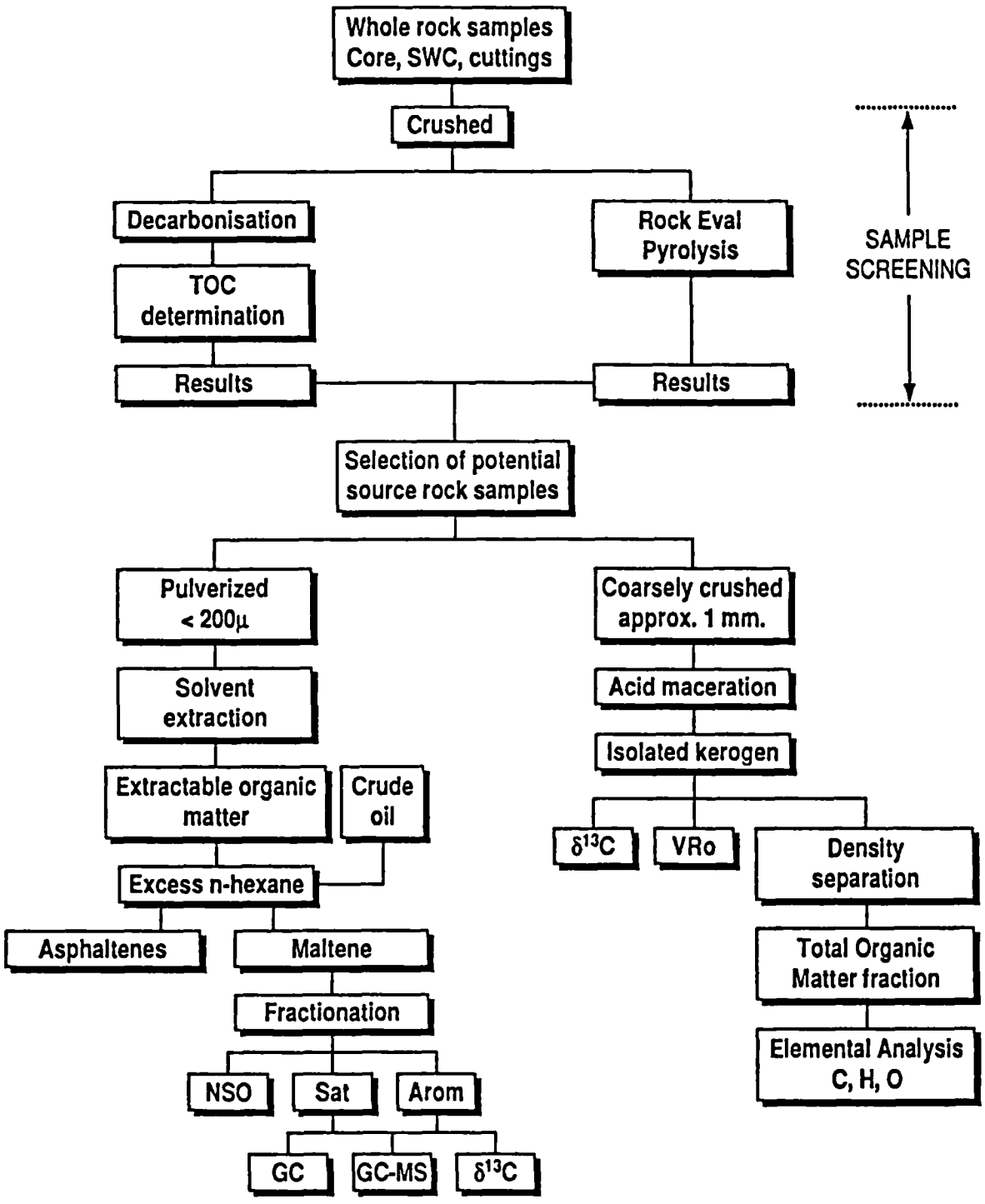


FIGURE 3.9 Flow diagram of the analytical procedures undertaken.

Table 3.3 Organic geochemical analyses performed - continued

Analysis	Sample Type	Information Retrieved	Samples analysed
Gas chromatography	Aliphatic fraction of sediment extracts	Organic matter type and maturity, environment of deposition	26
Gas chromatography-mass spectrometry	Aliphatic fraction of oils and sediment extracts	Organic matter type and maturity, environment of deposition	32
Stable carbon isotope ($\delta^{13}C$)	Kerogen Aliphatic and aromatic fractions from oils	Oil-source rock correlations	3 4

CHAPTER FOUR

REVIEW OF THE ORGANIC GEOCHEMICAL TECHNIQUES

4.1 Sample preparation

Ditch-cutting samples were placed in glass petri dishes for the elimination of commonly present metal shards with a magnet. Other contaminants such as drilling mud, nutshells and husks were picked with tweezers while observing through a microscope. A description of the sample was made before a portion is crushed with an agate mortar and pestle and kept in glass bottles prior to pyrolysis, and decarbonisation to determine the Total Organic Carbon (TOC) content.

Core and side-wall core samples were cleaned with a small stiff brush to eliminate foreign material adhering to them. The majority of samples were rather friable and most contaminants could be picked with tweezers. The samples were then described, crushed and stored in the same manner as the ditch-cuttings. Water-based drilling mud were used in all the seven wells included for analyses (PETRONAS : in-house well completion reports). This eliminates the possibility of hydrocarbon contamination from the mud and expels the need to solvent extract samples before pyrolysis and total organic carbon (TOC) determination. Detailed procedures for the methods described below can be found in **Appendix I.**

4.2 Whole rock analyses

Crushed whole rock samples were used for the determination of Total Organic Carbon content and Rock-Eval pyrolysis. These two analyses are the basic screening methods, allowing the selection of only significant samples for further investigation. The type of information derived are quantity of organic matter from TOC content determination, and organic matter quality, type and maturity from Rock-Eval pyrolysis.

4.2.1 Determination Of Organic Carbon Content

Total organic carbon (TOC) analysis measures the organic richness of a rock in weight percent organic carbon and is typically the first screening analysis completed in the evaluation of the hydrocarbon generating potential of a certain formation (Jarvie, 1991). A total organic carbon content of 0.5% for shales and 0.3% for carbonates are generally

accepted as the lower limits for effective source rocks (Gehman, 1962; Tissot & Welte, 1984).

Jones (1984) indicated that the minimum TOC values for potential carbonate and shale source rocks are approximately the same. This, however, cannot strictly be the case, because of the different nature of the rock types involved and their effects on hydrocarbon retention. The higher oil saturation threshold of shales, compared to carbonates, will undoubtedly influence their source rock rating. In this study, all the samples selected are mainly composed of varying proportions of shales, silty mudstones, siltstones and sandstones with negligible amounts of carbonates. The TOC cut-off values used here are of Peters (1986):

TOC Content (wt%)	Rating
0.0 - 0.5	Poor
0.5 - 1.0	Fair
1.0 - 2.0	Good
2.0 - 5.0	Very good
> 5.0	Excellent

A TOC value of 1 wt% means that in 100g of sediment sample, there is 1g of organic carbon. It is important to realise that the minimum value of organic carbon content for potential source rocks is only a necessary background value rather than a positive indication for a source rock. The TOC values express the organic richness of a sample and not its hydrocarbon potential; for example, a sample containing significant amounts of recycled or dead carbon will also have a high TOC value, just as a sample having excellent hydrocarbon generative organic matter will. In this study, the Leco IR-312 Carbon Analyser was used for the determination of total organic carbon contents of the sediments under investigation.

4.2.2 Rock-Eval Pyrolysis

Pyrolysis is a method that attempts to emulate nature's maturation processes at a much higher rate, resulting in the artificial maturation of kerogen. In this study, the IFP's Rock-Eval 5 instrument was used. This is a rapid (20 minutes per sample) quantitative method and provides information on sample characteristics with respect to the type of organic matter it contains, its hydrocarbon generation potential and its present level of maturity (Peters, 1986; Philp & Galvez-Sinibaldi, 1991). The equipment measures two peaks, S1 and S2, the temperature at which maximum hydrocarbon generation occurs, Tmax (°C) and it will calculate the Hydrogen Index if provided with the sample's TOC value prior to analysis (**Figure 4.1**). The Rock-Eval 5 equipment used was, however, not equipped for measuring the S3 oxygen peak.

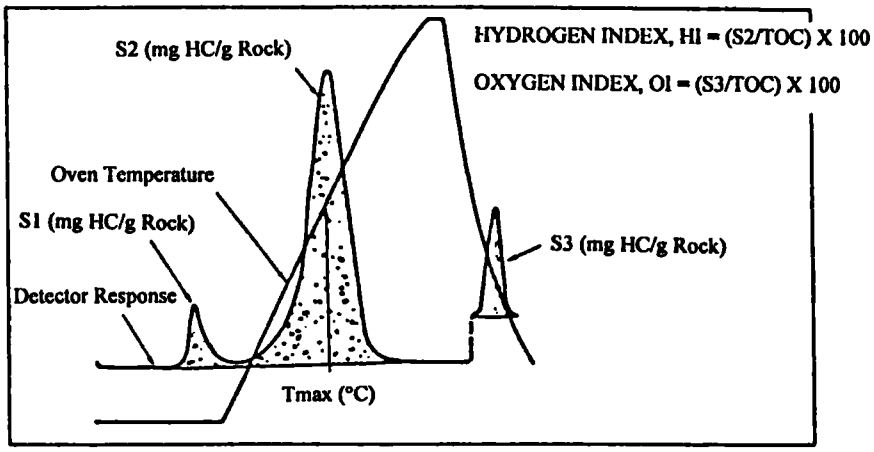


FIGURE 4.1 A general schematic diagram showing the release of hydrocarbons and CO_2 during pyrolysis, with time increasing from left to right. The primary parameters measured by the pyrolysis instrument are S1, S2, S3 and Tmax. The secondary parameters of Hydrogen Index (HI) and Production Index (PI) are calculated from the equation shown (from Peters, 1986).

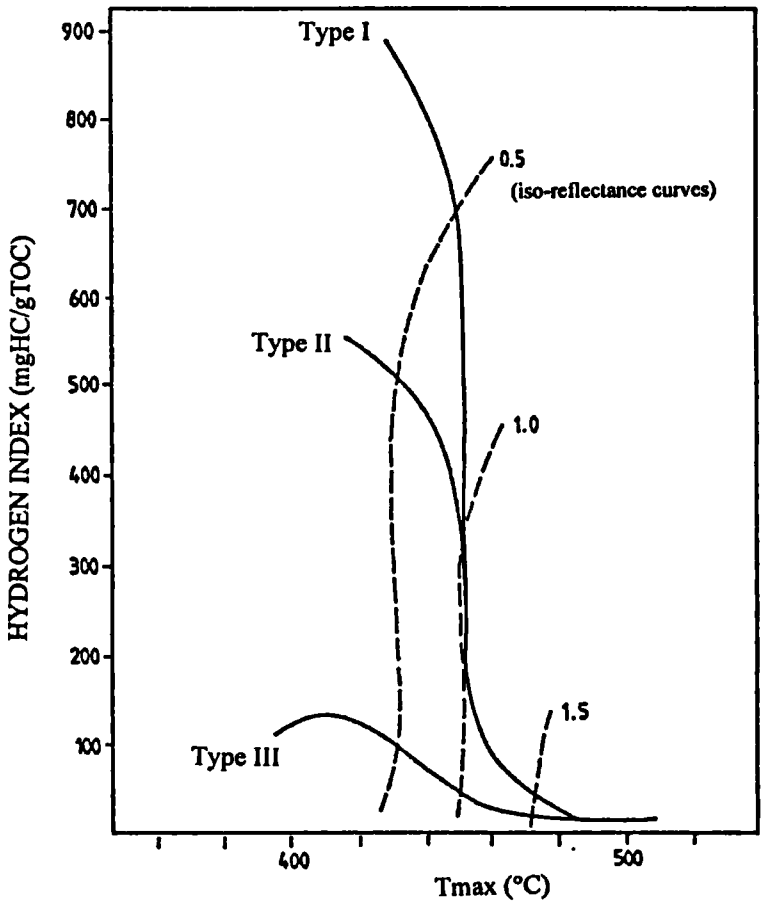


FIGURE 4.2 Plotting the Hydrogen Index (HI, mg HC/g TOC) against pyrolysis Tmax (°C) can be used as one method of determining kerogen type (from Parnell & Rahman, 1990).

BIBL
LONDON
UNIV

The S1 peak represents hydrocarbons that are already present in the sediments, volatilised at 300°C. These could be either indigenous or migrated hydrocarbons. The S2 peak corresponds to the amount of hydrocarbons generated from the thermal degradation of kerogen in the sample at temperatures ranging from 300°C to 600°C. Together, the S1 and S2 peaks represent the Hydrocarbon Generating Potential, also known as the Genetic Potential, of the sediments. Below is Tissot & Welte's (1984) classification scheme for genetic potentials :

Genetic Potential (mg/g)	**Source Potential**
< 2.0	Poor oil, some gas
2.0 - 6.0	Moderate
> 6.0	Good

The values, however, will not represent the sample's true genetic potential if the hydrocarbons measured by the S1 peak have migrated into the sample from elsewhere. The S2 peak, on the other hand, represents either the total hydrocarbon-generating potential if the samples analysed are immature, or the residual hydrocarbon-generating potential if the samples analysed are already in the hydrocarbon-generation zone. Note that the genetic potential cannot be used to predict the type of hydrocarbon (whether gaseous or liquid) produced during pyrolysis.

The **Hydrogen Index,** defined as **HI** = (S2/TOC) x 100, is used to determine the type and quality of the organic matter present in the sediments. The type of organic matter can be determined by plotting the Hydrogen Index values against the maximum temperature, Tmax (°C), where the organic matter can be classified into three possible groups : Type I, Type II and Type III **(Figure 4.2).** Generally, low Hydrogen Index values (< 200 mg HC/g TOC) typify Type III organic matter while higher values (> 200 mgHC/gTOC) are characteristic of Type I and Type II organic matter.

The **Production Index, PI** = S1/(S1+S2), also known as the **Transformation Ratio,** is often used to assess the relative thermal maturity of organic matter for it continuously increases as a function of depth. In the absence of migration, it measures the extent to which the genetic potential has been effectively realised. Plotting the variation of the transformation ratio against depth will help identify minute accumulations in the micro-reservoirs by their anomalously high values compared to the average curve. The maximum temperature, **Tmax,** recorded during pyrolysis corresponds to the temperature at which maximum generation of hydrocarbons occurred. It is related to the degree of thermal maturity of the sample. The cut-off values used in this study for the maturity interpretation are as follows :

Tmax (°C)	**Degree of thermal maturity**
< 420°C	Immature
420°C - 430°C	Late immature
430°C - 440°C	Marginal mature

440°C - 460°C	Mature (oil window)
> 460°C	Over mature (gas)

However, the Tmax values of samples with poor S2 peaks (< 0.2 mg/g) are considered to be inaccurate and should not be included when analysing the thermal maturity of the sediments for the following reason. The small quantities of pyrolysates produced by samples containing poor hydrocarbon-generating organic matter are thought to be prone to the adsorption capacity of the samples' mineral matrix, particularly by clayey-shaley matrix (Dembicki *et. al.*, 1983; Espitalie' *et. al.*, 1980; Peters, 1986). The adsorbed pyrolysates will only be released at higher temperatures inevitably giving misleading indications of the samples' maturity levels.

4.3 Solvent extraction

Soluble organic matter (bitumen) present in the samples was extracted by treating the samples with an azeotropic solvent mixture of dichloromethane and methanol at the ratio of 93:7, respectively. Using an azeotropic solvent will allow the extraction of a greater range of organic matter than a single solvent would. Furthermore, its boiling point is lower than that of single solvents, aiding the removal of the solvent without too much loss of the extracted organic matter (Kinghorn, pers. comm.). Only the C_{15+} and heavier hydrocarbons would be completely recovered during extraction. The lighter hydrocarbons (< C_{15}) have the same boiling point range as the organic solvent, and this results in their loss during solvent evaporation.

Solvent extraction was performed on samples with generally high TOC contents (> 1.0 wt%), high S1 peaks (> 0.2 mg/g) and high production index values (> 0.2 mg/g). The extracted bitumen is referred to as Extractable Organic Matter, EOM. It is also often called Total Soluble Extract (TSE) or Soluble Organic Matter (SOM). For evaluating the liquid hydrocarbon source potential, the following EOM scheme is available :

EOM (ppm)	**Potential**
< 300	Poor
300 - 1000	Fair
1000 - 2000	Good
> 2000	Excellent

The hydrocarbon content (saturate + aromatic) is also important indicator of liquid hydrocarbon source potential of the sediments. A source rock rating scheme based upon Philippi (1957) is given below :

Saturate + Aromatic (ppm)	**Potential**
0 - 50	Very poor
50 - 150	Poor
150 - 500	Fair

500 - 1000	Good
1000 - 5000	Very good
> 5000	Excellent

Ratios calculated from TOC, EOM and (Saturate + Aromatic) data are also useful in evaluating liquid hydrocarbon source potential and for identifying migrated, non-indigenous hydrocarbons. The following scheme is used for such purposes :

EOM/TOC (mg/g)	HC/TOC (mg/g)	Potential
< 5	< 3	Poor
5 - 10	3 - 6	Fair
10 - 15	6 - 9	Good
15 - 20	9 - 12	Excellent
> 25	> 20	Migrated HC

4.4 Extractable organic matter analyses

Extracted hydrocarbon fractions were analysed using gas chromatography and gas chromatography-mass spectrometry to obtain information on organic matter type, environment of deposition and level of maturity utilising chromatogram traces and biological markers (**Figure 4.3**).

4.4.1 Gas Chromatography

Saturated hydrocarbons analysed by gas chromatography determine the n-alkane and isoprenoid distributions. The shape of the n-alkane envelope changes with thermal maturity; immature sediments often have high concentrations of odd carbon-numbered n-alkanes which disappear with increasing thermal maturation. The Carbon Preference Index, CPI, is a convenient parameter for measuring thermal maturity and is calculated according to the equation of Bray & Evans (1961) :

$$CPI = 0.5 \left\{ \frac{\Sigma(nC_{25}\text{-}C_{33})}{\Sigma(nC_{26}\text{-}C_{34})} + \frac{\Sigma(nC_{25}\text{-}C_{33})}{n\Sigma(C_{24}\text{-}C_{32})} \right\}$$

Alternative equations put forward by (1) Louis (1967) and (2) Scalan & Smith (1970) can also be used:

(1) $$CPI = \left\{ \frac{2nC_{29}}{\Sigma(nC_{28} + nC_{30})} \right\}$$

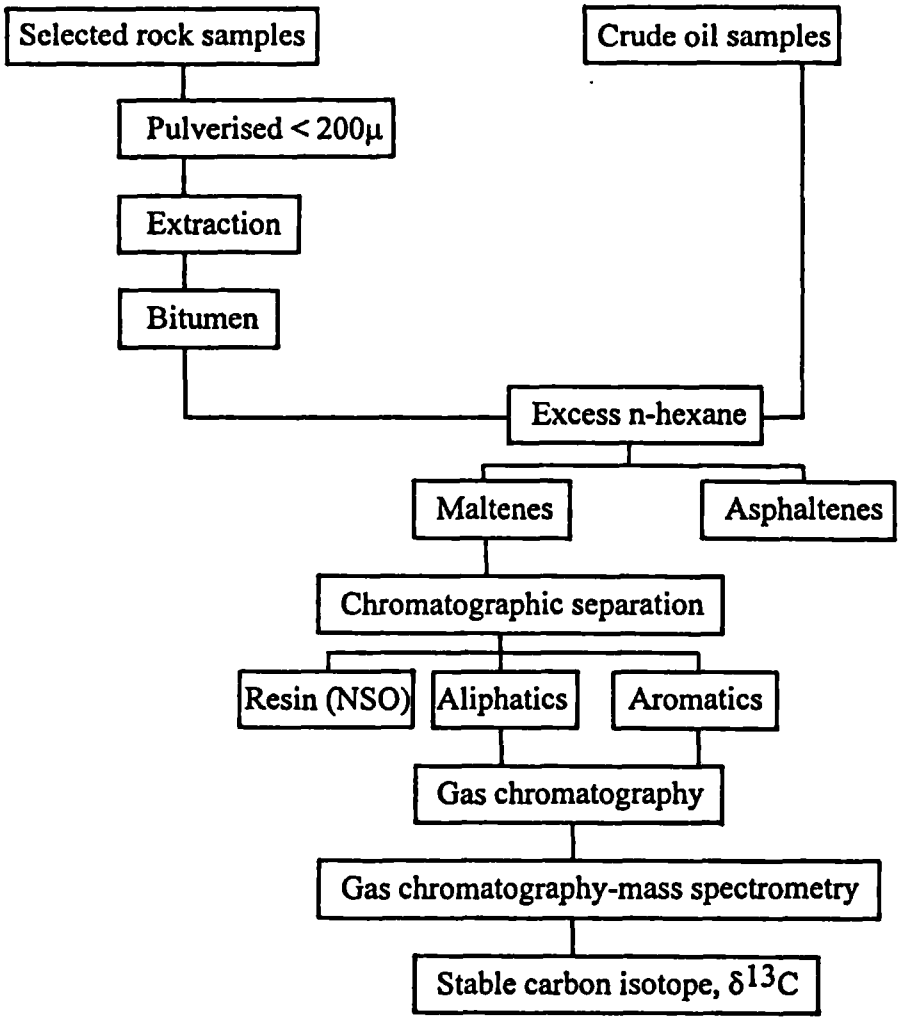


Figure 4.3 Analysis of bitumen and crude oil samples

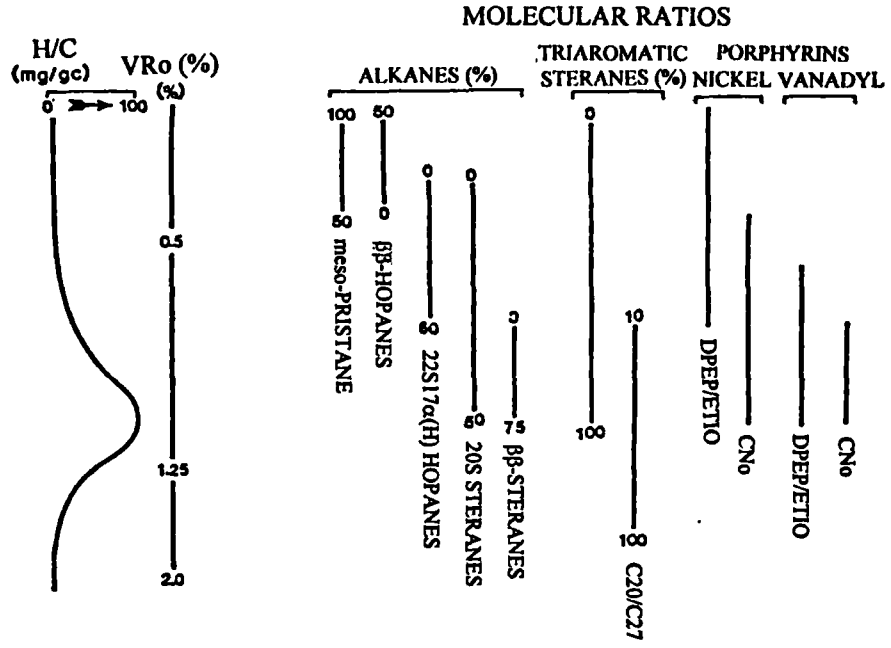


FIGURE 4.4 Approximate ranges of the sterane 20S/(20S+20R) and hopane 22S/(22S+22R), and other molecular ratios in relation to vitrinite reflectance values and yields of extractable hydrocarbon extracts (from Mackenzie & Maxwell, 1981).

(2) $$OEP = \left\{ \frac{C_i + 6C_{i+2} + C_{i+4}}{4C_{i+1} + 4C_{i+3}} \right\} (-1)^{i+1}$$

In general, the CPI decreases with increasing organic matter maturity until the sediment is in a state to produce hydrocarbons, when the CPI will be nearly unity and very similar to that of crude oils (Tissot & Welte, 1984).

Information about the type of organic matter in the sediments and its maturity can also be obtained from the chromatograms. According to Bray and Evans (1961, 1965), normal alkane distributions with odd numbered nC_{21} to nC_{35} alkanes as the predominant compounds are derived from cuticular waxes of land plants. Normal alkane distributions in which nC_{15}, nC_{17} and nC_{19} alkanes are the predominant compounds are considered to be derived from algal and/or bacterial sources (Nissenbaum *et. al.*, 1972). Brackish-water plants synthesize compounds in the intermediate carbon number range of C_{19}-C_{27} (Hunt, 1968, 1979). Where there are contributions from both land plants and algae/bacteria, the chromatogram will show abundance of the lower as well as higher molecular weight n-alkanes.

4.4.2 Gas Chromatography-Mass Spectrometry

Gas chromatography - mass spectrometry is an analytical technique used to study the occurrence and distribution of specific organic compounds in complex hydrocarbon mixtures (Noble, 1991). It is primarily used to characterise the distribution of trace organic substances known as biological markers, which are molecules that retain enough of their original chemical structure so that their biological origin is recognisable. The biomarker distribution patterns depend on the type of organic matter incorporated in the sediments and the subsequent chemical changes that occurs with sediment burial. These complex processes vary considerably form one depositional setting to another, resulting in very different biomarker distribution patterns and provide a tool for fingerprinting samples.

The use of biomarkers like steranes and triterpanes in petroleum geochemistry is now widespread (Mackenzie, 1984; Philp, 1985) resulting from improvements in equipment and techniques. By determining the distribution of steranes and triterpanes, it is possible to obtain information on depositional environment, maturation and migration history, biodegradation and thermal maturity. The distribution patterns are also used to correlate crude oils to their source rocks. The most common maturity ratios [reactant/(reactant + product)] used are:

1. Isomerisation at C-22 in the C_{31}-C_{35} 17α(H)21β(H)-hopanes. The ratio [22S/(22S+22R)] reaches equilibrium around the value of 0.6 (equivalent to VRo ≈ 0.75%, **Figure 4.4**) at the onset of hydrocarbon generation (Ensminger *et. al.*, 1974;

Seifert & Moldowan, 1980; Mackenzie & Maxwell, 1981; Mackenzie, 1984). In this study, the ratio is calculated using the C_{32} 17α(H)21β(H)-hopane.

2. Isomerisation at C-20 in the C_{29} steranes has a much wider range of application and reaches equilibrium at an estimated VRo ≈ 1.0% (**Figure 4.4**). The [20S/(20S+20R)] ratio at the C_{29} 5α(H)14α(H)17α(H)-steranes reaches equilibrium around the value of 0.54 (Mackenzie *et. al.*, 1980a; Seifert & Moldowan, 1981; Mackenzie & Maxwell, 1981). The C_{29} compound is used for calculating the ratio as it is least affected by co-elution with other compounds (Waples & Machihara, 1991).

In this study, the gas chromatography - mass spectrometry equipment was made available by British Gas, London Research Station. The set-up consisted of a 25m x 0.22mm i.d. fused silica column coated with a cross bonded non-polar phase (CP-Sil 5CB) in the gas chromatograph whilst the mass spectrometer (Finnigan TSQ 70 triple quadrupole) is set to monitor ions that are specific to certain classes of biomarkers. Here, the m/z 191 and m/z 217 were monitored for hopane and sterane distributions in order to calculate the biomarker ratios from hopane 22S and 22R, and sterane 20S and 20R epimers, whose stereo-chemistries are reportedly dependent on maturity level.

The main attractions of the GC-MS technique is that only very small amounts of sample are required for analysis and its simple analytical procedures (Kimble *et. al.*, 1974; Wardroper *et. al.*, 1977). Furthermore, the technique is insensitive to the length of time the sample has been stored in the warehouse or the physical condition of the samples (Noble, 1991). Ideally, core samples should be used to avoid sample cross-contamination. Result from biomarker analysis should still be supplemented by other geochemical data like gas-chromatograph profiles and stable carbon isotope ratios before any conclusions on extract/oil to source rock correlations are drawn.

4.4.3 Tandem Gas Chromatography-Mass Spectrometry

This method allows the complete separation of complex hydrocarbon compounds and is extremely powerful for correlative work and for ensuring that certain peaks used for maturity calculations are unaffected by the co-elution of other compounds. The Finnigan TSQ 70 mass spectrometer at the British Gas London Research Station was used for this study. The first quadrupole of the Finnigan TSQ 70 mass spectrometer is set to jump molecular ions of the hopanoid class of triterpenoid hydrocarbons or steranes. The collision gas is introduced in the second quadrupole to fragment the molecular ion and the third quadrupole is set to monitor the characteristic fragment ion of hopanes (m/z 191) or of steranes (m/z 217). The final reconstructed ion chromatogram (RIC) will consist entirely of hopane/sterane homologues. The main aim of using this technique is to ascertain that the C_{32} 17α(H)21β(H)-hopane and C_{29} 5α(H)14α(H)17α(H)-sterane peaks used for calculating the thermal maturity ratios are not

affected by co-elution of other compounds which, if they are, will give erroneous biomarker maturity ratios.

4.4.4 Stable Carbon Isotope, $\delta^{13}C_{extracts}$

The isotopic composition of an element is determined by firstly converting it quantitatively to a gaseous form (CO_2 for carbon), and then analysing the gas on a mass spectrometer (Sofer, 1991). Isotopic compositions are reported as δ values per mil (‰) defined as:

$$\delta\ (‰) = [(R_{sample} - R_{standard})/R_{standard}] \times 1000$$

where R_{sample} is the ratio of heavy-to-light isotope ($^{13}C/^{12}C$) and $R_{standard}$ is the respective ratio of an internationally-accepted standard, the Pee Dee Belemnite. Samples with ratios larger than the standard are said to have positive δ values; conversely, those with smaller ratios are negative. Isotopically more positive samples have more heavy isotope (^{13}C); isotopically negative samples have less ^{13}C. Thus, isotopically heavier is equivalent to isotopically positive, and isotopically lighter is equivalent to isotopically negative.

In this study, aliphatic and aromatic fractions from rock extracts and crude oils, as well as kerogen samples, were sent to Simon Laboratories in Llandudno, North Wales for the determination of their isotopic compositions. Using Stahl's (1977, 1978) isotope type curves, genetic association between kerogens, oils and extracts can be elucidated. Fuex (1977) suggested that in oil-source rock correlations, a genetic relationship is established when the isotopic composition of the fractions differ by less than 1 ‰. Sofer (1984), however, showed that non-marine oils can be isotopically different by as much as 4 ‰ and still be genetically associated. Yeh & Epstein (1981) and Sofer (1984) have shown that the isotopic composition of kerogen cannot be used as a depositional environment indicator.

4.5 Kerogen isolation

Treatment of crushed whole rock samples with hydrochloric (HCl) and hydrofluoric (HF) acids releases the insoluble organic matter (kerogen) for further investigations. A host of analyses **(Figure 4.5)** performed on isolated kerogens can provide information on kerogen type and its level of maturity, to be compared with results obtained from other analytical procedures.

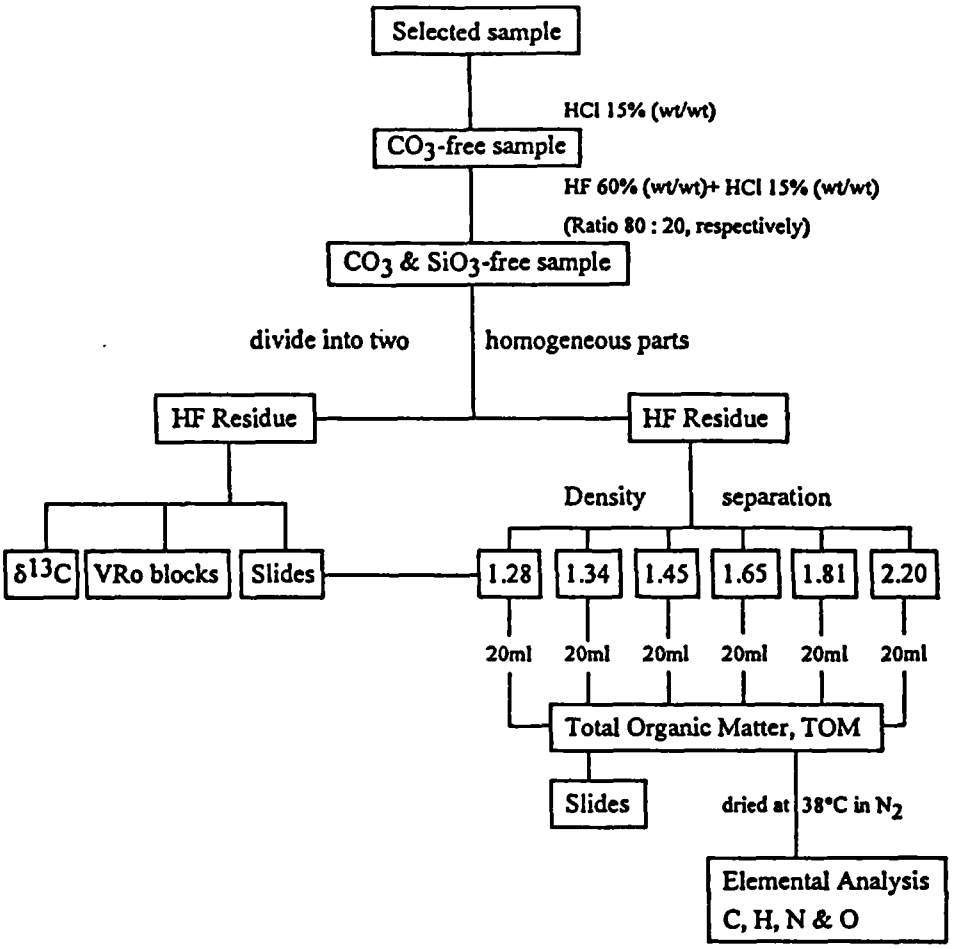


Figure 4.5 Analyses performed on isolated kerogen samples.

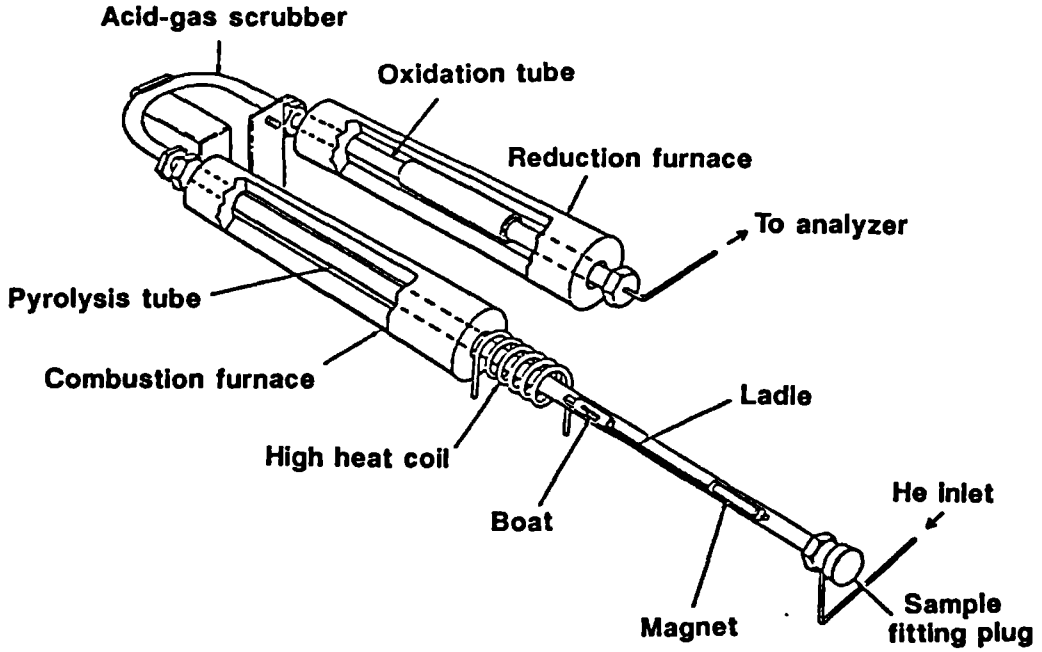


FIGURE 4.7 The combustion train used for oxygen analysis (Perkin-Elmer Handbook, 1986).

4.6 Isolated kerogen analyses

4.6.1 Density Separation

The density separation of different maceral groups making up the kerogen concentrate by sequential centrifuging in zinc bromide solutions of progressively higher specific gravities is based on the fact that the density of each component in a kerogen depends upon its chemical composition. Hydrogen-rich kerogens are lighter than those which are deficient in hydrogen and, as such, they will have lower specific gravities compared to their hydrogen-poor counterparts (Kinghorn & Rahman, 1980). Quantitative estimations of the respective fractions were made after the density separation procedure was completed. Slides of each density fraction and the hydrofluoric acid residue of each sample were made for kerogen typing and maturity determination by observation under transmitted, ultra-violet and reflected-light microscopes. Mineral-free Total Organic Matter (TOM) mixtures were prepared and left to dry in an oven at 38°C in a nitrogen atmosphere. Once dried, they are homogenised for elemental analysis.

4.6.2 Elemental Analysis

The Perkin-Elmer Model 240C Elemental Analyser was used to determine the elemental compositions of isolated kerogens. It determines carbon, hydrogen, nitrogen and oxygen contents of organic compounds, as burnt to CO_2, H_2O, and N_2. Combustion occurs in pure oxygen for CHN analyses and in helium for O_2 analysis. The products are analysed automatically in a self-integrating, steady-state, thermal conductivity analyser (Perkin-Elmer Handbook, 1986). Results are recorded with the Perkin-Elmer Data Station; blanks, sensitivity factors and analytical results are computed directly in weight percent (wt%). **Figure 4.6** shows a simplified diagram of the combustion train and analytical system for the carbon, hydrogen and nitrogen analysis, and **Figure 4.7** shows the combustion train used in oxygen analysis.

An investigation as to whether there were any significant difference in results when using Nickel boats, as opposed to Platinum boats, was carried out prior to analysis, using acetanilide standard for carbon/hydrogen/nitrogen (CHN) analysis and benzoic acid for oxygen analysis, as samples. Results show that there was not any, with the results varying only between 0.24% to 4.73% **(Table 4.1)**. The repeatability of results, controlled by the equipment's stability were also investigated **(Table 4.1)**. For every sample run, this repeatibility was determined prior to any kerogen sample analysis to ascertain the instrument's behaviour. Only when the equipment's stability has been determined (% variation < 5.00%) will sample analysis commence. To further confirm that the analytical conditions were consistent throughout the sample run, standards were analysed at the end of the sample run. Three repeat analyses were done for each kerogen sample, and the results presented in **Chapter 5** are average values calculated from the three repeated runs.

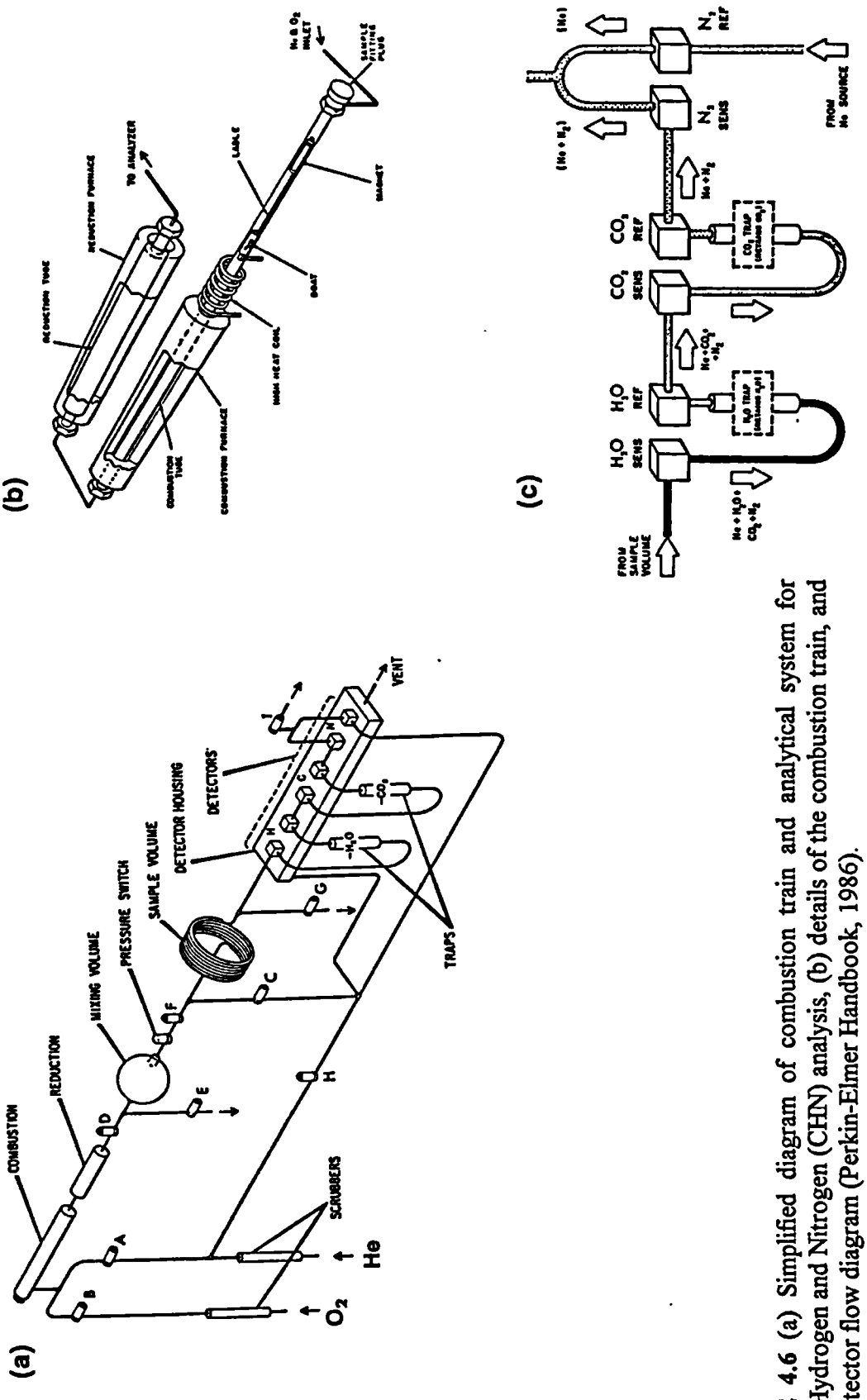


FIGURE 4.6 (a) Simplified diagram of combustion train and analytical system for Carbon, Hydrogen and Nitrogen (CHN) analysis, (b) details of the combustion train, and (c) the detector flow diagram (Perkin-Elmer Handbook, 1986).

4.6.3 Visual Examination

4.6.3a Kerogen typing

This involves viewing strewn slides made from kerogens isolated according to their specific gravities, as well as slides of the Total Organic Matter (TOM) fraction and the hydrofluoric acid residue under a transmitted and ultraviolet-light microscopes. 200 point counts were made per slide using a point counter to record the counts.

4.6.3b Vitrinite reflectance measurement

Vitrinite reflectance has been successfully demonstrated as a reliable indicator of organic maturation in sedimentary rocks and is widely used in the petroleum industry for the evaluation of kerogens. Reflectance is defined as the proportion of normal incident light reflected by a planar and polished surface of the substance under consideration (Senftle & Landis, 1991) and is expressed as a percentage of the light incident on the surface. For vitrinite reflectance, only the amount of light reflected in the green visible wavelength (546 nm) is measured. A stabilised light source, immersion oil with a refractive index of n=1.518 and a microscope photometer are used to compare the reflected intensities of vitrinite macerals to that of a standard. A tungsten filament lamp provides the incident white light on the sample.

In this study, vitrinite reflectance is measured from polished kerogen concentrates embedded in epoxy resin blocks. Due to the friable and fragmented nature of the samples, whole rock mounts could not be satisfactorily prepared and were therefore excluded from the vitrinite reflectance measurements, despite the obvious advantage of being able to make the distinction between *in situ* and recycled vitrinite particles. A total of 50 to 100 measurements were made per sample and histograms were drawn up in order to distinguish between the recycled and caved vitrinites from those that are *in situ*. It is important to compare the vitrinite reflectance maturity results with those of other techniques, especially when dealing with immature rocks and those in the early zone of oil generation. Furthermore, different types of vitrinite can affect the measurements obtained (Toxopeus, 1982; Price & Barker, 1985).

4.6.4 Stable Carbon Isotope, $\delta^{13}C_{kerogen}$

The isotopic composition of kerogen is probably the most important factor for determining the isotopic composition of the oil it generated (Sofer, 1991). Isotope compositions normally become less negative with increasing polarity from saturates to kerogens. Employing the Stahl (1977, 1978) isotopic type curves allows the estimation of isotopic composition of an oil generated from a given kerogen and vice-versa, thus aiding oil to source rock correlation. The kerogen samples, along with aliphatic and aromatic fractions of seven Sabah Basin oils from South Furious, Barton, Rusa Timur, St. Joseph, Tembungo, Erb West and Ketam areas (**Figure 1.5**), were sent to Simon Laboratories to determine their isotopic compositions.

Table 4.1 Comparison between the use of platinum and nickel boats when analysing elemental compositions.

(a) Standard compound : Acetanilide

Boat type		Platinum	Nickel	
Sensitivity factor				% variation
K_{Carbon}	1)	19.53	19.58	
	2)	19.54	19.56	
	3)	19.67	19.54	0.24
Average, μ		19.58	19.56	
Std. deviation, σ		0.06	0.02	
% variation		0.31	0.10	
$K_{Hydrogen}$	1)	54.58	54.60	
	2)	51.43	48.24	
	3)	51.26	55.25	4.73
Average, μ		52.42	52.70	
Std. deviation, σ		1.53	3.16	
% variation		2.92	6.00	
$K_{Nitrogen}$	1)	7.20	7.13	
	2)	7.28	7.29	
	3)	7.22	7.28	0.79
Average, μ		7.23	7.23	
Std. deviation, σ		0.03	0.07	
% variation		0.41	1.01	

(b) Standard compound : Benzoic acid

Boat type		Platinum	Nickel	
Sensitivity factor				% variation
K_{Oxygen}	1)	7.56	7.37	
	2)	7.63	7.79	
	3)	7.58	7.55	1.63
Average, μ		7.59	7.57	
Std. deviation, σ		0.03	0.17	
% variation		0.40	2.25	

CHAPTER FIVE

RESULTS FROM SAMPLE SCREENING AND KEROGEN ANALYSES

5.1 General characteristics of the dispersed organic matter : quantity, quality and maturity

5.1.1 Stage III

Deep marine sediments of Stage III were encountered by South Furious-2 and South Furious-3 wells. Drilling stopped after penetrating only 173m (567ft) and 18m (60ft) of Stage III sediments in South Furious-2 and South Furious-3, respectively, due to over-pressure. Caution must be exercised when making generalised conclusions on the hydrocarbon potential of these sediments because of the very limited section analysed, both areally and stratigraphically.

5.1.1a Organic Carbon Content

Total organic carbon (TOC) contents were found to range from 1.24-3.78 wt% (μ=2.24 wt%, σ=0.92 wt%) in South Furious-2. Only two samples were available from South Furious-3, which had TOC values of 1.51-1.70 wt%. The TOC values **(Table 5.1)** from both wells show that the penetrated Stage III sediments have good to very good organic carbon contents.

Table 5.1 Screening results for Stage III sediments (South Furious area only).

	Depth (m)	(ft)	TOC (wt%)	S1 (mg/g)	S2 (mg/g)	Tmax (°C)	PI	HI (mgHC/gTOC)
South Furious-2								
1.	1871	6138	3.33	0.17	2.10	418	0.07	63
2.	1880	6168	1.78	0.14	1.04	414	0.12	58
3.	1893	6211	1.26	0.08	0.68	420	0.11	54
4.	1921	6302	1.41	0.14	1.04	415	0.12	74
5.	1957	6421	1.60	0.16	1.43	418	0.10	89
6.	1969	6460	2.96	0.13	1.44	424	0.08	49
7.	1979	6493	3.78	0.22	2.82	407	0.07	75
8.	1988	6522	2.83	0.21	2.64	417	0.07	93
9.	1998	6555	1.24	0.11	0.72	418	0.13	53

Table 5.1 Screening results for Stage III sediments (South Furious area only) - continued.

Depth (m)	Depth (ft)	TOC (wt%)	S1 (mg/g)	S2 (mg/g)	Tmax (°C)	PI	HI (mgHC/gTOC)
South Furious-3							
10.	2310	7579	1.51	0.16	1.20	425	0.12	79
11.	2316	7598	1.70	0.21	1.62	424	0.11	95

5.1.1b Organic Matter Type And Quality

Rock-Eval pyrolysis revealed that samples from both wells only have low to moderate S2 yields **(Table 5.1)** ranging from 0.68-2.82 mg/g (μ=1.52 mg/g, σ=0.69 mg/g). Hydrogen Index values were correspondingly low with values < 100 mgHC/gTOC, suggesting poor kerogen-convertibility and essentially gas-prone kerogens. This is supported by **Figure 5.1**, a plot of Hydrogen Index vs Tmax which indicates that the Stage III sediments contain mainly terrigenous Type III organic matter.

Results from elemental analysis of six kerogen concentrates **(Table 5.2)** suggest that they are of Type III, with South Furious-3 samples having slightly higher H/C atomic ratios **(Figure 5.2)**. The sample positions in the van Krevelen diagram agree with their respective Hydrogen Index values **(Table 5.1)**.

Table 5.2 Elemental analysis results : Stage III (South Furious area only).

Depth (m)	Depth (ft)	H%	O%	C%	N%	H/C	O/C	Total % of (C+H+N+O)
South Furious-2								
1.	1871	6138	4.30	30.58	51.84	1.64	1.00	0.44	88.36
2.	1921	6302	4.41	29.62	52.43	1.60	1.01	0.42	88.06
3.	1957	6421	4.29	26.29	61.20	1.62	0.84	0.32	93.40
4.	1988	6522	4.45	28.83	64.44	1.68	0.83	0.34	99.40
South Furious-3								
5.	2310	7579	5.16	23.91	55.22	1.20	1.12	0.32	85.49
6.	2316	7598	5.24	22.46	52.04	1.19	1.21	0.32	80.93

Relative maceral abundance in South Furious-2 and South Furious-3 are determined from both visual kerogen analysis and density separation **(Table 5.3)**. Using a transmitted-light microscope, herbaceous organic particles comprising spores, pollen and cuticles are grouped as exinite while brown woody/structured matter are classified as vitrinite. Other black/oxidised forms, structured or otherwise, are grouped as inertinites. For density separation, the organic matter are classified as per Kinghorn and Rahman (1980) where those with density < 1.45 are grouped as sapropelic algae,

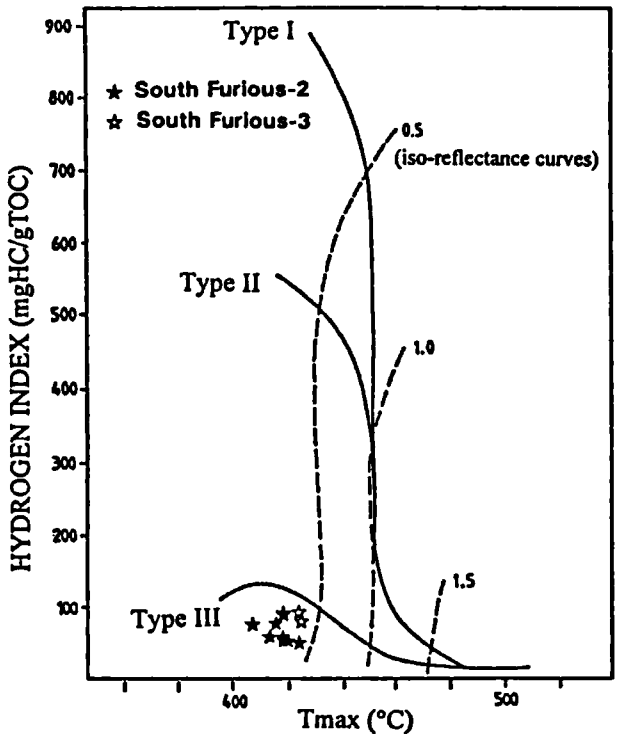


FIGURE 5.1 Hydrogen Index vs Tmax cross-plot (from Parnell & Rahman, 1990) for Stage III sediments.

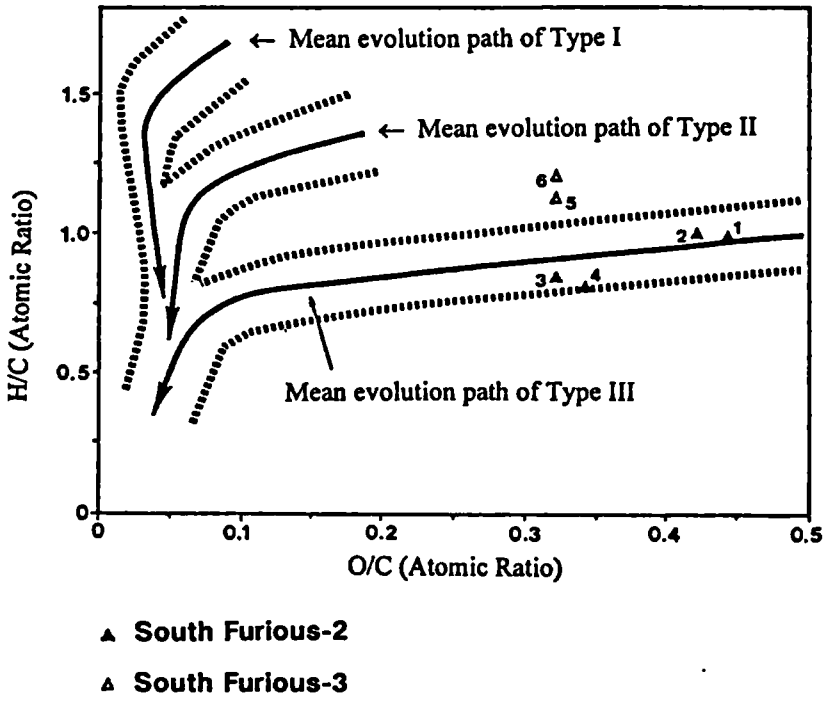


FIGURE 5.2 Elemental compositions of Stage III kerogens plotted on the van Krevelen diagram (from Durand, 1980).

1.45-1.65 as herbaceous, 1.81 as woody (vitrinite) and 2.20 as inertinite. In all the samples analysed, except for sample 1871m/6138ft, exinites are dominant, making up 60% or more of the total count **(Table 5.3)**. These exinites are degraded (see **Appendix II**), which accounts for the low Hydrogen Index values. Vitrinites are almost equal or slightly more in quantity than inertinites, except in sample 1871m/6138ft where inertinites are dominant.

Estimations of percentage composition by both optical means and density separation seem to have some degree of agreement between them **(Figure 5.3)**. Corresponding Hydrogen Index values also reflect the changes in composition, where Hydrogen Index increases with increasing exinite content. For sample 1871m/6138ft in South Furious-2 **(Table 5.3)**, the high TOC but low Hydrogen Index values illustrate the basic importance of knowing maceral composition. As emphasised by Tissot & Welte (1984), the type of organic matter is just as important as its quantity in determining the quality of source rocks. Having good TOC contents do not necessarily mean good hydrocarbon-generating potentials, for the organic carbon could be made up of poor quality organic matter, as shown by sample 1871m/6138ft.

Table 5.3 Visual analysis and density separation of kerogen concentrates : Stage III (South Furious area only).

	Depth		% (optical)			% (spec. grav.)				HI	TOC
	(m)	(ft)	Ex	Vit	In	1.45	1.65	1.81	2.20		
South Furious-2											
1.	1871	6138	30	25	44	5	20	60	15	63	3.33
2.	1921	6302	60	25	15	10	20	65	5	74	1.41
3.	1957	6421	20	65	15	5	15	70	10	89	1.60
4.	1988	6522	50	40	10	10	60	20	10	93	2.83
South Furious-3											
5.	2310	7579	66	17	17	5	80	10	5	79	1.51
6.	2316	7598	74	16	10	5	80	10	5	95	1.70

Key : Ex = Exinite, Vit = Vitrinite, In = Inertinite

C_{15+} saturate hydrocarbon chromatograms of South Furious-2 Stage III samples **(Figure 5.4, 5.5 & 5.6)** show the presence of high molecular weight n-alkanes, typical of waxy hydrocarbons derived from terrigenous organic matter (Hedberg, 1968; Tissot & Welte, 1984). The dominance of odd carbon-numbers in the nC_{25}-nC_{35} region of the distribution is also consistent with contribution from land plants (Chibnall *et. al.*, 1934). Further evidence is given by the high Pr/Phy ratios (> 2.0) and Pr/nC_{17} ratios (> 1.0) **(Table 5.4)** which indicate less anoxic conditions (Powell & McKirdy, 1973; Lijmbach, 1976) often present in deltaic/paralic or peat swamp environments of deposition.

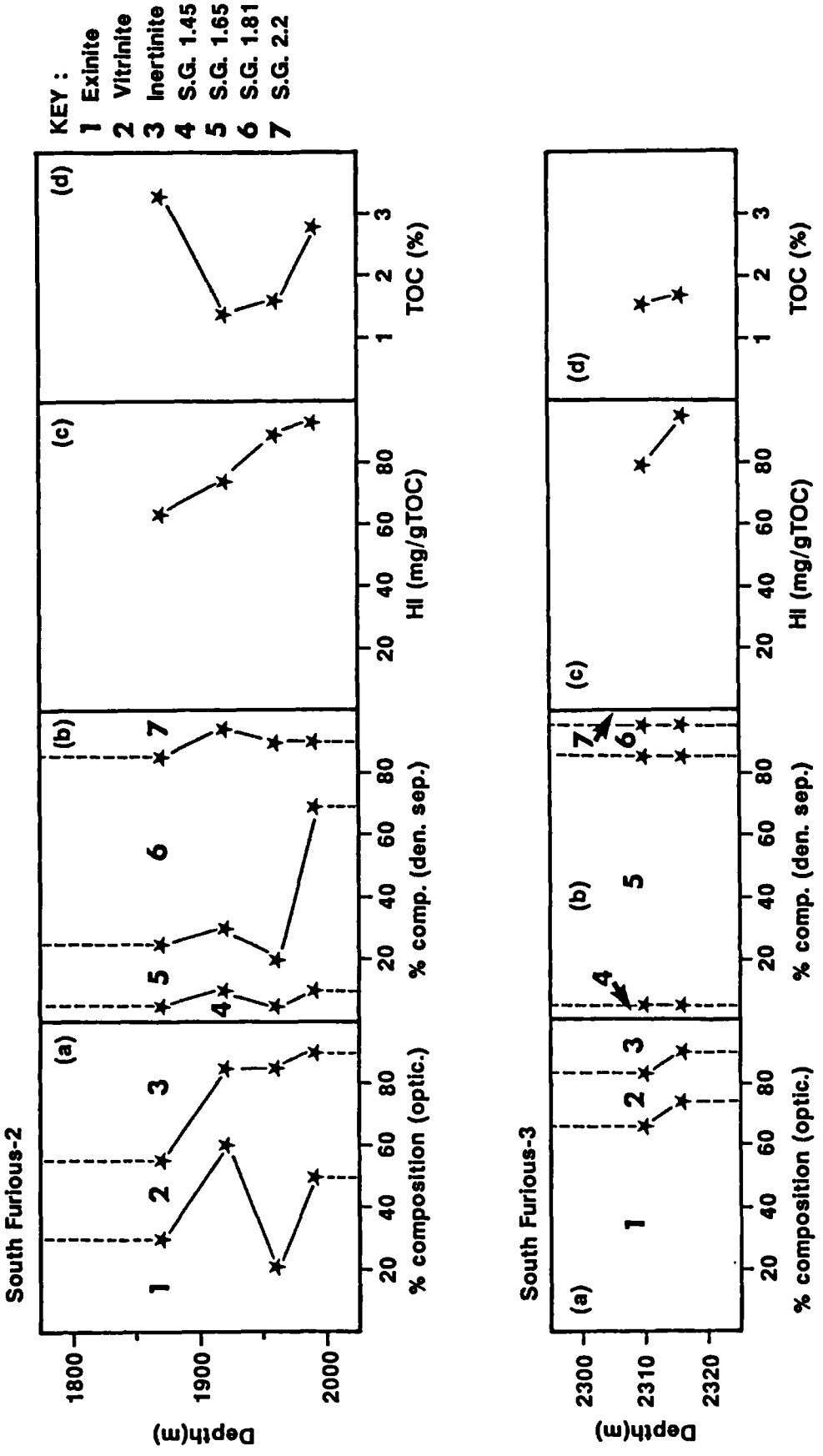


FIGURE 5.3 The variations in kerogen composition of South Furious-2 and South Furious-3 Stage III sediments from (a) organic petrography and (b) density separation. Also shown are the corresponding (c) Hydrogen Index and (d) Total Organic Carbon contents.

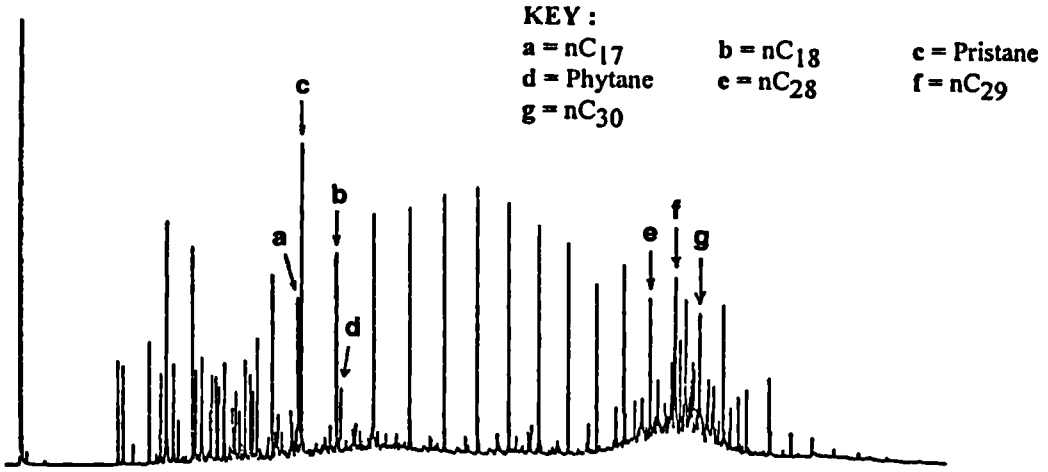


FIGURE 5.4 Gas chromatogram of Stage III South Furious-2 saturate fraction 1871m/6138ft.

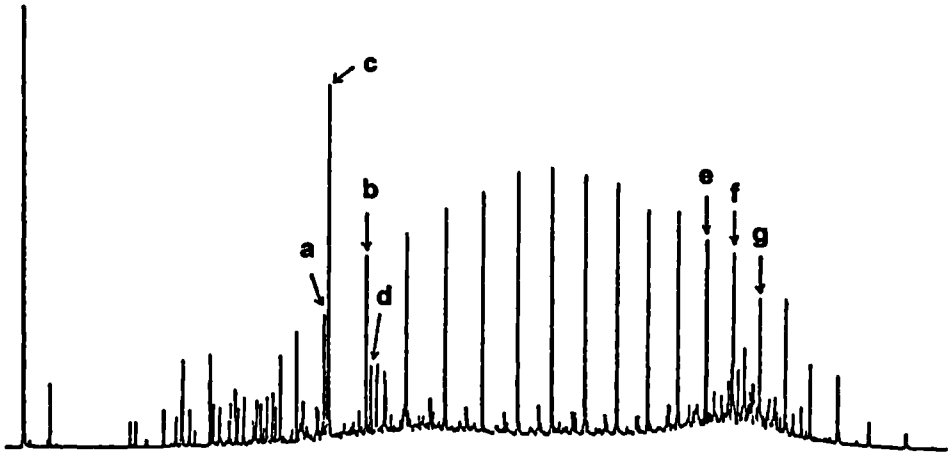


FIGURE 5.5 Gas chromatogram of Stage III South Furious-2 saturate fraction 1921m/6302ft.

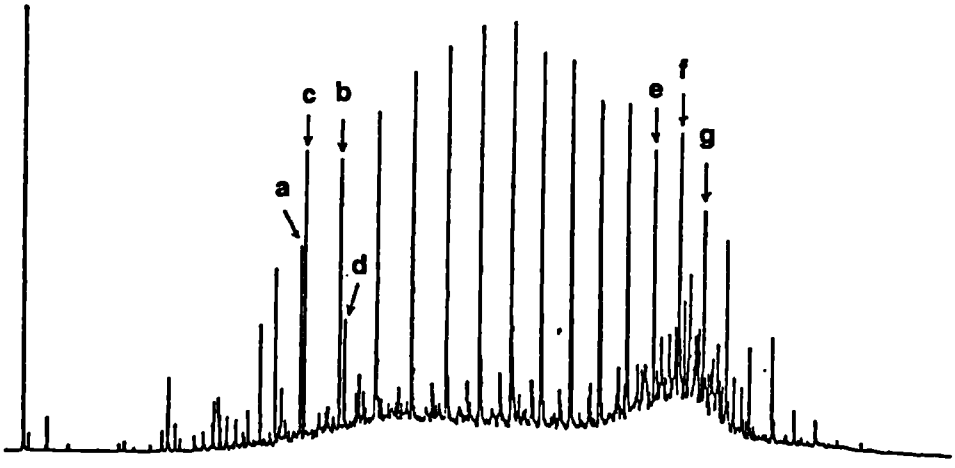


FIGURE 5.6 Gas chromatogram of Stage III South Furious-2 saturate fraction 1979m/6493ft.

Table 5.4 Isoprenoid ratios for Stage III sediments (South Furious area only).

	Depth (m)	(ft)	Pr/Phy	Pr/nC_{17}	CPI *
South Furious-2					
1.	1871	6138	4.8	2.0	1.2
2.	1921	6302	5.1	2.9	1.1
3.	1979	6493	2.6	1.5	1.2

* Louis (1967)

5.1.1c Organic Matter Maturity

In South Furious-2, production index values varying between 0.07-0.13 mg/g (μ=0.10 mg/g) correlate well with the Tmax results which range from 407-424°C (μ=417°C). Both parameters indicate the immaturity of the samples. Carbon Preference Index (CPI) values of 1.1-1.2 indicate that the extracts do not have strong odd carbon-number predominance, suggesting that they are approaching or very close to maturity **(Table 5.4)**. This contradicts with the Tmax and production index values which show the samples to be immature, thus inferring that the hydrocarbons present are most likely to be non-indigenous. Production index values of 0.12 and 0.11 mg/g for South Furious-3 samples indicate their immaturity **(Table 5.1)**. This is supported by pyrolysis Tmax values of 424 and 425°C (late immature zone 420-430°C). Gas chromatography was not performed for South Furious-3 because of small sample volume. Vitrinite reflectance measured on kerogen concentrate samples from both wells verify the immaturity of the penetrated Stage III sediments **(Table 5.5)**.

Table 5.5 Vitrinite reflectance : Stage III (South Furious area only).

	Depth (m)	(ft)	Measured VRo (%)	% Error
South Furious-2				
1.	1871	6138	0.45	±11
2.	1921	6302	0.46	±13
South Furious-3				
3.	2310	7579	0.40	±8
4.	2316	7598	0.40	±15

5.1.2 Sub-Stage IVA

Sub-Stage IVA sediments were encountered in South Furious-2, South Furious-3 and Rusa Timur-1 wells. In South Furious-2 and South Furious-3, they represent coastal-delta plain interbedded sand-siltstone-shale sequences. In Rusa Timur-1, sub-Stage IVA sediments are deep marine shales representing the distal equivalent of the sub-Stage IVA sediments in South Furious-2 and South Furious-3.

5.1.2a Organic Carbon Content

Total organic carbon contents range between 0.30-5.33 wt% (μ=1.44 wt%, σ=1.05 wt%) in South Furious-2; 0.57-14.32 wt% (μ=3.04 wt%, σ=2.43 wt%) in South Furious-3; and 0.72-0.91 wt% (μ=0.83 wt%, σ=0.07 wt%) in Rusa Timur-1 **(Table 5.6)**. TOC values are highest in lower coastal plain sediments of South Furious-2 and South Furious-3, and lowest in deep marine sediments of Rusa Timur-1. The influence of terrigenous source proximity is reflected by the decrease in organic matter quantity further offshore.

5.1.2b Organic Matter Type And Quality

Pyrolysis S2 yields for sub-Stage IVA sediments in South Furious-2 and South Furious-3 **(Table 5.6)** show that they have poor to moderate hydrocarbon-generating potentials. In South Furious-2, the S2 yields range from 0.08 - 3.70 mg/g (μ = 0.89 mg/g, σ = 0.87 mg/g) while in South Furious-3, they range from 0.12-22.34 mg/g (μ=2.31 mg/g, σ =3.28 mg/g).

Table 5.6 TOC and Pyrolysis results : sub-Stage IVA.

	Depth (m)	(ft)	TOC (wt%)	S1 (mg/g)	S2 (mg/g)	Tmax (°C)	PI	HI (mgHC/gTOC)
South Furious-2								
1.	446	1463	3.91	1.78	3.70	384	0.32	95
2.	636	2087	4.38	0.70	3.43	404	0.17	78
3.	881	2890	2.35	0.13	1.02	416	0.11	43
4.	919	3015	2.41	0.13	0.96	402	0.12	40
5.	976	3202	1.79	0.26	1.10	411	0.19	61
6.	991	3251	0.49	0.01	0.13	417	0.07	27
7.	992	3255	0.41	0.00	0.08	422	0.00	20
8.	999	3278	0.67	0.02	0.21	419	0.09	31
9.	1000	3281	0.80	0.03	0.22	418	0.12	28
10.	1002	3287	0.67	0.28	0.90	373	0.24	134
11.	1006	3301	1.60	0.07	2.92	438	0.02	183
12.	1062	3484	1.03	0.07	0.64	414	0.10	62
13.	1123	3684	0.68	0.16	0.57	417	0.22	84
14.	1131	3711	0.78	0.10	0.62	425	0.14	79
15.	1140	3740	2.19	0.48	1.04	413	0.32	47
16.	1156	3793	0.74	0.07	0.25	418	0.22	34
17.	1162	3812	0.52	0.17	0.25	390	0.40	48
18.	1165	3822	0.51	0.12	0.66	425	0.15	129
19.	1170	3839	1.03	0.32	1.02	370	0.24	99
20.	1179	3868	0.73	0.06	0.54	429	0.10	74
21.	1211	3973	1.14	0.11	0.50	416	0.18	44
22.	1215	3986	0.64	0.08	0.26	419	0.24	41
23.	1220	4003	2.30	0.45	0.62	382	0.42	27
24.	1238	4062	0.96	0.11	0.32	414	0.26	33
25.	1245	4085	0.87	0.27	0.72	363	0.27	83
26.	1267	4157	0.30	0.24	0.14	418	0.63	47
27.	1293	4242	2.73	0.29	1.54	416	0.16	56
28.	1294	4245	0.83	0.08	0.27	421	0.23	33

Table 5.6 TOC and Pyrolysis results : sub-Stage IVA - continued.

	Depth (m)	(ft)	TOC (wt%)	S1 (mg/g)	S2 (mg/g)	Tmax (°C)	PI	HI (mgHC/gTOC)
29.	1296	4252	0.76	0.05	0.40	424	0.11	53
30.	1298	4259	0.58	0.01	0.35	433	0.03	60
31.	1299	4262	0.60	0.02	0.22	421	0.08	37
32.	1427	4682	0.72	0.03	0.50	436	0.06	69
33.	1431	4695	0.68	0.02	0.44	425	0.04	65
34.	1461	4793	1.25	0.10	0.57	417	0.15	46
35.	1543	5062	0.67	0.05	0.36	425	0.12	54
36.	1602	5256	1.29	0.07	0.49	420	0.13	38
37.	1603	5259	1.32	0.07	0.54	416	0.11	41
38.	1604	5262	1.50	0.86	0.82	408	0.51	55
39.	1606	5269	1.06	0.04	0.30	416	0.12	28
41.	1644	5394	1.82	0.09	0.74	419	0.11	41
42.	1674	5492	2.52	0.09	1.35	419	0.06	54
43.	1720	5643	1.80	0.09	1.08	420	0.08	60
44.	1738	5702	2.82	0.57	3.15	416	0.15	112
45.	1756	5761	1.77	0.08	0.84	419	0.09	47
46.	1779	5837	5.33	0.24	3.14	413	0.07	59
47.	1793	5883	2.06	0.06	1.30	402	0.04	63
48.	1802	5912	1.09	0.03	0.40	422	0.07	37
49.	1811	5942	1.68	0.05	0.76	420	0.06	45
50.	1820	5971	2.63	0.14	1.36	414	0.09	52
South Furious-3								
51.	825	2707	1.25	0.08	0.38	408	0.17	30
52.	826	2710	5.85	0.40	2.48	397	0.14	42
53.	827	2713	2.07	0.12	0.76	402	0.14	37
54.	828	2717	0.65	0.02	0.12	416	0.14	18
55.	829	2720	0.64	0.03	0.16	417	0.16	25
56.	838	2749	0.61	0.03	0.36	426	0.08	59
57.	841	2759	0.68	0.05	0.24	427	0.17	35
58.	1340	4396	0.58	0.03	0.16	419	0.16	28
59.	1344	4409	1.02	0.05	0.36	413	0.12	35
60.	1346	4416	0.63	0.02	0.40	425	0.05	63
61.	1347	4419	0.72	0.04	0.30	413	0.12	42
62.	1350	4429	1.09	0.04	0.37	420	0.10	34
63.	1600	5249	0.58	0.03	0.22	425	0.12	38
64.	1602	5256	0.89	0.08	0.54	414	0.13	61
65.	1615	5299	0.58	0.03	0.32	434	0.09	55
66.	1616	5302	0.63	0.03	0.38	433	0.07	60
67.	1617	5305	0.57	0.02	0.38	433	0.05	67
68.	1618	5308	0.59	0.03	0.34	433	0.08	58
69.	1761	5778	3.27	0.08	1.54	450	0.05	47
70.	1807	5928	7.44	0.36	5.11	408	0.07	69
71.	1841	6040	1.51	0.06	0.66	410	0.08	44
72.	1848	6063	3.63	0.22	1.46	415	0.13	40
73.	1851	6073	2.96	0.17	1.24	420	0.12	42
74.	1888	6194	2.71	0.08	1.24	453	0.06	46
75.	1898	6227	2.63	0.44	1.90	417	0.19	72
76.	1906	6253	3.67	0.44	2.92	418	0.13	80
77.	1922	6306	2.01	0.12	1.20	426	0.09	60
78.	1946	6385	1.03	0.04	0.47	407	0.08	46
79.	1962	6437	4.45	0.17	2.62	440	0.06	59
80.	1969	6460	2.70	0.10	1.54	414	0.06	57

Table 5.6 TOC and Pyrolysis results : sub-Stage IVA - continued.

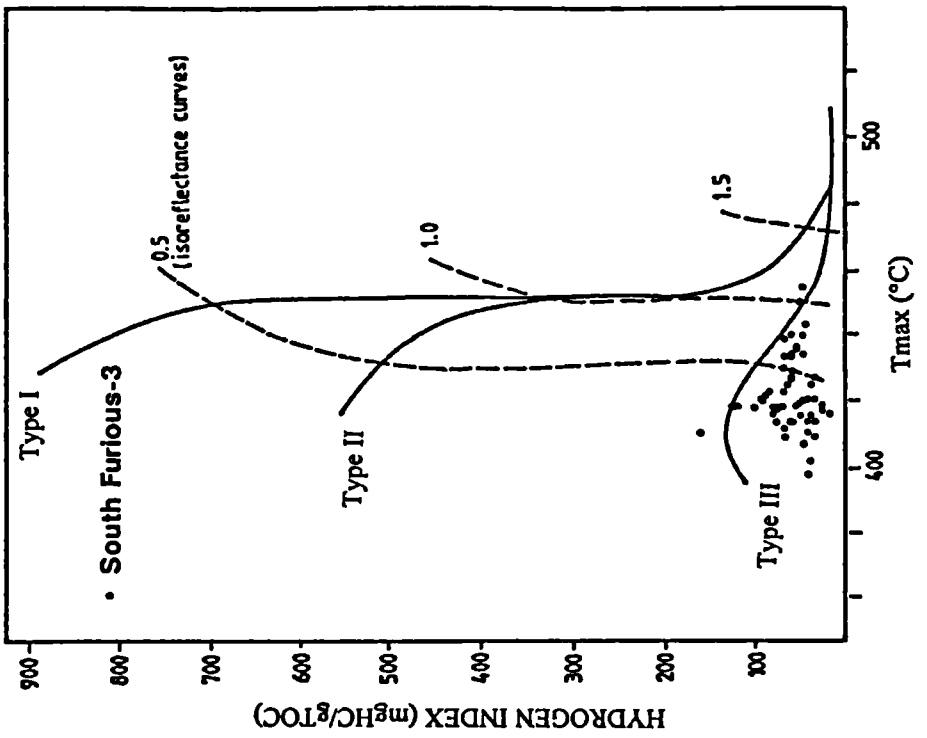
	Depth (m)	(ft)	TOC (wt%)	S1 (mg/g)	S2 (mg/g)	Tmax (°C)	PI	HI (mgHC/gTOC)
81.	1978	6490	3.93	0.28	2.66	422	0.10	68
82.	1997	6552	4.74	0.33	3.04	424	0.10	64
83.	2016	6614	1.75	0.09	0.80	433	0.10	46
84.	2035	6677	3.23	0.15	1.64	435	0.08	51
85.	2053	6736	3.14	0.10	1.60	434	0.06	51
86.	2059	6755	2.81	0.12	1.40	415	0.08	50
87.	2066	6778	2.07	0.08	0.90	443	0.08	43
88.	2096	6877	3.11	0.18	1.88	428	0.09	60
89.	2121	6959	1.42	0.07	0.95	438	0.07	67
90.	2127	6978	2.11	0.06	1.14	418	0.05	54
91.	2151	7057	2.31	0.11	1.02	419	0.10	44
92.	2157	7077	5.37	0.34	4.70	421	0.07	88
93.	2163	7096	4.80	0.32	3.10	411	0.09	65
94.	2185	7169	2.57	0.11	1.26	448	0.08	49
95.	2194	7198	2.10	0.12	1.34	425	0.08	64
96.	2203	7228	3.21	0.19	2.22	428	0.08	69
97.	2215	7267	2.29	0.15	1.22	419	0.11	53
98.	2218	7277	3.47	0.27	2.54	414	0.10	73
99.	2220	7283	8.35	0.72	10.20	417	0.07	122
100.	2227	7306	7.84	0.70	9.10	417	0.07	116
101.	2230	7316	5.50	0.53	6.51	417	0.08	118
102.	2252	7388	4.52	0.32	3.44	417	0.09	76
103.	2255	7398	3.38	0.39	3.16	421	0.11	93
104.	2258	7408	6.34	0.56	4.98	415	0.10	79
105.	2267	7438	3.81	0.22	2.88	418	0.07	76
106.	2270	7448	6.77	0.44	5.60	423	0.07	83
107.	2276	7467	4.20	0.24	2.76	417	0.08	66
108.	2282	7487	14.32	1.38	22.34	410	0.06	156
109.	2291	7516	1.90	0.28	4.86	418	0.13	98
110.	2304	7559	3.34	0.28	3.12	420	0.08	93
Rusa Timur-1								
111.	1909	6263	0.72	0.14	1.08	433	0.11	150
112.	1924	6312	0.89	0.13	1.00	424	0.12	112
113.	1967	6453	0.91	0.17	1.07	425	0.14	118
114.	2040	6693	0.87	0.23	1.56	424	0.13	79
115.	2055	6742	0.84	0.31	1.47	421	0.17	175
116.	2079	6821	0.76	0.22	1.46	425	0.13	192

Hydrogen Index values of these sediments range between 20-183 mgHC/gTOC (μ=59 mgHC/gTOC, σ=31 mgHC/gTOC) in South Furious-2, and 18-156 mgHC/gTOC (μ=61 mgHC/gTOC, σ=25 mgHC/gTOC) in South Furious-3. The more offshore located Rusa Timur-1 S2 yields vary between 1.00-1.56 mg/g (μ=1.27 mg/g, σ=0.23 mg/g). A correspondingly high average Hydrogen Index value of 154 mgHC/gTOC (range:112-192 mgHC/gTOC, σ=31 mgHC/gTOC) indicate that the sub-Stage IVA sediments in Rusa Timur-1 contain relatively more hydrogen-rich organic matter than the South Furious wells. The lower coastal plain sediments, however, have the highest S2 yield of 22.34 mg/g (**Table 5.6**, sample 2282m/7487ft, South Furious-3).

The high variability of S2 yields and Hydrogen Index values in South Furious-2 and South Furious-3, indicated by the large standard deviations, implies a high degree of organic matter mixing in such an environment. Conversely, the S2 yields and the standard deviation of the bathyal sediments are respectively more uniform and smaller. This is possibly due to preferential sorting resulting in similar types of organic matter being selectively grouped together. Hydrogen Index vs Tmax plot (**Figure 5.7**) and van Krevelen diagram (**Figure 5.8**) both show the prevailing organic matter type is mainly terrigenous Type III kerogen. Results from elemental analysis of isolated kerogens are shown in **Table 5.7**.

Table 5.7 Elemental analysis results : sub-Stage IVA.

	Depth (m)	(ft)	H%	O%	C%	N%	H/C	O/C	Total % of (C+H+N+O)
South Furious-2									
1.	446	1463	3.75	24.81	53.33	1.28	0.84	0.35	83.17
2.	636	2087	3.77	24.38	60.55	1.30	0.75	0.30	90.00
3.	1006	3301	3.90	22.63	51.92	1.35	0.90	0.33	79.80
4.	1156	3793	3.84	23.51	56.23	1.33	0.82	0.31	84.91
5.	1211	3973	4.38	22.29	51.67	1.42	1.02	0.32	79.76
6.	1294	4245	4.64	24.41	45.68	1.46	1.22	0.40	76.19
7.	1296	4252	4.12	20.16	57.64	1.37	0.86	0.26	83.29
8.	1602	5256	4.30	23.59	53.16	1.42	0.97	0.33	82.47
9.	1603	5259	4.24	23.07	57.06	1.36	0.89	0.30	85.73
10.	1604	5262	4.01	22.54	55.34	1.40	0.87	0.31	83.29
11.	1606	5269	3.40	20.73	48.13	1.48	0.85	0.32	73.74
12.	1674	5492	4.25	27.88	61.73	1.52	0.83	0.34	95.38
13.	1738	5702	5.14	27.78	62.11	1.46	0.99	0.34	96.49
14.	1779	5837	4.60	27.66	59.42	1.51	0.93	0.35	93.19
15.	1820	5971	4.30	28.97	61.42	1.58	0.84	0.35	96.27
South Furious-3									
16.	825	2707	4.21	22.53	47.09	1.51	1.07	0.36	75.34
17.	1350	4429	4.20	25.88	62.42	2.06	0.81	0.31	94.56
18.	1602	5256	4.26	23.43	51.66	1.71	0.99	0.34	81.06
19.	1617	5305	4.02	26.80	61.80	1.96	0.78	0.33	94.58
20.	1807	5928	4.11	27.74	60.74	1.68	0.81	0.34	94.27
21.	1962	6437	4.26	23.43	51.66	1.70	0.99	0.34	81.05
22.	1978	6490	4.19	27.14	60.82	1.41	0.83	0.33	93.56
23.	1997	6552	4.67	28.99	54.60	1.47	1.03	0.40	89.73
24.	2035	6677	4.38	28.16	63.90	1.70	0.82	0.33	98.14
25.	2096	6877	4.58	25.61	65.83	1.63	0.84	0.29	97.65
26.	2157	7077	4.74	25.65	65.77	1.35	0.86	0.29	97.51
27.	2218	7277	4.59	28.15	64.63	2.01	0.85	0.33	99.38
28.	2258	7408	4.64	23.07	64.35	1.50	0.87	0.27	94.30
29.	2282	7487	5.44	25.68	54.28	1.09	1.20	0.36	86.49
30.	2384	7820	4.86	25.09	66.85	1.38	0.87	0.28	98.18
Rusa Timur-1									
31.	1924	6312	4.37	27.70	57.12	2.02	0.92	0.36	91.21
32.	1967	6453	4.63	23.10	54.08	1.82	1.03	0.32	83.63
33.	2040	6693	5.12	20.19	67.56	2.03	0.91	0.22	94.90



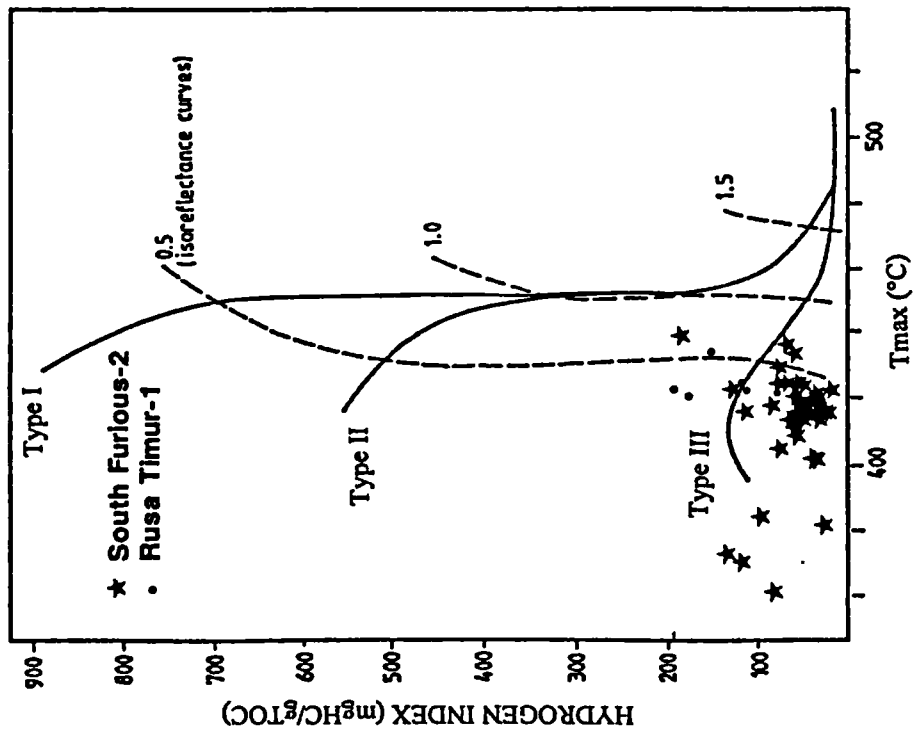


FIGURE 5.7 Hydrogen Index vs Tmax cross-plot (from Parnell & Rahman, 1990) for Stage IVA sediments.

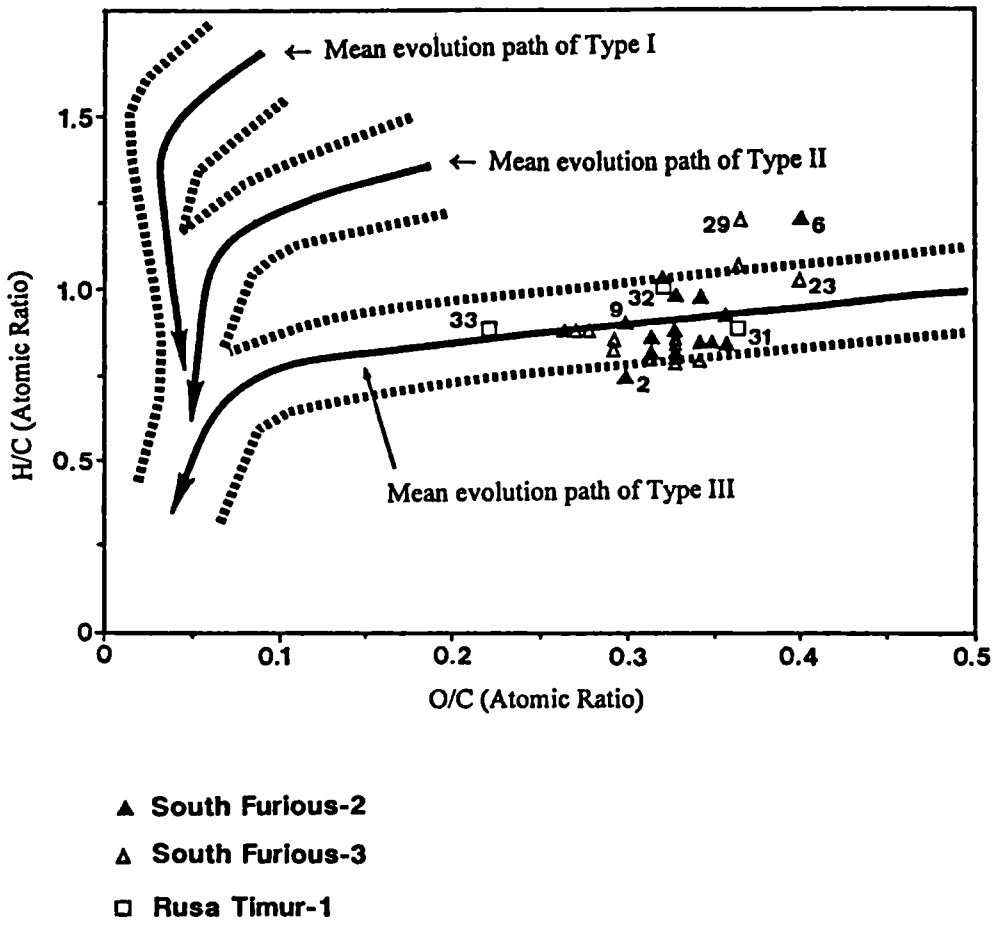


FIGURE 5.8 Elemental compositions of Stage IVA kerogens plotted on the van Krevelen diagram (from Durand, 1980).

Maceral abundance in sub-Stage IVA sediments was determined both visually and through density separation techniques. Results in **Table 5.8** show that percentage compositions estimated by both methods generally agree (**Figure 5.9**). Hydrogen Index values also seem to reflect maceral content variations, increasing or decreasing accordingly. Average percentage composition from both techniques indicate exinites to be dominant with some of them degraded (see **Appendix II**). This corresponds to the generally low Hydrogen Index values.

Table 5.8 Visual analysis and density separation of kerogen concentrates : sub-Stage IVA.

	Depth		% (optical)			% (spec. grav.)				HI	TOC
	(m)	(ft)	Ex	Vit	In	1.45	1.65	1.81	2.20		
South Furious-2											
1.	446	1463	15	20	65	5	5	20	70	95	3.91
2.	636	2087	18	55	27	5	15	70	10	78	4.38
3.	1006	3301	47	39	14	5	30	35	30	134	0.80
4.	1156	3793	10	38	52	0	10	45	45	34	0.74
5.	1211	3973	10	55	35	0	10	50	40	44	1.14
6.	1293	4242	47	34	19	5	50	40	5	56	2.73
7.	1296	4252	23	43	34	0	10	20	70	53	0.76
8.	1602	5256	59	22	19	10	60	30	0	38	1.29
9.	1603	5259	59	19	22	5	65	30	0	41	1.32
10.	1604	5262	60	21	19	5	65	20	10	55	1.50
11.	1606	5269	62	23	15	5	60	15	20	28	1.06
12.	1674	5492	14	62	24	5	15	70	10	54	2.52
13.	1738	5702	66	18	16	5	80	10	5	112	2.82
14.	1779	5837	62	20	18	5	60	35	0	59	5.33
15.	1820	5971	19	59	22	5	20	60	15	52	2.63
South Furious-3											
16.	825	2707	18	42	40	0	20	10	70	30	1.25
17.	1350	4429	63	18	19	10	65	10	15	34	1.09
18.	1602	5256	17	58	25	5	15	45	35	61	0.89
19.	1617	5305	19	47	34	5	20	55	20	67	0.57
20.	1807	5928	64	20	16	5	70	15	10	69	7.44
21.	1962	6437	21	47	32	0	10	40	50	61	0.89
22.	1978	6490	52	27	21	5	65	15	15	68	3.93
23.	1997	6552	68	18	14	5	75	15	5	64	4.74
24.	2035	6677	66	28	16	5	70	15	10	51	3.23
25.	2096	6877	67	19	14	15	55	15	15	60	3.11
26.	2157	7077	73	15	12	5	80	10	5	88	5.37
27.	2218	7277	62	24	14	5	65	25	5	73	3.47
28.	2258	7408	74	16	10	10	70	15	5	79	6.34
29.	2282	7487	79	10	11	5	90	5	0	156	14.32
30.	2304	7559	52	27	21	10	65	20	5	93	3.34
Rusa Timur-1											
31.	1924	6312	54	10	36	5	45	5	45	112	0.89
32.	1967	6453	41	24	35	5	40	40	15	118	0.91
33.	2040	6693	31	18	51	10	30	25	35	79	0.87

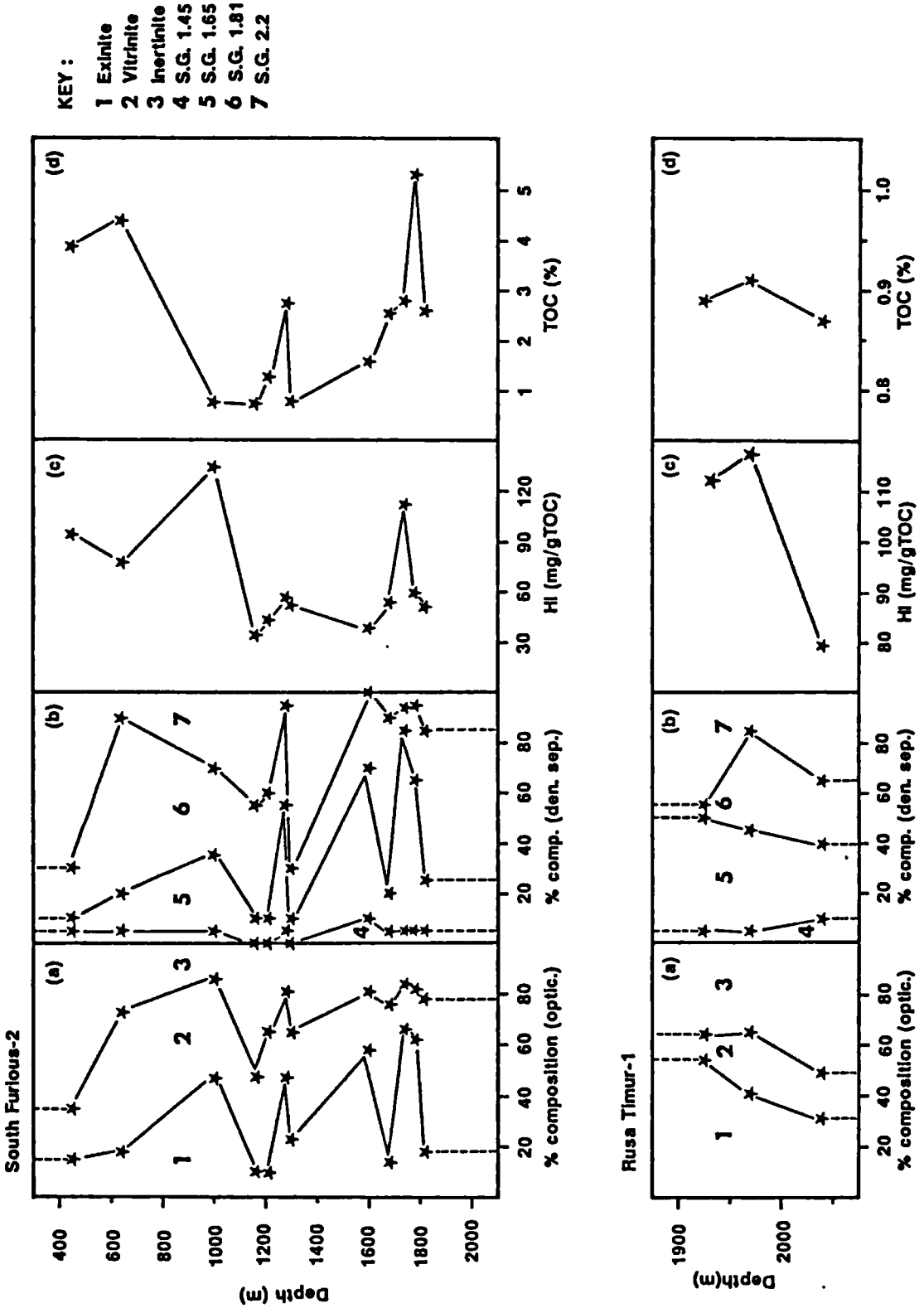


FIGURE 5.9 The variations in kerogen composition of South Furious-2, South Furious-3 and Rusa Timur-1 Stage IVA sediments from (a) organic petrography and (b) density separation. Also shown are the corresponding (c) Hydrogen Index and (d) Total Organic Carbon contents.

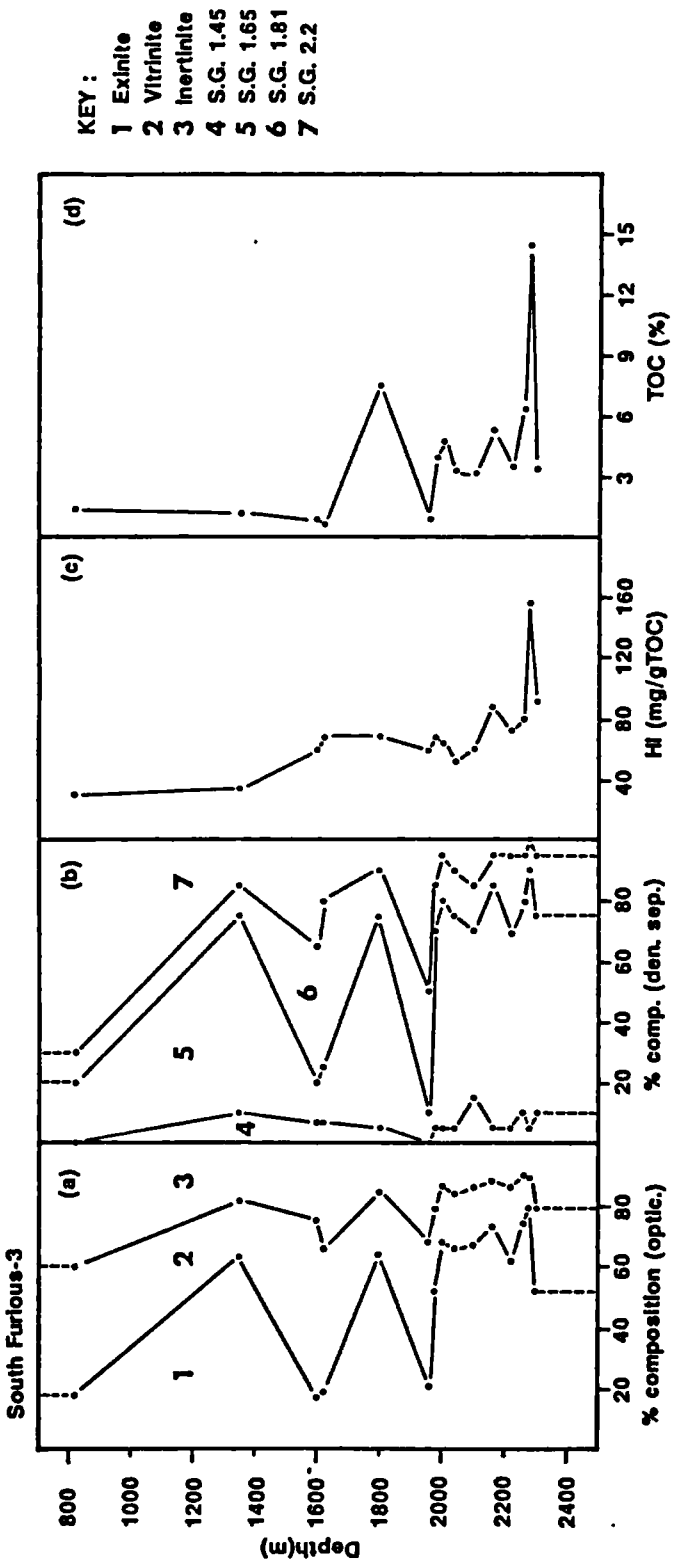


FIGURE 5.9 Continued.

C_{15+} saturate hydrocarbon distributions of sub-Stage IVA samples are shown in **Figures 5.10 - 5.16.** South Furious-2 sample 446m/1463ft shows a lack of lower molecular weight n-alkanes with pristane, phytane and the higher molecular weight nC_{28}, nC_{29} and nC_{30} alkanes being dominant **(Figure 5.10).** Pr/Phy and Pr/nC_{17} ratios of 2.1 and 4.9, respectively, **(Table 5.9)** indicate terrestrial, peat swamp or oxidising aquatic depositional environments. Sample 1006m/3301ft shows predominance of high molecular weight n-alkanes with a slight odd preference in the C_{26}-C_{35} region **(Figure 5.11).** This, together with high Pr/Phy and Pr/nC_{17} ratios, suggest input from land-plants deposited in an oxic environment. Sample 1293m/4242ft shows a shift to the lower molecular weight n-alkane region with a slight odd dominance in the C_{29}-C_{35} region, and a relatively higher nC_{17} peak **(Figure 5.12).** Pristane is, however, still more abundant than nC_{17} indicating that the main source of organic matter is terrigenous with a small contribution from algal and/or bacterial sources.

Table 5.9 Isoprenoid ratios for sub-Stage IVA.

	Depth (m)	(ft)	Pr/Phy	Pr/nC_{17}	CPI *
South Furious-2					
1.	446	1463	2.1	4.9	1.9
2.	1006	3301	2.4	3.1	1.1
3.	1293	4242	6.3	1.6	1.1
4.	1606	5269	4.0	4.2	1.5
5.	1738	5702	5.0	2.2	1.1
6.	1779	5837	5.4	3.6	1.3
Rusa Timur-1					
7.	2040	6693	2.8	1.0	1.1

* Louis (1967)

Gas chromatograms of sample 1606m/5269ft, 1738m/5702ft and 1779m/5837ft are very similar, except that sample 1606m/5269ft has a slightly larger naphthenic hump **(Figures 5.13, 5.14 & 5.15).** They all have high pristane peaks and exhibit odd carbon-number dominance in the C_{25}-C_{35} region which corresponds to the contributions from higher plants. The Pr/Phy and Pr/nC_{17} ratios **(Table 5.9)** indicate oxygenated depositional conditions often present in deltaic or paralic, or peat swamp environments. **Figure 5.16** is the gas chromatogram of the saturate hydrocarbon fraction from Rusa Timur-1 showing the presence of pristane, phytane, higher molecular weight n-alkanes and nC_{17} peaks being slightly larger than the pristane peaks, suggesting that both land plant material and algae/bacteria may have contributed to the organic matter input.

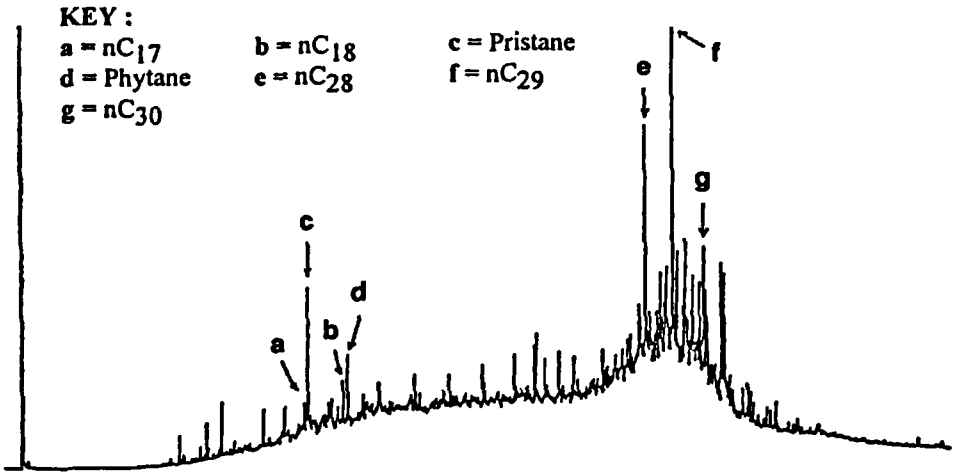


FIGURE 5.10 Gas chromatogram of Stage IVA South Furious-2 saturate fraction 446m/1463ft.



FIGURE 5.11 Gas chromatogram of Stage IVA South Furious-2 saturate fraction 1006m/3301ft.

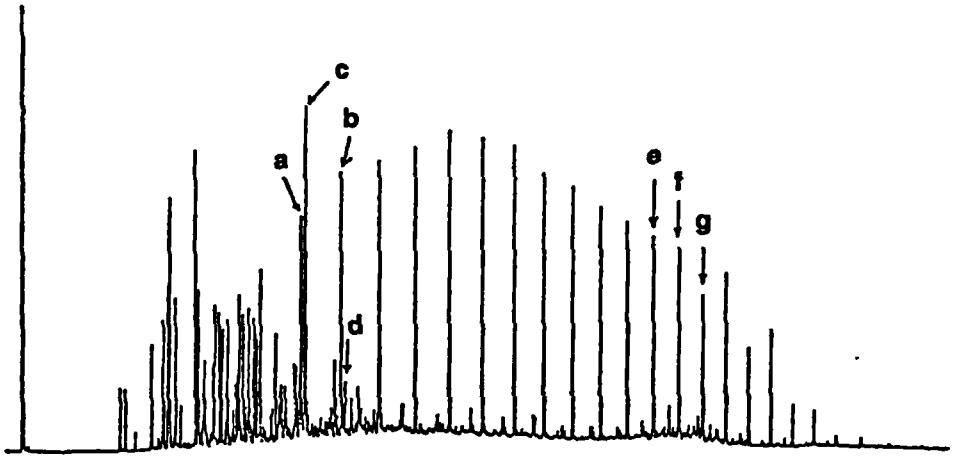


FIGURE 5.12 Gas chromatogram of Stage IVA South Furious-2 saturate fraction 1293m/4242ft.

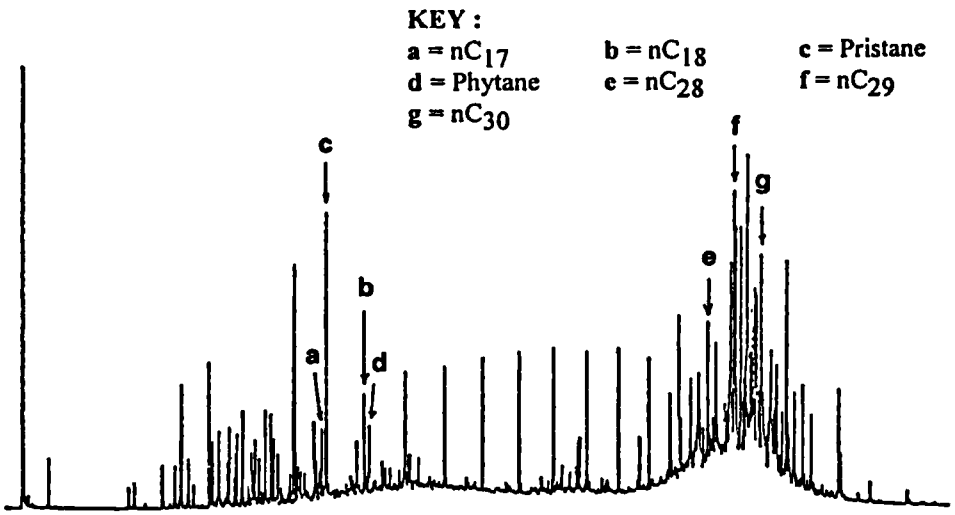


FIGURE 5.13 Gas chromatogram of Stage IVA South Furious-2 saturate fraction 1606m/5269ft.

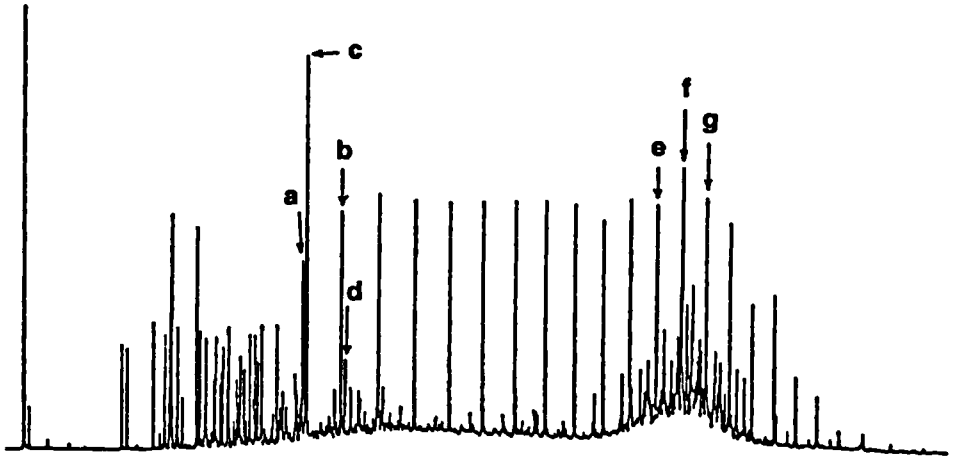


FIGURE 5.14 Gas chromatogram of Stage IVA South Furious-2 saturate fraction 1738m/5702ft.

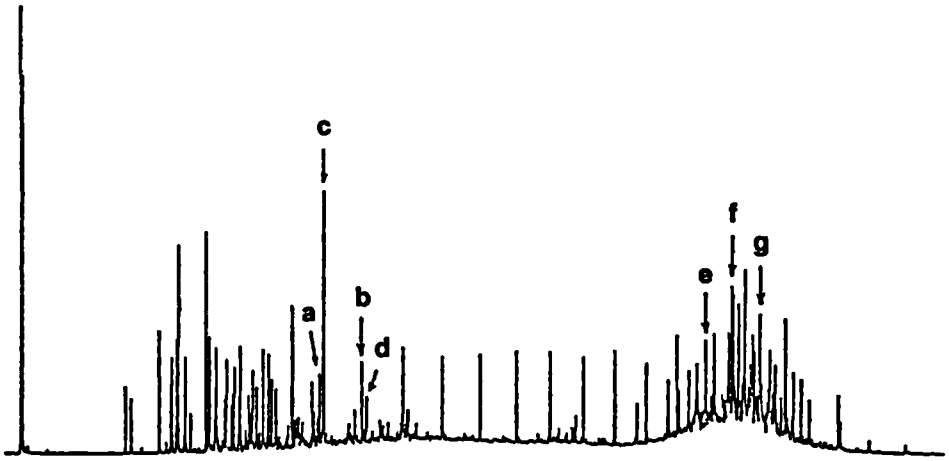


FIGURE 5.15 Gas chromatogram of Stage IVA South Furious-2 saturate fraction 1779m/5837ft.

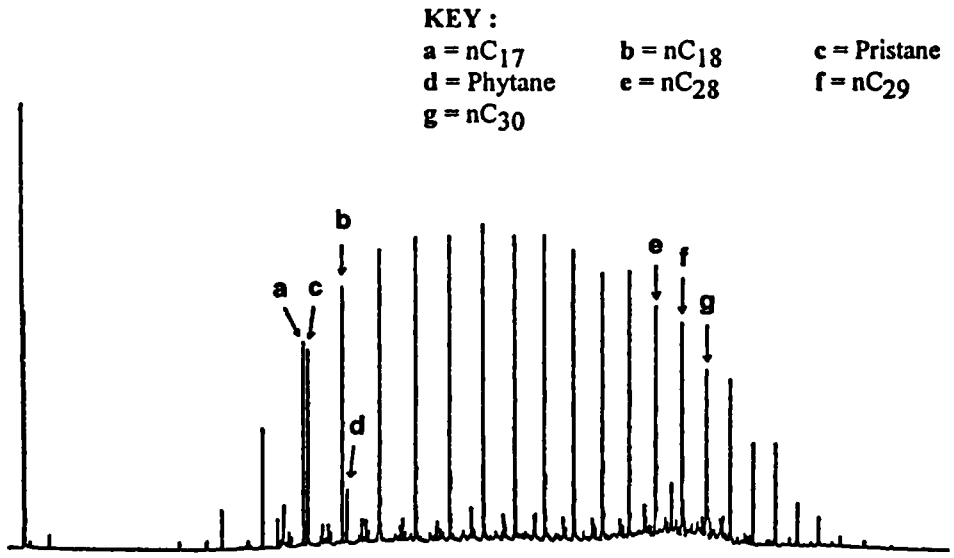


FIGURE 5.16 Gas chromatogram of Stage IVA Rusa Timur-1 saturate fraction 2040m/6693ft.

5.1.2c Organic Matter Maturity

In South Furious-2, production index values range between 0.00-0.63 mg/g (μ=0.16 mg/g), suggesting that hydrocarbon generation may have occurred at levels where the production index values >0.2 mg/g. However, the majority of the deeper samples have low (0.04-0.15 mg/g) production index values while shallow samples have relatively higher production index values. It is therefore likely that the hydrocarbons contributing to the S1 peak during pyrolysis of the shallower samples are non-indigenous. Tmax values range between 363-438°C (μ = 414°C), indicating that the samples are immature to marginal mature, with the majority in the immature (<420°C) and late immature (420-430°C) stages. The immaturity of the samples again verifies that the hydrocarbons present are non-indigenous.

CPI values **(Table 5.9)** suggest that the hydrocarbons are approaching maturity (no marked odd carbon-number dominance) except for the shallowest sample 446m/1463ft and sample 1606m/5269ft which had the slightly larger naphthenic hump. With the Tmax and CPI values contradicting each other, it is concluded that the hydrocarbons present in the samples have originated from elsewhere. In South Furious-3, production index values range from 0.04-0.19 mg/g (μ=0.10 mg/g) indicating that the samples are immature. Tmax values varying between 397-450°C (μ=422°C) indicate some samples may have attained higher maturity levels (mature zone: 440-460°C). However, the higher Tmax values are more likely to be the result of late pyrolysate release due to adsorption by the clayey-shaley mineral-matrix (Katz, 1983; Peters, 1986). Solvent extraction was not performed on the sub-Stage IVA sediments of South Furious-3 due to sample scarcity.

Production index values ranging from 0.11-0.17 mg/g (μ=0.13 mg/g) suggest that Rusa Timur-1 samples are immature. This is supported by pyrolysis Tmax values varying between 421-433°C (μ=425°C) indicating that the samples are mainly in the late immature stage (420-430°C). CPI value of 1.1 **(Table 5.9)** determined from the gas chromatogram of sample 2040m/6693ft saturate fraction **(Figure 5.16)** implies that the extract is mature. Based on the Tmax and CPI values, the sample extracts are all deemed to be non-indigenous. Vitrinite reflectance values verify the immature state of the penetrated sub-Stage IVA sediments **(Table 5.10)**.

Table 5.10 Vitrinite reflectance values : sub-Stage IVA.

	Depth (m)	Depth (ft)	Measured VRo (%)	% Error
South Furious-2				
1.	446	1463	0.38	±15
2.	1006	3301	0.41	±24
3.	1293	4242	0.36	±28
4.	1296	4252	0.36	±17
5.	1602	5256	0.37	±19

Table 5.10 Vitrinite reflectance values : sub-Stage IVA - continued.

	Depth (m)	(ft)	Measured VRo (%)	% Error
6.	1603	5259	0.38	±10
7.	1604	5262	0.41	±16
8.	1606	5269	0.40	±15
9.	1738	5702	0.37	±16
10.	1779	5837	0.43	±14
South Furious-3				
11.	825	2707	0.40	±18
12.	1962	6437	0.45	±9
13.	1997	6552	0.44	±11
14.	2282	7487	0.39	±13
Rusa Timur-1				
15.	1967	6453	0.50	±14

5.1.3 Sub-Stage IVB

Only Rusa Timur-1 penetrated sub-Stage IVB which is represented by deep marine sediments. In the South Furious area, sub-Stage IVB sediments were either eroded or not deposited, and in the Tembungo/Gajah Hitam areas, they were not penetrated. Generalisations about the hydrocarbon potential of this sub-Stage are therefore applicable only to the surrounding vicinity of Rusa Timur-1.

5.1.3a Organic Carbon Content

Total organic carbon contents range from 0.70-1.05 wt% (μ=0.84wt%, σ=0.11 wt%) **(Table 5.11)**. These values indicate that sub-Stage IVB sediments here contain only fair amounts of organic matter.

Table 5.11 TOC and Pyrolysis results : sub-Stage IVB.

	Depth (m)	(ft)	TOC (wt%)	S1 (mg/g)	S2 (mg/g)	Tmax (°C)	PI	HI (mgHC/gTOC)
Rusa Timur-1								
1.	1744	5722	0.75	0.12	1.02	428	0.11	136
2.	1775	5823	0.79	0.13	1.00	425	0.12	127
3.	1800	5906	0.88	0.52	1.68	413	0.24	191
4.	1814	5951	1.05	0.76	2.23	365	0.25	212
5.	1842	6043	0.93	0.24	1.14	423	0.17	123
6.	1866	6122	0.70	0.12	1.01	440	0.11	44
7.	1878	6161	0.81	0.17	1.06	423	0.14	131

5.1.3b Organic Matter Type And Quality

Poor to moderate S2 pyrolysis yields and Hydrogen Index values **(Table 5.11.)** indicate that kerogen-convertibility may be low, and the organic matter present is most likely to be gas-prone. There are, however, possible exceptions for samples 1800m/5906ft and 1814m/5951ft. Based on Hydrogen Index values (range:123-212 mgHC/gTOC) and S2 yields (range:1.68-2.23 mg/g), they may have the potential to generate some liquid hydrocarbons as well as gas, if sufficiently matured. Hydrogen Index vs Tmax plot **(Figure 5.17)** clearly shows the organic matter to be of terrigenous Type III. Elemental compositions of isolated kerogen samples **(Table 5.12, Figure 5.18)** plotted slightly outside the Type III kerogen band **(Table 5.11)**.

Table 5.12 Elemental analysis results : sub-Stage IVB.

	Depth (m)	(ft)	H%	O%	C%	N%	H/C	O/C	Total % of (C+H+N+O)
Rusa Timur-1									
1.	1744	5722	5.84	20.93	65.74	1.87	1.07	0.24	94.38
2.	1800	5906	4.86	23.25	59.94	1.93	0.97	0.29	89.98
3.	1814	5951	6.19	21.78	68.40	1.75	1.09	0.24	98.12
4.	1866	6122	5.23	21.14	61.10	1.84	1.03	0.26	89.31
5.	1878	6161	4.98	21.35	59.73	1.89	1.00	0.27	87.95

Visual inspection of strewn slides and density separation results generally support each other **(Table 5.13, Figure 5.19)**. Average percentage composition for the analysed sub-Stage IVB samples indicate the predominance of exinitic macerals. As in the previous sub-Stages III and IVA, these exinites were degraded (see **Appendix II**). The high percentage of terrestrial exinitic/herbaceous material in the deep marine sample 1814m/5951ft could have been brought about by preferential segregation and transportation based on their lower densities and resistance to degradation (Tissot & Welte, 1984; Frewin *et. al.*, 1993).

Thompson *et. al.* (1985) had suggested that the formation of allochthonous coals in the Mahakam Delta was due to the concentration of liptinitic organic matter by selective transportation. This is a probable mechanism to explain the presence of exinitic organic matter in the deep marine sediment samples of this study. Evidence for turbiditic/mass flow deposits, which is a transport mechanism for terrigenous particles into deeper waters, has been reported to occur within sub-Stage IVB sequence by Levell & Kasumajaya (1985). An argument against this type of selective concentration of herbaceous material was put forward by Cole (1987). He stated that the herbaceous organic matter are prone to oxidation and their transportation would only result in quality degradation. However, results from this study and that of Frewin *et. al.* (1993) indicate otherwise.

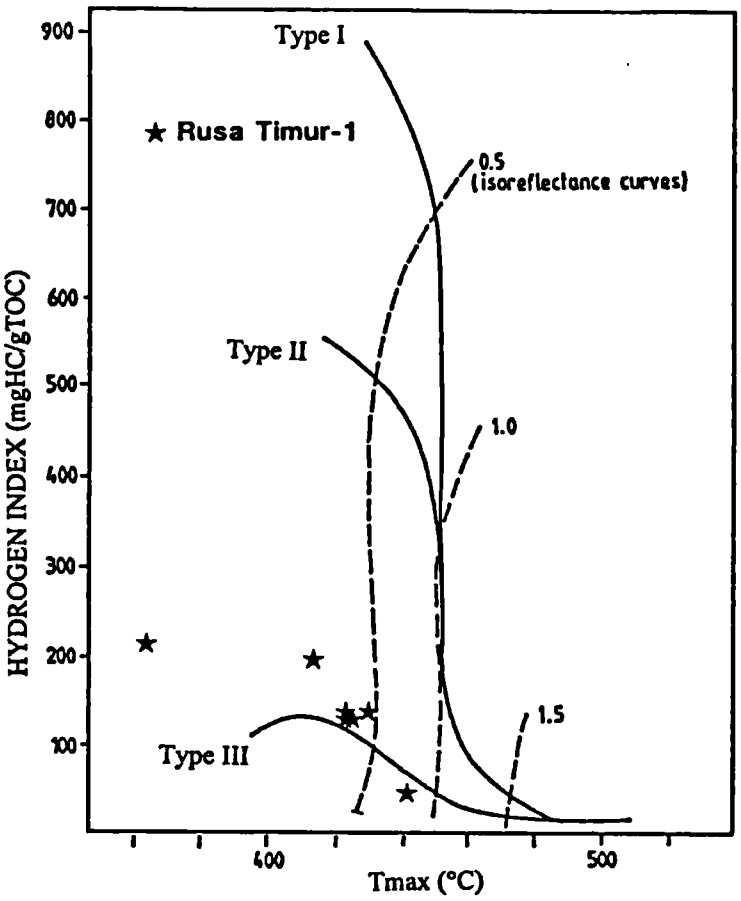


FIGURE 5.17 Hydrogen Index vs Tmax cross-plot (from Parnell & Rahman, 1990) for Stage IVB sediments.

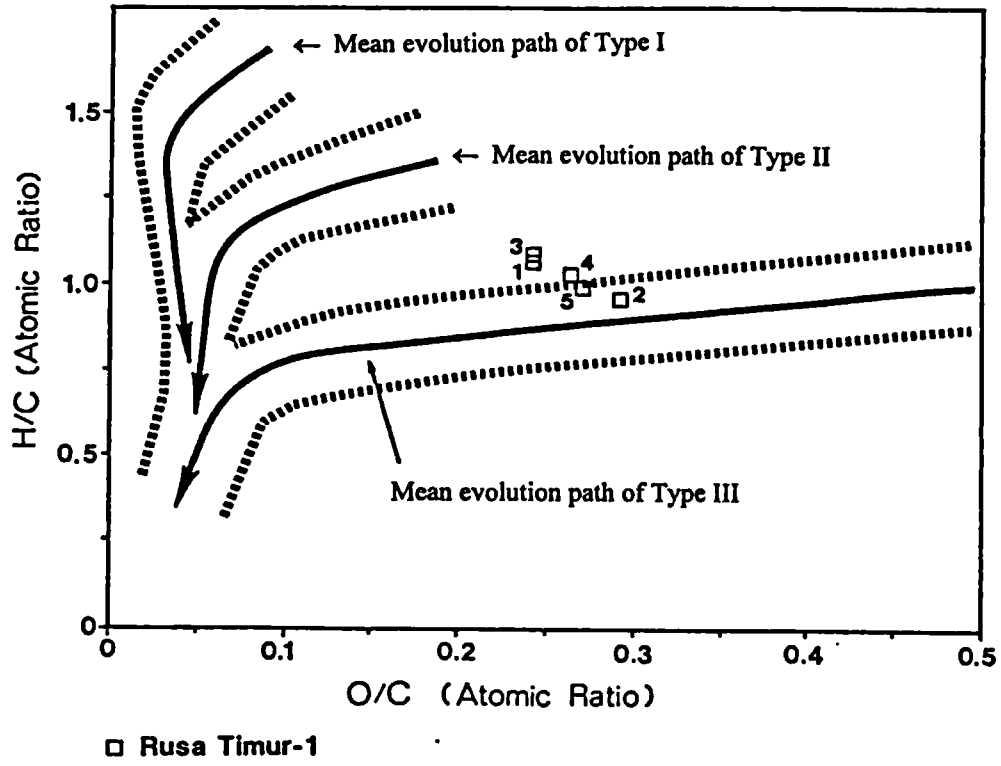


FIGURE 5.18 Elemental compositions of Stage IVB kerogens plotted on the van Krevelen diagram (from Durand, 1980).

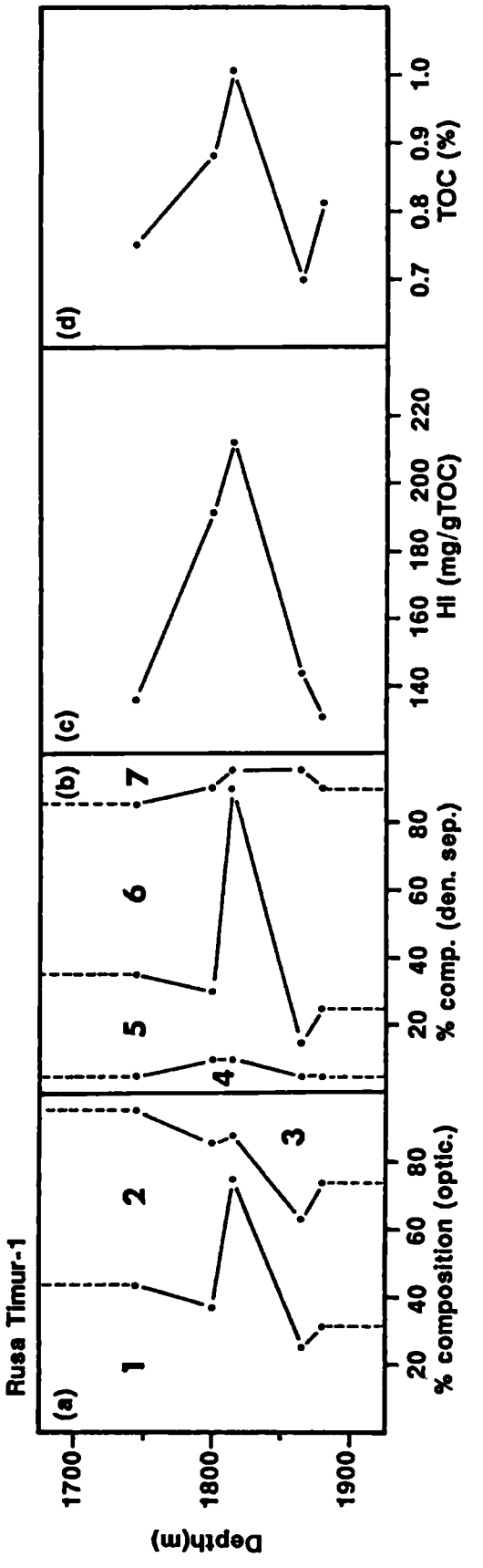


FIGURE 5.19 The variations in kerogen composition of Rusa Timur-1 Stage IVB sediments from (a) organic petrography and (b) density separation. Also shown are the corresponding (c) Hydrogen Index and (d) Total Organic Carbon contents.

Table 5.13 Visual analysis and density separation of kerogen concentrates : sub-Stage IVB.

	Depth (m)	(ft)	% (optical) Ex	Vit	In	% (spec. grav.) 1.45	1.65	1.81	2.20	HI	TOC
Rusa Timur-1											
1.	1744	5722	43	52	5	5	30	50	15	136	0.75
2.	1800	5906	37	49	14	10	20	60	10	191	0.88
3.	1814	5951	75	13	12	10	80	5	5	212	1.05
4.	1866	6122	25	38	37	5	10	80	5	144	0.70
5.	1878	6161	31	43	26	5	20	65	10	131	0.81

Key : Ex = Exinite, Vit = Vitrinite, In = Inertinite

The gas chromatogram trace of sample 1814m/5951ft saturate hydrocarbon shows the presence of pristane, phytane, higher molecular weight n-alkanes and nC_{17} peaks slightly larger than the pristane peaks (**Figure 5.20**). These suggest both land plant material and algae/bacteria may have contributed to the organic matter input. Pr/Phy ratio of 3.9 (**Table 5.14**) indicates oxic depositional conditions such as in deltaic/paralic and peat swamp environments. Hydrogen Index values of Rusa Timur-1 are slightly higher relative to the more proximal South Furious-2 and South Furious-3.

Table 5.14 Isoprenoid ratios for sub-Stage IVB.

	Depth (m)	(ft)	Pr/Phy	Pr/nC_{17}	CPI *
Rusa Timur-1					
1.	1814	5951	3.9	1.0	1.0

* Louis (1967)

5.1.3c Organic Matter Maturity

Production index values vary between 0.11-0.26 mg/g (μ=0.16 mg/g), indicating that the samples are generally immature (**Table 5.11**). Tmax values also infer immaturity (range:365-440°C, σ=417°C) with only one sample having a Tmax value of 440°C (between marginal mature [430-440°C] and mature zones [440-460°C]). The majority of samples are in the late immature zone (420-430°C). CPI value of 1.0 (**Table 5.14**) implies that the sample extract is mature, thus suggesting that it has migrated into the sediments from elsewhere. Vitrinite reflectance measurements (**Table 5.15**) confirm the immaturity of the sub-Stage IVB sediments.

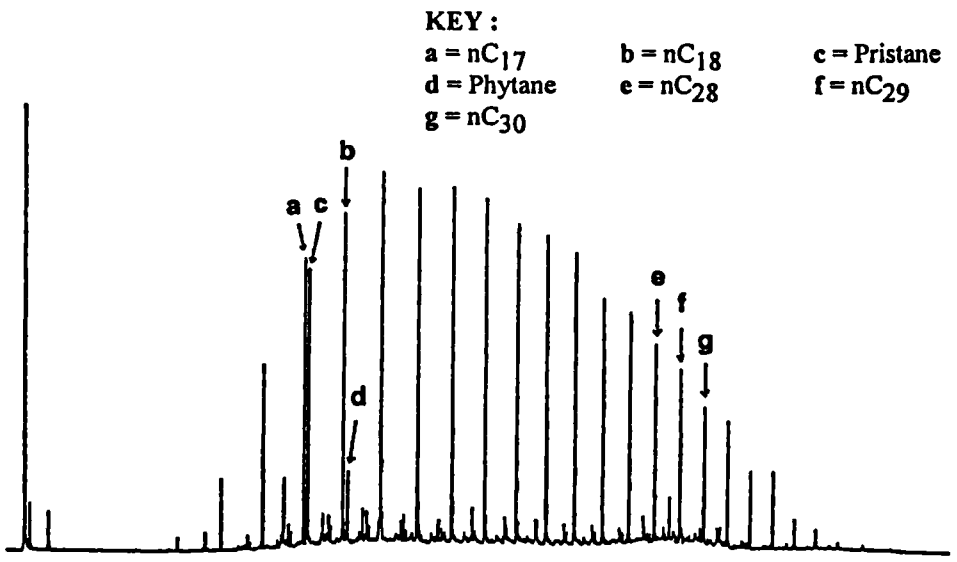


FIGURE 5.20 Gas chromatogram of Stage IVB Rusa Timur-1 saturate fraction 1814m/5951ft.

Table 5.15 Vitrinite reflectance values : sub-Stage IVB.

	Depth (m)	(ft)	Measured VRo (%)	% Error
Rusa Timur-1				
1.	1744	5722	0.40	±13
2.	1814	5951	0.43	±19
3.	1866	6122	0.46	±15
4.	1878	6161	0.46	±10

5.1.4 Sub-Stage IVC

Sub-Stage IVC is represented by deep marine sediments and is encountered in Tembungo-1, Tembungo-2, Tembungo-6, Rusa Timur-1 and Gajah Hitam-1 wells. Sand bodies present in the sequence are of turbiditic or mass flow/shelf slumping origin (Levell & Kasumajaya, 1985).

5.1.4a Organic Carbon Content

Total organic carbon contents range from 0.2-2.61 wt% (μ=0.76 wt%, σ=0.77 wt%) in Tembungo-1; 0.14-2.72 wt% (μ=1.00 wt%, σ=0.74 wt%) in Tembungo-2; 0.63-0.81 wt%, (μ=0.72 wt%, σ=0.09 wt%) in Tembungo-6; 0.40-0.71 wt% (μ=0.57 wt%, σ=0.09 wt%) in Rusa Timur-1; and 0.83-1.36 wt% (μ=1.00 wt%, σ=0.21 wt%) in Gajah Hitam-1 **(Table 5.16)**. These values indicate that sub-Stage IVC sediments contain poor to good amounts of organic carbon. Closer inshore, the large variations in Tembungo-1 and Tembungo-2 TOC contents reflect the mixed nature of organic matter fed into the basin. These were then transported further into the basin by turbidity currents and/or mass flow triggered by slumping of shelf sediments (Levell & Kasumajaya, 1985). Variability in TOC contents decreases towards the distal part of the basin, i.e. towards Rusa Timur and Gajah Hitam, indicating that a process of selective segregation of like organic material may have occurred.

Table 5.16 TOC and Pyrolysis results : sub-Stage IVC.

	Depth (m)	(ft)	TOC (wt%)	S1 (mg/g)	S2 (mg/g)	Tmax (°C)	PI	HI (mgHC/gTOC)
Tembungo-1								
1.	1888	6194	2.61	0.53	3.00	415	0.15	115
2.	1900	6234	0.57	0.04	0.31	440	0.11	54
3.	1931	6335	0.69	0.07	0.48	497	0.13	70
4.	1967	6453	0.20	0.05	0.34	417	0.13	170
5.	1984	6509	0.43	0.04	0.18	424	0.18	42
6.	2083	6834	0.23	0.02	0.13	437	0.13	57
7.	2169	7116	0.58	0.13	0.32	424	0.29	55

Table 5.16 TOC and Pyrolysis results : sub-Stage IVC - continued.

	Depth (m)	(ft)	TOC (wt%)	S1 (mg/g)	S2 (mg/g)	Tmax (°C)	PI	HI (mgHC/gTOC)
Tembungo-2								
8.	2068	6785	0.43	0.04	0.23	429	0.15	53
9.	2074	6804	0.47	0.05	0.25	429	0.17	53
10.	2079	6821	2.72	0.56	5.01	414	0.10	184
11.	2088	6850	1.32	0.16	2.12	422	0.07	161
12.	2098	6883	1.10	0.18	1.02	383	0.15	93
13.	2107	6913	1.31	0.26	4.38	422	0.06	334
14.	2116	6942	1.12	0.16	1.70	419	0.09	152
15.	2159	7083	0.42	0.57	0.67	403	0.46	160
16.	2241	7352	0.14	0.02	0.08	428	0.20	57
Tembungo-6								
17.	1874	6148	0.63	0.06	0.26	428	0.19	41
18.	1901	6237	0.81	0.15	0.68	427	0.18	84
Rusa Timur-1								
19.	1592	5223	0.89	0.47	1.42	409	0.25	160
20.	1619	5312	1.36	0.81	2.32	413	0.26	171
21.	1674	5492	0.88	0.34	1.31	426	0.21	149
22.	1738	5702	0.85	0.12	1.08	440	0.10	127
Gajah Hitam-1								
23.	1599	5246	0.53	0.00	0.32	435	0.00	60
24.	1602	5256	0.49	0.00	0.35	427	0.00	71
25.	1603	5259	0.49	0.00	0.38	447	0.00	78
26.	1604	5262	0.40	0.00	0.18	442	0.00	45
27.	1606	5269	0.51	0.00	0.27	435	0.00	53
28.	1608	5276	0.46	0.00	0.30	449	0.00	65
29.	1989	6526	0.57	0.03	0.98	432	0.03	172
30.	2014	6608	0.46	0.04	0.42	441	0.09	91
31.	2053	6736	0.59	0.04	0.48	436	0.08	81
32.	2108	6916	0.51	0.02	0.36	451	0.05	71
33.	2117	6946	0.61	0.03	0.46	435	0.06	75
34.	2126	6975	0.65	0.03	0.64	444	0.04	98
35.	2209	7247	0.56	0.04	0.55	436	0.07	98
36.	2276	7467	0.67	0.03	0.68	433	0.04	101
37.	2279	7477	0.63	0.04	0.63	433	0.06	100
38.	2318	7605	0.68	0.02	0.58	444	0.03	85
39.	2373	7785	0.67	0.02	0.54	450	0.04	81
40.	2392	7848	0.68	0.02	0.67	453	0.03	99
41.	2401	7877	0.71	0.02	0.58	439	0.03	82

5.1.4b Organic Matter Type And Quality

Pyrolysis S2 yields for sub-Stage IVC sediments in Tembungo-1, Tembungo-2 and Rusa Timur-1 are much more variable than those of Tembungo-6 and Gajah Hitam-1 **(Table 5.16)**. They also indicate that some of the sediments, principally those from Tembungo-1 (sample 1888m/6194ft), Tembungo-2 (samples 2079m/6821ft, 2088m/6850ft, 2107m/6913ft and 2116m/6942ft) and Rusa Timur-1 (samples 1592m/5223ft, 1619m/5312ft and 1674m/5492ft) have the potential to generate some

hydrocarbons if sufficiently matured. The relatively higher S2 yields (range:1.31-5.01 mg/g) together with correspondingly high Hydrogen Index values (115-334 mgHC/gTOC) suggest moderate kerogen-convertibility to possibly some liquid hydrocarbons as well as gas. The noticeably large variability in the pyrolysis S2 yields of Tembungo-1 and Tembungo-2 is a possible indication of pulses of sediment input via turbiditic/mass flows carrying highly mixed organic matter, possibly emphasised by an incomplete segregation of macerals. Hydrogen Index vs Tmax plot **(Figure 5.21)** and van Krevelen diagram **(Figure 5.22)** both show that the kerogen is mainly of Type III. Elemental analysis results are shown in **Table 5.17** below.

Table 5.17 Elemental analysis results : sub-Stage IVC.

	Depth (m)	(ft)	H%	O%	C%	N%	H/C	O/C	Total % of (C+H+N+O)
Tembungo-1									
1.	1984	6509	5.84	29.43	60.62	1.82	1.16	0.36	97.71
Tembungo-2									
2.	2074	6804	5.32	26.02	51.72	2.06	1.23	0.38	85.12
3.	2107	6883	6.51	28.42	63.17	1.74	1.24	0.34	99.84
Tembungo-6									
4.	1874	6148	4.63	23.71	59.64	1.99	0.93	0.30	89.97
5.	1901	6237	4.91	24.29	61.39	1.72	0.96	0.30	92.31
Rusa Timur-1									
6.	1592	5223	5.27	23.54	61.32	1.52	1.03	0.29	91.65
7.	1619	5312	5.48	19.70	56.39	1.54	1.17	0.26	83.11
8.	1674	5492	5.71	24.81	62.94	1.60	1.09	0.30	95.06
9.	1738	5702	4.89	22.99	60.86	1.64	0.96	0.28	90.38
Gajah Hitam-1									
10.	1606	5269	5.13	20.07	58.80	1.79	1.05	0.26	85.79
11.	1989	6526	5.36	21.90	64.05	1.82	1.00	0.26	93.13
12.	2117	6946	3.98	18.04	57.78	2.01	0.83	0.23	81.81
13.	2276	7467	4.11	19.61	58.81	1.92	0.84	0.25	84.45
14.	2401	7877	4.97	20.44	49.62	1.98	1.20	0.31	77.01

The organic matter type is supported by visual examination of strewn slides under transmitted-light microscope (see **Appendix II**) and density separation of isolated kerogens. Results from both techniques **(Table 5.18)** show a general agreement between maceral composition and Hydrogen Index **(Figure 5.23)**.

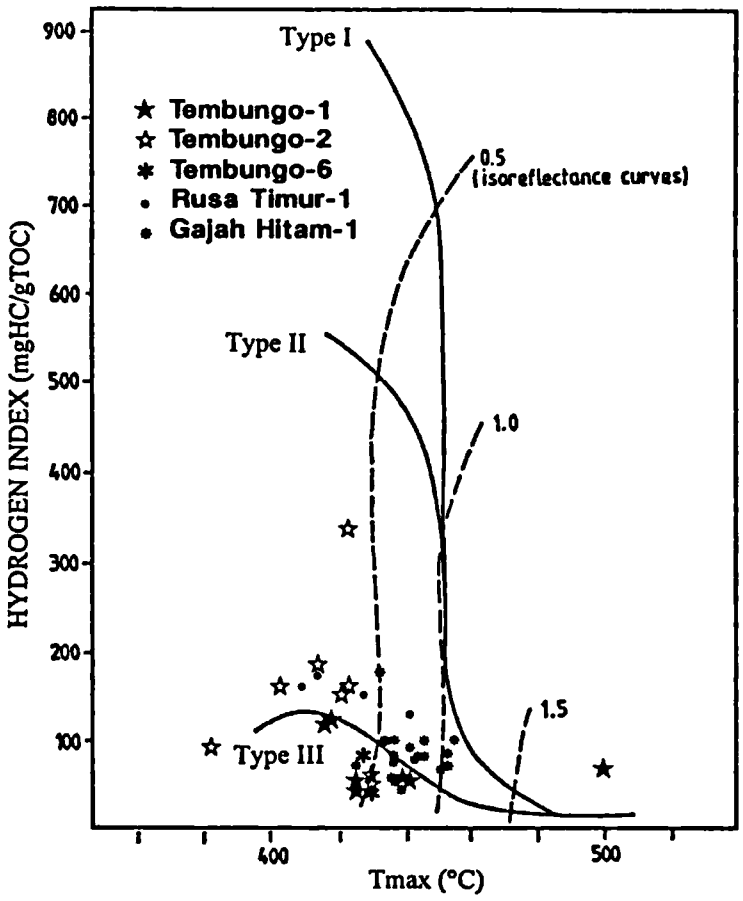


FIGURE 5.21 Hydrogen Index vs Tmax cross-plot (from Parnell & Rahman, 1990) for Stage IVC sediments.

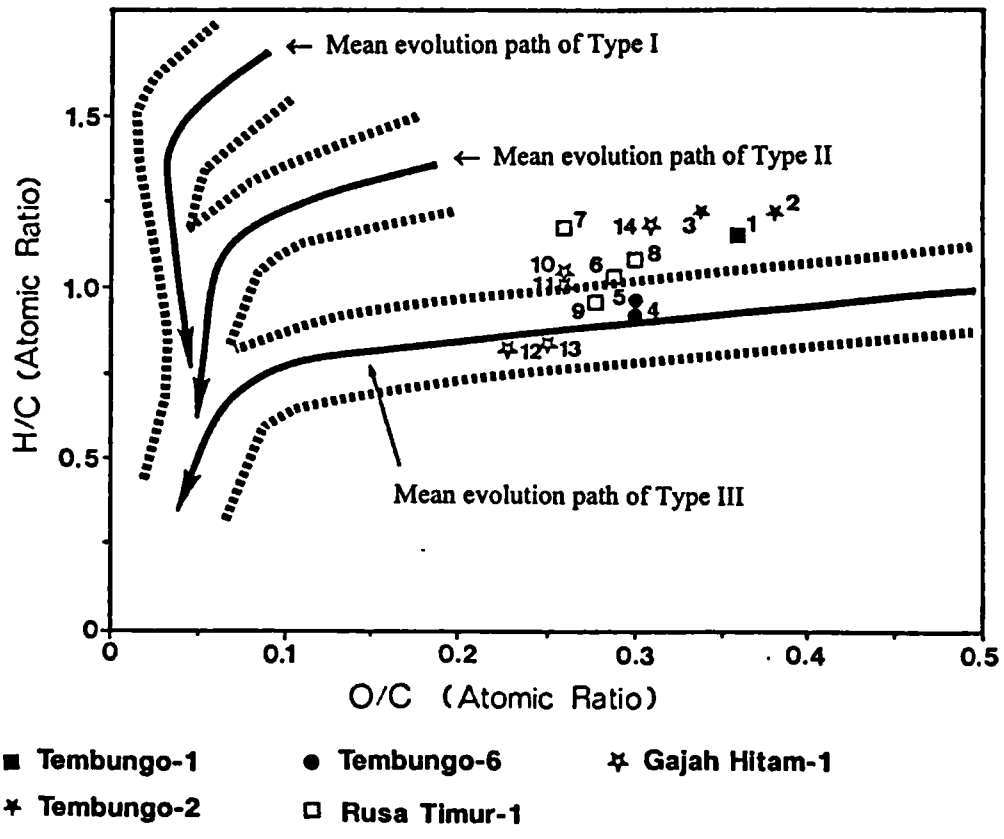


FIGURE 5.22 Elemental compositions of Stage IVC kerogens plotted on the van Krevelen diagram (from Durand, 1980).

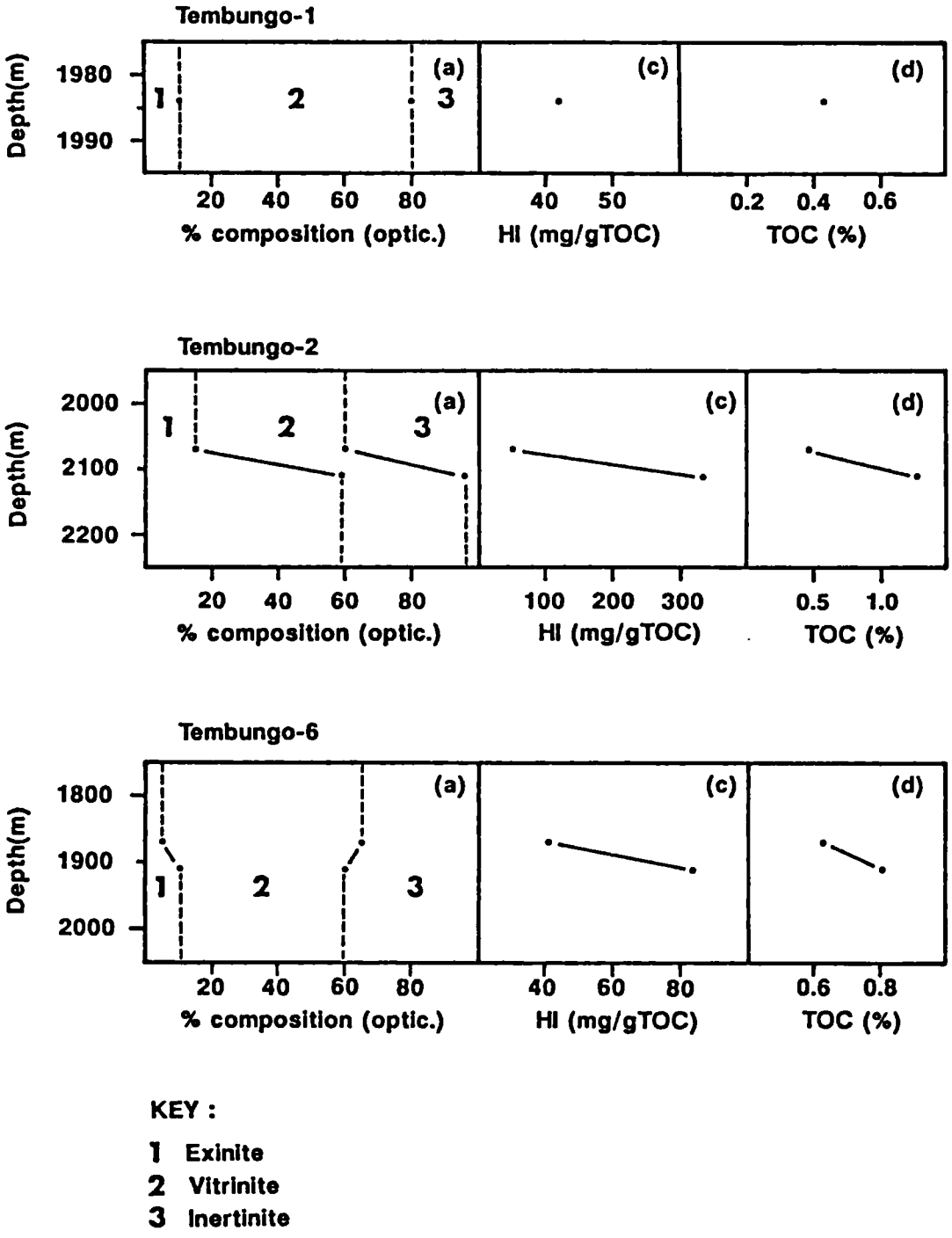


FIGURE 5.23 The variations in kerogen composition of Tembungo-1, Tembungo-2, Tembungo-6, Rusa Timur-1 and Gajah Hitam-1 Stage IVC sediments from (a) organic petrography and (b) density separation. Also shown are the corresponding (c) Hydrogen Index and (d) Total Organic Carbon contents.

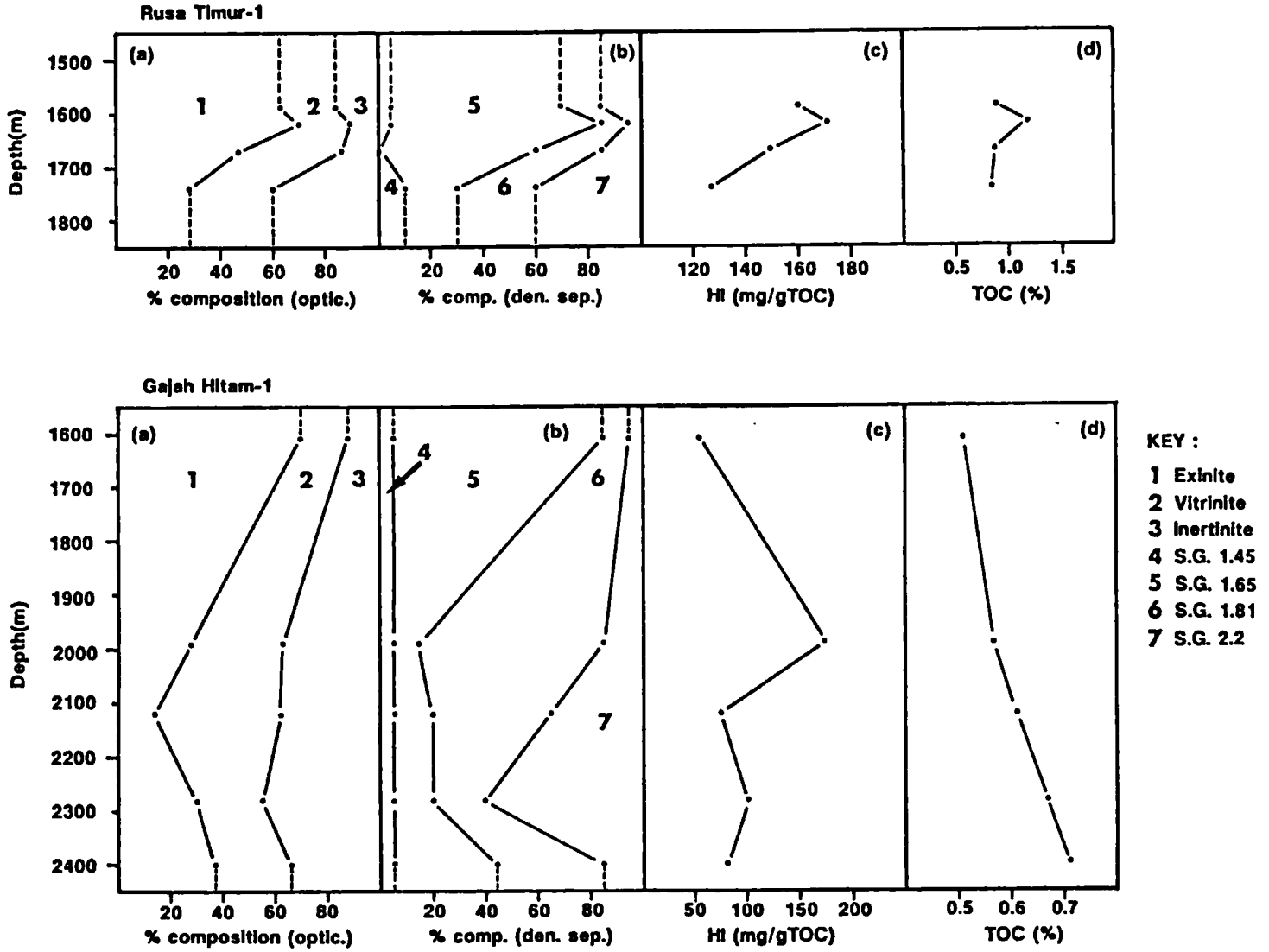


FIGURE 5.23 Continued.

Table 5.18 Visual analysis and density separation of kerogen concentrates : sub-Stage IVC.

	Depth (m)	(ft)	% (optical) Ex	Vit	In	% (spec. grav.) 1.45	1.65	1.81	2.20	HI	TOC
Tembungo-1											
1.	1984	6509	10	70	20	np.	np.	np	np.	42	0.43
Tembungo-2											
2.	2074	6804	15	45	40	np.	np.	np.	np.	53	0.47
3.	2107	6913	59	37	4	np.	np.	np.	np.	334	1.31
Tembungo-6											
4.	1874	6148	5	60	35	np.	np.	np.	np.	41	0.63
5.	1901	6237	10	50	40	np.	np.	np.	np.	84	0.81
Rusa Timur-1											
6.	1592	5223	63	21	16	5	65	15	15	160	0.89
7.	1619	5312	70	19	11	5	80	10	5	171	1.36
8.	1674	5492	47	39	14	0	60	25	15	149	0.88
9.	1738	5702	28	32	40	10	20	30	40	127	0.85
Gajah Hitam-1											
10.	1606	5269	70	14	16	5	80	10	5	53	0.51
11.	1989	6526	28	35	37	5	10	70	15	172	0.57
12.	2117	6946	14	48	38	5	15	45	35	75	0.61
13.	2276	7467	30	25	45	5	15	20	60	101	0.67
14.	2401	7877	37	29	34	5	40	40	15	82	0.71

Key : Ex = Exinite, Vit = Vitrinite, In = Inertinite

np. : density separation not performed due to inadequate amounts of kerogen recovered

Figures 5.24-5.27 are the gas-chromatograms of sub-Stage IVC saturate samples. The trace of sample 1901m/6237ft from Tembungo-6 **(Figure 5.24)** shows the presence of pristane, phytane and high molecular weight n-alkanes accompanied by an nC_{17} peak of equivalent height to the pristane peak. This indicates an organic matter input from a mainly terrestrial source with possibly some contributions from algal and/or bacterial sources (Tissot & Welte, 1984). Rusa Timur-1 sample 1619m/5312ft **(Figure 5.25)**, and Gajah Hitam-1 samples 2117m/6946ft **(Figure 5.26)** and 2401m/7877ft **(Figure 5.27)** all exhibit the presence of pristane and phytane peaks with the odd carbon-number predominance in the nC_{25}-nC_{35} region, consistent with input from land-derived organic matter. Pr/Phy ratios of > 2.0 **(Table 5.19)** indicate that deposition occurred in oxic conditions, similar to those present in terrestrial peat swamps or oxidising aquatic environments. They also have quite large nC_{17} peaks comparable to the pristane peaks suggesting the possibility of some contribution from algae and/or bacteria.

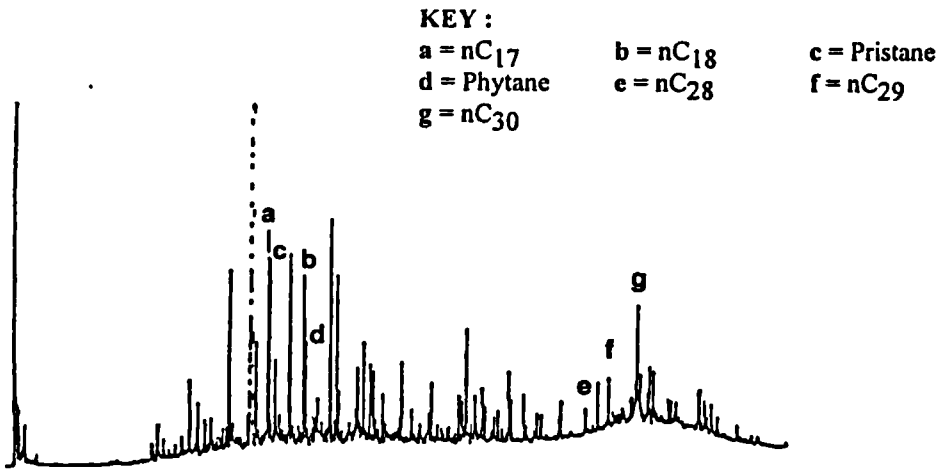


FIGURE 5.24 Gas chromatogram of Stage IVC Tembungo-6 saturate fraction 1901m/6237ft.

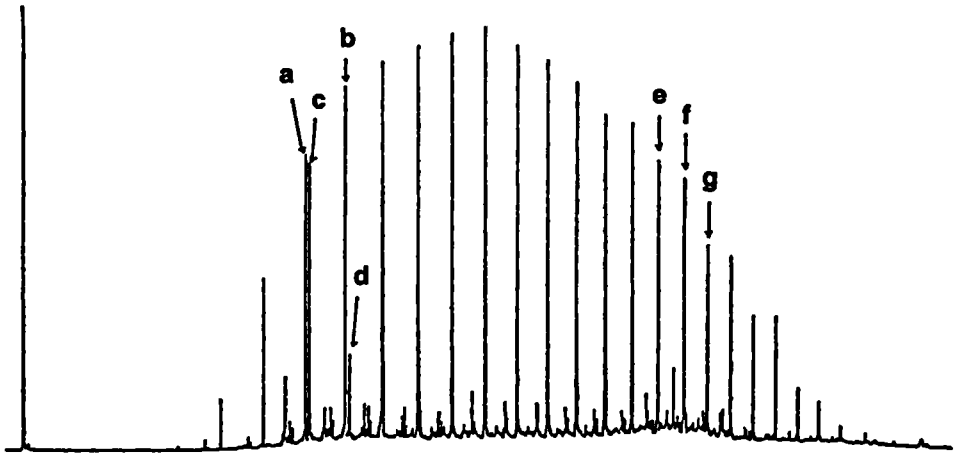


FIGURE 5.25 Gas chromatogram of Stage IVC Rusa Timur-1 saturate fraction 1619m/5312ft.

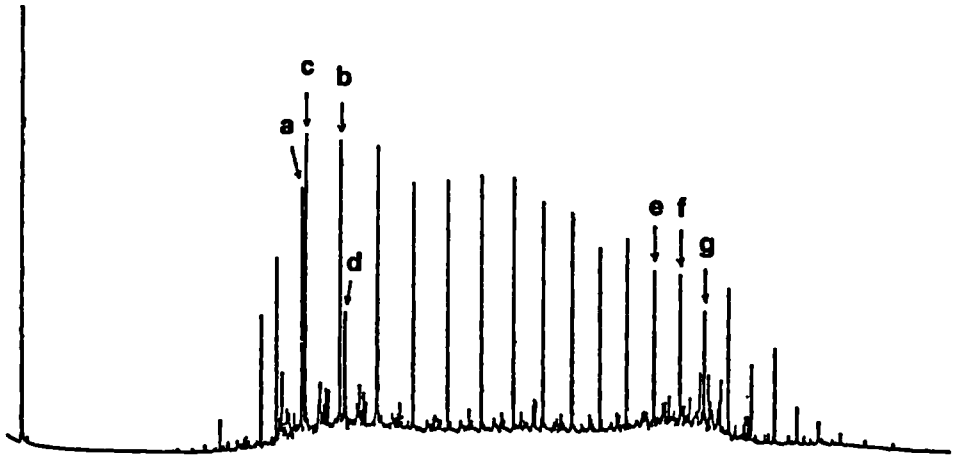


FIGURE 5.26 Gas chromatogram of Stage IVC Gajah Hitam-1 saturate fraction 2117m/6946ft.

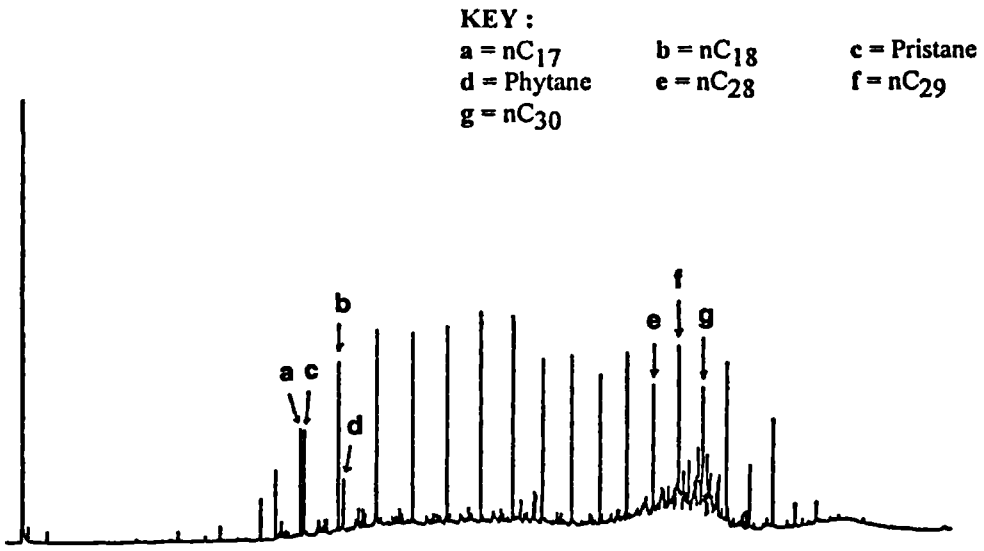


FIGURE 5.27 Gas chromatogram of Stage IVC Gajah Hitam-1 saturate fraction 2401m/7877ft.

5.1.4c Organic Matter Maturity

In Tembungo-1, production index values vary from 0.11-0.29 mg/g (μ=0.16 mg/g) indicating the majority of samples are immature, except for those with production index values > 0.2 mg/g. The average Tmax value of 436°C (marginal mature:430-440°C) also supports this. Production index values in Tembungo-2 range between 0.06-0.46 mg/g (μ=0.16 mg/g), suggesting the presence of free hydrocarbons in some of the samples. Their corresponding Tmax values, however, indicate that the samples have not been subjected to sufficient temperatures required to actually generate hydrocarbons, varying from 383-429°C (μ=417°C). It is therefore likely that the hydrocarbons detected have migrated into the sediments from elsewhere.

Table 5.19 Isoprenoid ratios for sub-Stage IVC.

	Depth (m)	Depth (ft)	Pr/Phy	Pr/nC_{17}	CPI *
Tembungo-6					
1.	1901	6237	1.9	1.0	0.8
Rusa Timur-1					
2.	1619	5312	3.4	1.0	1.1
Gajah Hitam-1					
3.	2117	6946	2.7	1.2	1.1
4.	2401	7877	2.1	1.0	1.3

* Louis (1967)

Acquisition of extracts from Tembungo-1 and Tembungo-2 was hampered by the lack and poor sample conditions, including core samples which were in a very weathered and friable state. Most of the available samples were spent during the screening analyses and as a result, solvent extraction was not possible. In Tembungo-6, production index values are 0.18 mg/g and 0.19 mg/g, indicating that the samples are possibly late immature. This is supported by their corresponding Tmax values of 427°C and 428°C which indicate that the samples are in the late immature zone (420-430°C). Solvent extraction was performed on sample 1901m/6237ft from Tembungo-6 but separation of the saturate, aromatic and NSO fractions was not attempted due to the very low yield of the maltene fraction (saturate+aromatic+NSO) after asphaltene precipitation. The undifferentiated maltene fraction was analysed by gas chromatography and **Figure 5.24** shows the resulting gas chromatogram. CPI value of 1.0 **(Table 5.19)** indicate that the extracted hydrocarbons are mature.

In Rusa Timur-1, production index values ranging between 0.10-0.26 mg/g (μ=0.21 mg/g) indicate that free hydrocarbons may be present within the samples. Tmax values, however, vary from 409-440°C (μ=422°C) indicating that most samples have not reached the level of maturity necessary for hydrocarbon generation. **Figure 5.25** shows

the gas chromatogram of saturate hydrocarbon sample 1619m/5312ft from Rusa Timur-1. CPI value of 1.1 **(Table 5.19)** suggests maturity, contradicting with the Tmax of 413° C. The sample is thus deemed to have been stained by migrating hydrocarbons.

Gajah Hitam-1 production index values range between 0.00-0.09 mg/g, clearly indicating that the samples are immature. Tmax values vary from 410-453°C (μ=439°C) show that some samples may be in the mature zone (440-460°C). There are two likely explanations for this. Firstly, assuming that the Tmax values reflect the true maturity level of samples, they are naturally poor in organic carbon (range:0.40-0.71 wt%) accompanied by poor initial hydrocarbon-generating potential (HI:45-172 mgHC/gTOC). No hydrocarbons can be produced even with increasing maturation, thus the low Production Index values. The second possible explanation is that the Tmax values recorded during pyrolysis may have been under the influence of mineral-matrix. The presence of clayey-shaley matrix can delay the release of pyrolysate to the detectors, resulting in the falsely high Tmax values (Katz, 1983; Peters, 1986). In the case of Gajah Hitam samples, the high Tmax is more likely to be the result of mineral matrix interference instead of high maturation level and vitrinite reflectance values generally support this **(Table 5.20)**.

Table 5.20 Vitrinite reflectance values : sub-Stage IVC.

	Depth (m)	Depth (ft)	Measured VRo (%)	% Error
Tembungo-1				
1.	1984	6509	0.41	±10
Tembungo-2				
2.	2074	6804	0.53	±11
3.	2107	6913	0.50	±8
Tembungo-6				
4.	1901	6237	0.46	±17
Rusa Timur-1				
5.	1592	5223	0.42	±10
6.	1619	5312	0.42	±7
7.	1674	5492	0.45	±12
8.	1738	5702	0.44	±14
Gajah Hitam-1				
9.	1606	5269	0.47	±17
10.	1989	6526	0.57	±18
11.	2401	7877	0.52	±21

Figure 5.26 and **5.27** are the gas chromatograms of saturate hydrocarbon samples 2117m/6946ft and 2401m/7877ft from Tembungo-1. CPI values of 1.1 and 1.3 suggest that the extract samples are approaching maturity **(Table 5.19)**.

5.1.5 Sub-Stage IVD

Five wells, Tembungo-1, Tembungo-2, Tembungo-6, Rusa Timur-1 and Gajah Hitam-1, penetrated the sub-Stage IVD sequence. The sediments were deposited in a variety of depositional environments depending upon their location in the basin. Palaeontological data from PETRONAS in-house reports were used to determine the range of depositional environments encountered by the individual wells **(Table 5.21)**.

Table 5.21 Depositional environment variations.

	Depth interval (m) *	Depositional Environment
Tembungo-1	523m (1716ft)-1437m (4715ft)	coastal to inner neritic
	1437m (4715ft)-1882m (6175ft)	deep marine
Tembungo-2	729m (2392ft)-1640m (5381ft)	coastal to inner neritic
	1640m (5381ft)-2117m (6946ft)	deep marine
Tembungo-6	542m (1778ft)-1231m (4039ft)	coastal to inner neritic
	1231m (4039ft)-1438m (4718ft)	middle neritic
	1438m (4718ft)-1853m (6079ft)	deep marine
Rusa Timur-1	703m (2306ft)-1504m (4934ft)	outer neritic
Gajah Hitam-1	274m (899ft)-1474m (4834ft)	outer neritic

* All depths are calculated from the sea-bed [i.e. log depth - (kelly bushing + water depth)].

5.1.5a Organic Carbon Content

i) Coastal to inner neritic

TOC contents of the coastal to inner neritic sediments range from 0.11-5.31 wt% (μ =1.01 wt%, σ=1.28 wt%) in Tembungo-1; 0.05-3.26 wt% (μ=0.79 wt%, σ=1.05 wt%) Tembungo-2; and 0.11-1.83 wt% (μ=0.49 wt%, σ=0.39 wt%) in Tembungo-6 **(Table 5.22)**. It is observed that TOC content variation as well as absolute organic carbon concentration decrease from Tembungo-1 to Tembungo-2 to Tembungo-6.

Table 5.22 TOC and Pyrolysis results : sub-Stage IVD (coastal to inner neritic sediments).

	Depth (m)	(ft)	TOC (wt%)	S1 (mg/g)	S2 (mg/g)	Tmax (°C)	PI	HI (mgHC/gTOC)
Tembungo-1								
1.	632	2073	1.44	0.25	0.50	379	0.33	35
2.	642	2106	1.19	0.34	0.47	372	0.42	39
3.	660	2165	0.59	0.04	0.13	403	0.24	22
4.	678	2224	0.30	0.02	0.08	434	0.20	27
5.	706	2316	0.85	0.23	0.70	373	0.25	82
6.	715	2346	1.94	0.61	0.90	372	0.40	46
7.	751	2464	4.02	0.42	3.46	378	0.11	86
8.	760	2493	0.20	0.01	0.05	427	0.17	25

Table 5.22 TOC and Pyrolysis results : sub-Stage IVD (coastal to inner neritic sediments) - continued.

	Depth (m)	Depth (ft)	TOC (wt%)	S1 (mg/g)	S2 (mg/g)	Tmax (°C)	PI	HI (mgHC/gTOC)
9.	788	2585	2.51	0.11	0.68	385	0.14	27
10.	806	2644	1.49	0.06	0.36	401	0.14	24
11.	815	2674	3.30	0.23	1.87	386	0.11	57
12.	824	2703	4.02	0.24	1.92	381	0.11	48
13.	834	2736	0.43	0.04	0.36	395	0.10	84
14.	843	2766	0.89	0.07	0.26	394	0.21	29
15.	888	2913	0.63	0.03	0.18	394	0.14	29
16.	907	2976	0.20	0.01	0.06	440	0.14	30
17.	925	3035	0.53	0.05	0.33	422	0.13	62
18.	952	3123	1.18	0.25	1.42	375	0.15	120
19.	962	3156	0.35	0.04	0.08	414	0.33	23
20.	983	3225	0.20	0.01	0.09	489	0.10	45
21.	992	3255	5.31	0.13	0.71	403	0.15	13
22.	1056	3465	0.76	0.12	0.33	414	0.27	43
23.	1084	3556	0.25	0.09	0.27	427	0.25	108
24.	1102	3615	0.28	0.08	0.37	374	0.18	132
25.	1138	3734	0.25	0.08	0.31	442	0.21	124
26.	1157	3796	0.11	0.01	0.03	394	0.25	27
27.	1166	3825	0.19	0.08	0.24	436	0.25	126
28.	1205	3953	0.23	0.02	0.13	439	0.13	57
29.	1242	4075	0.15	0.01	0.05	441	0.17	33
30.	1273	4177	0.18	0.01	0.06	461	0.14	33
31.	1303	4275	0.31	0.02	0.16	479	0.11	52
32.	1333	4373	0.46	0.04	0.18	435	0.18	39
33.	1364	4475	0.23	0.01	0.04	507	0.20	17
34.	1394	4573	0.21	0.02	0.12	500	0.14	57
35.	1425	4675	0.33	0.02	0.20	489	0.09	61
Tembungo-2								
37.	823	2700	0.15	0.01	0.03	448	0.25	20
38.	851	2792	0.16	0.01	0.04	444	0.20	25
39.	912	2992	0.39	0.01	0.14	428	0.07	36
40.	976	3202	0.23	0.13	0.72	369	0.15	313
41.	1003	3291	0.19	0.02	0.19	423	0.10	100
42.	1040	3412	0.16	0.00	0.01	432	0.00	6
43.	1104	3622	0.14	0.02	0.09	431	0.18	64
44.	1159	3802	2.48	0.19	2.33	424	0.08	94
45.	1168	3832	1.85	1.69	2.81	383	0.38	152
46.	1177	3862	2.00	0.52	5.15	385	0.09	258
47.	1204	3950	0.12	0.02	0.01	385	0.67	8
48.	1287	4222	0.14	0.01	0.03	408	0.25	21
49.	1323	4341	0.06	0.01	0.01	301	0.50	17
50.	1378	4521	0.12	0.01	0.03	385	0.25	25
51.	1415	4642	0.06	0.01	0.03	362	0.25	50
52.	1470	4823	0.05	0.01	0.01	340	0.50	20
53.	1497	4911	0.86	0.11	1.42	388	0.07	165
54.	1515	4970	3.03	0.20	2.49	377	0.07	82

Table 5.22 TOC and Pyrolysis results : sub-Stage IVD (coastal to inner neritic sediments) - continued.

	Depth (m)	(ft)	TOC (wt%)	S1 (mg/g)	S2 (mg/g)	Tmax (°C)	PI	HI (mgHC/gTOC)
Tembungo-6								
55.	1534	5033	3.26	0.41	4.65	378	0.08	143
56.	1543	5062	0.39	0.02	0.39	437	0.05	100
57.	704	2310	0.14	0.01	0.02	382	0.33	14
58.	740	2428	0.13	0.01	0.01	340	0.50	8
59.	777	2549	0.15	0.02	0.02	345	0.50	13
60.	813	2667	0.52	0.02	0.07	457	0.22	13
61.	822	2697	0.16	0.01	0.03	343	0.33	13
62.	832	2730	0.11	0.01	0.01	318	0.50	9
63.	841	2759	0.35	0.03	0.12	429	0.20	34
64.	850	2789	0.74	0.25	1.46	473	0.15	197
65.	859	2818	0.28	0.02	0.07	434	0.22	25
66.	868	2848	0.42	0.03	0.15	429	0.17	36
67.	877	2877	0.96	0.03	0.25	429	0.11	26
68.	887	2910	0.42	0.05	0.18	424	0.22	43
69.	923	3028	0.32	0.02	0.08	429	0.20	25
70.	960	3150	0.47	0.04	0.21	431	0.16	45
71.	987	3238	0.45	0.06	0.16	429	0.27	36
72.	1005	3297	0.74	0.02	0.21	384	0.09	28
73.	1170	3839	0.43	0.01	0.07	439	0.13	16
74.	1179	3868	1.83	0.07	0.66	428	0.10	36
75.	1188	3898	0.90	0.07	0.40	433	0.15	44
76.	1197	3927	0.54	0.02	0.29	437	0.06	54
77.	1216	3990	0.20	0.01	0.03	425	0.25	15

ii) Middle neritic

Only Tembungo-6 penetrated middle neritic sediments. TOC contents range from 0.16-0.90 wt% (μ=0.54 wt%, σ=0.19 wt%), indicating poor to fair amounts of organic carbon **(Table 5.23)**.

Table 5.23 TOC and Pyrolysis results : sub-Stage IVD (middle neritic sediments).

	Depth (m)	(ft)	TOC (wt%)	S1 (mg/g)	S2 (mg/g)	Tmax (°C)	PI	HI (mgHC/gTOC)
Tembungo-6								
1.	1252	4108	0.52	0.04	0.30	376	0.12	58
2.	1289	4229	0.48	0.05	0.26	426	0.16	54
3.	1325	4347	0.16	0.04	0.12	435	0.25	75
4.	1362	4469	0.52	0.07	0.34	428	0.17	65
5.	1389	4557	0.60	0.08	0.31	431	0.21	52
6.	1399	4590	0.90	0.08	0.29	433	0.22	32
7.	1408	4619	0.54	0.05	0.27	435	0.16	50
8.	1435	4708	0.58	0.08	0.36	429	0.18	62

iii) Outer neritic

Sub-Stage IVD sediments encountered by Rusa Timur-1 and Gajah Hitam-1 were deposited in an outer neritic setting. Total organic carbon contents range from 0.53-1.24 wt% (μ=0.87 wt%, σ=0.37 wt%) in Rusa Timur-1; and from 0.65-0.98 wt% (μ=0.82 wt% and σ=0.10 wt%) in Gajah Hitam-1 **(Table 5.24)**. Both wells have very similar, poor to fair, organic carbon contents.

Table 5.24 TOC and Pyrolysis results : sub-Stage IVD (outer neritic sediments).

	Depth (m)	(ft)	TOC (wt%)	S1 (mg/g)	S2 (mg/g)	Tmax (°C)	PI	HI (mgHC/gTOC)
Rusa Timur-1								
1.	772	2533	1.80	0.53	11.48	410	0.04	638
2.	790	2592	1.05	0.59	5.10	414	0.10	486
3.	875	2871	0.53	0.00	0.17	425	0.00	32
4.	877	2877	0.66	0.00	0.21	426	0.00	32
5.	879	2884	0.62	0.00	0.27	417	0.00	44
6.	882	2894	0.59	0.00	0.33	448	0.00	56
7.	884	2900	0.65	0.00	0.28	425	0.00	43
8.	885	2904	0.58	0.00	0.26	440	0.00	45
9.	1406	4613	1.24	0.75	2.60	411	0.22	210
10.	1424	4672	0.93	0.31	1.32	428	0.19	142
11.	1497	4911	0.91	0.39	1.16	418	0.25	127
Gajah Hitam-1								
12.	489	1604	0.65	0.00	0.16	412	0.00	25
13.	493	1617	0.89	0.00	0.32	410	0.00	36
14.	497	1631	0.82	0.00	0.49	427	0.00	60
15.	499	1637	0.76	0.00	0.28	436	0.00	37
16.	524	1719	0.81	0.00	0.24	425	0.00	30
17.	529	1734	0.98	0.01	0.95	438	0.01	97

iv) Bathyal

Deep marine sediments were penetrated by Tembungo-1, Tembungo-2 and Tembungo-6. TOC contents range from 0.25-5.42 wt% (μ=1.12 wt%, σ=1.14 wt%) in Tembungo-1; 0.46-1.94 wt% (μ=0.68 wt%, σ=0.42 wt%) in Tembungo-2; and 0.27-0.73wt%(μ =0.51wt%, σ=0.15wt%) in Tembungo-6 **(Table 5.25)**. The decrease in TOC variability is accompanied by lower absolute organic carbon contents.

Table 5.25 TOC and Pyrolysis results : sub-Stage IVD (bathyal sediments).

	Depth (m)	(ft)	TOC (wt%)	S1 (mg/g)	S2 (mg/g)	Tmax (°C)	PI	HI (mgHC/gTOC)
Tembungo-1								
1.	1455	4774	0.40	0.02	0.13	462	0.13	33
2.	1486	4875	0.25	0.02	0.05	441	0.29	20
3.	1516	4974	0.41	0.05	0.44	436	0.10	107
4.	1547	5075	0.74	0.03	0.29	487	0.09	39

Table 5.25 TOC and Pyrolysis results : sub-Stage IVD (bathyal sediments) - continued.

	Depth (m)	(ft)	TOC (wt%)	S1 (mg/g)	S2 (mg/g)	Tmax (°C)	PI	HI (mgHC/gTOC)
5.	1565	5135	1.37	0.04	0.14	421	0.22	10
6.	1608	5276	0.62	0.02	0.24	492	0.08	39
7.	1638	5374	0.33	0.01	0.13	499	0.07	39
8.	1650	5413	0.26	0.11	0.20	428	0.35	77
9.	1663	5456	0.96	0.11	1.08	406	0.09	113
10.	1681	5515	1.31	0.13	0.74	411	0.15	56
11.	1699	5574	0.26	0.04	0.18	471	0.18	69
12.	1718	5636	0.56	0.03	0.27	448	0.10	48
13.	1748	5735	0.39	0.02	0.24	496	0.08	62
14.	1772	5814	0.27	0.05	0.17	419	0.23	63
15.	1809	5935	0.63	0.04	0.33	434	0.11	52
16.	1821	5974	2.33	0.26	1.15	416	0.18	49
17.	1839	6033	3.10	0.19	1.76	419	0.10	57
18.	1858	6096	2.62	0.53	4.89	409	0.10	187
19.	1870	6135	4.42	0.26	1.77	400	0.13	40
Tembungo-2								
20.	1790	5873	1.94	0.11	0.57	438	0.16	29
21.	1823	5981	0.68	0.28	0.86	417	0.25	126
22.	1965	6447	0.59	0.04	0.43	434	0.09	73
23.	1973	6473	0.75	0.08	0.49	430	0.14	65
24.	1994	6542	0.63	0.07	0.38	432	0.16	60
25.	1998	6555	0.29	0.04	0.29	434	0.12	100
26.	2002	6568	0.62	0.03	0.37	440	0.08	60
27.	2021	6631	0.46	0.04	0.30	436	0.12	65
28.	2025	6644	0.49	0.05	0.37	432	0.12	76
29.	2059	6755	0.47	0.05	0.21	428	0.19	45
30.	2065	6775	0.51	0.05	0.40	431	0.11	78
Tembungo-6								
31.	1462	4797	0.52	0.06	0.23	434	0.21	44
32.	1508	4948	0.53	0.08	0.33	431	0.20	62
33.	1545	5069	0.69	0.07	0.46	430	0.13	67
34.	1581	5187	0.73	0.05	0.31	430	0.14	42
35.	1618	5308	0.60	0.03	0.29	431	0.09	48
36.	1655	5430	0.39	0.01	0.08	446	0.11	21
37.	1691	5548	0.46	0.05	0.22	405	0.19	48
38.	1728	5669	0.71	0.12	0.56	427	0.18	79
39.	1764	5787	0.27	0.01	0.08	467	0.11	30
40.	1801	5909	0.35	0.01	0.09	424	0.10	26
41.	1837	6027	0.41	0.01	0.07	429	0.13	17

5.1.5b Organic Matter Type And Quality

Hydrogen Index vs Tmax plot (**Figure 5.28**) and van Krevelen diagram (**Figure 5.29**) for all sub-Stage IVD samples, regardless of palaeodepositional environment, indicate that the organic carbon present are mainly terrigenous Type III kerogen (see **Appendix II**). Elemental analysis results (**Table 5.26**) are confirmed by visual kerogen typing (**Table 5.27**) which shows the predominance of vitrinites. Density separation was not

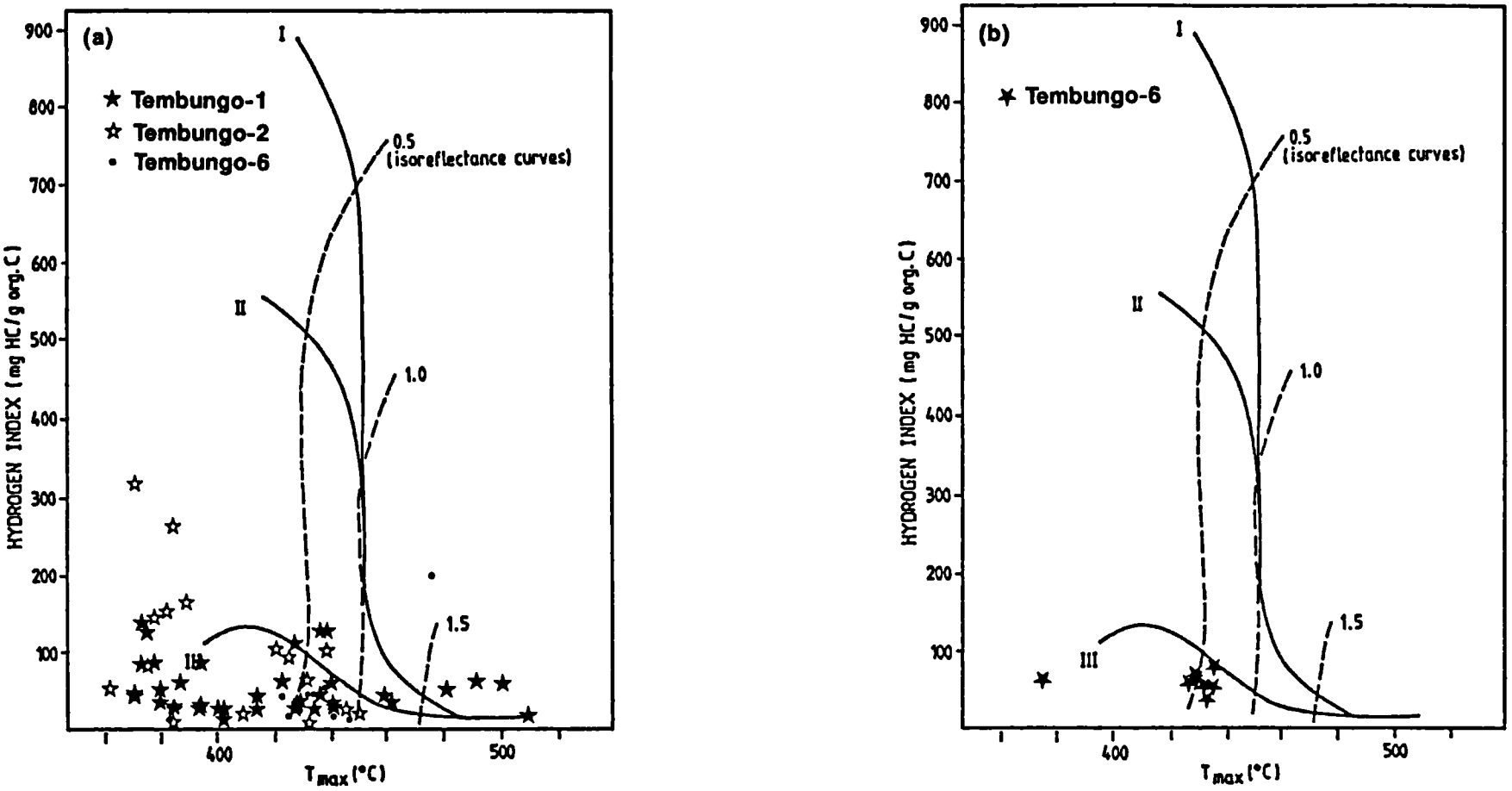
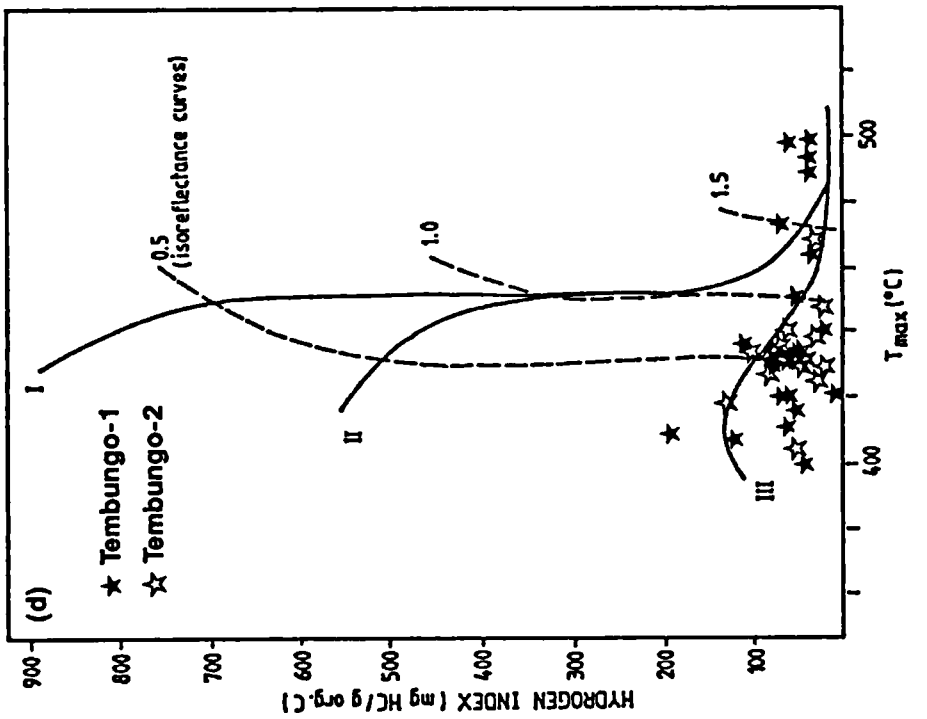


FIGURE 5.28 Hydrogen Index vs Tmax cross-plot (from Parnell & Rahman, 1990) for Stage IVD sediments according to palaeoenvironments: **(a)** coastal-inner neritic, **(b)** middle neritic, **(c)** outer neritic and **(d)** bathyal.



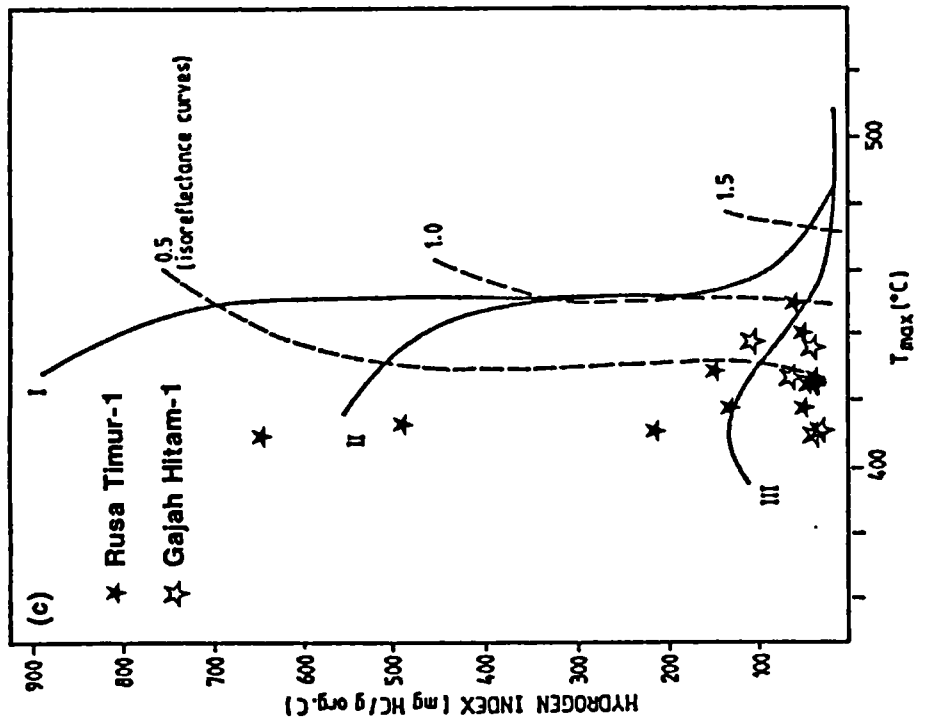


FIGURE 5.28 Continued.

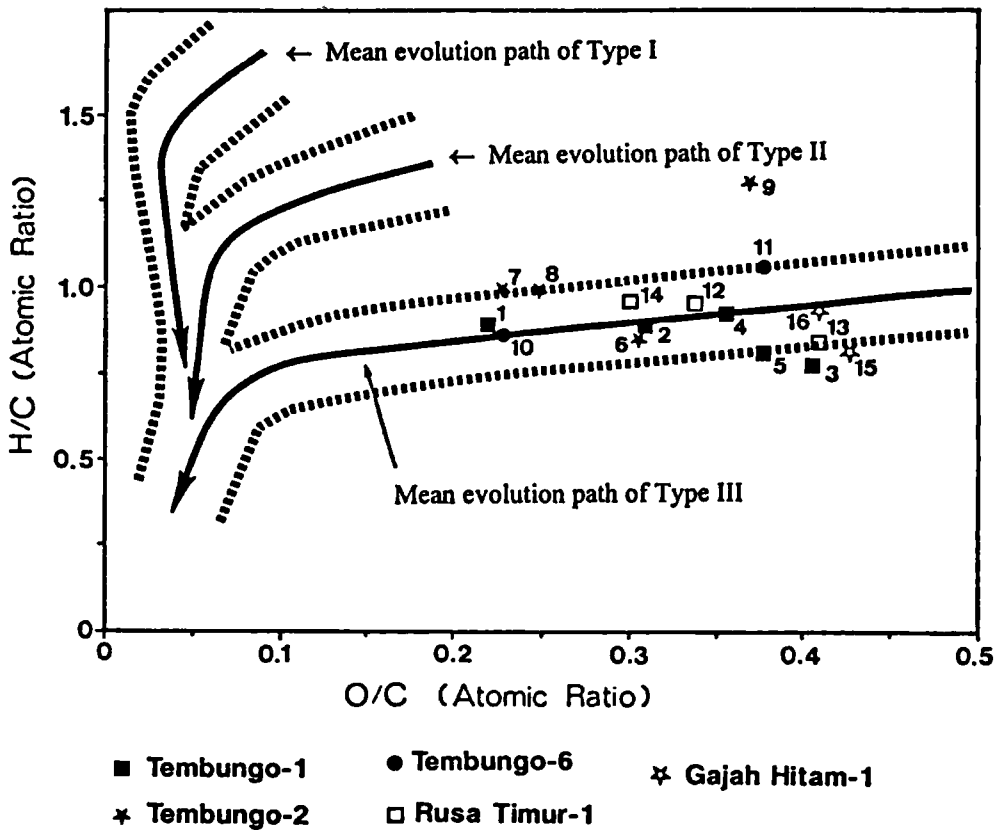


FIGURE 5.29 Elemental compositions of Stage IVD kerogens plotted on the van Krevelen diagram (from Durand, 1980).

attempted on isolated kerogen samples from Tembungo-1, Tembungo-2 and Tembungo-6 because of their insufficient quantities, thus preventing this technique to be performed satisfactorily (Rahman, pers. comm.). As a result, only samples from Rusa Timur-1 and Gajah Hitam-1 were subjected to density separation. A plot of depth vs maceral composition with the corresponding Hydrogen Index values indicate general agreement with each other **(Figure 5.30)**.

Table 5.26 Elemental analysis results : sub-Stage IVD.

	Depth (m)	(ft)	H%	O%	C%	N%	H/C	O/C	Total % of (C+H+N+O)
Tembungo-1									
1.	888	2913	5.32	21.36	71.09	1.70	0.90	0.22	99.47
2.	983	3225	4.82	26.37	64.21	1.68	0.90	0.31	97.08
3.	1565	5135	3.64	30.60	56.16	1.75	0.78	0.41	92.15
4.	1809	5935	4.38	27.44	56.79	1.45	0.92	0.36	90.06
5.	1870	6135	4.18	30.84	60.37	1.40	0.83	0.38	96.79
Tembungo-2									
6.	1177	3862	4.26	24.72	59.28	1.10	0.86	0.31	89.36
7.	1534	5033	5.09	18.96	60.94	1.08	1.00	0.23	86.07
8.	1994	6542	5.02	20.06	59.84	1.17	1.00	0.25	86.09
9.	2025	6644	6.75	30.30	61.50	1.12	1.32	0.37	99.67
Tembungo-6									
10.	868	2848	3.24	13.68	44.64	1.60	0.87	0.23	63.16
11.	1188	3898	3.84	21.71	43.26	1.41	1.07	0.38	70.22
Rusa Timur-1									
12.	877	2877	4.59	25.71	57.16	1.65	0.96	0.34	89.11
13.	885	2904	3.90	30.13	55.14	1.64	0.85	0.41	90.81
14.	1406	4613	4.80	23.64	59.93	1.59	0.96	0.30	89.96
Gajah Hitam-1									
15.	493	1617	3.48	29.26	50.51	1.68	0.83	0.43	84.93
16.	529	1736	4.33	30.47	55.25	1.65	0.94	0.41	91.70

Table 5.27 Visual analysis and density separation of kerogen concentrates : sub-Stage IVD.

	Depth (m)	(ft)	% (optical) Ex	Vit	In	% (spec. grav.) 1.45	1.65	1.81	2.20	HI	TOC
Tembungo-1											
1.	888	2913	10	70	20	np.	np.	np.	np.	27	2.51
2.	983	3225	20	70	10	np.	np.	np.	np.	45	0.20
3.	1565	5135	10	80	10	np.	np.	np.	np.	10	1.37
4.	1809	5935	15	65	20	np.	np.	np.	np.	52	0.63
5.	1870	6135	15	65	20	np.	np.	np.	np.	40	4.42
Tembungo-2											
6.	1177	3862	44	32	24	np.	np.	np.	np.	258	2.00

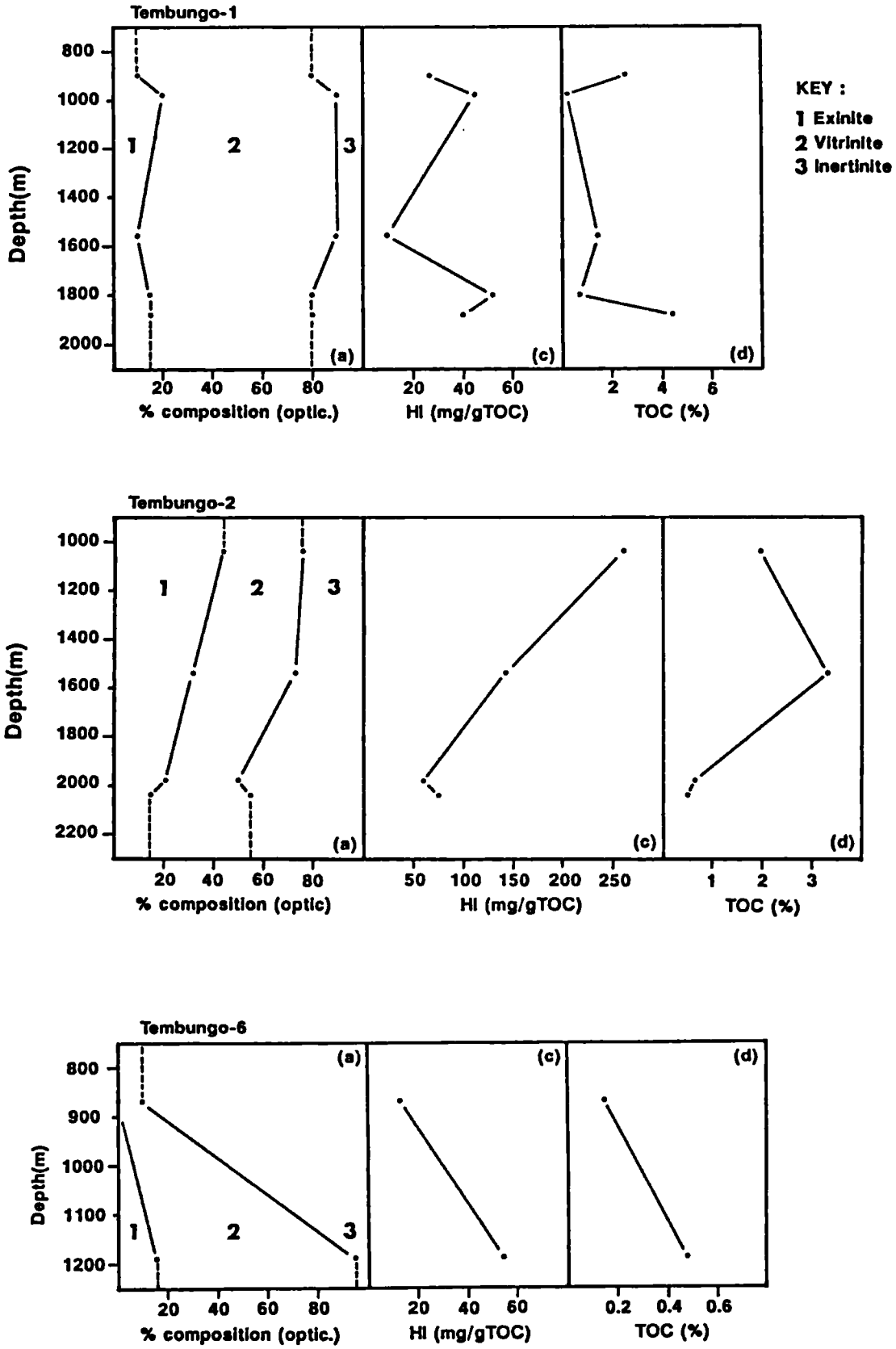


FIGURE 5.30 The variations in kerogen composition of Tembungo-1, Tembungo-2, Tembungo-6, Rusa Timur-1 and Gajah Hitam-1 Stage IVD sediments from (a) organic petrography and (b) density separation. Also shown are the corresponding (c) Hydrogen Index and (d) Total Organic Carbon contents.

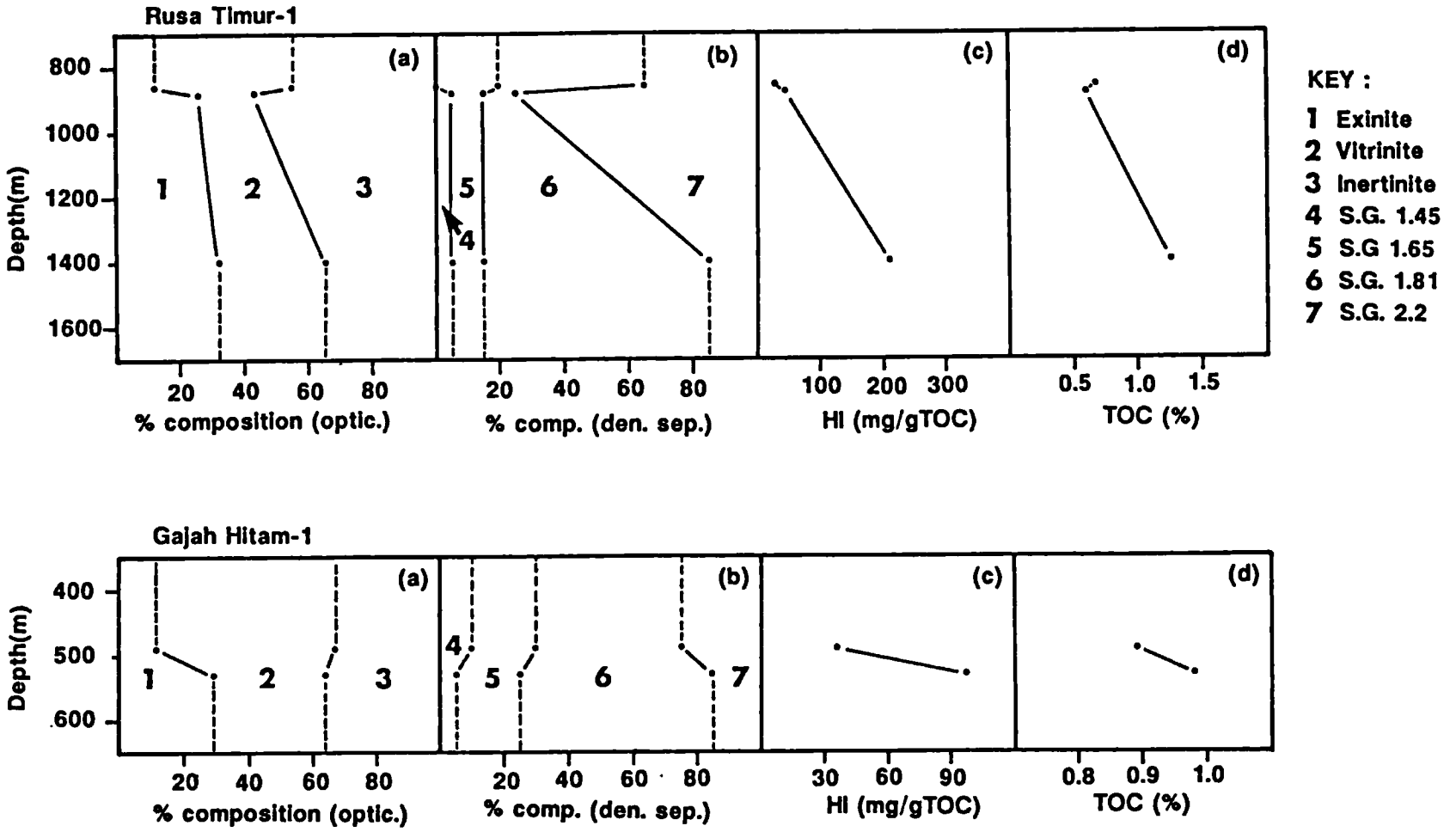


FIGURE 5.30 Continued.

Table 5.27 Visual analysis and density separation of kerogen concentrates : sub-Stage IVD - continued.

	Depth (m)	(ft)	% (optical) Ex	Vit	In	% (spec. grav.) 1.45	1.65	1.81	2.20	HI	TOC
Tembungo-6											
7.	1534	5033	32	41	27	np.	np.	np.	np.	143	3.26
8.	1994	6542	20	30	50	np.	np.	np.	np.	60	0.63
9.	2025	6644	15	40	45	np.	np.	np.	np.	75	0.49
10.	868	2848	0	10	90	np.	np.	np.	np.	13	0.15
11.	1188	3898	15	80	5	np.	np.	np.	np.	54	0.48
Rusa Timur-1											
12.	877	2877	12	43	45	0	20	45	35	32	0.66
13.	885	2904	26	17	57	5	10	10	75	45	0.58
14.	1406	4613	32	33	34	5	10	70	15	210	1.24
Gajah Hitam-1											
15.	493	1617	11	56	33	10	20	45	25	36	0.89
16.	529	1736	29	35	36	5	20	60	15	97	0.98

Key : Ex = Exinite, Vit = Vitrinite, In = Inertinite
np. : density separation not performed due to inadequate amounts of kerogen recovered

Gas chromatogram trace of Tembungo-1 saturate sample 1809m/5935ft (**Figure 5.31**) shows significant contributions from land-plants by the presence of pristane, phytane and n-alkanes in the high molecular weight region. However, the nC_{17} peak is also present in a slightly higher concentration than pristane, which may be due to input from algae and/or bacteria. Pr/Phy and Pr/nC_{17} ratios (**Table 5.28**) suggest that organic matter deposition may have occurred in a marginally anoxic environment. Gas chromatogram of Tembungo-2 saturate sample 1994m/6542ft (**Figure 5.32**) shows the presence of pristane, phytane and high molecular weight n-alkanes, again indicating organic matter input from land plants. Pr/Phy and Pr/nC_{17} ratios (**Table 5.28**) both suggest that the organic matter was deposited in oxic conditions such as those present in deltaic/paralic and peat swamp environments.

Figures 5.33 and **5.34** are gas chromatograms of saturate hydrocarbon fractions of Rusa Timur-1 samples 772m/2533ft and 1406m/4613ft. They all show the presence of pristane, phytane, higher molecular weight n-alkanes and nC_{17} peaks slightly larger than the pristane peaks. These suggest that both land plant material and algae/bacteria may have contributed to the organic matter input. Pr/Phy ratios (**Table 5.28**) indicate oxic depositional conditions such as in deltaic/paralic and peat swamp environments. Lack of samples, primarily due to poor recovery and preservation, impeded solvent extraction to be performed on sub-Stage IVD samples of Tembungo-6 and Gajah Hitam-1.

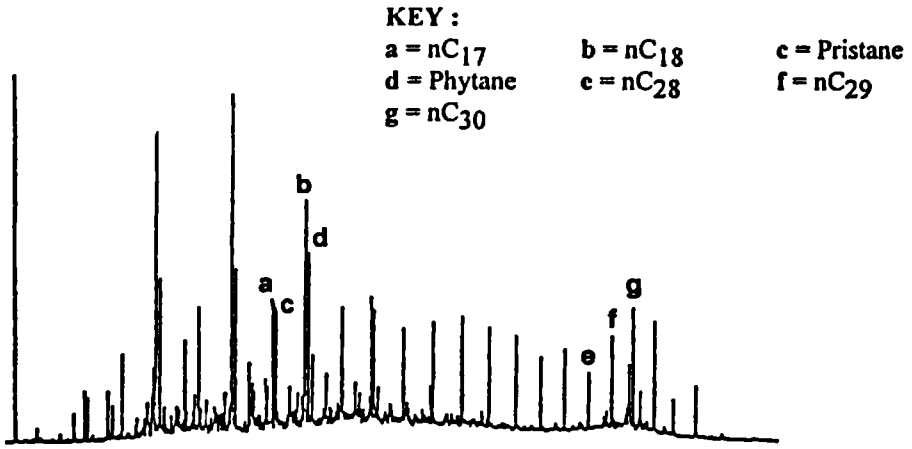


FIGURE 5.31 Gas chromatogram of Stage IVD Tembungo-1 saturate fraction 1809m/5935ft.

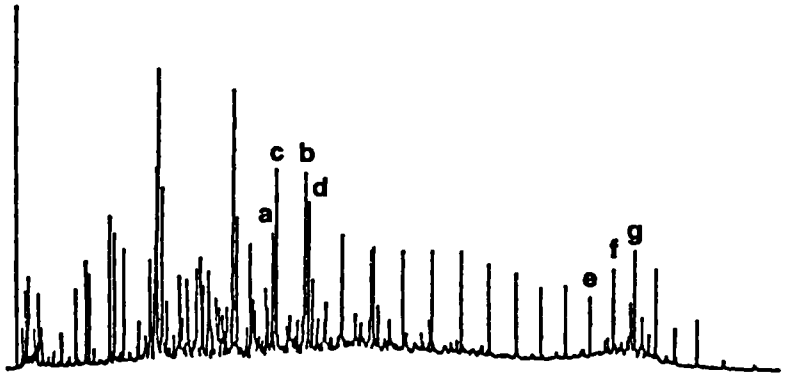


FIGURE 5.32 Gas chromatogram of Stage IVD Tembungo-2 saturate fraction 1994m/6542ft.

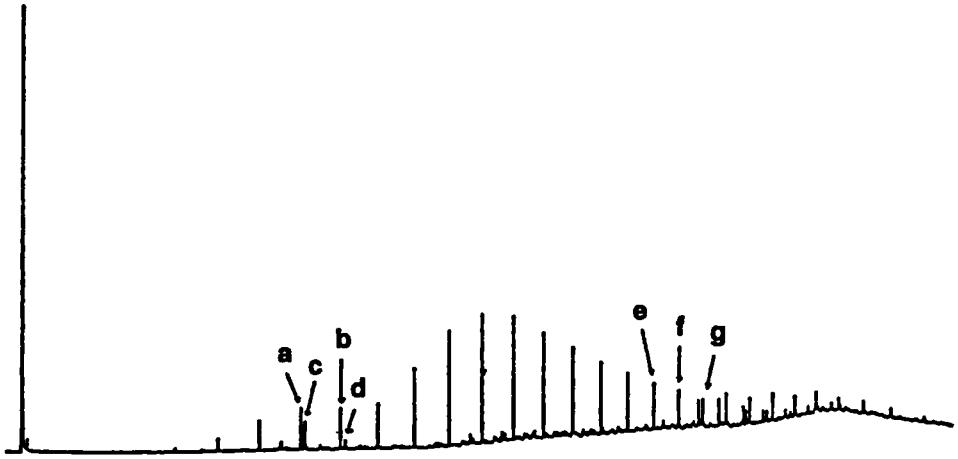


FIGURE 5.33 Gas chromatogram of Stage IVD Rusa Timur-1 saturate fraction 772m/2533ft.

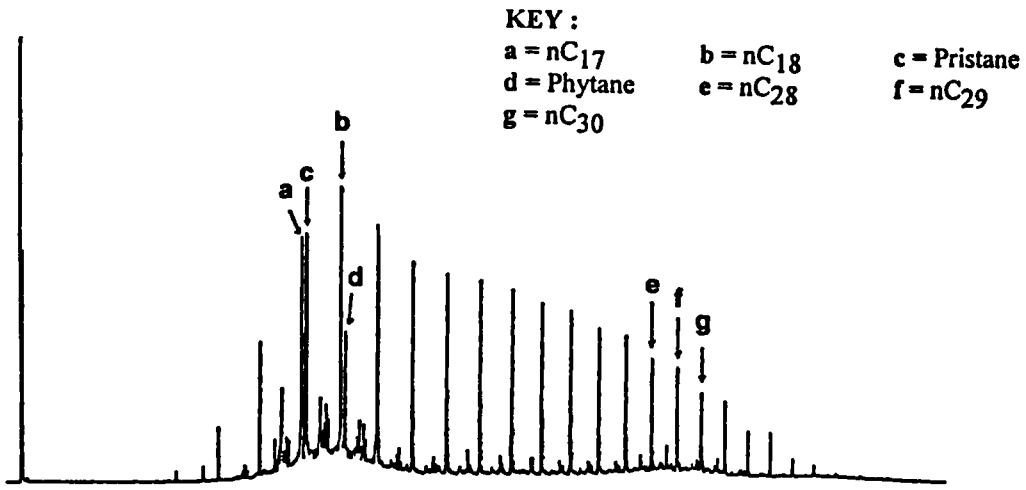


FIGURE 5.34 Gas chromatogram of Stage IVD Rusa Timur-1 saturate fraction 1406m/4613ft.

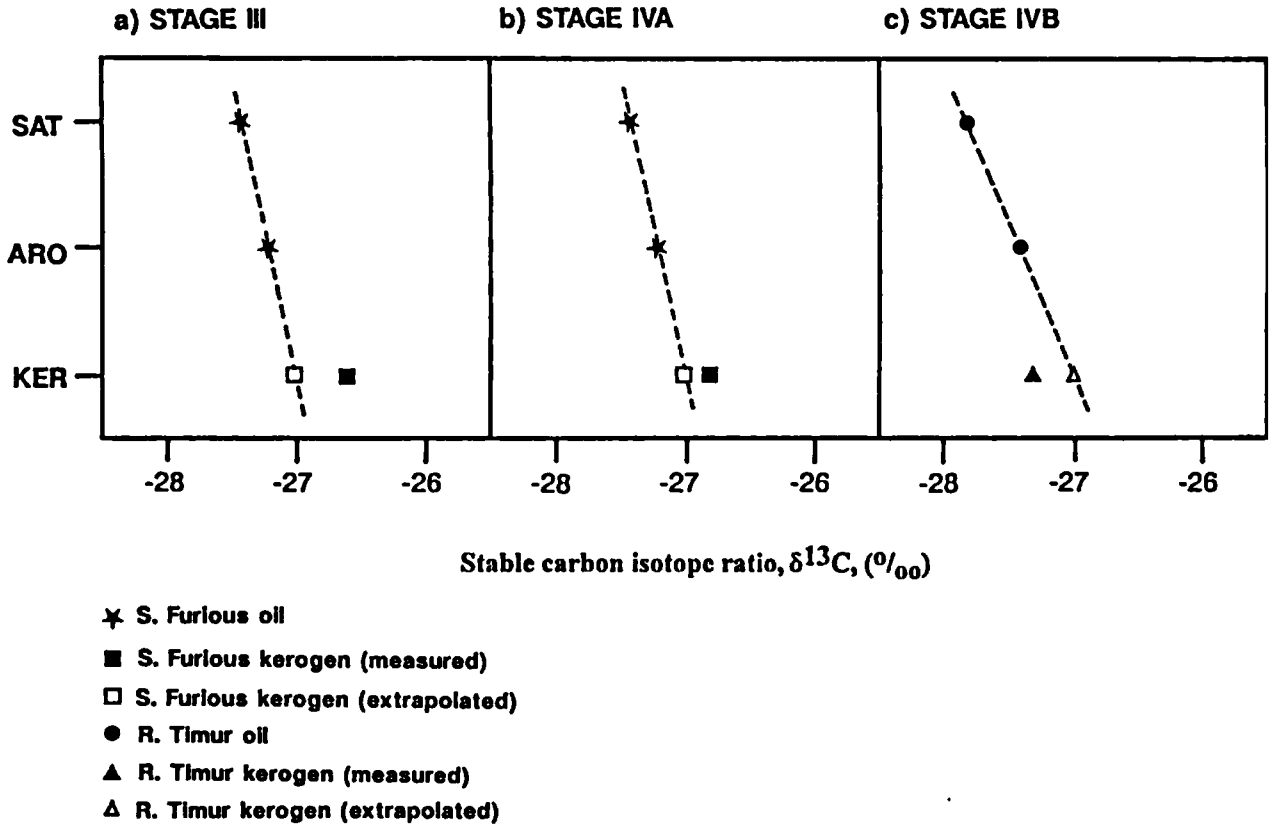


FIGURE 5.35 Isotope type-curves (Stahl, 1978) for South Furious and Rusa Timur oils, and kerogens from (a) Stage III, (b) Stage IVA and (c) Stage IVB sediments.

5.1.5c Organic Matter Maturity

Production index values varying between 0.07-0.42 mg/g (μ 0.17 mg/g) in Tembungo-1 suggest the presence of free hydrocarbons. Tmax values range from 372-507°C (μ=427° C) indicating that the majority of samples are in the late immature zone (420-430°C). Samples with Tmax values in the mature (440-460°C) and overmature (>460°C) zones have low corresponding S2 yields (0.04-0.31mg/g). The high Tmax values are thus most likely the result of delayed pyrolysates release due to adsorption by the clayey-shaley mineral matrix, rather than reflecting the true maturity levels of the samples (Katz, 1983; Peters, 1986). **Figure 5.31** shows the gas chromatogram of Tembungo-1 saturate sample 1809m/5935ft whose CPI value of 1.0 **(Table 5.28)** indicates it to be mature.

Table 5.28 Isoprenoid ratios for sub-Stage IVD.

	Depth (m)	(ft)	Pr/Phy	Pr/nC_{17}	CPI *
Tembungo-1					
1.	1809	5935	0.7	1.0	1.0
Tembungo-2					
2.	1994	6542	1.2	1.5	1.2
Rusa Timur-1					
3.	772	2533	3.2	0.7	1.0
4.	1406	4613	1.9	1.0	1.1

* Louis (1967)

In Tembungo-2, production index values varying from 0.00-0.67 mg/g (μ=0.18 mg/g) indicate the presence of free hydrocarbons. Tmax values, however, indicate that the samples are mostly immature, ranging between 301-448°C (μ=409°C). Again, samples with Tmax values in the mature zone (440-460°C) have very low corresponding S2 yields (0.3-0.37mg/g) that they could not have generated the hydrocarbons even if they had reached the temperature threshold for hydrocarbon generation. The free hydrocarbons detected are therefore likely to be migrated hydrocarbons. CPI value of 1.2 **(Table 5.28)** calculated from the gas chromatogram of sample 1994m/6542ft saturate fraction **(Figure 5.32)** indicates that it has a slight odd carbon-number preference. Production index values in Tembungo-6 vary between 0.06-0.50 mg/g, indicating the presence of free hydrocarbons. However, as the majority of the samples are immature, with Tmax values ranging from 318-473°C (μ=419°C), and have very poor S2 yields and Hydrogen Index values, the hydrocarbons present could not have been generated *in -situ.*

Sample immaturity in Rusa Timur-1 are indicated by production index values ranging between 0.00-0.25 mg/g (μ=0.07 mg/g). Tmax values varying from 411-448°C

(μ=426°C) also implies general immaturity. There are samples with Tmax values in the marginal mature (430-440°C) and mature (440-460°C) zones. However, since they are the shallower samples, the high Tmax values are more likely to be the result of mineral matrix interference. CPI values of 1.0 and 1.1 **(Table 5.28)** calculated from the gas chromatograms of samples 772m/2533ft **(Figure 5.33)** and 1406m/4613ft **(Figure 5.34)** imply that they are mature, contradicting the Tmax indication of immaturity. It is therefore likely the sediments have been stained by migrating hydrocarbons. In Gajah Hitam-1, production index values of mainly 0.00 mg/g indicate that the samples are immature. Tmax values generally reflect this, ranging from 410-438°C (μ=425°C) except for two samples, 499m/1637ft and 529m/1734ft, which seem to be marginally mature. Based on their poor production index, S2 yields and Hydrogen Index values, the high Tmax of the two samples are the result of mineral matrix effects during pyrolysis. Evidence of immaturity of sub-Stage IVD sediments was further provided by vitrinite reflectance values **(Table 5.29)**.

Table 5.29 Vitrinite reflectance values : sub-Stage IVD.

	Depth (m)	(ft)	Measured VRo (%)	% Error
Tembungo-1				
1.	888	2913	0.28	±29
2.	983	3225	0.34	±21
3.	1565	5135	0.31	±26
4.	1809	5935	0.30	±17
5.	1870	6135	0.31	±23
Tembungo-2				
6.	1994	6542	0.41	±5
7.	2025	6644	0.42	±10
Tembungo-6				
8.	868	2848	0.37	±27
9.	1188	3898	0.50	±18
Rusa Timur-1				
10.	877	2877	0.36	±15
11.	1406	4613	0.39	±13
Gajah Hitam-1				
12.	529	1736	0.40	±10

5.2 Extractable organic matter

Sediment source potentials can be estimated from the quantity of extractable organic matter, EOM (Hunt, 1979; Tissot & Welte, 1984). In this study, however, source potentials of the analysed sediments were not estimated using their EOM quantities due to the migrated origin of the hydrocarbon extracts. This was established from the incompatibility of high production index and low Tmax values, and supported by

correspondingly low vitrinite reflectance values. Results based on non-indigenous hydrocarbons would not reflect the true hydrocarbon-generating potentials of the sediments.

5.3 Stable carbon isotope ratios, $\delta^{13}C$

Isotopic type-curves of Stahl (1977, 1978) show the relationship between isotopic compositions of kerogen and those of oils and extracts, making them useful in oil-source correlation studies. With increasing polarity from saturates to kerogens, isotopic compositions become less negative, i.e. isotopically heavier. According to Yen (1972), the carbon isotope ratio between genetically associated kerogens and oil fractions vary in the following manner:

$$\delta^{13}C_{kerogen} \geq \delta^{13}C_{asphaltenes} \geq \delta^{13}C_{NSO} \geq \delta^{13}C_{aromatics} \geq \delta^{13}C_{saturates}$$

(isotopically heaviest and most positive) — (isotopically lightest and most negative)

Maturation and migration tend to make saturate and aromatic fractions isotopically heavier (Sofer, 1991). However, genetic relationship between kerogens and oils can be established when their isotopic compositions differ by <1‰ (Fuex, 1977). Plotting the isotopic compositions of Stage III and sub-Stages IVA and IVB kerogen samples, and the saturate and aromatic fractions of South Furious and Rusa Timur oils **(Table 5.30)** on Stahl's type-curves **(Figure 5.35)**, it can be seen that there are genetic associations between :

- South Furious oil and kerogens of Stage III and sub-Stage IVA in the South Furious area
- Rusa Timur oil and sub-Stage IVB kerogen in the Rusa Timur area

The very similar isotopic values of the kerogens **(Table 5.30)** suggest that they may have originated from the same source, which is supported by visual kerogen study where the organic matter present are all land-derived. To further ascertain these observations, differences between measured and extrapolated kerogen carbon isotope ratios, where:

$$\Delta_K = (\delta^{13}C \text{ kerogen})_{measured} - (\delta^{13}C \text{ kerogen})_{extrapolated} \quad \text{(Stahl, 1978)}$$

are investigated. This is based on the premise that if the oil and kerogen are genetically related, then the difference between the carbon isotope ratios will reflect the degree of genetic 'closeness' between them. Results from this study show that kerogens of Stages III, IVA and IVB has Δ_K values between 2σ standard deviations, which is taken to

indicate the range of isotopic differences for genetically associated oil-kerogen pairs **(Figure 5.36)**. The same principle is extended to the saturate and aromatic fractions by calculating $\Delta_{K\text{-}SAT}$ and $\Delta_{K\text{-}ARO}$. Differences between measured kerogen isotope ratio and the saturate and aromatic fractions will be small if the fractions had been generated by the kerogen (Stahl, 1978). Here, hydrocarbon fractions of Stages III, IVA and IVB are shown to be genetically-related with their respective kerogen samples, varying between 2σ standard deviations **(Figure 5.37)**.

Table 5.30 Stable carbon isotope ratios.

Stage / Sub-Stage	Kerogen (‰)	Oil	
		Saturates (‰)	Aromatics (‰)
IVB (Rusa Timur)	-27.3	-27.8	-27.4
IVA (South Furious)	-26.8	-27.4	-27.2
III (South Furious)	-26.6	-27.4	-27.2

5.4 Source rock considerations

As the result of their immature status, none of the samples analysed have contributed to the present hydrocarbon accumulations in Sabah Basin. Results from TOC determination and Rock-Eval pyrolysis screening methods were interpreted according to the current guidelines followed by the industry. All analytical parameters, including those obtained from gas-chromatography, show a characteristically terrestrial organic matter fingerprint. Both geochemical and petrographic data point to a predominantly detrital terrestrial origin of the dispersed organic matter in the Stage III and Stage IV sediments of Sabah Basin. Evidence for the terrigenous origin are :

- predominance of high molecular weight n-alkanes in most gas chromatograms, typical of waxy oils derived from higher land plants.
- low Hydrogen Index values and H/C ratios
- high O/C ratios
- high Pr/Phy (>2) and Pr/nC_{17} (>1) ratios indicating that deposition and preservation took place in oxygenated environments often prevailing in deltas and peat swamps (Powell & McKirdy, 1973; Lijmbach, 1976; Didyk *et. al.*, 1978).
- maceral compositions consistent with higher plant source-mixture of structured woody material (vitrinite), degraded cuticular fragments, pollen and spores which make up the exinite group. Opaque organic matter (inertinites) are generally considered detrital and continental in origin.

$\Delta_K = (\delta^{13}C \text{ kerogen})_{measured} - (\delta^{13}C \text{ kerogen})_{extrapolated}$ (Stahl, 1978)

1) STAGE IVB

$(\delta^{13}C \text{ kerogen})_{measured} = -27.3\ ^{o}/_{oo}$

$(\delta^{13}C \text{ kerogen})_{extrapolated} = -27.0\ ^{o}/_{oo}$

$\Delta_K = -27.3 - (-27.0) = -0.3\ ^{o}/_{oo}$

2) STAGE IVA

$(\delta^{13}C \text{ kerogen})_{measured} = -26.8\ ^{o}/_{oo}$

$(\delta^{13}C \text{ kerogen})_{extrapolated} = -27.0\ ^{o}/_{oo}$

$\Delta_K = -26.8 - (-27.0) = 0.2\ ^{o}/_{oo}$

3) STAGE III

$(\delta^{13}C \text{ kerogen})_{measured} = -26.6\ ^{o}/_{oo}$

$(\delta^{13}C \text{ kerogen})_{extrapolated} = -27.0\ ^{o}/_{oo}$

$\Delta_K = -26.6 - (-27.0) = 0.4\ ^{o}/_{oo}$

$\therefore \Delta_K = 0.1\ ^{o}/_{oo}$

$\sigma = 0.29\ ^{o}/_{oo}$

$2\sigma = 0.58\ ^{o}/_{oo}$

For the kerogen and oil to be genetically related, the Δ_K values should be within 2σ limits (Stahl, 1978)

where: Lower limit = $0.1 - 0.58 = -0.48\ ^{o}/_{oo}$

Upper limit = $0.1 + 0.58 = 0.68\ ^{o}/_{oo}$

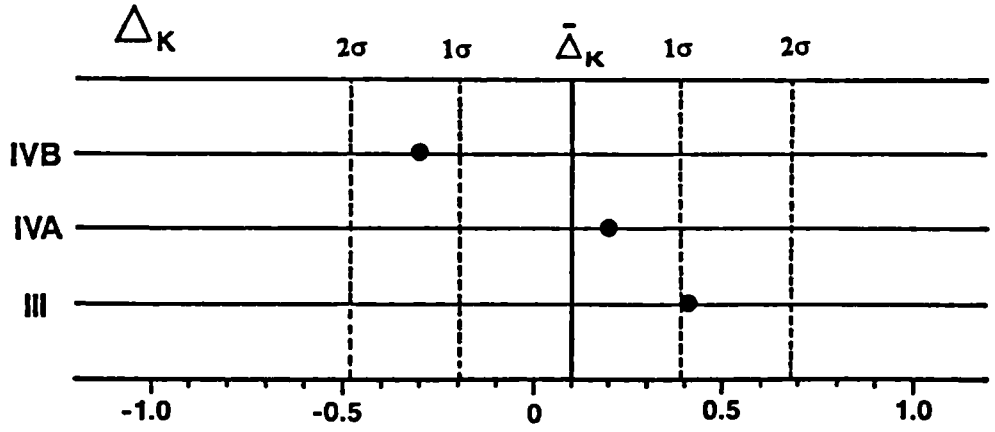


FIGURE 5.36 Δ_K values of Stage III (South Furious area), Stage IVA (South Furious area) and Stage IVB (Rusa Timur-1 area) kerogens.

$\Delta_{K\text{-}SAT} = (\delta^{13}C \text{ kerogen})_{measured} - (\delta^{13}C \text{ saturates})_{measured}$

$\Delta_{K\text{-}ARO} = (\delta^{13}C \text{ kerogen})_{measured} - (\delta^{13}C \text{ aromatics})_{measured}$

(after Stahl, 1978)

1) STAGE IVB

$(\delta^{13}C \text{ kerogen})_{measured} = -27.3\ ^{o}/_{oo}$

$(\delta^{13}C \text{ saturates})_{measured} = -27.8\ ^{o}/_{oo}$

$(\delta^{13}C \text{ aromatics})_{measured} = -27.4\ ^{o}/_{oo}$

$\Delta_{K\text{-}SAT} = -27.3 - (-27.8) = 0.5\ ^{o}/_{oo}$

$\Delta_{K\text{-}ARO} = -27.3 - (-27.4) = 0.1\ ^{o}/_{oo}$

2) STAGE IVA

$(\delta^{13}C \text{ kerogen})_{measured} = -26.8\ ^{o}/_{oo}$

$(\delta^{13}C \text{ saturates})_{measured} = -27.4\ ^{o}/_{oo}$

$(\delta^{13}C \text{ aromatics})_{measured} = -27.2\ ^{o}/_{oo}$

$\Delta_{K\text{-}SAT} = -26.8 - (-27.4) = 0.6\ ^{o}/_{oo}$

$\Delta_{K\text{-}ARO} = -26.8 - (-27.2) = 0.4\ ^{o}/_{oo}$

3) STAGE III

$(\delta^{13}C \text{ kerogen})_{measured} = -26.6\ ^{o}/_{oo}$

$(\delta^{13}C \text{ saturates})_{measured} = -27.4\ ^{o}/_{oo}$

$(\delta^{13}C \text{ aromatics})_{measured} = -27.2\ ^{o}/_{oo}$

$\Delta_{K\text{-}SAT} = -26.6 - (-27.4) = 0.8\ ^{o}/_{oo}$

$\Delta_{K\text{-}ARO} = -26.6 - (-27.2) = 0.6\ ^{o}/_{oo}$

$\therefore \Delta_{K\text{-}SAT} = 0.63$

$1\sigma = 0.12\ ^{o}/_{oo}$

$2\sigma = 0.24\ ^{o}/_{oo}$

$\therefore \Delta_{K\text{-}ARO} = 0.37$

$1\sigma = 0.21\ ^{o}/_{oo}$

$2\sigma = 0.42\ ^{o}/_{oo}$

For the kerogen and oil to be genetically related, the $\Delta_{K\text{-}SAT}$ and $\Delta_{K\text{-}ARO}$ values should be within 2σ limits (Stahl, 1978) where:

$\Delta_{K\text{-}SAT}$: Lower limit = 0.63 - 0.24 = $0.39\ ^{o}/_{oo}$

Upper limit = 0.63 + 0.24 = $0.87\ ^{o}/_{oo}$

$\Delta_{K\text{-}ARO}$: Lower limit = 0.37 - 0.42 = $-0.05\ ^{o}/_{oo}$

Upper limit = 0.37 + 0.42 = $0.79\ ^{o}/_{oo}$

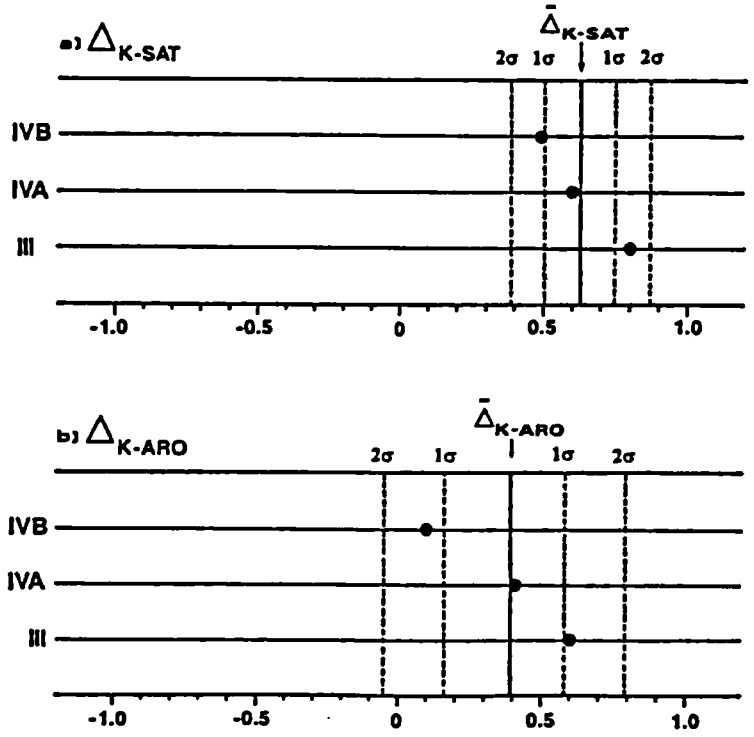


FIGURE 5.37 (a) $\Delta_{K\text{-}SAT}$ and (b) $\Delta_{K\text{-}ARO}$ values of Stage III (South Furious area), Stage IVA (South Furious area) and Stage IVB (Rusa Timur area) kerogens and hydrocarbon fractions.

- the almost total absence of marine organic matter even in the deep marine sequences, apart from some foraminifera linings (useful as a paralic/marine environment indicator) and traces of amorphous organic matter (<1%)

Analyses of deeper sediments are hampered by the fact that no well has penetrated Stage I and Stage II sediments. Even for the Stage III sediments, only the top was penetrated by the South Furious wells. For Stage IV sediments, those younger than sub-Stage IVD are excluded from the analyses for they are thought to be too young and therefore, immature. This assumption was proven to be correct by the low pyrolysis Tmax values obtained for even the deepest samples analysed. Bulk analyses results indicate that Stage III and Stage IV sediments investigated in this study have generally poor to marginal source quality with gas being the major product, based on the generally low Hydrogen Index values. This does not explain the presence of hydrocarbons in the Sabah Basin. There are several conditions which can cause the Hydrogen Index values to be low :

a) The over maturity of the kerogen in the samples

As kerogen goes through the oil generation window towards the over-mature zone, its hydrogen content will reduce due to maturation and hydrocarbon-generation process. Pyrolysis of over mature kerogens will yield small S2 peaks which, in turn, results in low corresponding Hydrogen Index values. In this study, however, over mature kerogens cannot be the reason for the low Hydrogen Index values as Tmax values indicate that the sediments are generally immature, with most of them being in the immature (<420°C) and the marginally-mature zones (430-440°C). Elemental compositions and vitrinite reflectance values of kerogens confirm that none of the samples analysed have reached the oil generation window.

b) The sediments analysed do not possess any source potential

One can also say that the low Hydrogen Index values may actually be due to the non-source potential of the sediments under investigation which, in effect, suggests that the source for Sabah Basin hydrocarbons is located deeper in the unpenetrated pile of Tertiary sediments. Results from Stage III samples of the South Furious wells indicate that it is very much like the rest of the sediments overlying it in terms of the quantity and quality of organic matter. This, however, only applies directly to the top of Stage III; inferring this to the rest of the unpenetrated Stage III sequence may, or may not, be strictly valid.

The chance of acquiring samples of the deeper Stage III and older sediments is rather remote as the industry presently considers it as the economic basement. Only with the failure to identify any source rock horizons in the overlying sequences should the Stage III, and possibly older Stage II sediments, be seriously considered as having

hydrocarbon-source potentials. As such, any assumptions about their source rock potentials will be rather limited and in the realms of uncertainty due to the present lack of information.

c) Intermixing between good and poor quality kerogen, with the poor quality kerogen being relatively more abundant.

Hydrogen Index is calculated from the S2 peak obtained from pyrolysis of crushed whole rock sample and dividing that value by the sample's TOC content. Being a bulk parameter, the resulting Hydrogen Index value may not reflect the true kerogen composition, especially in situations where the presence of good quality kerogen is overwhelmed by the abundance of dead organic carbon. Evidence from petrographic studies of kerogen concentrates indicate that kerogen intermixing (Case *(c)*) is the most likely reason for the low Hydrogen Index values obtained (**Appendix II**). Kerogen intermixing is also reflected by Hydrogen Index values of Stages III and IVA of the South Furious wells. Being in a more proximal location compared to Tembungo, Rusa Timur and Gajah Hitam areas, South Furious must have received copious amounts of organic matter from land which were likely to be of a mixed nature in terms of their source potentials. Degradation of good quality organic matter is more efficient in this relatively more oxic environment and cause the good quality organic matter to be 'masked' by the more abundant poor quality organic matter. This inevitably results in the 'down-grading' of Hydrogen Index values of the sediments.

The deep marine sub-Stage IVA sediments of Rusa Timur, for comparison, has a relatively higher average Hydrogen Index value (**Table 5.31**). Since only input from higher plants was observed in all the samples, the slight increase in hydrogen content of Rusa Timur's sub-Stage IVA is attributed to the preferential sorting of good quality land-derived organic matter (hydrogen-rich protective coatings like waxes, cuticles and resins) from the poor ones before being deposited in the sediments.

Table 5.31 Average screening results.

Well	Stage / Sub-Stage	TOC (wt%)	Generation Potential (mg/g)	Hydrogen Index (mg/gTOC)	Tmax (°C)
T1		1.05	0.69	68	427
T2		0.75	0.95	80	409
T6	IVD	0.52	0.30	48	419
RT1		0.87	2.34	169	426
GH1		0.82	0.41	47	425
T1		0.78	0.81	80	436
T2		1.00	1.94	138	417
T6	IVC	0.72	0.58	62	428
RT1		1.00	1.97	152	422
GH1		0.84	0.50	85	440

Table 5.31 Average screening results - continued.

Well	Stage / Sub-Stage	TOC (wt%)	Generation Potential (mg/g)	Hydrogen Index (mg/gTOC)	Tmax (°C)
RT1	IVB	0.84	1.60	142	425
SF2		1.44	1.08	59	414
SF3	IVA	3.07	2.52	62	422
RT1		0.83	1.47	154	425
SF2	III	2.24	1.70	68	417
SF3		1.60	1.60	87	425

5.5 Summary

Analytical results have shown that coastal plain sediments which form the bulk of sub-Stage IVA sediments in the South Furious area represents the main potential source rocks responsible for the hydrocarbon accumulations in Sabah Basin. Other potential source rocks within the Stage IV sediments are the deep marine sediments containing land-derived organic matter of sub-Stage IVB in the Rusa Timur area, sub-Stage IVC in Tembungo and Rusa Timur areas and sub-Stage IVD in the Rusa Timur area **(Table 5.31)**. The source potential of the deep marine Stage III sediments do not seem to differ very much from sub-Stage IVA. However, more samples from Stage III need to be analysed for this preliminary indications can be confirmed.

The hydrocarbon generating potentials of these potential source rocks are only poor to marginal, with the majority of samples indicated to have genetic potentials less than sufficient to give rise to commercial hydrocarbon accumulations (Hunt, 1979; Tissot & Welte, 1984; Kinghorn, 1983, Peters, 1986). Poor source rocks have been shown to be capable of generating significant quantities of hydrocarbons, where they were effective at an overall lower organic matter quality than generally considered essential. This type of source rocks, composed mainly of terrigenous organic matter of low to moderate oil-generating potential, include the Mahakam Delta, Kalimantan (Combaz & de Matharel, 1978; Hoffman *et. al.*, 1984), Australian basins (Thomas, 1982; Thompson *et. al.*, 1985; Shanmugam, 1985; Philp & Gilbert, 1986; Powell *et. al.*, 1991; Powell & Boreham, 1991), Indonesian basins (Robinson, 1987; Noble *et. al.*, 1991) and the Niger Delta (Bustin, 1988).

In Sabah Basin, the generally poor hydrocarbon-generating potentials are compensated by the approximately 2000m thick (South Furious, sub-Stage IVA) of low-yield source rocks present, with effective migration and drainage provided by numerous interbedded sandstones and possible rapid hydrocarbon generation due to high sedimentation and burial rates resulting from both sedimentary and tectonic loading (Azim-Ibrahim, 1994).

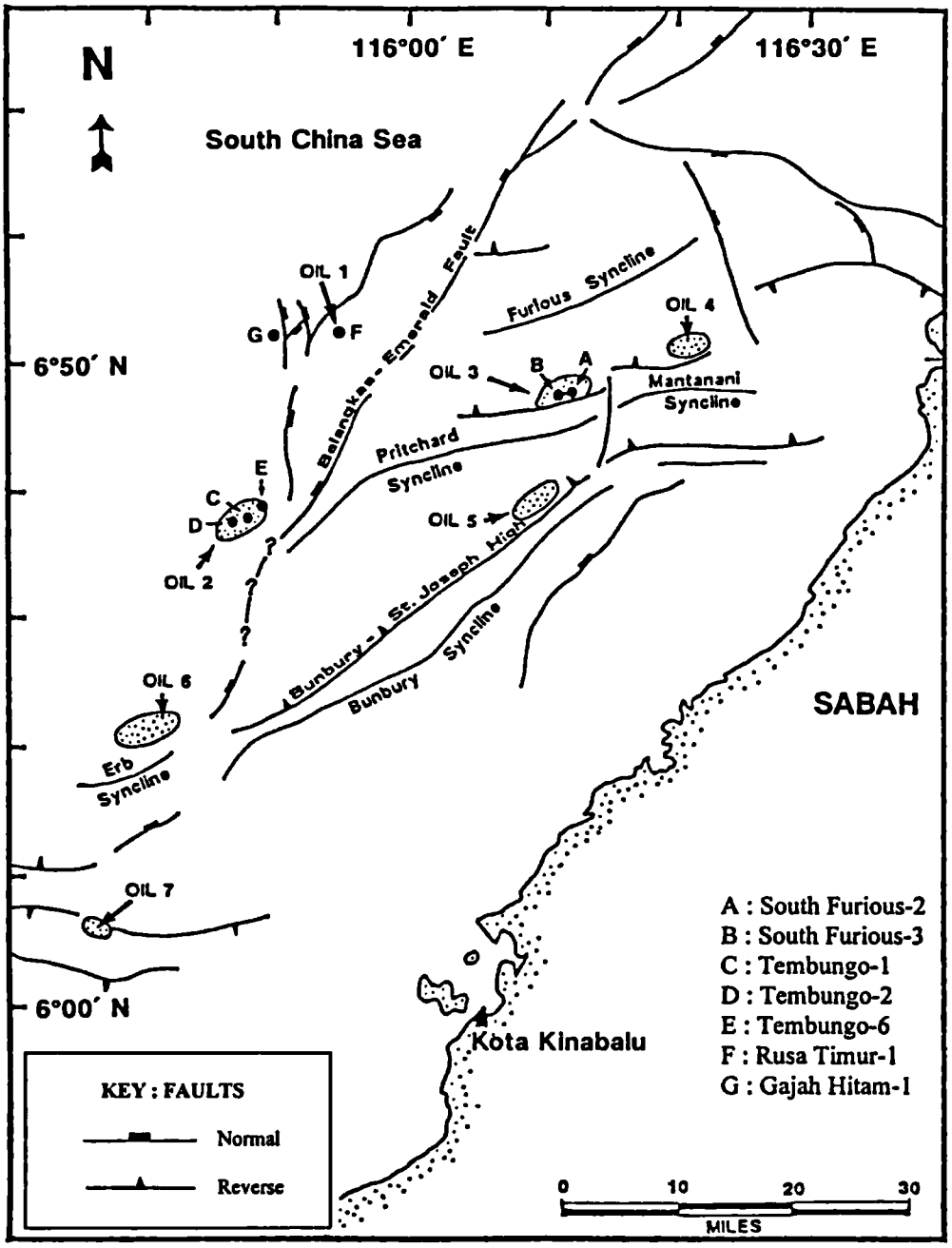
CHAPTER SIX.

BIOLOGICAL MARKER ANALYSIS FROM GAS CHROMATOGRAPHY-MASS SPECTROMETRY

6.1 Introduction

Gas chromatography-mass spectrometry allows the characterisation of oils and sediment extracts at the molecular level and provides data which can be utilised for oil-oil and oil-extract correlations, maturity level determinations as well as providing information on depositional environment conditions. The success of this method is attributed to its ability to gather reliable information from small sample volumes. General guidelines for interpreting results from mass fragmentograms have been laid out by various workers (Philp; 1985; Seifert & Moldowan; 1986; Waples & Machihara, 1991). However, being a relatively young science, some exceptions to, and deviations from, the guidelines have been reported (Grantham, 1986b; Wang *et. al.*, 1991; Anuar *et. al.*, 1993). It is expected that, as this method is used by more researchers, a clearer picture on biomarker behaviour with respect to depositional conditions, burial and thermal maturation will emerge. As a precaution to erroneous interpretations, results from the biomarker analyses here are supplemented with data obtained from the other geochemical methods utilised in this study.

Seven oil samples from different areas in the Sabah Basin - Rusa Timur (Oil 1), Tembungo (Oil 2), South Furious (Oil 3), Barton (Oil 4), St. Joseph (Oil 5), Erb West (Oil 6) and Ketam (Oil 7) **(Figure 6.1)** - and twenty-six sediment extract samples from six wells (South Furious-2, South Furious-3, Tembungo-1, Tembungo-2, Rusa Timur-1 and Gajah Hitam-1) were analysed, monitoring for triterpanes (m/z 191) and steranes (m/z 217). The sediment extracts are thought to be non-indigenous hydrocarbons based on the incompatibility of high Production Index values with low pyrolysis Tmax and vitrinite reflectance values, indicating the sediments from which the hydrocarbons were extracted are immature. Furthermore, Carbon Preference Index (CPI) values determined from two different methods (Bray & Evans, 1961; Louis, 1967), and Odd Even Preference (OEP) values (Scalan & Smith, 1970) vary between 1.0-1.2, thus providing evidence that the extracts are mature hydrocarbons which have stained the immature sediments during their migration from elsewhere. As a result of this 'false bitumen', oil-sediment extract correlation will not be attempted for they will be



KEY: OIL 1 = Rusa Timur
OIL 2 = Tembungo
OIL 3 = South Furious
OIL 4 = Barton
OIL 5 = St. Joseph
OIL 6 = Erb West
OIL 7 = Ketam

FIGURE 6.1 Well and oil sample locations, Sabah Basin, Malaysia.

incorrect. The aims for this biological marker study are therefore limited to determining the source of organic matter input, the maturity levels of the oils and observing any influence of migrated hydrocarbons on maturity ratios determined from sediment extracts.

6.2 Triterpane fingerprints of the sediment extracts and oils

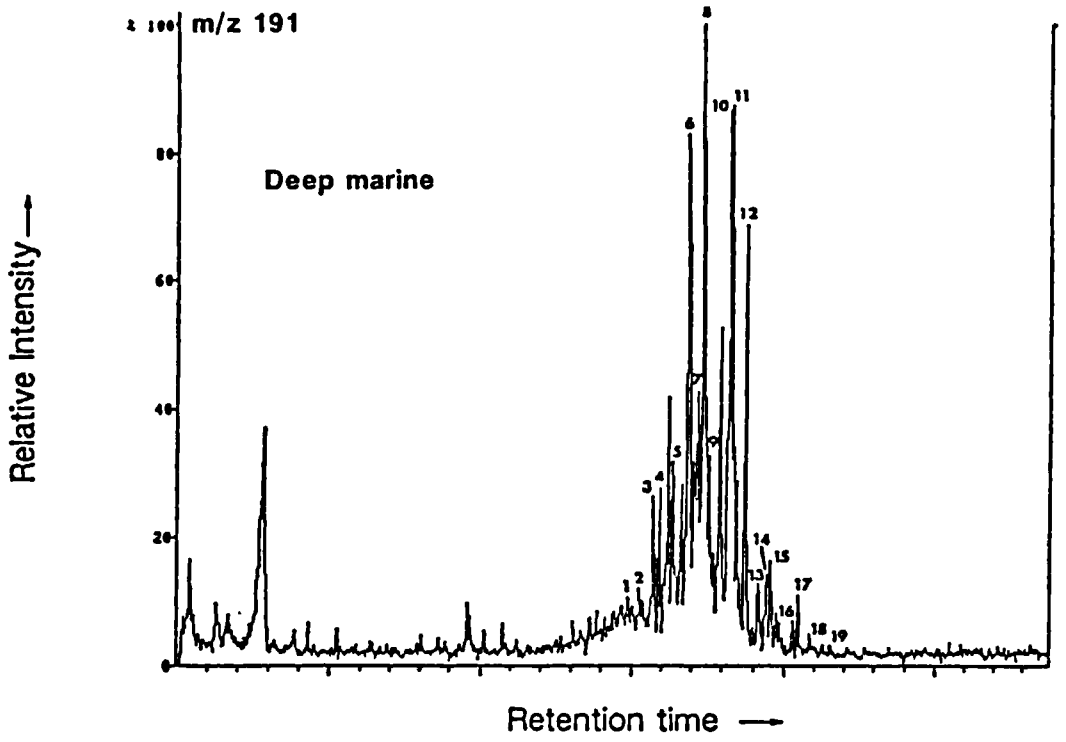
6.2.1 Results : Sediment Extracts of Stage III

Three sediment extracts were obtained from South Furious-2 well. The resulting m/z 191 triterpane mass fragmentograms are shown in **Figure 6.2**, displaying the dominance of regular 17α(H)-hopane; the key to peak identities is given in **Table 6.1**. In sample 1871m (6138ft), the C_{29} 17α(H)-hopane (norhopane, peak 8) predominates over the C_{30} 17α(H)-hopane (peak 11). This situation is reversed in sample 1921m (6302ft) where the C_{30} 17α(H)-hopane is more abundant than the C_{29} 17α(H)-norhopane. Sample 1979m (6493ft) again shows a variation with these two peaks occurring in almost equal abundance. These slight differences can be attributed to minor variations in the source material (Seifert & Moldowan, 1978). The optical analysis of isolated kerogen from samples 1871m (6138ft) and 1921m (6302ft) showed differences in the relative amounts of exinite, vitrinite and inertinite **(Table 5.3)**. Sample 1871m (6138ft) has 30% exinite, 25% vitrinite and 45% inertinite while sample 1921m (6302ft) has 60% exinite, 25% vitrinite and 15% inertinite. It should also be noted that an unknown triterpane, peak 6, is dominant in samples 1921m (6302ft) and 1979m (6493ft).

TABLE 6.1 Key to peak identities for triterpane (m/z 191) and sterane (m/z 217) mass fragmentograms shown in this study.

Triterpane m/z 191 distribution	
Peak No.	Compound
1	Resin W (cis-cis-trans bicadinane)
2	Ts
3	Tm
4	Resin T (trans-trans-trans bicadinane)
5	Resin R
6	Unknown C_{30}-triterpenoid
7	Unknown C_{30}-triterpenoid
8	C_{29} 17α(H)21β(H)-hopane
9	Unknown C_{30}-triterpene
10	18α(H)-oleanane
11	C_{30} 17α(H)21β(H)-hopane
12	C_{30} 17β(H)21α(H)-hopane (moretane)
13	Unknown C_{30}-triterpenoid
14	C_{31} 17α(H)21β(H)-homohopane, 22S
15	C_{31} 17α(H)21β(H)-homohopane, 22R
16	C_{32} 17α(H)21β(H)-bishomohopane, 22S

(a) 1871m/6138ft



(b) 1921m/6302ft

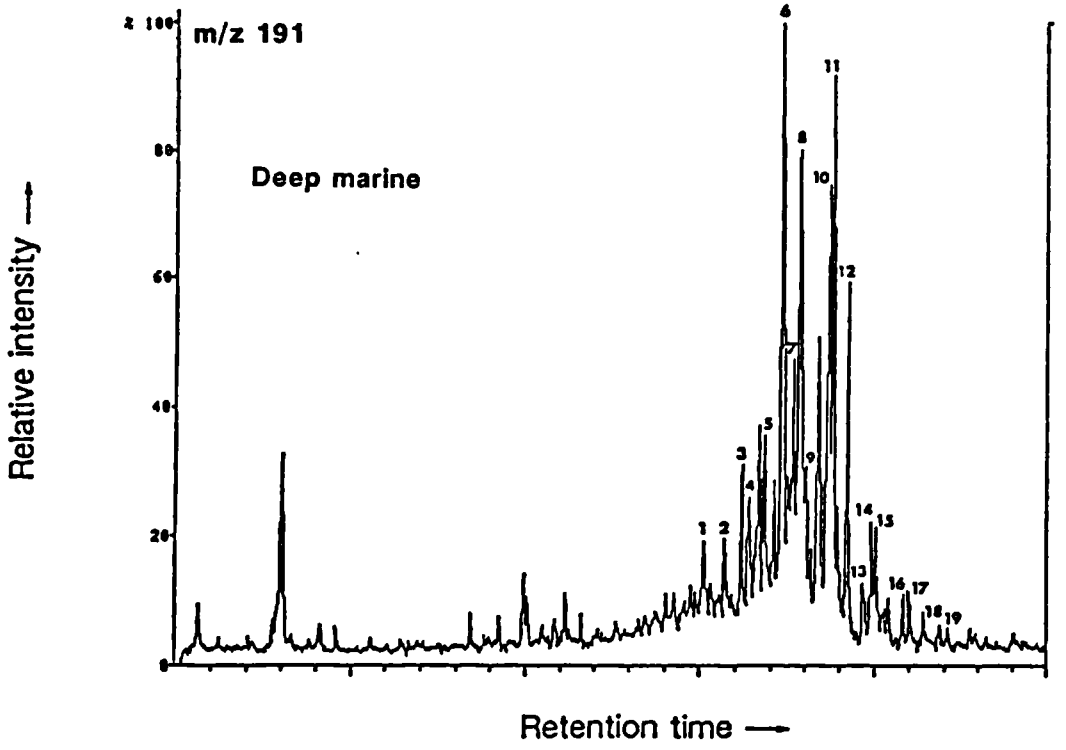


FIGURE 6.2 Triterpane (m/z 191) distributions of Stage III sediment extract samples obtained from South Furious-2 well, (a) 1871m/6138ft, (b) 1921m/6302ft and (c) 1979m/6493ft.

(c) 1979m/6493ft

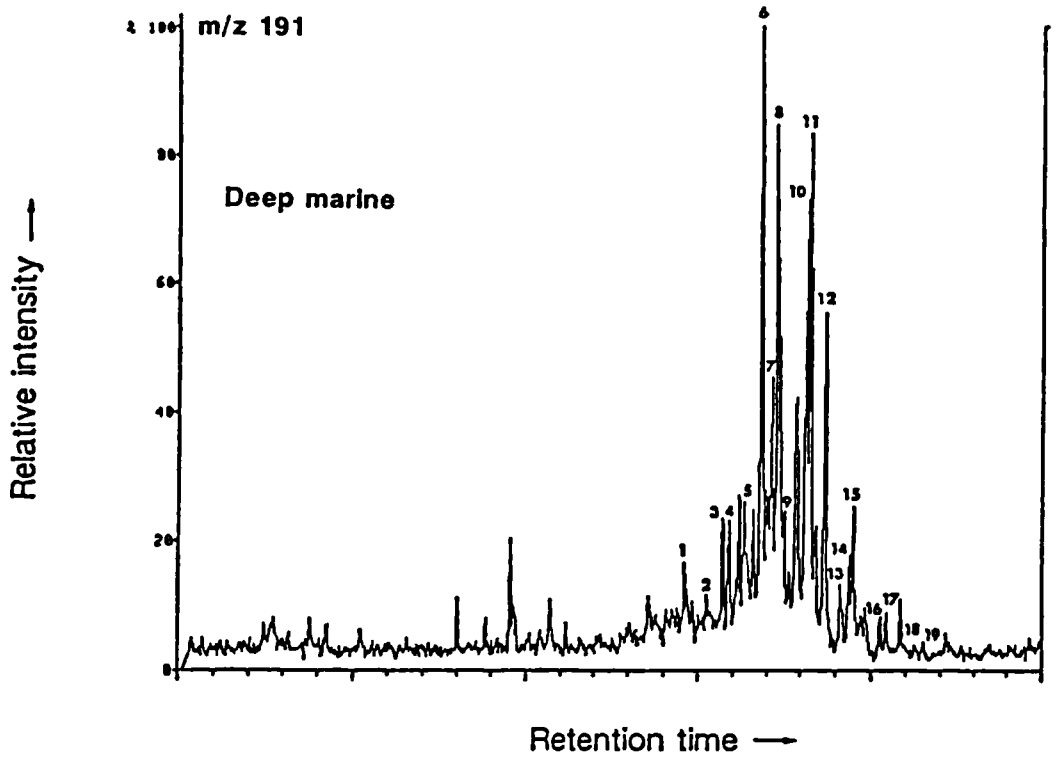


FIGURE 6.2 Continued

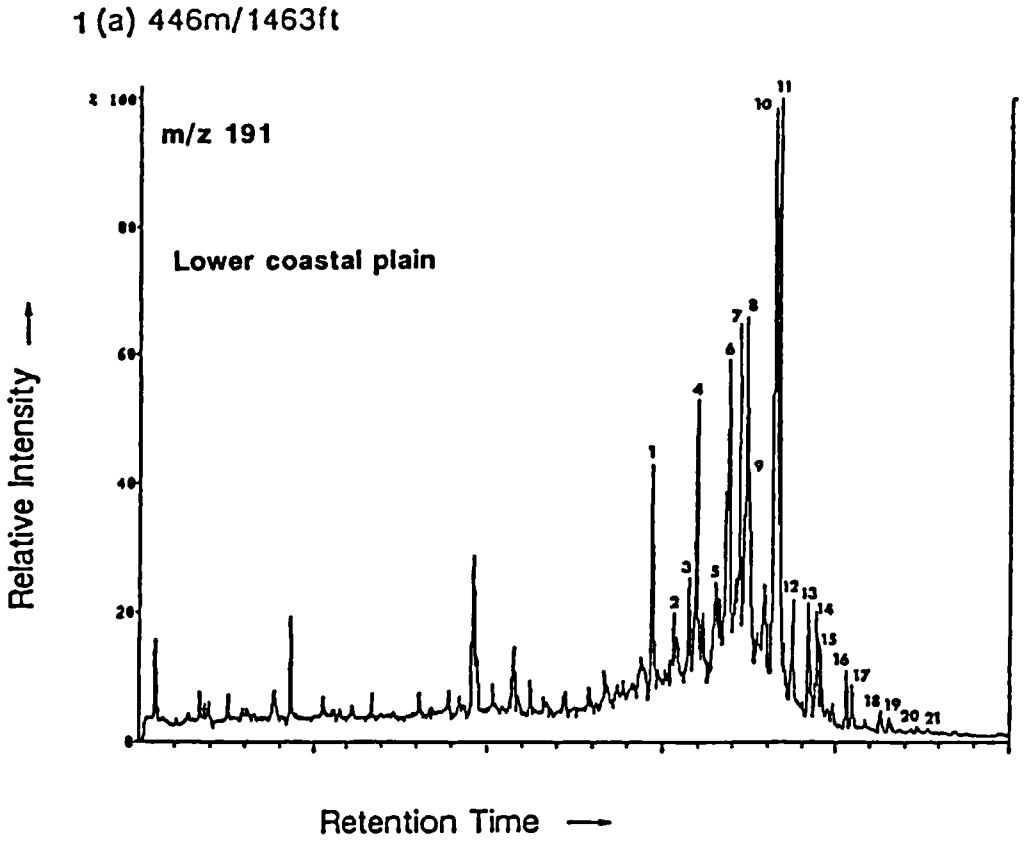
TABLE 6.1 Key to peak identities for triterpane (m/z 191) and sterane (m/z 217) mass fragmentograms shown in this study - continued.

Triterpane m/z 191 distribution	
Peak No.	Compound
17	C_{32} 17α(H)21β(H)-bishomohopane, 22R
18	C_{33} 17α(H)21β(H)-trishomohopane, 22S
19	C_{33} 17α(H)21β(H)-trishomohopane, 22R
20	C_{34} 17α(H)21β(H)-tetrakishomohopane, 22S
21	C_{34} 17α(H)21β(H)-tetrakishomohopane, 22R
22	C_{35} 17α(H)21β(H)-pentakishomohopane, 22S
23	C_{35} 17α(H)21β(H)-pentakishomohopane, 22R
Sterane m/z 217 distribution	
Peak No.	Compound
24	Resin W (cis-cis-trans bicadinane)
25	Resin T (trans-trans-trans bicadinane)
26	C_{29} 5α(H)14α(H)17α(H)-cholestane, 20S
27	C_{29} 5α(H)14β(H)17β(H)-isocholestane, 20R
28	C_{29} 5α(H)14β(H)17β(H)-isocholestane, 20S
29	C_{29} 5α(H)14α(H)17α(H)-cholestane, 20R

The presence of oleanane and resins W, T and R in all three samples provide evidence of input from land-derived organic matter. Resins W and T were identified by van Aarssen *et. al.* (1990, 1992) as pentacyclic triterpanes known as bicadinanes, derived from dammar resins which originate from resin-producing tropical plants such as *Dipterocarpaceae*. Oleananes arise from the geological transformation of pentacyclic triterpenoids typical of higher plants (Ekweozor & Udo, 1988). They have been identified in rocks and oils from the Far East (Wang *et. al.*, 1991), Southeast Asia (Grantham *et. al.*, 1983; Jamil *et. al.*, 1991; Anuar *et. al.*, 1993), Niger Delta (Nwachukwu & Chukwura, 1986) and Brazil (Mello *et. al.*, 1988a, 1988b).

6.2.2 Results : Sediment Extracts of Sub-Stage IVA

Seven samples from South Furious-2 and six from South Furious-3, representing lower coastal plain sediments, and one sample from Rusa Timur-1, representing bathyal sediments, were extracted. Their triterpane distributions are shown in **Figure 6.3.** Samples 446m (1463ft), 1002m (3287ft) and 1293m (4242ft) of South Furious-2, and sample 2040m (6693ft) of Rusa Timur-1 are quite similar to each other, except for the dominance of oleanane over C_{30} hopane, the absence of Ts (peak 2) and Tm (peak 3) in sample 2040m (6693ft). The presence of terrestrially-derived peaks in bathyal sediments has also been reported in southern Nigerian basins where oleananes were found to be present in marine litho-units (Ekweozor & Udo, 1988). Their resistance to biodegradation and low densities are largely responsible for their preservation and



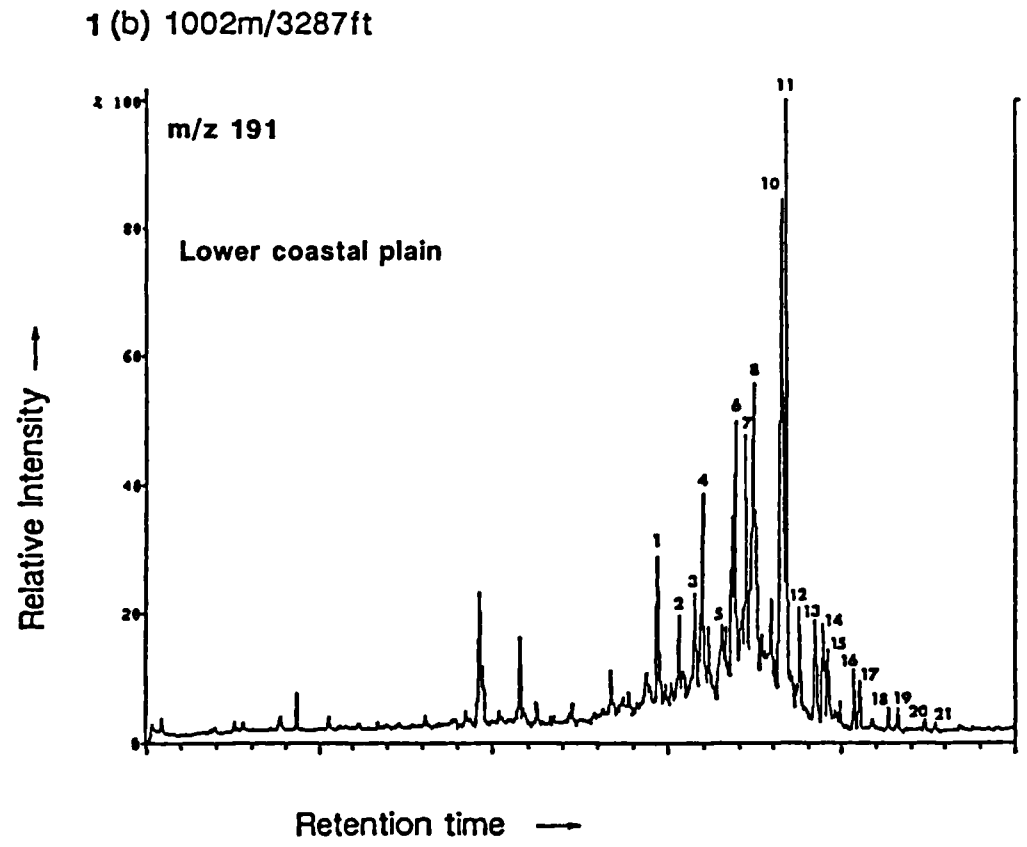
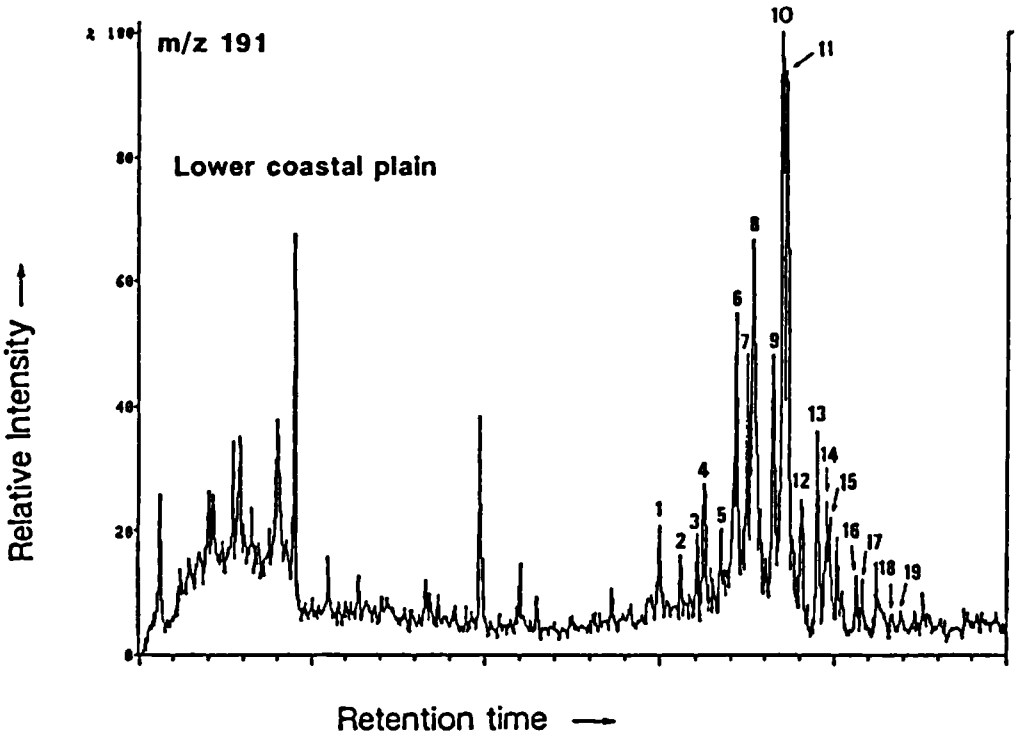


FIGURE 6.3 Triterpane (m/z 91) distributions of Stage IVA sediment extract samples obtained from (1) South Furious-2 well (a to g), (2) South Furious-3 well (a to f) and (3) Rusa Timur-1 well (a).

1(c) 1293m/4242ft



1(d) 1603m/5259ft

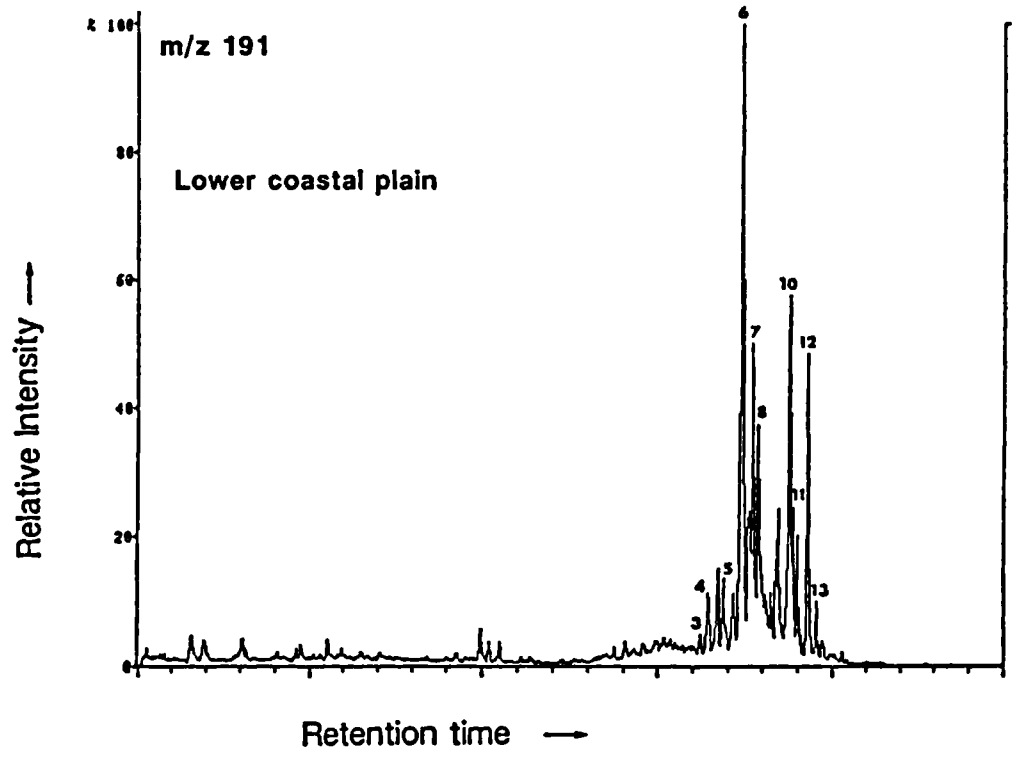
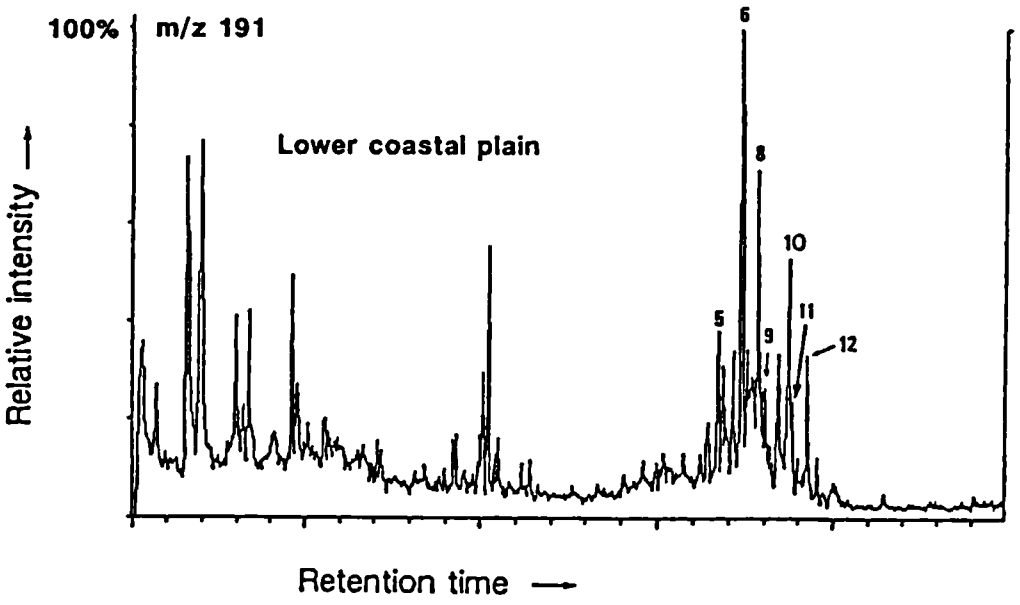


FIGURE 6.3 Continued.

1(e) 1644m/5394ft



1 (f) 1738m/5702ft

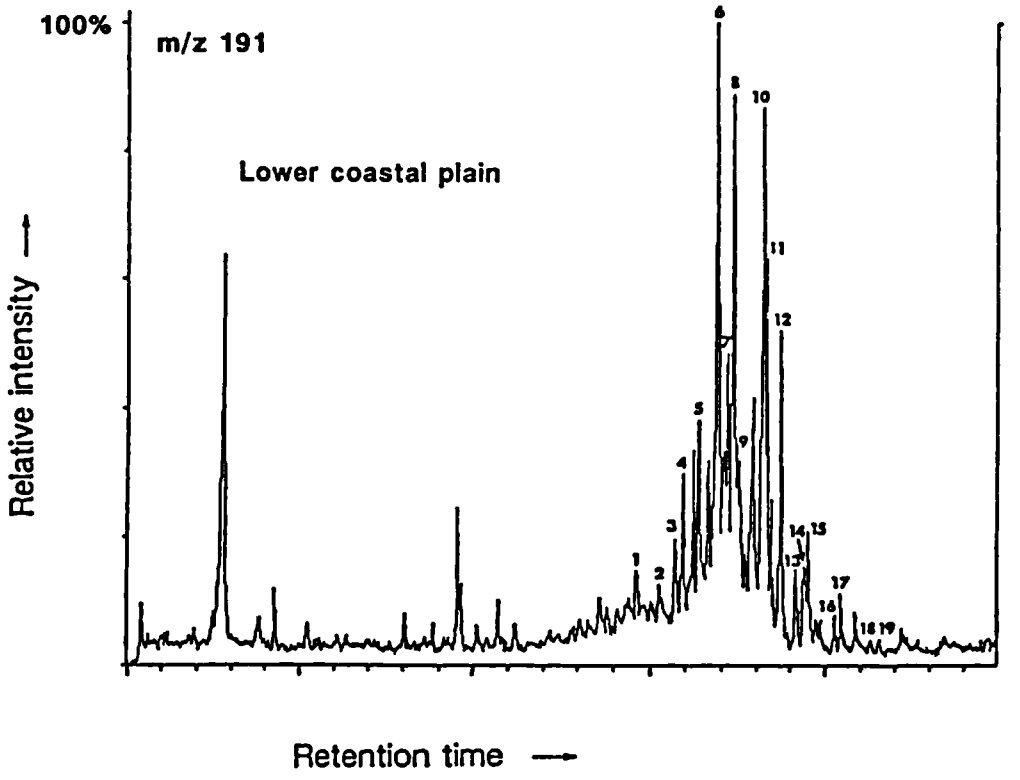


FIGURE 6.3 Continued.

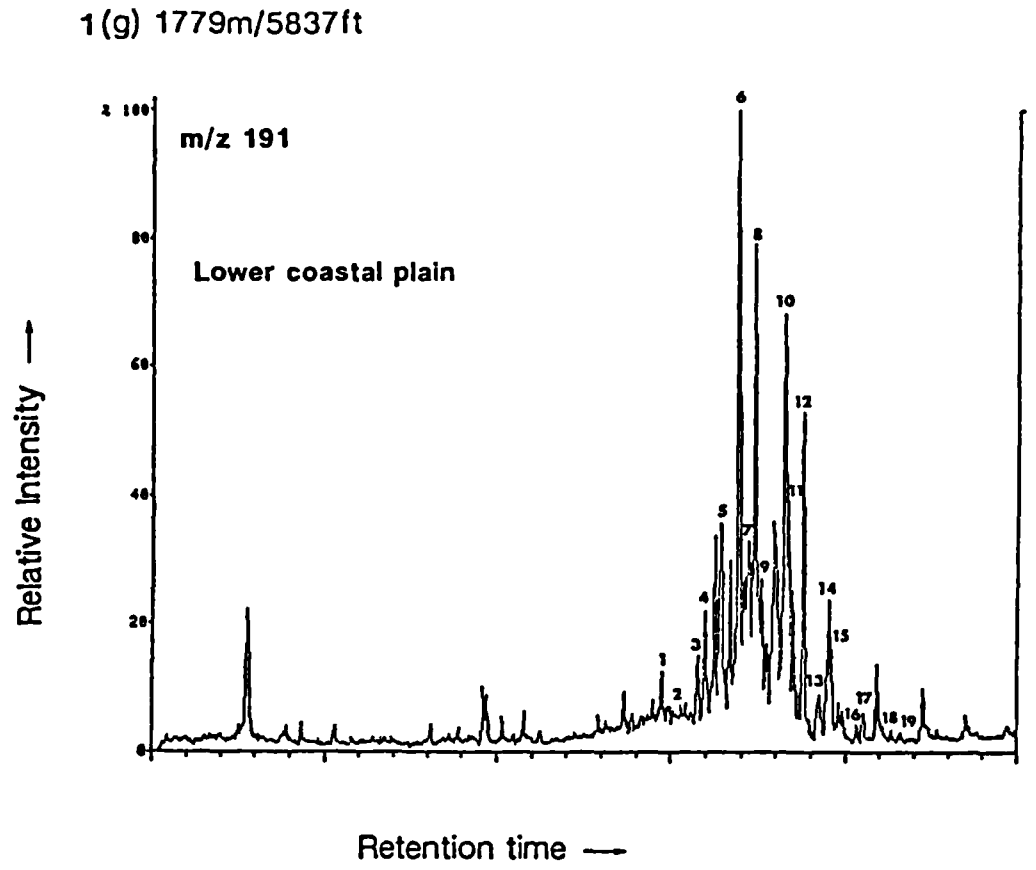
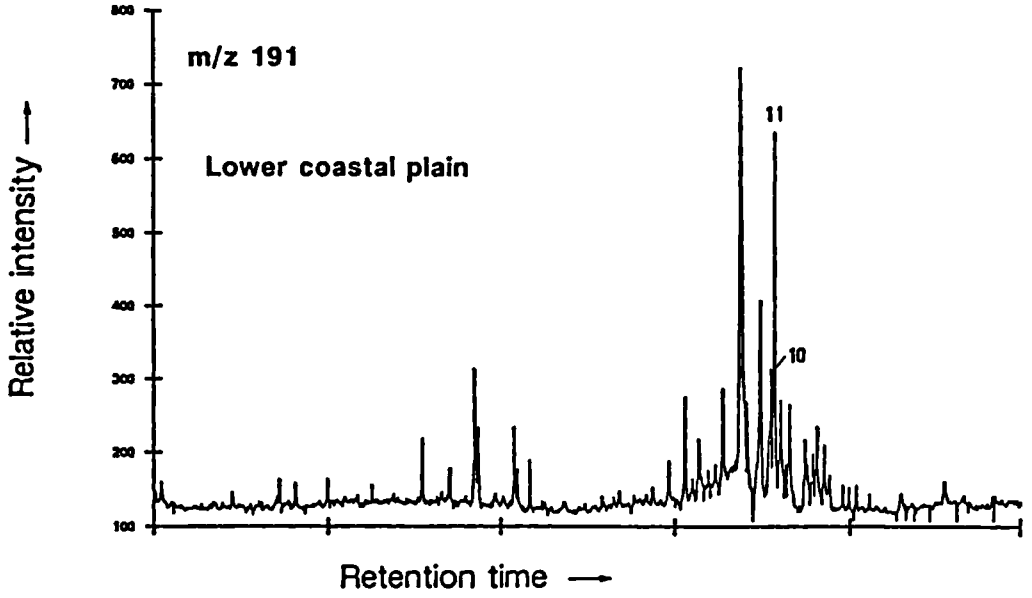


FIGURE 6.3 Continued.

2(b) 841m/2759ft



2(c) 1346m/4416ft

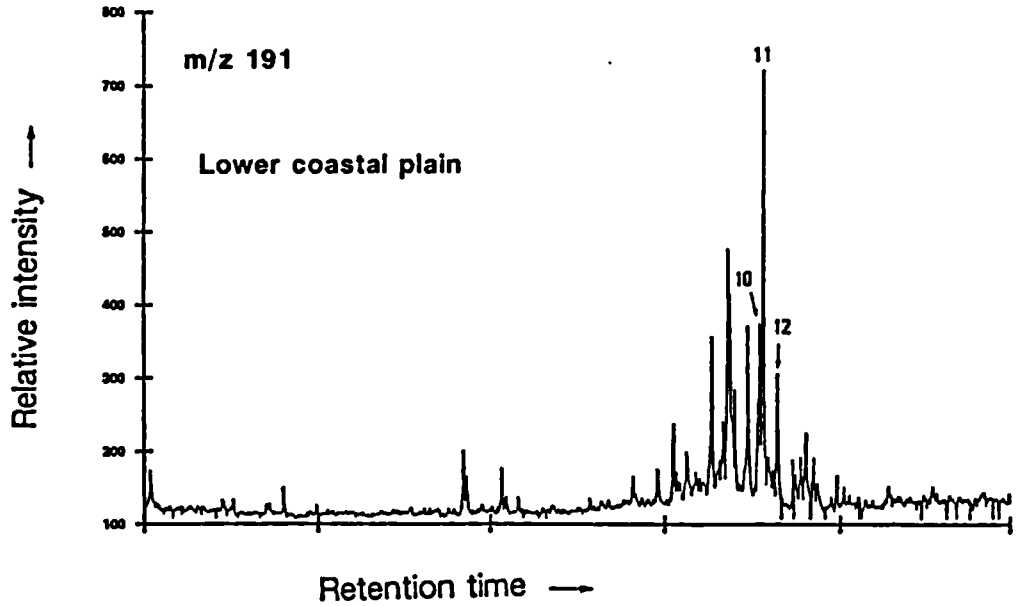
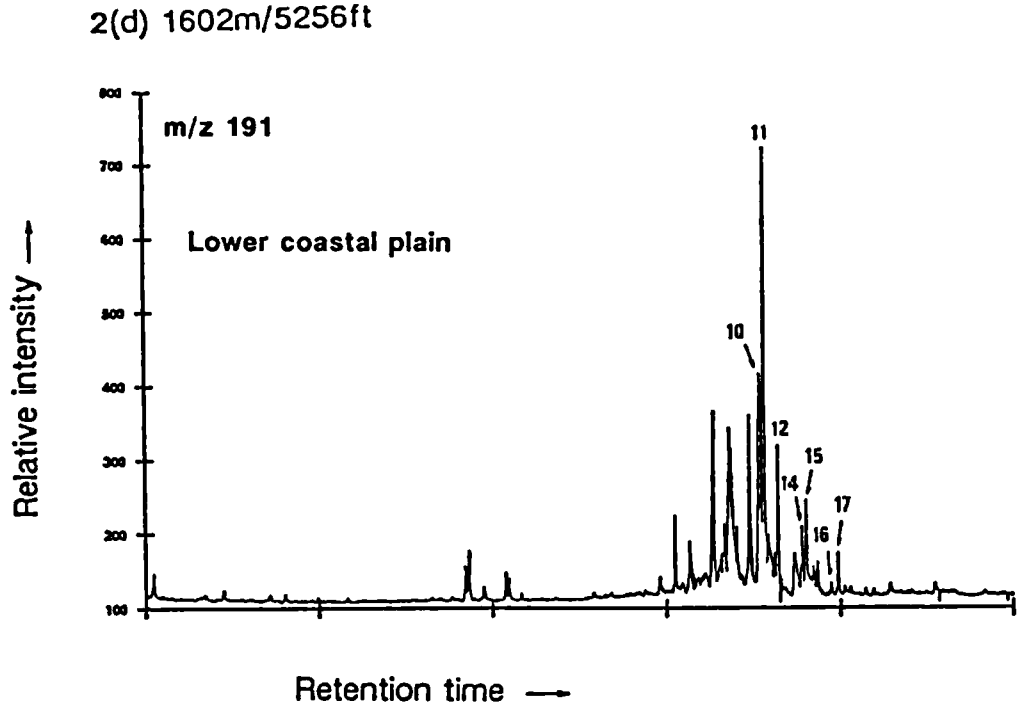


FIGURE 6.3 Continued.



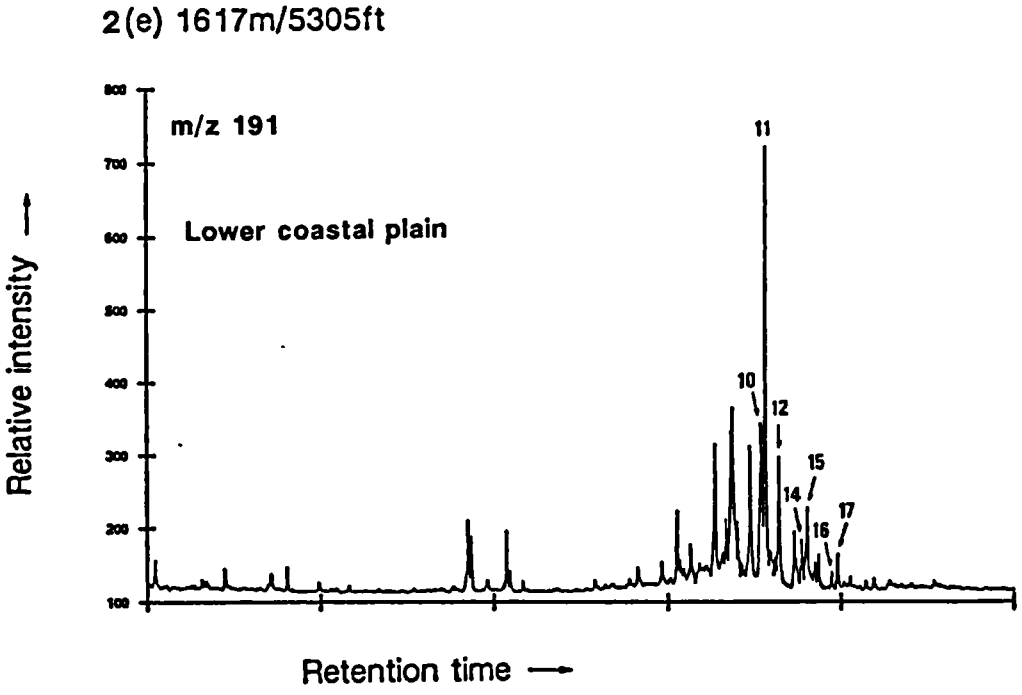
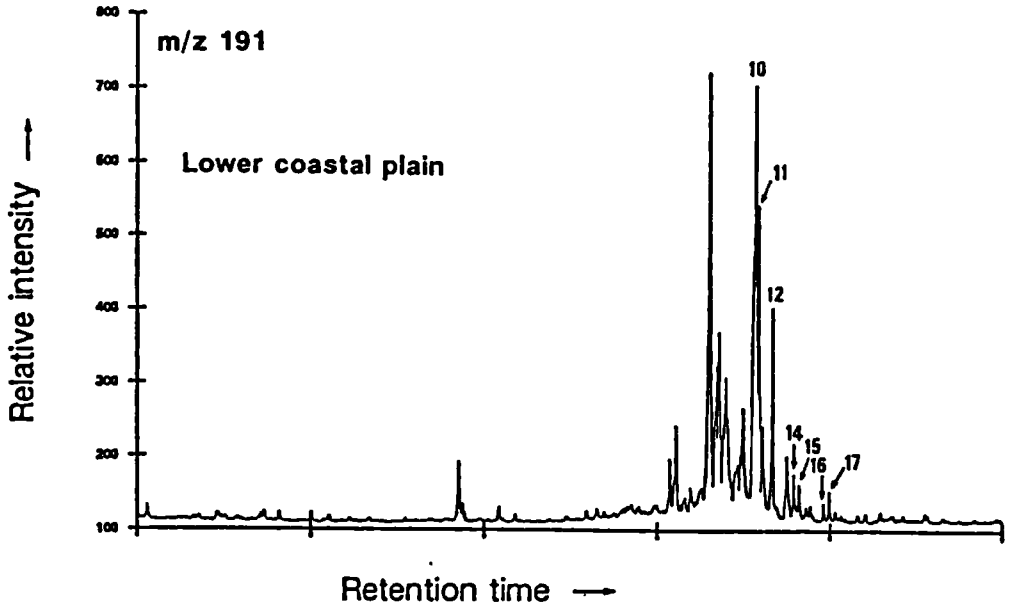


FIGURE 6.3 Continued.

2 (f) 2291m/7516ft



3(a) 2040m/6693ft

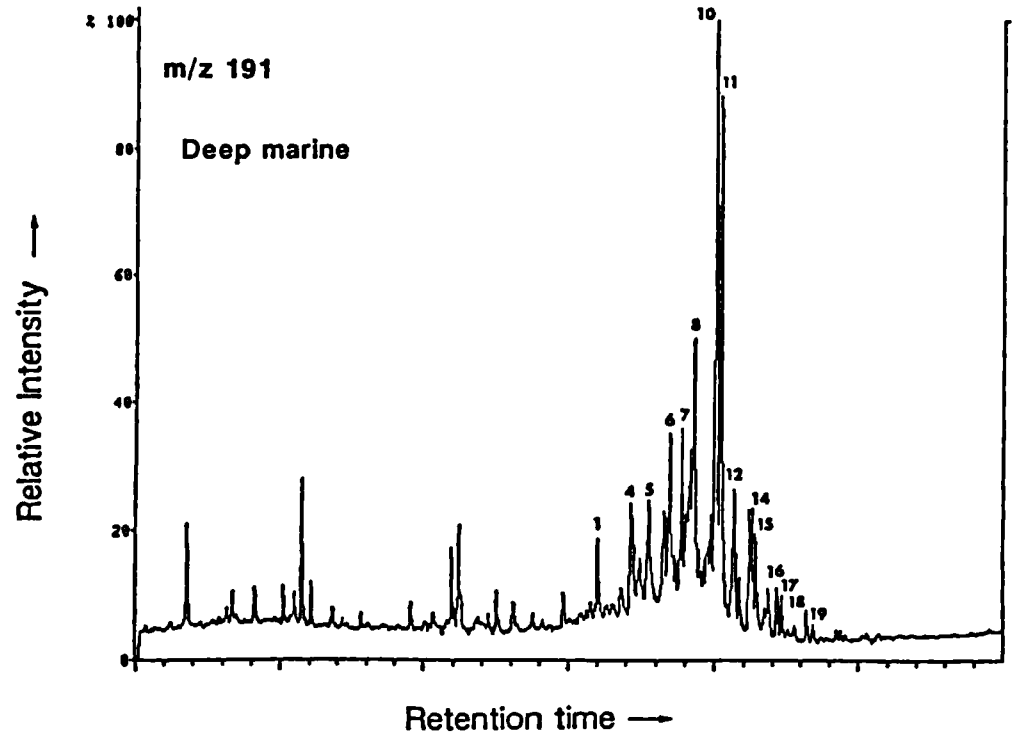


FIGURE 6.3 Continued.

incorporation into marine sediments. The remaining three samples, 1603m (5259ft), 1738m (5702ft) and 1779m (5837ft), all from South Furious-2, are similar by having the unknown triterpenoid (peak 6) as the most dominant peak. Samples 1603m (5259ft) and 1644m (5394ft) are slightly different by the absence of the homohopanes. The peak distributions of the six South Furious-3 samples are comparable with each other and with those of South Furious-2 and Rusa Timur-1. All the samples contain oleanane and resin peaks. **Figure 6.4** is the partial mass chromatograms for bicadinanes in sample 1002m/3287ft (sub-Stage IVA, South Furious-2) compared to those published by van Aarssen *et. al.* (1992), ascertaining the presence of bicadinanes in these samples (peak identities for **Figure 6.4** are in **Table 6.2**). The extracts also show the minor presence of tricyclic peaks, in all cases in lesser abundance compared to the pentacyclics.

Table 6.2 Key to **Figure 6.4**

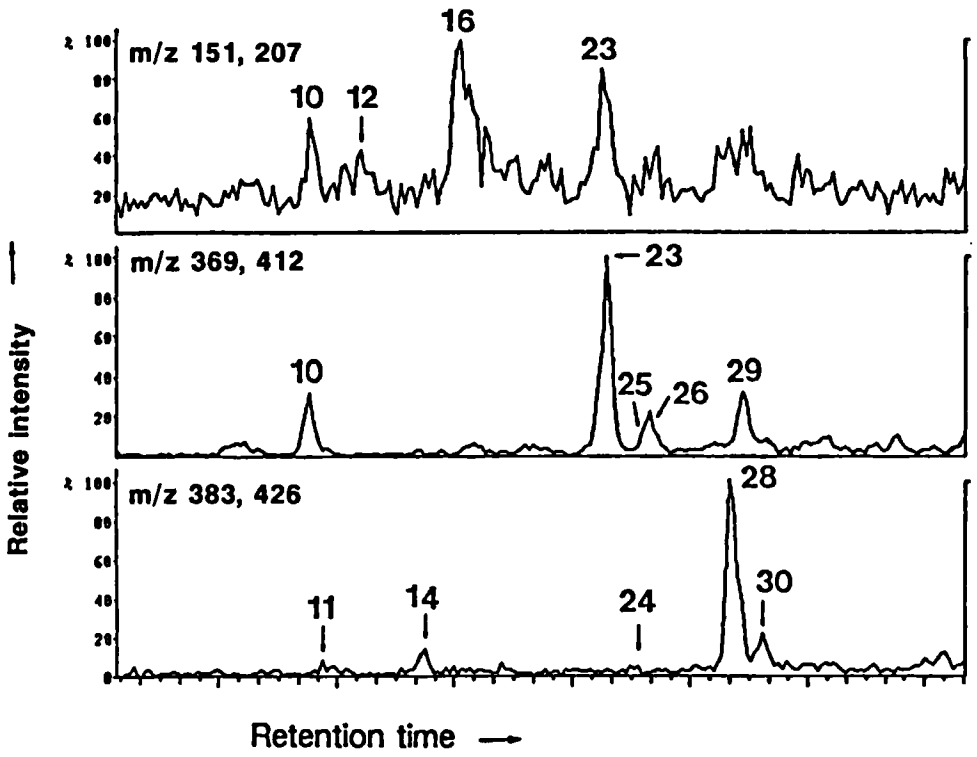
Peak No.	Compound
10	Resin W (cis-cis-trans bicadinane)
11	C_{31} bicadinane
12	C_{30} seco-bicadinane
14	C_{31} bicadinane
16	C_{30} seco-bicadinane
23	Resin T (trans-trans-trans bicadinane)
24	C_{31} bicadinane
25	C_{30} bicadinane
26	C_{30} bicadinane
28	C_{31} bicadinane
29	C_{30} bicadinane
30	C_{31} bicadinane

6.2.3 Results : Sediment Extracts of Sub-Stage IVB

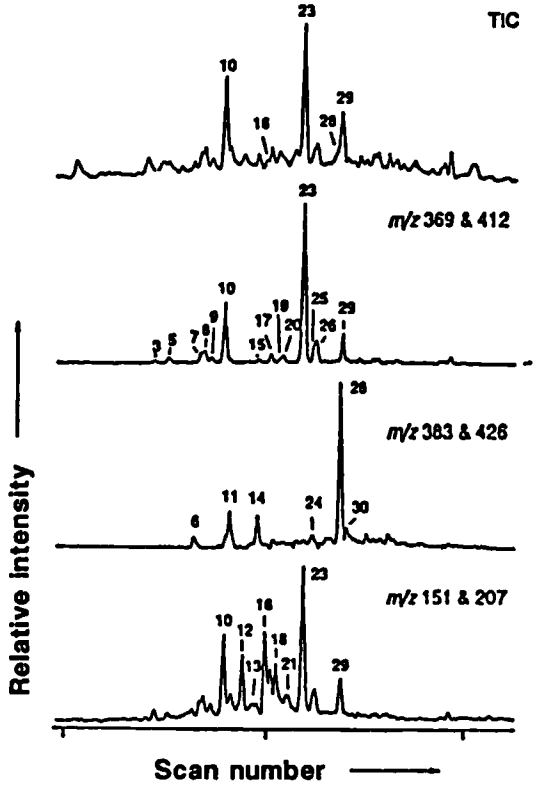
Only one sub-Stage IVB sample (1814m/5951ft) was obtained for extraction. This came from Rusa Timur-1 and represents deep marine shales. The triterpane distribution is shown in **Figure 6.5**, showing characteristics resembling those of the previous sub-Stages. The oleanane peak dominates the fragmentogram with some tricyclics present.

6.2.4 Results : Sediment Extracts of Sub-Stage IVC

Four extract samples, (one each from Tembungo-6 and Rusa Timur-1, and two from Gajah Hitam-1), were obtained but only three were analysed for their biomarker distributions (one from Rusa Timur-1 and two from Gajah Hitam-1). The sample from Tembungo-6 was not analysed because of its small volume which hindered satisfactory fractionation. The triterpane distributions are generally comparable (**Figure 6.6**), with all three samples showing the C_{30} 17α(H)-hopane (peak 11) to be dominant and the presence of some tricyclics. Sample 2117m (6946ft) has a rather large Tm peak (peak 3), and oleanane (peak 10) and resins (peaks 1, 4 and 5) are present in all the samples.



(a) Sample 1002m/3287ft (Stage IVA)



(b) Prabumulih crude sample, Sumatra, Indonesia (from van Aarssen et al, 1992)

FIGURE 6.4 Comparison between the resulting partial mass chromatograms of m/z 151 and 207, indicating seco-bicadinanes, m/z 369 and 412, indicating bicadinanes and m/z 383 and 426, indicating homobicadinanes of **(a)** South Furious-2 Stage IVA extract sample 1002m/3287ft from this study and **(b)** the published data of van Aarssen *et. al.* (1992).

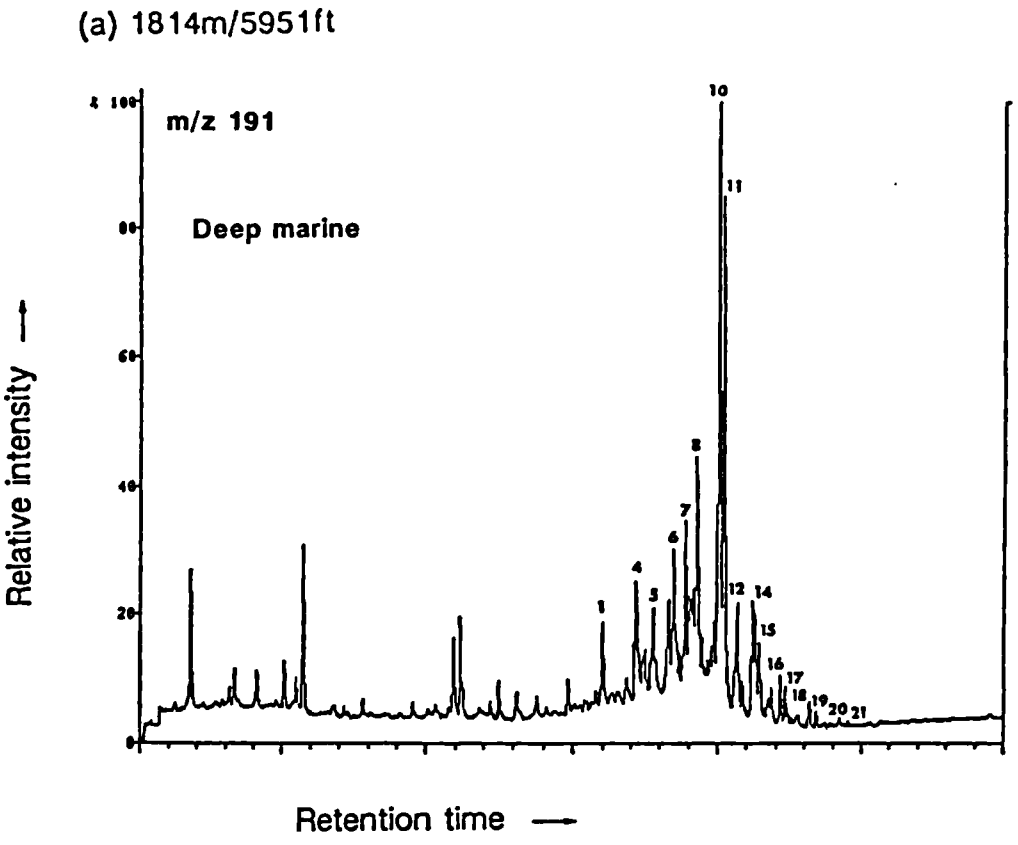


FIGURE 6.5 Triterpane (m/z 191) distribution of a Stage IVB sediment extract sample obtained from Rusa Timur-1 well.

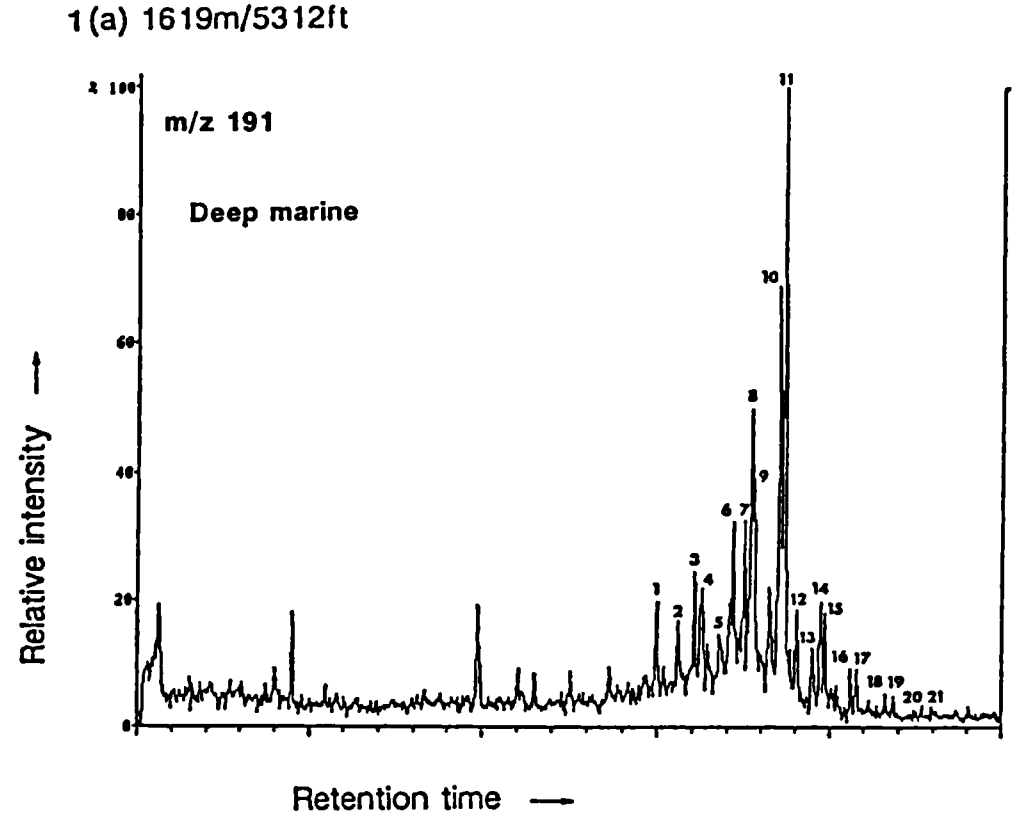
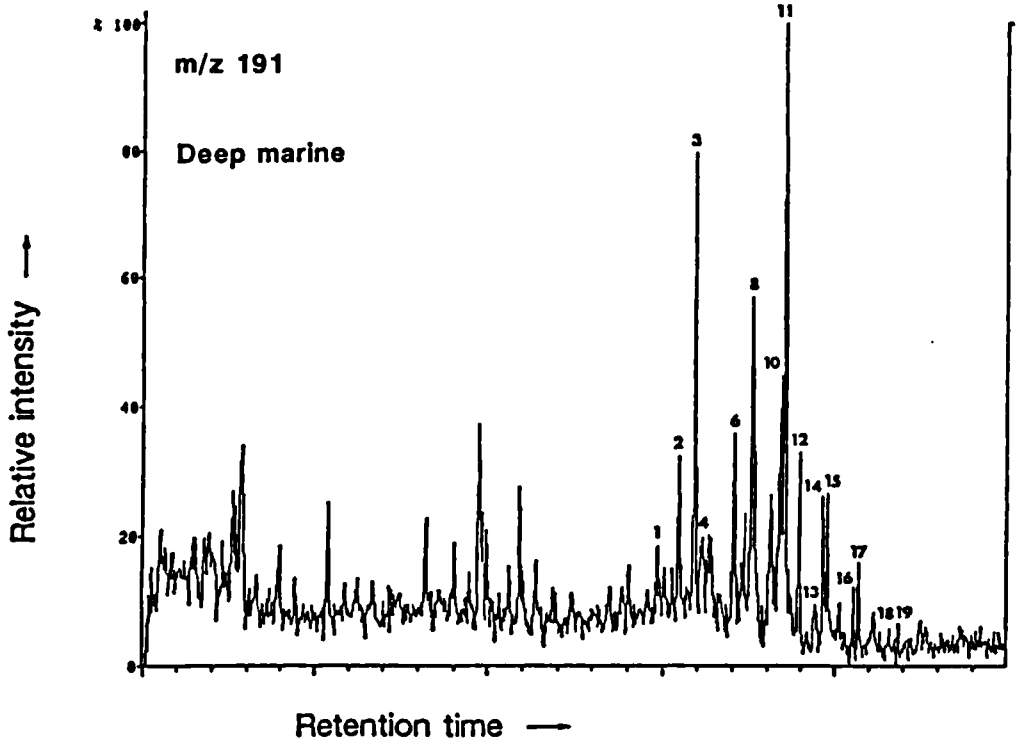


FIGURE 6.6 Triterpane (m/z 191) distributions of Stage IVC sediment extract samples obtained from (1) Rusa Timur-1 well (a) and (2) Gajah Hitam-1 well (a to b).

2(a) 2117m/6946ft



2(b) 2401m/7877ft

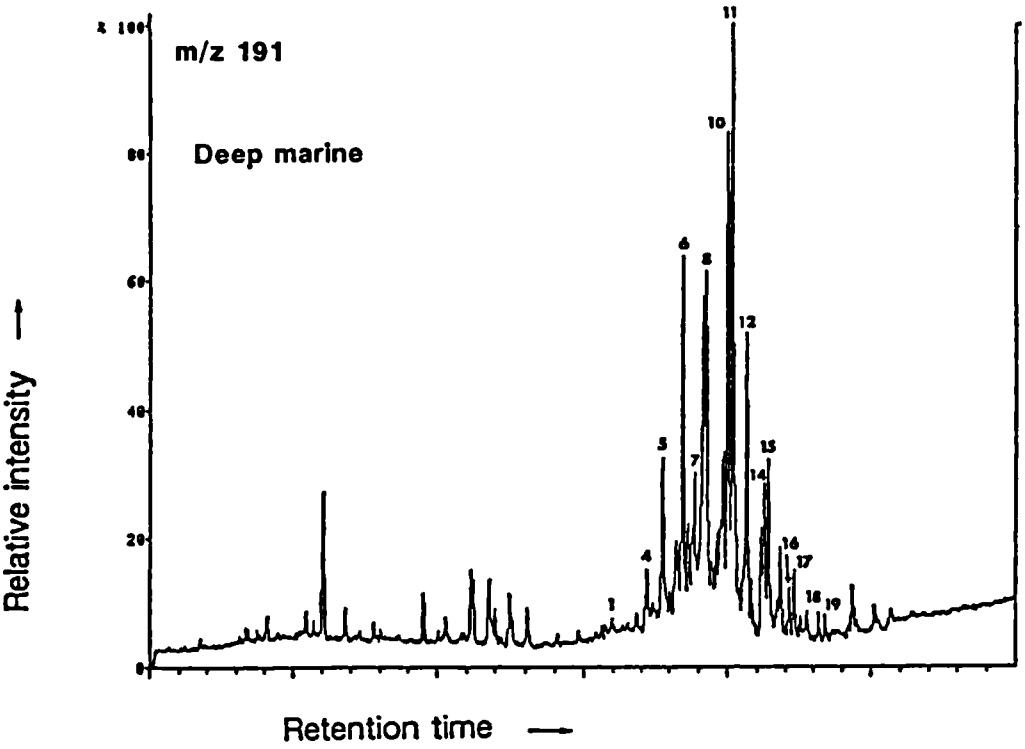


FIGURE 6.6 Continued.

6.2.5 Results : Sediment Extracts of Sub-Stage IVD

Two extract samples from Rusa Timur-1, and one each from Tembungo-1 and Tembungo-2 were analysed. Sample 772m (2533ft) from Rusa Timur-1 differs from the other sub-Stage IVD samples, as well as from the rest of the samples, with the noticeable absence of the oleanane peak (**Figure 6.7**). However, it still displays resins T (peak 4) and R (peak 5). C_{30} 17α(H)-hopane (peak 11) is dominant in the sub-Stage IVD samples with some tricyclics being present.

6.2.6 Results : Oil Samples

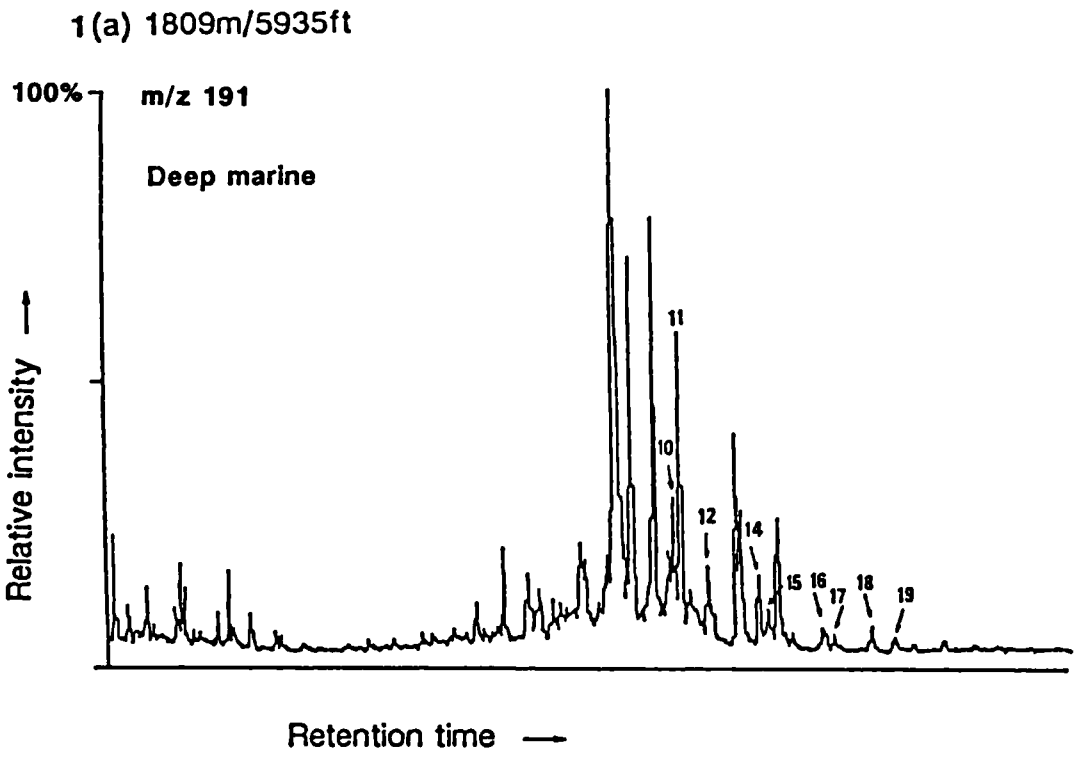
The triterpane distributions of oil samples from seven different fields in Sabah Basin are shown in **Figure 6.8**. The consistently similar m/z 191 traces for the oils suggest that they are likely to have been generated by the same source rock, or by source rocks which are of similar, or comparable, nature i.e. containing Type III, land-derived organic matter. All the oils contain resins W, T and R (peaks 1, 4, and 5, respectively) and oleanane (peak 10) which are compounds commonly associated with higher land-plants.

6.3 Sterane fingerprints of sediment extracts and oils

6.3.1 Results : Sediment Extracts of Stage III

The m/z 217 fragmentograms of Stage III sediment extracts are quite similar to each other, all exhibiting the dominance of C_{29} regular steranes over the C_{27} and C_{28} species (**Figure 6.9**). There are also resin-derived cycloalkane peaks (peaks 24 and 25) which are believed to originate from non-steranes that yield large m/z 217 peaks (Waples & Machihara, 1991). It is interesting to note that these peaks coincide with those of resins W, T and R in the m/z 191 mass fragmentograms, shown to be pentacyclic triterpanes (van Aarssen *et. al.*, 1990, 1992). Here, we have compounds with bicadinane partial mass chromatograms which also give responses in the m/z 217 mass fragmentograms.

Comet *et. al.* (1989) suggested that some of the resin-derived cycloalkanes may be bicadinanes and evidence from this study seem to support the suggestion. The occurrence of these resins has been reported in oils derived from coals/coaly shales and in coal extracts (Thompson *et. al.*, 1985; Comet *et. al.*, 1989; Jamil *et. al.*, 1990). There are two ways to avoid confusing the resin peaks with those of the steranes. Overlaying the m/z 191 fragmentogram over its corresponding m/z 217 trace will allow identification of the resin peaks. Alternatively, they can be identified by monitoring the parent-daughter ion m/z 412 → m/z 217.



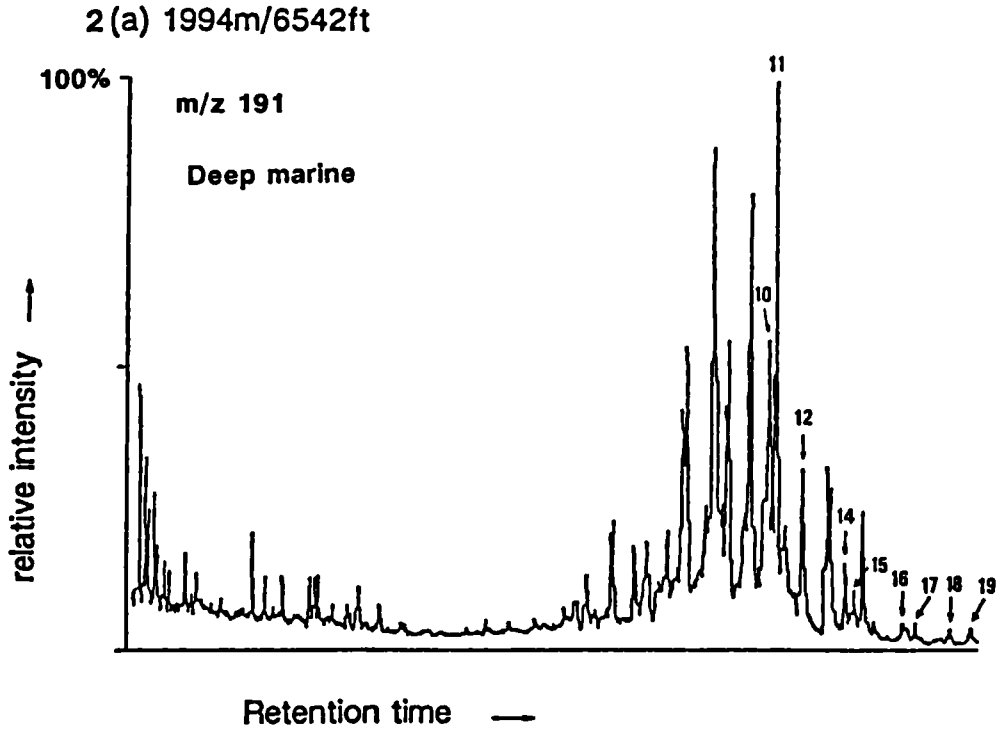
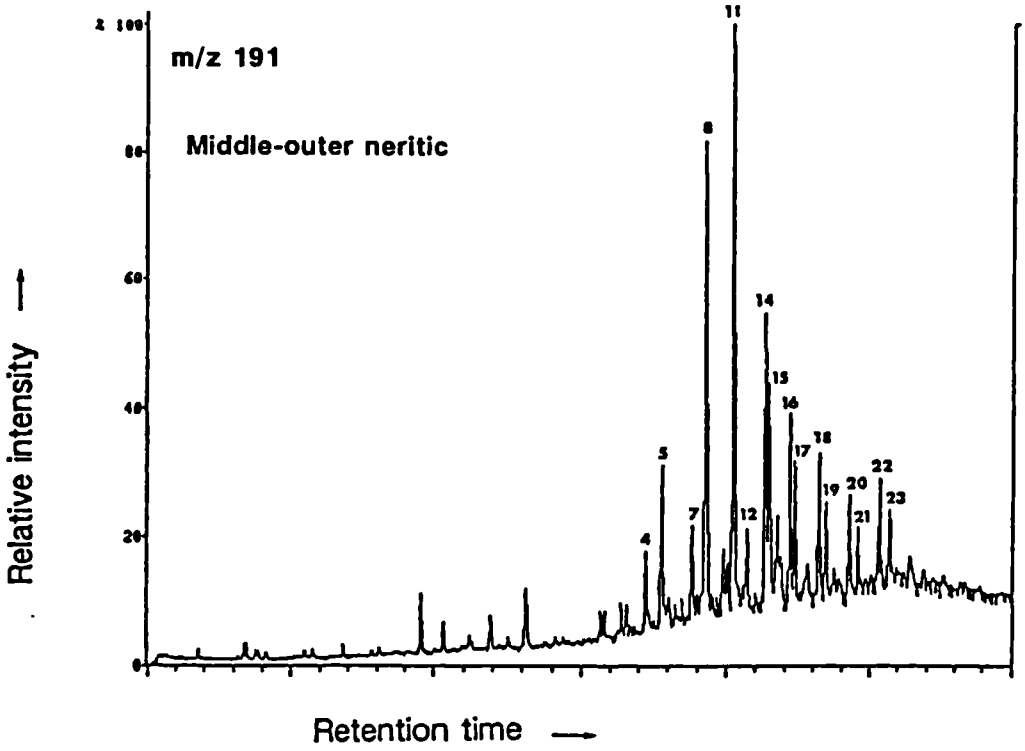


FIGURE 6.7 Triterpane (m/z 191) distributions of Stage IVD sediment extract samples obtained from (1) Tembungo-1 well (a), (2) Tembungo-2 well (a) and (3) Rusa Timur-1 well (a to b).

3(a) 772m/2533ft



3(b) 1406m/4613ft

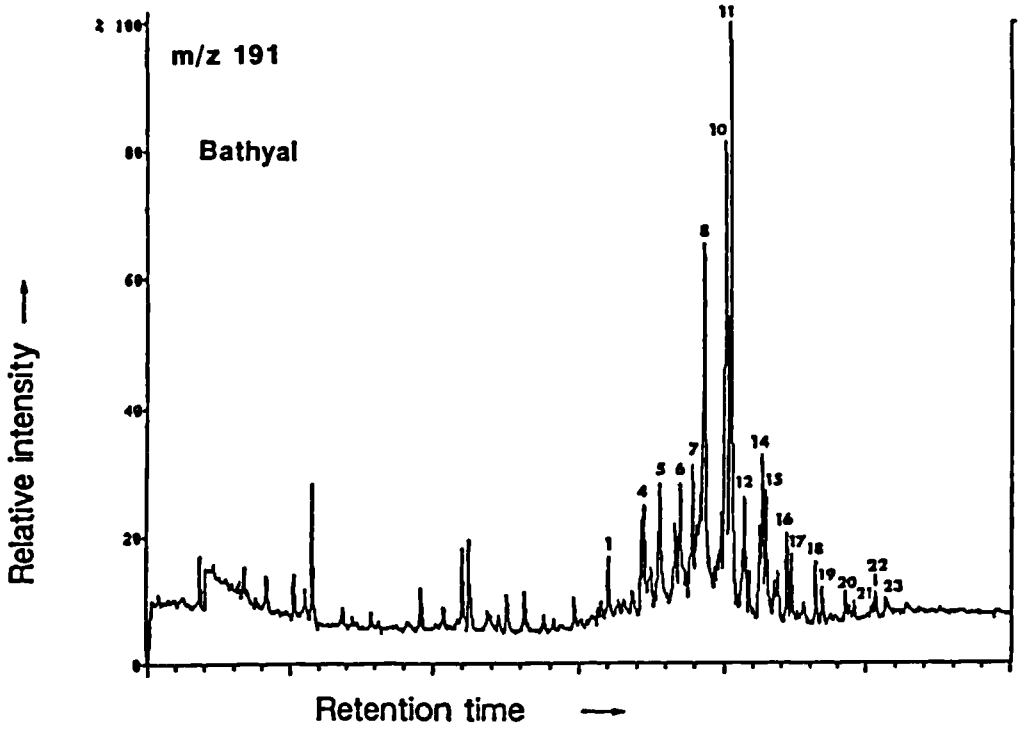


FIGURE 6.7 Continued.

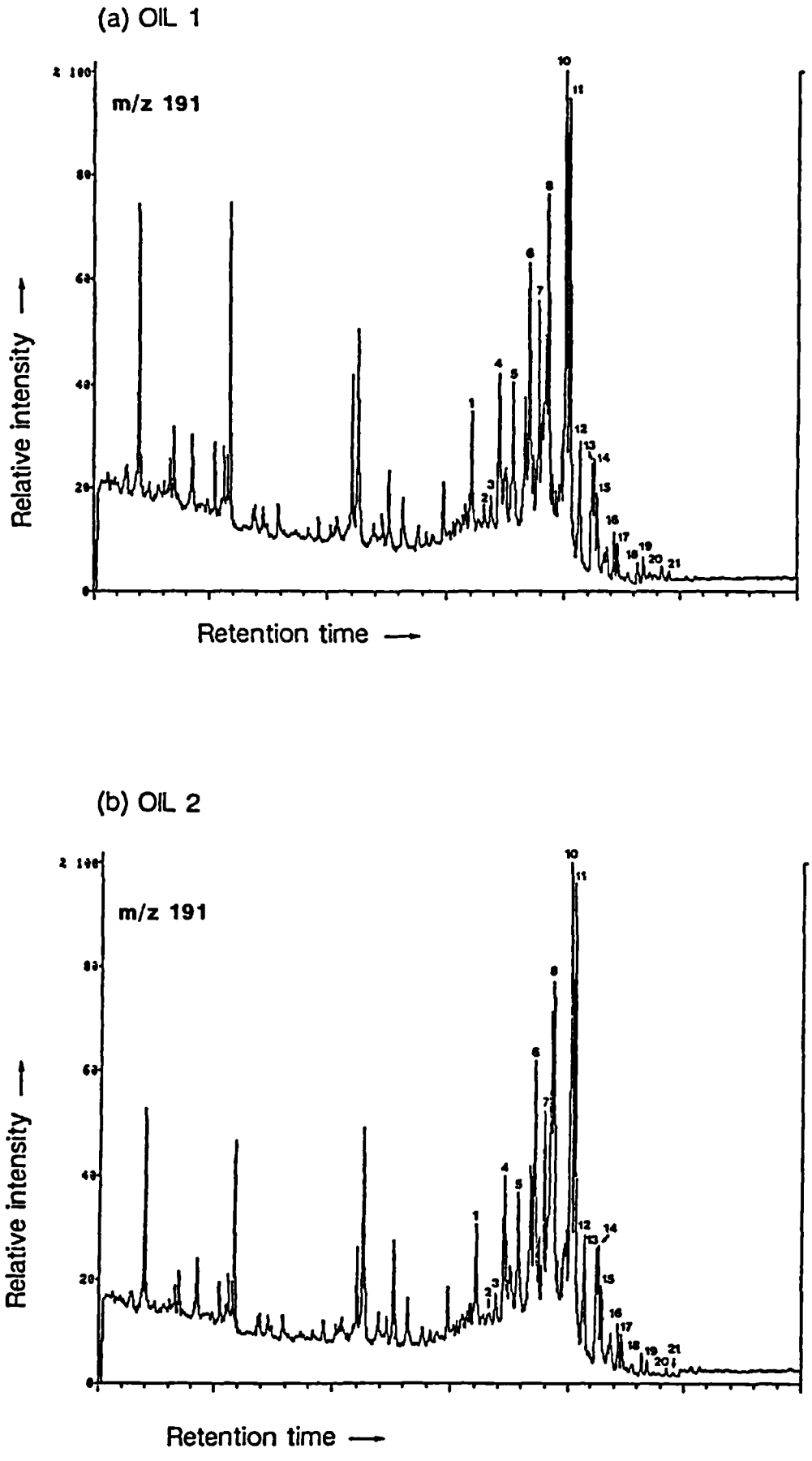
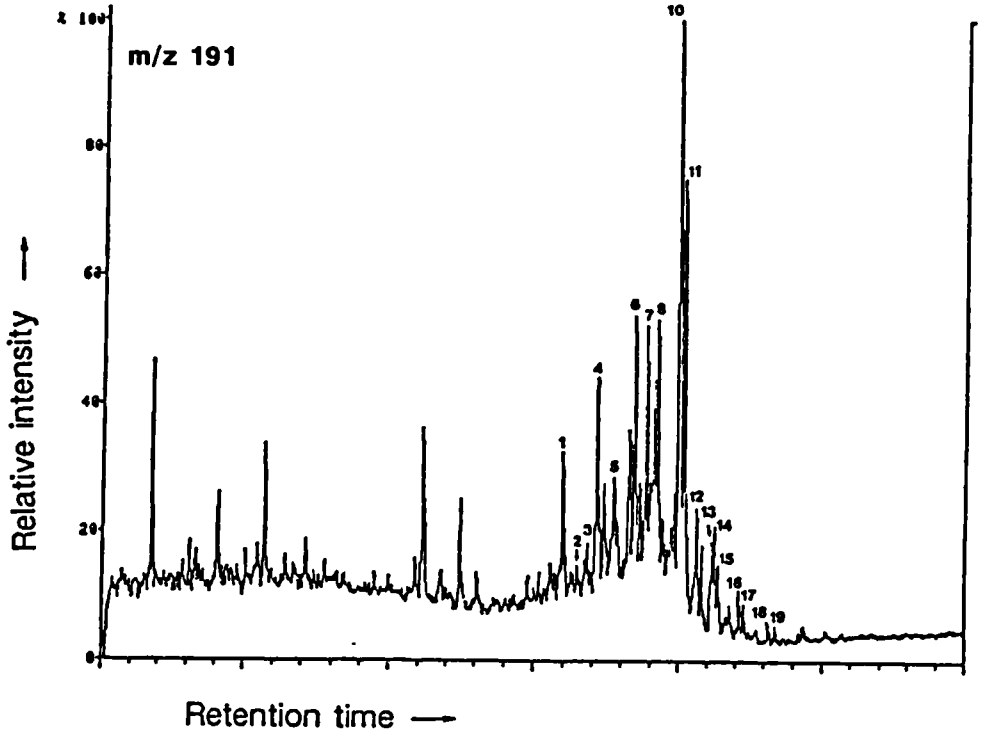


FIGURE 6.8 Triterpane (m/z 191) distributions of the seven oil samples collected from different locations in the Sabah Basin. Refer to **Figure 6.1** for locations.

(c) OIL 3



(d) OIL 4

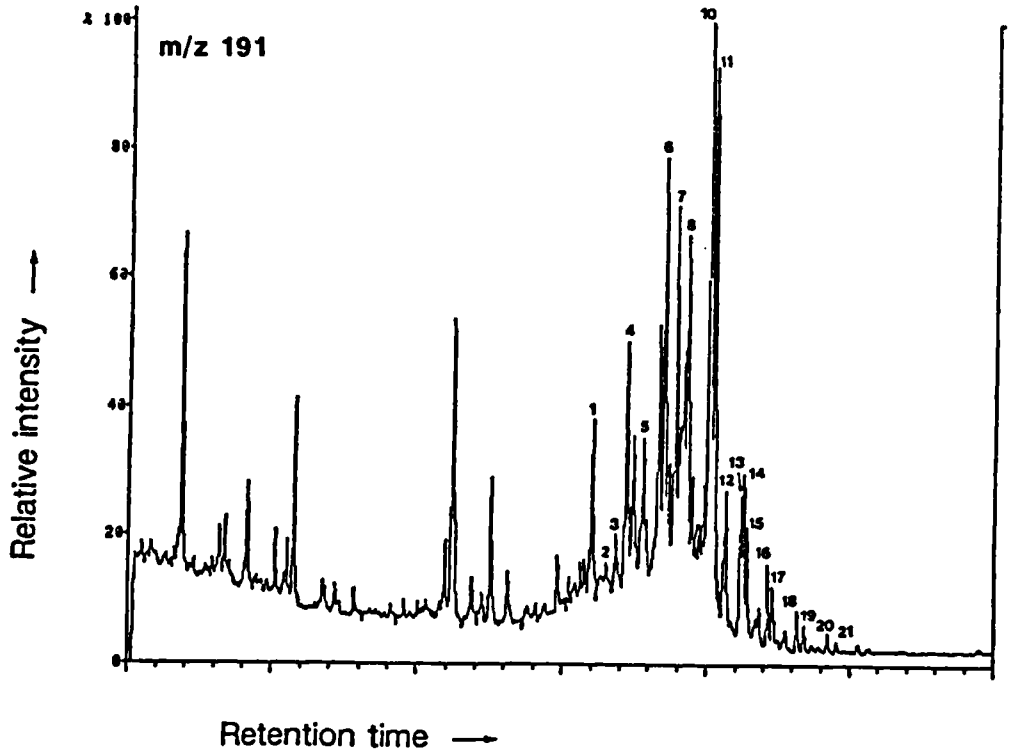
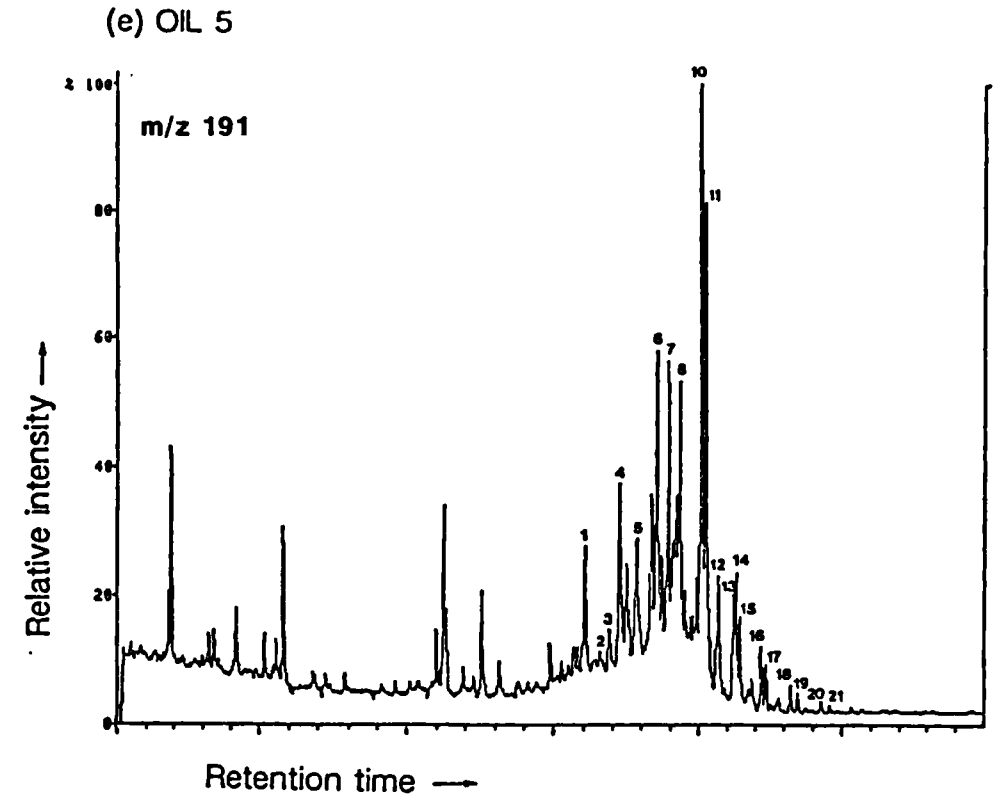


FIGURE 6.8 Continued.



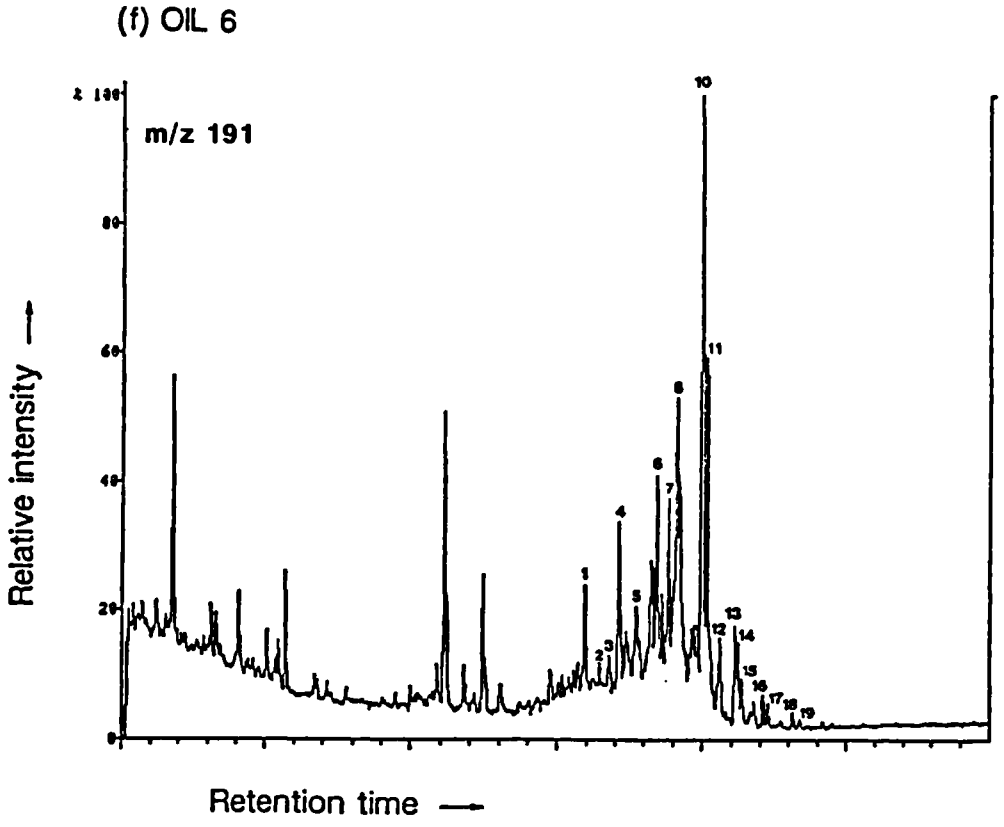


FIGURE 6.8 Continued.

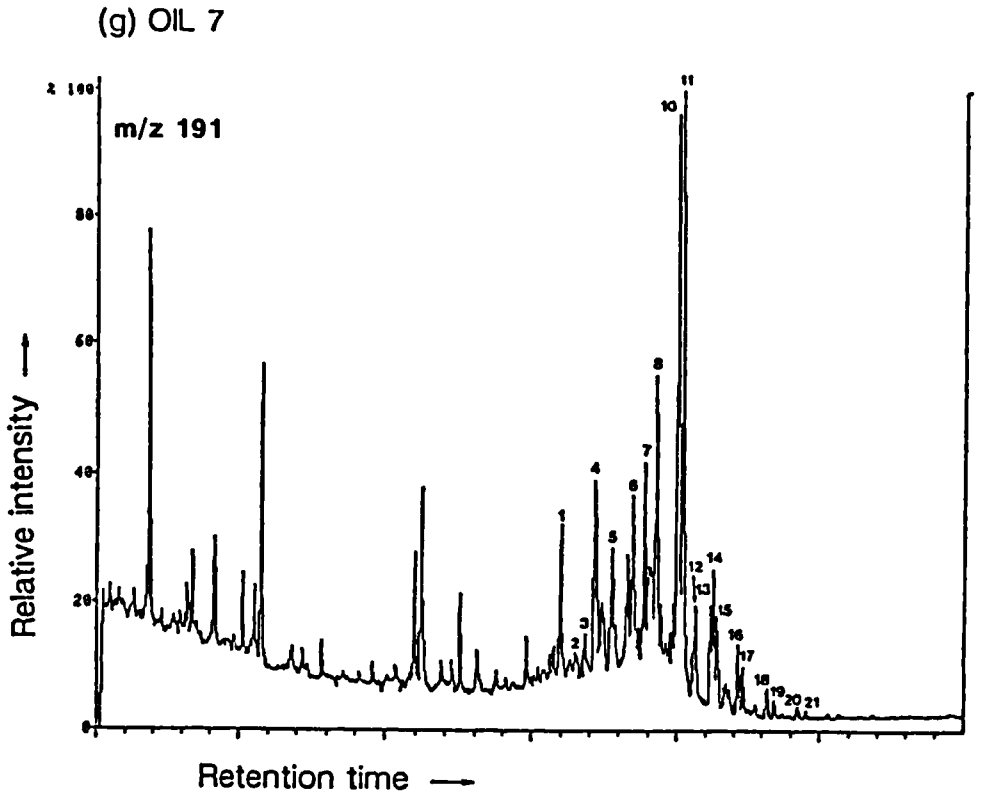


FIGURE 6.8 Continued.

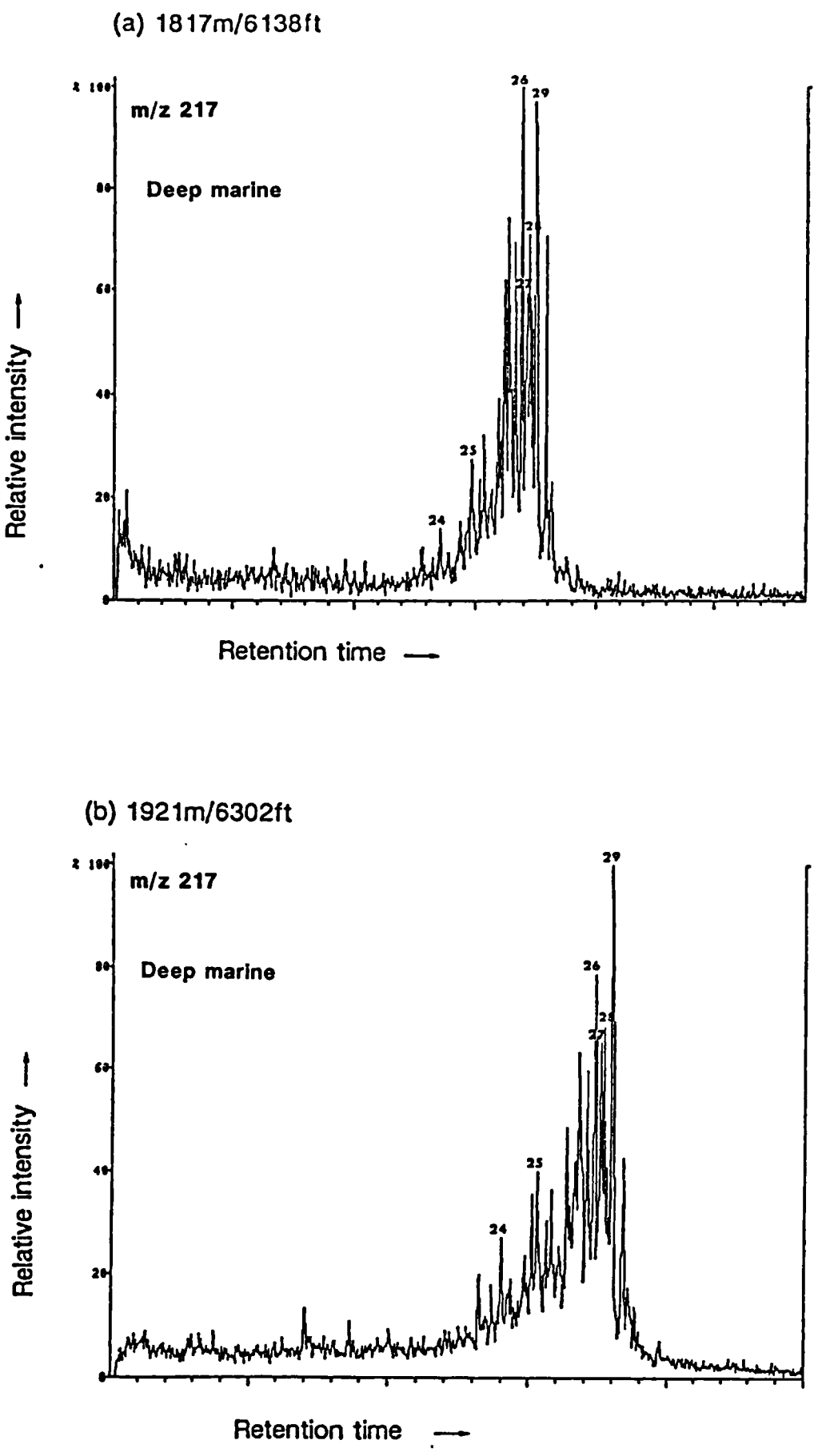


FIGURE 6.9 Sterane (m/z 217) distributions for Stage III sediment extract samples obtained from South Furious-2 well (a) 1871m/6138ft, (b) 1921m/6302ft and (c) 1979m/6493ft.

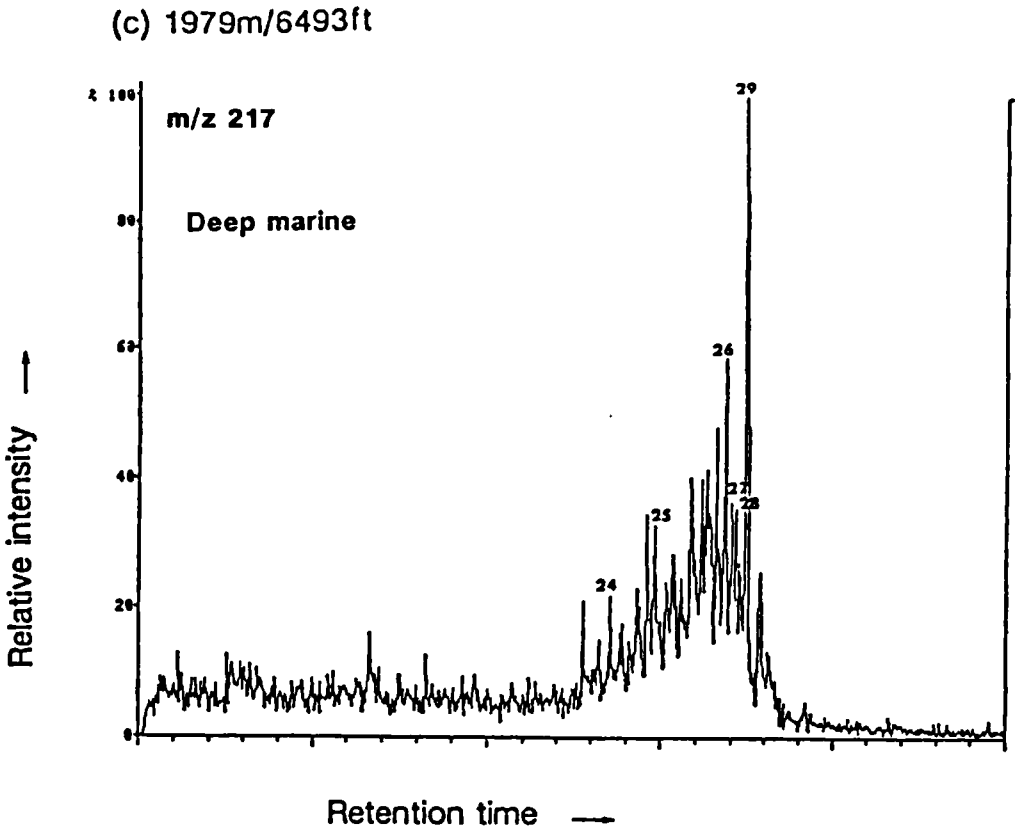


FIGURE 6.9 Continued.

6.3.2 Results : Sediment Extracts of Sub-Stage IVA

Sterane distributions **(Figure 6.10)** of South Furious-2 samples 446m (1463ft) and 1002m (3287ft) are almost identical, as are South Furious-2 samples 1738m (5702ft) and 1779m (5837ft). The trace of sample 2040m (6693ft) from Rusa Timur-1 closely resembles those of South Furious-2 samples 446m (1463ft) and 1002m (3287ft) except for its higher C_{29}-20R peak (peak 29), while sample 1603m (5259ft) closely resembles South Furious-2 samples 1738m (5702ft) and 1779m (5837ft) except for its slightly smaller C_{29}-ββ peaks (peaks 27 and 28). Sample 1293m (4242ft) of South Furious-2 compare well with all six extract samples from South Furious-3. All the samples have resins W and T (peaks 1 and 4), with the largest peaks occurring in South Furious-2 samples 446m (1463ft) and 1002m (3287ft), and Rusa Timur-1 sample 2040m (6693ft). They also exhibit $C_{29} > C_{27}$ and C_{28}, except in sample 446m (1463ft), where they seem to occur in comparable concentrations. Only sample 1644m (5394ft) of South Furious-2 differs slightly from the rest of the sub-Stage IVA sterane distributions by having a large C_{29} 5α(H)14α(H)17α(H)-cholestane (20S) (peak 26).

6.3.3 Results : Sediment Extracts of Sub-Stage IVB

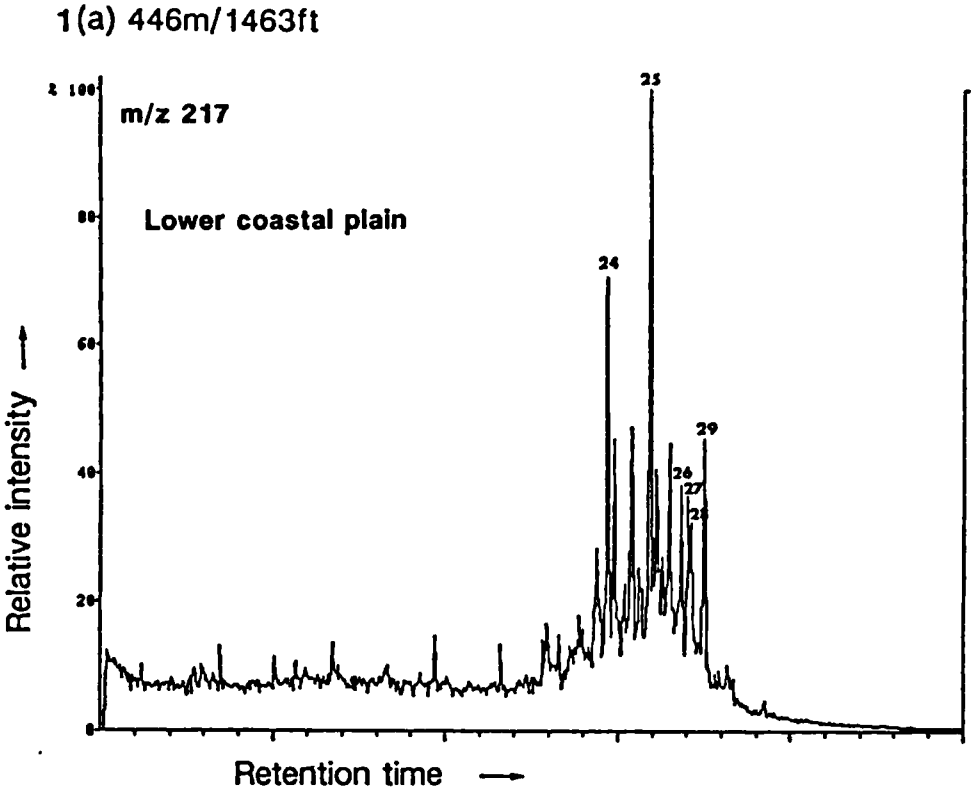
The only extract available from this sub-Stage, sample 1814m (5951ft) of Rusa Timur-1, exhibits a large resin T (peak 25) and the dominance of C_{29} regular steranes over the C_{27} and C_{28} species **(Figure 6.11)**.

6.3.4 Results : Sediment Extracts of Sub-Stage IVC

The m/z 217 sterane distributions of sub-Stage IVC sediment extracts **(Figure 6.12)** show the presence of resins W and T (peaks 1 and 4), except for Gajah Hitam-1 sample 2117m (6946ft) whose response is rather weak, possibly due to a dilute sample. The weakness in the response made the identification of the resin peaks difficult. The C_{29} regular steranes are generally present in greater abundance than the C_{27} or C_{28} species, and evidence from Hydrogen Index, elemental composition and visual analysis support a terrigenous source of organic matter input.

6.3.5 Results : Sediment Extracts of Sub-Stage IVD

Sterane distributions of Tembungo-1 and Tembungo-2 samples are very similar to each other, with C_{29} regular steranes predominating over C_{27} and C_{28} species. The sterane trace of Rusa Timur-1 sample 772m (2533ft) differs from all previous samples by not exhibiting any resins. Instead, it contains C_{30} regular sterane peaks **(Figure 6.13)** which have been reported to occur in post-Silurian samples deposited in marine environments (Moldowan *et. al.*, 1985; Mello *et. al.*, 1988a, b). Evidence from Hydrogen Index, elemental and visual analyses indicate contribution mainly from higher land plants. In Rusa Timur-1 sample 1406m (4613ft), the C_{29}-regular sterane



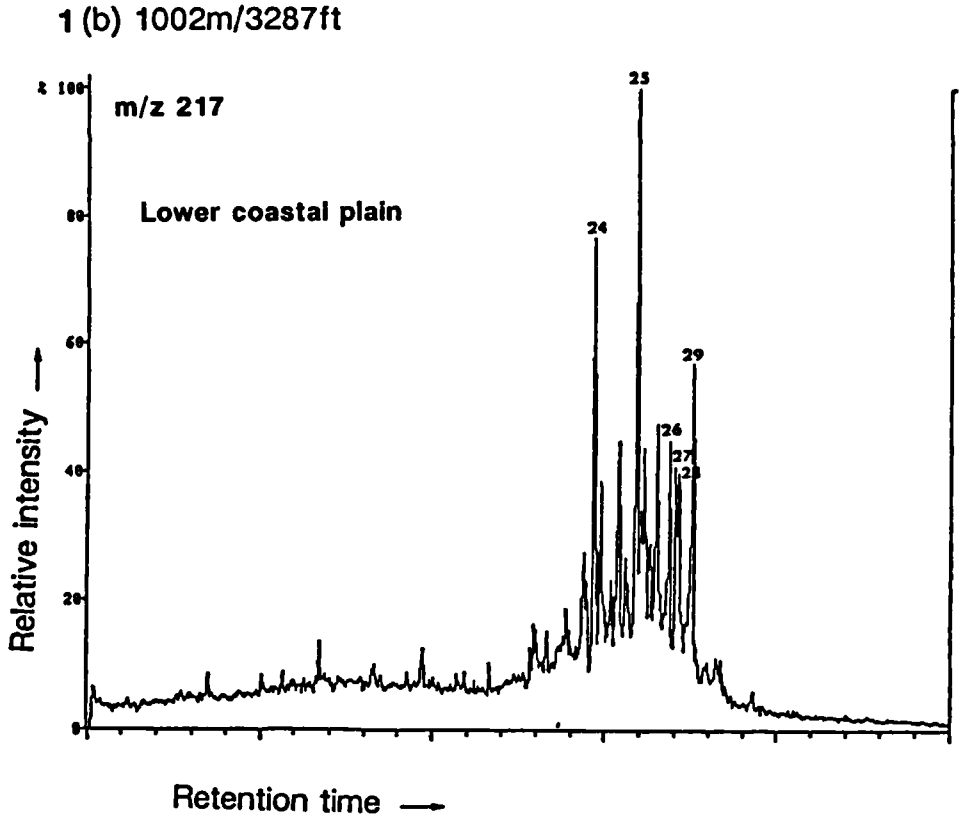
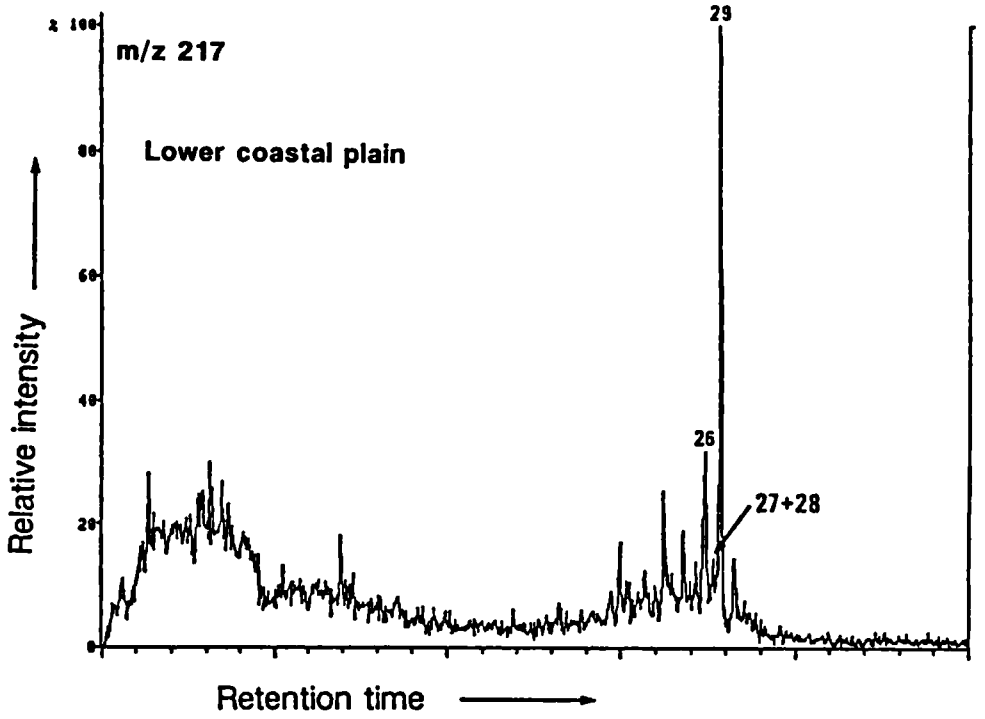


FIGURE 6.10 Sterane (m/z 217) distributions of Stage IVA sediment extract samples obtained from (1) South Furious-2 well (a to g), (2) South Furious-3 well (a to f) and (3) Rusa Timur-1 well F (a).

1(c) 1293m/4242ft



1(d) 1603m/5259ft

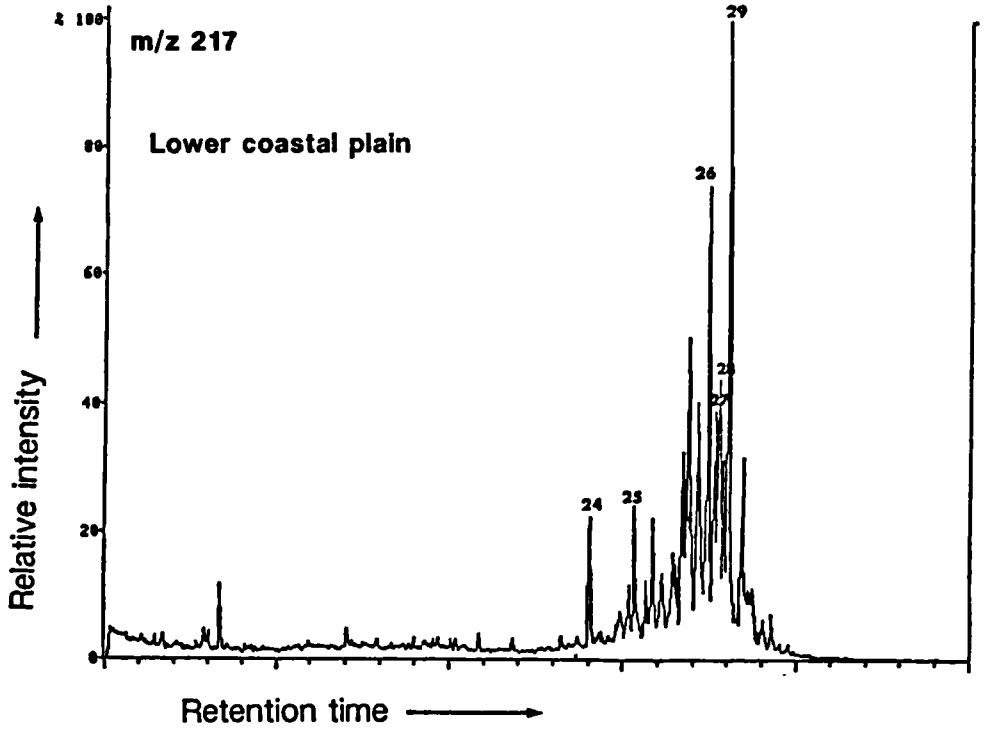
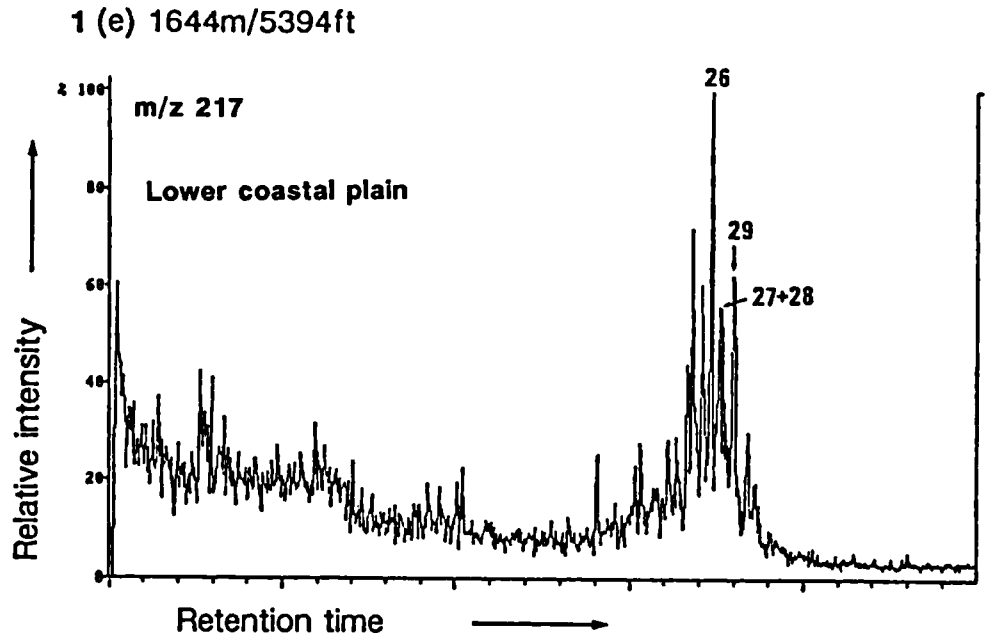


FIGURE 6.10 Continued.



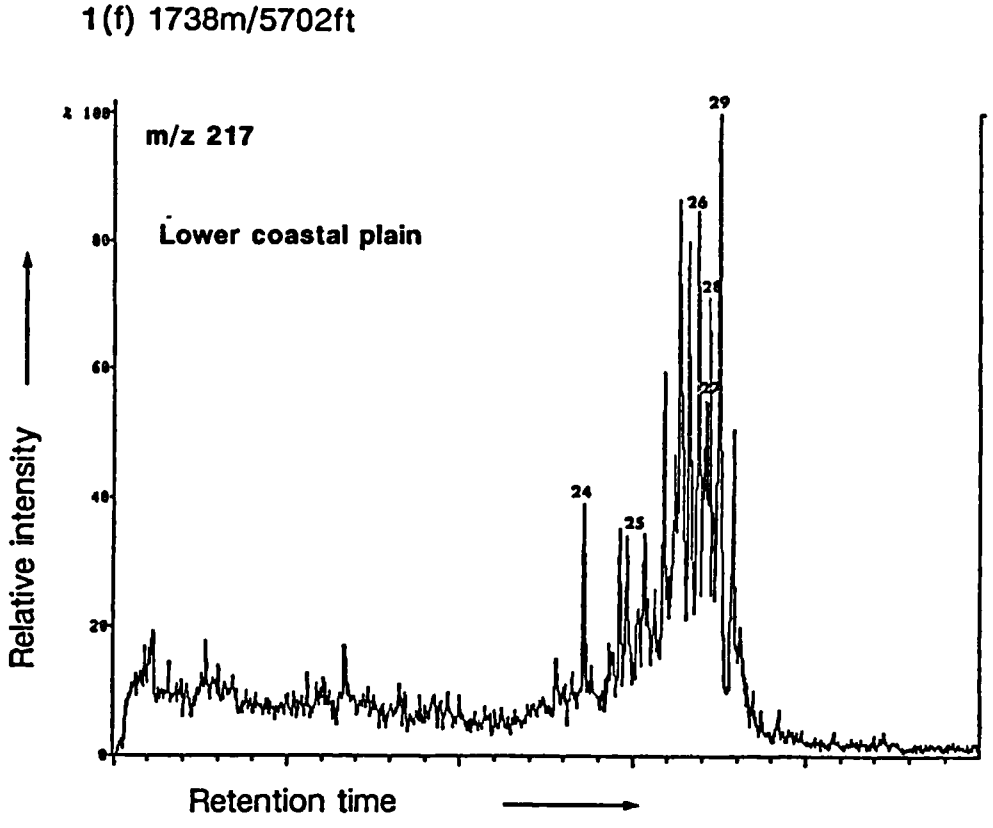
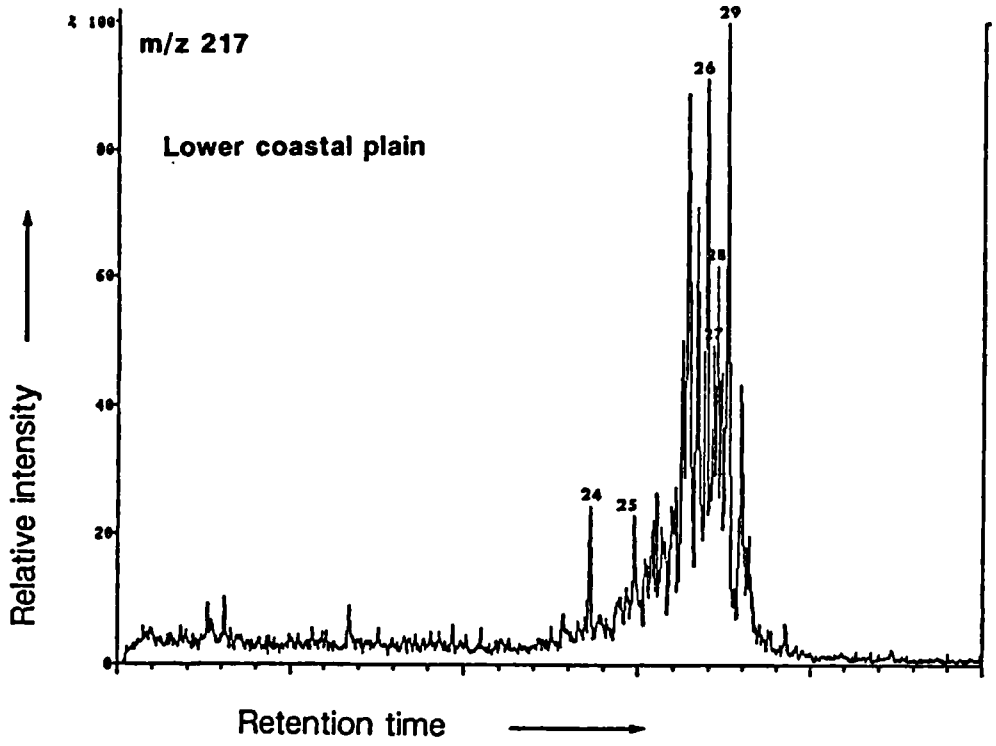


FIGURE 6.10 Continued.

1(g) 1779m/5837ft



2 (a) 826m/2710ft

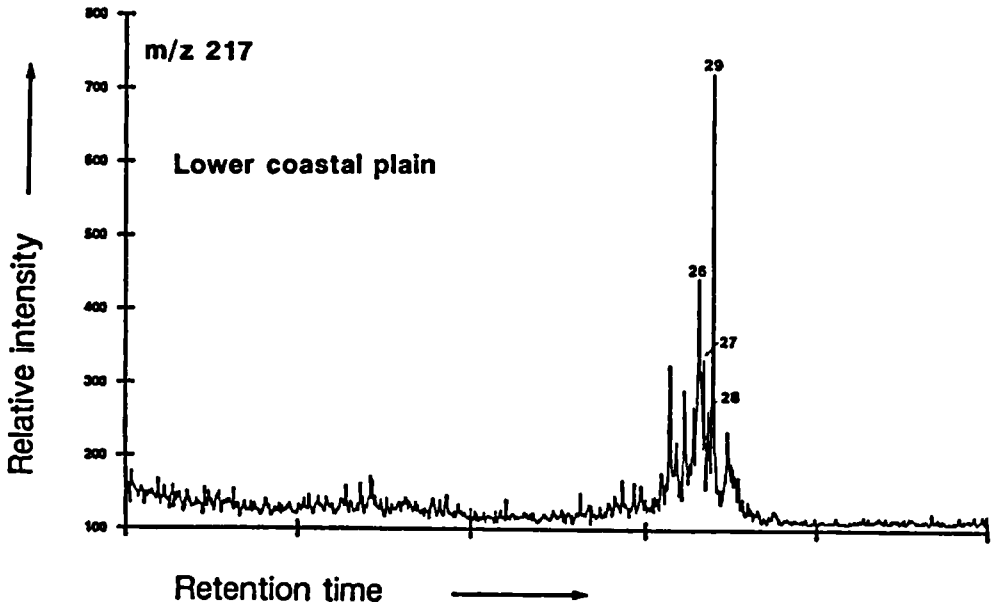
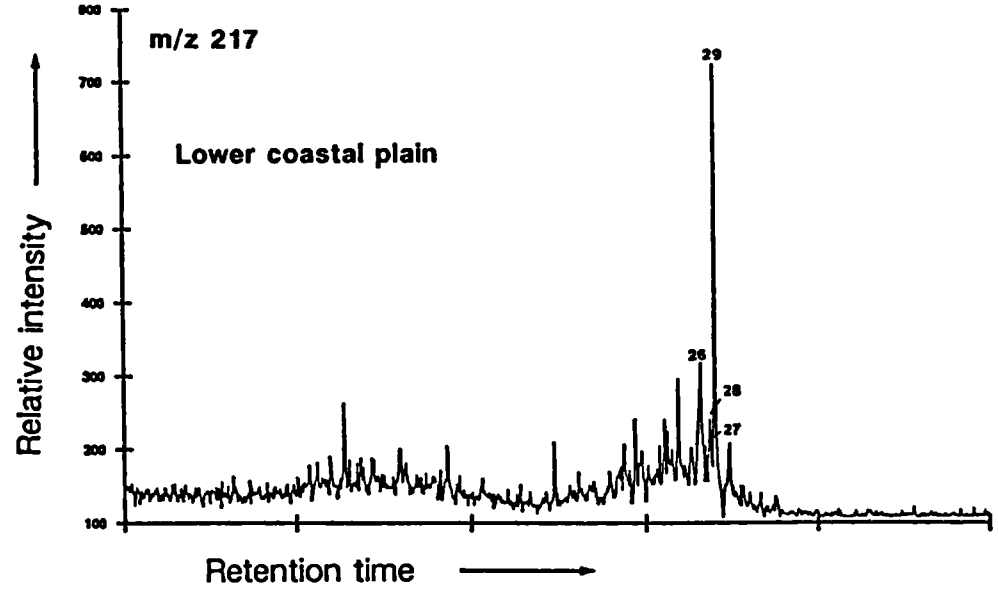


FIGURE 6.10 Continued.

2(b) 841m/2759ft



2(c) 1346m/4416ft

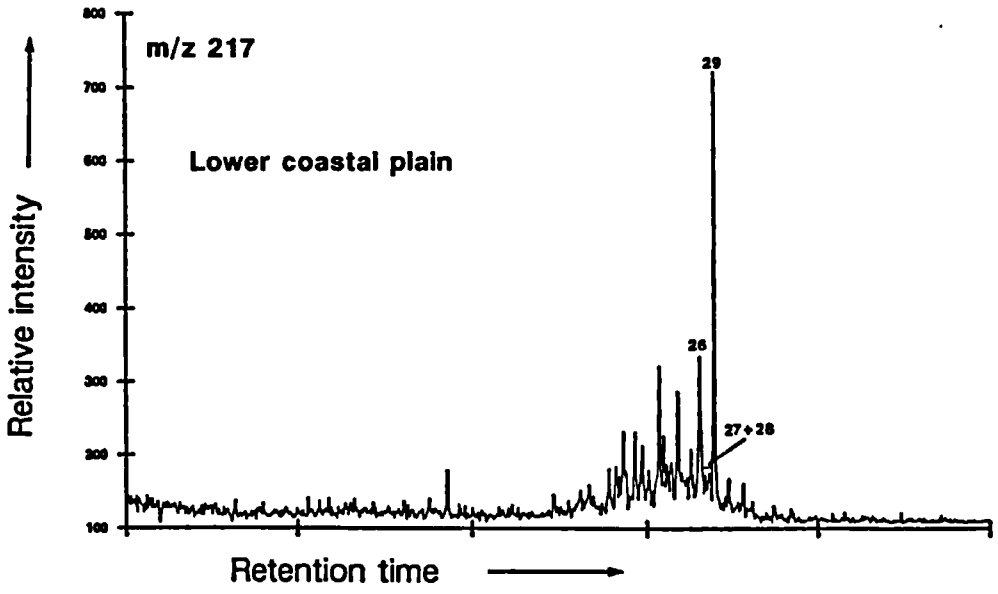
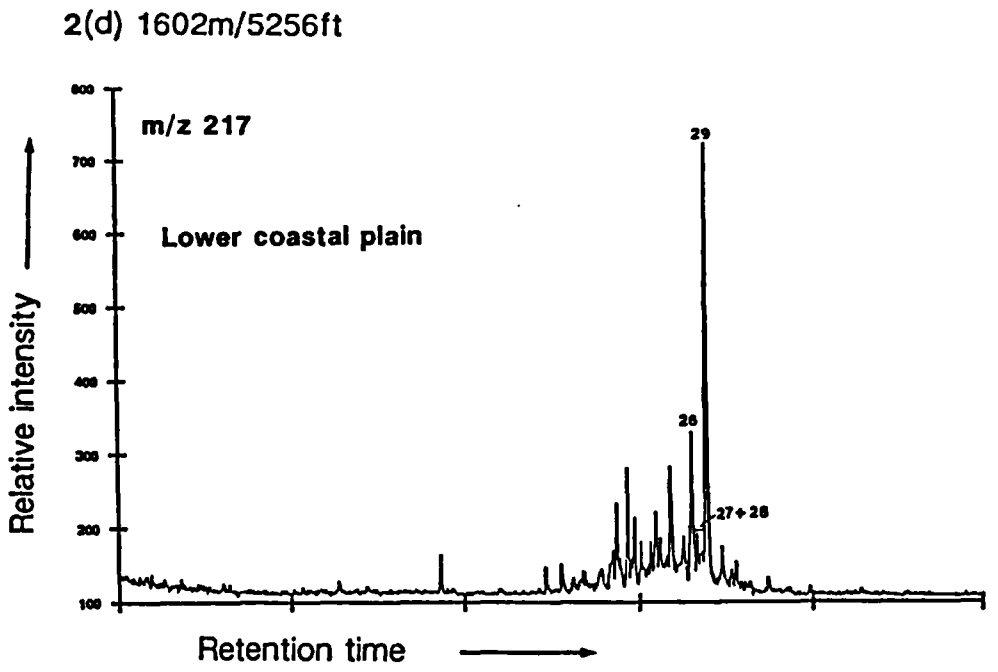


FIGURE 6.10 Continued.



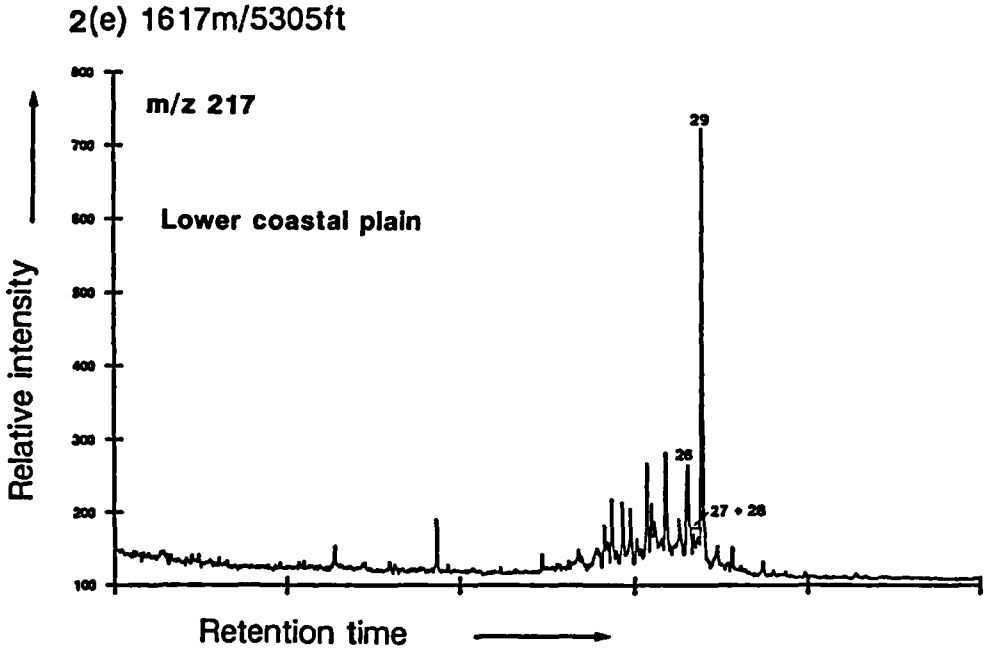
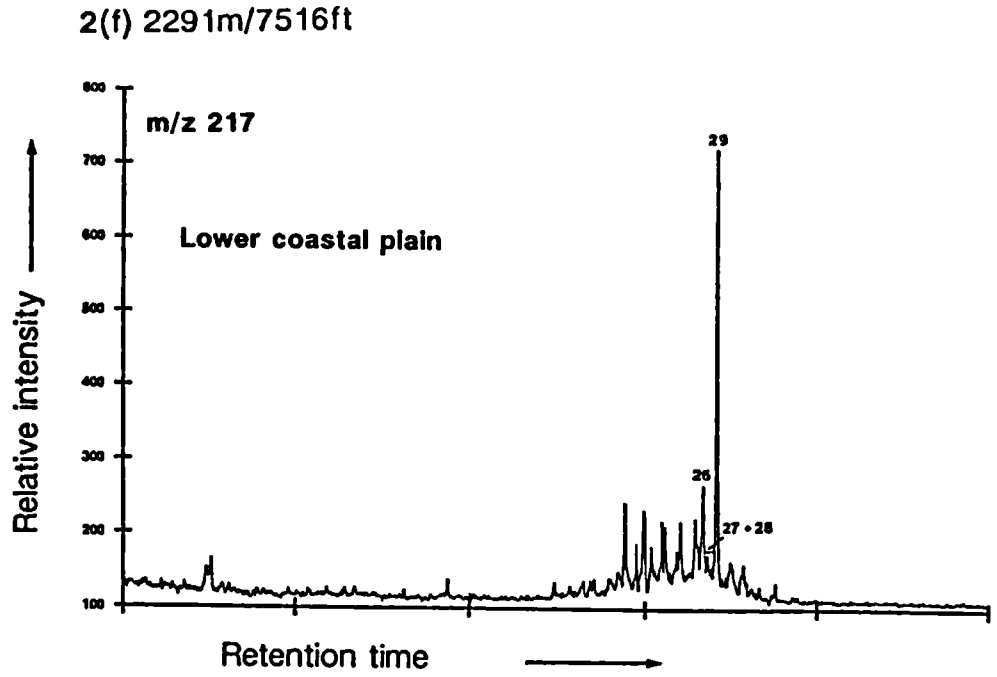


FIGURE 6.10 Continued.



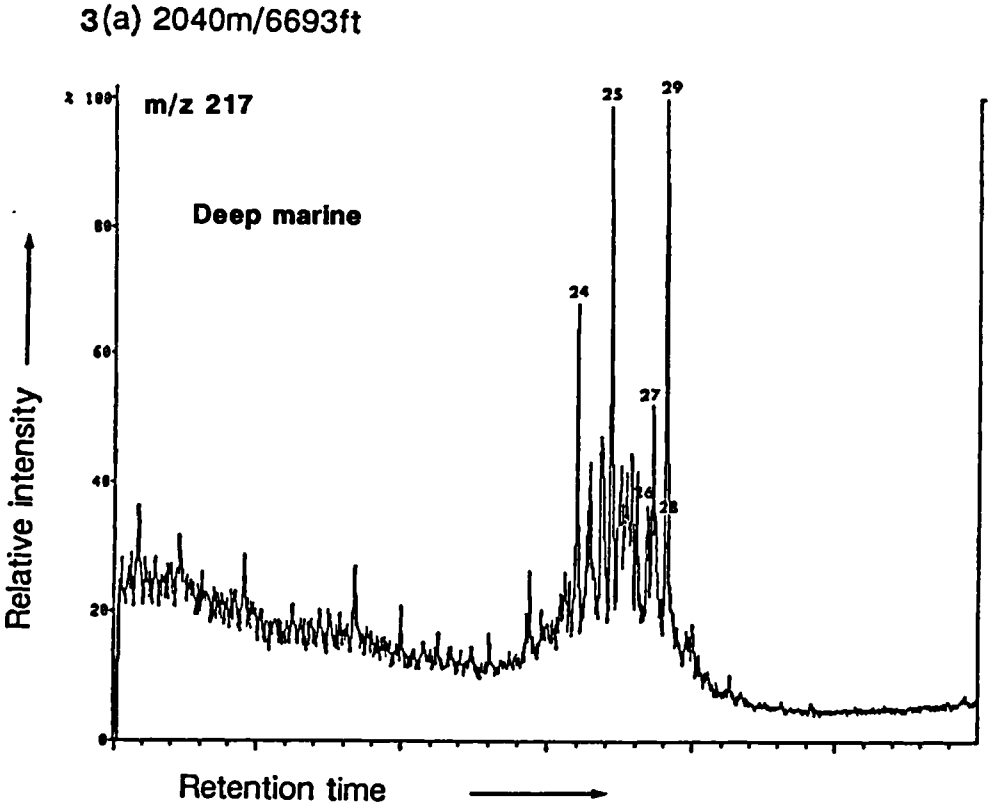


FIGURE 6.10 Continued.

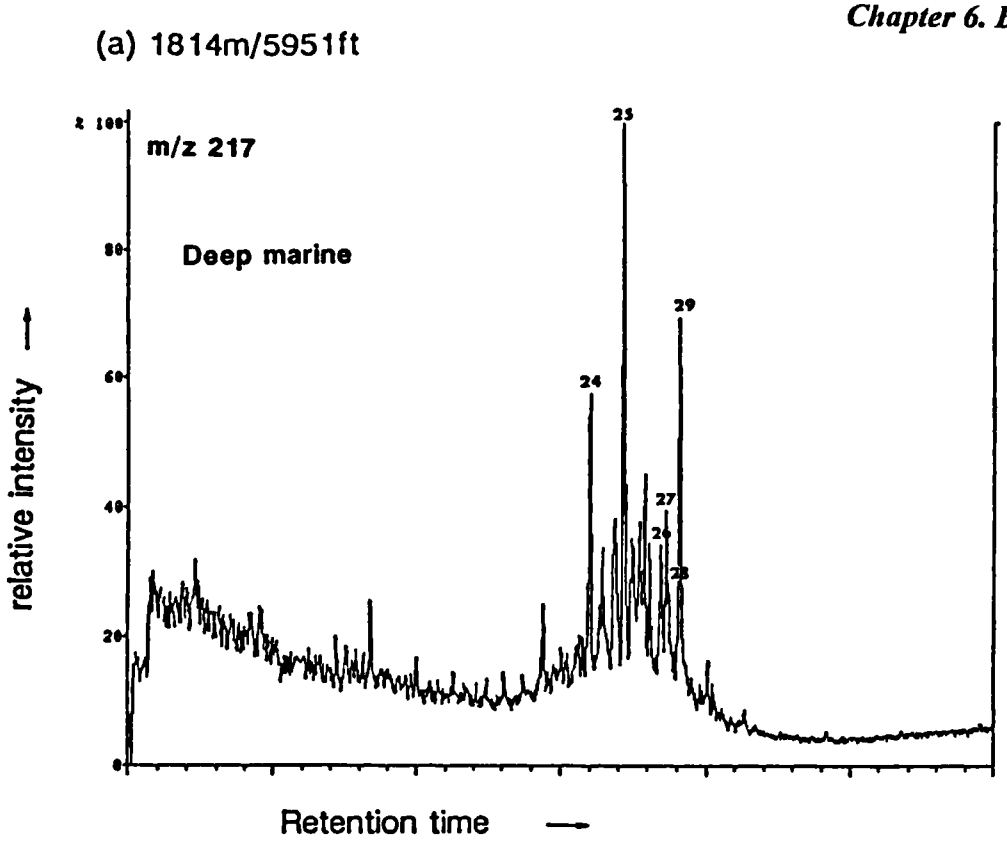


FIGURE 6.11 Sterane (m/z 217) distribution of a Stage IVB sediment extract sample obtained from Rusa Timur-1 well.

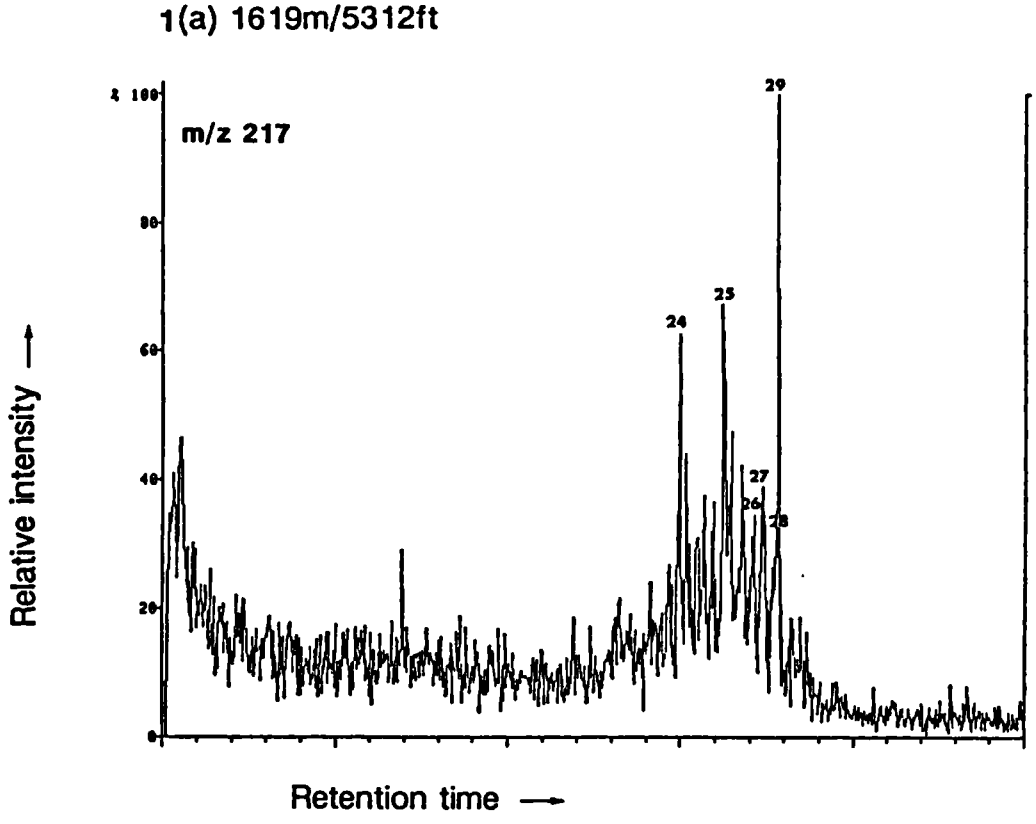
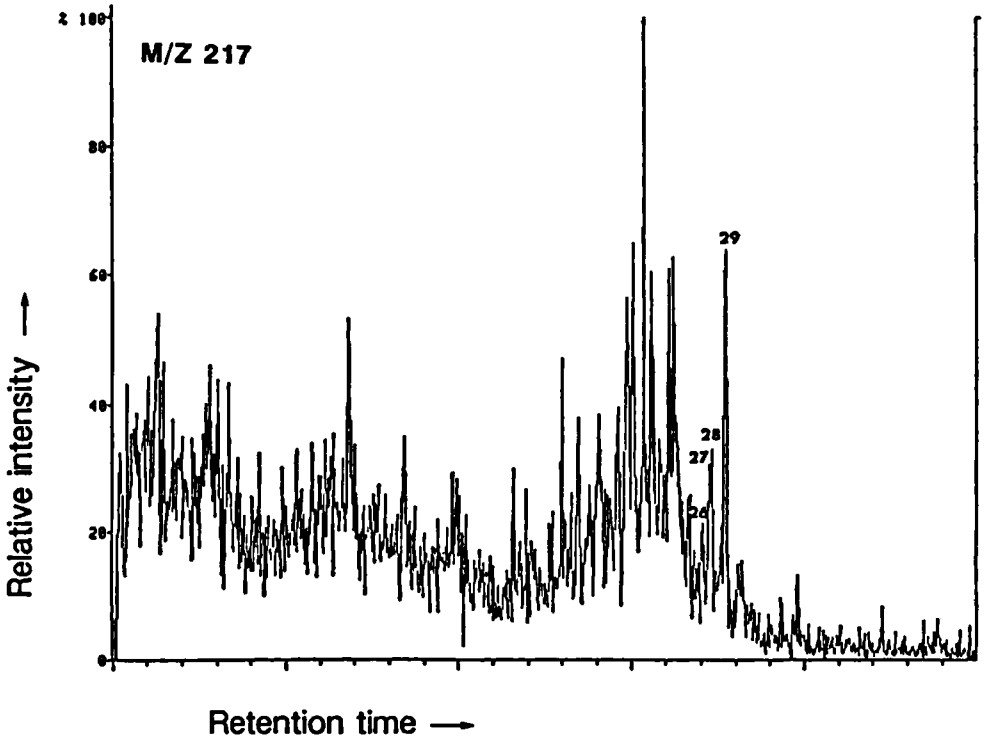


FIGURE 6.12 Sterane (m/z 217) distributions of Stage IVC sediment extract samples obtained from (1) Rusa Timur-1 well (a) and (2) Gajah Hitam-1 well (a to b).

2(a) 2117m/6946ft



2(b) 2401m/7877ft

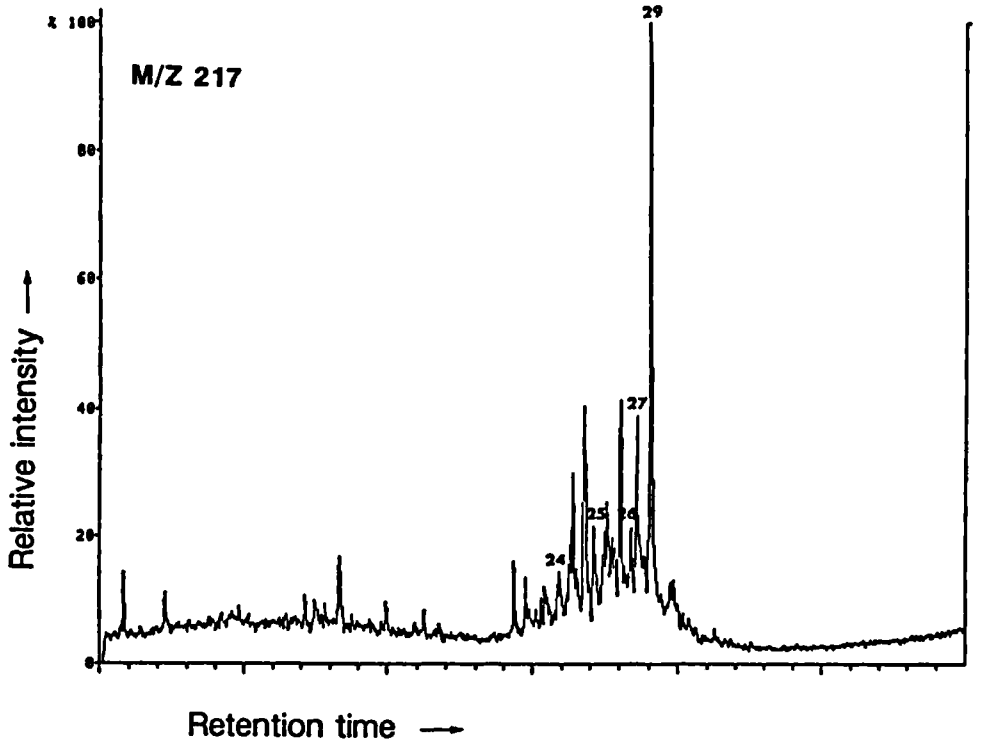
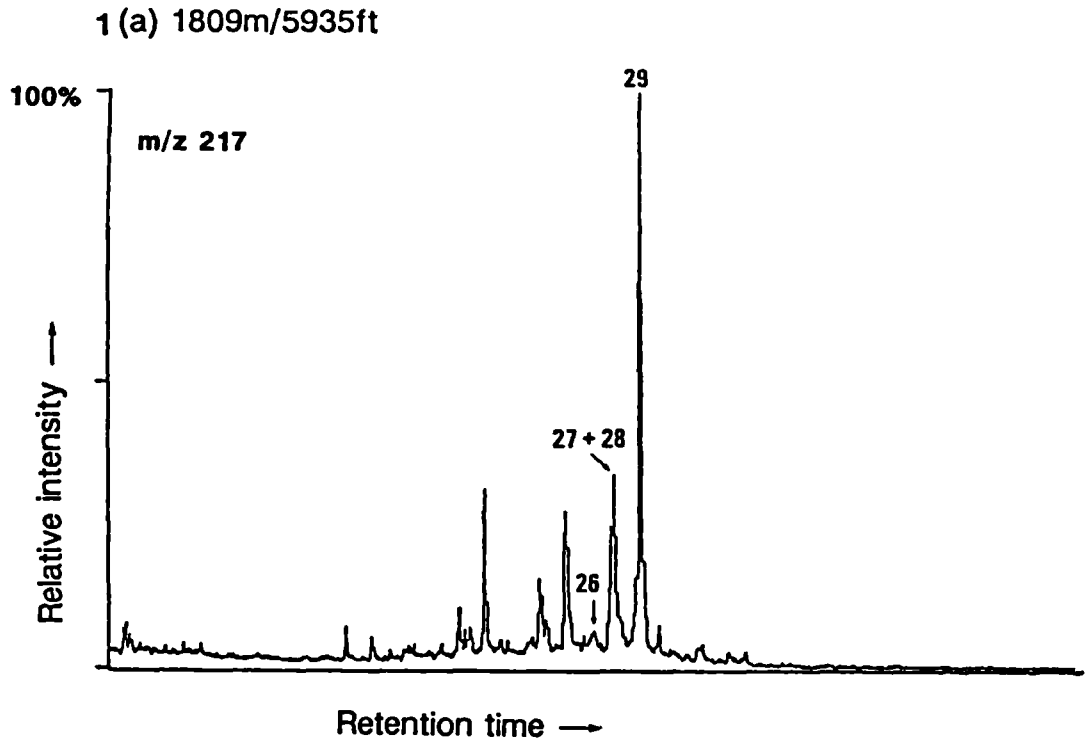


FIGURE 6.12 Continued.



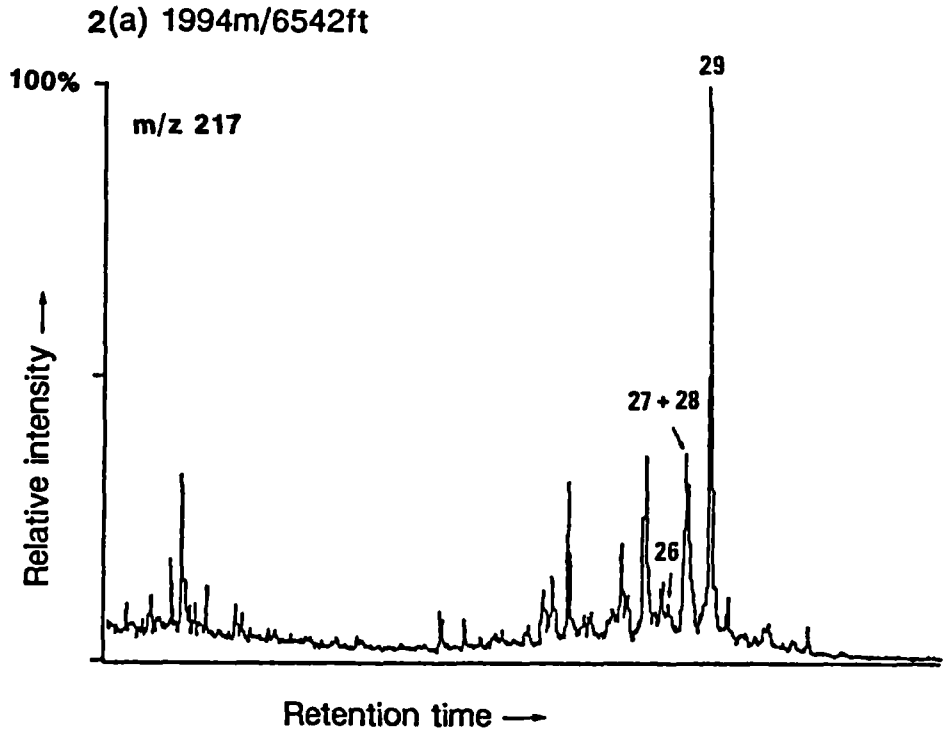
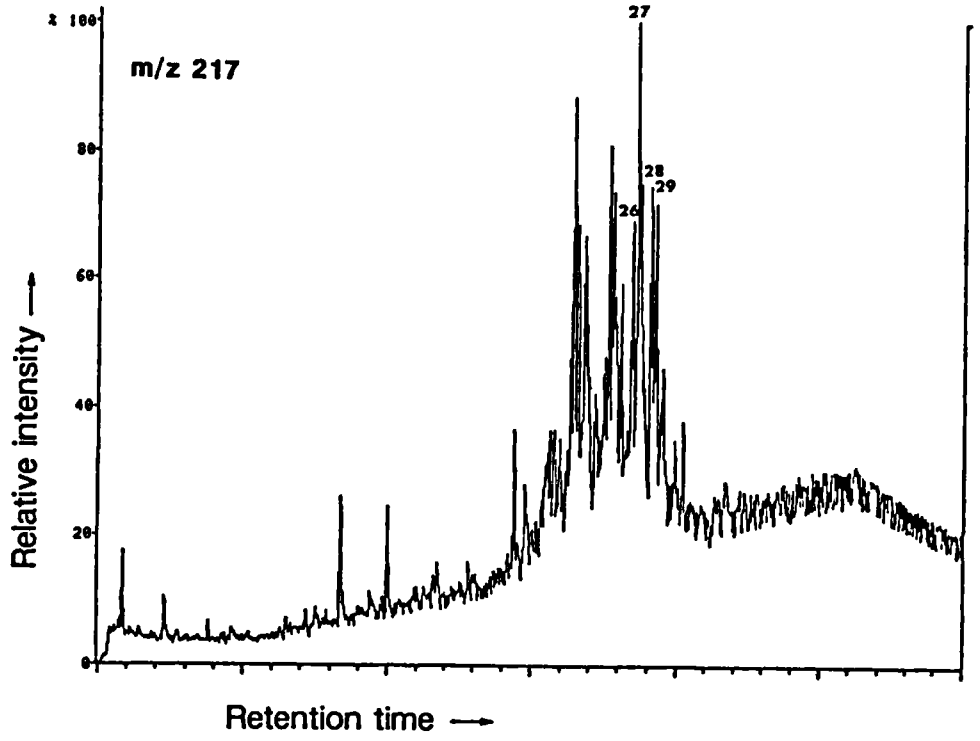


FIGURE 6.13 Sterane (m/z 217) distributions of Stage IVD sediment extract samples obtained from (1) Tembungo-1 well (a), (2) Tembungo-2 well (a) and (3) Rusa Timur-1 well (a to b).

3(a) 772m/2533ft



3(b) 1406m/4613ft

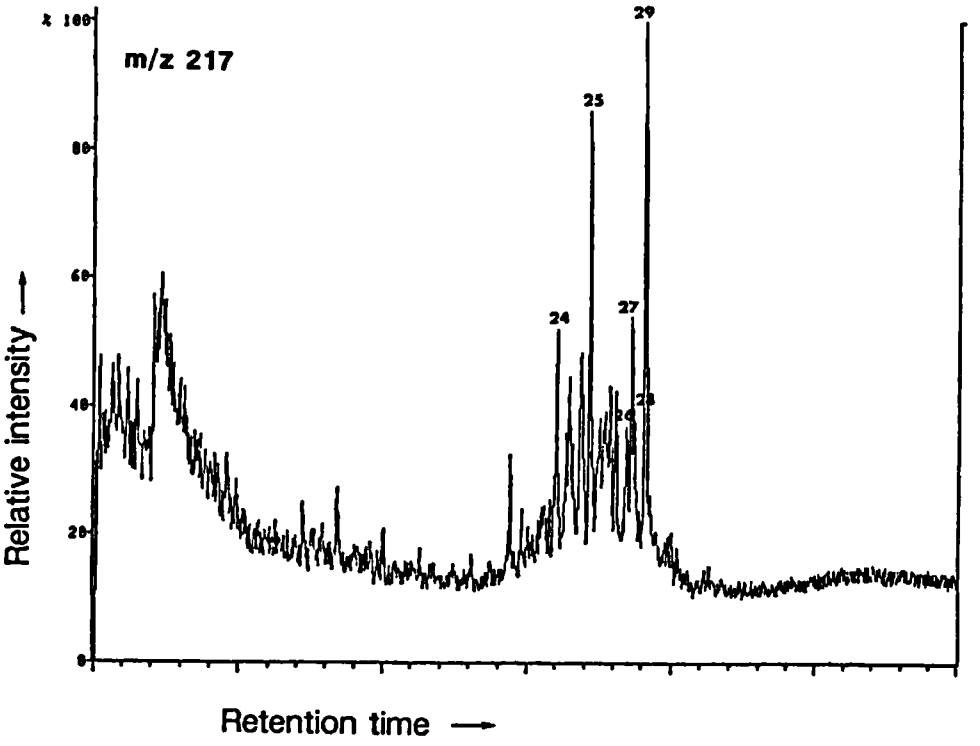


FIGURE 6.13 Continued.

re-established as the dominant peak with the co-occurrence of resins W and T (peaks 1 and 4).

6.3.6 Results : Oil Samples

All the oils have dominant resin peaks, indicating contribution from terrigenous organic matter (**Figure 6.14**). The C_{29}-regular steranes, however, do not show general dominance over the C_{27} and C_{28} species. Instead, they occur in relatively comparable quantities. Only Oil 1 (Rusa Timur) and Oil 2 (Tembungo) exhibit the dominance of C_{29} species over the C_{27} and C_{28}, with large ββ-peaks. The samples also exhibit very minor C_{30}-regular steranes peaks. It is very likely that these peaks reflect the marine sedimentary environment rather than the actual source of the oils, which are primarily terrigenous organic matter transported into marine environments by rivers and turbidity currents. In some cases, oil samples produced from deltaic-lower coastal plain sediments can show minor marine indications, for example, those deposited in brackish environments where mixing of marine and fresh water occur. Some marine algae may be washed in by the tide, creating a mixed environment with respect to organic matter type with the terrigenous organic matter predominating. These conditions can occur in mangrove and back-mangrove swamps, lagoons as well as delta fronts.

6.4 Organic facies as indicated by the biological markers

6.4.1 Introduction

Biomarkers are derived from biological precursor molecules in specific organisms living in specific environments. As such, they can be used to indicate the environmental conditions in which they existed. Generally, steranes are indicators of both terrestrial and aquatic photosynthetic biota, while triterpanes are indicators of depositional and diagenetic conditions, being derived mainly from bacteria (Waples & Machihara, 1990, 1991; Seifert & Moldowan, 1978, 1980, 1981, 1986). When interpreting organic facies, it is necessary to be aware of the factors that can affect the resulting biomarker distributions :

- the multiple origins of biomarker precursors, thus complicating organic facies interpretation
- the 'average' biomarker signature of the organic facies given by ditch-cutting samples, which are naturally prone to contamination
- the representativeness of core samples analysed
- oil samples that have been sourced by a number of source rocks, resulting in a mixture of biomarkers bearing information on the different sources

Furthermore, rapid organic facies variations both vertically and laterally make generalised organic facies interpretation inaccurate. Due to the various potential pitfalls, results from other geochemical methods are jointly used with biomarker data before any conclusions on organic facies are drawn. The following discussion is set out

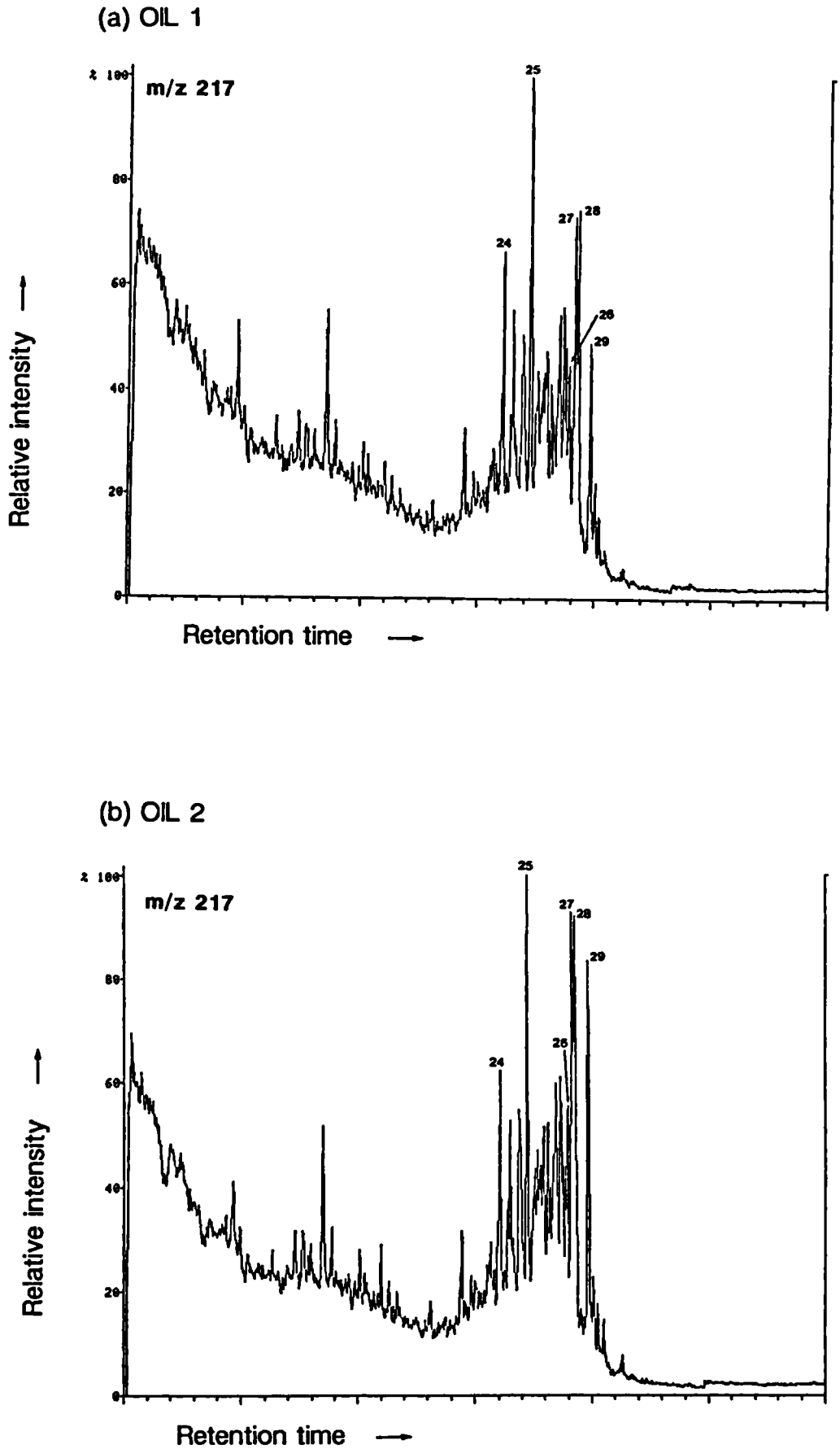
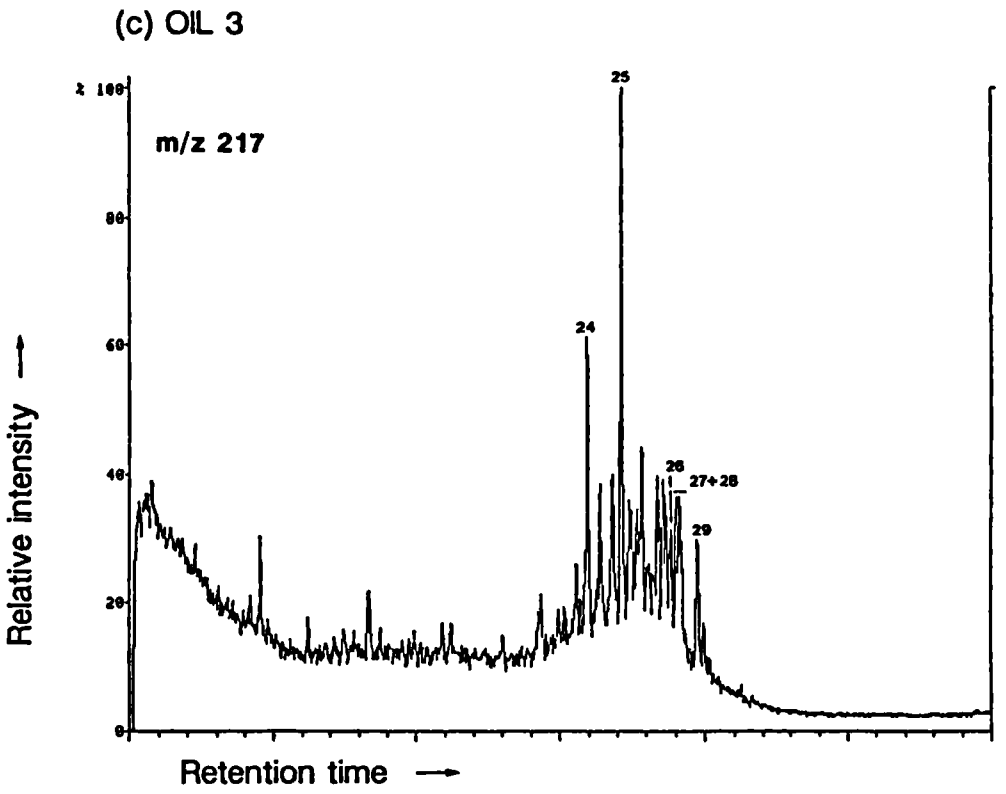


FIGURE 6.14 Sterane (m/z 217) distributions of the seven oil samples collected from different locations in the Sabah Basin. Refer to **Figure 6.1** for locations.



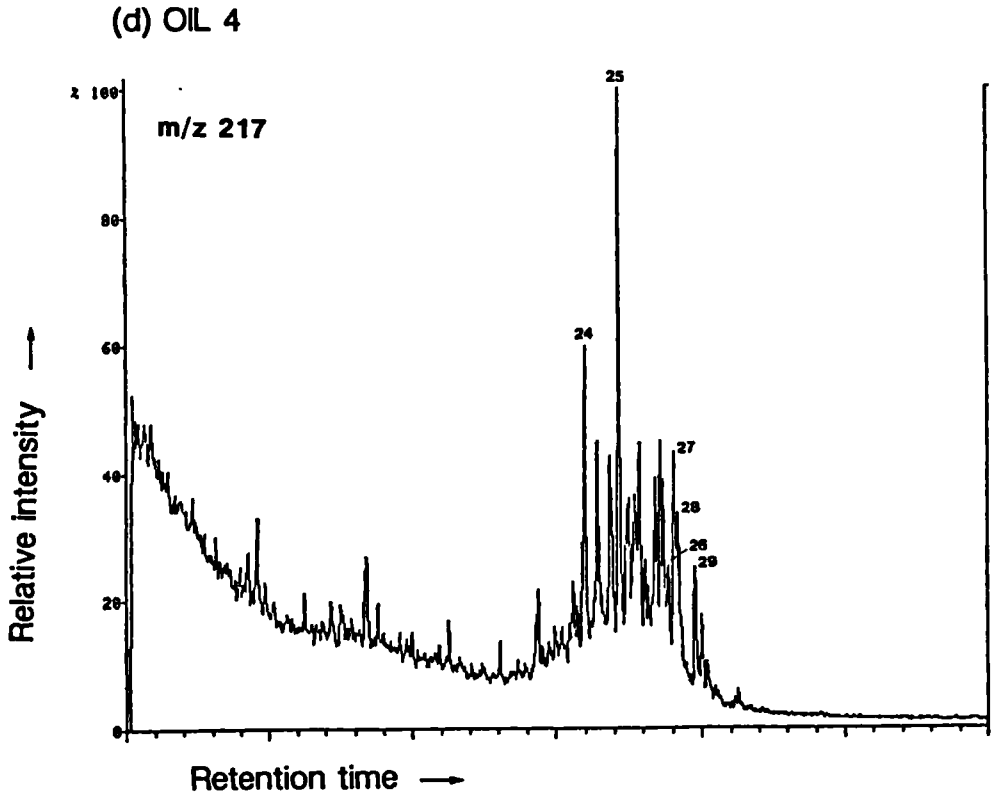
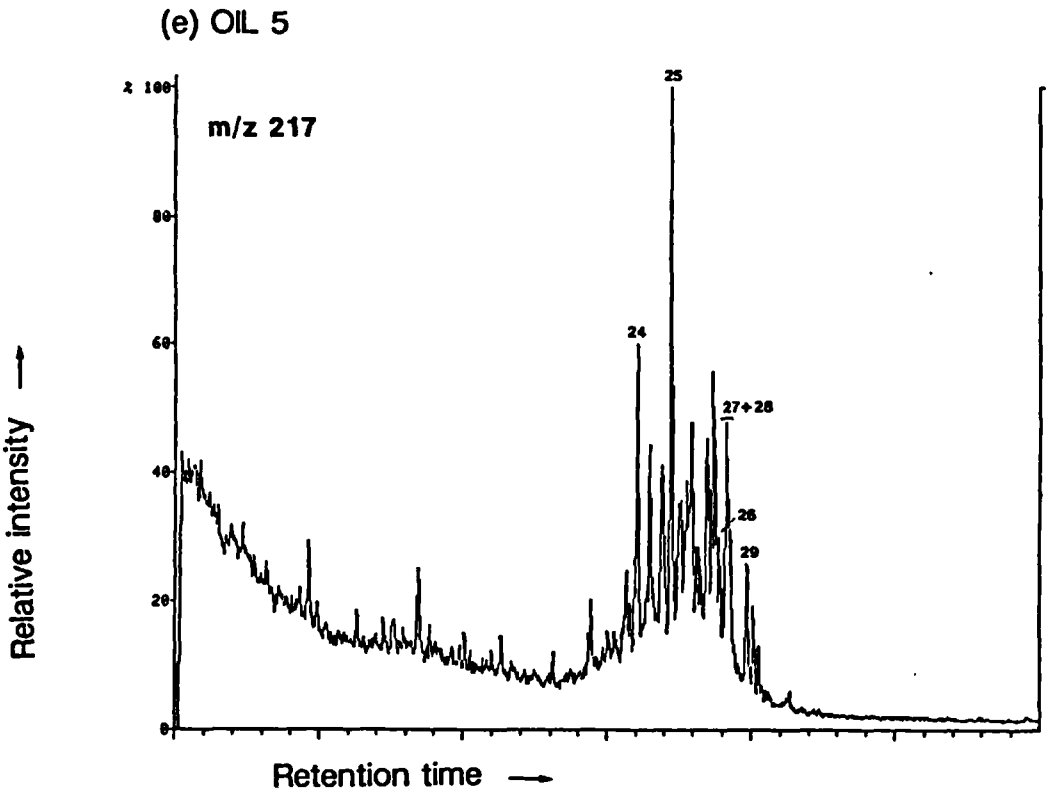


FIGURE 6.14 Continued.



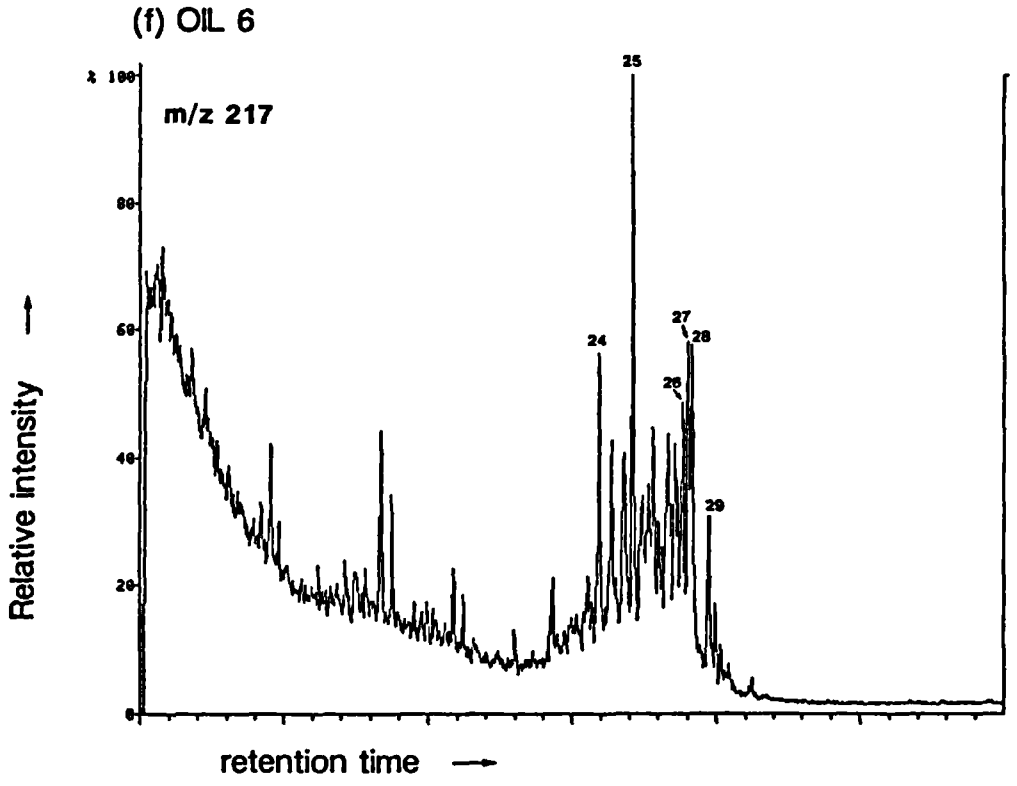


FIGURE 6.14 Continued.

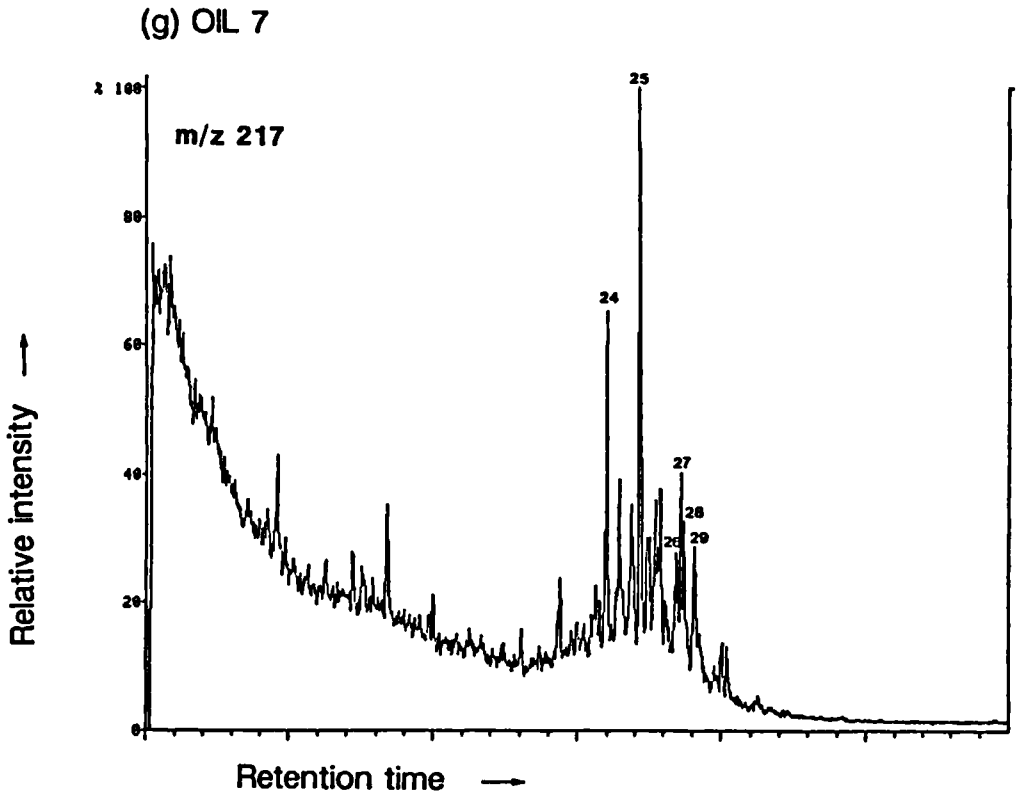


FIGURE 6.14 Continued.

according to wells grouped together according to their basinal locations : South Furious-1 and South Furious-3, Tembungo-1, Tembungo-2 and Tembungo-6, and Rusa Timur-1 and Gajah Hitam-1. The biomarker peak distributions are then compared with the pre-determined palaeo-environmental divisions based on benthic foraminifera (PETRONAS in-house reports).

6.4.2 Results : Sediment Extracts of South Furious-2 and South Furious-3

Seven and six extract samples were obtained from South Furious-2 and South Furious-3, respectively. They generally show similar biomarker distributions characterised by the presence of resins W, T and R, oleanane, C_{31}-C_{35} extended hopanes (homohopanes) and some unknown triterpanes in the m/z 191 mass fragmentograms (**Figures 6.2**, and **6.3(1)** and **(2)**). The resins and oleanane peaks provide evidence for terrestrial source input. Furthermore, the regularly decreasing peak heights of the C_{31}-C_{35} members usually represent clastic facies (Waples & Machihara, 1991), and Villar *et. al.* (1988) reported that the C_{31} member are associated with peats and coals. The concentration of the C_{31} hopane correlate well with pristane/phytane ratios which have been related to diagenetic conditions in coal swamps (ten Haven *et. al.*, 1987).

The m/z 217 mass fragmentograms from both wells are also comparable with each other. They generally show C_{29} regular sterane predominating, except where a large resin peak (W or T) is present (**Figures 6.9**, and **6.10(1)** and **(2)**). Many workers advocate care when using Huang & Meinschein's (1979) triangular diagram to determine source input, which proposed that a predominance of C_{27} regular steranes indicates marine input while a predominance of C_{29} regular steranes indicates land-derived organic matter input. The reservation was voiced when it was discovered that some marine organisms also contain C_{29} compounds (Volkman, 1986, 1988; Nichols *et. al.*, 1990). In this case, however, together with the evidence from the m/z 191 mass fragmentograms and results from the prior suite of organic geochemical analyses, it is believed that the predominance of C_{29}-regular steranes in these samples acknowledge input from higher land plants. Huang & Meinschein's scheme has been used with success, for example, Robinson (1987) found C_{29} regular steranes dominant in oils originating from a fluvio-deltaic environment in Indonesia, providing evidence for land-derived organic matter as the source.

The palaeo-environment as determined from benthic foraminifera found in the well samples indicate a bathyal sequence (Stage III) overlain by a thick deltaic-lower coastal plain sequence (sub-Stage IVA). Both the m/z 191 and m/z 217 fragmentograms generally do not show any significant differences accompanying this environmental change, except that the Stage III bathyal samples exhibit relatively smaller concentrations of C_{31}-C_{35} homohopane members (**Figures 6.2**, and **6.3(1)** and **(2)**). The presence of resins and oleanane peaks in the Stage III samples suggest input from land-derived organic matter. An important factor that needs to be taken into account

when interpreting Stage III samples is that all the samples analysed are ditch-cuttings and they could possibly be contaminated by cuttings from the overlying deltaic-lower coastal plain sediments of sub-Stage IVA.

Furthermore, only a short interval of Stage III was penetrated by both wells (173m/567ft in South Furious-2 and 18m/60ft in South Furious-3), which makes the possibility of getting a non-representative sample from Stage III even more likely. Therefore, interpretations for Stage III are inconclusive. The author intends to direct some future work towards ascertaining the organic geochemical character of Stage III sediments using samples from other wells in Sabah Basin which had penetrated thicker sections of the Stage III sequence.

6.4.3 Results : Sediment Extracts of Tembungo-1, Tembungo-2 and Tembungo-6

Only extract samples from Tembungo-1 and Tembungo-2 were analysed; these came from bathyal sediments of sub-Stage IVD. The Tembungo-6 extract was not analysed by GC-MS due to a sample volume too small to allow the separation of individual fractions. Compounds present in the m/z 191 mass fragmentograms are generally similar, except that the Tembungo-1 sample is dominated by C_{29} hopane and has relatively smaller oleanane, C_{30} hopane and unknown triterpane peaks (**Figure 6.7(1)** and **(2)**). The m/z 217 mass fragmentograms are also very comparable, with C_{29} regular steranes predominating (**Figure 6.13(1)** and **(2)**). All these provide indications of a terrigenous source input, a conclusion supported by the previous organic geochemical analyses results. The presence of terrestrial organic matter in bathyal sediments is the result of transportation into the deep marine environment by shelf-slumpings and turbidity currents. Turbidite occurrences have been reported in sub-Stages IVB and IVC by Levell & Kasumajaya (1985).

6.4.4 Results : Sediment Extracts of Rusa Timur-1 and Gajah Hitam-1

Five and two samples from Rusa Timur-1 and Gajah Hitam-1, respectively, were analysed. Rusa Timur-1 samples are from sub-Stages IVA, IVB, IVC and IVD while Gajah Hitam-1 samples are from sub-Stage IVC. Palaeo-environmental divisions from benthic foraminifera indicate that sub-Stages IVA, IVB, IVC and the lower part of IVD in Rusa Timur-1 are deep marine, and the upper part of IVD as middle-outer neritic. In Gajah Hitam-1, the sub-Stage IVD is represented by outer neritic sediments and the sub-Stage IVC by deep marine sediments.

The m/z 191 mass fragmentograms from Rusa Timur-1, in general, show similar biomarker distributions (**Figures 6.3(3), 6.5, 6.6** and **6.7(3)**). However, sample 772m (2533ft) from sub-Stage IVD is slightly different from the other samples because it does not have an oleanane peak (**Figure 6.7(3a)**), which is seen in all other samples analysed in this study. Resin W is also absent. Apart from these, the rest of the biomarker compounds present suggest land derived organic matter input with the presence of

resins T and R, and the general decreasing trend of the C_{31}-C_{35} homohopane members indicating clastic facies (Waples & Machihara, 1991). Tricyclic triterpanes have been reported to occur in relatively small amounts, or absent, in Indonesian non-marine oils originating from organic matter deposited in fluvio-deltaic environment (Robinson, 1987). The presence of a C_{24} tetracyclic triterpane in this sample also reflects its terrestrial origin (Philp & Gilbert, 1986). The m/z 217 mass fragmentograms for samples from both wells are again relatively similar in character, with C_{29} regular steranes predominating over other compounds (**Figures 6.10(3), 6.11, 6.12** and **6.13(3)**). In some samples, the resin peak is larger than the C_{29} peak. The only difference between these traces is that sample 772m (2533ft) contains C_{30} regular sterane peaks.

There are no obvious distinctions between samples from the different sub-Stages, suggesting a consistent input of land derived organic matter throughout the sediment deposition. The transport mechanism of terrestrial organic matter into deeper water areas has been attributed to shelf slumpings and turbidity currents. It is, however, rather odd that marine indicators are either absent or present in minor amounts in the deep marine sediments. This phenomenon is discussed more fully in **Chapter 8.**

6.4.5 Results : Oil Samples

Seven oils from different locations in the basin (**Figure 6.1**) were analysed for their biomarker distributions. Their mass fragmentograms show very similar general biomarker distribution; all possess dominant oleanane and C_{30}-hopane peaks in the m/z 191 fragmentograms (**Figure 6.8**). They also exhibit some tricyclic triterpane peaks relatively larger than those present in all of the sediment extracts analysed. Tricyclic terpanes were reported by Aquino Neto *et. al.* (1983) to be present in all oils not derived from terrestrial organic matter and that tricyclics have microbial or algal origin. These tricyclics, however, do not predominate over the regular and extended hopanes and, based on evidence from other geochemical analyses, these oils are more likely to have been generated by land-derived organic matter.

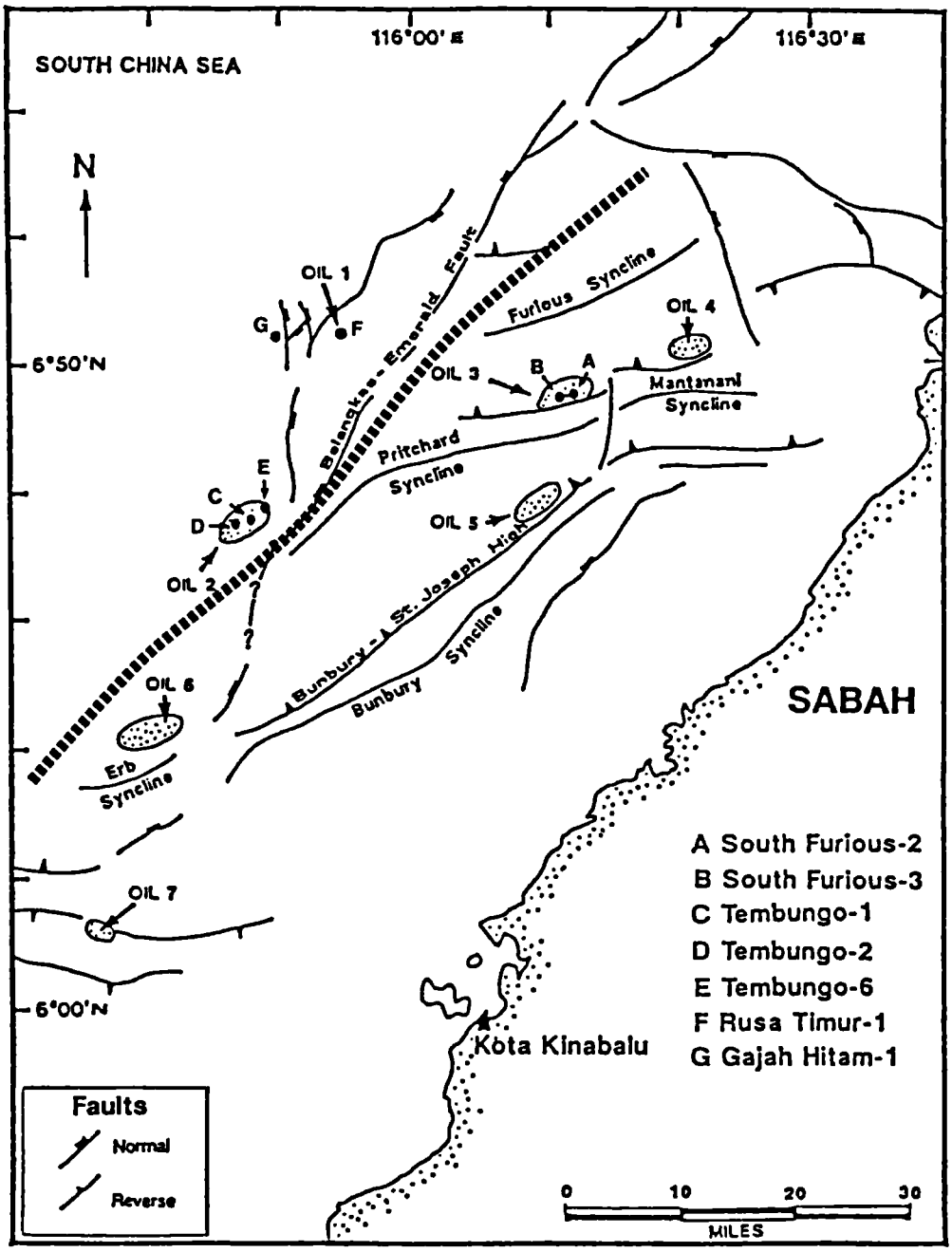
The m/z 217 fragmentograms are also very similar to each other (**Figure 6.14**), with the Rusa Timur and Tembungo oils (Oils 1 and 2, respectively) showing slight differences with their relatively larger C_{29}-ββ peaks. The C_{30} regular steranes are present in Rusa Timur and Tembungo oils in greater amounts than the other oil samples. Moldowan *et. al.* (1985) and Mello *et. al.* (1988a, 1988b) proposed that these compounds are only present in post-Silurian samples deposited in marine environments. Using this proposal, it would seem that Rusa Timur and Tembungo oils originated from terrestrial organic matter deposited in relatively more marine environments while the rest of the oils were derived from similar organic matter deposited in relatively less marine environments. This deduction seems to show a general agreement with the depositional palaeoenvironment of sub-Stage IVA. Oils from the 'inner belt' (South

Furious, Barton, St. Joseph, Erb West and Ketam oils) originated from land-derived organic matter deposited in paralic/deltaic-lower coastal plain environments of sub-Stage IVA while the two 'outer' oils (Rusa Timur and Tembungo oils) were produced by terrigenous organic matter deposited in predominantly bathyal environments **(Figure 6.15)**.

It has been proposed that the triterpane/sterane ratio is an organic matter source indicator where oils generated from terrigenous organic matter commonly have high triterpane/sterane ratios, as in the Gippsland Basin (Philp & Gilbert, 1986), Mahakam Delta (Hoffman *et. al.*, 1984), Taiwan oils (Philp *et. al.*, 1990) and some oils from the West and Central African rift system (Genik, 1993). Oils sourced from kerogens of marine origin will conversely have lower triterpane/sterane ratios. Waples & Machihara (1991) expressed concern in the method of calculating this ratio because presently, there is no uniformity over which hopane and sterane peaks are to be used for the calculation of the ratio. In this study, the triterpane/sterane ratio of the oils are calculated by taking the abundance ratio of the largest triterpane peak to the largest sterane peak. The resulting triterpane/sterane ratios for the seven oils are :

Oil Sample	**Triterpane/Sterane Ratio**
Rusa Timur	3 : 1
Tembungo	3 : 1
South Furious	7 : 1
Barton	5 : 1
St. Joseph	5 : 1
Erb West	5 : 1
Ketam	8 : 1

From the hopane/sterane ratio comparative chart **(Figure 6.16)** in Genik (1993), these oils generally plot in the paralic oil zone. The lowest ratios are from Rusa Timur and Tembungo oils, which are from the deeper water parts of the basin compared to the rest of the oil samples **(Figure 6.15)**. This is further evidence for the preservation of land-plant organic matter in more marine depositional environments, and concurs with the relatively higher C_{30} regular sterane concentrations. Unfortunately, this seems to indicate that the triterpane/sterane ratio may be affected by depositional environment conditions when it is defined as a source indicator. For example, Rusa Timur and Tembungo oils are classified as marine-paralic oils on the hopane/sterane ratio comparative chart **(Figure 6.16)**, but it has been established by other organic geochemical parameters that these oils have been produced from terrigenous, Type III kerogen. The complex relationship between organic facies and the triterpane/sterane ratio (Waples & Machihara, 1991) may have been underestimated. It is also possible that differences in the resulting ratios are caused by the selection of different hopane and sterane peaks for the calculations. To enable the use of this ratio with more certainty, it is therefore necessary to conform to some sort of uniformity, or



KEY: OIL 1 = Rusa Timur
OIL 2 = Tembungo
OIL 3 = South Furious
OIL 4 = Barton
OIL 5 = St. Joseph
OIL 6 = Erb West
OIL 7 = Ketam

FIGURE 6.15 The dividing line between the 'inner' and 'outer' oils based on the relative abundance of C_{30} regular steranes and triterpane/sterane ratios. Oil 1 (Rusa Timur) and Oil 2 (Tembungo) are deduced to have been generated by land-derived organic matter deposited in deep-marine environments while the other oils were sourced by terrestrial organic matter deposited in deltaic-lower coastal plain environments.

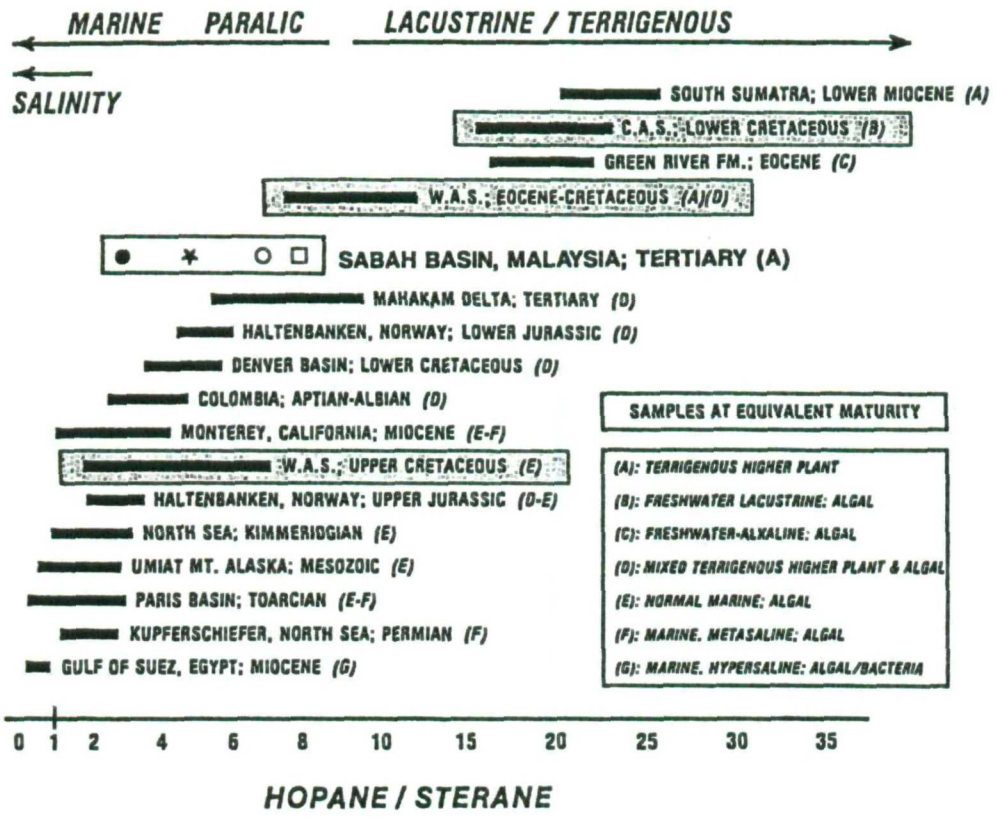


FIGURE 6.16 Comparative chart of hopane/sterane ratios in oils sourced from marine, paralic and lacustrine/terrigenous kerogens (modified from Genik, 1993).

standardisation, in terms of peak selection. This will eliminate result discrepancies caused by using different peaks, making the ratio universally applicable and useful for comparing oils from all over the world.

Oil-sediment extract correlation is not attempted here because of the 'false bitumen' situation. As a result of the extracts being contaminated by migrating hydrocarbons, oil-source rock correlation now depends rather heavily on carbon isotopic compositions of the kerogens and hydrocarbon fractions of the oils.

6.5 Biomarkers as thermal maturity indicators

6.5.1 Introduction

Biomarkers in the mobile bitumen fraction can only be used as maturity indicators if the bitumen is indigenous (Waples & Machihara, 1991). Maturity determination from biomarkers should ideally be supported by those obtained from other geochemical techniques. Kerogen analysis is considered to be the most reliable because, once deposited, the kerogen is immobile and the maturity results will therefore reflect the maturity level of the sediment in which it is in.

6.5.1a Steranes

i) 20S/[20S+20R] epimer ratios

In immature sediments, steranes occur exclusively in the 20R configuration. With increasing maturation, the proportion of 20S molecules increases as the 20R molecules change configuration (**Figure 6.17**). Eventually, the isomerisation leads to an equilibrium state where the ratio of 20S/[20S+20R] becomes 55 : 45. This ratio reaches equilibrium value prior to the onset of intense hydrocarbon generation (VRo $\approx$ 1.0%) after which no further changes occur. Theoretically, any of the C_{27}, C_{28} or C_{29} steranes can be used for maturity calculations. However, sterane mixtures are highly complex, with peaks overlapping in the fragmentogram. The C_{29} sterane is the least affected by co-elution (Waples & Machihara, 1991), providing the most accurate maturity measurement and is used for the maturity calculations in this study.

6.5.1b Triterpanes

i) 22S/[22S+22R]

The biologically produced 22R form of the C_{31}-C_{35} extended 17α(H)-hopane transforms into the 22S form with maturation (**Figure 6.18**). Increasing maturation results in an equilibrium mixture of 22S and 22R epimers with an approximate ratio of 60:40. Equilibrium is reached very rapidly (VRo $\approx$ 0.6%), making the effective range of this ratio limited to immature sediments. Any of the C_{31}-C_{35} 17α(H)-extended hopanes can be used for calculating the 22S/(22S+22R) ratio; in this study the C_{32} homologue was used.

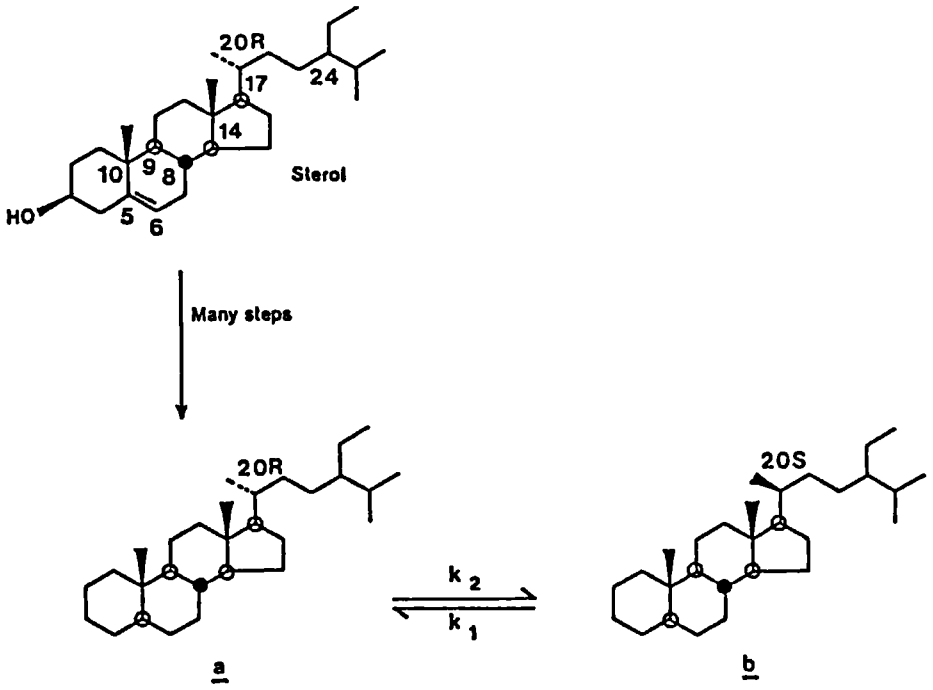


FIGURE 6.17 The transformation of sterane 20R to the 20S configuration (from Mackenzie & McKenzie, 1983).

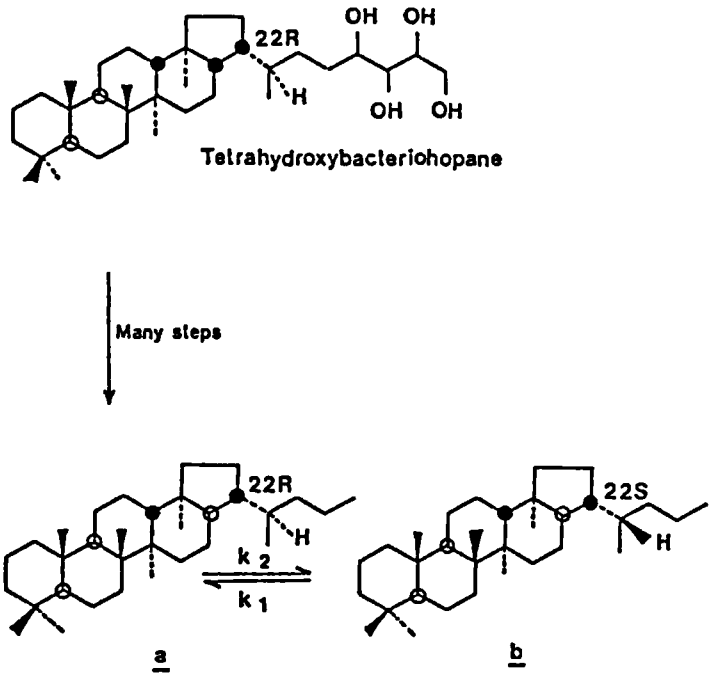


FIGURE 6.18 The transformation of triterpane 22R to the 22S configuration (from Mackenzie & McKenzie, 1983).

ii) Moretane/Hopane

The decrease in moretane concentration with maturity occurs more rapidly than the 17α (H)-hopanes, being less stable (Kvenvolden & Simoneit, 1990). Its usefulness is, thus, limited to immature sediments (VRo < 0.60%).

iii) Tm/Ts

With increasing maturity, the relative concentration of Tm gradually decreases, resulting in the apparent increase in Ts concentration. This ratio begin to decrease quite late during maturation i.e. VRo > 0.90% (van Graas, 1990) and in principle, the ratio should be able to supplement maturation determinations at maturity levels above 0.75% VRo. The Tm/Ts ratios, however, has been reported to be facies-related (Snowdon *et. al.*, 1987; Rullkotter & Marzi, 1988), possibly due to the natural variation in original Ts content (Waples & Machihara, 1991).

iv) Oleanane Parameter : $\frac{18\alpha(H)\text{-oleanane} + 18\beta(H)\text{-oleanane}}{[(18\alpha(H)\text{-oleanane} + 18\beta(H)\text{-oleanane}) + C_{30}\text{-hopane}]}$

This ratio has been shown to increase with depth (Ekweozor & Udo, 1988; Ekweozor & Telnaes, 1990) and peaks near the onset of intense oil generation before decreasing with further maturation.

v) 18α(H)-Oleanane/18β(H)-Oleanane

Maturation converts 18β(H)-oleanane to 18α(H)-oleanane. With increasing maturation, this ratio increases over a maturity range from approximately 0.6% VRo to peak oil generation (Riva *et. al.*, 1988).

6.5.2 Results : Sediment Extracts

Biomarker maturity ratios calculated from m/z 191 triterpane and m/z 217 sterane mass fragmentograms are listed according to the wells in **Table 6.3**. As was mentioned earlier, these biomarker ratios cannot be used for determining sediment maturity levels due to possible intermixing between biomarkers present in the residual migrated hydrocarbons and the *in situ* biomarkers. It is also interesting to note that the 20S/[20S+20R] sterane and 22S/[22S+22R] triterpane ratios were highly correlatable to production index values (**Figure 6.19**). The sediments analysed are all immature, as established from pyrolysis Tmax and vitrinite reflectance values; the unidentified compounds in the m/z 191 mass fragmentograms are probably ββ-hopanes found only in samples of very low maturity (Waples & Machihara, 1991). The production index values can then be used to indicate the extent of contamination by migrating hydrocarbons.

It is proposed here that if contamination by the residual migrated hydrocarbons is low, then the resulting 20S/[20S+20R] sterane and 22S/[22S+22R] biomarker ratios

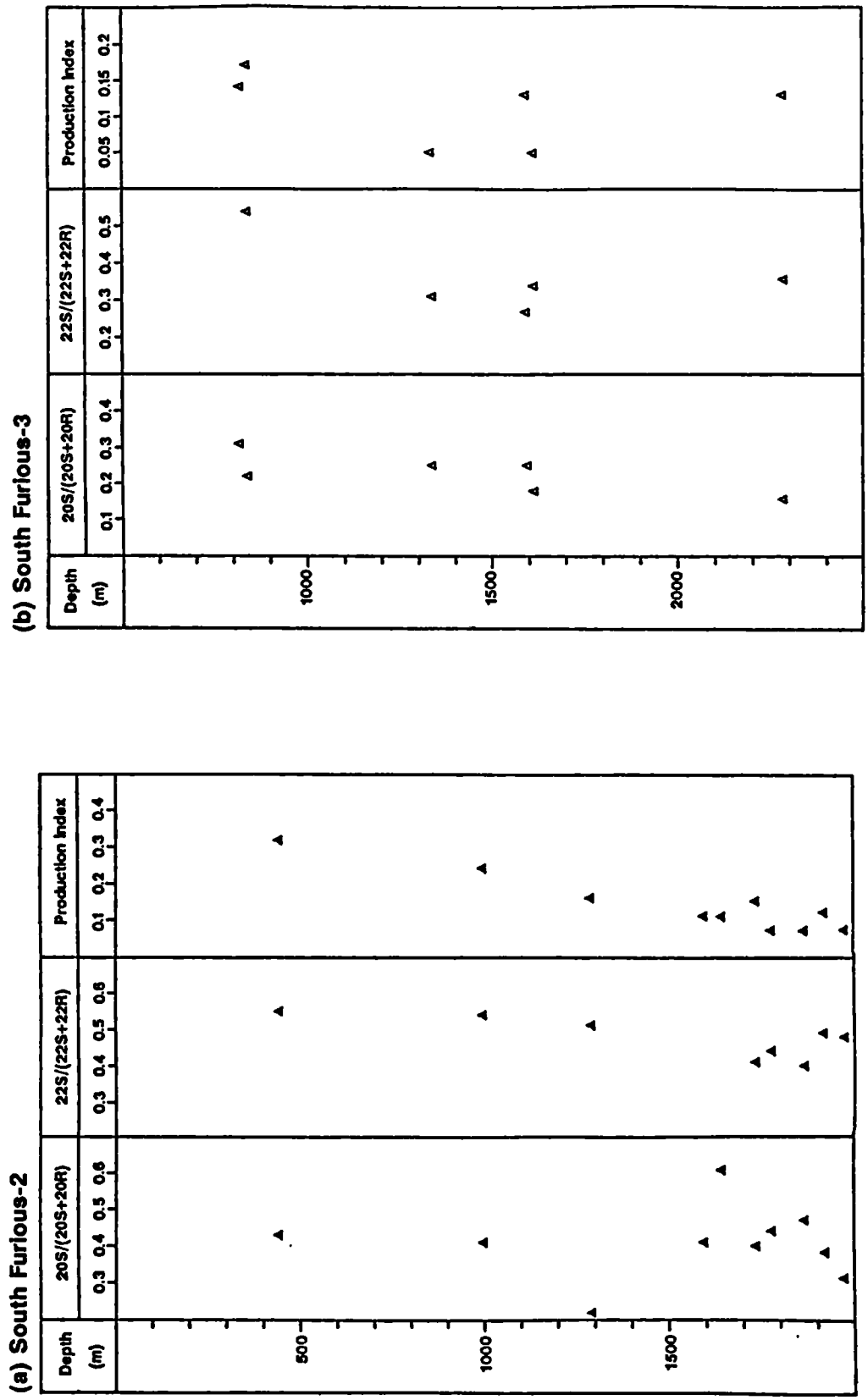
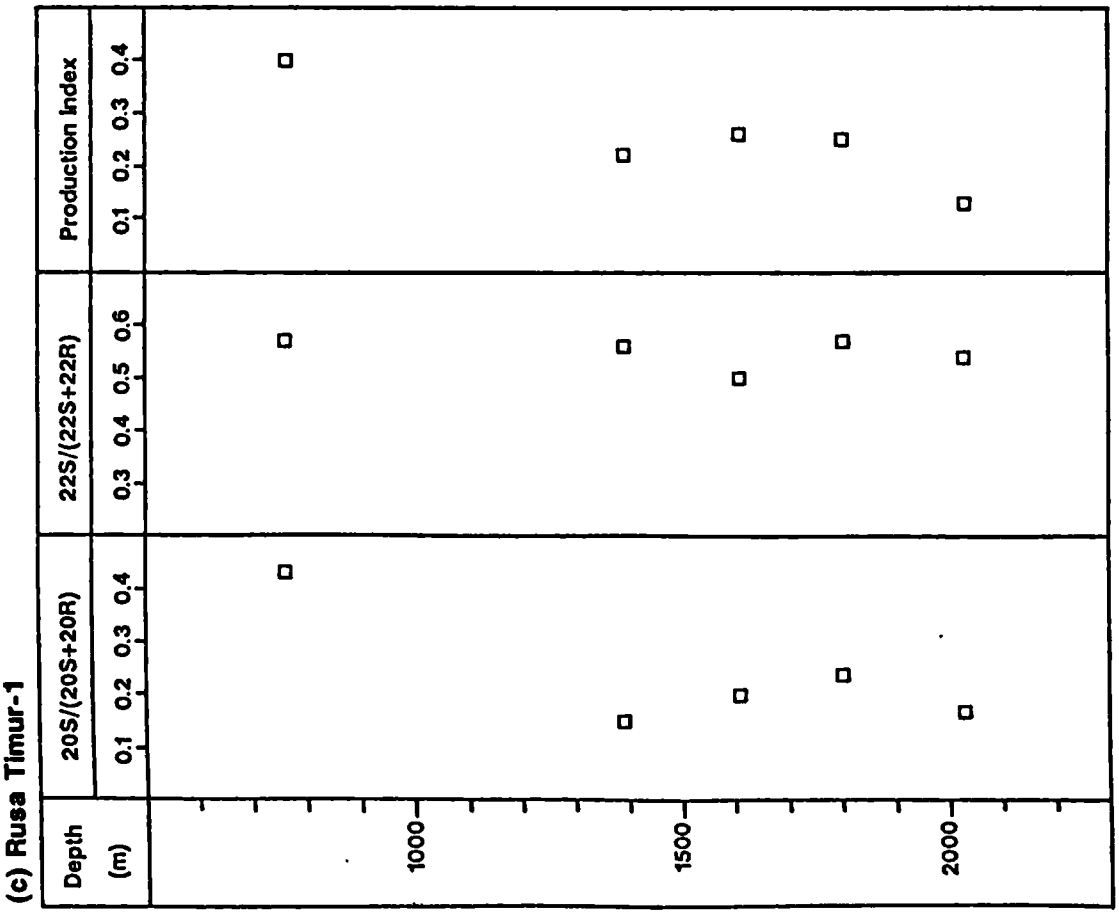


FIGURE 6.19 Comparison between the sterane 20S/(20S+20R) and triterpane 22S/(22S+22R) biomarker maturity ratios with the production index values for (a) South Furious-2, (b) South Furious-3, (c) Rusa Timur-1 and (d) Gajah Hitam-1.



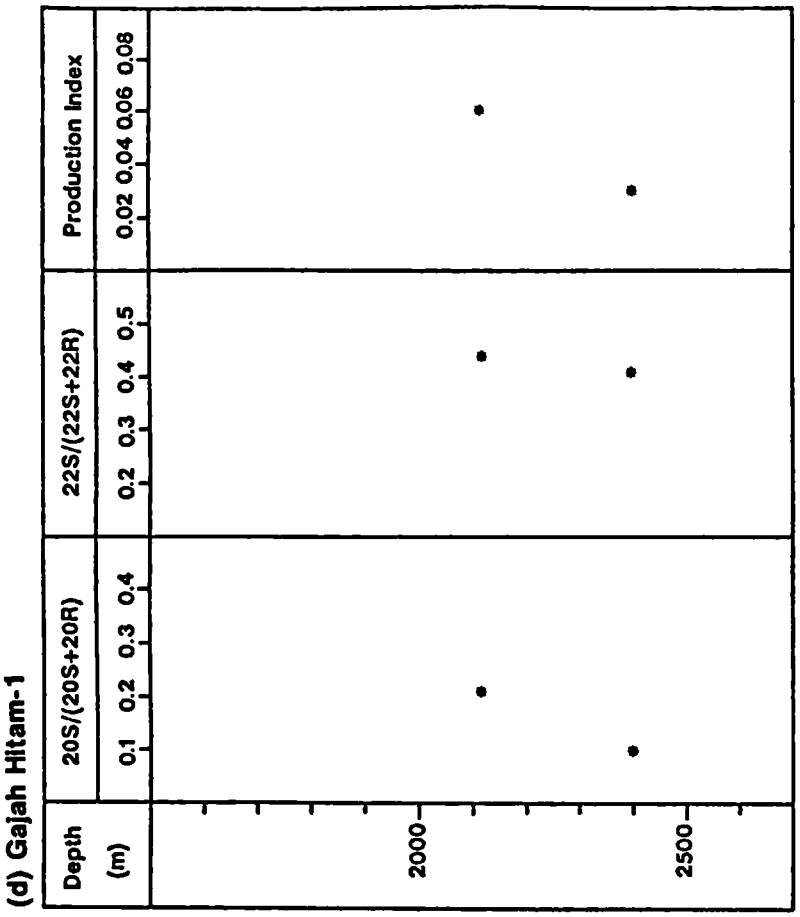


FIGURE 6.19 Continued.

will be correspondingly low, since the biomarkers present will be more representative of the immature sediments from which they were extracted. Conversely, if contamination by residual migrated hydrocarbon is high, then the ratios will be correspondingly high, reflecting the maturity level already attained by the sediments that generated the hydrocarbons. The immature *in situ* biomarkers will be present but in relatively smaller concentrations compared to when contamination is low. **Figure 6.19** shows the maturity ratios from 20S/[20S+20R] sterane and 22S/[22S+22R] triterpane fluctuating with increasing depth, resulting in an overall trend of decreasing with depth. Maturity is indicated to be highest in the shallower samples when they should naturally be the least mature. This trend is taken as an indication of the upward direction of hydrocarbon migration. The true sediment maturity is taken to be the lowest ratio value obtained, where the effects of contamination from migrated hydrocarbons is minimal.

Table 6.3 Results from the thermal maturity parameters for the sediment extract samples of **(a)** South Furious-2, **(b)** South Furious-3, **(c)** Tembungo-1, **(d)** Tembungo-2, **(e)** Rusa Timur-1 and **(f)** Gajah Hitam-1 wells.

(a) South Furious-2

Sample depth	Stage	Thermal Maturity Parameters						
		1	2	3	4	5	6	7
1) 446m/1463ft	IVA	0.43	0.55	0.17	1.19	n.a.	0.50	0.32
2) 1002m/3287ft	IVA	0.41	0.54	0.17	1.25	1.57	0.46	0.24
3) 1293m/4242ft	IVA	0.21	0.51	0.22	1.41	n.a.	0.52	0.16
4) 1603m/5259ft	IVA	0.41.	n.d	2.33	n.d.	0.15	0.73	0.11
5) 1644m/5394ft	IVA	0.61	n.d.	1.52	n.d.	0.29	0.73	0.11
6) 1738m/5702ft	IVA	0.40	0.41	0.92	1.96	0.68	0.60	0.15
7) 1779m/5837ft	IVA	0.44	0.44	2.82	4.17	0.36	0.66	0.07
8) 1871m/6138ft	III	0.47	0.40	0.80	3.85	0.49	0.50	0.07
9) 1921m/6302ft	III	0.38	0.49	0.65	2.04	n.a.	0.45	0.12
10) 1979m/6493ft	III	0.31	0.48	0.67	3.03	n.a.	0.46	0.07

(b) South Furious-3

Sample depth	Stage	Thermal Maturity Parameters						
		1	2	3	4	5	6	7
1) 826m/2710ft	IVA	0.31	n.d.	0.97	2.63	n.a.	0.68	0.14
2) 841m/2759ft	IVA	0.22	0.54	0.25	2.44	n.a.	0.18	0.17
3) 1346m/4416ft	IVA	0.25	0.31	0.30	2.00	n.a.	0.29	0.05
4) 1602m/5256ft	IVA	0.25	0.27	0.31	4.00	n.a.	0.33	0.13
5) 1617m/5305ft	IVA	0.18	0.34	0.28	3.03	n.a.	0.27	0.05
6) 2291m/7516ft	IVA	0.16	0.36	0.67	n.d.	n.a.	0.56	0.13

Table 6.3 Results from the thermal maturity parameters for the sediment extract samples of **(a)** South Furious-2, **(b)** South Furious-3, **(c)** Tembungo-1, **(d)** Tembungo-2, **(e)** Rusa Timur-1 and **(f)** Gajah Hitam-1 wells - continued.

(c) Tembungo-1

Sample depth	Stage	Thermal Maturity Parameters						
		1	2	3	4	5	6	7
1) 1809m/5935ft	IVD	0.05	0.64	0.24	n.d.	n.a.	0.30	0.11

(d) Tembungo-2

Sample depth	Stage	Thermal Maturity Parameters						
		1	2	3	4	5	6	7
1) 1994m/6542ft	IVD	0.05	0.64	0.30	n.d.	n.a.	0.32	0.16

(e) Rusa Timur-1

Sample depth	Stage	Thermal Maturity Parameters						
		1	2	3	4	5	6	7
1) 772m/2533ft	IVD	0.43	0.57	0.13	n.d.	n.a.	-	0.40
2).1406m/4613ft	IVD	0.15	0.56	0.20	n.d.	n.a.	0.43	0.22
3) 1619m/5312ft	IVC	0.20	0.50	0.07	1.56	n.a.	0.40	0.26
4) 1814m/5951ft	IVB	0.24	0.57	0.22	n.d.	n.a.	0.54	0.25
5) 2040m/6693ft	IVA	0.17	0.54	0.26	n.d.	n.a.	0.51	0.13

(f) Gajah Hitam-1

Sample depth	Stage	Thermal Maturity Parameters						
		1	2	3	4	5	6	7
1) 2117m/6946ft	IVC	0.21	0.44	0.30	2.94	n.a.	0.29	0.06
2) 2401m/7877ft	IVC	0.10	0.41	0.50	n.d.	n.a.	0.46	0.03

Key :

1	Sterane 20S/(20S+20R)	2	Triterpane 22S/(22S+22R)
3	Moretane/C_{30}-hopane	4	Tm/Ts
5	18α(H)/18β(H)	6	Oleanane Parameter
7	Production Index	n.a.	not analysed
n.d.	not determinable		

Oleananes have been used as maturity indicators (Riva *et. al.*, 1988; Ekweozor & Udo, 1988; Ekweozor & Telnaes, 1990). In this study, it was initially attempted to separate the two oleanane peaks, 18α(H)-oleanane and 18β(H)-oleanane, and use Riva *et. al.*'s maturity ratio of 18α(H)-oleanane/18β(H)-oleanane, reported to increase with increasing thermal maturation. To quickly ascertain the decreasing maturity trend with depth as indicated by the sterane and triterpane epimer ratios, the shallowest and deepest samples from South Furious-2 were analysed first. The complete analytical

results **(Table 6.3, Figure 6.20)** for South Furious-2 samples, in general, support this trend. Further analysis for the separation of the 18α(H)-oleanane and 18β(H)-oleanane of the rest of the samples were, unfortunately, hindered by some problems faced after the replacement of the GC-MS column. To overcome this problem, an alternative oleanane ratio is used. The **Oleanane Parameter** was proposed by Ekweozor & Udo (1988) where :

$$\textbf{Oleanane Parameter} = \frac{(18\alpha(H)\text{-oleanane} + 18\beta(H)\text{-oleanane})}{[(18\alpha(H)\text{-oleanane} + 18\beta(H)\text{-oleanane}) + C_{30}\text{-hopane}]}$$

According to Ekweozor & Telnaes (1990), the Oleanane Parameter is useful throughout the oil generation window as it increases with depth, peaks at the maximum hydrocarbon generation stage and then uniformly declines. The Oleanane Parameter is calculated for the samples analysed in this study, bearing in mind that the resulting values will not reflect the true maturity levels of the sediments. This exercise is to observe whether the oleananes are similarly affected by migrated hydrocarbons in the same way as the previous 20S/[20S+20R] sterane and 22S/[22S+22R] triterpane ratios.

It is expected that the Oleanane Parameter will show a trend of decreasing with depth without a peak value, based on the immature status of the samples. However, results show that the Oleanane Parameter does have peak values, particularly in South Furious-2 and Rusa Timur-1 wells **(Figure 6.20)**, and behaves in similar fashion as that reported by Ekweozor & Telnaes (1990). The major differences here are firstly, this trend occurs in sediments indicated to be immature by other maturity parameters; secondly, the absolute values obtained for the Oleanane Parameter, ranging between 0.18 - 0.73, are generally much larger than the 0.1 - 0.4 value range reported by Ekweozor & Udo (1988) and Ekweozor & Telnaes (1990).

Moretane/C_{30}-hopane ratios should decrease with increasing thermal maturation. Here, they do not indicate the sediments' maturity levels; instead, their fluctuating nature with depth **(Figure 6.21)** provide evidence for the influence of residual migrated hydrocarbons. The Tm/Ts ratio is reported to decrease with increasing maturity (Philp, 1985; Jones & Philp, 1990). Here again, the effects of residual migrated hydrocarbons on the biomarker ratio is apparent. With increasing residual hydrocarbon content relative to the *in situ* biomarkers, which has been established to occur in the shallower samples as a result of upward migratory movement of the hydrocarbons, the Tm/Ts values of South Furious-2 and South Furious-3 generally decrease. This is the reverse of the expected trend of decreasing with depth **(Figure 6.21)**.

6.5.3 Results : Oil Samples

Biomarker maturity ratios calculated for the oils are presented in **Table 6.4**. In general, the oils have 20S/[20S+20R] sterane ratios < 0.55, 22S/[22S+22R] triterpane ratios ≤ 0.60 and moretane/hopane ratios > 0.10. Study of Tertiary oils by Grantham (1986b) revealed higher moretane/hopane ratios compared to those determined from older oils,

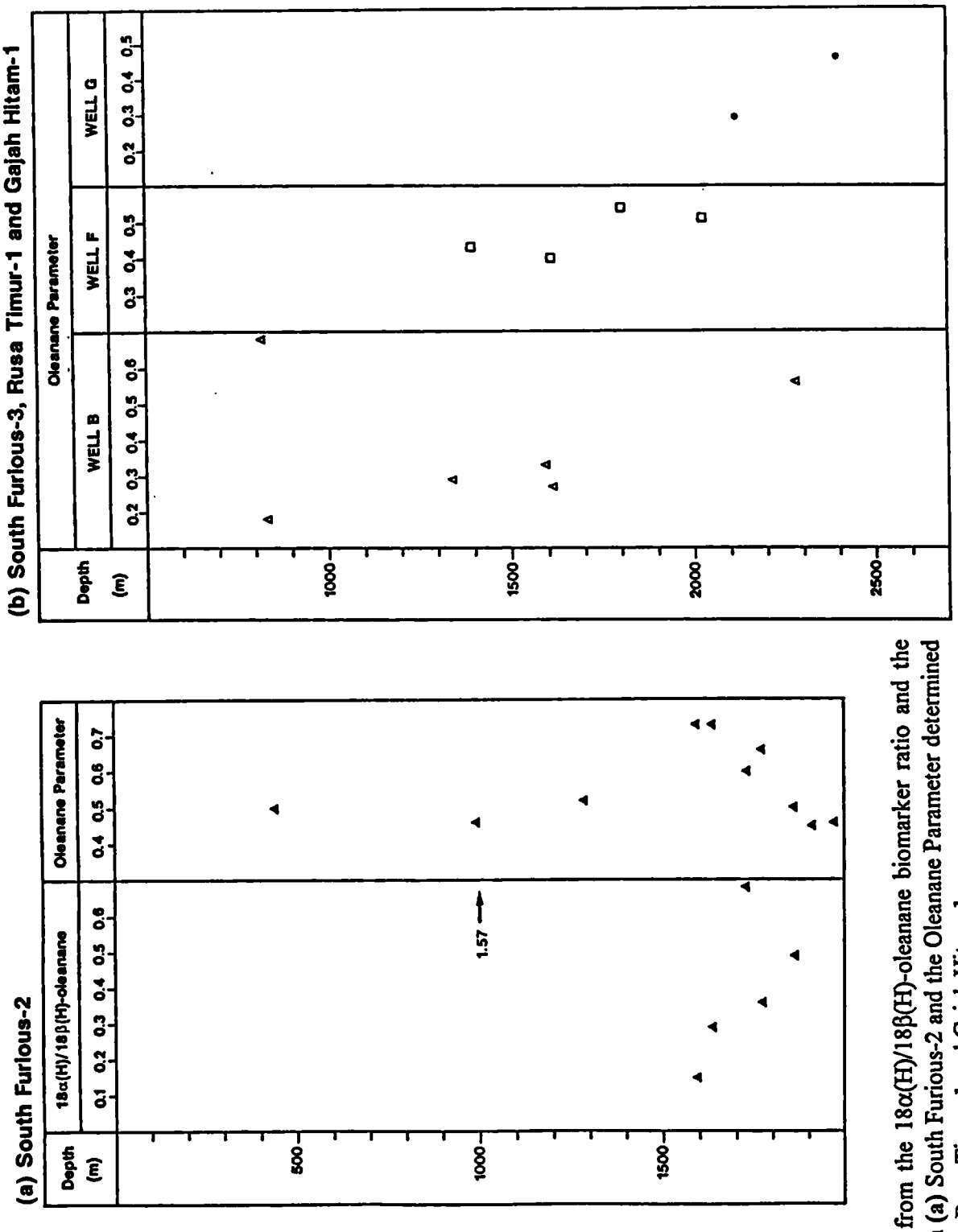


FIGURE 6.20 Results from the 18α(H)/18β(H)-oleanane biomarker ratio and the Oleanane Parameter from (a) South Furious-2 and the Oleanane Parameter determined from (b) South Furious-3, Rusa Timur-1 and Gajah Hitam-1.

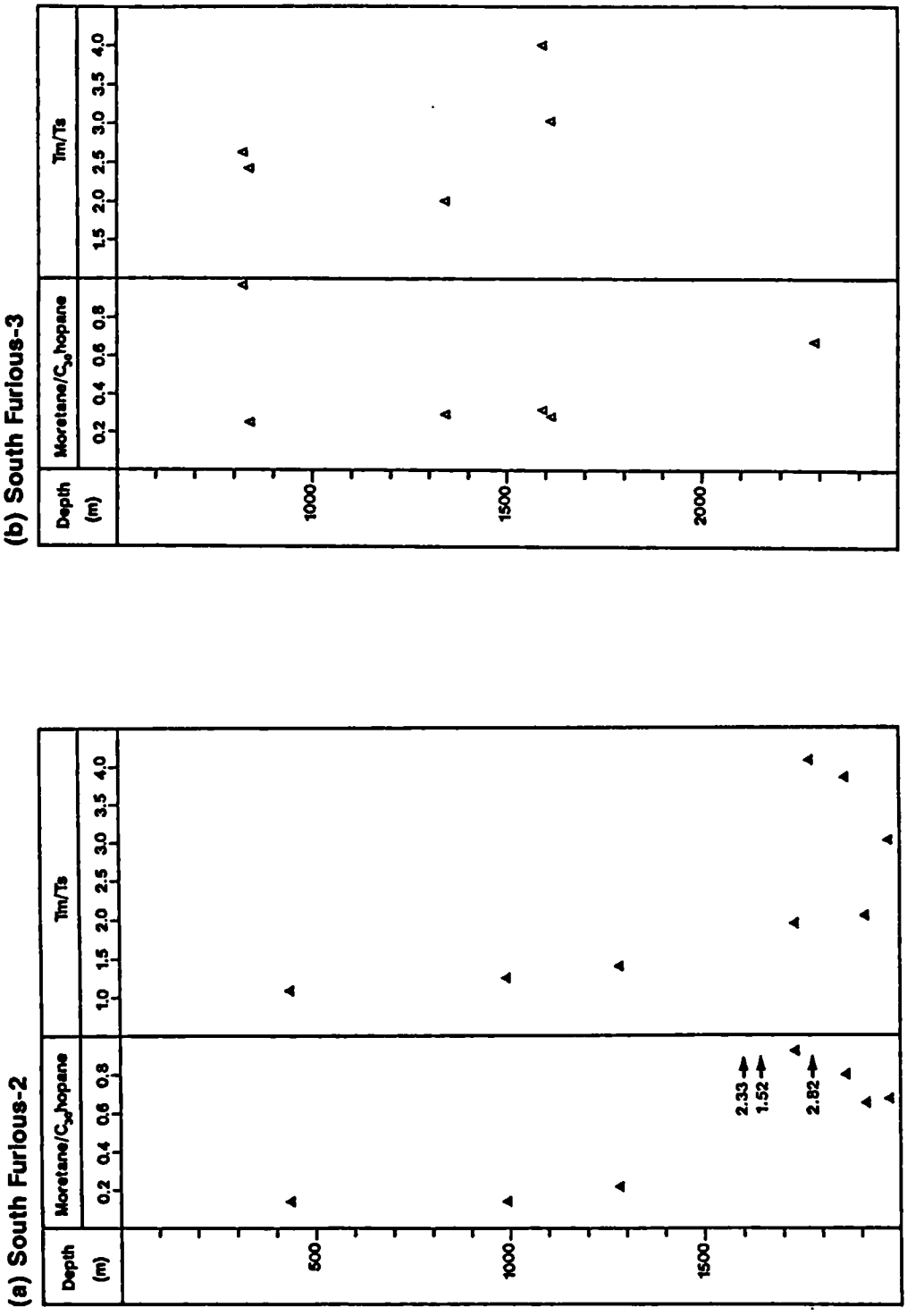
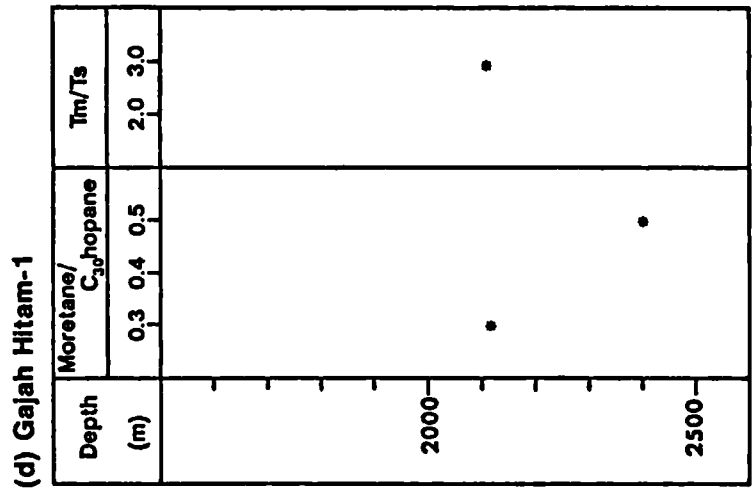


FIGURE 6.21 The moretane/C_{30}-hopane and Tm/Ts biomarker ratios for (a) South Furious-2, (b) South Furious-3, (c) Tembungo-1 and (d) Gajah Hitam-1.



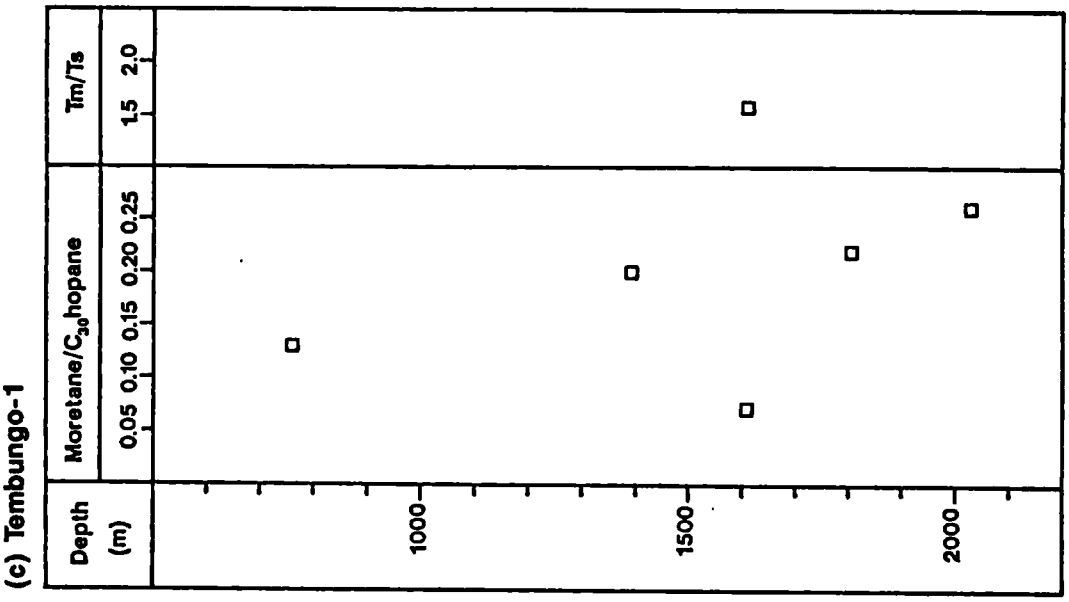


FIGURE 6.21 Continued.

ranging between 0.1 and 0.3 with values of 0.15 to 0.20 being common. Moretane/hopane values obtained from the oil samples in this study also support the observations of Grantham (1986b) with values ranging between 0.12 and 0.27.

In the same paper, Grantham also noted that the 20S/[20S+20R] sterane ratios of the Tertiary oils appear to be retarded, not quite reaching the expected equilibrium value of 0.55. He underlined the significance of time in sterane isomerisation, thus confirming observations of earlier workers whose researches had indicated the differing rates of sterane epimerisation and kerogen maturation (Mackenzie & McKenzie, 1983; Mackenzie, 1984; Rullkotter & Marzi, 1988). Grantham proposed that the rapid sedimentation rates often experienced by young Tertiary basins may have influenced the chemical reactions of the biomarkers, resulting in retardation of the epimerisation process. Again, the 20S/[20S+20R] sterane ratios of the Sabah Basin oils concur, with values much lower than the equilibrium value of 0.55, ranging between 0.29 and 0.53 **(Table 6.4).**

The 22S/[22S+22R] triterpane ratios were calculated from the C_{32} homologue. Even though the ratios determined from the oils are less than the expected equilibrium value of 0.60, they are very close to it, with values ranging from 0.57 to 0.59. They somehow appear to be unaffected by the yet unclear processes which caused the retardation of the sterane epimer ratio. It is therefore proposed here that, for Tertiary oils, the 22S/[22S+22R] biomarker ratio is a relatively more reliable maturity indicator than the 20S/[20S+20R]-sterane and moretane/hopane biomarker ratios. The question as to why only the triterpane 22S/[22S+22R] epimer is unaffected remains to be answered. Further investigations may clarify the possible underlying reasons for the different behaviours of the two biomarker ratios.

Table 6.4 Results from the thermal maturity paramcters for the seven oil samples.

Oil No.	Thermal Maturity Parameters					
	1	2	3	4	5	6
1	0.38	0.57	0.27	2.63	n.a.	0.50
2	0.29	0.57	0.26	2.63	n.a.	0.50
3	0.39	0.59	0.25	1.56	n.a.	0.57
4	0.40	0.57	0.26	2.00	n.a.	0.51
5	0.45	0.59	0.25	2.38	n.a.	0.55
6	0.53	0.58	0.14	3.45	n.a.	0.64
7	0.40	0.59	0.12	1.79	n.a.	0.48

Key :

1	Sterane 20S/(20S+20R)	**2**	Triterpane 22S/(22S+22R)
3	Moretane/C_{30}-hopane	**4**	Tm/Ts
5	18α(H)/18β(H)	**6**	Oleanane Parameter
n.a.	not analysed		

The Oleanane Parameter theoretically should provide information on the maturity level of the source rock at which the hydrocarbons were expelled. There is, however, a

problem in correlating the absolute Oleanane Parameter values obtained from the Sabah oils with vitrinite reflectance, as they are generally higher **(Table 6.4)** than those reported by Ekweozor & Udo (1988) and Ekweozor & Telnaes (1990). Vitrinite reflectance equivalent values, therefore, cannot be directly determined. This goes to emphasise the need to obtain more information on the behaviour of oleananes in general, in order to be able to confidently use, or reject altogether, the oleanane ratios as maturity indicators.

6.6 Pattern recognition within a multivariate data set : Principal components analysis

6.6.1 Introduction

Data analysis generally becomes more complex as the number of input data, or variables, increases. A pictorial way of looking at the data through graphs is limited to a maximum of three variables at one time. In organic geochemical analyses, more often than not , the input data are very large, generated by the highly sophisticated instruments used which supply a wealth of data for each analysed sample. When faced with the final data table consisting of numerous rows and columns, the process of data interpretation, or information extraction, can be a confusing one which can also be influenced by the interpreter's bias towards certain variables. To overcome this problem and to confirm, or refute, interpretations made earlier, biomarker data of the oil and extract samples were subjected to principal component analysis using the PC-based programme SIRIUS, Version 2.3 of Karstang & Kvalheim (1991).

Principal component analysis provides a way of analysing multivariate data sets more efficiently by treating all the data together, in contrast to other techniques which only treat one, two, or at the most, three variables at any one time (Christie *et. al.*, 1984). To analyse the relationship between all variables concurrently, the variables must be plotted in a variable space which has as many dimensions as there are variables. This will give a unique point representation for each sample and the inter-relation between samples can then be described in terms of their resulting positions.

Once the data are plotted in a multi-dimensional variable space, extraction of information can be made. The principal component method reduces the multi-dimensionality of the data by extracting the minimum number of principal components, also known as eigenvectors, which best span the data. Basically, the directions of large data point scatter in this hyper-space are also the directions of high information density. In principal component analysis, the original data set is decomposed into a principal component described by 'loadings' and 'scores', and a residual matrix **(Figure 6.22)**. The loading refers to the contribution of a variable on the principal component; the higher the loading, the larger the effect, and vice-versa. The score represents the

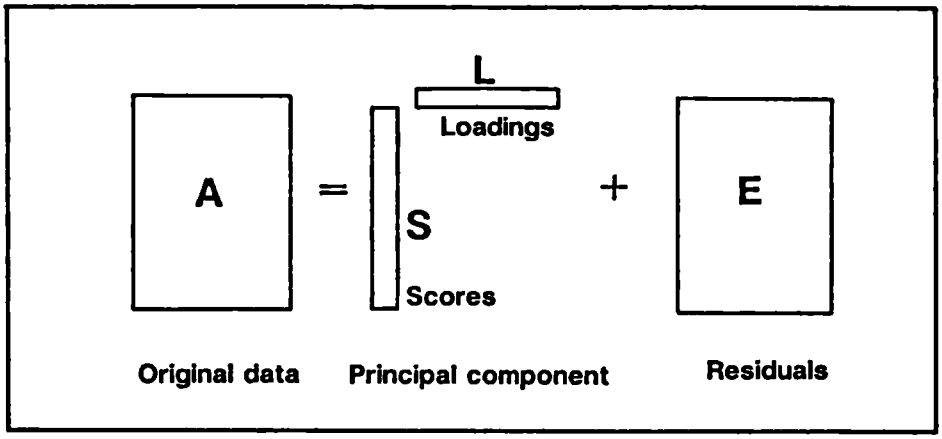


FIGURE 6.22 The decomposition of the original data matrix, A, into the score, S and loading, L matrices. E is the residual matrix (Christie, pers. comm.).

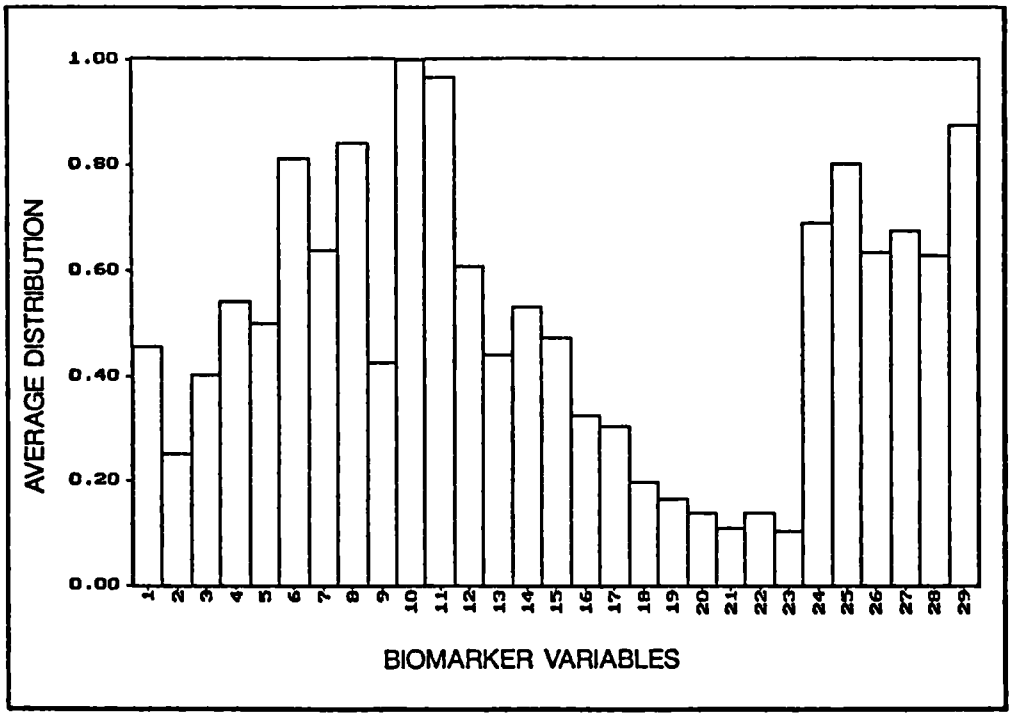


FIGURE 6.23 The average distribution of the 29 normalised biomarker peak heights for the 17 sediment extract and 7 oil samples included in the multivariate analysis.

location of each sample along the principal component and thus explains the relationship between samples.

Each principal component represents a given and specific process. The direction of the first principal component, PC 1, coincides with the direction of the largest point scatter. As such, it corresponds to the most important variation within the data set and thus, represents the process which has the strongest influence in the data set. The residual variances in the data set after the extraction of PC 1 are then used to calculate the second most important principal component, PC 2, whose direction is similar to the direction of largest point scatter perpendicular to PC 1. Variances along the principal components quantify the percentages of total information within the data set that they account for. Plotting PC 1 against PC 2 will therefore provide the highest possible information density compared to any other two-dimensional plane projections. The cross-validation technique of Wold (1978) incorporated in the SIRIUS programme assesses the significance of individual principal components.

The principal component method of analysing large data sets have been successfully applied to organic geochemistry, for example, in oil-oil (Hughes *et. al.*, 1985, Telnaes & Dahl, 1986) and oil-source rock (Telnaes & Cooper, 1991) correlations, distinguishing palaeo-depositional environments (Mello *et. al.*, 1988; Jiamo *et. al.*, 1990; Telnaes & Isaksen, 1993), the prediction of source rock burial and oil generation depths (Christie *et. al.*, 1993), kerogen characterisation (Oygard *et. al.*, 1988) and the determination of maturity levels from alkylated phenanthrene distributions (Budzinski *et. al.*, 1993).

6.6.2 Input Data

Peak heights from triterpane m/z 191 and sterane m/z 217 mass fragmentograms of 17 extract samples (from South Furious-2, Rusa Timur-1 and Gajah Hitam-1 wells) and 7 oil samples (Rusa Timur : Oil 1, Tembungo : Oil 2, South Furious : Oil 3, Barton : Oil 4, St. Joseph : Oil 5, Erb West : Oil 6 and Ketam : Oil 7) were used for the multivariate data analysis. The peak heights of each sample are block-normalised, i.e. triterpane and sterane peaks are normalised separately (Christie, pers. comm.), and the normalised values are then expressed as their logarithm to balance the general log-normal distribution found among biomarkers (Kvalheim, 1985). This data pre-treatment is comparable to Telnaes & Cooper (1991) in their Haltenbanken example for the correlation of oils with an immature source rock equivalent.

6.6.3 Results : Principal Component Analysis Of Oils And Sediment Extracts

24 samples and 29 variables were analysed (**Tables 6.5 - 6.7**) and **Figure 6.23** shows the average distribution of the log-normalised peak heights of the biomarker variables (for peak identification, see **Table 6.1**). The first three principal components were extracted where PC 1 accounted for 36.0% of the total information present in the data

set, while PC 2 and PC 3 each accounted for 13.5% and 9.4%, respectively. All three principal components explained close to 60% of the total information held by the data set. The contribution of each variable to the principal components can be viewed on the loading plots **(Figure 6.24)** while the inter-relationship between samples are shown in the score plot of PC 1 against PC 2 **(Figure 6.25)**.

TABLE 6.5 The raw biomarker peak height data of South Furious-2 samples used in the multivariate analyses of the 17 sediment extract and 7 oil samples.

Biomarker peaks	South Furious-2 sample codes									
	A1	A2	A3	A4	A5	A6	A7	A8	A9	A10
1	6.1	3.9	2.5	0.01	0.01	1.2	1.4	0.7	2.0	1.6
2	1.5	2.1	1.7	0.01	0.01	1.0	0.4	1.0	2.0	0.8
3	2.3	2.5	2.3	0.5	0.01	2.1	1.8	3.6	3.9	2.9
4	7.0	5.1	3.5	1.1	0.01	3.2	2.8	3.9	2.8	2.9
5	1.9	1.2	1.9	1.9	4.4	4.4	4.7	3.9	4.1	2.7
6	7.4	6.5	7.1	16.1	13.6	13.9	14.5	12.0	14.1	14.4
7	8.1	5.7	5.3	6.8	0.01	4.8	2.7	3.2	4.1	4.2
8	8.5	7.3	8.1	4.7	8.3	12.1	10.4	13.5	9.6	11.7
9	4.6	0.01	1.3	0.01	1.9	2.5	1.8	2.4	1.7	1.4
10	15.1	12.9	14.4	9.1	6.8	12.9	9.9	12.8	10.4	10.3
11	15.3	15.0	13.3	3.4	2.5	8.8	4.9	12.9	13.3	12.1
12	2.6	2.6	2.9	8.0	0.01	8.0	8.2	10.9	9.0	8.4
13	3.0	2.7	5.2	1.5	0.01	2.1	1.1	1.7	0.9	1.6
14	2.2	2.5	3.2	0.01	0.01	2.1	3.6	1.8	2.9	2.2
15	1.8	1.9	2.8	0.01	0.01	3.0	2.1	2.2	2.8	3.5
16	1.6	1.6	1.0	0.01	0.01	1.0	0.5	0.9	1.4	0.9
17	1.2	1.3	0.9	0.01	0.01	1.5	0.8	1.7	1.4	1.0
18	0.6	0.7	0.5	0.01	0.01	0.4	0.3	0.4	0.6	0.4
19	0.4	0.6	0.6	0.01	0.01	0.4	0.3	0.4	0.5	0.5
20	0.2	0.4	0.01	0.01	0.01	0.01	0.01	0.01	0.01	0.01
21	0.1	0.3	0.01	0.01	0.01	0.01	0.01	0.01	0.01	0.01
22	0.01	0.01	0.01	0.01	0.01	0.01	0.01	0.01	0.01	0.01
23	0.01	0.01	0.01	0.01	0.01	0.01	0.01	0.01	0.01	0.01
24	9.7	11.1	2.0	3.5	2.5	5.0	3.5	1.7	2.9	2.3
25	13.7	13.4	3.0	3.5	2.4	4.0	2.8	3.2	4.1	3.6
26	4.2	5.1	4.2	11.0	10.5	9.6	11.8	13.1	9.6	7.2
27	4.2	4.9	0.8	3.8	4.9	5.2	4.1	6.5	6.8	3.5
28	3.5	4.7	1.0	4.6	4.8	8.0	6.3	8.4	7.3	3.3
29	6.0	8.0	15.4	15.1	6.0	13.9	14.2	13.6	13.4	14.6

Table 6.6 The raw biomarker peak height data of Rusa Timur-1 and Gajah Hitam-1 samples used in the multivariate analyses of the 17 sediment extract and 7 oil samples.

Biomarker peaks	Rusa Timur-1 sample codes					Gajah Hitam-1 sample codes	
	F1	F2	F3	F4	F5	G1	G2
1	0.01	1.6	2.6	2.2	2.1	1.9	0.4
2	0.01	0.01	2.0	0.01	0.01	4.1	0.01
3	0.01	0.01	2.9	0.01	0.01	12.3	0.01
4	2.1	2.0	2.6	2.9	2.6	2.1	1.3

Table 6.6 The raw biomarker peak height data of Rusa Timur-1 and Gajah Hitam-1 samples used in the multivariate analyses of the 17 sediment extract and 7 oil samples - continued.

Biomarker peaks	Rusa Timur-1 sample codes F1	F2	F3	F4	F5	Gajah Hitam-1 sample codes G1	G2
5	4.2	3.3	1.1	2.2	2.7	0.01	4.2
6	0.01	2.8	3.9	3.2	3.9	5.1	9.0
7	2.0	3.0	4.0	3.8	3.8	0.01	2.7
8	12.6	8.9	7.1	4.8	6.2	8.5	8.1
9	0.01	0.01	5.3	0.01	0.01	0.01	0.01
10	0.01	11.7	10.5	15.3	15.1	6.3	11.9
11	15.5	14.8	15.8	12.8	13.1	15.7	14.7
12	2.1	3.0	2.2	2.8	3.4	4.9	7.5
13	0.01	0.01	1.6	0.01	0.01	1.8	0.01
14	7.5	4.3	2.9	3.1	3.3	3.8	3.9
15	5.7	3.3	2.6	2.0	2.6	3.9	4.6
16	5.1	2.4	1.3	1.3	1.4	2.0	1.3
17	3.9	1.9	1.2	1.0	1.2	2.6	1.8
18	3.8	1.8	0.7	0.8	0.9	0.8	0.8
19	2.6	1.1	0.6	0.5	0.5	0.9	0.8
20	2.7	0.8	0.4	0.3	0.3	0.8	0.01
21	1.8	0.6	0.3	0.2	0.3	0.7	0.01
22	3.0	0.7	0.01	0.01	0.01	0.01	0.01
23	2.0	0.5	0.01	0.01	0.01	0.01	0.01
24	0.01	5.9	8.5	7.4	8.9	0.01	1.3
25	2.3	11.4	7.5	14.3	13.5	0.01	2.3
26	6.1	2.5	3.6	3.1	2.6	2.4	1.6
27	11.6	5.4	5.1	3.9	5.3	3.9	4.8
28	7.3	2.6	4.1	1.9	2.4	4.3	1.0
29	8.1	14.0	15.8	9.7	14.4	9.2	15.3

Table 6.7 The raw biomarker peak height data of the seven oil samples used in the multivariate analyses of the 17 sediment extract and 7 oil samples.

Biomarker peaks	Oil 1	Oil 2	Oil 3	Oil 4	Oil 5	Oil 6	Oil 7
1	3.9	3.4	3.9	4.7	3.4	2.8	4.1
2	0.4	0.4	0.8	0.6	0.5	0.3	0.6
3	1.1	1.0	1.3	1.5	1.1	0.9	1.1
4	4.6	4.3	5.5	6.0	4.4	4.3	4.8
5	4.7	3.9	2.6	3.5	3.1	1.9	3.3
6	7.3	6.9	6.5	9.6	7.0	4.7	3.8
7	6.2	5.0	5.8	8.1	6.6	4.1	4.7
8	9.8	9.7	6.0	6.1	6.1	7.0	6.6
9	0.01	0.01	0.01	0.01	0.01	0.01	0.01
10	14.4	14.4	14.9	14.8	15.0	15.6	14.9
11	13.6	13.7	10.7	13.6	11.8	8.7	15.5
12	3.9	3.7	2.7	3.4	3.1	2.0	2.5
13	3.6	3.9	2.4	3.8	2.9	2.6	2.7

Table 6.7 The raw biomarker peak height data of the seven oil samples used in the multivariate analyses of the 17 sediment extract and 7 oil samples - continued.

Biomarker peaks	Oil 1	Oil 2	Oil 3	Oil 4	Oil 5	Oil 6	Oil 7
14	3.8	4.0	2.9	4.4	3.5	2.2	3.7
15	2.6	2.6	1.8	3.0	2.3	1.2	2.5
16	1.6	1.5	1.3	2.1	1.8	0.9	1.9
17	1.2	1.2	1.0	1.5	1.3	0.7	1.3
18	0.7	0.8	0.6	1.1	0.8	0.5	0.8
19	0.8	0.5	0.5	0.7	0.6	0.3	0.5
20	0.5	0.3	0.2	0.6	0.3	0.2	0.4
21	0.3	0.2	0.4	0.4	0.2	0.1	0.3
22	0.2	0.2	0.01	0.3	0.2	0.01	0.1
23	0.2	0.2	0.01	0.1	0.1	0.01	0.1
24	8.0	7.4	8.0	8.0	8.0	7.6	8.9
25	13.5	13.3	14.2	14.4	14.3	14.5	14.6
26	3.4	5.1	2.2	1.5	2.0	5.1	2.1
27	9.7	12.5	3.8	5.4	6.1	7.3	4.2
28	9.9	12.3	3.8	3.8	6.1	7.2	3.0
29	6.6	12.1	3.4	3.1	3.2	4.1	3.4

The PC 1 loading plot shows an overwhelming contribution (high loading value) from the higher land-plant derived Resins W (peak 24) and T (peak 25) compared to the rest of the variables **(Figure 6.24(a))**. It is therefore interpreted that PC 1 explains the variations of resin content in the samples. In the loading plot of PC 2, there is a general negative correlation between the loading values of steranes to those of the triterpanes **(Figure 6.24(b))**. PC 2 is thus related to the relative amounts of steranes and triterpanes in the samples.

PC 3's loading pattern seem to be influenced by some maturation processes **(Figure 6.24(c))**. The loading plot shows high loading values of ββ - steranes (peaks 27 and 28) which predominate at high maturity levels in petroleum (Philp, 1985; Waples & Machihara, 1991) being negatively correlated to sterane αα - 20R species (peak 29). The unknown triterpane (peak 7), known to be present in very immature samples (Waples & Machihara, 1991), have a high negative loading against the homohopanes (peaks 14 to 23). Moretane (peak 12), also known to convert into hopanes with increasing maturity, are negatively correlated to the homohopanes as well. The negative compatibility of Ts (peak 2) and Tm (peak 3) peaks also indicate that PC 3 reflects maturation processes.

Score plots aid the visualisation of sample inter-relationships **(Figure 6.25)**; samples that plot close together are considered to be very similar to each other, while those that do not, are different. The scores of PC 1 versus PC 2 account for about 50% of the total information in the data set and shows the separation of the 24 samples into 4 groups, with a sub-grouping in Group 1 **(Figure 6.25(a))**. Generally, extract samples from the same well group together, with an exception in Group 3, where samples A3 (South

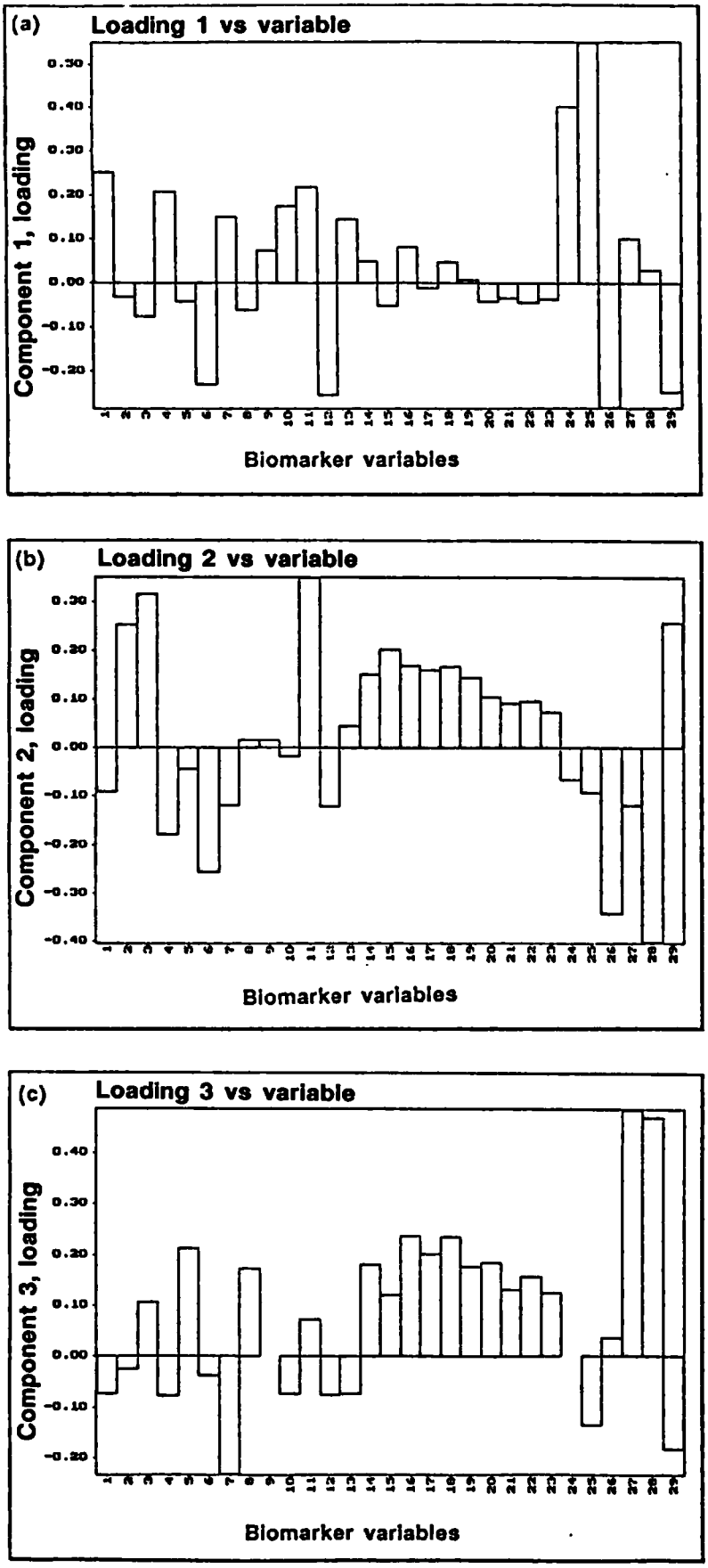


FIGURE 6.24 Loading plots for the first three principal components versus biomarker variables (a) PC 1, 36.0% (b) PC 2, 13.5% and (c) PC 3, 9.4%, accounting for 58.9% of the total information within the data set. Refer to **Table 6.1** for key to biomarker variables.

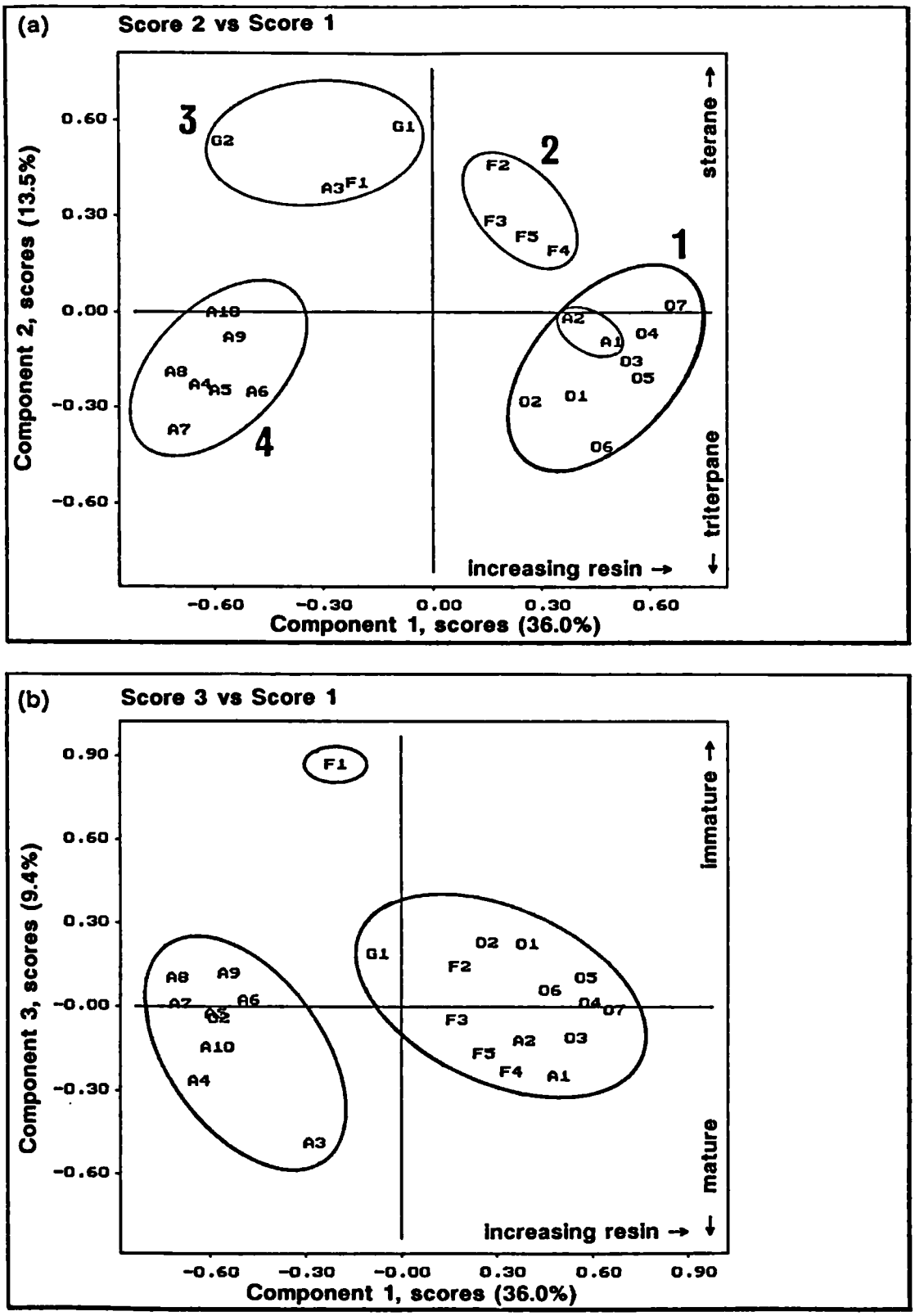


FIGURE 6.25 Sample score plots : (a) the scores of PC 1 versus PC 2 and (b) the scores of PC 1 versus PC 3.

Furious-2) and F1 (Rusa Timur-1) are grouped together with samples from Gajah Hitam-1. The oils too are grouped together, along with two South Furious-2 samples, A1 and A2. PC 1 was established to explain the resin content variations within the samples. Upon re-examining the data set, it was observed that the oils had the largest land-plant derived resin peaks, as well as the two shallowest samples A1 and A2, from South Furious-2.

Therefore, along the first principal component, resin contents increase to the right and decrease to the left. Listing the samples in the order of decreasing resin content : All oils, samples A1 and A2 (South Furious-2) > samples F2, F3, F4 and F5 (Rusa Timur-1) > samples G1 and G2 (Gajah Hitam-1), sample F1 (Rusa Timur-1), sample A3 (South Furious-2) > samples A4, A5, A6, A7, A8, A9 and A10 (South Furious-2).

The presence of high resin peaks in the oils are most likely be due to their relatively higher convertibility into hydrocarbons compared to other land-derived organic matter (Snowdon, 1980). The two shallowest South Furious-2 samples, A1 and A2, are included in the oil group possibly because they possess the most oil-like properties, which concurs with the explanation in **Section 6.5.2** for the likely cause of the reverse maturity trends of the biomarker parameters. Rusa Timur-1 and Gajah Hitam-1 samples (outer neritic - bathyal sediments) are shown to possess more resins than the majority of the South Furious-2 samples. This can be explained by the selective enrichment process which favourably concentrates the more resistant leaf cuticles and plant waxes as well as resins, and transport them further into shelf and deeper water environments, aided by their low densities. Conversely, South Furious-2 samples, which are of deltaic to lower coastal plain origin, do not experience such an enrichment process, with the different organic matter components being highly mixed up. The resins in these sediments are, in effect, overwhelmed by other terrigenous debris.

Along the second principal component **(Figure 6.25(a))**, it is the relative amounts of steranes and triterpanes which dictates the sample groupings. The steranes originate from marine phytoplankton while the terpanes in shales and crude oils are generally limited to compounds which are apparently derived from bacterial membrane lipids (Ourisson *et. al.*, 1984). In the order of increasing triterpane contents, the samples are arranged in the following sequence : samples G1 and G2 (Gajah Hitam-1), sample F1 (Rusa Timur-1) and sample A3 (South Furious-2) < samples F2, F3, F4 and F5 (Rusa Timur-1) < samples A1, A2, A4, A5, A6, A7, A8, A9 and A10 (South Furious-2), and all the oils. This is also the general order of increasing triterpane : sterane ratio, indicating that the organic matter giving rise to the oils and South Furious-2 extract samples were deposited in a relatively more terrigenous-influenced depositional environment compared to those responsible for Rusa Timur-1 and Gajah Hitam-1 extract samples.

The resulting clusters suggest that the oils have very similar triterpane contents with samples from South Furious-2 but differ in their resin contents. Similarly, samples from

Rusa Timur-1 and Gajah Hitam-1, which are of outer neritic to bathyal origin, have comparable triterpane contents but differ slightly in their resin contents. As expected, samples from Rusa Timur-1 and Gajah Hitam-1 are well separated from South Furious-2 samples which are of deltaic to lower coastal plain origin.

The score plot of PC 1 versus PC 3 explains 45% of the total information available within the data set (**Figure 6.25(b)**). Along PC 3, which reflects maturation processes, the direction of maturity increase is determined using the 22S/(22S+22R) triterpane ratio of the oils and the timing of hydrocarbon generation calculated from the TTI_{ARR} method of Hunt & Hennet (1992) addressed in **Chapter 7**. For Oil 1 (Rusa Timur), the timing of hydrocarbon generation is 5.6 Ma and for Oil 3 (South Furious), it is 8 Ma. Using this information, the direction of maturity increase is from top to bottom (**Figure 6.25(b)**). In general, the resulting clusters show that there is very little difference in the maturity levels of the sample extracts and the oils, supporting the migrated origin of the hydrocarbons in the sediment extracts.

6.6.4 Results : Principal Component Analysis Of Oil Samples

Two principal components were extracted from a data set consisting of 7 oil samples and 24 biomarker variables (**Table 6.7**). PC 1 and PC 2 account for 60.4% and 24.2%, respectively, explaining a sum total of 84.6% of the total variation in the data set. The average distribution of the log-normalised variable peak heights are shown in **Figure 6.26**. The loading plot of the first PC (**Figure 6.27(a)**) shows a negative correlation between triterpanes/resins and steranes. It therefore signifies the relative amounts of steranes and triterpanes/resins, indicating the extent of input from bacteria (triterpanes), higher land-plants (resins) as well as marine phytoplankton (steranes).

The loading plot of the second PC (**Figure 6.27(b)**) shows a very strong positive correlation between oleanane, Resin W and Resin T peaks, all of which are negatively correlated with other triterpanes. PC 2 therefore indicates the relative amounts of input from higher land-plants and from bacteria, signified by the oleanane and resins, and other triterpane species, respectively.

The inter-relationships between the seven oil samples are shown in the score plot of PC 1 versus PC 2 (**Figure 6.28**), where they are generally separated into 3 groups ; **Group 1 :** Oils 1 (Rusa Timur) and 2 (Tembungo), **Group 2 :** Oil 6 (Erb West), and **Group 3 :** Oils 3 (South Furious), 4 (Barton), 5 (Bunbury) and 7 (Ketam). Along the first principal component, which accounts for the relative amounts of triterpanes and steranes in the oils, the groupings clearly mark out the palaeo-depositional environments of the oils' source rocks. Listing the oils in the order of increasing triterpane contents : Oils 1 and 2 < Oil 6 < Oils 3, 4, 5 and 7. This is also the general direction of increasing triterpane : sterane ratio which is commonly used as a palaeo-depositional environment indicator.

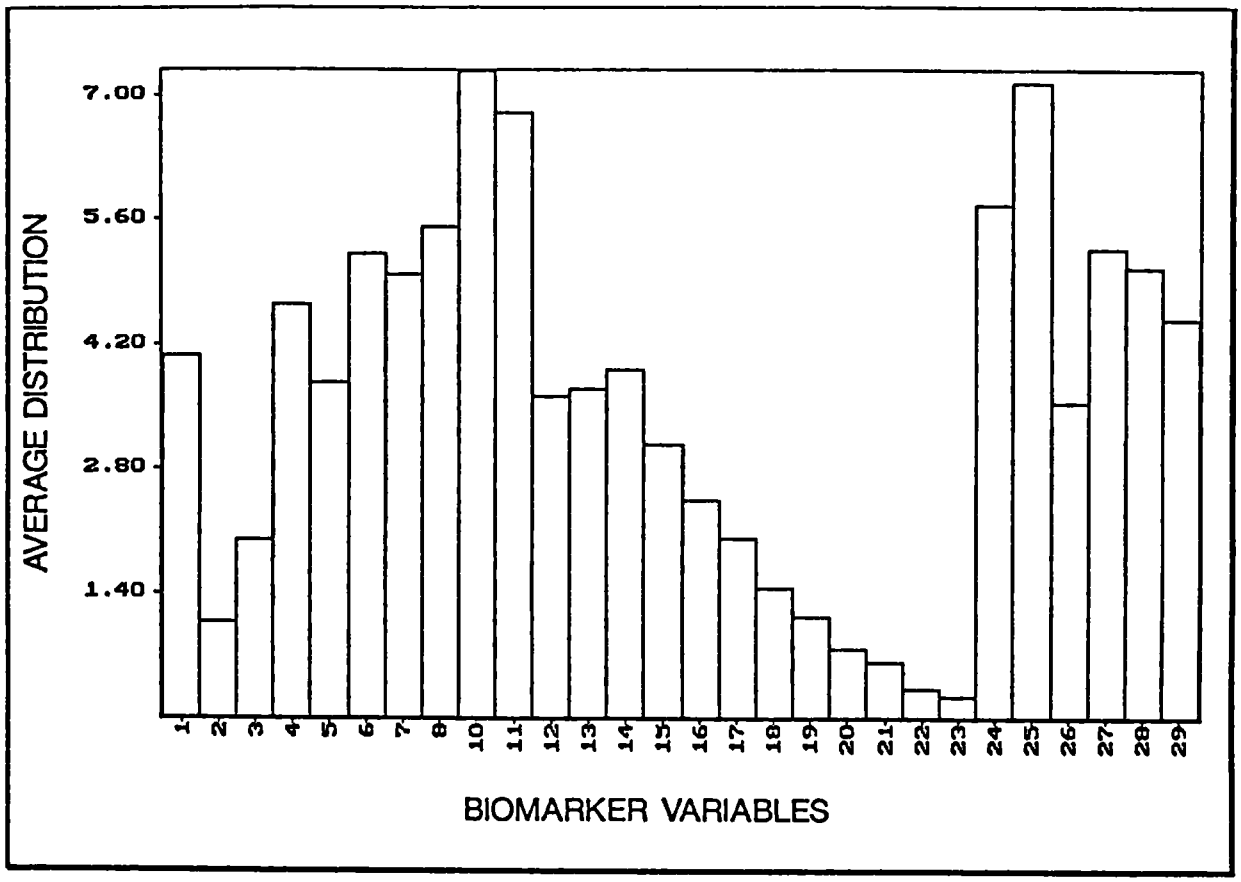


FIGURE 6.26 The average distribution of the 29 normalised biomarker peak heights for the multivariate analysis of the 7 oil samples.

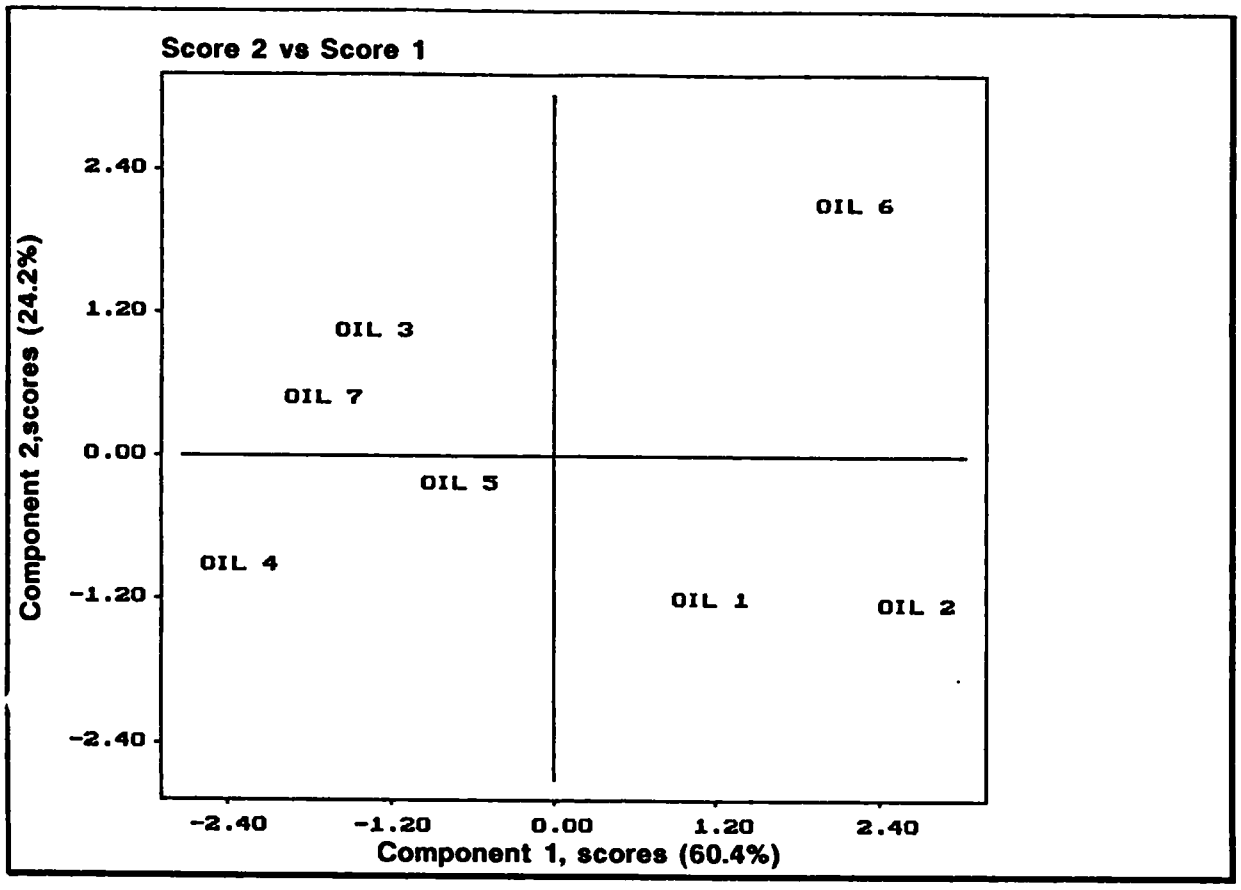


FIGURE 6.28 The sample scores of PC 1 versus PC 2.

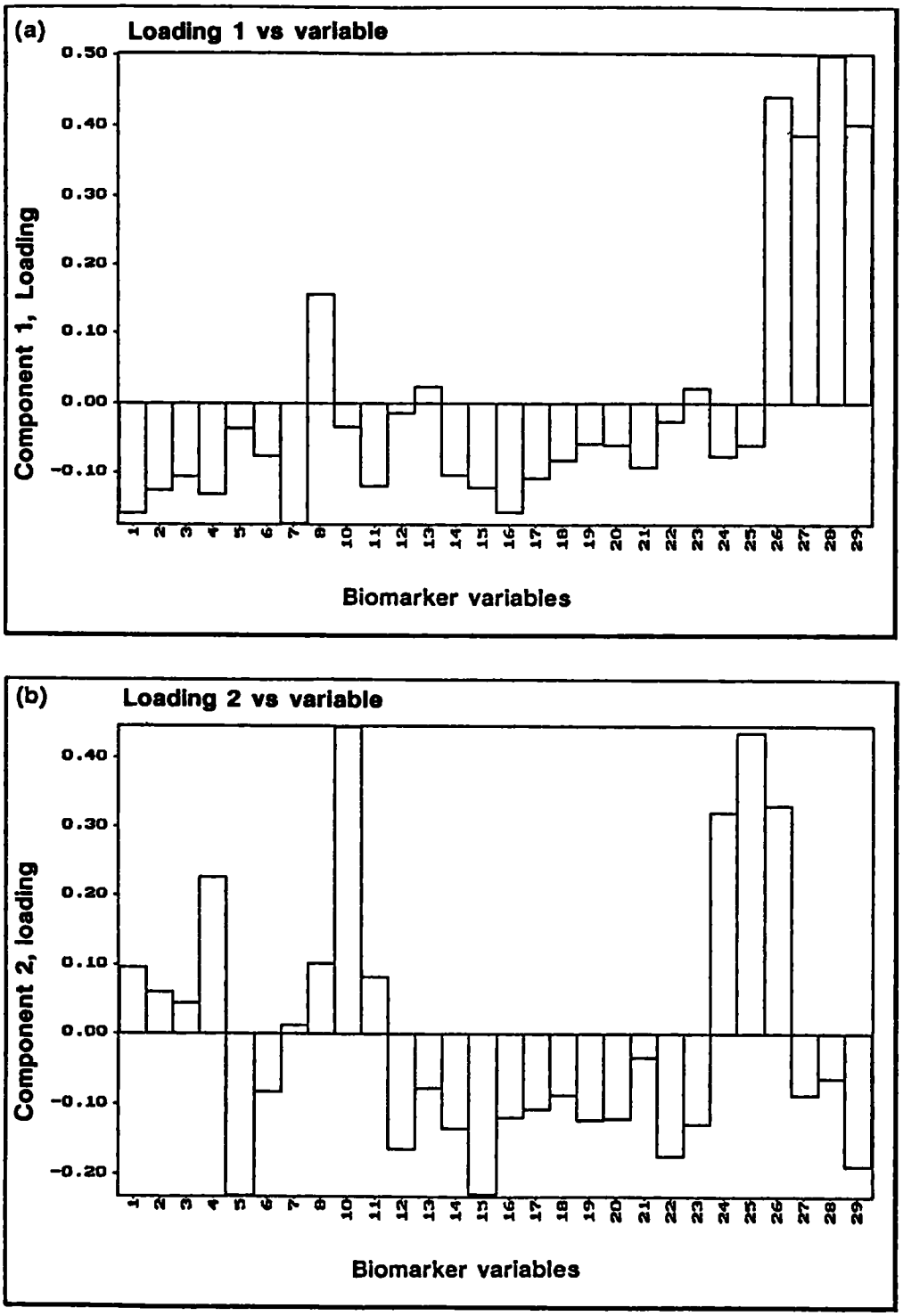


FIGURE 6.27 Loading plots for the first two principal components versus biomarker variables (a) PC 1, 60.4% and (b) PC 2, 24.2%, accounting for 84.6% of the total variation within the data set. Refer to **Table 6.1** for key to biomarker variables.

Palaeontological data from PETRONAS in-house reports indicate that the source rocks for Rusa Timur and Tembungo oils were deposited in deep marine to bathyal settings, holomarine inner neritic for the Erb West oil, and lower coastal/delta plain to fluviomarine inner neritic for South Furious, Barton, Bunbury and Ketam oils. Therefore, along the first principal component, the oils are separated into groups relating to the palaeo-depositional environments of their source rocks.

The scores of PC 2 indicate an increasing contribution from higher land-plant derived resins from bottom upwards (**Figure 6.28**), with Rusa Timur and Tembungo oils having relatively lesser oleanane, Resin W and Resin T compared to the Erb West oil. In the order of increasing resin and oleanane contents, the oils are arranged as follows : Rusa Timur and Tembungo oils < Erb West oil < Bunbury oil < Ketam oil < South Furious oil < Erb West oil. The difference in resin and oleanane contents between these oils are, however, not very significant for it was established in their analysis together with the sediment extracts that they generally have similar resin and oleanane contents (Group 1 : Score plot PC 1 vs. PC 2, **Figure 6.25(a)**). It can also be seen from Group 1 in the score plot that Rusa Timur and Tembungo oils have slightly less resin and oleanane contents compared to the rest of the oils.

6.7 Summary

Biomarker studies using oil samples and sediment extracts from wells located in the northern part of Sabah Basin show that the organic matter source for the basin's hydrocarbons to be dominantly terrigenous, indicated by high triterpane/sterane ratios, the presence of compounds diagnostic of land-derived organic matter such as oleanane, and Resins W, T and R, and the general predominance of C_{29} regular steranes over C_{27} and C_{28} species. The consistently similar mass fragmentograms of both m/z 191 and m/z 217 suggest that the oils and sediment extracts originated either from the same source rock, or from different source rocks with similar chemical compositions. The relative similarity of peak distributions in samples from different environments suggests that detrital plant components from similar types of higher land plants were re-distributed by sedimentary/transport processes to each depositional setting.

For the oils, the 20S/[20S+20R]-sterane biomarker maturity ratios are lower than the equilibrium value of 0.55 and moretane/hopane ratios > 0.10. This supports the apparent retardation of the isomerisation process previously reported by Grantham (1986b) to occur in Far Eastern Tertiary oils. The triterpane 22S/[22S+22R] ratio, on the other hand, appears to reflect the expected maturity levels of the oils. The majority of the extracted sediments are shown to be immature by pyrolysis Tmax, vitrinite reflectance and kerogen elemental composition, indicating that the extracted hydrocarbons have migrated into the sediments from elsewhere. Therefore, biomarker ratios from the extracts cannot be used to determine the true maturity levels of the sediments as the *in. situ* biomarkers will have been mixed with those already present in the migrating

hydrocarbons. Variations of biomarker maturity ratios with depth resemble those of the Production Index in all the studied wells, thus confirming the influence of non-indigenous residual hydrocarbons on the biomarker maturity ratios.

Principal components analyses of sediment extract and oil samples biomarker data concur, and thus confirm, observations made earlier. Firstly, maturity is not shown to be a major distinguishing factor between samples, thus supporting the migrated, non-indigenous nature of the hydrocarbons in the sediment samples; and secondly, Rusa Timur and Tembungo oils are slightly different from the rest of the oils with their relatively lower overall triterpane contents and relatively smaller contributions from oleananc, Resin W and Resin T.

CHAPTER SEVEN

THERMAL MATURATION OF SEDIMENTARY ORGANIC MATTER

7.1 Introduction

The objective of thermal maturation modelling is to determine the timing of hydrocarbon generation. This quantitative approach is performed as a function of time and temperature for each sedimentary sequence in the basin where the effects of time and temperature are calculated and used for the prediction of maturation products. Several methods have been proposed by various workers and among the earliest models are those of Lopatin (1971, 1976) and Hood *et. al.* (1975). These models are based on the assumption that oil generation depends on both the temperature to which the kerogen has been heated, and the duration of the heating. The Arrhenius equation, shown below, expresses in theoretical terms the exponential temperature dependence of the rate of a chemical reaction, such as the rate of kerogen decomposition to form oil.

$$k = Ae^{(-Ea/RT)}$$

where k is the reaction rate constant (1/my), A is the pre-exponential or frequency factor (1/my), Ea is the activation energy (kJ/mol), R is the universal/ideal gas constant, and T is the temperature in Kelvins (°C + 273).

Waples (1980) presented the time-temperature index (TTI) of maturity, first introduced by Lopatin (1971). The method calculates the TTI based on the time of residence in a given temperature range. To do this, the burial history and geothermal gradient are needed. The Lopatin model, however, does not take into account the types of organic matter nor does it take into account the different generative potential and kinetics of organic matter during thermal degradation. The calculation is also oversimplified by the hypothesis that the chemical reaction approximately double for every 10°C rise in temperature (Tissot, 1984; Waples, 1984). This assumption is true only for reactions with activation energies in the range 42-84 kJ/mol (Tissot, 1984). For the rupturing of the weaker bonds, these values are acceptable; but when stronger carbon-carbon bonds are involved, where much higher activation energies are required, it is doubtful that these activation energies are adequate. At peak oil generation, activation energies in the range of 168-294 kJ/mol are common (Tissot & Espitalie,

1975). This may correspond to reaction rates multiplied by a factor of 4 to 10, instead of 2, for a 10°C rise in the corresponding temperature range.

Quigley *et. al.* (1987) voiced rather strong reservations on the use of Lopatin's TTI approach for the calculation of the hydrocarbon generation window. They found that for heating rates greater than 1°C/Ma, Lopatin's TTI underestimates the extent of oil generation, while for heating rates less than 1°C/Ma, it will over estimate the extent of oil generation. They emphasised that TTI must be calibrated with other thermal maturity indicators for each area since it is not a universal description of organic maturation. Calling the Lopatin TTI approach 'an unsophisticated piece of science', they urged workers to adopt a more rigorous kinetic description of oil and gas formation. The findings of Wood (1988) support the observations of Quigley *et. al.* (1987). He, too, came to similar conclusions when comparing the TTI results based on the Arrhenius equation (TTI_{ARR}) to those from the Lopatin method (TTI_{LOP}). He demonstrated that TTI_{ARR} modelled the hydrocarbon generation from the different kerogen types more accurately than TTI_{LOP}.

Wood (1988) used kinetic parameters that simulate vitrinite reflectance data (Ea = 218kJ/mol, A = 5.45 x 10^{26}/my) to calculate the maturity indicator ΣTTI_{ARR} and correlate the stages of petroleum generation associated with it. He applied this method to a series of burial histories representing examples of thermal evolution in a variety of tectonic environments. Of interest to this study is his Example 4 : Low to High Burial Rates/Moderate Temperature Gradient, depicting foreland basins associated with thrust tectonics. This model is applicable to Sabah Basin which has been identified as a foreland basin by Azim-Ibrahim (1994). Furthermore, with the organic matter type in the basin being land-derived Type III, the kinetic parameters used by Wood (1988) will closely depict the organic matter maturation in the basin. He concluded that for foreland basins, the ΣTTI_{ARR} and ΣTTI_{LOP} give similar maturity estimates, and that similar conclusions on maturation history would be drawn from the results of both techniques.

A graphic method, comprising a number of graphs constructed based on the Arrhenius equation for the different types of kerogens, for defining the position of the hydrocarbon window was developed by Hunt *et. al.* (1991) and Hunt & Hennet (1992) to simplify the calculations of ΣTTI_{ARR}. Results from the application of the TTI graphs for kerogen Types I, II and III, as well as a graph for the conversion of oil to gas, is reported to closely match the oil window indicated by maturation indicators other than the Lopatin method for fast reacting kerogens. However, for medium and slow reacting Type II kerogens and for medium reacting Type I and Type III kerogen at moderate heating rates, both the Arrhenius-based TTI and Lopatin TTI values defined approximately the same oil window (Hunt & Hennet, 1992). This concurs with the observations of Wood (1988).

Hunt & Hennet (1992) used the Palaeocene age Tent Island Formation from the Beaufort-Mackenzie Basin, northern Canada (Issler & Snowdon, 1990) as the Type III

source rock sample. The kinetic parameters for this source rock sample (**Table 7.1**) are similar to those of the Miocene coals and coaly shales of the Mahakam Delta, Indonesia (Tissot *et. al.*, 1987). The time-temperature index graphs for Type III organic matter and for the conversion of oil to gas of Hunt & Hennet (1992) are thus used to calculate the position of the hydrocarbon generation window for the sediments under investigation in the Sabah Basin.

Table 7.1 Arrhenius kinetic parameters used by Hunt & Hennet (1992) for the construction of the TTI graphs for each kerogen type. Note the degree of variations within kerogen Types I and II.

Arrhenius kinetic parameters (E and A) for generation of expelled hydrocarbons from source rocks with varying amounts of organic sulphur.

Kerogens			Standard samples			
Type	Reaction rate	Source	E (kJ/mol)	A (1/my)	S_{org} (wt%)	Atomic S/C
IA	fast	Green R., Colorado	194	1.01×10^{25}	2.2	0.011
IB	medium	Green R., Utah	219	8.87×10^{26}	1.3	0.007
IC	slow	Green R.,	269	7.48×10^{30}	1.4	0.007
IIA	fast	Monterey	144	7.017×10^{20}	11	0.055
IIB	medium-fast	Phosphoria	179	4.223×10^{23}	9	0.045
IIC	medium	Alum	201	1.546×10^{25}	7.4	0.036
IID	slow	Woodford	218	5.656×10^{26}	5.4	0.024
III	medium	Tent Island, Canada	230	3.98×10^{27}	-	-

Thermal maturation of the sediments under study were also modelled using the BasinMod programme developed by the Platte River Associates (Version 2.97, 1992). The geothermal gradient used in this study was assumed to be invariant (28°C/km, Hutchison, 1989) during the basin's subsidence history. Organic matter composition were taken into account during the calculation of the hydrocarbon generation window. The kinetic model of the programme calculates multiple parallel reactions that occur as organic matter undergoes thermal degradation to hydrocarbons, i.e. from kerogens into oil and gas, and oil into gas and residues. Each chemical reaction has its own kinetic parameters for bond rupture (activation energy, Ea) and the Arrhenius constant, A (frequency factor). This model provides one of the best representations of the complex series of chemical reactions that occur in hydrocarbon generation to date.

7.2 Burial history

A modular one-dimensional basin modelling system developed by the Platte River Associates, Inc. has been used for this purpose. The software allows the integration of geological and geochemical data to provide burial histories, determine the depth to, and timing of, hydrocarbon generation using any kerogen mixtures. The software calculates thermal maturity based on the theory of time and temperature while the kinetic module allows the estimation of hydrocarbon generation with respect to time and temperature. Determination of kinetic parameters are documented by Braun & Burnham (1987), Burnham *et. al.* (1987, 1988), Burhnam & Sweeney (1989) and Sweeney & Burnham (1990). The resulting model is limited by how well the geological and thermal histories of the basin are known, and how well the kinetic model describes the real behaviour of organic matter during burial over geological time.

In this study, the BasinMod programme was used to plot the burial history curves and temperature grids for the Sabah Basin sediments under study. These include the sediments penetrated by the seven wells and the sedimentary sequences in the Pritchard and Furious Synclines, as well as those in the graben between Rusa Timur-1 and Belangkas area (**Figure 7.1**).

7.2.1 Input Data

For basic analysis, the data required for each sedimentary sequence are the surface temperature (in °C), formation top, formation thickness, ages at the formation boundaries and the geothermal gradient. Vitrinite reflectance and palynofacies data (relative proportions of kerogen types present) are also included for the thermal modelling. **Tables 7.2** to **7.11** display the input data used to generate the burial history curves in this study.

Table 7.2 South Furious-2: Data for burial history and thermal maturation modelling

Stage	Age* (Ma)	Formation Top (m)	Formation Thickness (m)	Lithology (%) Sst	Slst	Shale	CO_3
IVF/IVG	4.1	0	57	30	0	30	40
IVD	8.5	57	233	0	0	100	0
IVC	10.3	290	134	0	0	100	0
IVA	14.5	424	1411	41	14	45	0
III	15.0	1835	173	0	0	100	0
Total depth		2008					

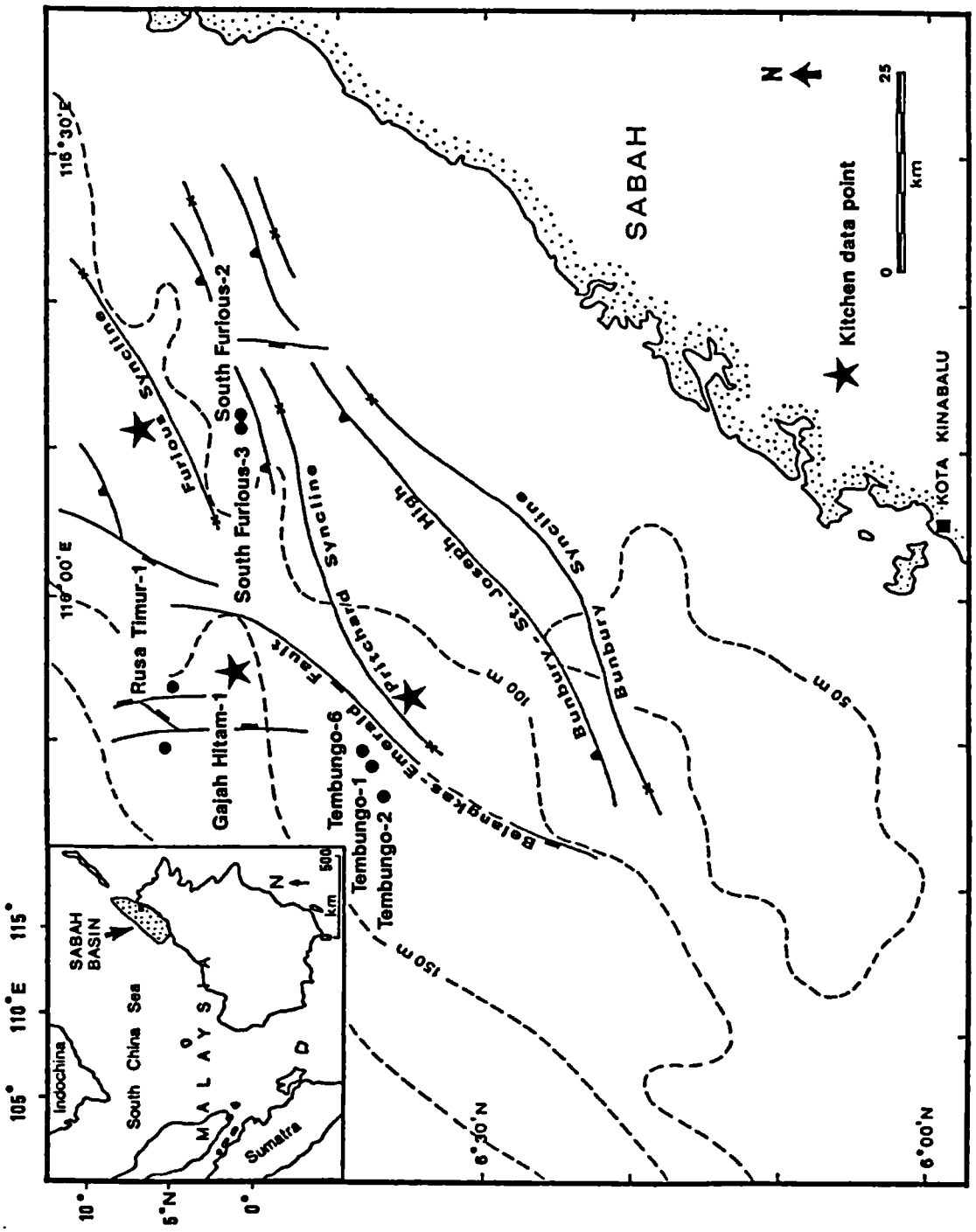


FIGURE 7.1 Well locations and three data points taken in the hydrocarbon kitchens.

Table 7.3 South Furious-3 : Data for burial history and thermal maturation modelling

Stage	Age* (Ma)	Formation Top (m)	Formation Thickness (m)	Lithology (%) Sst	Slst	Shale	CO_3
IVF/IVG	4.1	0	72	50	0	0	50
IVC/IVD	10.3	72	317	8	12	80	0
IVA	14.5	389	1915	36	15	49	0
III	15.0	2304	18	0	0	100	0
Total depth		2322					

Table 7.4 Tembungo-1 : Data for burial history and thermal maturation modelling

Stage	Age* (Ma)	Formation Top (m)	Formation Thickness (m)	Lithology (%) Sst	Slst	Shale	CO_3
IVG	1.6	0	190	0	0	95	5
IVF	4.1	190	65	27	0	73	0
IVE	6.8	255	353	3	28	57	12
IVD	8.5	608	1280	35	6	58	1
IVC	9.0	1888	300	16	9	75	0
Total depth		2188					

Table 7.5 Tembungo-2 : Data for burial history and thermal maturation modelling

Stage	Age* (Ma)	Formation Top (m)	Formation Thickness (m)	Lithology (%) Sst	Slst	Shale	CO_3
IVG	1.6	0	211	2	4	88	6
IVF	4.1	211	82	0	0	97	3
IVE	6.8	293	524	4	0	69	27
IVD	8.5	817	1250	40	8	51	1
IVC	9.0	2067	174	1	1	98	0
Total depth		2241					

Table 7.6 Tembungo-6 : Data for burial history and thermal maturation modelling

Stage	Age* (Ma)	Formation Top (m)	Formation Thickness (m)	Lithology (%) Sst	Slst	Shale	CO_3
IVG	1.6	0	201	0	0	100	0
IVF	4.1	201	105	0	0	100	0
IVE	6.8	306	328	2	6	84	8
IVD	8.5	634	1219	29	25	46	0
IVC	9.0	1853	61	20	80	0	0
Total depth		1914					

Surface temperature : 25°C
Geothermal gradient : 28°C/km (Hutchison, 1989)
* The boundary ages used are taken from Johnson & Huong (1990).

Table 7.7 Rusa Timur-1 : Data for burial history and thermal maturation modelling

Stage	Age* (Ma)	Formation Top (m)	Formation Thickness (m)	Lithology (%) Sst	Slst	Shale	CO_3
IVE/IVF	6.8	0	790	15	0	85	0
IVD	8.5	790	801	67	0	33	0
IVC	10.3	1591	235	3	0	97	0
IVB	11.2	1826	165	15	0	85	0
IVA	12.0	1991	217	2	0	98	0
Total depth		2208					

Table 7.8 Gajah Hitam-1 : Data for burial history and thermal maturation modelling

Stage	Age* (Ma)	Formation Top (m)	Formation Thickness (m)	Lithology (%) Sst	Slst	Shale	CO_3
IVE/IVF	6.8	0	274	0	0	100	0
IVD	8.5	274	1200	53	0	47	0
IVC	10.3	1474	933	37	0	63	0
Total depth		2407					

Table 7.9 Pritchard Syncline : Data for burial history and thermal maturation modelling

Stage	Age* (Ma)	Formation Top (m)	Formation Thickness (m)	Sst	Lithology (%) Slst	Shale	CO_3
IVG	1.6	0	250				
IVF	4.1	250	300				
IVE	6.8	550	550				
IVD	8.5	1100	300		No data		
IVC	10.3	1600	1650				
IVB	11.2	3250	950				
IVA	14.5	4200	1600				
Total depth		5800					

Table 7.10 Furious Syncline : Data for burial history and thermal maturation modelling

Stage	Age* (Ma)	Formation Top (m)	Formation Thickness (m)	Sst	Lithology (%) Slst	Shale	CO_3
IVF/IVG	4.1	0	200				
IVE	6.8	200	600				
IVD	8.5	8000	800				
IVC	10.3	1600	900		No data		
IVB	11.2	2500	1300				
IVA	14.5	3800	2000				
Total depth		5800					

Table 7.11 Graben between Rusa Timur-1 and Belangkas : Data for burial history and thermal maturation modelling

Stage	Age* (Ma)	Formation Top (m)	Formation Thickness (m)	Lithology (%) Sst	Slst	Shale	CO_3
IVG	1.6	0	330				
IVF	4.1	330	285				
IVE	6.8	615	900				
IVD	8.5	1515	1210		No data		
IVC	10.3	2725	440				
IVB	11.2	3165	560				
IVA	14.5	3725	1860				
Total depth		5585					

Surface temperature : 25°C
Geothermal gradient : 28°C/km (Hutchison, 1989)
* The boundary ages used are taken from Johnson & Huong (1990).

The duration taken to deposit the 10-12 km thick of Middle - Upper Miocene sedimentary pile in the Sabah Basin was only 14.5 Ma, where sedimentation rates can be as high as 500-1000m/Ma (Azim-Ibrahim, 1994). Ideally, missing sections should be estimated and included in the thermal modelling. This can be done only if the duration of the unconformity and sedimentation rates are known. Vitrinite reflectance versus depth profiles can also be used for the purpose of estimating the thickness of the missing section. In this instance, however, the thickness of the missing sections cannot be calculated using the first method because of a technical limitation involved in the determination of the duration of the unconformity. The time duration of the unconformities cannot be determined from the present biostratigraphic scheme due to inadequate age resolution. The occurrence of the unconformities within one biostratigraphic zone does not permit the estimation of their time durations. A biostratigraphic scheme with higher age resolution, i.e. with more closely divided age zones, is required before this can be done. Such a scheme is presently unavailable.

The plots of vitrinite reflectance versus depth, too, do not provide a means of estimating the eroded thickness as they all do not exhibit any of the characteristic 'jumps' often associated with the presence of unconformities (**Figure 7.2**). As a result of these limitations, the unconformities here are treated as normal conformable boundaries in the thermal modelling. This will affect the results of the modelling but it is believed that the effects are minor and do not cause any drastic differences in the conclusions made if the eroded thickness had been included. This assumption is based on several reasons.

Firstly, the wells that will be most affected by the under estimation of the sediment thickness are South Furious-2 and South Furious-3 where actual erosion occurred. Assuming that the sedimentation rate in the South Furious area reached 500m/Ma and based on a probable erosion interval of 0.5 Ma (Azim-Ibrahim, pers. comm.), the

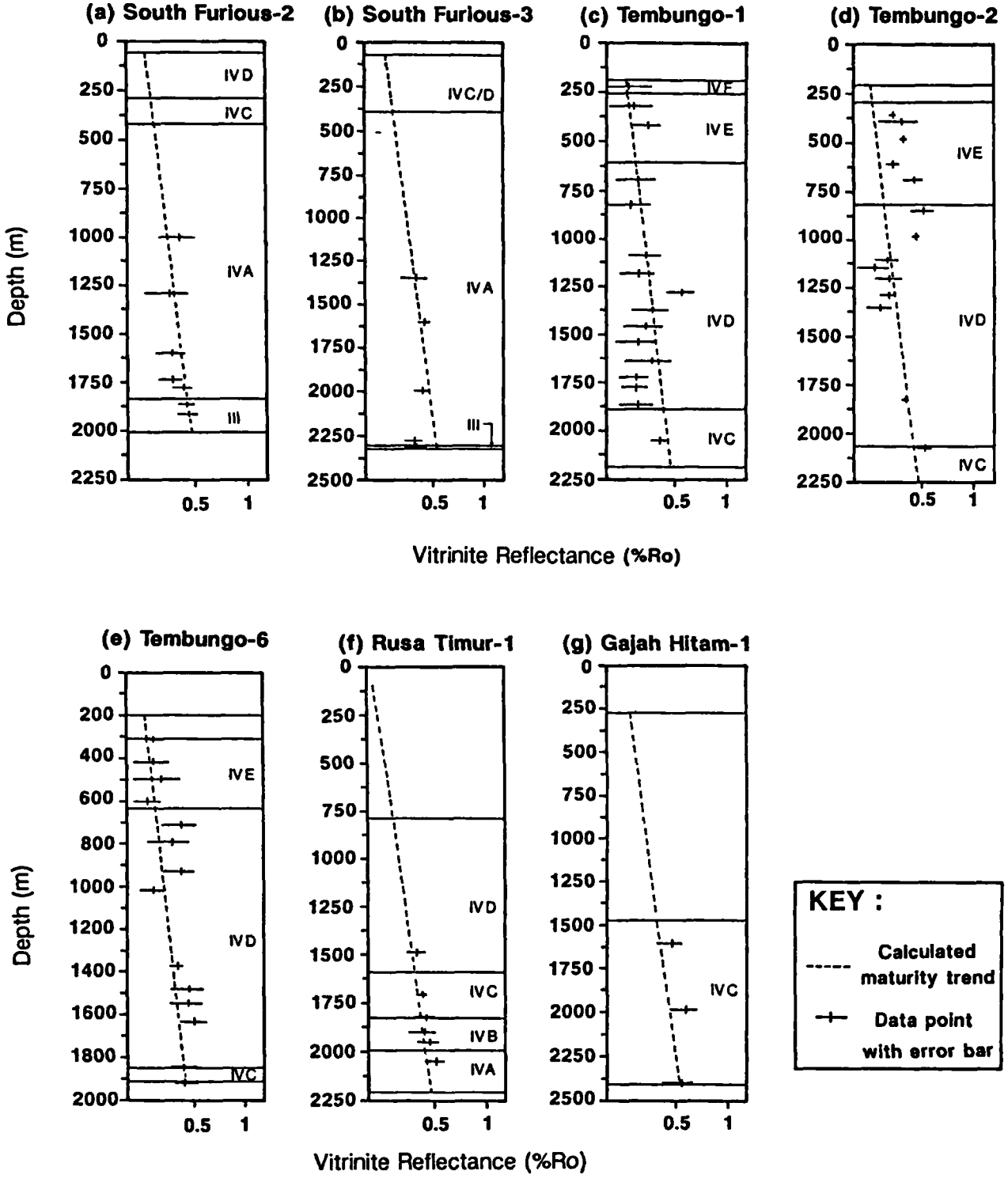


FIGURE 7.2 Measured vitrinite reflectance versus depth profiles for **(a)** South Furious-2, **(b)** South Furious-3, **(c)** Tembungo-1, **(d)** Tembungo-2, **(e)** Tembungo-6, **(f)** Rusa Timur-1 and **(g)** Gajah Hitam-1.

missing section would only amount to 250m. Adding this extra thickness during the thermal modelling will not greatly affect the general thermal history of the sediments in the South Furious area. In the other five wells, the boundaries between the Stages and sub-Stages represent disconformities (i.e. correlative conformities) rather than actual erosional surfaces; as such, deposition in these wells occurred continuously. The scenario is the same for the Pritchard and Furious Synclines, as well as the graben located between Rusa Timur-1 and Belangkas area. Therefore, based on this reasoning, the results from the maturity modelling are thought to be representative of the area under study.

7.3 Timing of hydrocarbon generation

Results from three different methods of determining the timing of hydrocarbon generation are compared. The following section documents the results from :

- Lopatin's (1971, 1976) TTI approach
- Hunt & Hennet's (1992) Arrhenius-based TTI method
- BasinMod's (1992) kinetic modelling

7.3.1 Lopatin's TTI Method

To perform maturity calculations using the Lopatin method, time and temperature factors need to be defined for each temperature interval shown in the burial history plots. The time factor is simply defined as the length of time in million years spent by the sediment in each temperature interval. The temperature factor, conversely, increases exponentially with increasing temperature. Lopatin (1971, 1976) defined the temperature factor, γ, as $\gamma = 2n$, where n is the index value (**Table 7.12**). The γ factor reflects the exponential dependence of maturity on temperature. The Total TTI which gives the total maturity of the sediment is sum total of the interval TTI, i.e.

$$\text{Total TTI} = \sum_{n=\min}^{n=\max} (\text{Time factor, Tn}) \times (\text{Temperature factor, } \gamma)$$

For land-derived Type III organic matter, Total TTI guidelines used for locating the hydrocarbon generation window are :

Total TTI	Stage
15	Onset of hydrocarbon generation
160	End of hydrocarbon generation

(Waples, 1985)

Table 7.12 Relation between sediment temperature, the index value, n, and the temperature factor, γ (from Waples, 1985)

Temperature Range (°C)	n	Temperature Factor, $\gamma=2^n$
20-30	-8	256^{-1}
30-40	-7	128^{-1}
40-50	-6	64^{-1}
50-60	-5	32^{-1}
60-70	-4	16^{-1}
70-80	-3	8^{-1}
80-90	-2	4^{-1}
90-100	-1	2^{-1}
100-110	0	1
110-120	1	2
120-130	2	4
130-140	3	8
140-150	4	16
150-160	5	32
160-170	6	64
170-180	7	128
180-190	8	256

7.3.1a Well Results

Using the information in **Tables 7.2** to **7.8**, the family of burial history curves for the sediments in the seven wells are constructed (**Figure 7.3**). Interval TTI values are calculated for each 10°C temperature range, and are summed up to obtain the Total TTI values which indicate the level of maturity of a particular sedimentary layer. Results from the calculations of the Lopatin TTI values indicate that the sediments penetrated by all the seven wells are still within the immature stage (**Tables 7.13** to **7.19**). Evidence from other maturity parameters (pyrolysis Tmax, vitrinite reflectance and kerogen elemental composition) concur with this.

Table 7.13 Summary of Lopatin TTI calculations for South Furious-2

Stage	Temp. Range	Temp. Factor	Time Factor	TTI	ΣTTI	Oil Window	Time (Ma)
IVE/IVF	20-30	256^{-1}	3.9	0.015	0.015		0
IVD	20-30	256^{-1}	3.3	0.013	0.013		5.2
	30-40	128^{-1}	5.2	0.041	0.054		0
IVC	20-30	256^{-1}	2.5	0.010	0.010		7.8
	30-40	128^{-1}	7.8	0.061	0.071		0
IVA	20-30	256^{-1}	0.5	0.002	0.002		14.0
	30-40	128^{-1}	1.1	0.009	0.011		12.9
	40-50	64^{-1}	1.1	0.017	0.028		11.8

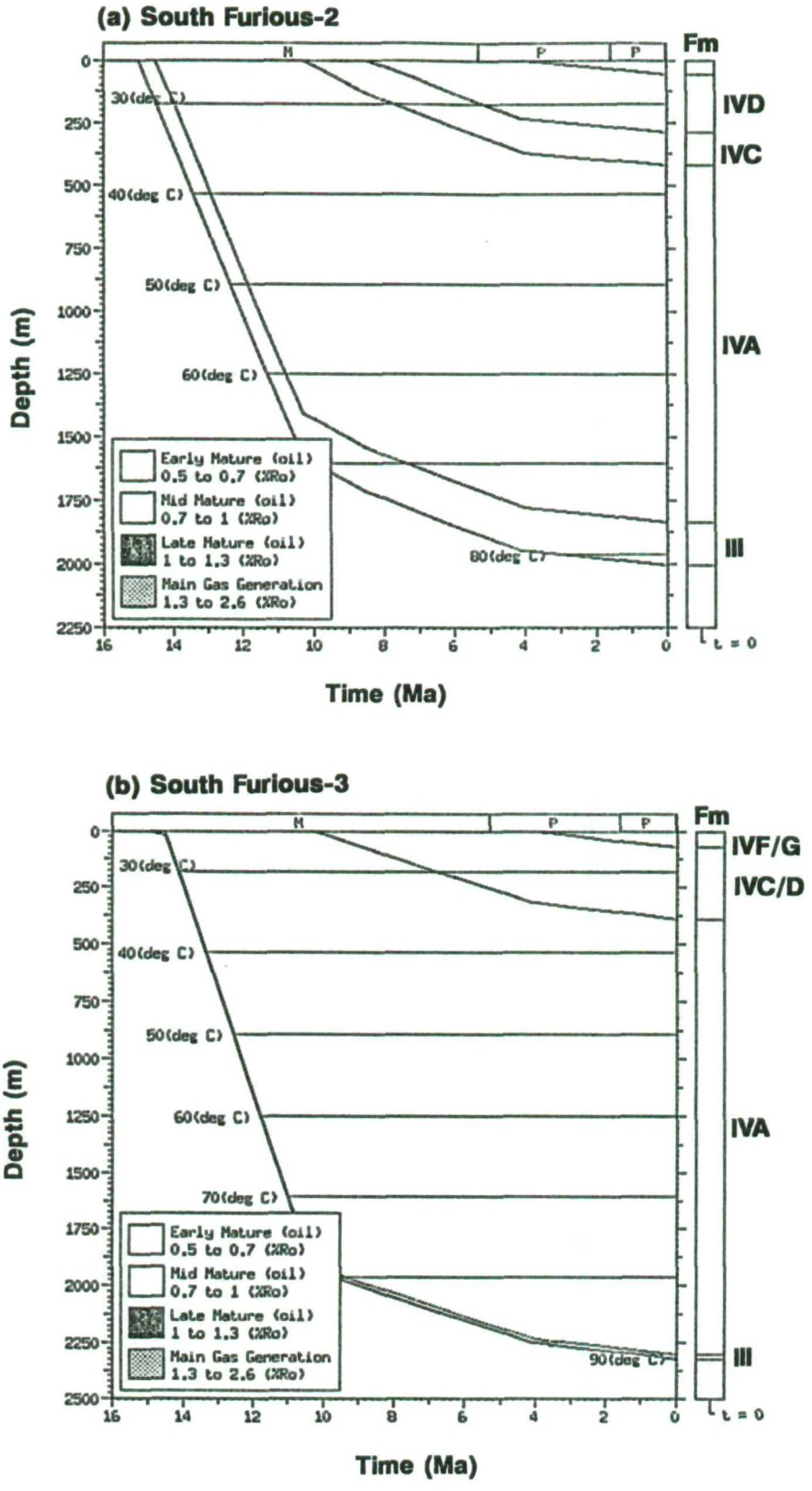
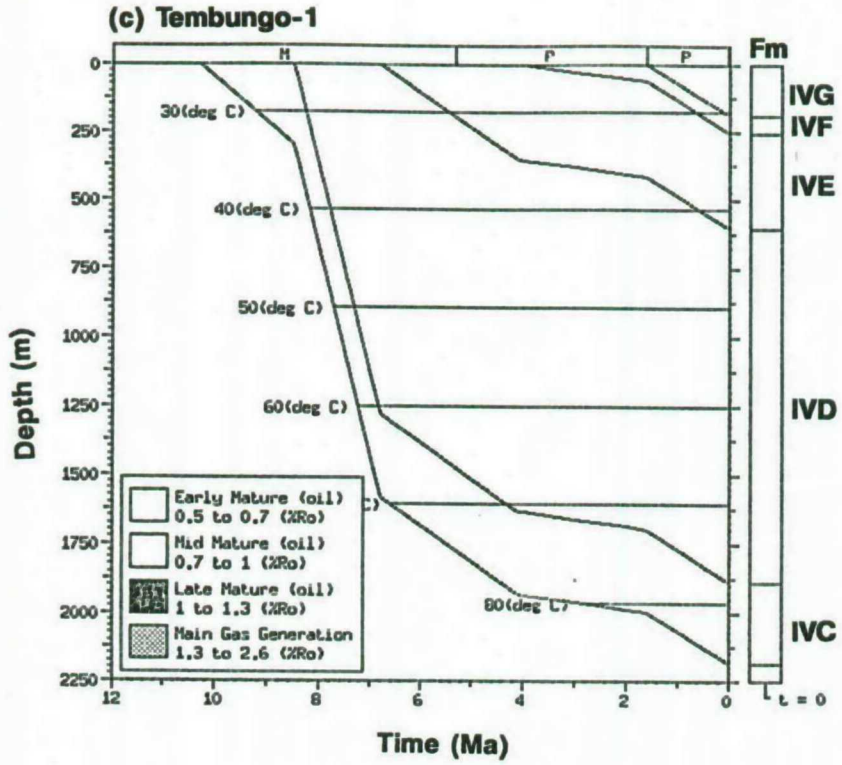


FIGURE 7.3 The burial history curves for the sedimentary sequences in **(a)** South Furious-2, **(b)** South Furious-3, **(c)** Tembungo-1, **(d)** Tembungo-2, **(e)** Tembungo-6, **(f)** Rusa Timur-1 and **(g)** Gajah Hitam-1.



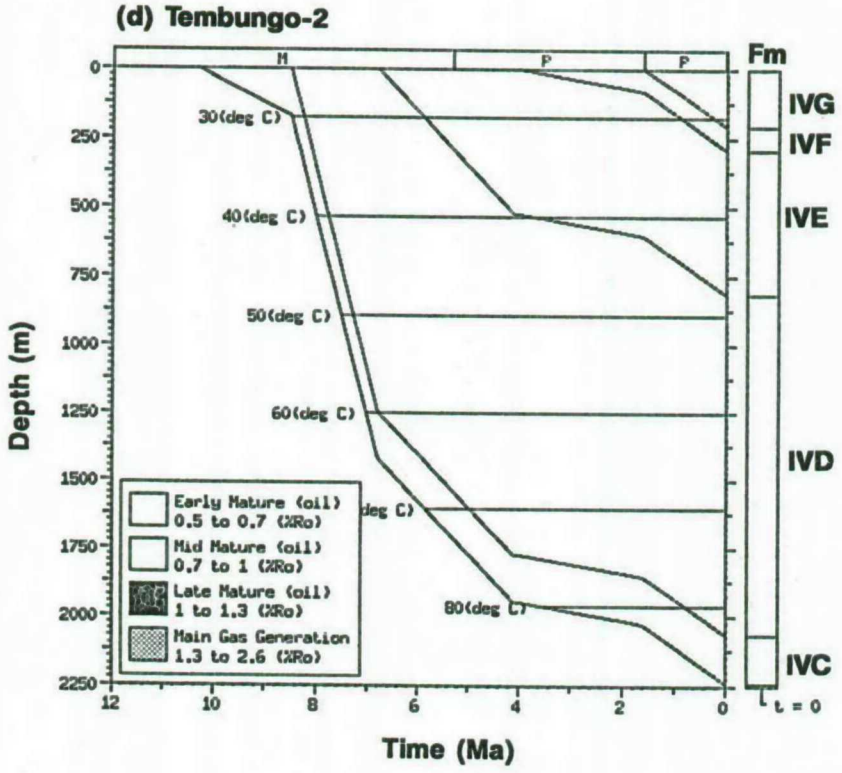
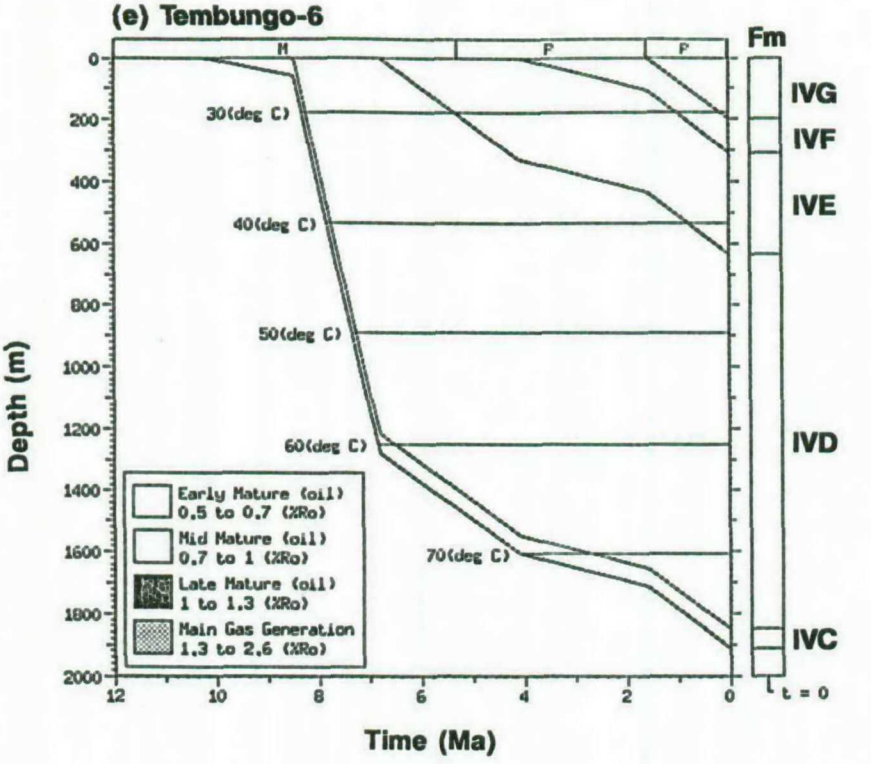


FIGURE 7.3 Continued.



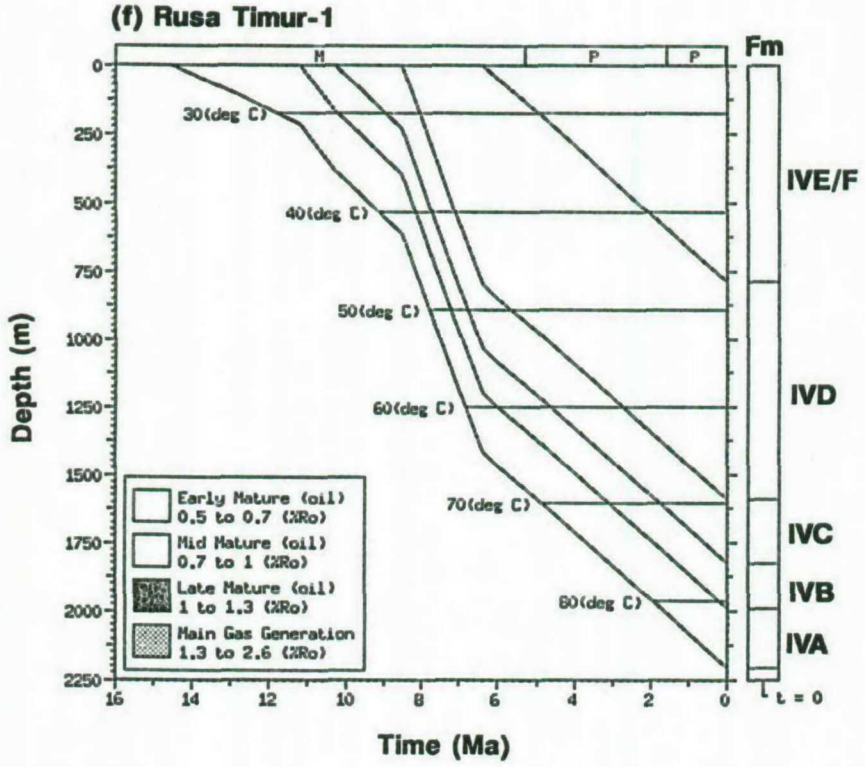


FIGURE 7.3 Continued.

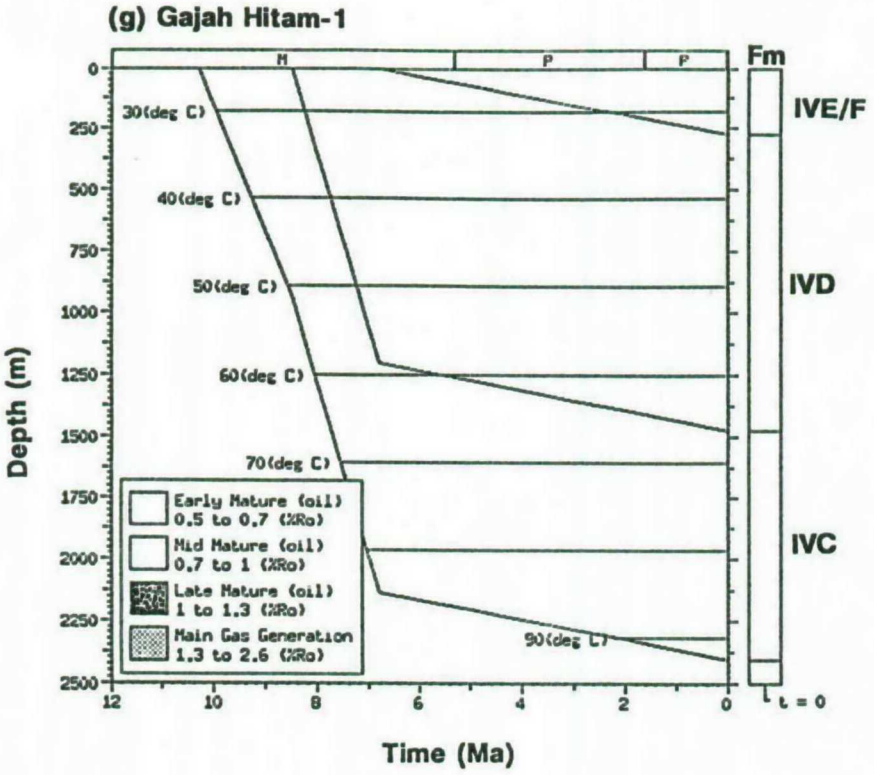


FIGURE 7.3 Continued.

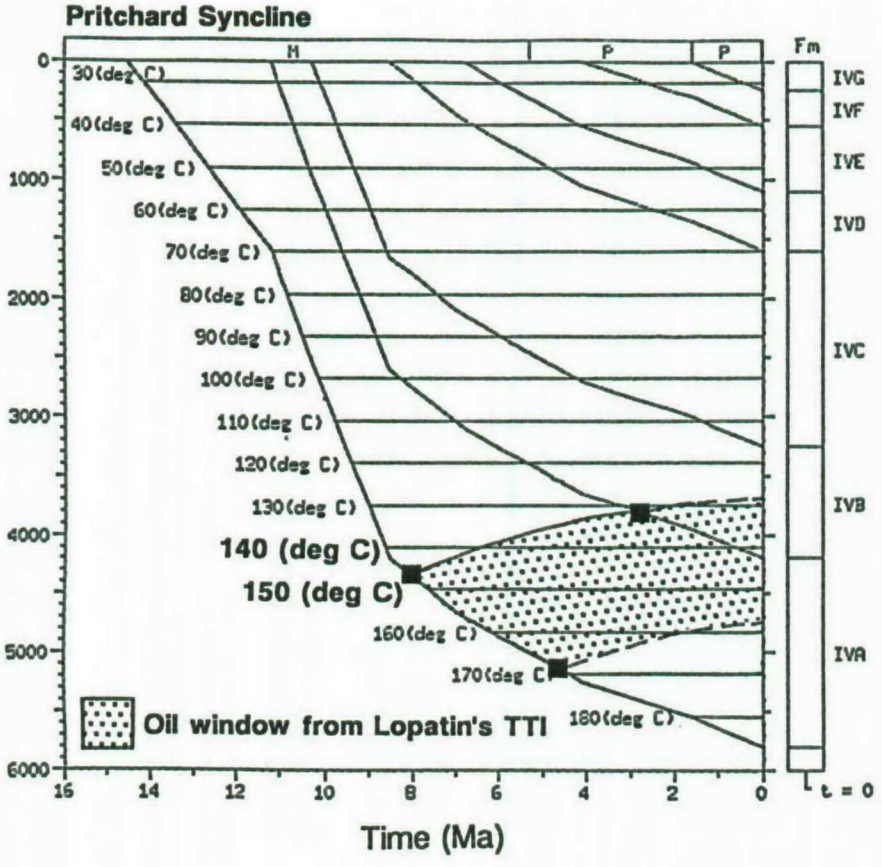


FIGURE 7.4 Hydrocarbon generation window in the Pritchard Syncline determined from Lopatin's TTI method.

Table 7.13 Summary of Lopatin TTI calculations for South Furious-2 - continued

Stage	Temp. Range	Temp. Factor	Time Factor	TTI	ΣTTI	Oil Window	Time (Ma)
	50-60	32^{-1}	1.0	0.031	0.059		10.8
	60-70	16^{-1}	3.8	0.238	0.297		7.4
	70-80	8^{-1}	7.4	0.925	1.240		0
III	20-30	256^{-1}	0.6	0.002	0.002		14.4
	30-40	128^{-1}	1.0	0.008	0.010		13.4
	40-50	64^{-1}	1.0	0.016	0.026		12.4
	50-60	32^{-1}	1.0	0.031	0.057		11.4
	60-70	16^{-1}	1.0	0.063	0.120		10.4
	70-80	8^{-1}	7.6	0.950	1.070		2.8
	80-90	4^{-1}	2.8	0.700	1.770		0

Table 7.14 Summary of Lopatin TTI calculations for South Furious-3

Stage	Temp. Range	Temp. Factor	Time Factor	TTI	ΣTTI	Oil Window	Time (Ma)
IVE/IVF	20-30	256^{-1}	4.0	0.016	0.016		0
IVC/IVD	20-30	256^{-1}	3.4	0.013	0.013		6.8
	30-40	128^{-1}	6.8	0.053	0.066		0
IVA	20-30	256^{-1}	0.5	0.002	0.002		14.0
	30-40	128^{-1}	0.7	0.005	0.007		13.3
	40-50	64^{-1}	1.2	0.019	0.026		12.5
	50-60	32^{-1}	0.8	0.025	0.051		11.7
	60-70	16^{-1}	0.8	0.050	0.101		10.9
	70-80	8^{-1}	1.5	0.188	0.289		9.4
	80-90	4^{-1}	9.4	2.350	2.639		0
III	20-30	256^{-1}	0.8	0.003	0.003		14.2
	30-40	128^{-1}	0.8	0.006	0.009		13.4
	40-50	64^{-1}	0.8	0.013	0.022		12.6
	50-60	32^{-1}	0.8	0.025	0.047		11.8
	60-70	16^{-1}	0.8	0.050	0.097		11.0
	70-80	8^{-1}	0.8	0.100	0.197		10.2
	80-90	4^{-1}	10.2	2.550	2.747		0

Table 7.15 Summary of Lopatin TTI calculations for Tembungo-1.

Stage	Temp. Range	Temp. Factor	Time Factor	TTI	ΣTTI	Oil Window	Time (Ma)
IVG	20-30	256^{-1}	1.5	0.006	0.006		0.1
	30-40	128^{-1}	0.1	0.001	0.007		0
IVF	20-30	256^{-1}	3.4	0.013	0.013		0.6
	30-40	128^{-1}	0.6	0.005	0.018		0

Table 7.15 Summary of Lopatin TTI calculations for Tembungo-1 - continued.

Stage	Temp. Range	Temp. Factor	Time Factor	TTI	ΣTTI	Oil Window	Time (Ma)
IVE	20-30	256^{-1}	1.4	0.005	0.005		5.4
	30-40	128^{-1}	4.8	0.038	0.043		0.6
	40-50	64^{-1}	0.6	0.009	0.052		0
IVD	20-30	256^{-1}	0.2	0.001	0.001		8.3
	30-40	128^{-1}	0.5	0.004	0.005		7.8
	40-50	64^{-1}	0.5	0.008	0.013		7.3
	50-60	32^{-1}	0.5	0.016	0.029		6.8
	60-70	16^{-1}	2.5	0.156	0.185		4.3
	70-80	8^{-1}	4.3	0.538	0.723		0
IVC	20-30	256^{-1}	1.0	0.004	0.004		9.3
	30-40	128^{-1}	1.1	0.009	0.013		8.2
	40-50	64^{-1}	0.5	0.008	0.021		7.7
	50-60	32^{-1}	0.5	0.016	0.037		7.2
	60-70	16^{-1}	0.6	0.038	0.075		6.6
	70-80	8^{-1}	3.7	0.463	0.538.		2.9
	80-90	4^{-1}	2.9	0.725	1.263		0

Table 7.16 Summary of Lopatin TTI calculations for sediments in Tembungo-2

Stage	Temp. Range	Temp. Factor	Time Factor	TTI	ΣTTI	Oil Window	Time (Ma)
IVG	20-30	256^{-1}	1.4	0.005	0.005		0.2
	30-40	128^{-1}	0.2	0.002	0.007		0
IVF	20-30	256^{-1}	3.1	0.012	0.012		0.9
	30-40	128^{-1}	0.9	0.007	0.019		0
IVE	20-30	256^{-1}	0.9	0.004	0.004		5.9
	30-40	128^{-1}	2.2	0.017	0.021		3.7
	40-50	64^{-1}	3.7	0.058	0.079		0
IVD	20-30	256^{-1}	0.2	0.001	0.001		8.5
	30-40	128^{-1}	0.5	0.004	0.005		7.8
	40-50	64^{-1}	0.5	0.008	0.013		7.3
	50-60	32^{-1}	0.5	0.016	0.029		6.8
	60-70	16^{-1}	1.8	0.113	0.142		5.0
	70-80	8^{-1}	4.2	0.525	0.667		0.8
	80-90	4^{-1}	0.8	0.200	0.867		0
IVC	20-30	256^{-1}	1.8	0.007	0.007		8.5
	30-40	128^{-1}	0.5	0.004	0.011		8.0
	40-50	64^{-1}	0.4	0.006	0.017		7.6
	50-60	32^{-1}	0.6	0.019	0.036		7.0
	60-70	16^{-1}	1.2	0.075	0.111		5.8
	70-80	8^{-1}	2.4	0.300	0.411		3.4
	80-90	4^{-1}	3.4	0.850	1.261		0

Table 7.17 Summary of Lopatin TTI calculations for sediments in Tembungo-6.

Stage	Temp. Range	Temp. Factor	Time Factor	TTI	ΣTTI	Oil Window	Time (Ma)
IVG	20-30	256^{-1}	1.4	0.005	0.005		0.2
	30-40	128^{-1}	0.2	0.002	0.007		0
IVF	20-30	256^{-1}	3.0	0.012	0.012		1.1
	30-40	128^{-1}	1.1	0.009	0.021		0
IVE	20-30	256^{-1}	1.4	0.005	0.005		5.4
	30-40	128^{-1}	4.6	0.036	0.041		0.8
	40-50	64^{-1}	0.8	0.013	0.054		0
IVD	20-30	256^{-1}	0.3	0.001	0.001		8.3
	30-40	128^{-1}	0.6	0.005	0.006		7.7
	40-50	64^{-1}	0.4	0.006	0.012		7.3
	50-60	32^{-1}	0.8	0.025	0.037		6.5
	60-70	16^{-1}	3.8	0.238	0.275		2.7
	70-80	8^{-1}	2.7	0.338	0.613		0
IVC	20-30	256^{-1}	1.9	0.004	0.004		8.4
	30-40	128^{-1}	0.6	0.005	0.009		7.8
	40-50	64^{-1}	0.4	0.006	0.015		7.4
	50-60	32^{-1}	0.6	0.019	0.034		6.8
	60-70	16^{-1}	2.7	0.169	0.203		4.1
	70-80	8^{-1}	4.1	0.513	0.716		0

Table 7.18 Summary of Lopatin TTI calculations for sediments in Rusa Timur-1.

Stage	Temp. Range	Temp. Factor	Time Factor	TTI	ΣTTI	Oil Window	Time (Ma)
IVE/IVF	20-30	256^{-1}	1.4	0.005	0.005		5.0
	30-40	128^{-1}	2.9	0.023	0.028		2.1
	40-50	64^{-1}	2.1	0.033	0.061		0
IVD	20-30	256^{-1}	0.6	0.002	0.002		8.0
	30-40	128^{-1}	1.1	0.009	0.011		7.1
	40-50	64^{-1}	1.5	0.023	0.034		5.6
	50-60	32^{-1}	2.8	0.088	0.122		2.8
	60-70	16^{-1}	2.8	0.175	0.297		0
IVC	20-30	256^{-1}	1.3	0.005	0.005		9.0
	30-40	128^{-1}	1.2	0.009	0.014		7.8
	40-50	64^{-1}	1.0	0.016	0.030		6.8
	50-60	32^{-1}	2.2	0.069	0.099		4.6
	60-70	16^{-1}	2.8	0.175	0.274		1.8
	70-80	8^{-1}	1.8	0.225	0.499		0
IVB	20-30	256^{-1}	1.0	0.004	0.004		10.2
	30-40	128^{-1}	2.0	0.016	0.020		8.2
	40-50	64^{-1}	1.0	0.016	0.036		7.2
	50-60	32^{-1}	1.2	0.038	0.074		6.0
	60-70	16^{-1}	2.9	0.181	0.255		3.1

Table 7.18 Summary of Lopatin TTI calculations for sediments in Rusa Timur-1 - continued.

Stage	Temp. Range	Temp. Factor	Time Factor	TTI	ΣTTI	Oil Window	Time (Ma)
	70-80	8^{-1}	2.9	0.363	0.618		0.2
	80-90	4^{-1}	0.2	0.050	0.668		0
IVA	20-30	256^{-1}	2.7	0.011	0.011		11.8
	30-40	128^{-1}	2.6	0.020	0.031		9.2
	40-50	64^{-1}	1.4	0.022	0.053		7.8
	50-60	32^{-1}	1.0	0.031	0.084		6.8
	60-70	16^{-1}	1.9	0.119	0.203		4.9
	70-80	8^{-1}	2.9	0.363	0.566		2.0
	80-90	4^{-1}	2.0	0.500	1.066		0

TABLE 7.19 Summary of Lopatin TTI calculations for sediments in Gajah Hitam-1.

Stage	Temp. Range	Temp. Factor	Time Factor	TTI	ΣTTI	Oil Window	Time (Ma)
IVE/IVF	20-30	256^{-1}	4.5	0.018	0.018		2.3
	30-40	128^{-1}	2.3	0.018	0.036		0
IVD	20-30	256^{-1}	0.3	0.001	0.001		8.2
	30-40	128^{-1}	0.4	0.003	0.004		7.8
	40-50	64^{-1}	0.6	0.009	0.013		7.2
	50-60	32^{-1}	1.6	0.050	0.063		5.6
	60-70	16^{-1}	5.6	0.350	0.413		0
IVC	20-30	256^{-1}	0.3	0.001	0.001		10.0
	30-40	128^{-1}	0.7	0.005	0.006		9.3
	40-50	64^{-1}	0.7	0.011	0.017		8.6
	50-60	32^{-1}	0.6	0.019	0.036		8.0
	60-70	16^{-1}	0.2	0.013	0.049		7.8
	70-80	8^{-1}	0.8	0.100	0.149		7.0
	80-90	4^{-1}	5.1	1.275	1.424		2.1
	90-100	2^{-1}	2.1	1.050	2.474		0

7.3.1b Hydrocarbon Kitchen 1 : Pritchard Syncline

Data for the Pritchard Syncline (**Table 7.9**) are taken from a seismic cross-section whose location is shown in **Figure 7.1**. The Stage and sub-Stage boundaries identified by Azim-Ibrahim (1994) are used here. Taking TTI=15 as the onset of hydrocarbon generation and TTI=160 as the upper limit of hydrocarbon generation, Lopatin's method indicates that the sub-Stage IVA sediments began generating hydrocarbons around 8.0 my and ceased producing around 4.6 my ago (**Table 7.20, Figure 7.4**). It also shows that the sub-Stage IVB sediments entered the hydrocarbon generation window around 3.0 my ago and are presently within the oil window. The rest of the younger sediments are still immature.

Table 7.20 Summary of Lopatin TTI calculations for sediments in the Pritchard Syncline.

Stage	Temp. Range	Temp. Factor	Time Factor	TTI	ΣTTI	Oil Window	Time (Ma)
IVG	20-30	256^{-1}	1.1	0.004	0.004		0.5
	30-40	128^{-1}	0.5	0.004	0.008		0
IVF	20-30	256^{-1}	1.5	0.006	0.006		2.6
	30-40	128^{-1}	2.6	0.020	0.026		0
IVE	20-30	256^{-1}	0.8	0.003	0.003		6.0
	30-40	128^{-1}	1.8	0.014	0.017		4.2
	40-50	64^{-1}	2.9	0.045	0.062		1.3
	50-60	32^{-1}	1.3	0.041	0.103		0
IVD	20-30	256^{-1}	0.6	0.002	0.002		8.0
	30-40	128^{-1}	1.4	0.011	0.013		6.6
	40-50	64^{-1}	1.8	0.028	0.041		4.8
	50-60	32^{-1}	2.4	0.075	0.116		2.4
	60-70	16^{-1}	2.4	0.150	0.226		0
IVC	20-30	256^{-1}	0.2	0.001	0.001		10.2
	30-40	128^{-1}	0.5	0.004	0.005		9.7
	40-50	64^{-1}	0.4	0.006	0.011		9.3
	50-60	32^{-1}	0.3	0.009	0.020		9.0
	60-70	16^{-1}	0.4	0.025	0.045		8.6
	70-80	8^{-1}	1.2	0.150	0.195		7.4
	80-90	4^{-1}	1.9	0.475	0.670		5.5
	90-100	2^{-1}	1.3	0.650	1.320		4.2
	100-110	1	2.8	2.800	4.120		1.4
	110-120	2	1.4	2.800	6.920		0
IVB	20-30	256^{-1}	0.2	0.001	0.001		11.0
	30-40	128^{-1}	0.4	0.003	0.004		10.6
	40-50	64^{-1}	0.2	0.003	0.007		10.4
	50-60	32^{-1}	0.4	0.013	0.020		10.0
	60-70	16^{-1}	0.4	0.025	0.045		9.6
	70-80	8^{-1}	0.4	0.050	0.085		9.2
	80-90	4^{-1}	0.4	0.100	0.195		8.8
	90-100	2^{-1}	0.5	0.250	0.445		8.3
	100-110	1	1.3	1.300	1.745		7.0
	110-120	2	1.6	3.200	4.945		5.4
	120-130	4	2.1	8.400	13.35	B	3.3
	130-140	8	2.7	21.60	34.95	↓	0.6
	140-150	16	0.6	9.600	44.55		0
IVA	20-30	256^{-1}	0.3	0.001	0.001		14.2
	30-40	128^{-1}	0.8	0.006	0.007		13.4
	40-50	64^{-1}	0.8	0.013	0.020		12.6
	50-60	32^{-1}	0.7	0.022	0.042		11.9
	60-70	16^{-1}	0.7	0.044	0.085		11.2
	70-80	8^{-1}	0.4	0.050	0.135		10.8
	80-90	4^{-1}	0.3	0.075	0.211		10.5
	90-100	2^{-1}	0.3	0.150	0.370		10.2

Table 7.20 Summary of Lopatin TTI calculations for sediments in the Pritchard Syncline - continued.

Stage	Temp. Range	Temp. Factor	Time Factor	TTI	ΣTTI	Oil Window	Time (Ma)
	100-110	1	0.4	0.400	0.770		9.8
	110-120	2	0.4	0.800	1.570		9.4
	120-130	4	0.4	1.600	3.170		9.0
	130-140	8	0.4	3.200	6.370	B	8.6
	140-150	16	1.0	16.00	22.37	↓	7.6
	150-160	32	1.4	44.80	67.17		6.2
	160-170	64	1.8	115.2	182.4	E	4.4
	170-180	128	2.8	358.4	540.8		1.6
	180-190	256	1.6	409.6	950.4		0

* B = beginning and E = end of oil generation window.

7.3.1c Hydrocarbon Kitchen 2 : Furious Syncline

A seismic section taken across the Furious Syncline (**Figure 7.1**) was used to determine the depths to the tops of the Stages/sub-Stages; the boundary identifications are again taken from Azim-Ibrahim (1994). The sub-Stage IVA sediments here entered the oil window around 8.4 my ago (**Table 7.21, Figure 7.5**), slightly earlier than those in the Pritchard Syncline. Hydrocarbon generation from the sub-Stage IVA sediments ceased around 5.9 my. For the sub-Stage IVB sediments, hydrocarbon generation began around 2.6 my ago and are still producing. The younger overlying sediments of sub-Stages IVC-IVG are presently immature.

Table 7.21 Summary of Lopatin TTI calculations for sediments in the Furious Syncline.

Stage	Temp. Range	Temp. Factor	Time Factor	TTI	ΣTTI	Oil Window	Time (Ma)
IVF/IVG	20-30	256^{-1}	4.0	0.016	0.016		0
IVE	20-30	256^{-1}	0.8	0.003	0.003		6.0
	30-40	128^{-1}	1.6	0.013	0.016		4.4
	40-50	64^{-1}	4.4	0.069	0.085		0
IVD	20-30	256^{-1}	0.4	0.002	0.002		8.2
	30-40	128^{-1}	0.8	0.006	0.008		7.4
	40-50	64^{-1}	1.0	0.016	0.024		6.4
	50-60	32^{-1}	1.6	0.050	0.074		4.8
	60-70	16^{-1}	4.8	0.300	0.374		0
IVC	20-30	256^{-1}	0.4	0.002	0.002		9.9
	30-40	128^{-1}	0.7	0.005	0.007		9.2
	40-50	64^{-1}	0.6	0.009	0.016		8.6
	50-60	32^{-1}	0.8	0.025	0.041		7.8
	60-70	16^{-1}	0.8	0.050	0.091		7.0

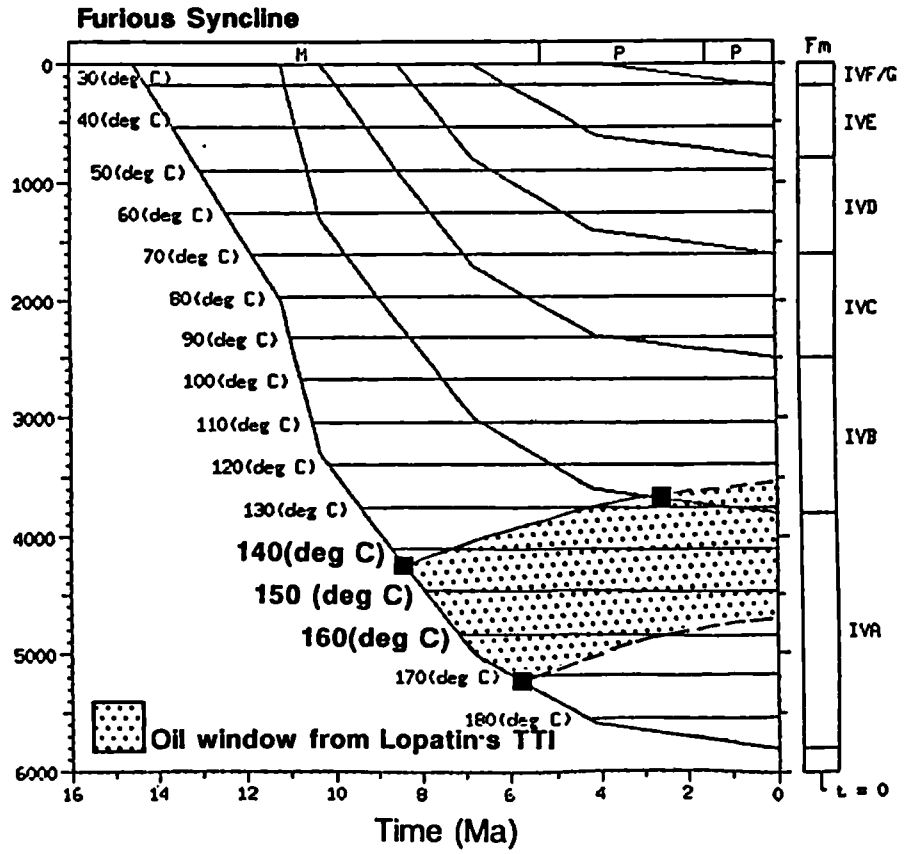


FIGURE 7.5 Hydrocarbon generation window in the Furious Syncline determined from Lopatin's TTI method.

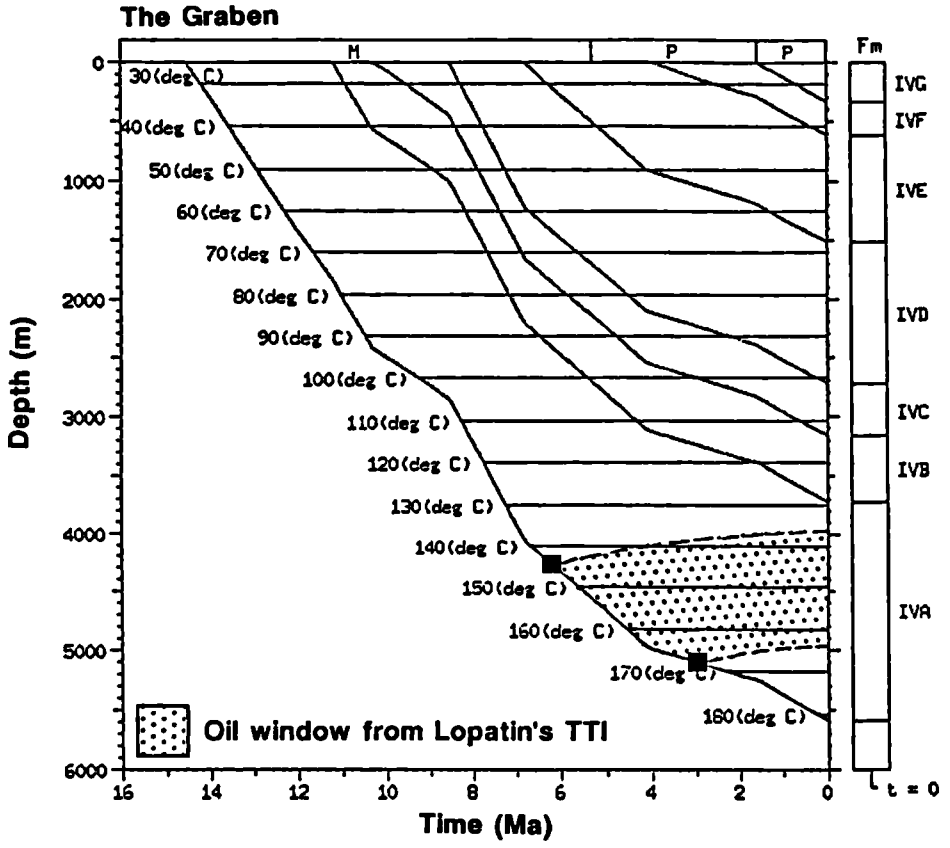


FIGURE 7.6 Hydrocarbon generation window in The Graben located between Rusa Timur-1 and Belangkas area determined from Lopatin's TTI method.

Table 7.21 Summary of Lopatin TTI calculations for sediments in the Furious Syncline - continued.

Stage	Temp. Range	Temp. Factor	Time Factor	TTI	ΣTTI	Oil Window	Time (Ma)
	70-80	8^{-1}	1.4	0.175	0.266		5.6
	80-90	4^{-1}	1.8	0.450	0.716		3.8
	90-100	2^{-1}	3.8	1.900	2.616		0
IVB	20-30	256^{-1}	0.2	0.001	0.001		11.0
	30-40	128^{-1}	0.2	0.002	0.003		10.8
	40-50	64^{-1}	0.2	0.003	0.006		10.6
	50-60	32^{-1}	0.2	0.006	0.012		10.4
	70-80	8^{-1}	0.7	0.088	0.144		9.0
	60-70	16^{-1}	0.7	0.044	0.056		9.7
	80-90	4^{-1}	0.8	0.200	0.344		8.2
	90-100	2^{-1}	0.7	0.350	0.694		7.5
	100-110	1	0.9	0.900	1.594		6.6
	110-120	2	1.5	3.000	4.594	B	5.1
	120-130	4	4.1	16.40	20.99	↓	1.0
	130-140	8	1.0	8.000	28.99		0
IVA	20-30	256^{-1}	0.3	0.001	0.001		14.2
	30-40	128^{-1}	0.6	0.005	0.006		13.6
	40-50	64^{-1}	0.6	0.009	0.015		13.0
	50-60	32^{-1}	0.5	0.016	0.040		12.5
	60-70	16^{-1}	0.7	0.044	0.075		11.8
	70-80	8^{-1}	0.6	0.075	0.150		11.2
	80-90	4^{-1}	0.2	0.050	0.200		11.0
	90-100	2^{-1}	0.2	0.100	0.300		10.8
	100-110	1	0.3	0.300	0.600		10.5
	110-120	2	0.4	0.800	1.400		10.1
	120-130	4	0.7	2.800	4.200		9.4
	130-140	8	0.7	5.600	9.800	B	8.7
	140-150	16	0.7	11.20	21.00		8.0
	150-160	32	0.8	25.60	46.60	↓	7.2
	160-170	64	1.6	102.4	149.0		6.0
	170-180	128	1.6	204.8	353.8	E	4.4
	180-190	256	4.4	1126	1470		0

7.3.1d Hydrocarbon Kitchen 3 : The Graben

As for the previous hydrocarbon kitchens, data for the thermal modelling of the sediments in the graben were obtained from a seismic section (**Figure 7.1**). Stage and sub-Stage boundaries identified by Azim-Ibrahim (1994) are used. The sub-Stage IVA sediments entered the oil generation window around 6.3 my ago and left it around 3.0 my (**Table 7.22, Figure 7.6**). Lopatin's TTI values indicate that the sub-Stage IVB sediments are just about to enter the oil window, with the overlying sediments being still immature.

Table 7.22 Summary of Lopatin TTI calculations for sediments in the graben located between Rusa Timur-1 and Belangkas.

Stage	Temp. Range	Temp. Factor	Time Factor	TTI	ΣTTI	Oil Window	Time (Ma)
IVG	20-30	256^{-1}	0.8	0.003	0.003		0.8
	30-40	128^{-1}	0.8	0.006	0.009		0
IVF	20-30	256^{-1}	1.4	0.005	0.005		2.6
	30-40	128^{-1}	2.2	0.017	0.022		0.4
	40-50	64^{-1}	0.4	0.006	0.028		0
IVE	20-30	256^{-1}	0.5	0.002	0.002		6.3
	30-40	128^{-1}	1.1	0.009	0.011		5.2
	40-50	64^{-1}	1.0	0.016	0.027		4.2
	50-60	32^{-1}	2.8	0.088	2.131		1.4
	60-70	16^{-1}	1.4	0.088	2.219		0
IVD	20-30	256^{-1}	0.3	0.001	0.001		8.3
	30-40	128^{-1}	0.5	0.004	0.005		7.8
	40-50	64^{-1}	0.5	0.008	0.013		7.3
	50-60	32^{-1}	0.5	0.016	0.029		6.8
	60-70	16^{-1}	1.2	0.075	0.104		5.6
	70-80	8^{-1}	1.1	0.138	0.144		4.5
	80-90	4^{-1}	2.3	0.575	0.242		2.2
	90-100	2^{-1}	2.0	1.000	1.817		0.2
	100-110	1	0.2	0.200	2.017		0
IVC	20-30	256^{-1}	0.8	0.003	0.003		9.6
	30-40	128^{-1}	1.2	0.009	0.012		8.4
	40-50	64^{-1}	0.5	0.008	0.020		7.9
	50-60	32^{-1}	0.5	0.016	0.036		7.4
	60-70	16^{-1}	0.5	0.031	0.067		6.9
	70-80	8^{-1}	1.0	0.125	0.192		5.9
	80-90	4^{-1}	1.1	0.275	0.467		4.8
	90-100	2^{-1}	1.8	0.900	1.367		3.0
	100-110	1	2.4	2.400	3.767		0.6
	110-120	2	0.6	1.200	4.967		0
IVB	20-30	256^{-1}	0.3	0.001	0.001		11.0
	30-40	128^{-1}	0.6	0.005	0.006		10.4
	40-50	64^{-1}	0.6	0.009	0.015		9.0
	50-60	32^{-1}	1.2	0.038	0.053		8.2
	60-70	16^{-1}	0.5	0.031	0.084		7.7
	70-80	8^{-1}	0.5	0.063	0.147		7.2
	80-90	4^{-1}	0.7	0.175	0.322		6.5
	90-100	2^{-1}	1.0	0.500	0.822		5.5
	100-110	1	1.1	1.100	1.922		4.4
	110-120	2	0.7	1.400	3.322		1.7
	120-130	4	1.7	6.800	10.12		0
IVA	20-30	256^{-1}	0.3	0.001	0.001		14.2
	30-40	128^{-1}	0.6	0.005	0.006		13.6
	40-50	64^{-1}	0.6	0.009	0.015		13.0
	50-60	32^{-1}	0.6	0.019	0.034		12.4

Table 7.22 Summary of Lopatin TTI calculations for sediments in the graben located between Rusa Timur-1 and Belangkas - continued.

Stage	Temp. Range	Temp. Factor	Time Factor	TTI	ΣTTI	Oil Window	Time (Ma)
	60-70	16^{-1}	0.7	0.044	0.078		11.7
	70-80	8^{-1}	0.7	0.088	0.166		11.0
	80-90	4^{-1}	0.6	0.150	0.316		10.4
	90-100	2^{-1}	1.1	0.550	0.866		9.3
	100-110	1	1.1	1.100	1.966		8.2
	110-120	2	0.4	0.800	2.766		7.8
	120-130	4	0.6	2.400	5.166		7.2
	130-140	8	0.5	4.000	9.166	B	6.7
	140-150	16	1.1	17.60	26.77	↓	5.6
	150-160	32	1.0	32.00	58.77		4.6
	160-170	64	2.4	153.6	212.4	E	2.2
	170-180	128	2.0	256.0	468.4		0.2
	180-190	256	0.2	51.20	519.6		0

7.3.2 Arrhenius-based TTI Values

Calculations of the Arrhenius-based TTI values (TTI_{ARR}) for the sedimentary sequences under investigation here are compared with the results of Lopatin's TTI method. If, as Hunt & Hennet (1992) observed, results from both methods are very similar, then performing the simple maturation modelling according to the Lopatin method is justifiable for the Sabah Basin for quick thermal analyses, providing that the kerogen type remains as land-derived Type III organic matter.

The calculation of the Arrhenius-based TTI values are similar to the Lopatin method, where addition of the TTI_{ARR} values for each 10°C interval in the burial history curve of the sediments gives a summation index Σ TTI_{ARR}, which is the cumulative effect of time and temperature experienced by the sediments (Hunt & Hennet, 1992). Interval TTI_{ARR} values are determined for each temperature range using the relevant graph for kerogen Type III kinetics (**Figure 7.7**) and the graph for the conversion of oil to gas (**Figure 7.8**). The summation index Σ TTI_{ARR} can then be used to determine the stage of hydrocarbon generation and the maximum percentage of hydrocarbon already generated by using the graph in **Figure 7.9**. The guideline for interpreting the TTI_{ARR} values are :

TTI_{ARR}	Stage
1	Onset of hydrocarbon generation
460	End of hydrocarbon generation

(from Hunt & Hennet, 1992)

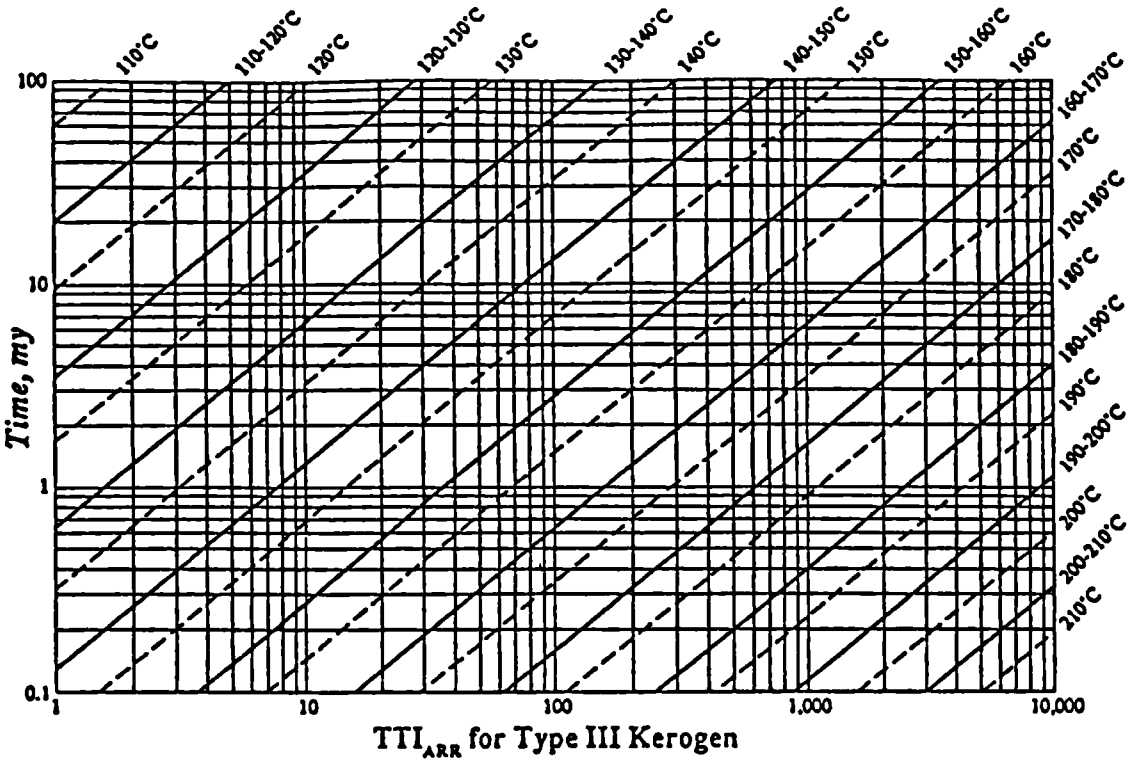


FIGURE 7.7 Graph showing relationship between time, temperature and TTI_{ARR} for kerogen Type III kinetics as represented by the Tent Island Formation of the Beaufort-Mackenzie Basin of Canada (from Hunt & Hennet, 1992).

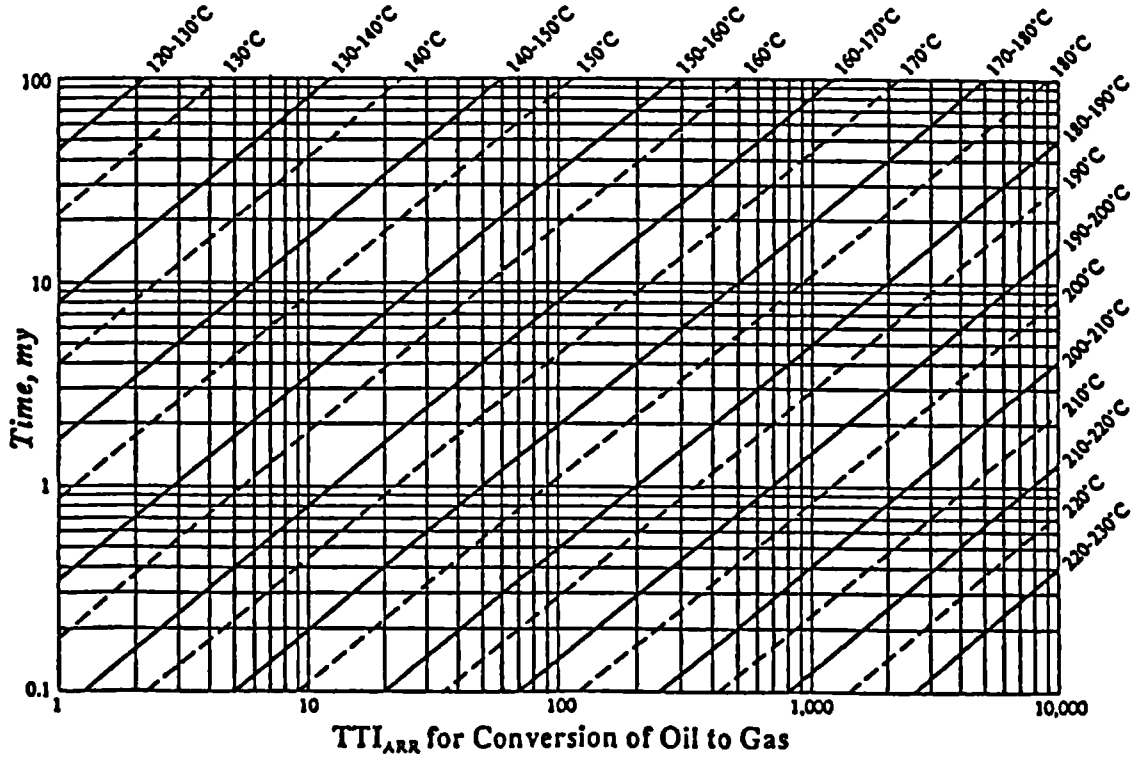


FIGURE 7.8 Graph showing relationship between time, temperature and TTI_{ARR} for the conversion of oil to gas (E = 230 kJ/mol and A = 3.17×10^{21} my) (from Hunt & Hennet, 1992).

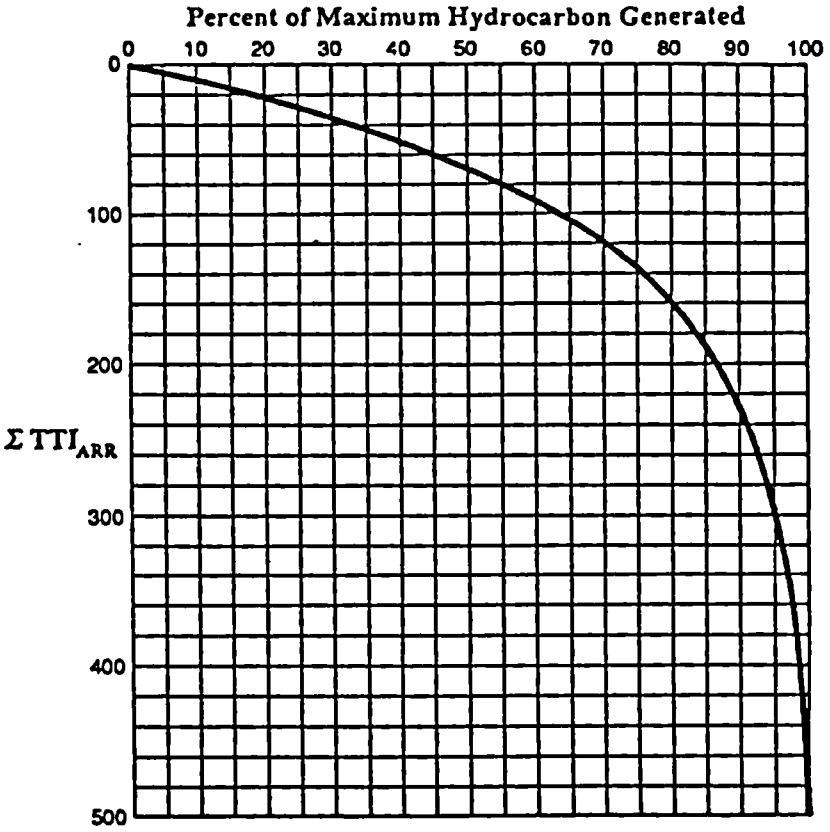


FIGURE 7.9 Graph showing the relationship between TTI_{ARR} and percent of hydrocarbon generated (from Hunt & Hennet, 1992).

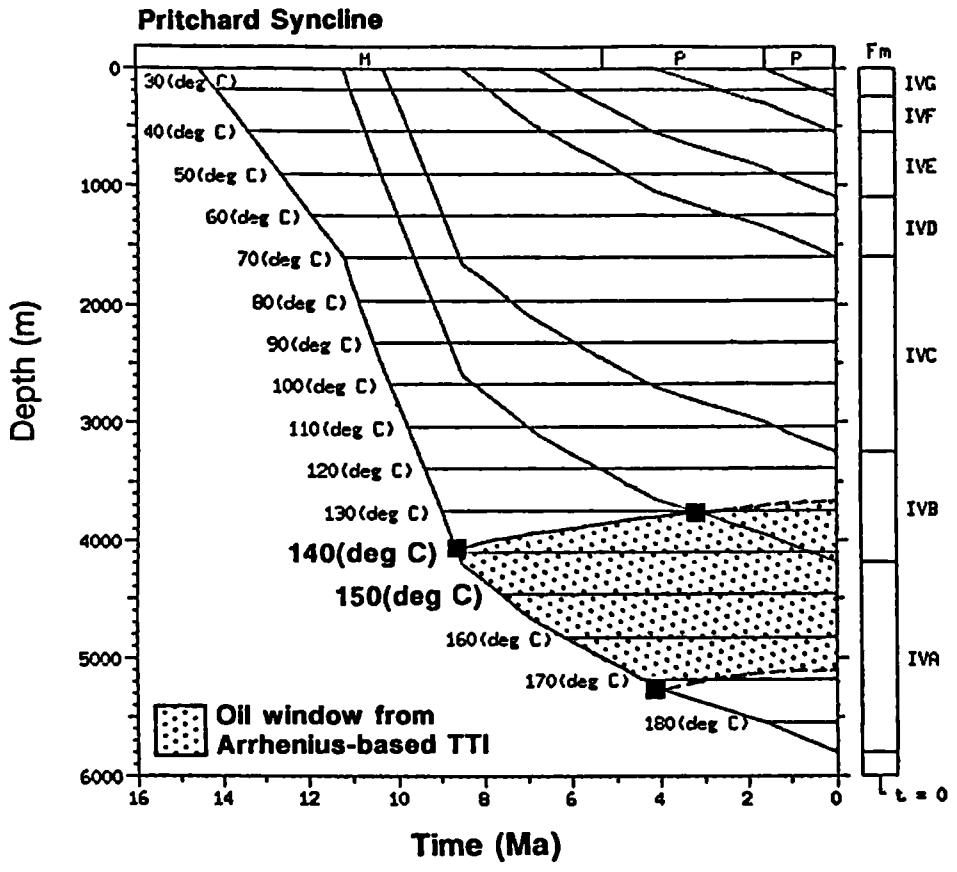


FIGURE 7.10 Hydrocarbon generation window in the Pritchard Syncline determined from the Arrhenius-based TTI method.

7.3.2a Well Results

From their burial history curves shown earlier, it can be seen that the sediments in all the seven wells have not reached the lowest temperature required (110°C) for the calculation of the TTI_{ARR} values. They are, therefore, still immature and this indication is well supported by data from pyrolysis Tmax, vitrinite reflectance values, palynomorph colour as well as the kerogen elemental compositions.

7.3.2b Hydrocarbon Kitchen 1 : Pritchard Syncline

Applying the Arrhenius TTI to sediments in the Pritchard Syncline shows that the sub-Stage IVC and younger sequences are presently immature, while the sub-Stage IVB entered the oil generation window around 3.3 Ma ago and has only generated about 10% of its total hydrocarbon generating capacity (**Table 7.23, Figure 7.10**). No gas is currently being produced from the sub-stage IVB sediments. The sub-Stage IVA sediments are now well within the oil window, having entered it around 8.6 Ma, and left it around 4.2 Ma ago. Both the oil and gas generating capacities of the lowermost parts of sub-Stage IVA sediments in this particular location in the Pritchard syncline have been depleted, indicating that they are within the overmature zone. The upper parts of sub-Stage IVA are presently still generating some hydrocarbons.

Table 7.23 Arrhenius TTI values for oil and gas generation in the Pritchard Syncline using kerogen Type III and oil to gas kinetics.

Stage	Temp. Range (°C)	Exposure Time (Ma)	Type III TTI	Type III ΣTTI	Oil * Window	Oil to gas TTI	Oil to gas ΣTTI	Gas • Window
IVC	110-120	1.4	0	0				
IVB	110-120	1.6	0	0				
	120-130	2.1	0	0		0	0	No gas
	130-140	2.7	4.5	4.5	B	0	0	generated
	140-150	0.6	4.7	9.2	↓	0	0	as yet
IVA	110-120	0.4	0	0				
	120-130	0.4	0	0		0	0	
	130-140	0.4	0	0		0	0	
	140-150	1.0	8	8	B	0	0	
	150-160	1.4	50	58	↓	4	4	B
	160-170	1.8	280	338		22	26	↓
	170-180	2.8	1900	2238	E	150	176	
	180-190	1.6	3500	5738		300	476	E

* B = beginning and E = end of oil generation window.

• B = beginning and E = end of conversion of oil to gas.

7.3.2c Hydrocarbon Kitchen 2 : Furious Syncline

The sub-Stage IVB sequence here have generated about 3% of its total hydrocarbon generating capacity following its entry into the oil window around 2.6 Ma ago (**Table 7.24, Figure 7.11**). Gas production from the cracking of oil has not yet begun. As in the Pritchard Syncline, the sub-Stage IVA sediments in this particular location span through the onset (8.7 Ma, 4100m) and end (5.7 Ma, 5250m) of the oil window. Oil and gas are presently being generated from parts of the sequence that have not reached the overmature stage.

Table 7.24 Arrhenius TTI values for oil and gas generation in the Furious Syncline using kerogen Type III and oil to gas kinetics.

Stage	Temp. Range (°C)	Exposure Time (Ma)	Type III TTI	Type III ΣTTI	Oil * Window	Oil to gas TTI	Oil to gas ΣTTI	Gas • Window
IVB	110-120	1.5	0	0				
	120-130	4.1	1.3	1.3	B	0	0	No gas
	130-140	1.0	1.6	2.9	↓	0	0	generated
								as yet
IVA	110-120	0.4	0	0				
	120-130	0.7	0	0		0	0	
	130-140	0.7	1.1	1.1	B	0	0	
	140-150	0.7	5.3	6.4		0	0	
	150-160	0.8	29	35	↓	2.3	2.3	B
	160-170	1.6	240	275		18	20	↓
	170-180	1.6	900	1175	E	700	720	E
	180-190	4.4	> 10,000		900	1620		

* **B** = beginning and **E** = end of oil generation window.
• **B** = beginning and **E** = end of conversion of oil to gas.

7.3.26 Hydrocarbon Kitchen 3 : The Graben

Only the sub-Stage IVA sediments are mature here, having entered the hydrocarbon generation window around 5.6 Ma at 4480m (**Table 7.25, Figure 7.12**). The end of the oil window occurred 2.1 Ma ago at 5200m. 83% of the total gas generating capacity of the sub-Stage IVA sequence here have been realised at present.

Table 7.25 Arrhenius TTI values for oil and gas generation in the graben between Rusa Timur-1 and Belangkas using kerogen Type III and oil to gas kinetics.

Stage	Temp. Range (°C)	Exposure Time (Ma)	Type III TTI	Type III ΣTTI	Oil * Window	Oil to gas TTI	Oil to gas ΣTTI	Gas • Window
IVC	110-120	0.6	0	0				
IVB	110-120	0.7	0	0				

Table 7.25 Arrhenius TTI values for oil and gas generation in the graben between Rusa Timur-1 and Belangkas using kerogen Type III and oil to gas kinetics - continued.

Stage	Temp. Range (°C)	Exposure Time (Ma)	Type III TTI	Type III ΣTTI	Oil * Window	Oil to gas TTI	Oil to gas ΣTTI	Gas • Window
	120-130	1.7	0	0				
IVA	110-120	0.4	0	0				
	120-130	0.6	0	0		0	0	
	130-140	0.5	0	0		0	0	
	140-150	1.1	8	8	B	1.3	1.3	B
	150-160	1.0	36	44	↓	2.9	4.2	
	160-170	2.4	380	424		30	34	↓
	170-180	2.0	1250	1674	E	100	134	
	180-190	0.2	500	2174		40	174	

* **B** = beginning and **E** = end of oil generation window.
• **B** = beginning and **E** = end of conversion of oil to gas.

7.3.3 BasinMod Kinetic Modelling

Additional input data on the relative proportions of kerogen types and total organic carbon contents for each sub-Stage were included for BasinMod kinetic modelling. These data are available from visual organic matter typing and TOC determination performed earlier.

7.3.3a Well Results

Sediments in all the seven wells have not reached the hydrocarbon generation window according to the thermal modelling results from the BasinMod programme, which agrees with all other maturity indicators.

7.3.3b Hydrocarbon Kitchen 1 : Pritchard Syncline

Using a kerogen mix of 85% Type III and 15% Type IV, and TOC values of 1.5% for sub-Stage IVD, 1.0% for sub-Stage IVC, 1.5% for sub-Stage IVB and 2.5% for sub-Stage IVA, the main phase of oil generation in the Pritchard Syncline is presently between 4100m - 5100m (**Figure 7.13**), within the 120°C-130°C temperature range. The sub-Stage IVA sequence here have realised between 25% to 90% of its total hydrocarbon generating potential. About 50% of the sub-Stage IVB sediments are presently in the early maturation zone.

7.3.3c Hydrocarbon Kitchen 2 : Furious Syncline

Similar kerogen mix and TOC content values as the Pritchard Syncline are used for the sediments in the Furious Syncline. The kinetic modelling results show that the main oil generation phase here occurs between 4000m - 5100m, within the temperature range of 130°C-140°C (**Figure 7.14**). The lowermost part of the sub-Stage IVA sediments have

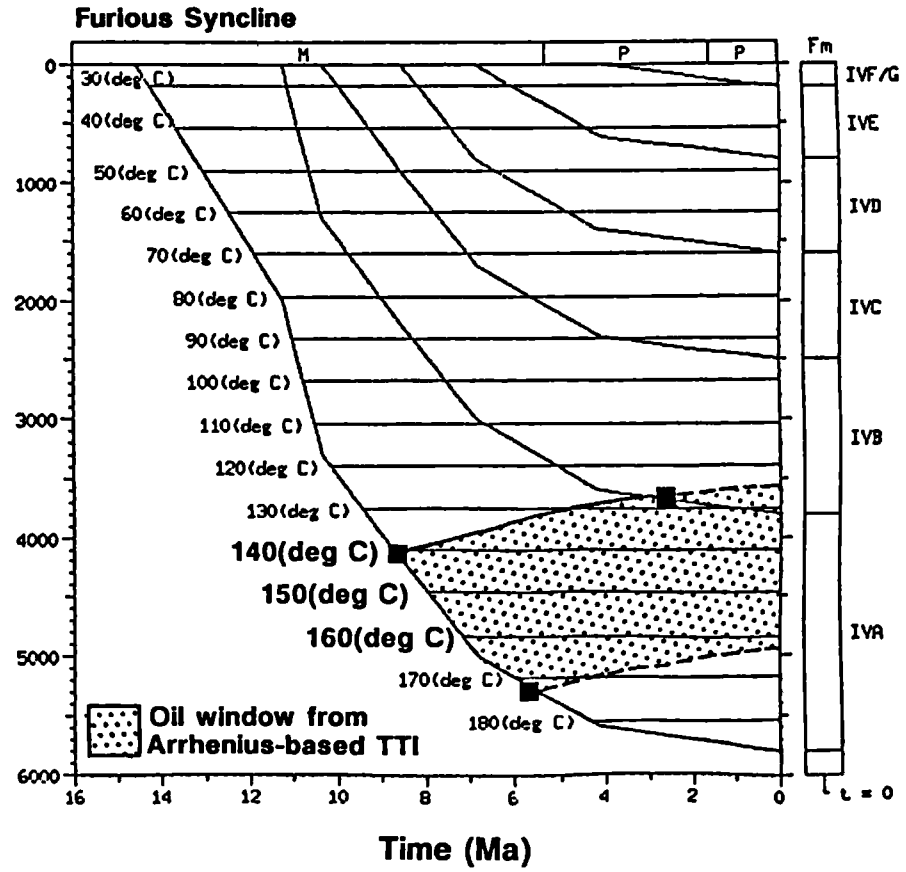


FIGURE 7.11 Hydrocarbon generation window in the Furious Syncline determined from the Arrhenius-based TTI method.

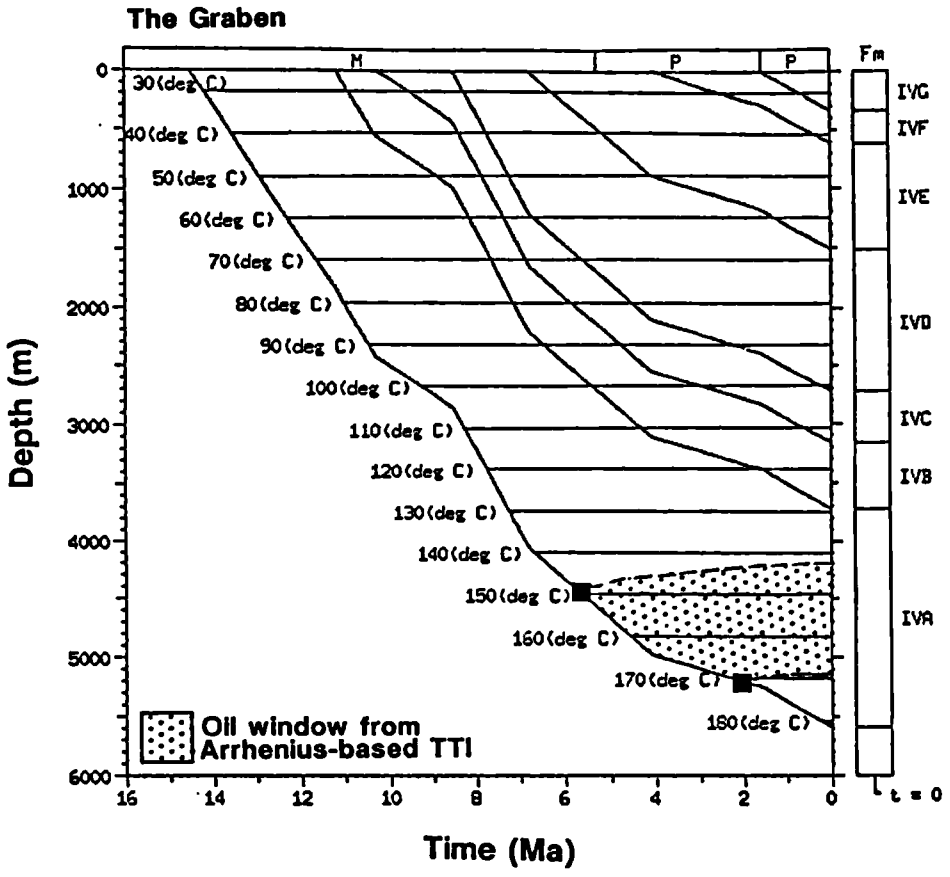


FIGURE 7.12 Hydrocarbon generation window in the graben located between Rusa Timur-1 and Belangkas area determined from the Arrhenius-based TTI method.

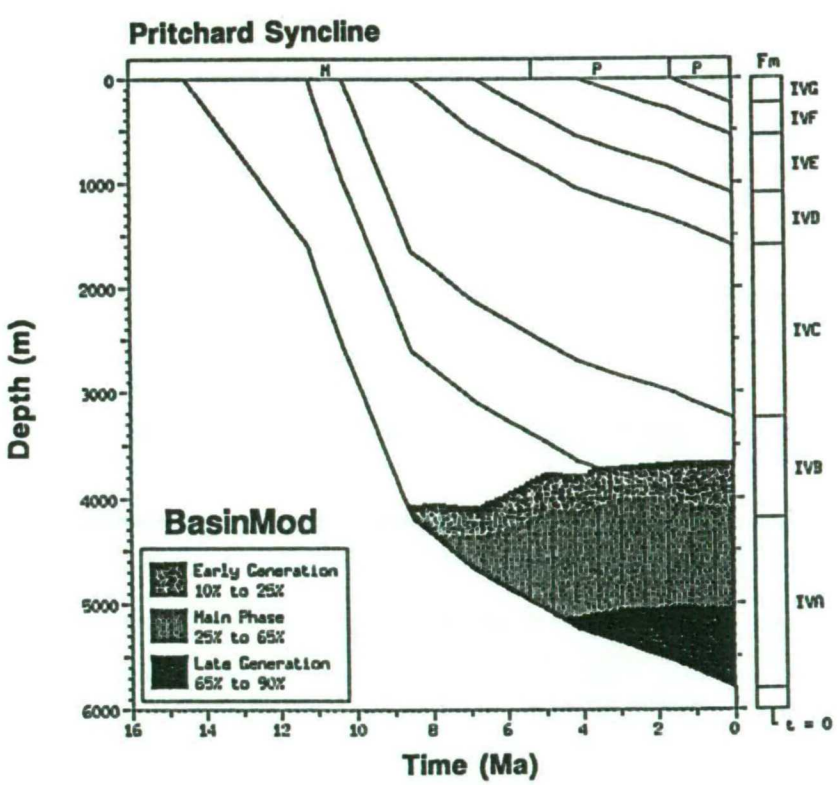


FIGURE 7.13 Hydrocarbon generation window in the Pritchard Syncline determined by BasinMod kinetic modelling.

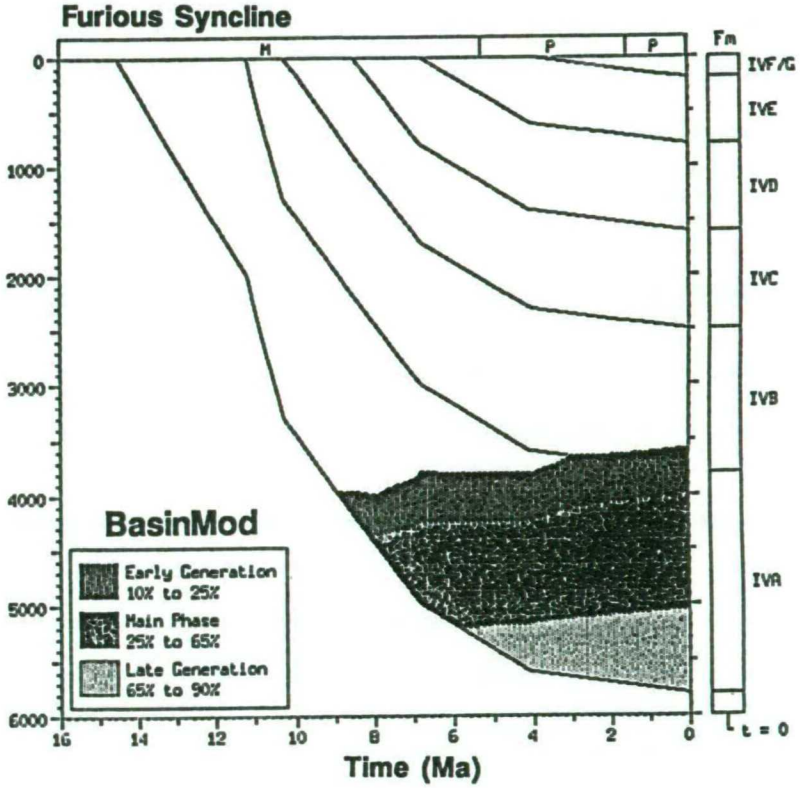


FIGURE 7.14 Hydrocarbon generation window in the Furious Syncline determined by BasinMod kinetic modelling.

almost depleted the hydrocarbon generating capacity with 65% to 90% hydrocarbons already produced. The topmost part of sub-Stage IVA are presently in the upper part of the oil generation window, along with part of the sub-Stage IVB sediments.

7.3.3d Hydrocarbon Kitchen 3 : The Graben

Sub-Stage IVA sediments span the whole of the hydrocarbon generation window which is located between 3750m - 5300m (**Figure 7.15**), beginning in the 130°C-140°C temperature range. The lowermost 10% of sub-Stage IVA sediments have entered the late generation stage with the remaining 90% are almost equally divided into the early and main hydrocarbon generation zones. Sub-Stage IVB sediments and younger sediments are presently immature.

7.4 Discussion

All the seven wells, drilled on anticlinal structures, have not penetrated any mature sediments. As a result, it is necessary to extrapolate the sediments in the wells to areas where they would have entered the necessary thermal zones to produce hydrocarbons. This was done by using the correlations made by Azim-Ibrahim (1994) of the sedimentary Stage boundaries into three hydrocarbon kitchens present in the area, which are the Pritchard and Furious Synclines, and The Graben. Sub-Stage IVA sequence, deemed to be the most likely source rock, has been subjected to the required temperatures in all three locations.

At present, some of the lower parts of the sequence are already in the overmature zone, or are producing gas, while the upper parts are still producing oil and gas. In the Pritchard Syncline (**Figure 7.10**), about 45% of the sub-Stage IVA sediments are presently overmature, with the remaining 55% in various stages of hydrocarbon generation, from early to end. About 50% of sub-Stage IVB have entered the early oil generation zone. These conditions are very similar in the Furious Syncline (**Figure 7.11**) where the only difference is that, due to a much thicker sub-Stage IVA sequence, only 10% of the sub-Stage IVB have entered the oil window. In the Graben, the hydrocarbon generation window is indicated to span within the sub-Stage IVA sediments alone (**Figure 7.12**). About 20% of the sub-Stage IVA sequence are presently overmature and another 25% still immature.

For Sabah Basin, the simple Lopatin method gives comparable results, and thus similar conclusions, to the more sophisticated BasinMod programme and the more scientifically-sound Arrhenius-based TTI method (**Figures 7.16, 7.17** and **7.18**). It is therefore recommended that the Arrhenius-based TTI graphs of Hunt & Hennet (1992) be used, if one cannot get access to a basin modelling package because of its simple and straightforward application which is in the same manner as calculating Lopatin's TTI values. Workers familiar with the Lopatin method will not face any difficulties in adapting the TTI graphs, and the sound basis for the construction of the graphs, where

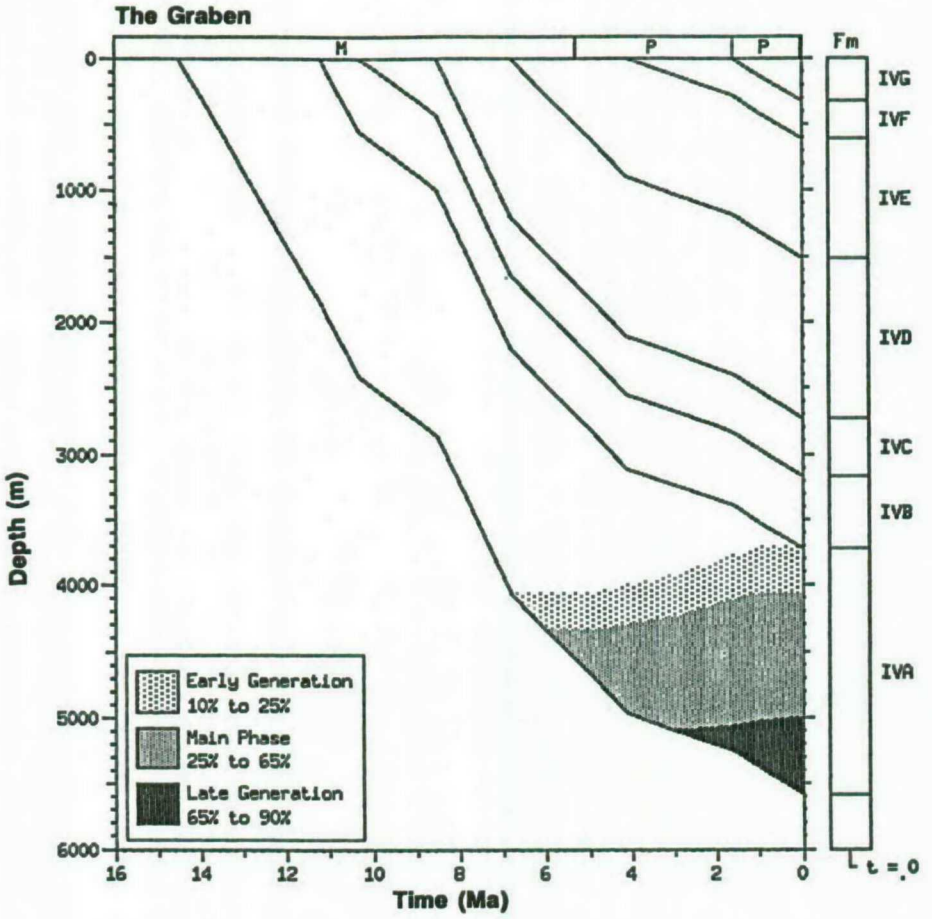


FIGURE 7.15 Hydrocarbon generation window in The Graben determined by BasinMod kinetic modelling.

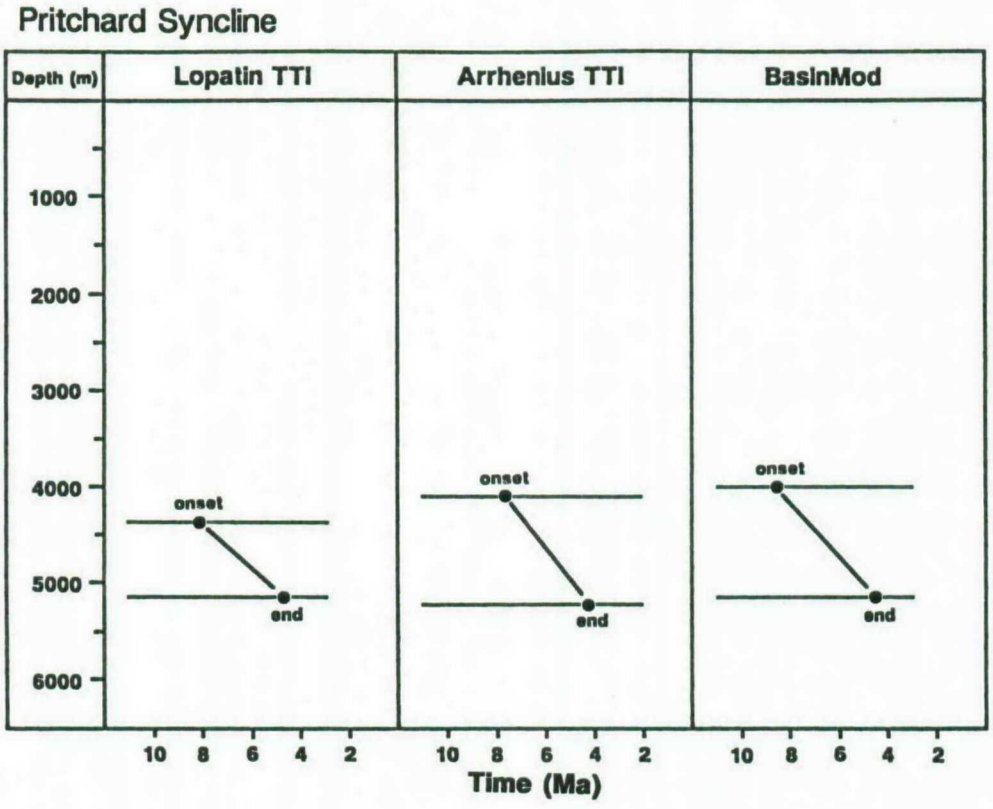


FIGURE 7.16 Comparisons between the location of the oil window in the Pritchard Syncline determined by the different methods used.

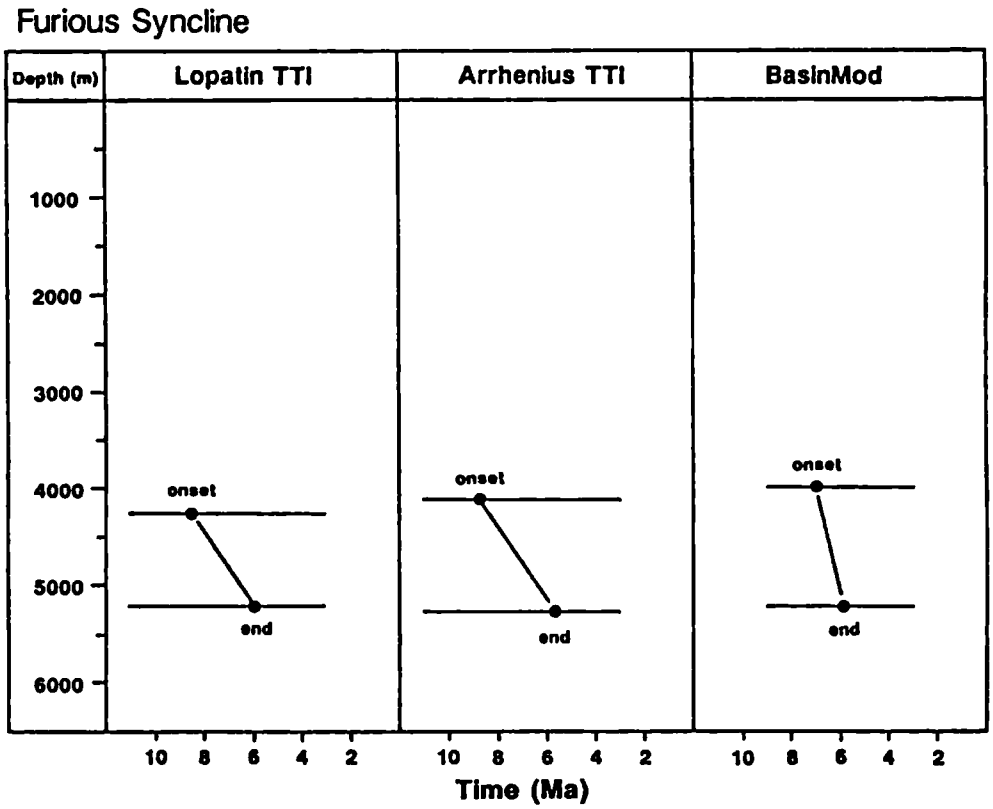


FIGURE 7.17 Comparisons between the location of the oil window in the Furious Syncline determined by the different methods used.

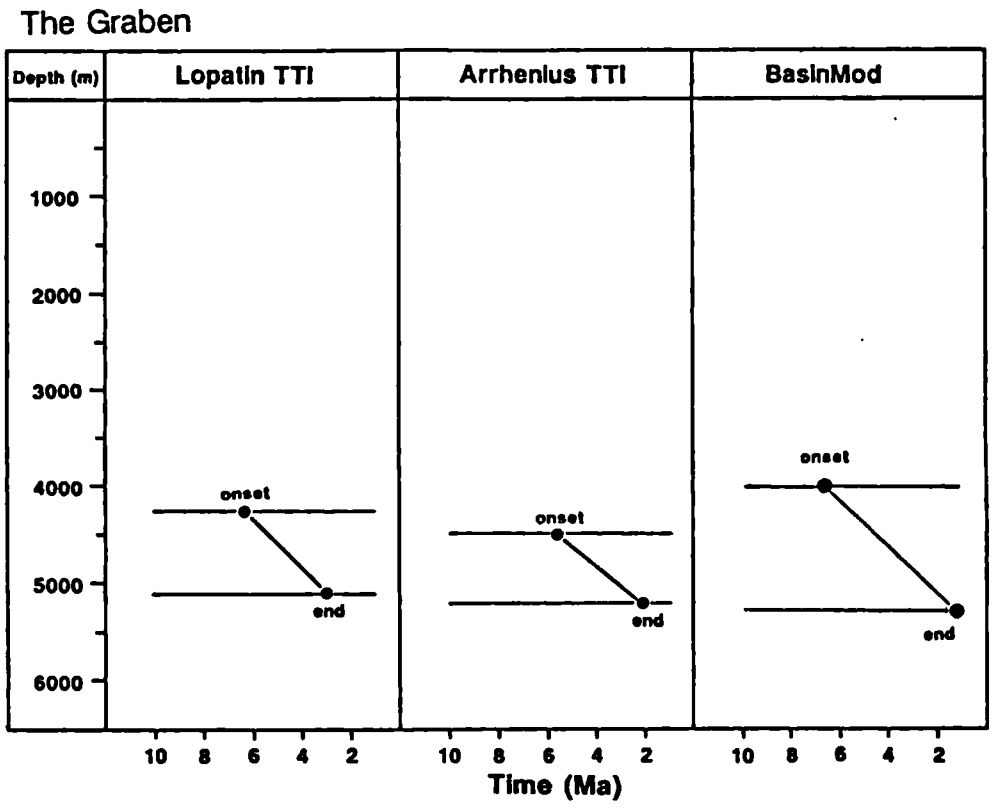


FIGURE 7.18 Comparisons between the location of the oil window in The Graben determined by the different methods used.

the various kinetic parameters for the different kerogen types were taken into account, will eliminate any of the uncertainties and problems faced by Lopatin's TTI method.

Timing of hydrocarbon generation determined from the three methods, despite generally agreeing with each other, do not concur with vitrinite reflectance values which indicated the oil generation window to begin between 2000-2500m depth. This is much shallower than depths indicated by modelling. The two implications from this discrepancy are either the vitrinite reflectance measurements were made on a population of recycled vitrinites, or that there are inherent shortcomings in the modelling methods. Here, results from the Arrhenius-based TTI method are taken as the most reliable. Furthermore, the vitrinite reflectance measurements were made on isolated kerogens, not on rock samples. In order to obtain reflectance measurements on *in situ* vitrinites, it is thus necessary to attempt mounting rock samples cut parallel to bedding in resin. As mentioned previously, the friability of the rocks made this very difficult to do. However, fresh effort in finding better quality samples has to be done to obtain representative vitrinite reflectance values.

Wood's (1988) TTI_{ARR} values were calculated based on kinetic parameters simulating vitrinite reflectance data with Ea = 218kJ/mol and A = 5.45 $x10^{26}$/my, while Hunt & Hennet (1992) used Type III kerogen sample from the Tent Island Formation, Canada which had similar kinetic parameters as the coals and coaly shales of the Mahakam Delta, Indonesia (Ea = 230kJ/mol, A = 3.98 x 10^{27}/my). It may seem that there exists some variations in the kinetic parameters within the Type III kerogen group. However, it is believed that these variations are not as important as those for the Type II kerogen group (Hunt *et. al.*, 1991; Hunt & Hennet, 1992) because the results from Wood (1988) based on vitrinites, and those from Hunt & Hennet (1992), based on a Mahakam Delta Type III equivalent (rich in cuticles/cutinites) are comparable. Similar conclusions are derived from both workers using what can be classified as the two 'end members' of the Type III kerogen : woody/vitrinite-rich and cutinite-rich. Refinement, or the further division, of the Type III kerogen according to different kinetic parameters will not be particularly useful for modelling purposes but will be purely of academical interest.

7.5 Summary

For marginal and poor source rocks, such as those in the Sabah Basin, rapid maturation is considered to be an important factor contributing to commercial oil accumulations. Once deposited, it is imperative that the organic matter be removed from the oxidation zone as quickly as possible to preserve whatever little hydrocarbon generating potential they possess. This requirement is fulfilled in the Sabah Basin where rapid tectonic subsidence, coupled with high sedimentation rates commonly exceeding 200m/Ma (Azim-Ibrahim, 1994), enabled the quick removal of the Type III organic matter from

shallow depths. This resulted in a fairly rapid passage of the strata past the oxidation zone and through the oil window, generating most of the hydrocarbons in a short time.

In the Pritchard Syncline, the oil window occurs between 4000m-5230m for the sub-Stage IVA sediments and corresponds to a time duration of 4.4 Ma (**Table 7.26(a)**). In the Furious Syncline, the oil window is located between 4100m-5250m, corresponding to a time duration of 3.0 Ma (**Table 7.26(b)**), while in the Graben, the oil window occurs between 4480m-5200m, corresponding to a time duration of 3.5 Ma (**Table 7.26(c)**). This is one of the possible reasons why the marginal/poor source rocks in the Sabah Basin has been successful, where the fast 'cooking' of the organic matter had generated enough hydrocarbons to instigate their expulsion. The greater the quantity of hydrocarbons available for migration at a particular time, the greater the likelihood of migration and formation of commercial accumulations. The intimate arrangement of numerous interbedded sandstones with the deltaic-lower coastal plain carbonaceous shales of sub-Stage IVA promoted efficient expulsion. For the three locations selected in the hydrocarbon kitchens, the onset of hydrocarbon generation determined by the three methods differed by less than 1 Ma (**Table 7.27**).

Table 7.26 Summary of thermal modelling results from Lopatin TTI, Arrhenius-based TTI and BasinMod kinetic modelling for a) the Pritchard Syncline, b) the Furious Syncline and c) the graben.

a) Pritchard Syncline

Stage	Oil Window	Methods: Lopatin Temp. Range	Lopatin Depth (m)	Lopatin Time (Ma)	Arrhenius Temp. Range	Arrhenius Depth (m)	Arrhenius Time (Ma)	BasinMod Temp. Range	BasinMod Depth (m)	BasinMod Time (Ma)
IVB	Onset	130-140	3800	2.8	130-140	3750	3.3	120-130	3700	3.9
	End	-	-	-	-	-	-	-	-	-
IVA	Onset	140-150	4380	8.0	130-140	4000	8.6	130-140	4000	8.6
	End	160-170	5150	4.6	170-180	5230	4.2	160-170	5150	4.6

b) Furious Syncline

Stage	Oil Window	Methods: Lopatin Temp. Range	Lopatin Depth (m)	Lopatin Time (Ma)	Arrhenius Temp. Range	Arrhenius Depth (m)	Arrhenius Time (Ma)	BasinMod Temp. Range	BasinMod Depth (m)	BasinMod Time (Ma)
IVB	Onset	120-130	3700	2.6	120-130	3700	2.6	120-130	3650	3.1
	End	-	-	-	-	-	-	-	-	-

b) Furious Syncline - continued

Stage	Oil Window	Methods: Lopatin Temp. Range	Lopatin Depth (m)	Lopatin Time (Ma)	Arrhenius Temp. Range	Arrhenius Depth (m)	Arrhenius Time (Ma)	BasinMod Temp. Range	BasinMod Depth (m)	BasinMod Time (Ma)
IVA	Onset	140-150	4250	8.4	130-140	4100	8.7	130-140	3970	9.0
	End	170-180	5200	5.9	170-180	5250	5.7	170-180	5200	5.9

c) The Graben

Stage	Oil Window	Methods: Lopatin Temp. Range	Lopatin Depth (m)	Lopatin Time (Ma)	Arrhenius Temp. Range	Arrhenius Depth (m)	Arrhenius Time (Ma)	BasinMod Temp. Range	BasinMod Depth (m)	BasinMod Time (Ma)
IVA	Onset	140-150	4250	6.3	140-150	4480	5.6	130-140	4100	6.0
	End	160-170	5100	3.0	170-180	5200	2.1	170-180	5300	1.4

Table 7.27 Timing of hydrocarbon generation in the three kitchen areas determined from TTI_{LOP}, TTI_{ARR} and BasinMod.

Kitchen area	Method	Begin time for hydrocarbon generation (Ma)	
Pritchard Syncline	TTI_{LOP}	8.0	
	TTI_{ARR}	8.6	Largest difference :
	BasinMod	8.6	0.6 Ma
Furious Syncline	TTI_{LOP}	8.4	
	TTI_{ARR}	8.7	Largest difference :
	BasinMod	9.0	0.6 Ma
Graben	TTI_{LOP}	6.3	
	TTI_{ARR}	5.6	Largest difference :
	BasinMod	6.0	0.7 Ma

In general, hydrocarbon generation generally begun around 8 - 9 Ma in the Pritchard and Furious Synclines, and around 6 Ma in the Graben. Hydrocarbon generation from the lower parts of sub-Stage IVA sediments ceased around 4 - 6 Ma in the Synclines and around 1 -3 Ma in the Graben.

CHAPTER EIGHT

ORGANIC MATTER DEPOSITION AND PRESERVATION

8.1 Introduction

This chapter discusses the deposition and preservation mechanisms of the Sabah Basin source rocks. It includes outlining the palaeoclimate and palaeodepositional environments thought to prevail during the Middle-Late Miocene times based upon present day observations. Arguments on the importance of anoxia for the preservation of organic-rich beds are taken into account when analysing the possible conditions responsible for the preservation of the Sabah Basin source rocks. The variations of organic matter type and abundance in different palaeoenvironments are also discussed. Finally, simple source rock distribution maps are derived based on the palaeoenvironments.

8.2 Climate and vegetation

The present day climate in the NW Borneo region is a uniformly wet, hot and very humid tropical climate. Temperatures range between 70°F to 90°F with high humidity, up to 97% in the early morning (Grant, 1984). Most of the region is covered with primary equatorial rain forest with peat swamp forests on the coastal alluvium. Much of the coast and tidal rivers are lined by extensive mangrove belts and *nypa-palm* forests. Palaeobotanists and palynologists working in the tropical Cainozoic believe that there has not been any major changes of floras at the generic level during the Neogene in the lower latitudes (Traverse, 1988; Williams *et. al.*, 1985; Leopold, 1969). As a result,

" not only do we have in the spores/pollen flora evidence of plants referable to modern genera, but in a broad way, it is reasonable to draw palaeo-ecological conclusions from them "

Traverse, 1988

Therefore, in this study, the present day climate, vegetation and depositional environments are used as a model during the Neogene period in the Sabah Basin.

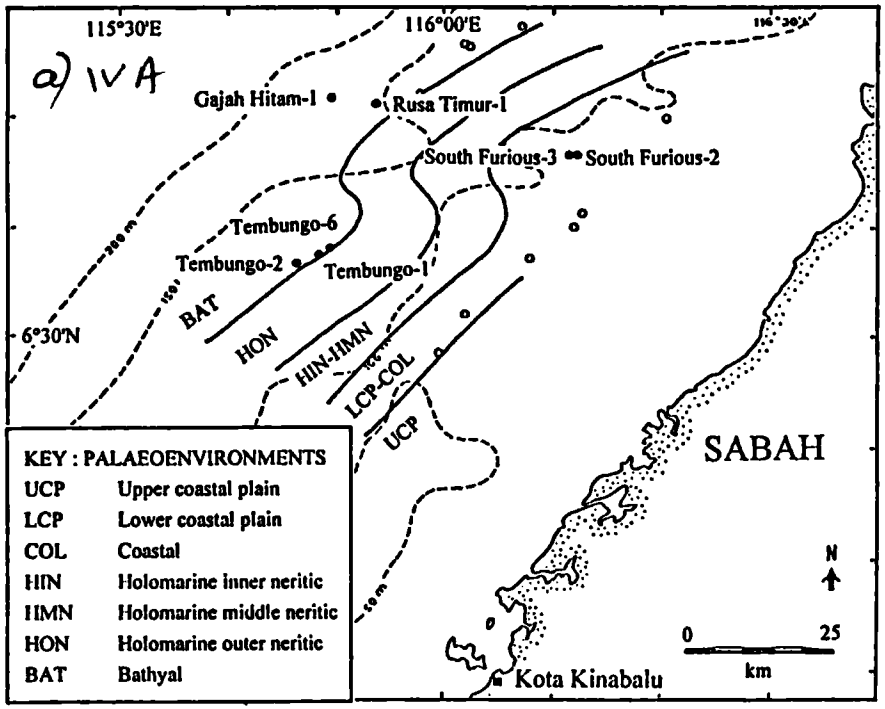
8.3 Neogene sedimentation

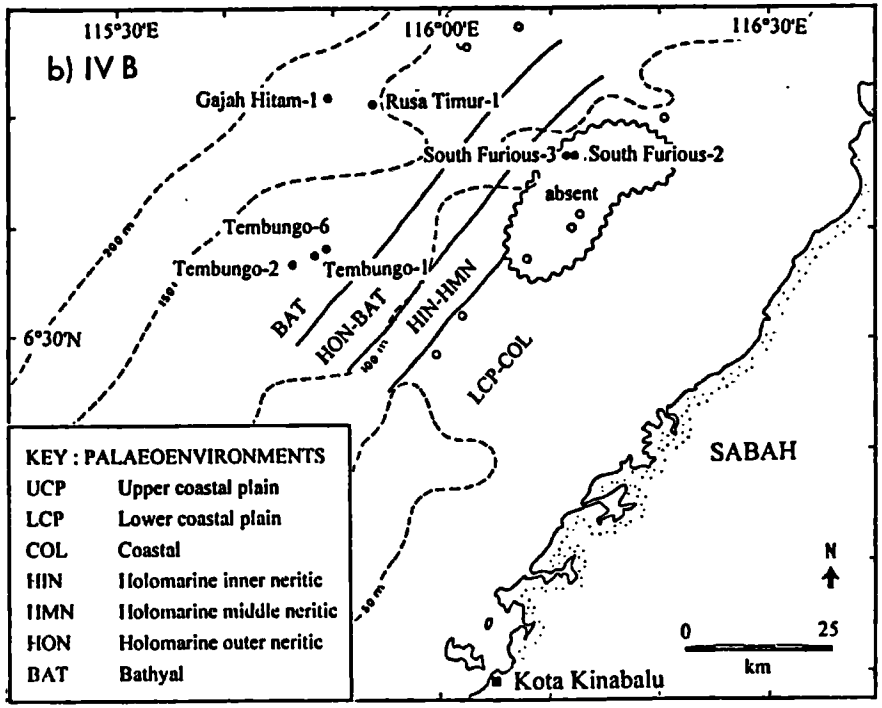
During the Neogene, sedimentation in the Sabah Basin occurred within a range of depositional environments, ranging from coastal plain on the landward margin of the basin to deep marine towards the South China Sea. A schematic illustration of the main depositional environments was shown in **Figure 2.12.** This model is based on the modern day setting and their identification in ancient sequences can be done according to palynological and palaeontological zonations (Ho, 1978).

Deposition of sub-Stage IVA sediments began following the uplift of the Crocker Accretionary Prism, which also brought about a relative sea-level drop. Large amounts of sediments were eroded and transported from the SE to the NW, and deposited in the basin. Depositional environments throughout the sub-Stage IVA time were largely alluvial to deep marine environments present further into the basin **(Figure 8.1).** According to previous well log interpretations of Shell, the sub-Stage IVB sediments are generally absent along the Bunbury - St. Joseph High. In the South Furious area, they are present as deep marine sediments. However, a recent well drilled by British Gas in the Bunbury-St. Joseph High area penetrated lower coastal plain sediments in sub-Stage IVB (Cocksedge & Carr, pers. comm.).

Re-interpretation of stage boundaries for several wells along the Bunbury-St. Joseph High by Azim-Ibrahim (1994) indicated that some of the previously identified sub-Stage IVA sequence actually included the sub-Stage IVB sequence. The boundary between sub-Stages IVA and IVB was not identified before probably because of the similar lithology of the two stages. Therefore, during the sub-Stage IVB time, lower coastal plain sediments were deposited in the proximal areas with deep marine sediments deposited further offshore **(Figure 8.1).** Both the sedimentation and tectonic subsidence rates were high during most of the sub-Stage IVA and sub-Stage IVB times, 500-1000m/my and 300-500m/my, respectively , leading to the accumulation of an immensely thick (> 2000m) sedimentary sequence.

The Bunbury-St. Joseph High began to form during the deposition of the sub-Stage IVB sediments (Levell; 1987, Johnson *et. al.*, 1989). Persisting unstable shelf conditions led to the feeding of coastal - coastal plain sands and shales into the deeper parts of the basin via shelf slumpings. Slump scar occurrences have been documented by Levell & Kasumajaya (1985). Shallow marine/storm dominated settings during the sub-Stage IVC time was prevalent in the inner parts of the basin (Johnson *et. al.*, 1989). Active slumping continues to be a source of sediments to the deeper parts of the basin. These sediment flows resulted in the creation of both basin-slope and basin-floor turbidites in deep marine environments. This type of deposition prevailed to the sub-Stage IVD time **(Figure 8.1).** Both the tectonic subsidence and sedimentation rates slowed down relative to the previous stages during the sedimentation at the end of sub-Stage IVC (Azim-Ibrahim, 1994).





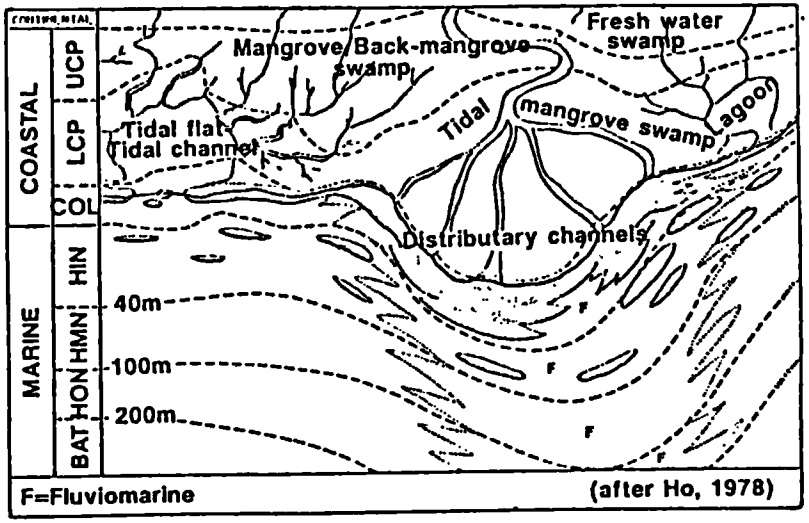
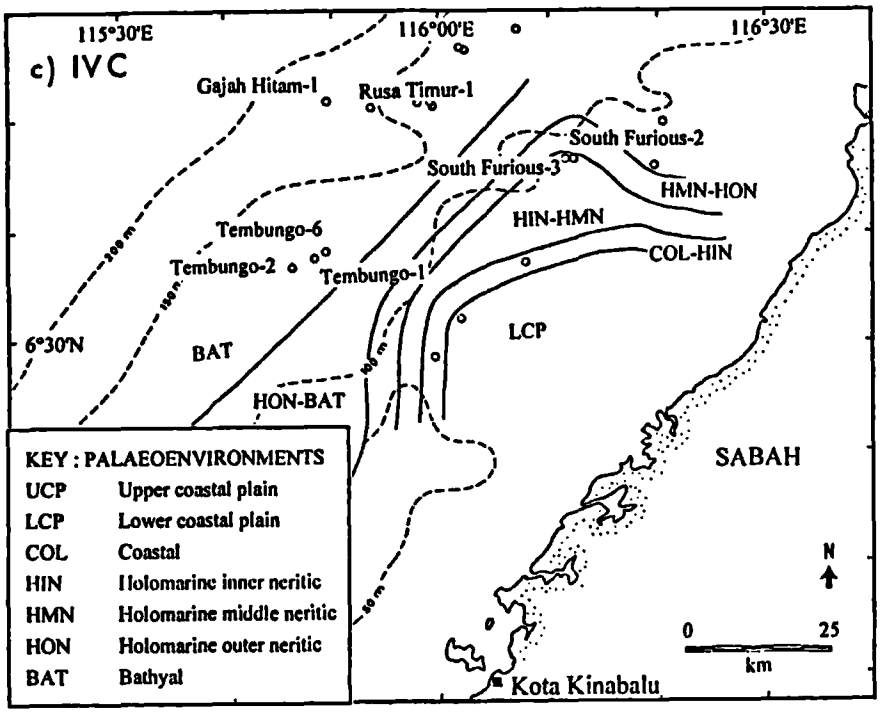
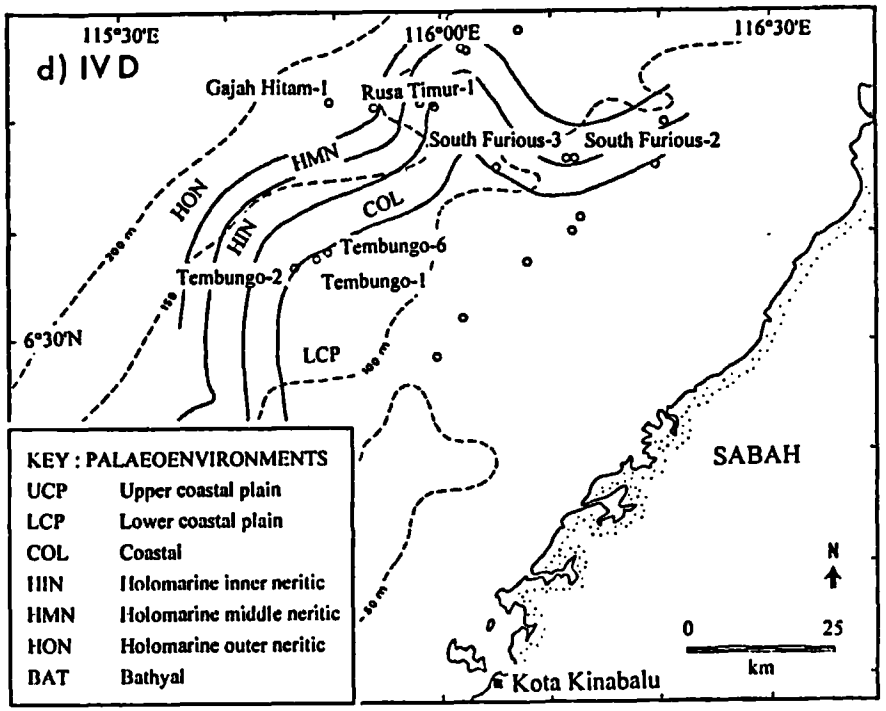


FIGURE 8.1 Palaeoenvironmental changes throughout the deposition of the Middle to Upper Miocene sediments in Sabah Basin, (a) IVA, (b) IVB, (c) IVC and (d) IVD. The palaeoenvironments shown are for the top of each sedimentary Stage, and the palaeoenvironmental interpretations were based upon PETRONAS in-house biostratigraphic reports.





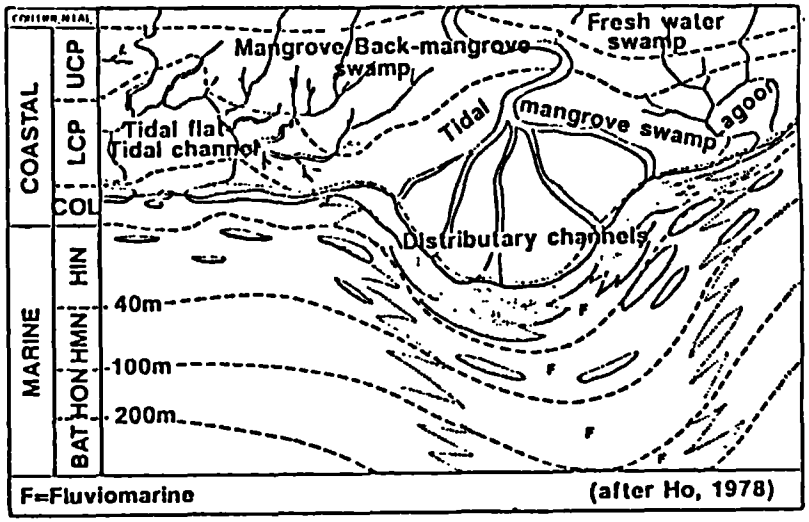


FIGURE 8.1 Continued.

8.4 Organic matter production and preservation

8.4.1 Organic Matter Production In Sabah Basin

Stable climatic conditions prevailing throughout the Neogene (Traverse, 1988; Williams *et. al.*, 1985; Leopold, 1969) allows the interpolation of hot, humid and ever wet tropical climate with high primary terrigenous productivity, similar to the present day, during the deposition of the Middle to Upper Miocene sequences. Based on present day vegetation, the type of organic matter available and fed in the basin would have been dominated by mangrove and *nypa-palm* products (Potter *et. al.*, 1984), as well as those brought in by rivers draining the hinterland regions. The present day marine surface productivity in the region is estimated by Berger *et. al.* (1989) to range between 60 - 90 $gC\ m^{-2}\ yr^{-1}$.

8.4.2 Organic Matter Preservation Conditions In General

There are presently two schools of thought concerning the conditions necessary for the preservation of organic matter. Numerous workers such as Demaison & Moore (1980), Demaison *et. al.* (1984), Emerson & Hedges (1988), Canfield (1989) and Paropkari *et. al.* (1993) support the idea of oxygen as the dominant oxidant and that depleted oxygen contents (anoxia) are essential for organic matter preservation. On the other hand, there are also workers who have found evidence that water column anoxia is not essential for the preservation of organic matter (Pedersen & Calvert, 1990) as indicated by the non-enhancement of organic carbon accumulation in oxygen-deficient conditions in the Black Sea (Calvert *et. al.*, 1991), the Oman margin (Pedersen *et. al.*, 1992) and the Gulf of California (Calvert *et. al.*, 1992). Sediment accumulation rate (Ibach, 1982; Kuehl *et. al.*, 1993) and hydrodynamic factors such as winnowing and associated reworking (Pedersen *et. al.*, 1992) have been linked with the success or failure of organic matter preservation.

In the Sabah Basin, deposition of terrigenous organic matter mostly occur in oxic lower coastal plain or deltaic environments, as well as marine environments. Present day South China Sea has basically open ocean conditions, with well mixed, cold bottom waters (**Figure 8.2**). It is well oxygenated due to replenishment by the Western North Pacific Intermediate Water (Linsley *et. al.*, 1985). The early diagenetic degradation process subjected to dead organic matter involves organic matter oxidation occurring in the sequence of decreasing free-energy yield, i.e. **1.** Anaerobic oxidation > **2.** Denitrification ≥ **3.** Iodate reduction > **4.** Manganese oxide reduction > **5.** Ferric oxide reduction > **6.** Sulphate reduction > **7.** Methanogenesis/fermentation :

$$CH_2O + O_2 \rightarrow CO_2 + H_2O \quad (1)$$

$$5CH_2O + 4NO_3^- \rightarrow 2N_2 + 4HCO_3^- + CO_2 + 6H_2O \quad (2)$$

$$3CH_2O + 2IO_3^- \rightarrow 2I^- + 3CO_2 + 3H_2O \quad (3)$$

$$CH_2O + 3CO_2 + H_2O + 2MnO_2 \rightarrow 2Mn^{2+} + 4HCO_3^- \quad (4)$$

$$CH_2O + 7CO_2 + 4Fe(OH)_3 \rightarrow 4Fe^{2+} + 8HCO_3^- + 3H_2O \quad (5)$$

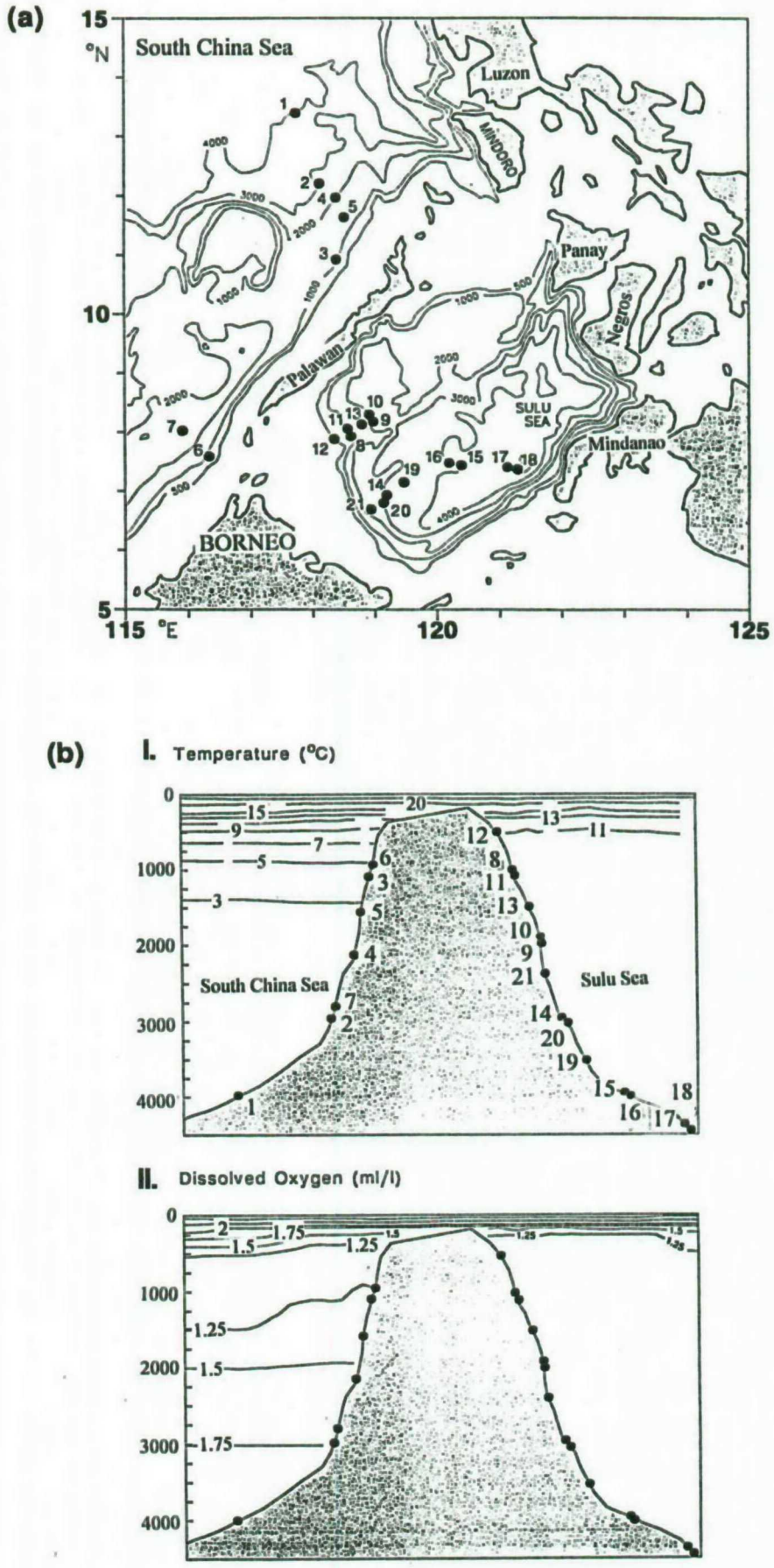


FIGURE 8. 2 (a) Bathymetric chart of Kuehl et al's (1993) study area. Of interest here are the sample locations of box cores No. 6 and No. 7 whose results will have some significance for the Sabah Basin. (b) Temperature and dissolved oxygen distributions across the Palawan sill with depth distribution of the box cores. (From Kuehl et al, 1993).

$$2CH_2O + SO_4^{2-} \rightarrow H_2S + HCO_3^- \quad (6)$$

$$2CH_2O \rightarrow CH_4 + CO_2 \quad (7)$$

Elderfield (1985).

These processes generally proceed in the following sequence with increasing depths (**Figure 8.3**). They show that the oxidation of organic matter does not stop with the depletion of oxygen. In the absence of oxygen, oxidation continues using different electron acceptors (oxidants) such as the nitrates and sulphates. Fermentation (methanogenesis) continues to degrade the organic matter when all the oxidants are consumed, but this process is very slow (Berner, 1980; Pedersen & Calvert, 1990). A common assumption is that organic matter degrades much faster in oxic compared to anoxic conditions. However, as pointed out by Pedersen & Calvert (1990), evidence for it is scanty. Studies by Lee (1992), Henrichs & Reeburgh (1987), Henrichs & Farrington (1987), Westrich & Berner (1984) and Otsuki & Hanya (1972a, 1972b) provided evidence for the lack of difference in the organic carbon decomposition rates in oxic and anoxic waters, thus negating the theory that anoxic decomposition is inherently slower than oxic decomposition. Anaerobic organisms as well as aerobic organism are just as important for organic matter degradation. The main difference between the two is that anaerobes are less effective at breaking down complex organic molecules, thus resulting in a relatively smaller degree of degradation (Pedersen & Calvert, 1990). The lack of a major difference in the decomposition rates between anoxic and oxic conditions necessitates further alternative explanations for the controls on organic carbon preservation.

Several possibilities have been documented; for example, Demaison & Moore (1980) and Suess (1980) indicated that the transit distance of the organic matter to the sea bed can adversely affect its preservation where longer residence time in the water column will increase exposure to oxidative processes; Pedersen & Calvert (1990) emphasised on the importance of high primary productivity; Lee (1992) proposed that the differences in the numbers and diversity of organisms grazing upon bacteria between oxic and anoxic sediments may explain part of the difference in organic carbon preservation rates; and Kuehl *et. al.* (1993) concluded that sedimentation rates are important.

8.4.3 Organic Matter Preservation In Sabah Basin

It is perceived that the success of source rock preservation in Sabah Basin is mainly the result of a balanced interplay between high sediment accumulation rates and concomitant high terrigenous organic matter input from the lush vegetation of the warm and ever wet tropical conditions. High sedimentation rates have been reported to result in enhanced preservation of deposited organic matter (Muller & Suess, 1979; Henrichs & Reeburgh, 1987; Berner, 1989; Canfield, 1989; Ingall & van Capellen, 1990; Calvert *et. al.*, 1991).

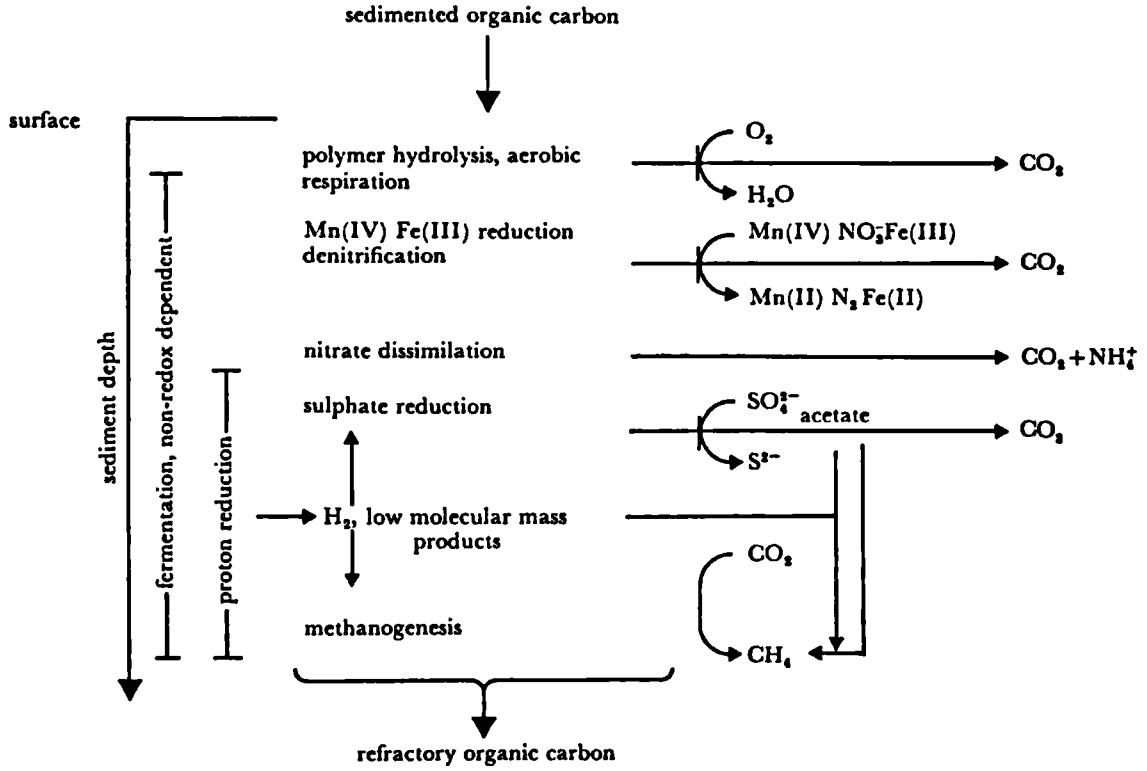


FIGURE 8.3 Depth distribution and interactions of decomposition processes in buried sediments. (From Jones, 1985).

In Sabah Basin, the rapid sedimentation that occurred between 10 - 15 Ma (**Figure 8.4**) played a major role in the preservation process by quickly removing deposited organic matter away from the oxic conditions of the water and sediments. This limits the extent of degradation experienced by the organic matter, which is especially important when the organic matter being deposited is comparatively the least oil prone (Type III) compared to other types of organic matter (Types I and II). The hydrogen-rich parts contributed by waxes derived from exinites, suberinite and resins constitute only a small percentage of the total volume of deposited organic matter transported. Rapid burial is therefore critical for their preservation. These lipid-rich plant counterparts are most likely to have been contributed by the mangrove belts along the coast and tidal rivers; the waxes and cuticles of mangroves have recently been found to be inherently very resistant to degradation (Frewin *et. al.*, 1993).

Another factor that helps promote the preservation of organic matter in these generally oxic conditions is the presence of tannin in the waters of the mangrove and back-mangrove swamps, and in lagoonal areas (**Figure 2.12**). Tannin is a natural aromatic substance widely distributed in higher plants and they appear to play a role in the healing process of plants and the lignification of the cell walls (Hunt, 1979). When parts of dead tree trunks, leaves and branches are immersed in these waters, the tannin is dissolved and acts as a bactericide creating bacteria-free water columns (Tissot & Welte, 1984) that effectively impede any ensuing degradation of deposited organic matter by bacteria.

It is equally important for the amount of organic carbon preserved to be adequate to avoid the dilution effect (Ibach, 1982) and make the deposition of a source rock possible. In the Sabah Basin, the quantity of organic matter preserved within the sediments generally satisfy the requirements for organic carbon concentration to merit further investigation. The drawback is that the preserved organic matter are of poor to marginal quality, based on the present classification schemes for Hydrogen Index and hydrocarbon Generating Potential from Rock-Eval pyrolysis (see **Chapter 5**). The rapid rate of sedimentation is finely balanced between diluting the organic matter concentration too much to render them useless as hydrocarbon sources, and aiding the preservation of the terrigenous organic matter by removing them quickly from the oxidation zone. The part played by the high primary organic productivity in this tropical region is considerable to counterbalance dilution effects.

Therefore, both productivity and rapid sedimentation are equally important during the deposition of the Sabah Basin source rocks. The poor to marginal source rock quality is compensated by its thickness, i.e. quantity versus quality, which is further aided in its success as a source rock by the presence of numerous intercalated sandstones acting as permeable conduits for the generated hydrocarbons.

High primary terrigenous productivity inevitably results in the deposition of large amounts of Type III organic matter. Their degradation utilises the oxidants and creates

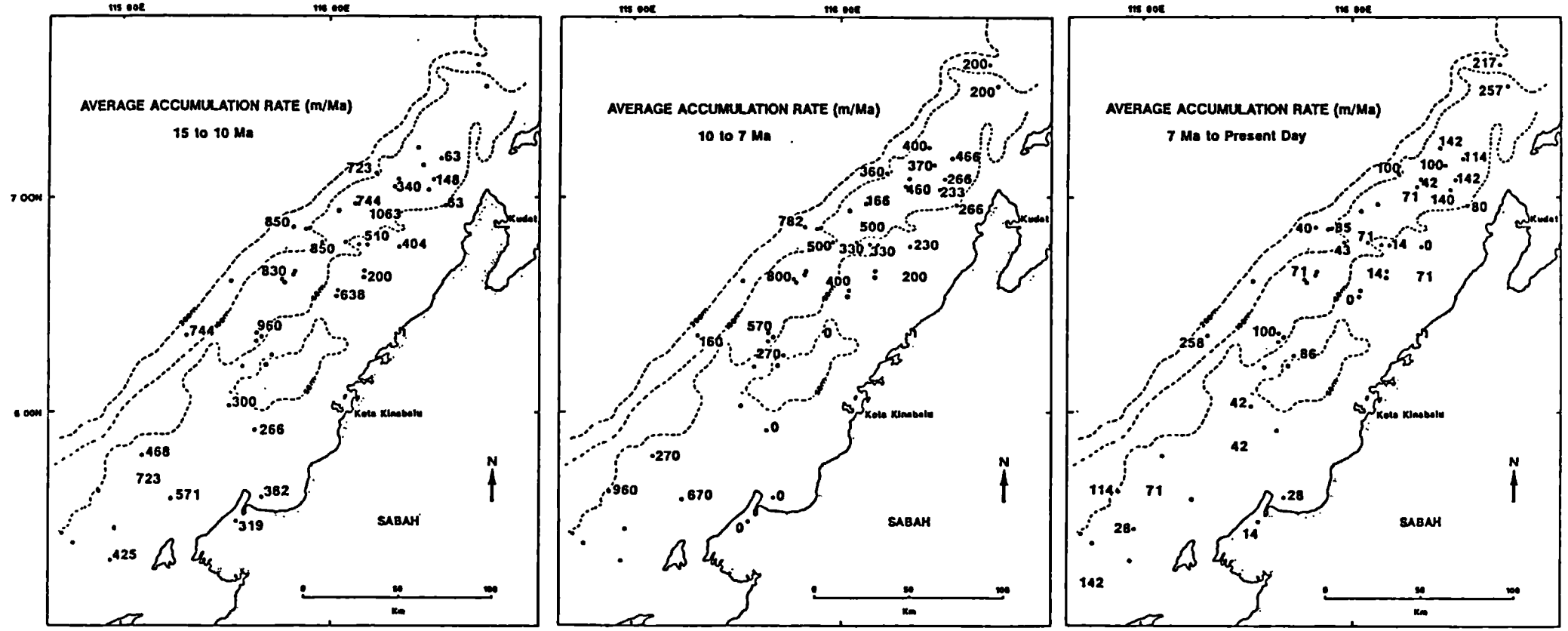


FIGURE 8.4 Average sediment accumulation rates in Sabah Basin throughout the Neogene (Azim-Ibrahim, 1994).

local zones of anoxia. Even though the rate of oxidation in the anoxic conditions may not be any different from oxic conditions (Lee, 1992), the degradation process is less efficient in anoxic compared to oxic conditions (Pedersen & Calvert, 1990). Furthermore, grazing by organisms is relatively more inefficient at high production rates, allowing more organic carbon to have the opportunity to be preserved. However, in the study area, it is believed that the role of anoxia in source rock preservation is of secondary importance compared to primary productivity and sediment accumulation rate. In oxic depositional environments such as the Sabah Basin, it is essential that the organic matter is rapidly removed from the zone of oxidation to avoid quality degradation. This requirement is fulfilled by the high sedimentation rate occurring between 10-15 Ma.

It is also essential that the organic matter productivity is high so as to avoid being diluted. Being in a tropical setting, this requirement is also satisfied. The nature of organic matter input, i.e., lipid-rich mangrove waxes and cuticles, also contribute to their preservability by being more resistant to degradation (Frewin *et. al.*, 1993). Lee (1992) and Harvey *et. al.* (1986) have reported that the rates of organic matter decomposition can depend on their compositions. Therefore, in areas with high productivity and high sedimentation rates such as the Sabah Basin, anoxic conditions are relatively less important for the deposition and preservation of organic-rich sediments. It is the high burial rate paralleled by high organic matter input that resulted in the successful preservation of source rock quality sediments here. Anoxia will be most important for source rock preservation in areas with low organic matter productivity and low sedimentation rates.

Results from this study indicate that the organic matter preserved in the sediments are mainly derived from higher land plants, with marine organic matter input being insignificant even in the marine sediments. This leads to the question why marine organic matter was not preserved in the sediments as was the land derived organic matter. Based on the study of Kuehl *et. al.* (1993), only between 0.06% - 0.17% of the actual amounts of marine organic carbon presently end up being preserved. Comparing the percentages of preserved marine organic carbon of the South China Sea with the Sulu Sea, marine productivity levels being similar, Kuehl *et. al.* (1993) concluded that the relatively lower preservation of organic carbon in the present day South China Sea is due to its lower sediment accumulation rate (27 - 30m/my) compared to the Sulu Sea (50 - 123m/my) (**Figure 8.5**). He also observed that organic carbon concentrations generally decrease with increasing water depth. Assuming uniform productivity, the observed depth dependent decrease results at least partly from oxidation and/or biological consumption, related to residence time in the oxic water column.

With the constant climatic conditions throughout the Neogene, the marine surface primary productivity is assumed to be similar to the present day. The only difference between the present day and the Neogene depositional systems is that the sediment

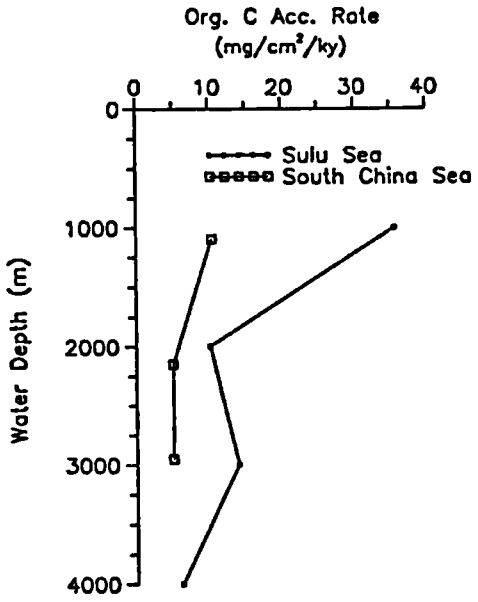


FIGURE 8.5 Organic carbon accumulation rates are higher by 2-3 times in the Sulu Sea compared to the South China Sea (From Kuehl et al, 1993).

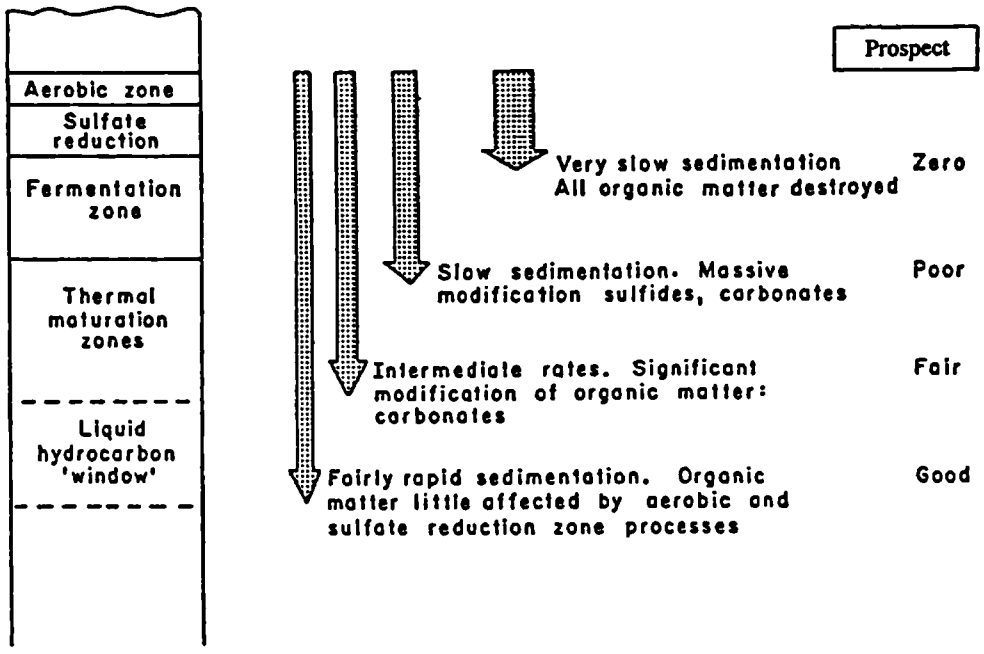


FIGURE 8.6 Increasing sedimentation rate results in the better preservation of organic matter by the rapid passage through the near-surface zone of microbial degradation (From Ibach, 1982). However, organic productivity must be simultaneously high to counterbalance the effect of sediment volume and thus avoid dilution.

accumulation rate was very much higher, varying between 500-1000m/Ma (Azim-Ibrahim, 1994) **(Figure 8.4)**. Following the argument of Kuehl *et. al.* (1993), this increase in sedimentation rate should, to a certain extent, aid the preservation of the marine organic carbon. Ibach (1982) concluded that for oil-prone organic matter, higher sedimentation rates can enhance preservation, owing to the relative inefficiency of near-surface degradation at the higher burial rates **(Figure 8.6)**. This is, however, not the case for the marine organic matter in the Sabah Basin. The absence of marine organic matter in the marine sediments of Sabah Basin leads to the conclusion that the very high sedimentation rates have resulted in their dilution and led to their 'scarcity'. The question now is why the dilution effects are relatively more severe for the marine organic matter compared to its land derived counterpart.

Several factors may be responsible for the reduction of the marine organic matter quantity prior to its deposition. Non-preservation of marine organic matter in the generally oxic conditions of Sabah Basin, which prevailed throughout the Neogene, is most likely due to their nature of being most prone to oxidation and bacterial degradation. Marine organic matter are by nature preferentially removed by organisms (Waples, 1985) because of their high lipid contents. The oxic nature of the Sabah waters greatly reduced the preservation chances of the marine organic matter. Also, the longer transit time experienced by the marine organic matter in the oxic water column before reaching the sea bed, subjects it to longer exposures to degradation processes. As a result of this decrease in quantity, any marine organic matter left available for deposition becomes diluted in concentration by the high sedimentation rates.

On the other hand, the land-derived organic matter transported out to the marine environments comprise very resistant cuticles and waxes of mangrove origin. Their resistance to degradation (Frewin *et. al.*, 1993) allows them to be better preserved than their marine counterparts. In the nearshore areas, it is the high primary terrigenous organic productivity that has inhibited the excess dilution of land-derived organic matter. There is no doubt that some extent of dilution must have occurred but, with high productivity counterbalancing the high sedimentation rates, sediments with adequate organic contents and hydrocarbon generating potentials to be classified as source rocks were successfully deposited. In general, even though the marine sediments may have organic matter of better quality, i.e. lipid rich waxes and cuticles versus unsorted terrigenous organic matter, the overall effect is that both the lower coastal/delta plain and marine sediments have generally comparable hydrocarbon generating potentials, if not slightly lower in the latter (see **Chapter 5**).

Finally, it has to be noted here that the general concept of organic matter preservation being enhanced by increased sedimentation rates may have been taken for granted. It is important to realise that sedimentation rates and bacterial activities are on two different time-scales; the first being a geological scale and the second being a biological scale. Working with a sedimentation rate of 1000m/Ma, a piece of organic

matter will only be covered by 0.1cm thick of sediments after one year. For it to be covered by 1 metre of sediments will take 1000 years, giving ample time for micro-organisms to work on it. It is, therefore, entirely probable that the organic matter is degraded before it finally leaves the oxic sedimentary environment. The sedimentation rate used for the calculation here, 1000m/Ma, is extremely high and most often occur in young, Tertiary basins. In general, sedimentation rates are much lower than this, which leaves some doubt on the validity of high burial rates being quoted as responsible for the preservation of the less resistant Types I and II organic matter.

8.5 Variation in organic matter quality and quantity

The abundance and type of organic matter in Sabah Basin vary with their environment of deposition (**Figure 8.7**). An apparent inter-relationship exists between the quantity of organic matter supplied to a depositional environment and the concentration of organic matter incorporated in the sediment. In general, supply of organic matter is greatest in areas of high primary productivity, such as along continental margins, around land masses and areas of upwelling. However, this supply factor becomes modified by processes responsible for conservation and concentration of organic matter, and by those responsible for dilution and destruction.

The majority of land-derived organic matter in Sabah Basin are allochthonous i.e. foreign to their environment of deposition, except for those deposited in coastal plain settings where they can be either allochthonous or autochthonous. The importance of allochthonous organic matter is illustrated by the occurrence of hydrocarbon-generating allochthonous coals in the Mahakam Delta (Thompson *et. al.*, 1985). Roman (1974) documented the presence of great quantities of pollen in the bottom sediments of the Black Sea, exemplifying the importance of allochthonous organic matter in modern sediments. The marine Black Sea sediments contained more land-derived than marine particles among the microscopically identifiable fraction of organic matter.

8.5.1 Organic Matter Variation Pattern With Environmental Depth Zones

Environmental depth zones (Bustin, 1988) defined by the micropalaeontological studies of Hedgpeth (1957a) are adapted here (**Figure 8.7**). Four zones are differentiated :

1. Lower coastal plain : above high tide
2. Coastal to inner neritic : 0 - 50m
3. Middle to outer neritic : 50 - 250m
4. Bathyal : > 250m

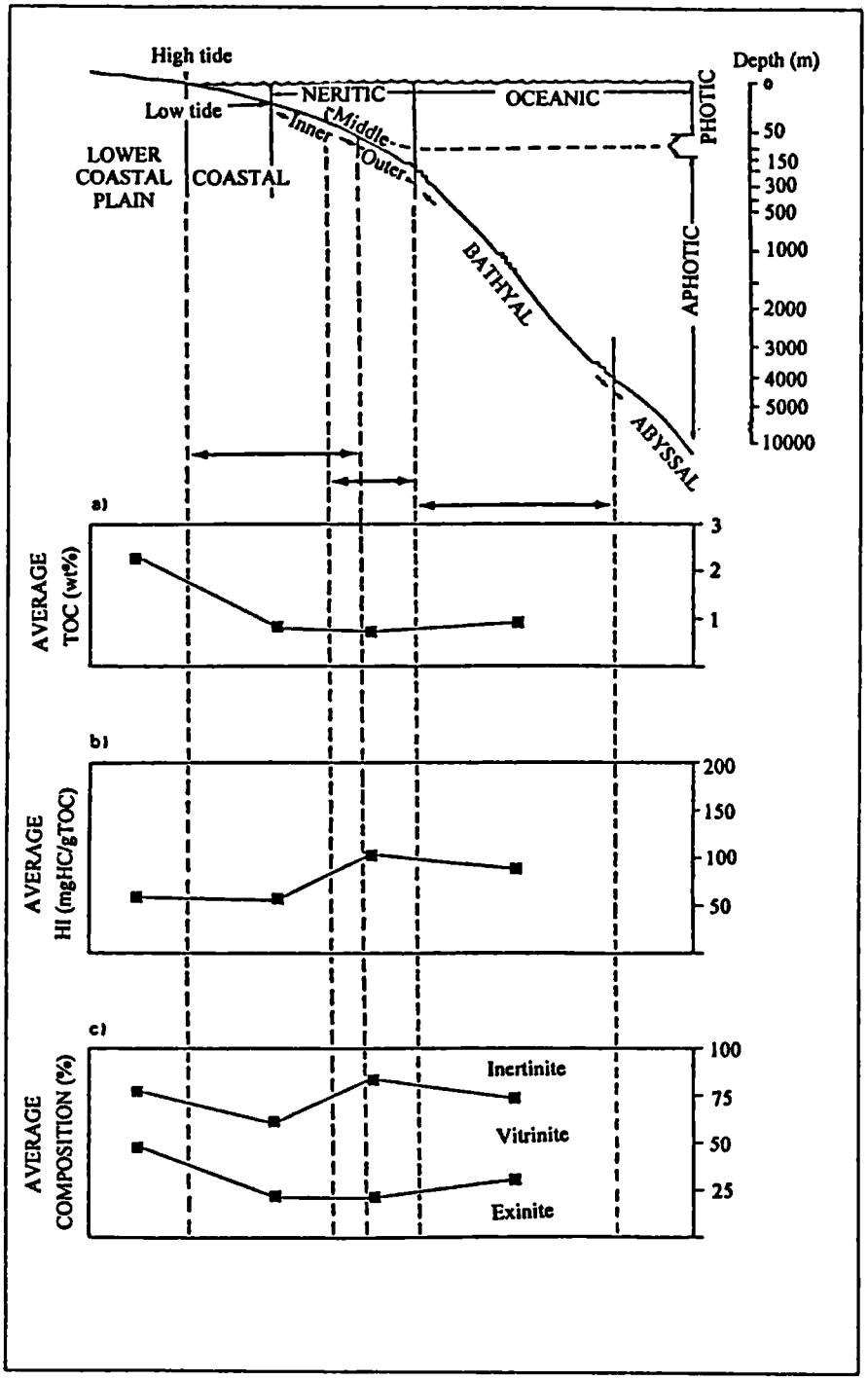


FIGURE 8.7 Variations in (a) average TOC (wt%), (b) average Hydrogen Index, HI (mgHC/gTOC) and (c) average organic matter compositions with palaeodepositional environments of Hedgpeth (1957a) (From Anuar *et. al.*, 1993).

The lower coastal plain depth zone has the highest average total organic carbon (TOC) content. There appears to be little variation in the average TOC content in the other depth zones, save for a slight increases towards the deeper environment **(Figure 8.7)**. The average Hydrogen Index value decreases slightly from the lower coastal plain depth zone to the coastal-inner neritic depth zone, then increases in the middle-outer neritic depth zone followed by a slight decrease in the bathyal depth zone. The increase in the average Hydrogen Index value in the middle neritic-outer neritic zone corresponds with a low average TOC. This suggests that the increase in the average Hydrogen Index is the result of more hydrogen-rich organic matter being present in the sediments. An increased quantity of hydrogen-rich organic matter in the middle neritic-outer neritic zone is the result of selective transportation of hydrogen-rich parts of land plants, such as leaf cuticles, waxes, resins, pollen and spores, and not due to input from marine organic matter.

Meade *et. al.* (1975) and Milliman *et. al.* (1975) recognised the importance of suspended organic matter with respect to transportation and sedimentation of organic matter. Organic matter that are rich in hydrogen are relatively lower in density compared to those that are hydrogen-poor (Kinghorn & Rahman, 1980). As such, the lipid fraction of organic matter behaves differently in sedimentary processes than non-lipid material. Being low in density, they can more easily stay in suspension and be carried away into quiet waters. The lipid fraction has been reported as very resistant to mechanical and biological weathering (Tissot & Welte, 1984; Thompson *et. al.*, 1985).

Suberin and cutin are two types of lipids present in plants that act as protective tissues. Suberin is formed and deposited inside plant tissues and cell walls while cutin and waxes are deposited mainly on the outer side of plant cells, for example on the surfaces of pollen, spores and leaves. Both suberin and cutin are highly resistant to microbial attack, oxidation or chemical treatment (Tissot & Welte, 1984). The properties of the hydrogen-rich organic matter, being low in density, highly insoluble in water together with the resistance to mechanical and chemical degradation, are held as largely responsible for the contribution of terrestrial plant material to the marine sediments.

The variations in palynofacies with the environmental depth zones show exinites predominating in the lower coastal plain, possibly reflecting source proximity more than anything else, while structured woody material like vitrinite being the major component in the middle neritic to the bathyal depth zone **(Figure 8.7)**. The coastal-inner neritic zone has the highest inertinite content. This is in agreement with a high energy environment which invariably leads to high organic matter susceptibility to oxidation. There is also an observed increase in the exinite content towards the deeper depth zones after an initial decrease in the coastal-inner neritic zone. This is seen as supporting the selective transportation mechanism discussed above.

8.5.2. Origin Of Variation

The variation in abundance and characteristics of the dispersed organic matter with the environmental depth zones mainly reflects the deposition of land-derived organic detritus being controlled to some extent by sedimentary processes and by the nature of the organic matter. The most significant variation in the organic matter is between the lower coastal plain and the coastal to inner neritic depth zones. The lower coastal plain zone is characterised by a significantly higher average total organic carbon (TOC) content with the highest Hydrogen Index values occurring in carbonaceous shales.

The decrease in the average TOC contents from the lower coastal plain to the coastal-inner neritic zones reflects the possibility of organic matter erosion, dilution by mineral matter accompanying transport and deposition, as well as oxidation. Although a substantial decrease occurs in the average TOC content from the lower coastal plain to the coastal-inner neritic depth zones, no significant variations occur from the coastal-inner neritic to the bathyal depth zones. The absence of significant decline in average TOC contents may reflect a broadly homogeneous dispersion and deposition of detrital organic matter.

The decrease in the average Hydrogen Index value of the lower coastal plain zone to the coastal-inner neritic zone (**Figure 8.7**) is very likely due to the oxidation of organic matter which is very feasible in the high energy coastal-inner neritic environment. Oxidation, including microbial degradation of organic matter results in the decrease of hydrogen and carbon contents, and a relative increase in oxygen content (Bustin, 1988). A sharp increase in the average Hydrogen Index value from coastal-inner neritic to middle-outer neritic zones followed by a slight decrease towards the bathyal depth zone is thought to be due to the relative increase in exinite content as a result of the selective transport mechanism. Low density hydrogen-rich material transported further offshore while high density, hydrogen-poor organic matter like degraded vitrinites and inertinites, are deposited nearer inshore.

A wider dispersal of hydrogen-rich material is possible due to its lower density (Stach *et. al.*, 1982) and lower deposition rate. Relative to other macerals, the nearshore sediments would be impoverished in liptinitic material and would have a low Hydrogen Index value. The variation in maceral content parallels the variation in the average Hydrogen Index values. It also supports the selective transport mechanism by showing a gradual increase in the exinite content following a decrease in the coastal- inner neritic depth zone.

8.5.3 Implications For Source Rock Distribution

Based on the results of this study, Sabah Basin hydrocarbons were generated by higher land-plant derived, Type III organic matter. The deposition and preservation of the organic matter occurred in three palaeoenvironments, which are :

1. The *in situ* deposition of organic matter in the coastal plain areas. Depositional environments suitable for the formation of source beds in the coastal plains include inter-channel swamp areas most often dominated by mangroves and nypa-palms, back-mangrove swamps, lagoonal areas and inter-distributary areas where organic rich clays or peats are deposited.
2. The fluviomarine environments - deltaic settings.
3. The continental shelf - deep marine environment.

Of the three, source rocks deposited in the first and second palaeoenvironments are the most significant for the generation of hydrocarbon in commercial quantities. In these depositional settings, the lateral continuity of the source beds are likely to be irregular. However, the irregularities in source rock occurrence is compensated by the presence of interbedded sandstones which, upon maturation of the source rocks, provide efficient migration paths.

Although results from organic geochemical analyses in this study classify them as poor to marginal source rocks, according to present standards (Hydrogen Index, Generation Potential), the discoveries of several producing oil and/or gas fields offshore Sabah, one of which (Samarang Field) qualifies as a giant discovery (>100 million bbl of oil) based on the American Association of Petroleum Geologists' classification (Scherer, 1980), attest to their success as source rocks. The high sediment accumulation rate and primary productivity (resulting in relatively lower degree of organic matter degradation), along with the nature of the sedimentary sequence where sandstones, siltstones and carbonaceous shales interbed, are deemed as the key to the success of the coastal plain - fluviomarine source rocks.

The third palaeoenvironment for source rock deposition in the Sabah Basin is the continental shelf - deep marine setting. Evidence for this comes from the analysis of deep marine samples from Rusa Timur-1 and Gajah Hitam-1 wells. Hydrogen-rich and low density waxes, cuticles, resins, pollen and spores had seemingly been preferentially transported and concentrated out into the deep marine environments for deposition (**Figure 8.7**). Results show that their hydrocarbon generation potentials are generally comparable to those of the coastal plain - fluviomarine source rocks. Oil samples from Rusa Timur-1 well indicate that they have been produced by Type III organic matter, with no significant contributions from marine organic matter (see **Chapter 6**).

Simple source rock distribution maps, based on the palaeoenvironments, during the Neogene sedimentation in the Sabah Basin, are shown in **Figure 8.8**. Sub-Stages IVC and IVD are not shown because they are presently immature, even in the hydrocarbon kitchens, and thus do not contribute to the present hydrocarbon accumulations found in offshore Sabah.

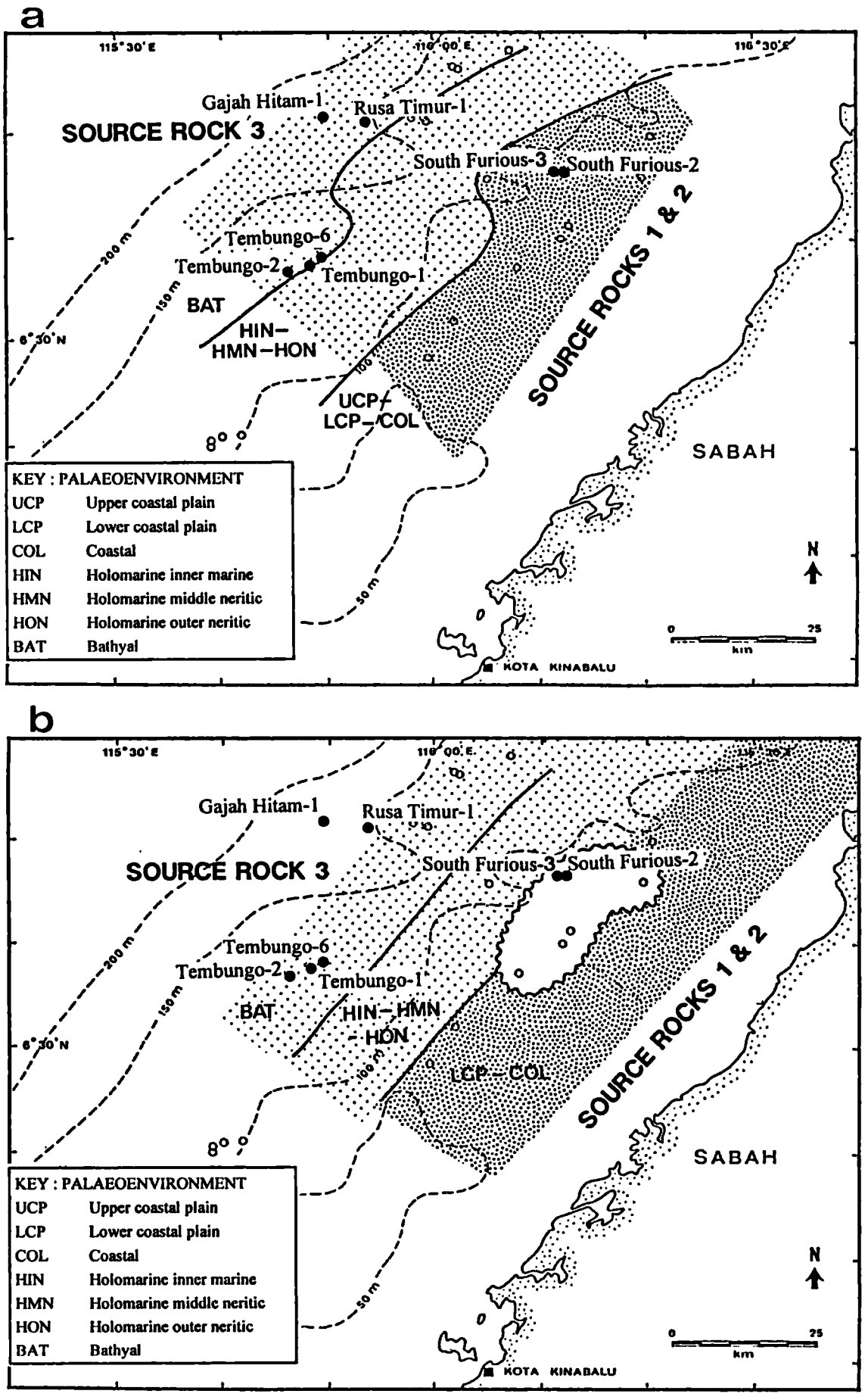


FIGURE 8.8 Simplified source rock distribution map for (a) Stage IVA and (b) Stage IVB.

8.6 SUMMARY

From this study, lower coastal plain and marine sediments containing higher land-plant derived organic matter are the most likely source for the Sabah Basin hydrocarbons. It seems that the source rocks of Sabah Basin are not restricted to any particular Stage or sub-Stage, but rather by sedimentary facies, and partly by the sedimentary process of exinite enrichment. The source rocks characteristics are:

- Type III kerogen.
- Poor hydrocarbon generation potentials by current standards used.
- The success of the source rocks is attributed to its thickness, rapid burial and maturation accompanied by migration pathways supplied by numerous intercalated sandstones.

High primary terrigenous productivity, high sediment accumulation rates and the nature of the organic matter are the primary controls for the successful deposition and preservation of the Sabah Basin source rocks. Anoxic depositional conditions only play a secondary role in the preservation of organic-rich sediments here.

In general, it is believed that all these parameters, productivity, burial rate, oxygen-deficient conditions and organic matter composition, all play a role in the successful preservation of organic matter. However, the extent to which each of these factors are important depends on the conditions of the basin. For example, in a basin with rapid sedimentation rates such as the Sabah Basin, the development of anoxia is not as important since the organic matter will be quickly removed from the zone of oxidation. It is also important that primary organic productivity is high so as to avoid the dilution effects reported by Ibach (1982). Based on the results of this study, and on the actual presence of hydrocarbons in commercial quantities in Sabah Basin, this mechanism for source rock preservation can be successful.

Conversely, in areas where organic productivity is high but sedimentation rate is low, anoxia will contribute to the preservation of organic matter by rendering the degradation process to be less efficient. However, in areas where organic productivity and sedimentation rate are low, then the development of anoxia is paramount for the preservation of organic-rich sediments. When organic productivity is low and sedimentation rate is high, the most likely outcome is dilution of the organic matter concentration resulting in lower overall oil generation potential of the sediments. In areas where both anoxia and high primary productivity co-occur, the failure of enhanced organic carbon preservation may be due to post-depositional redistribution of the organic matter by hydrodynamic influences such as sediment winnowing and reworking (bioturbation), for example, the Oman Margin (Pedersen *et. al.*, 1992).

Therefore, to attempt singling out a parameter as the primary control on general organic carbon preservation is basically unnecessary. One has to take into account all the parameters and investigate the actual extent of contribution from each parameter. Different parameters will have varying degrees of importance in different depositional

basins. It is the consequence of having favourable interactions between the parameters that culminates in the successful preservation of hydrocarbon source rocks.

CHAPTER NINE

CONCLUSIONS AND FUTURE WORK

For a highly petroliferous area, it is rather peculiar that until now source beds of mappable extent have not been found in NW Borneo's Sabah - Brunei - Sarawak Tertiary basins. This dissertation attempts to address this enigma through organic geochemical analyses of sediments in the northern part of Sabah Basin. The principal aims are to : 1) identify horizons of source rock quality, 2) correlate oils to kerogen isolated from the most probable source rocks, 3) determine the timing of hydrocarbon generation through maturity modelling, and 4) elucidate the primary controls of organic matter deposition and preservation of the study area.

Based on cumulative results, coastal plain and marine sediments containing terrigenous organic matter represent the most likely source rocks for the hydrocarbon accumulations in the study area. The Sabah Basin source rocks do not seem to be time-related and restricted to any particular Stage or sub-Stage, but rather to sedimentary facies and partly to preferential enrichment of liptinitic organic matter. As a result of rapid sedimentation rates and consistently high terrigenous organic productivity in an ever wet tropical setting, conditions promoting the successful preservation of source rocks prevailed in Sabah Basin during the Neogene.

Within the study area, coastal plain sediments constitute the bulk of sub-Stage IVA in South Furious. Organic geochemical results indicate that the sub-Stage IVA sediments generally have poor to marginal source potentials. Despite this, the almost 2000m thick of closely interbedded sandstone and carbonaceous shale sequence compensates its lack of quality with quantity. Persisting shelf instability during the sub-Stages IVB and IVC times fed the basin with terrigenous organic matter via sediment slumpings and turbiditic flows. This resulted in the incorporation of land-derived organic matter in marine sediments, while marine organic matter failed to be preserved due to their relatively higher degradability compared to land-derived exinitic matter, and the oxicity of the Sabah Basin waters throughout the Neogene. The Tembungo accumulation most likely originated from this type of source rock since the underlying sediments are largely deposited in marine settings, based on palaeoenvironmental changes during Stage IV. Therefore, in the study area, the coastal plain sediments of sub-Stage IVA are deemed as the source rocks for the South Furious hydrocarbons,

while marine sediments containing preferentially-enriched terrestrial organic matter are responsible for generating the Tembungo accumulation. No significant discoveries are yet found in the Rusa Timur area despite comparable source potentials (Rusa Timur-1, sub-Stage IVA) with those of the coastal plain sediments, and the fact that the sub-Stage IVA sediments there are also presently within the oil window in the adjacent graben. The Rusa Timur and Gajah Hitam structures are densely faulted and it is, thus, possible that the generated hydrocarbons have been lost through fault leakage.

Evidence from both geochemical and petrographic studies consistently indicate land-derived Type III organic matter as the hydrocarbon source. Being the least oil-prone kerogen compared to Types I and II, the deposition and preservation mechanisms are important to determine the success or failure of the Type III organic matter to become hydrocarbon sources. The rapid subsidence, due to both tectonic and sedimentary loadings, experienced by Sabah Basin between 10 - 15 Ma not only enhanced preservation but also ensured their rapid maturation. The fast hydrocarbon generation (duration between 3.0 - 4.4 Ma) serves to facilitate their release by reaching the hydrocarbon expulsion barrier quicker.

Mass fragmentograms of both triterpane m/z 191 and sterane m/z 217 are also consistently comparable, suggesting that the hydrocarbons were most likely generated by source rocks with similar chemical compositions. Biomarker maturity ratios of the sediment extracts are not applicable for the determination of sediment maturity levels as they are influenced by migrating hydrocarbons.This was evidenced by the almost synchronous variation with depth between the biomarker maturity ratio and the production index. The 20S/[20S+20R] biomarker maturity ratio values of the oils are lower than its reported equilibrium value and appears to support the apparent retardation of the isomerisation process. Conversely, the triterpane 22S/[22+22R] ratio did not seem to be affected in the same way.

Two biomarker data groups, oils + sediment extracts, and oils only, were statistically analysed by the principal components method. The two most important factors controlling data variation within the first group (oils + sediment extracts) are resin content and the relative quantities of triterpanes to steranes. Maturity differences were not significant enough to allow separation between oils and extracts, and this confirms the non-indigenous nature of the sediment extracts. Data variation in the second group (oils only) is most importantly attributed to deviations in relative triterpane and sterane quantities, and to input from oleanane and resins as opposed to other triterpane sources. The oils were separated into three groups, with each group representing the palaeodepositional environment of their source rocks.

Maturity modelling by Lopatin's TTI, Hunt & Hennet's Arrhenius-based TTI_{ARR} and BasinMod's kinetic module indicate that sub-Stage IVA sediments are presently at various stages of maturity in the Pritchard and Furious Synclines. In both synclines, the oil window is located between 4000m - 5000m depth. Hydrocarbon generation from the

sub-Stage IVA sediments began around 8 - 9 Ma in both synclines and ceased between 4 - 6 Ma. In the Graben, sub-Stage IVA sediments entered the oil generation window between 5 -6 Ma and ceased around 1 - 3 Ma. Sub-Stage IVB sediments entered the hydrocarbon window in both synclines around 3 - 4 Ma but are still immature in the Graben. It is noted here that when dealing with Type III kerogen, results from the three methods do not differ very significantly. Hunt & Hennet's Arrhenius-based TTI graphs are easy to use and readily available, and are therefore recommended for the quick location of hydrocarbon windows.

Future Work

This study has not been able to disqualify the Stage III sediments conclusively as potential source rocks. The limited data made available from this study indicate that, in terms of organic carbon contents and hydrocarbon generating potentials, they are very similar to the younger sub-Stage IVA-IVD sedimentary sequences. Vitrinite reflectance measurements made on isolated kerogen samples indicate that they are still immature, with VRo values ranging between 0.40% - 0.46%. This is quite interesting because Stage III is regarded as the present economic basement and is generally believed to be highly deformed and over mature. It would be beneficial to follow up this study with a project geared towards ascertaining the source rock potential of Stage III sediments. To do this, it would be necessary to collect samples from wells in Sabah Basin that had penetrated thicker sequences of Stage III sediments and subject them to organic geochemical analyses. Additionally, outcrop samples of sedimentary formations which are equivalent to Stage III, for example, Temburong Formation (Middle - Early Oligocene), Meligan Formation (Middle - Early Oligocene) and Setap Shale Formation (Early Miocene - Recent) can be collected and analysed likewise. All these formations outcrop in the southern parts of Sabah, Brunei as well as the northern parts of Sarawak.

Extensive analysis of isolated kerogen through pyrolysis-gas chromatography (Py-GC) and pyrolysis-gas chromatography-mass spectrometry (Py-GC-MS) would also be useful to enable direct comparisons between the end product of artificial maturation and the actual oils be made, thus allowing kerogen-oil correlation to be firmly established.

REFERENCES

Almond, J., Vincent, P. & Williams, L. R. (1990). The application of detailed reservoir geological studies in the D18 Field, Balingian Province, offshore Sarawak. *Bull. Geological Society of Malaysia*, 27, 137-160.

Anuar, A., Kinghorn, R. R. F., Cocksedge, M. J. & Carr, A. D. (1993). Source rock evaluation and thermal maturity of Middle-Late Miocene sequence in the northern part of Sabah Basin, Malaysia. **In,** K. Oygard (Ed.) Poster sessions from the 16th International Meeting on Organic Geochemistry, Stavanger; European Association of Organic Geochemists. Extended abstract, 67-72.

Aquino Neto, F. R., Trendel, J. M., Restle, A., Connan, J. & Albrecht, P. A. (1983). Occurrence and formation of tricyclic and tetracyclic terpanes in sediments and petroleums.**In,** M. Bjoroy *et. al.* (Eds.) *Advances in Organic Geochemistry 1981*, 659-667.

ASCOPE (1981). Tertiary sedimentary basins of the Gulf of Thailand and South China Sea : stratigraphy, structure and hydrocarbon occurrences. ASEAN Council on Petroleum, Jakarta.

Azim-Ibrahim, N. (1994). Major controls on the development of sedimentary sequence - Sabah Basin, Northwest Borneo. PhD. Thesis, University of Cambridge.

Bally, A. W. & Snelson, S. (1980). Realms of subsidence. Facts and principles of world petroleum occurrence. *Canadian Soc. of Petroleum Geologists.* **In,** A. D. Miall (Ed.) Memoirs 6, 9-94.

Berger, W. H., Smetacek, V. S. & Wefer, G. (1989). Ocean productivity and palaeoproductivity - an overview. **In,** W. H. Berger, V. S. Smetacek & G. Wefer (Eds.) Productivity of the ocean : present and past. Wiley, New York, 1-34.

Berner, R. A. (1980). Early diagenesis : A theoretical approach. Princeton, New Jersey, Princeton University Press, 241p.

Berner, R. A. (1989). Biogeochemical cycles of carbon and sulfur and their effects on atmospheric oxygen over Phanerozoic time. *Palaeogeogr., Palaeoclimatol. & Palaeoecol.*, 75, 97-122.

Bol, A. J. & van Hoorn, B. (1980). Structural styles in western Sabah offshore. *Bull. Geological Society of Malaysia*, 12, 1-16.

Bray, E. E. & Evans, E. D. (1961). Distribution of n-paraffins as a clue to recognition of source beds. *Geochimica et Cosmochimica Acta*, 22, 2-15.

Bray, E. E. & Evans, E. D. (1965). Hydrocarbons in non reservoir-rock source beds : Part 1. *American Association of Petroleum Geologists Bull.*, 49(3), 248-257.

Braun, R. L. & Burnham, A. K. (1987). Analysis of chemical reaction kinetics using a distribution of activation energies and simpler models. *Energy and Fuels*, 1, 153-161.

Budzinski, H., Garrigues, P., Radke, M., Connan, J. & Loudin, J. (1993). Alkylated phenanthrene distributions as maturity and source indicators in crude oils, rocks and artificially matured samples. **In,** K. Oygard (Ed.) Poster sessions from the 16th International Meeting on Organic Geochemistry, Stavanger; European Association of Organic Geochemists. Extended abstract, 120-124.

Burnham, A. K. & Sweeney, J. J. (1989). A chemical kinetic model of vitrinite maturation and reflectance. *Geochimica et Cosmochimica Acta*, 53, 2649-2657.

Burnham, A. K., Braun, R. L., Gregg, H. R. & Samoun, A. (1987). Comparison of methods for measuring kerogen pyrolysis rates and fiiting kinetic parameters.*Energy and Fuels*, 1, 452-458.

Burnham, A. K., Braun, R. L. & Samoun, A. (1988). Further comparison of methods for measuring kerogen pyrolysis rates and fitting kinetic parameters.**In,** L. Mattavelli & L. Novelli (Eds.) *Advances in Organic Geochemistry 1987*, 13, 839-845..

Bustin, R. M. (1988). Sedimentology and characteristics of dispersed organic matter in Tertiary Niger Delta : origin of source rocks in a deltaic environment. *American Association of Petroleum Geologists Bull.*, 72(3), 277-298.

Calvert, S. E., Karlin, R. E., Toolin, L. J., Donahue, D. J., Southon, J. R. & Vogel, J. S. (1991). Low organic carbon accumulation rates in Black Sea sediments. *Nature*, 350, 692-695.

Calvert, S. E., Bustin, R. M. & Pedersen, T. F. (1992). Lack of evidence for enhanced preservation of sedimentary organic matter in the oxygen minimum of the Gulf of California. *Geology*, 20, 757-760.

Canfield, D. E. (1989). Sulfate reduction and oxic respiration in marine sediments ; Implications for organic carbon preservation in euxinic environments.*Deep Sea Research*, 36, 121-138.

Chibnall, A. C., Piper, S. H., Pollard, A., Williams, E. F. & Sahai, P. N. (1934). Constitution of primary alcohols, fatty acids, and paraffins present in pla..nt and insect waxes. *Biochem. Jour.*, 28, 2189.

Christie, O. H. J., Esbensen, K., Meyer, T. & Wold, S. (1984). Aspects of pattern recognition in organic geochemistry. *Organic Geochemistry*, 6, 885-891.

Christie, O. H. J., Cornford, C., Endresen, U., Auxietre, J-L., Pittion, J-L. & Noyau, A. (1993). Prediction of North Sea source rock burial depth and oil generation depth, and a migration distance modelling technique, based on sterane and triterpane data. **In,** K. Oygard (Ed.) Poster sessions from the 16th International Meeting on Organic Geochemistry, Stavanger; European Association of Organic Geochemists. Extended abstract, 212-216.

Cole, J. M. (1987). Some fresh/brackish water depositional environments in the S. E. Asian Tertiary with emphasis on coal bearing & lacustrine deposits and their source rock potential.**In,** Proc. Indonesian Petroleum Association 16th Annual Convention : Jakarta, Indonesian Petroleum Association, 429-449.

Combaz, A. & de Matharel, M. (1978). Organic sedimentation and genesis of petroleum in Mahakam Delta, Borneo. *American Association of Petroleum Geologists Bull.*, 62, 1684-1695.

Comet, P. A., Ooi Siew Tin & Yap Ai Bee (1989). C-GC-MS and its application to crude oil analysis. *Bull. Geological Society of Malaysia*, 25, 1-25.

Demaison, G. J., Holck, A. J. J., Jones, R. W. & Moore, G. T. (1984). Predictive source bed stratigraphy : A guide to regional petroleum occurrence.**In,** Proceedings 11th World Petroleum Congress, Vol. 2 : Geology, Exploration, Reserves. John Wiley & Sons, 17-29.

Demaison, G. J. & Moore, G. T. (1980). Anoxic environments and oil source bed genesis. *American Association of Petroleum Geologists Bull.*, 64, 1179-1209.

Dembicki, H., Horsfield, B. & Ho, T. Y. (1983). Source rock evaluation by pyrolysis-gas chromatography. *American Association of Petroleum Geologists Bull.*, 67, 1094-1103.

Didyk, B. M., Simoneit, B. R. T., Brassell, S. C. & Eglinton, G. (1978). Organic geochemical indications of palaeo-environmental conditions of sedimentation. *Nature*, 272, 216-222.

Durand, B. (1980). Sedimentary organic matter and kerogen. Definition and quantitative importance of kerogen. **In,** B. Durand (Ed.) Kerogen : Insoluble organic matter from sedimentary rock. Editions Technip, Paris, 13-34. Reproduced in E. A. Beaumont & N. H. Foster (1988) Geochemistry, Treatise of Petroleum Geology, Reprint Series No. 8, 81-102.

Ekweozor, C. M. & Telnaes, n. (1990). Oleanane parameter : verification by quantitative study of the biomarker occurrence in sediments of the Niger Delta. *Organic Geochemistry*, 16, 401-413.

Ekweozor, C. M. & Udo, O. T. (1988). The oleananes : origin, maturation and limits of occurrence in Southern Nigeria sedimentary basins. **In,** L. Mattavelli & L. Novelli (Eds.) *Advances in Organic Geochemistry 1987*, 131-140.

Elderfield, H. (1985). Element cycling in bottom sediments. **In,** G. Eglinton (Ed.) Geochemistry of buried sediments. *Phil. Trans. R. Soc. Lond.*, A, 315, 19-23.

Ellenor, D. W. (1984). The oil and gas resources of Brunei. **In,** D. M. D. James (Ed.) The geology and hydrocarbon resources of Negara Brunei Darussalam. Special publication of Muzium Brunei and Brunei Shell Petroleum Company, 103-134.

Emerson, S. K. & Hedges, J. I. (1988). Processes controlling the organic carbon content of open ocean sediments. *Paleoceanography*, 3, 621-634.

Ensminger, A., van Dorsselaer, A., Spyckerelle, C., Albrecht, P. & Ourisson, G. (1974). Pentacyclic triterpanes of the hopane type as ubiquitous geochemical markers : Origin and significance. **In,** B. Tissot & F. Bienner (Eds.) *Advances in Organic Geochemistry 1973*, 245-260.

Espitalie, J., Madec, M. & Tissot, B. (1980). Role of mineral matrix in kerogen pyrolysis : Influence on petroleum generation and migration. *American Association of Petroleum Geologists Bull.*, 64, 59-66.

Frewin, N. L., Killops, S. D., van Bergen, P. F., de Leeuw, J. W. & Collinson, M. E. (1993). Preservation potential of biomacromolecules of higher plant cuticles in Florida Bay. **In,** K. Oygard (Ed.) Poster sessions from the 16th International Meeting on Organic Geochemistry, Stavanger. European Association of Organic Geochemists. Extended abstract, 566-569.

Fuex, A. N. (1977). The use of stable carbon isotopes in hydrocarbon exploration. *Jour. Geochemical Exploration*, 7, 155-188.

Gehman, H. M. (1962). Organic matter in limestones. *Geochimica et Cosmochimica Acta*, 26, 885-894.

Genik, G. J. (1993). Petroleum geology of Cretaceous-Tertiary rift basins in Niger, Chad and Central African Republic. *American Association of Petroleum Geologists Bull.*, 77, 8, 1405-1434.

Grant, C. K. (1984). Geographical overview. **In,** D. M. D. James (Ed.) The geology and hydrocarbon resources of Negara Brunei Darussalam. Muzium Brunei, 164p.

Grantham, P. J. (1986b). Sterane isomerisation and moretane/hopane ratios in crude oils derived from Tertiary source rocks. *Organic Geochemistry*, 9. 293-304.

Grantham, P. J., Posthuma, J. & Baak, A. (1983). Triterpanes in a number of Far Eastern crude oils. **In,** M. Bjoroy *et. al.* (Eds.) *Advances in Organic Geochemistry 1981*, 675-683.

Haq, B. U., Hardenbol, J. & Vail, P. R. (1987). Chronology of fluctuating sea levels since the Triassic. *Science*, 235, 1156-1167.

Hamilton, W. (1979). Tectonics of the Indonesian region. US Geol. Surv., Prof. Paper 1078, 345p.

Harvey, H. R., Fallon, R. D. & Patton, J. S. (1986). The effect of organic matter and oxygen on the degradation of bacterial membrane lipids in marine sediments. *Geochimimica. et Cosmochimica. Acta*, 50, 795-804.

Hedberg, H. D. (1968). Significance of high-wax oils with respect to genesis of petroleum. *American Association of Petroleum Geologists Bull.*, 52(5), 736-750.

Hedgpeth, J. W. (1957a). Classification of marine environments. *Memoir Geological Society of America*, 67(1), 17-28.

Henrichs, S. M. & Reeburgh, W. S. (1987). Anacrobic mineralisation of marine sediment organic matter : Rates and the role of anaerobic processes in the oceanic carbon economy. *Geomicrobiol. Jour.*, 5, 191-237.

Henrichs, S. M. & Farrington, J. W. (1987). Early diagenesis of amino acids and organic matter in two coastal sediments. *Geochimimica et Cosmochimica. Acta*, 51, 1-15.

Herron, S. L. (1991). *In situ* evaluation of potential source rock by wireline logs. **In,** R. K. Merrill (Ed.) Source and migration processes and evaluation techniques.*American Association of Petroleum Geoologists*, Treatise of Petroleum Geology, Handbook of Petroleum Geology, 127-134.

Ho Kiam Fui (1978). Stratigraphic framework for oil exploration in Sarawak.*Bull. Geological Society of Malaysia*, 14, 19-58.

Hoffman, C. F., Mackenzie, A. S. Lewis, C. A, Maxwell. J. E. Oudin, J. L., Durand. B. and Vandenbroucke, M. (1984). A biological marker study of coals, shales and oils from the Mahakam Delta, Kalimantan, Indonesia. *Chemical Geology*, 42, 1-23.

Holloway, N. H. (1981). The north Palawan block, Philippines : Its relation to the Asian mainland and its role in the evolution of the South China Sea. *Bull. Geological Society of Malaysia*, 14, 19-58.

Holloway, N. H. (1982). North Palawan block, Philippines : Its relation to the Asian mainland and role in evolution of South China Sea. *American Association of Petroleum Geologists Bull.*, 66(9), 1355-1383.

Hood, A., Gutjahr, C. C. M. & Heacock, R. L. (1975). Organic metamorphism and the generation of petroleum. *American Association of Petroleum Geologists Bull.*, 59, 986-996.

Huang, W. Y. & Meinschein, W. G. (1979). Sterols as ecological indicators. *Geochimica et Cosmochimica Acta*, 43, 739-745.

Hughes, W. B., Holba, A. G. Miller, D. E. & Richardson, J. S. (1985). Geochemistry of greater Ekofisk crude oils. **In,** B. M. Thomas *et al.* (Eds.) Petroleum geochemistry in exploration of the Norwegian shelf. Proceedings of a Norwegian Petroleum Society (NPF) conference ' Organic Geochemistry in Exploration of the Norwegian Shelf', Stavanger, 75-92.

Hunt, J. M. (1968). How gas and oil form and migrate. *World Oil*, 167, 140-150.

Hunt, J. M. (1979). Petroleum geochemistry and geology. W. H. Freeman, San Francisco, 617p.

Hunt, J. M. & Hennet, R. J.-C. (1992). Modelling petroleum generation in sedimentary basins. **In,** J. K. Whelan & J. W. Farrington (Eds.) Organic matter : Productivity, Accumulation, and Preservation in Recent and Ancient Sediments, 20-52.

Hunt, J. M., Lewan, M. D. & Hennet, R. J.-C. (1991). Modeling oil generation with time-temperature index graph based on the Arrhenius Equation. *American Association of Petroleum Geologists Bull.*, 75(4), 797-807.

Hutchison, C. S. (1984). Is there a satisfactory classification for Southeast Asian Tertiary basins? Offshore S. E. Asia Conference Proc., 5, *SEAPEX*, Singapore, 6.64-6.76.

Hutchison, C. S. (1989). Geological evolution of Southeast Asia. Oxford Monographs on Geology and Geophysics, No. 13, 368p.

Ibach, L. E. J. (1982). Relationship between sedimentation rate and total organic carbon content in ancient marine sediments. *American Association of Petroleum Geologists Bull.*, 66(2), 170-188.

Ingall, E. D. & van Capellen, P. (1990). Relation between sedimentation rate and burial of organic phosphorus and organic carbon in marine sediments. *Geochimimica et Cosmochimica Acta*, 54, 373-386.

Issler, R. D. & Snowdon, L. R. (1990). Hydrocarbon generation kinetics and thermal modelling, Beaufort-Mackenzie Basin. *Bull. Canadian Petroleum Geology*, 38, 1-16.

James, D. M. D. (1984). Regional geological setting. **In,** D. M. D. James (Ed.) The geology and hydrocarbon resources of Negara Brunei Darussalam. Special publication of Muzium Brunei and Brunei Shell Petroleum Company, 34-42.

Jamil, A. S. A., Anwar, M. L & Kiang, E. S. P. (1991). Geochemistry of selected crude oils from Sabah and Sarawak. *Bull. Geological Society of Malaysia*, 28, 123-149.

Jarvie, D. M. (1991). Total organic carbon (TOC) analysis. **In,** R. K. Merrill (Ed.) Source and migration processes and evaluation techniques. Treatise of Petroleum Geology, Handbook of Petroleum Geology, 113-119.

Jiamo, F., Guoying, S., Jiayou, X., Eglinton, G., Gowar, A. P. Rongfen, J., Shanfa, F. & Pingan, P. (1990). Application of biological markers in the assessment of paleoenvironments of Chinese non-marine sediments. *Organic Geochemistry*, 16, No. 4-6, 760-779. **In,** B. Durand & F. Behar (Eds.) *Advances in Organic Geochemistry 1989.*

Johnson, H. D., Chapman, J. W. & Ranggon, J. (1989). Structural and stratigraphic configuration of the Late Miocene Stage IVC reservoirs in the St. Joseph Field, offshore Sabah, NW Borneo. *Bull. Geological Society of Malaysia*, 25, 79-118.

Johnson, H. D. & Huong, J. (1991). Geological field guide to Labuan Island, Sabah. Unpublished report, Sabah Shell Petroleum Company Limited.

Jones, J. G. (1985). Microbes and microbial processes in sediments. **In,** G. Eglinton (Ed.) Geochemistry of buried sediments. *Phil. Trans. R. Soc. Lond.*, A, 315, 19-23.

Jones, P. J. & Philp, R. P. (1990). Oils and source rocks from Pauls Valley, Anadarko Basin, Oklahoma, USA. *Applied Geochemistry*, 5, 429-448.

Jones, R. W. (1984). Comparison of carbonate and shale source rocks. **In,** J. G. Palacas (Ed.) Petroleum Geochemistry and Source Rock Potential of Carbonate Rocks. *American Association of Petroleum Geologists Bull.*, Studies in Geology No. 18.

Karstang, T. V. & Kvalheim, O. M. (1991). SIRIUS - A Multivariate Analysis Program for Calibration and Classification, Pattern Recognition Systems, Version 2.3, Bergen, Norway.

Katz, B. J. (1983). Limitations of Rock-Eval pyrolysis for typing organic matter. *Organic Geochemistry*, 4, 195-199.

Kimble, B. J., Maxwell, J. R., Philp, R. P., Eglinton, P., Albrecht, P., Ensminger, A., Arpino, P. & Ourisson, G. (1974). Tri and tetraterpenoid hydrocarbons in the Messel oil shale. *Geochimimica et Cosmochimica Acta*, 38, 1165-1181.

Kinghorn, R. R. F. (1983). An introduction to the physics and chemistry of petroleum. John Wiley & Sons, 420p.

Kinghorn, R. R. F. & Rahman, M. (1980). The density separation of different maceral groups of organic matter dispersed in sedimentary rocks. *Journal of Petroleum Geology*, 2(4), 449-454.

Kingston. D. R., Dishroon, C. P. & Williams, P. A. (1983). Global basin classification system. *American Association of Petroleum Geologists Bull.*,67, 2175-2193.

Kuehl, S. A., Fuglseth, T. J. & Thunell, R. C. (1993). Sediment mixing and sediment accumulation rates in the Sulu and South China Seas : Implications for organic carbon preservation in deep-sea environments. *Marine Geology*, 111, 15-35.

Kvalheim, O. M. (1985). Scaling of analytical data. *Analytical Chimica Acta*, 177, 71-79.

Kvenvolden, K. A. & Simoneit, B. R. T. (1990). Hydrothermally derived petroleum : examples from Guaymas Basin, Gulf of California, and Escanaba Trough, northeast Pacific Ocean. *American Association of Petroleum Geologists Bull.*, 74, 223-237.

Lee, C. (1992). Controls on organic carbon preservation : the use of stratified water bodies to compare intrinsic rates of decomposition in oxic and anoxic systems. *Geochimimica et Cosmochimica Acta*, 56, 3323-3335.

Leopold, E. B. (1969). Late Cenozoic palynology. **In,** R. M. Tschudy & R. A. Scott (Eds.) Aspects of palynology - An introduction to plant microfossils in time. John Wiley & Sons, Inc., 377-438.

Letouzey, J., Sage, L. & Muller, C. (1988). Geological and structural map of Eastern Asia : Introductory notes, *American Association of Petroleum Geologists.*

Levell, B. K. (1987). The nature and significance of regional unconformities in the hydrocarbon-bearing Neogene sequence, offshore West Sabah. *Bull. Geological Society of Malaysia*, 21, 55-90.

Levell, B. K. & Kasumajaya, A. (1985). Slumping of the Late Miocene shelf edge, offshore West Sabah : A review of a turbidite basin edge. *Bull. Geological Society of Malaysia*, 18, 1-30.

Lijmbach, G. W. M. (1976). On the origin of petroleum : Ninth World Petroleum Congress Proceedings, 1975. Vol. 2. Applied Science Publishers Ltd, London, 357-369.

Linsley, B., Thunell, R., Morgan, C. & Williams, D. (1985). Oxygen minimum expansion in the Sulu Sea, western equatorial Pacific, during the last glacial low stand of sea level. *Marine Micropaleontology*, 9, 395-418.

Lopatin, N. V. (1971). Temperature and geological time as factors of carbonification. *Akad. Nauk SSSR. Izv. Ser. Geol.*, 3, 95-106.

Lopatin, N. V. (1976). The determination of the influence of temperature and geologic time on the catagenesis processes of coalification and oil-gas formation. **In,** Research on organic matter of modern and fossil deposits. Moscow, *Akad. Nauk SSSR, Izdatel'stvo, 'Nauka'*, 361-366.

Louis, M. (1967). Cours de geochimie du petrole; cours de l'Ecole Nationale Superieure du Petrole et des Moteurs : Paris, Inst. Francais Petrole, Editions Technip, 295p.

Mackenzie, A. S., Patience, R. L., Maxwell, J. E., Vandenbroucke, M. & Durand, B. (1980a). Molecular parameters of maturation in the Toarcian shales, Paris basin France. I. Changes in the configurations of acyclic isoprenoid alkanes, steranes and triterpanes. *Geochimimica et Cosmochimica Acta*, 44, 1709-1721.

Mackenzie, A. S. & McKenzie, D. H. (1983). Isomerization and aromatization of hydrocarbons in sedimentary basins formed by extension. *Geological Magazine*, 120(5), 417-528.

Mackenzie, A. S. & Maxwell, J. E. (1981). Assessment of thermal maturation in sedimentary rocks by molecular measurements. **In,** J. Brooks (Ed.) Organic maturation studies and fossil fuel exploration, 239-254.

Mackenzie, A. S. (1984). Application of biological markers in petrogeochemistry. **In,** J. Brooks & D. Welte (Eds.) Advances in Petroleum Geochemistry, 1, 115-214.

Meade R. H., Sachs, P. L., Manheim, F. T., Hathaway, J. C., Spencer, D. W. (1975). Sources of suspended matters in waters of the middle Atlantic bight. *Sedimentary Petrology*, 45, 171-188.

Mello, M. R., Gaglianone, P. C., Brassell, S. C. & Maxwell, J. R. (1988a). Geochemical and biological marker assessment of depositional palaeoenvironments using Brazilian offshore oils. *Marine and Petroleum Geology*, 5, 205-223.

Mello, M. R., Telnaes, N., Gaglianone, P. C., Chicarelli, M. I., Brassell, S. C. & Maxwell, J. R. (1988b). Organic geochemical characterisation of depositional palaeoenvironments of source rocks and oils in Brazilian marginal basins. *Organic Geochemistry*, 13, No. 1-3, 31-45. **In,** L. Mattavelli & L. Novelli (Eds.) *Advances in Organic Geochemistry 1987.*

Meyer, B. L. & Nederlof, M. H. (1984). Identification of source rocks on wireline logs by density/resistivity and sonic transit time/resistivity crossplots. *American Association of Petroleum Geologists Bull.*, 68(2), 121-129.

Milliman, J. D., Summerhayes, C. P., Baretto, H. T. (1975). Oceanography and suspended matter off the Amazon River. *Sedimentary Petrology*, 45, 189-206.

Moldowan, J. M., Seifert, W. K. & Gallegos, E. J. (1985). Relationship between petroleum composition and depositional environment of petroleum source rocks.*American Association of Petroleum Geologists Bull.*, 69, 1255-1268.

Muller, P. J. & Suess, E. (1979). Productivity, sedimentation rate and sedimentary organic matter in the oceans - organic carbon preservation. *Deep Sea Research*, 27A, 1347-1362.

Nichols, P. D., Palmisano, A. C., Rayner, M. S., Smith, G. A. & White, D. C. (1990). Occurrence of novel C_{30} sterols in Antarctic sea-ice diatom communities during a spring bloom. *Organic Geochemistry*, 15, 503-508.

Nissenbaum, A., Baedecker, M. J. & Kaplan, I. R. (1972). Studies on dissolved organic matter from interstitial water of a reducing marine fjord.**In**, H. R. von Gaertner & H. Wehner (Eds.) *Advances in Organic Geochemistry 1971*, 427-440.

Noble, R. A., Wu, C. H. & Atkinson, C. D. (1991). Petroleum generation and migration from Talang Akar coals and shales offshore N. W. Java, Indonesia. *Org. Geochemistry*, 17(3),363-374.

Noble, R. A. (1991). Geochemical techniques in relation to organic matter. **In**, R. K. Merrill (Ed.) Source and migration processes and evaluation techniques. *American Association of Petroleum Geologists*, Treatise of Petroleum Geology, Handbook of Petroleum Geology, 97-102.

Nwachukwu, J. I. & Chukwura, P. I. (1986). Organic matter of Agbada Formation, Niger Delta, Nigeria. *American Association of Petroleum Geologists Bull.*, 70(1), 48-55.

Otsuki, A. & Hanya, T. (1972a). Production of dissolved organic matter from dead green algal cells. I. Aerobic microbial decomposition. *Limnol. Oceanogr.*, 17, 248-256.

Otsuki, A. & Hanya, T. (1972b). Production of dissolved organic matter from dead green algal cells. II. Anaerobic microbial decomposition. *Limnol. Oceanogr.*, 17, 258-264.

Ourisson, G., Albrecht, P. & Rohmer, M. (1984). The microbial origin of fossil fuels. *Scientific American*, 251(2), 44-51.

Oygard, K., Larter, S. & Sentfle, J. (1988). The control of maturity and kerogen type on quantitative analytical pyrolysis data. *Organic Geochemistry*, 13, No. 4-6, 1153-1162. **In**, L. Mattavelli & L. Novelli (Eds.) *Advances in Organic Geochemistry 1987.*

Parnell, J & Rahman, M. (1990). Source rock evaluation of Devonian lacustrine carbonates, Northern Scotland. Geologic Notes, *American Association of Petroleum Geologists Bull.*, 74(3), 345-351.

Paropkari, A. L., Prakash Babu, C. & Mascarenhas, A. (1993). New evidence for enhanced preservation of organic carbon in contact with oxygen minimum zone in the western continental slope of India. *Marine Geology*, 111, 7-13.

Pautot, G., Rangin, C., Briais, A., Tapponier, P., Beuzart, P. Lenicolais, G., Mathieu, X., Wu, J., Han, S., Li, H., Lu, Y. & Zhao, J. (1986). Spreading direction in the central South China Sea. *Nature*, 321, 150-154.

Pedersen, T. F. & Calvert, S. E. (1990). Anoxia vs productivity : What controls the formation of organic carbon rich sediments and sedimentary rocks? *American Association of Petroleum Geologists Bull.*, 74, 454-466.

Pedersen, T. F., Shimmield, G. B. & Price, N. B. (1992) Lack of association between the oxygen minimum and the quality and content of organic matter in sediments on the Oman margin. *Geochimimica. et Cosmochimica. Acta*, 56, 545-551.

Perkin Elmer Handbook (1986). Instructions : Oxygen Analysis Kit. The Perkin Elmer Corp., Norwalk Connecticut, USA, 13p.

Peters, K. E. (1986). Guidelines for evaluating petroleum source rocks using programmed pyrolysis. *American Association of Petroleum Geologists Bull.*, 70, 318-329.

Philippi, G. T. (1957). Identification of oil-source beds by chemical means. **In,** Proc. 20th International Geological Congress, Mexico City, 1956, Sec. 3, 25-38.

Philp, R. P. & Gilbert, T. D. (1986). Biomarker distributions in oils predominantly derived from terrigenous source material. **In,** D. Leythaeuser & J. Rullkotter (Eds.) *Advances in Organic Geochemistry 1985*, 73-84.

Philp, R. P. & Galvez-Sinibaldi, A. (1991). Characterisation of organic matter by various pyrolysis techniques. **In,** R. K. Merrill (Ed.) Source and Migration Processes and Evaluation Techniques. *American Association of Petroleum Geologists Bull.*, Treatise of Petroleum Geology, Handbook of Petroleum Geology, 107-112.

Philp, R. P. (1985). Biological markers in fossil fuel production. Mass Spectrometry Reviews, 4, 1-54. Reprinted in E. A. Beaumont & N. H. Forster (Eds.) (1988) Geochemistry - Treatise of Petroleum Geology, *American Association of Petroleum Geologists,* Reprint Series No 8.

Potter, T. L., Johns, D. R. & de Natris, T. B. G. (1984). Lithostratigraphy. **In,** D. M. D. James (Ed.) The geology and hydrocarbon resources of Negara Brunei Darussalam. Special publication of Muzium Brunei and Brunei Shell Petroleum Company, 43-75.

Powell, T. G., Boreham, C. J., Smyth, M., Russell, N. & Cook, A. C. (1991). Petroleum source rock assessment in non-marine sequences : pyrolysis and petrographic analysis of Australian coals and carbonaceous shales. *Org. Geochemistry*, 17(3), 375-394.

Powell, T. G. & McKirdy, D. M. (1973). The effect of source material, rock type and diagenesis in the n-alkane content of sediments. *Geochimica et Cosmochimica Acta*, 37, 623-633.

Price, L. C. & Barker, C. E. (1985). Suppression of vitrinite reflectance in amorphous rich kerogen-a major unrecognized problem. *Jour. Petroleum Geology*, 8, 59-84.

Quigley, T. M. & Mackenzie, A. S. (1987). Kinetic theory of petroleum generation. **In,** B. Doligez (Ed.) Migration of hydrocarbons in sedimentary basins. Editions Technip, Paris, 649-665.

Rice-Oxley, E. D. (1991). Palaeoenvironments of the Lower Miocene to Pliocene sediments in offshore NW Sabah area. *Bull. Geological Society of Malaysia*, 28, 165-194.

Rijks, E. J. K. (1981). Baram Delta geology and hydrocarbon occurrence. *Bull. Geological Society of Malaysia*, 14, 1-18.

Riva, A., Caccialanza, P. G. & Quagliaroli, F. (1988). Recognition of 18β(H) oleanane in several crudes and Tertiary-Upper Cretaceous sediments. **In,** L. Mattavelli & L. Novelli (Eds.) *Advances in Organic Geochemistry 1987*, 671-675.

Robinson, K. M. (1987). An overview of source rocks and oils in Indonesia. **In,** Proc. Indonesian Petroleum Association 16th Annual Convention, Vol 1 : Jakarta, Indonesian Petroleum Association, 97-122.

Roman, St. (1974). Palynoplanktonic analysis of some Black Sea cores. **In,** E. T. Degens & D. A. Ross (Eds.) The Black Sea - Geology, Chemistry and Biology. *American Association of Petroleum Geologists Bull., Memoir 20*, 396-406.

Ru, K. & Pigott, J. D. (1986). Episodic rifting and subsidence in the South China Sea. *American Association of Petroleum Geologists Bull.*, 70, 1136-1155.

Rullkotter, J. & Marzi, R. (1988). Natural and artificial maturation of biological markers in a Toarcian shale from northern Germany. **In,** L. Mattavelli & L. Novelli (Eds.) *Advances in Organic Geochemistry 1987*, 639-645.

Scalan, R. S. & Smith, J. E. (1970). An improved measure of the odd-even predominance in the normal alkanes of sediment extracts and petroleum. *Geochimica et Cosmochimica Acta*, 34(6), 611-623.

Scherer, F. C. (1980). Exploration in East Malaysia over the past decade. **In,** M. T. Halbouty (Ed.) Giant oil and gas fields of the decade 1968-1978. *American Association of Petroleum Geologists Bull. Memoir, 30*, 423-440.

Seifert, W. K. & Moldowan, J. M. (1978). Application of steranes, terpanes and monoaromatics to the maturation, migration and source of crude oils. *Geochimica et Cosmochimica Acta*, 42, 77-95.

Seifert, W. K. & Moldowan, J. M. (1980). The effect of thermal stress on source rock quality as measured by hopane stereochemistry. **In,** A. G. Douglas & J. R. Maxwell (Eds.) *Advances in Organic Geochemistry 1979*, 229-237.

Seifert, W. K. & Moldowan, J. M. (1981). Paleoreconstruction by biological markers. *Geochimica et Cosmochimica Acta*, 45, 783-794.

Seifert, W. K. & Moldowan, J. M. (1986). Use of biological markers in petroleum exploration. **In,** R. B. Johns (Ed.) Biological markers in the sedimentary record : Methods in geochemistry and geophysics, 24, 261-290.

Senftle, J. T. & Landis, C. R. (1991) Vitrinite reflectance as a tool to assess thermal maturity. **In,** R. K. Merrill (Ed.) Source and migration processes and evaluation techniques, *American Association of Petroleum Geologists*, Treatise of Petroleum Geology, Handbook of Petroleum Geology, 119-125.

Shanmugam, G. (1985). Significance of coniferous rain forests and related organic matter in generating commercial quantities of oil, Gippsland Basin, Australia. *American Association of Petroleum Geologists Bull.*, 69, 1241-1254.

Snowdon, L. R. (1980). Resinite - a potential petroleum source in the Upper Cretaceous and Tertiary Beaufort-Mackenzie Basin. **In,** A. D. Miall (Ed.) Facts and principles of world petroleum occurrence. *Canadian Society of Petroleum Geologists*, Memoir 6, 509-520.

Snowdon, L. R., Brooks, P. W., Williams, G. K. & Goodarzi, F. (1987). Correlation of the Canol Formation source rock with oil from Norman Wells. *Organic Geochemistry*, 11, 529-548.

Sofer, Z. (1991). Stable isotopes in petroleum exploration. In, R. K. Merrill (Ed.) Source and migration processes and evaluation techniques, *American Association of Petroleum Geologists*, Treatise of Petroleum Geology, Handbook of Petroleum Geology, 103-106.

Sofer, Z. (1984). Stable carbon isotope composition of crude oils : Application to source depositional environments and petroleum alteration. *American Association of Petroleum Geologists Bull.*, 68, 31-49.

Stach, E., Mackowsky, M. T., Teichmuller, M., Taylor, G. H., Chandra, D. & Teichmuller, R. (1982). Stach's textbook of coal petrology. 3rd edition, Berlin, 535p.

Stahl, W. J. (1977). Carbon and nitrogen isotopes in hydrocarbon research and exploration. *Chem. Geol.*, 20, 121-149.

Stahl, W. J. (1978). Source rock-crude oil correlation by isotopic type curves. *Geochimica et Cosmochimica Acta*, 42, 1573-1577.

Suess, E. (1980). Particulate organic carbon flux in the oceans - surface productivity and oxygen utilisation. *Nature*, 288, 260-263.

Sweeney, J. J. & Burhnam, A. K. (1990). Evaluation of a simple model of of vitrinite reflectance based on chemical kinetics. *American Association of Petroleum Geologists Bull.*, 74, 1559-1570.

Tapponier, P., Peltzer, G. & Armijo, R. (1986). On the mechanics of the collision between India and Asia. **In**, M. P. Coward & A. C. Ries (Eds.) Collision Tectonics, *Geol. Soc. Spec. Publ. 19*, 115-157.

Taylor, B. & Hayes, D. E (1980). The tectonic evolution of the South China basin. : The tectonic and geologic evolution of Southeast Asian seas and islands. **In**, D. E Hayes (Ed.) *Geophysical Monograph* 23, American Geophysical Union, 89-104.

Telnaes, N. & Dahl, B. (1986). Oil-oil correlation using multivariate techniques. *Organic Geochemistry*, 10, 425-432. **In**, D. Leythaeuser & J. Rullkotter (Eds.) *Advances in Organic Geochemistry 1985.*

Telnaes, N. & Cooper, B. S. (1991). Oil-source rock correlation using biological markers, Norwegian continental shelf. *Marine and Petroleum Geology*, 8, 302-310.

Telnaes, N. & Isaksen, G. H. (1993). Classification of depositional environments using multivariate analysis of biomarker distributions. **In**, K. Oygard (Ed.) Poster sessions from the 16th International Meeting on Organic Geochemistry, Stavanger; European Association of Organic Geochemists. Extended abstract, 409-412.

ten haven, H. L., de Leeuw, J. W., Rullkotter, J. & Sinninghe-Damste, J. S. (1987). Restricted utility of the pristane/phytane ratio as a palaeoenvironmental indicator.*Nature*, 330, 641-643.

Thomas, B. M (1982). Land plant source rocks for oil and their significance in Australian basins. *Australian Petroleum Exploration Asssociation Jour.*, 22(1), 164-178.

Thompson, S., Cooper, B. S., Morley, R. J. and Barnard, P.C. (1985). Oil generating coals. **In**, B. M. Thomas *et al.* (eds.) Petroleum geochemistry in exploration of the Norwegian shelf. Graham & Trotman, London, 59-73.

Tissot, B. P. & Espitalie', J. (1975). L'evolution thermique de la matie're organique des se'diments : applications d'une simulation mathe'matique. Rev. Inst. Fr. Pe'trole, 30, 743-777.

Tissot, B. P. (1984). Recent advances in petroleum geochemistry applied to hydrocarbon exploration. *American Association of Petroleum Geologists Bull.*, 68(5), 545-563.

Tissot, B. P. & Welte, D. H. (1984). Petroleum formation and occurrence : A new approach to oil and gas exploration. Springer-Verlag, 699p.

Tissot, B., Pelet, R & Ungerer, P. H. (1987). Thermal history of sedimentary basins, maturation indices, and kinetics of oil and gas generation. *American Association of Petroleum Geologists Bull.*, 71, 1445-1466.

Toxopeus, Buiskool-, J. M. A. (1982). Selection criteria for the use of vitrinite reflectance as a maturity tool in petroleum exploration. *Jour. Petroleum Geology*, 5, 215.

Traverse, A. (1988). Paleopalynology. Allen & Unwin, Inc., 600p.

van Aarssen, B. G. K., Cox, H. C., Hoogendoorn, P. & de Leeuw, J. W. (1990). A cadinane biopolymer in fossil and extant dammar resins as a source for cadinanes and bicadinanes in crude oils from South East Asia. *Geochimica et Cosmochimica Acta*, 54, 3021-3031.

van Aarssen, B. G. K., Hessels, J. K. C., Abbink, O. A. & de Leeuw, J. W. (1992). The occurrence of polycyclic sesqui-, tri- and oligoterpenoids derived from a resinous polymeric cadinene in crude oils from southeast Asia. *Geochimica et Cosmochimica Acta*, 56, 1231-1246.

van Graas, G. W. (1990). Biomarker maturity parameters for high maturities : calibration of the working range up to the oil/condensate threshold. *Organic Geochemistry*, 16, 1025-1032.

Villar, H. J., Puttmann, W. & Wolf, M. (1988). Organic geochemistry and petrography of Tertiary coals and carbonaceous shales from Argentina. **In,** L. Mattavelli & L. Novelli (Eds.) *Advances in Organic Geochemistry 1987*, 1011-1021.

Volkman, J. K. (1986). A review of sterol biomarkers for marine and terrigenous organic matter. *Organic Geochemistry*, 9, 83-99.

Volkman, J. K. (1988). Biological marker compounds as indicators of the depositional environments of petroleum source rocks. **In,** A. J. Fleet *et. al.* (Eds.) Lacustrine petroleum source rocks, 103-122.

Wang, T., Chen, S. & Lin, J. (1991). Distribution of bitumen biomarkers in dry gas reservoirs and its application in dry gas migration. **In,** D. Manning (Ed.) Organic Geochemistry : Advances and applications in energy and the natural environment, *15th European Association of Organic Geochemists Meeting*. Extended abstract, 214-218.

Waples, D. W. (1980). Time and temperature in petroleum formation : Application of Lopatin's method to petroleum exploration. *American Association of Petroleum Geologists Bull.*, 64, 916-926.

Waples, D. W. (1985). Geochemistry in petroleum exploration. Boston, International Human Resources Development Corporation (IHRDC), 232p.

Waples, D. W. & Machihara, T. (1990). Application of sterane and triterpane biomarkers in petroleum exploration. *Bull. Canadian Petroleum Geology*, 38, 357-380.

Waples, D. W. & Machihara, T. (1991). Biomarkers for geologists - a practical guide to the application of steranes and triterpanes in petroleum geology. *American Association of Petroleum Geologists Bull.*, Methods in Exploration Series, No. 9, 91p.

Wardroper, A. M. K., Brooks, P. W., Humbertston, M. J. & Maxwell, J. R. (1977). Analysis of steranes and triterpanes in geolipid extracts by automatic classification of mass spectra, *Geochimica et Cosmochimica Acta*, 41, 499-510.

Westrich, J. T. & Berner, R. A. (1984). The role of sedimentary organic matter in bacterial sulfate reduction : The G model tested. *Limnol. Oceanogr.*, 29, 236-249.

Whittle, A. P. & Short, G. A. (1978). The petroleum geology of the Tembungo Field, east Malaysia. Proc. SEAPEX Conf., 18p.

Williams, H. H. et al (1985). The Palaeogene rift basin source rocks of Central Sumatra. **In,** Proc. Indonesian Petroleum Association 14th Annual Convention, Vol II : Jakarta, Indonesian Petroleum Association, 57-90.

Wold, S. (1978). Crossvalidatory estimation of the number of components in factor and principal components models. *Technometrics*, 20, 397-405.

Wood, D. A. (1988). Relationship between thermal maturity indices calculated using Arrhenius equation and Lopatin method : implications for petroleum exploration. *American Association of Petroleum Geologists Bull.*, 72(2), 115-134.

Yeh, H. W. & Epstein, S. (1981). Hydrogen and carbon isotopes of petroleum related organic matter. *Geochimica et Cosmochimica Acta*, 45, 753-762.

Yen, T. F. (1972). Terrestrial and extra terrestrial stable organic molecules. **In,** R. F. Landel & A. Rembaum (Eds.) Chemistry in Space Research, 105-153.

APPENDIX I

Organic Geochemical Techniques

I.1 DETERMINATION OF TOTAL ORGANIC CARBON CONTENT

I.1a Sample Preparation

About 2g of sample was weighed into a labelled centrifuge tube of known weight. 15% HCl (960ml of HCl SG 1.18 wt% + 1540ml deionised water) was carefully added to the samples. After waiting for effervescence to slow down, they were stood in an ultrasonic bath for 5 minutes. Having ensured that the acid was mixed properly with the sample, deionised water was added to the tubes which were then centrifuged for 10 minutes at 2000 rotations per minute (rpm). The tubes were removed from the centrifuge and the dilute acid decanted. The acidification procedure was repeated until all reaction had ceased. Once effervescence has totally stopped, deionised water was added to the tubes.

After centrifuging, the dilute acid was decanted, the sample mixed with distilled water and centrifuged again. This process was repeated until the liquid contents of the tube were neutral to pH indicator paper. As much deionised water as possible was drained off without any loss of the decarbonated sample. The samples were placed overnight in an oven at 40°C for drying. Once out of the oven, the samples were left to cool, then weighed. The drying and weighing process was repeated until weight of (sample + tube) becomes constant. From the recorded weight of the decarbonated sample, the carbonate content of each sample was calculated using the following equation:

$$\%CO_3 = \frac{\text{initial sample wt. - decarbonated sample wt.}}{\text{initial sample weight}} \times 100\%$$

About 100mg of the decarbonated sample was used for combustion in the Leco-IR 312 Carbon Analyzer. The total organic carbon content of the sample was then determined by adjusting the Leco result with the original sample weight to give the percentage weight of carbon:

$$\text{TOC (wt\%)} = \frac{\text{Leco result} \times \text{decarbonated sample weight}}{\text{initial sample weight}}$$

I.2 ROCK-EVAL PYROLYSIS

About 100mg of crushed whole rock sample was weighed and placed in the Rock-Eval 5 pyrolysis crucible which was then inserted into the instrument's furnace for combustion in an oxygen-free environment. The sample was heated over a specially programmed temperature

range of 300°C-600°C and the pyrolysates produced were swept away by the carrier gas (nitrogen) to the flame ionisation detector (FID) which measured the quantity of carbon.

I.3 SOLVENT EXTRACTION

I.3a Sample Selection and Preparation

Soxhlet extraction was performed on samples with high TOC contents (> 1.0 wt%), S1 peaks (> 0.2 mg/g) and production index values (> 0.2 mg/g). At least 15-25g of crushed sample was required for the extraction. All the samples were finely crushed using an agate mortar and pestle, and sieved using Endecotts Ltd. brass framed stainless steel mesh test sieve with an aperture size of 180 microns.

I.3b Sample Extraction

The sieved samples were placed in pre-extracted Whatman's double-thickness cellulose extraction thimbles (25 mm x 80 mm). They were then covered with pre-extracted cotton wool to ensure that the samples remained in the thimbles during extraction. The thimbles were placed in clean soxhlet extractors. 125ml of solvent was put in 250ml round bottom flask (solvent reservoir) together with some anti-bumping granules (boiling chips) to avoid too vigorous boiling, and copper granules for the removal of any free sulphur present in the samples. The extractor was assembled, enough solvent was added to cover the thimble and the condenser fitted. With the coolant flowing through the condenser, the heating mantle was switched on. The sample was extracted for at least 48 hours (4 x 12 hour durations) at 40°C. Fresh anti-bumping agents were added to the flask each time before re-commencing the extraction. More copper granules can also be added to the solvent at this time, if required.

I.3c Evaporation of Excess Solvent Using the Rotavapor

After the extraction was completed, the flask containing the extract (sample + solvent) was cooled and the solvent remaining in the extractor was added to that in the round bottom flask. The extracted residue left in the extraction thimbles was dried and saved for kerogen isolation procedure. The bulk of the solvent was evaporated on a rotary vacuum evaporator at a water-bath temperature of about 40°C. If necessary, more copper granules can be added for further sulphur reduction.

I.3d Sample Filtering

Once the volume of the extract had been considerably reduced, it was filtered twice; firstly, through a cotton-wool packed test tube, and secondly, through a filter paper, into a clean flask. The filter paper should be thoroughly washed with dichloromethane to flush all extract from it. The double filtering is important to ensure that neither the sample (those that may have been too finely crushed and have filtered through the extraction thimble walls) nor the reduced sulphur are collected as part of the Extractable Organic Matter, EOM, thus giving an incorrect EOM yield. The boiling chips and copper granules left in the flask were washed with dichloromethane 2-3 times to ensure that all the EOM had been retrieved. The extract was evaporated again to remove the excess solvent.

I.3e Determination of Extractable Organic Matter

After evaporation, the concentrated extract was transferred into a test tube of known weight. To determine the extractable organic matter (EOM), the extract was blow-dried with a stream of nitrogen on a heating block at 40°C until constant weight was achieved. This process removes all solvents, upon removal of which constant weight will be achieved. The extract weight, EOM, was recorded as ppm of the whole rock sample.

I.3f Separation Of The Saturates, Aromatics And NSOs From The Asphaltenes Using Excess N-Hexane

The separation of the maltene (aliphatics, aromatics and NSOs) and the asphaltene portions of the samples was achieved by adding excess n-hexane solvent to the test tube. After 5 minutes in an ultrasonic bath for the removal of any sample adhering to the test tube walls, they were centrifuged for 5 minutes. The asphaltenes precipitated out of solution and sunk to the bottom of the test tube while the maltene portion dissolved in the n-hexane solvent. The (maltene + solvent) was transferred into a clean test tube of known weight using a pipette. This treatment was repeated until the n-hexane was clear to ensure that all the maltene portion had been removed from the EOM sample. The solvent was evaporated off from the maltene by blowing with a stream of nitrogen. The remaining asphaltene + n-hexane solvent residue in the original test tube was blow dried by a nitrogen stream on a heating block and weighed. This process was repeated until a constant weight was achieved, which represented the asphaltene portion of the EOM. The asphaltene content was calculated as wt% of the original EOM. Ideally, the weights of the maltene and the asphaltene portions should add up to the weight of the EOM, i.e.

$$EOM = Maltene + Asphaltene$$

I.3g Fractionation of Bitumen

The maltene portion was separated into saturates, aromatics and NSO's by thin-layer chromatography. Glass plates were thinly coated with a silica-gel layer; the coating can be either 0.25, 0.5 or 1 mm thick depending upon the quantity of the maltene being separated. For 50mg or less of maltene weight, 0.5 mm thickness was used. For alkene/alkane separation, the silica gel contained 2.5% silver nitrate.

I.3h Preparation Of Plates For Thin-Layer Chromatography

For 20 x 20 cm plates:

0.50mm thick 60g silica gel + 120cm^3 water
0.25mm thick 30g silica gel + 60cm^3 water

The glass plates must be thoroughly clean for the silica-gel coating. After drying, the prepared silica-gel plates were dipped in dichloromethane to aid better separation of the aromatics, saturates and NSO's. The plates were placed in an oven at 110°C for about an hour before using to activate the silica-gel.

I.3i Sample Spotting

Having cleaned the edges of the prepared plate, a 1 inch strip was divided off on the left hand side for the standard. A standard solution of phenanthrene (0.2g) + std. alkanes (10-20 µl) + dichloromethane (200 µl) was spotted on the prepared strip. A concentrated solution of the

maltene portion in dichloromethane was then applied to the base of the plate with a pipette as a continuous line using a spotting guide. The plate was left to developed in a TLC tank containing petroleum spirit. After separation, the plate was sprayed with Rhodamine (6B) solution and left to dry before viewing under ultraviolet light. The appropriate areas on the plate corresponding to the required fractions were marked (from bottom up : NSO's, aromatics and saturates), referring to the standard strip for the respective boundaries. The silica-gel coating of the different fractions was then scraped off onto aluminium foil for temporary storage. The fractions were then individually eluted from the silica-gel by washing through a short column into 200ml round-bottom flasks. The short column was an open-ended test tube packed with cotton wool, followed by 2.5cm (1 inch) of silica-gel (35-70 mesh) and topped by the scraped silica-gel containing the sample. Each fraction was eluted with their respective solvents, which are methanol for the NSO's, petroleum spirit (ether) for the saturates and dichloromethane for the aromatics. Approximately 150ml of solvent was used for the elution of each fraction. The collected fractions were then evaporated using the rotavapor to remove the excess solvents. The water bath temperatures for the different solvents were as follows:

Solvent	**Temperature**
Methanol	65°C
Petroleum spirit	40.0 - 60.0°C (45°C)
Dichloromethane	40°C

When the volume of the fraction had considerably reduced, it was transferred into a weighed borosilicate glass specimen vial with a screw-on cap and blow-dried with a nitrogen stream to remove the remaining solvent until constant weight was achieved. The amount of the individual fractions are reported in ppm or weight percent.

I.4 GAS-CHROMATOGRAPHY

Analyses of the saturated hydrocarbon fractions were performed using a HP 5890A Gas Chromatograph equipped with a Flame Ionisation Detector (FID) and a 50 m x 0.31 mm fused silica capillary column coated with cross-linked methyl silicone (OV-1). The aromatic hydrocarbon fractions were analysed using a HP 5880A Gas Chromatograph equipped with a Flame Photometric Detector (FPD) and a Flame Ionisation Detector (FID), and two 50 m x 0.31 mm fused silica capillary column coated with cross-linked 5% phenyl methyl silicone (SE-54). The analytical conditions are as follows :

Injection port temperature	:	250°C
Detector port temperature	:	250°C
Initial time	:	2 min.
Final time	:	20 min.
Initial oven temperature	:	80°C
Final oven temperature	:	280°C
Programme rate	:	2°C/min.
Carrier gas	:	Helium
Flow rate	:	3 ml/min
Split ratio	:	10 : 1

The respective fractions were diluted with a small amount of dichloromethane prior to injection into the gas-chromatograph.

I.5 GAS-CHROMATOGRAPHY-MASS SPECTROMETRY

The gas chromatography-mass spectrometry technique provides biomarker profiles which give information on maturity and palaeo-environmental conditions at the time of deposition. The method uses the Varian 3400 capillary gas chromatograph equipped with an autosampler and data system using a temperature programme of 50°C for 1 minute then 5°C per minute to 320° C. A 25m x 0.22mm i.d. fused silica column coated with a cross bonded non-polar phase (CP-Sil 5B) was used. The Finnigan TSQ 70 triple quadrupole mass spectrometer was set to monitor and measure the triterpane (m/z 191) and sterane (m/z 217) biomarkers. A variety of other ions were used where necessary.

I.6 TANDEM GAS CHROMATOGRAPHY-MASS SPECTROMETRY

The TSQ 70 mass spectrometer can be operated in the GC-MS-MS mode if required, which enables the complete separation of complex mixtures. In this study, the main use for this method was to definitely ascertain the no co-elution of other compounds interfered with the compounds used for the maturity calculations. This problem mainly affects the steranes, therefore the equipment was set to monitor the sterane parent ions m/z 372, m/z 386 and m/z 400 for C_{27}, C_{28} and C_{29}, respectively. Also monitored was m/z 412 for resins as there were indications of resin peaks showing through the m/z 217 fragmentogram.

I.7 KEROGEN ISOLATION

The kerogen isolation procedure was performed in a fume cupboard on batches of ten samples per treatment. It involves the use of concentrated hydrochloric (15% HCl) and hydrofluoric (60% HF) acids for the elimination of carbonates and silicates, respectively. These acids are extremely hazardous as they are toxic and highly corrosive to the skin and the respiratory system (hence the use of the fume cupboard). Protective clothing (a plastic apron worn over a laboratory coat), a face mask, and thick gloves should be worn at all times when handling these chemicals. The stringent precautionary requirements when handling both chemicals should be strictly adhered to. When using hydrofluoric acid, it is also necessary for another person who is trained in the use of hydrofluoric acid to be present; this is to ensure that assistance will be close at hand should an accident occur.

I.7a Sample Preparation

About 20-30g of each sample, broken up into pieces of approximately 1mm size using a mortar and pestle to increase the surface area for reaction, were placed into tall polypropylene beakers. Hydrofluoric acid necessitates the use of polypropylene beakers because they are resistant to the acid's corrosive nature.

I.7b Addition of HCl

100ml of 15% HCl was added to the samples and stirred carefully with polypropylene rods. The samples were gently crushed using the stirring rods (note down any reactions). Using 15% hydrochloric acid will eliminate dolomite and siderite present in the samples. The samples were then left for two hours before being re-stirred and left overnight.

I.7c Sample Neutralisation

Decant as much spent hydrochloric acid as possible, carefully avoiding any sample loss, into a waste bottle for later neutralisation. Once the acid have been decanted, deionised water was added to the samples which were stirred and left to settle for at least three hours before the dilute acid washings were decanted into a bucket. Usually, three to four washes are required to fully neutralise the samples, depending upon how much of the spent hydrochloric acid was initially decanted off. Litmus paper was used to check the samples' neutrality.

I.7d HCl Waste Neutralisation

The concentrated hydrochloric acid wastes were neutralised according to the following procedure while waiting for the samples to settle from the first wash. Approximately 250ml of the concentrated hydrochloric acid waste was added to a bucket which was half full of water. The solution was well mixed using a stirrer; it was gently stirred whilst a 50% sodium hydroxide solution (1 part sodium hydroxide and 2 parts of water, by volume) was poured into it. Take care to continue stirring to disperse the heat generated during the exothermic neutralisation reaction. The solution's acidity level was checked with litmus paper. Once the waste was neutralised, it was left for about one hour to allow any sludge formed to settle before disposing the clear, neutral solution into the drainhole. The neutral sludge left behind was stored in a plastic container and allowed to dry out in a fume cupboard. This procedure was repeated until all the concentrated hydrochloric wastes were neutralised. With the diluted hydrochloric wastes from the sample washes, the procedure was exactly similar. The only difference was that they do not have to be diluted prior to the addition of caustic soda solution, as opposed to the concentrated waste. The waste container must also be neutralised by rinsing it with the sodium hydroxide solution.

I.7e Addition of HF

50ml of hydrofluoric acid were then added to the samples very carefully to prevent spillages, and were stirred gently. A small amount of 15% hydrochloric acid was added to the samples in order to avoid the formation of fluoro-silicates which would be difficult to eliminate once formed. Any free ions in the solution would react with the hydrochloric acid to form chlorides which could be easily disposed during sample washing for they are soluble in water. The samples were left for two hours, then re-stirred and left to settle overnight. The spent hydrofluoric acid was carefully decanted off as much as possible without sample loss into a HF acid waste container. Fresh hydrofluoric acid and a small amount of 15% hydrochloric acid were added to the samples, and the samples stirred carefully. They were re-stirred after two hours, then left to settle overnight. Again, the spent hydrofluoric acid was decanted into the HF acid waste bottle. It is advisable to attempt decanting off as much hydrofluoric acid as possible

at this stage because this will help reduce the number of sample washes required to neutralise the samples.

I.7f Sample Neutralisation

The samples were washed with deionised water, left for a minimum of three hours to settle before decanting the dilute hydrochloric (FLUORIC) acid solution into a bucket and re-washed. The samples' neutrality were checked after every wash with litmus paper. Commonly, three to four washes were necessary before the samples are fully neutralised.

I.7g HF Waste Neutralisation

While waiting for the samples to settle between washes, the hydrofluoric acid wastes should be neutralised, much in the same way as the hydrochloric acid waste neutralisation procedure. The main differences were that, no more than 100ml of concentrated hydrofluoric acid waste should be added to the bucket half-full of water for each neutralisation, and a thirty-minute time lapse was required between additions of the sodium hydroxide solution to the diluted waste. The reason for this is that the neutralisation of hydrofluoric acid waste generates much more heat energy during the exothermic reaction compared to hydrochloric acid waste. Rushing the neutralisation process of hydrofluoric acid waste by adding too much sodium hydroxide solution too quickly will result in the generation of too much heat energy which the bucket cannot possibly withstand, leading to a potentially dangerous 'blow-out'.

I.7h Storage of Isolated Kerogen

After being neutralised, the carbonate- and silicate-free kerogen were transferred into labelled plastic tubes. They were then divided into two portions after vigorously shaking the tube before quickly separating them to ensure homogeneity between the two divided portions; one for the density separation analysis, while the other for mounting on resin blocks for vitrinite reflectance measurements and for making slides for observation under a transmitted-light microscope.

I.8 DENSITY SEPARATION

Six zinc bromide solutions of different specific gravities of 1.28, 1.34, 1.45, 1.65, 1.81 to 2.20 were used for the density separation. Below are the ratios of zinc bromide to hydrochloric acid to make up the necessary solutions:

		$ZnBr_2$ [76% (wt/wt)]	:	0.1N hydrochloric acid*
	1) S.G. 2.2	10	:	3
		$ZnBr_2$ (S.G. 2.2)	:	**0.1N hydrochloric acid**
	2) S.G. 1.28	1	:	4
	3) S.G. 1.34	1	:	3
	4) S.G. 1.45	1	:	2
	5) S.G. 1.65	1	:	1
	6) S.G. 1.81	1	:	0.5
		HCl [36% (wt/wt)]	:	**deionised water**
*	0.1N HCl	22ml	:	228 ml

The specific gravities of the zinc bromide solutions were checked using the specific gravity bottle to obtain the weights of deionised water and the respective zinc bromide solutions. The specific gravity of a particular zinc bromide solution is given by ratio of the weight of the zinc bromide solution to that of the deionised water, i.e.

$$\text{Specific Gravity} = \frac{\text{weight of } ZnBr_2 \text{ solution}}{\text{weight of deionised water}}$$

I.8a Density Separation with SG 1.28 $ZnBr_2$ solution

Starting with $ZnBr_2$ solution of S.G. 1.28, the kerogen concentrates were sequentially centrifuged with $ZnBr_2$ solutions of higher densities. Firstly, the kerogen samples were centrifuged for 10 minutes at 2000 rotations per minute (rpm) to dewater them. The deionised water was carefully discarded to avoid any sample loss. About 10ml of $ZnBr_2$ solution of S.G. 1.28 was then added to the samples and shaken vigorously to ensure that the kerogen were thoroughly dispersed in the $ZnBr_2$ solution. The samples were centrifuged for 20 minutes at 2000 rpm for the density separation to take place.

I.8b Separation of 'float' and 'sink'

The sample tubes were gently removed from the centrifuge; note whether there were any separations into 'float' and 'sink' portions, and whether the separations were clear or indistinct (indicated by colloidal $ZnBr_2$ column). The kerogens may, or may not, have separated depending upon their compositions. After using a small spatula to release parts of the 'float' portion which may be adhering to the sides of the tubes, the $ZnBr_2$ solution and the 'float' were slowly poured into a new, labelled sample tube, being very careful not to disturb the bottom 'sink' portion.

I.8c Washing of 'sink' and 'float' with 0.1N HCl

Once the 'float' had been separated from the 'sink', they were both washed three times with 0.1N hydrochloric acid to remove the $ZnBr_2$ solution S.G. 1.28, centrifuged at 2000 rpm for 10 minutes per each wash.

I.8d Sample Neutralisation

The 'float' was neutralised with deionised water and left aside for slide making. The 'sink' does not have to be neutralised; after the third washing with 0.1N hydrochloric acid, as much acid as possible was discarded without losing any of the sample. 10ml of the next $ZnBr_2$ solution ie S.G. 1.34 was added and the above procedure was repeated. The final 'sink' portion of $ZnBr_2$ solution S.G. 2.20 must be neutralised and retained, should any future need for its inspection arise.

I.8e Slides

Quantitative estimations of the respective fractions were made after the density separation procedure was completed. Slides of each density fraction and the hydrofluoric acid residue of each sample were made for kerogen typing and maturity determination by observation under transmitted-light and reflected-light microscopes.

I.8f Total Organic Matter Fraction

Mineral-free Total Organic Matter (TOM) mixtures were prepared for determination of kerogen elemental composition by mixing equal proportions (20ml) of each density fraction together. At least two slides of each TOM mixture were made. The TOM mixtures were then dewatered and left to dry in an oven at 38°C in a nitrogen atmosphere. Once these are dry, they are crushed for elemental analysis.

I.9 PETROGRAPHIC EXAMINATION

I.9a Kerogen Typing

Strewn slides made from the hydrofluoric acid residues, Total Organic Matter fractions and the density separation fractions were observed under transmitted- and ultraviolet light using a Leitz MPV2 microscope at the British Gas London Research Station. Point counting was done to determine the kerogen composition using a ten channel point counter. Eight channels were used and labelled as such: amorphous (fluorescing), amorphous (non-fluorescing), black woody particles, brown woody particles, palynomorphs (spores and pollen), membraneous particles (cuticular fragments), marine structures (foraminifera linings) and fungal spores.

I.9b Vitrinite Reflectance Measurement

The resin blocks were made at the British Gas London Research Station. Dried kerogen concentrates were put into pre-labelled 5mm diameter glass bottles. The resin mix (100ml epoxy resin + 25 drops of hardener) were prepared and poured into the bottles, just enough to cover the kerogen. The resin and kerogen were mixed well with a glass stirrer, then left to set. Once set, more resin mix were poured into the bottles until about 3/4 of the bottle height. These were left overnight to set.

The bottles containing the 'kerogen core' were individually wrapped in a piece of clean cloth and were broken using a steel mortar and pestle. Extreme caution was exercised when doing this; protective glasses and thick gloves were essential. Once released, the kerogen cores were cleaned of any adhering glasss fragments and immediately placed in labelled block moulds to avoid sample mix-up. About 1 cm of resin mix was then poured into the block mould while holding the core upright in the middle of the mould. Once set, more resin mix was poured to fill up the moulds and left to harden before being removed from the moulds for polishing. It is important for the sample numbers to be immediately engraved on the resin blocks once out of their moulds.

Block polishing involved seven stages, the first three used decreasing grades of carborundum paper while the last four used optical finishing alumina powders of 5 micron, 1 micron, 0.3 micron and 0.03 micron grades. After polishing, the resin blocks were left to dry in an oven at 30°C before making any vitrinite reflectance measurements. This is because it is thought that water may suppress vitrinite reflectance (Carr, pers. comm., 1992).

The vitrinite reflectance values were measured on a Leitz MPV2 photometric microscope in immersion oil with a refractive index of 1.518. Calibration of the microscope was made using spinel (reflectance of 0.415%) and ytrium aluminium garnet (reflectance of 0.917%). Sample

measurements were made in white light following calibration. The reflectance is measured using a green filter with a peak transmission of 546 nm. The majority of the measurements were made on vitrinitic wisps while rounded vitrinite particles were avoided. A total of 50 to 100 measurements were made per sample and histograms were drawn based on the results to determine the average vitrinite reflectance value of the sample.

I.10 ELEMENTAL ANALYSIS

I.10a Carbon, Hydrogen and Nitrogen Analyses

About 2 to 3 micrograms of the dried Total Organic Matter (TOM) fraction were weighed out in clean nickel boats and kept in a desicator, ready for analysis. The time duration for the complete elemental analysis of one sample is 12 minutes. Conditioning and blank runs should precede all analytical runs and the sensitivity factors for carbon, hydrogen and nitrogen were then determined from an accurately weighed acetanilide standard compound of microanalytical grade. The sensitivity factors are used for calculating the carbon, hydrogen and nitrogen contents of the kerogen samples analysed.

To begin the analysis, the nickel boat containing the sample is placed into the magnetically operated ladle and inserted into the sample entrance. After replacing the stopper and pressing the START button, helium gas will flush the entire system with for about 90 seconds. This is followed by the flushing of the combustion train is with oxygen for 30 seconds. When the INJ-COMB button lights up, the sample boat is inserted into the combustion chamber; pressing the INJ-COMB button will initiate the sample combustion in helium (oven temperature : 975°C± 25°C). The gases produced from the combustion will then pass through the oxidation furnace temperature : 670°C ±25°C). The reduced gases proceeds through the H_2O and CO_2 traps to the detectors (Perkin Elmer Handbook, 1986). The Data Station records the results in weight per cent (wt%) element.

I.10b Oxygen Analysis

As with the CHN analysis, conditioning and blank runs were made prior to sample analysis. For oxygen analysis, the standard compound used is microanalytical grade benzoic acid. About 2 to 3 micrograms of sample were pyrolysed in helium at 975°C over platinised carbon where the resulting oxygen is converted to carbon monoxide. The carbon monoxide and the other gases pass through free copper at 900°C and through an external U-tube of Colorcarb where the acid gases are removed. The carbon monoxide and remaining gasses pass through copper oxide at 670°C where the CO is converted to CO_2 and all the basic gases are removed by a water trap (Perkin Elmer Handbook, 1986). The results are recorded by the Perkin Elmer 240 Data Station.

APPENDIX II

Photographs of isolated kerogen

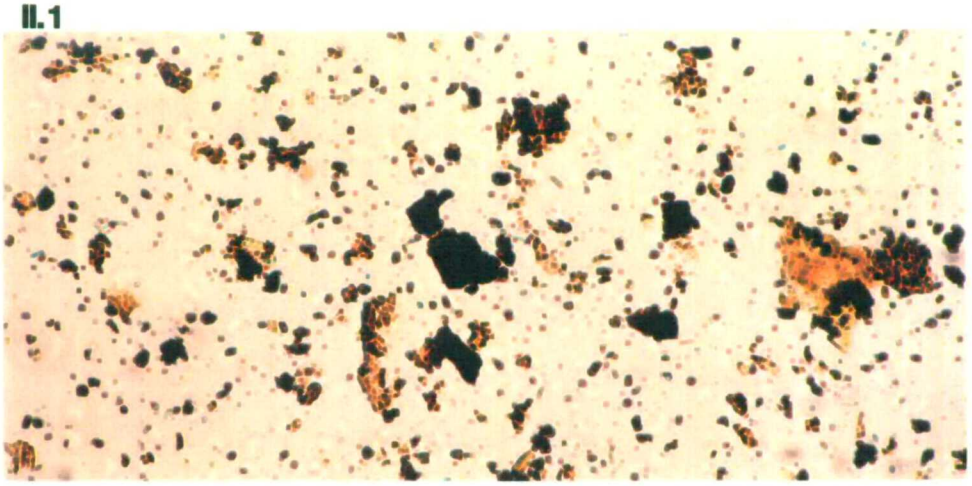
FIGURE II.1 Sample : South Furious-2, Stage III. Organic matter seen under transmitted white-light. Magnification : 200x.

FIGURE II.2 Sample : South Furious-2, sub-Stage IVA. Organic matter seen under transmitted white-light. Magnification : 200x.

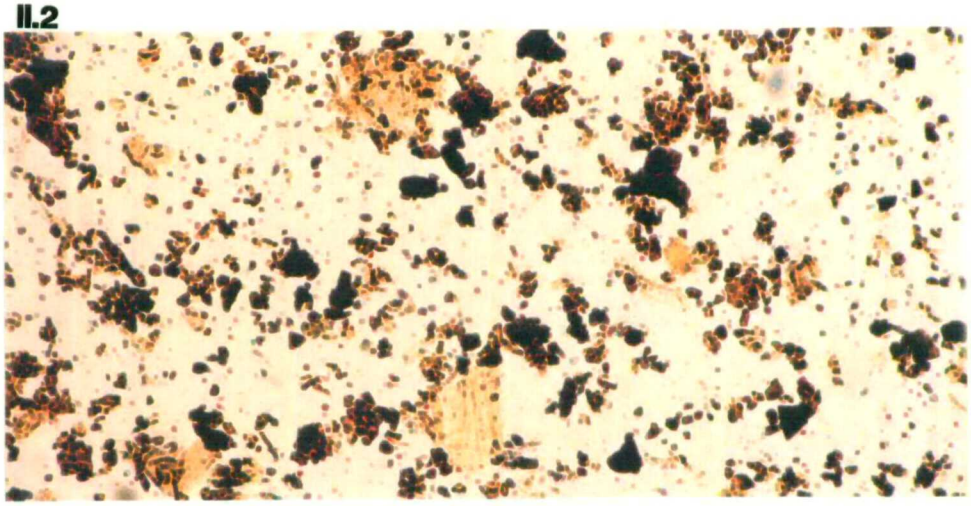
FIGURE II.3 Sample : South Furious-3, Stage III. Organic matter seen under transmitted white-light. Magnification : 400x.

FIGURE II.4 Sample : South Furious-3, sub-Stage IVA. Organic matter seen under transmitted white-light. Magnification : 200x.

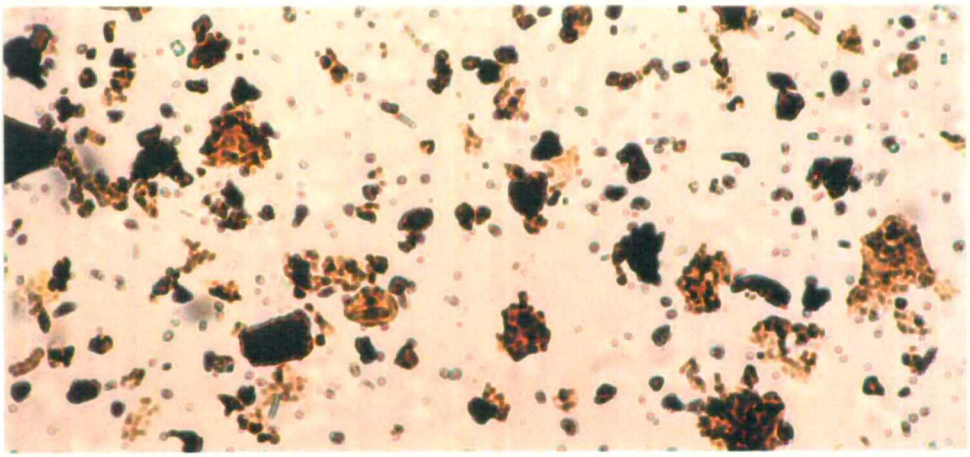
II.1



II.2



II.3



II.4

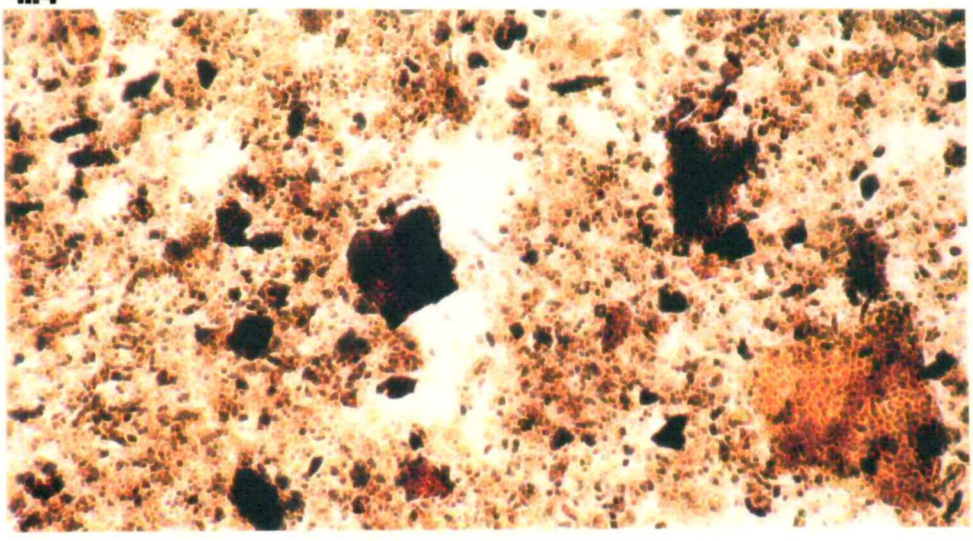


FIGURE II.5 Sample : Rusa Timur-1, sub-Stage IVA. **(a)** Fluorescing organic matter under ultra-violet light. **(b)** similar view as in **(a)** under transmitted white-light, showing some amorphous characteristics. The 'amorphousness' is thought to be due to degradation of Type III organic matter. Magnification : 400x.

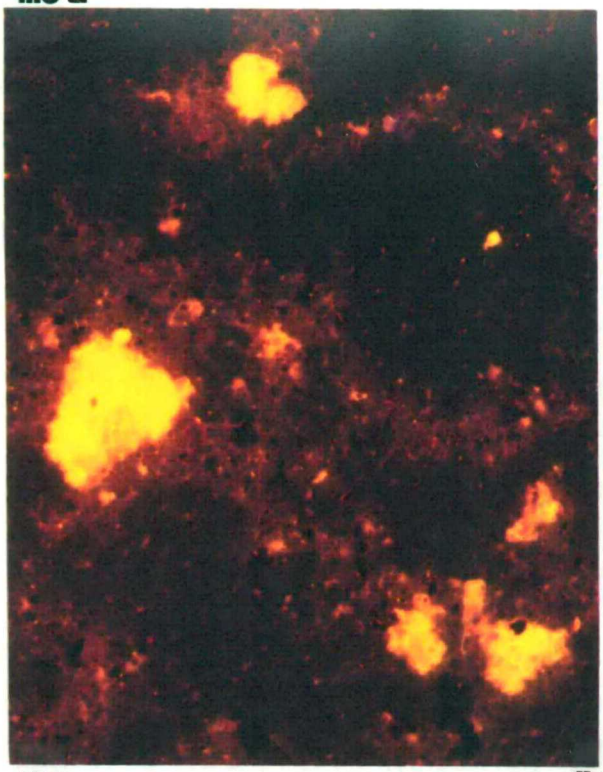
FIGURE II.6 Sample : Rusa Timur-1, sub-Stage IVA. Organic matter seen under transmitted white-light. Magnification : 400x.

FIGURE II.7 Sample : Rusa Timur-1, sub-Stage IVB. Cuticular fragments (arrow) seen under transmitted white-light. magnification : 400x.

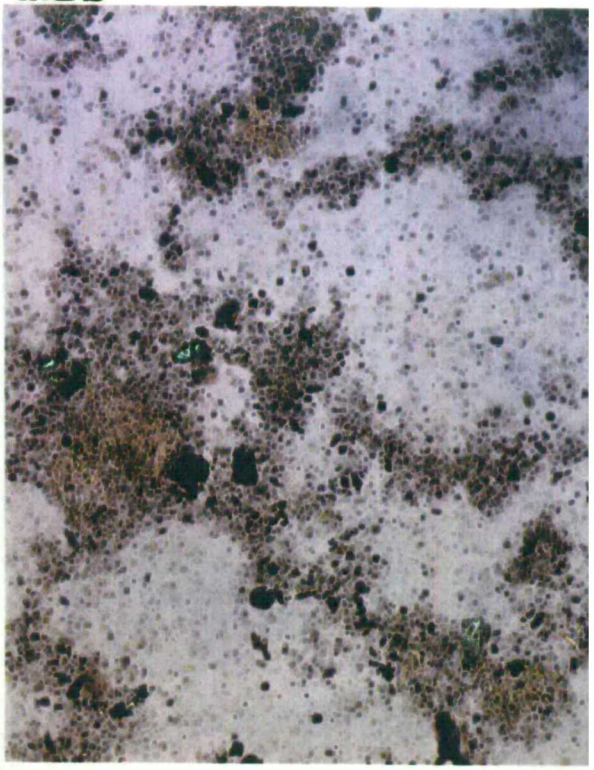
FIGURE II.8 Sample : Rusa Timur-1, sub-Stage IVB. A resinous particle under transmitted white-light. Magnification : 100x.

FIGURE II.9 Sample : Gajah Hitam-1, sub-Stage IVC. Degraded cuticular fragments seen under transmitted white-light. Magnification : 400x.

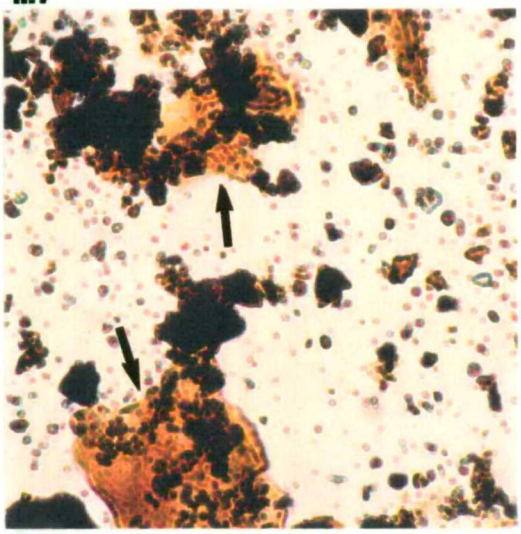
II.5 a



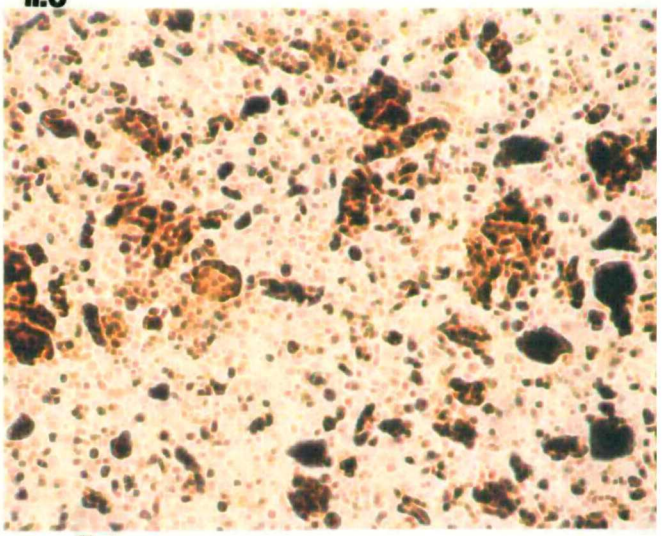
II.5b



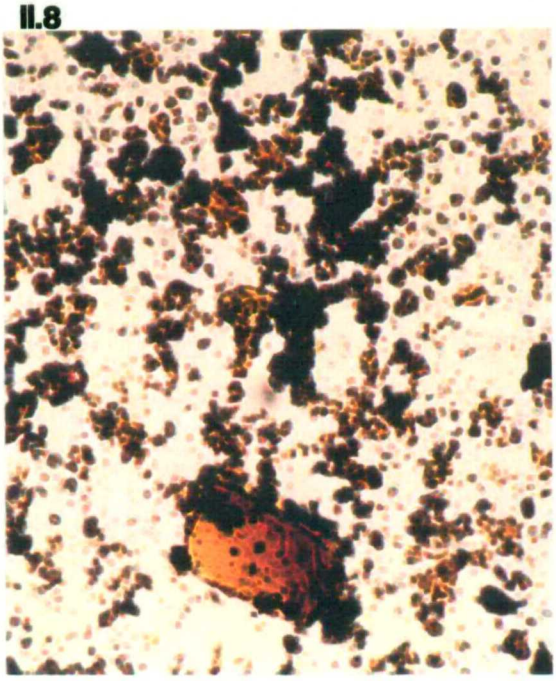
II.7



II.6



II.8



II.9

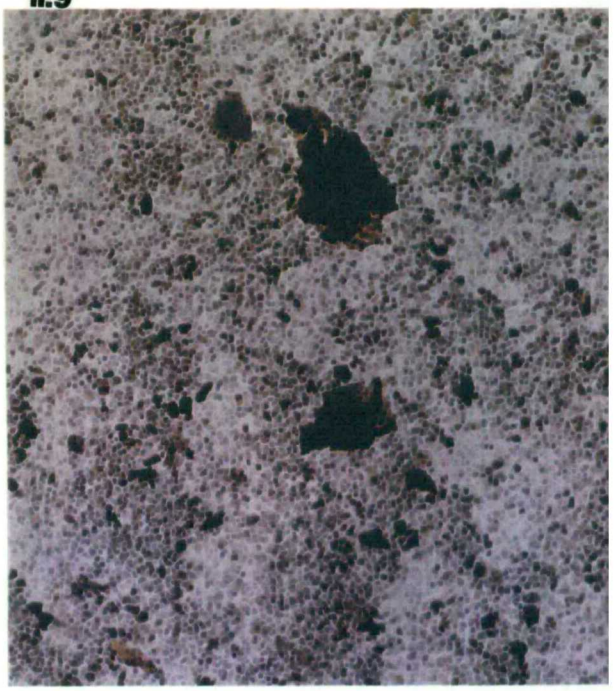
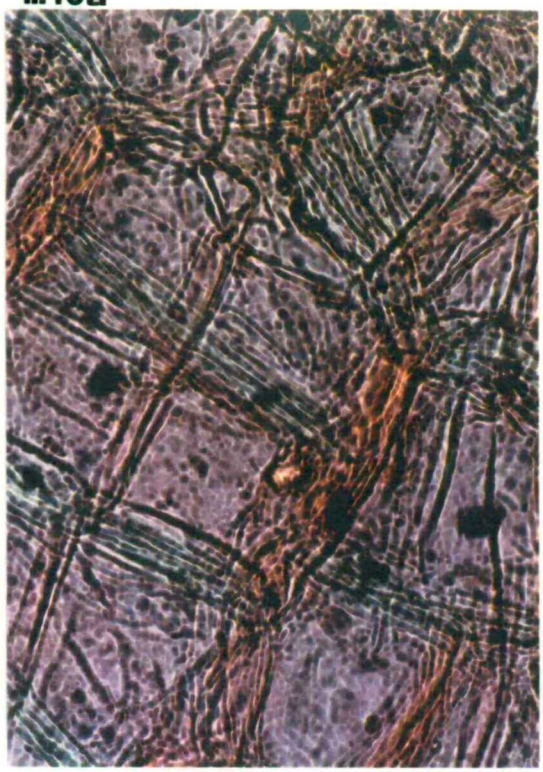


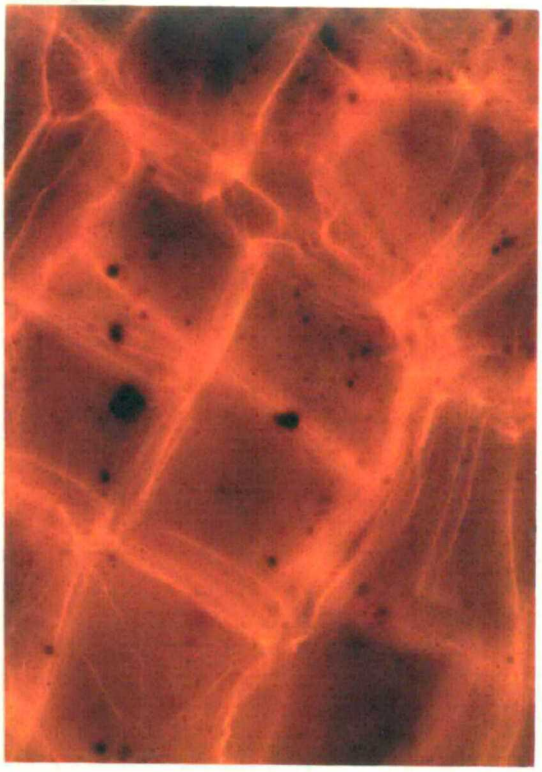
FIGURE II.10 Sample : South Furious-3, sub-Stage IVA. **(a)** Cellular structure of a cuticle seen under transmitted white-light. **(b)** The same cuticular fragment fluorescing under ultra-violet light. Magnification : 1200x.

FIGURE II.11 Sample : South Furious-2, sub-Stage IVA. **(a)** An organic matter particle seen as opaque under transmitted white-light but fluoresces under ultra-violet light, as shown in**(b)**. Magnification : 1000x.

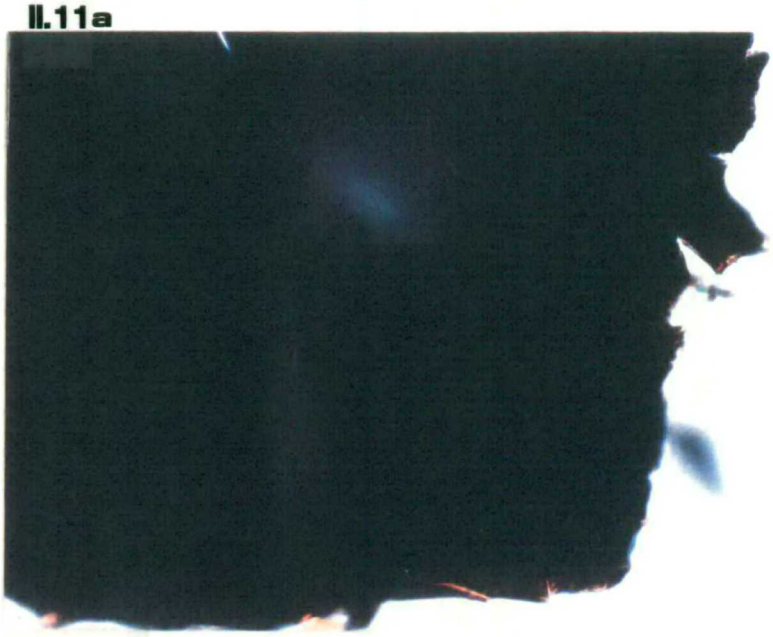
II.10a



II.10b



II.11a



II.11b

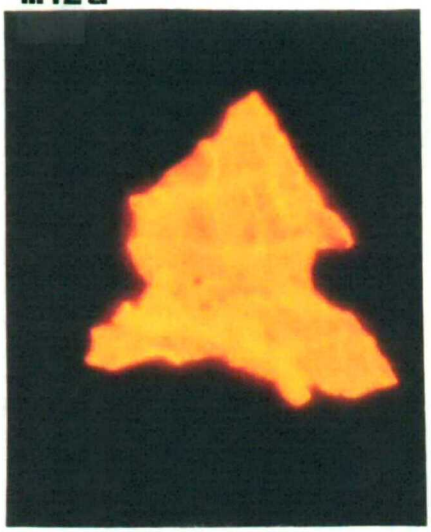


FIGURE II.12 Sample : South Furious-2, Stage III. **(a)** A piece of cuticle fluorescing under ultra-violet light **(b)** The same cuticle under transmitted white-light; its cellular structure can be easily observed. Magnification = 1250x.

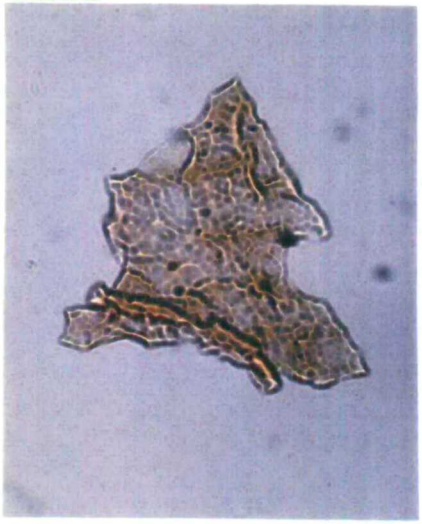
FIGURE II.13 Sample : Rusa Timur-1, sub-Stage IVA. **(a)** Hydrocarbon globules seen being expelled from an amorphous organic matter under ultra-violet light. The 'amorphousness' is though to be the result of mechanical degradation of terrigenous organic matter as no organic geochemical evidence has been found for marine input **(b)** The same organic matter under transmitted white light. Magnification = 1250x.

FIGURE II.14 Sample : Rusa Timur-1, sub-Stage IVA. **(a)** A resinous particle fluorescing under ultra-violet light **(b)** The same particle seen under transmitted white-light. Magnification = 1250x.

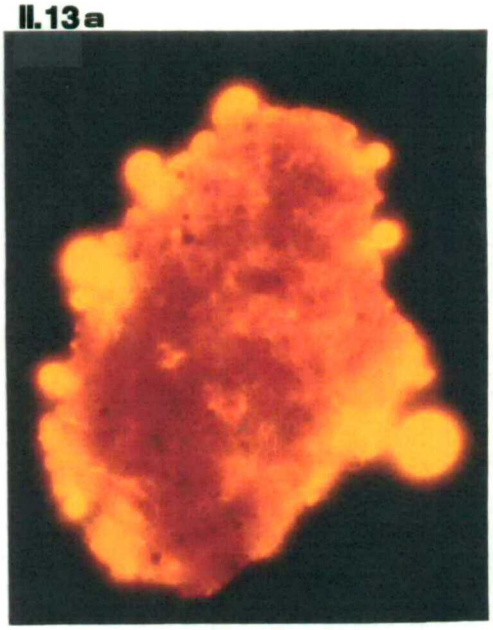
II.12a



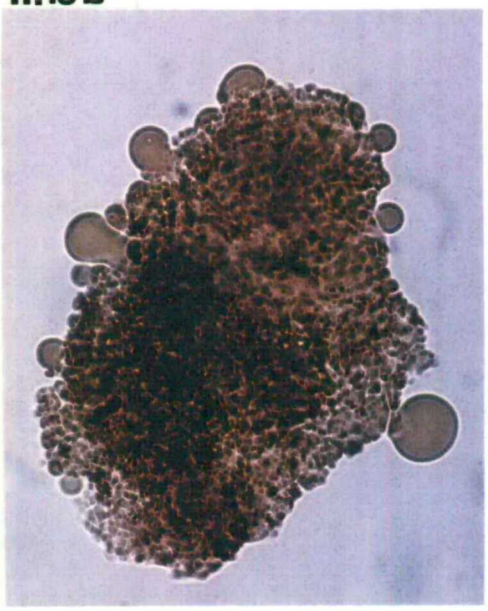
II.12b



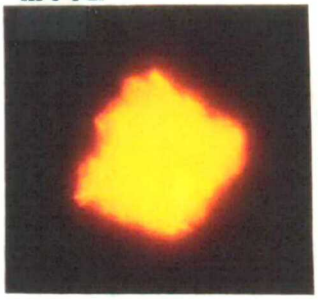
II.13a



II.13b



II.14a



II.14b

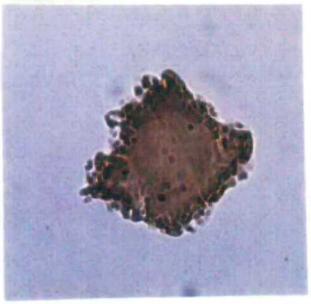


FIGURE II.15 Sample : South Furious-3, Stage III. The greenish-yellow colour of the palynomorph (indicated by arrow) indicates sediment immaturity. Transmitted-light, magnification = 400x.

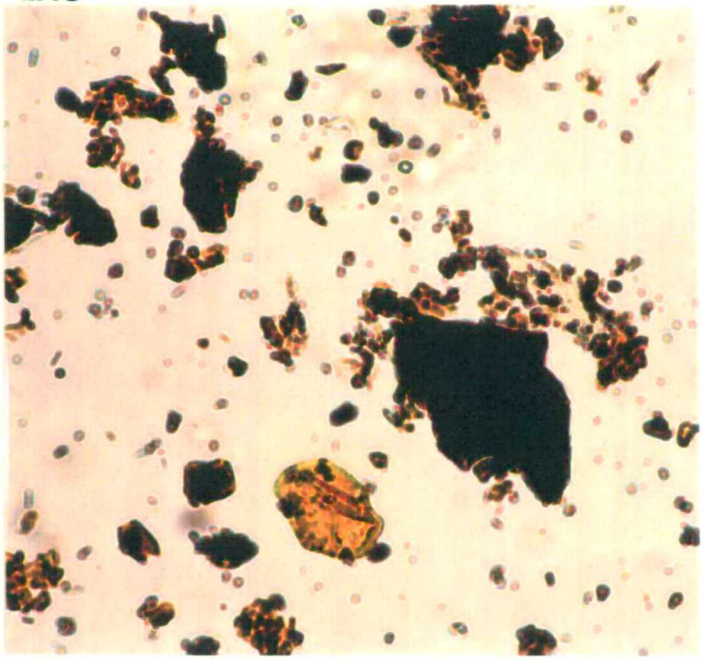
FIGURE II.16 Sample : South Furious-2, sub-Stage IVA. An example of a large woody particle. Transmitted-light, magnification = 200x.

FIGURE II.17 Sample : South Furious-2, sub-Stage IVA. A broken palynomorph; its pale green colour indicates the immaturity of the sediments. Transmitted-light, magnification = 400x.

FIGURE II.18 Sample : South Furious-3, sub-Stage IVA. An example of a mangrove pollen, *Sonneratia*. Transmitted-light, magnification = 400x.

FIGURE II.19 Sample : South Furious-2, sub-Stage IVA. Foraminiferal lining. Its occurrence is very rare in sediments analysed in this study. Transmitted-light, magnification = 400x.

II.15



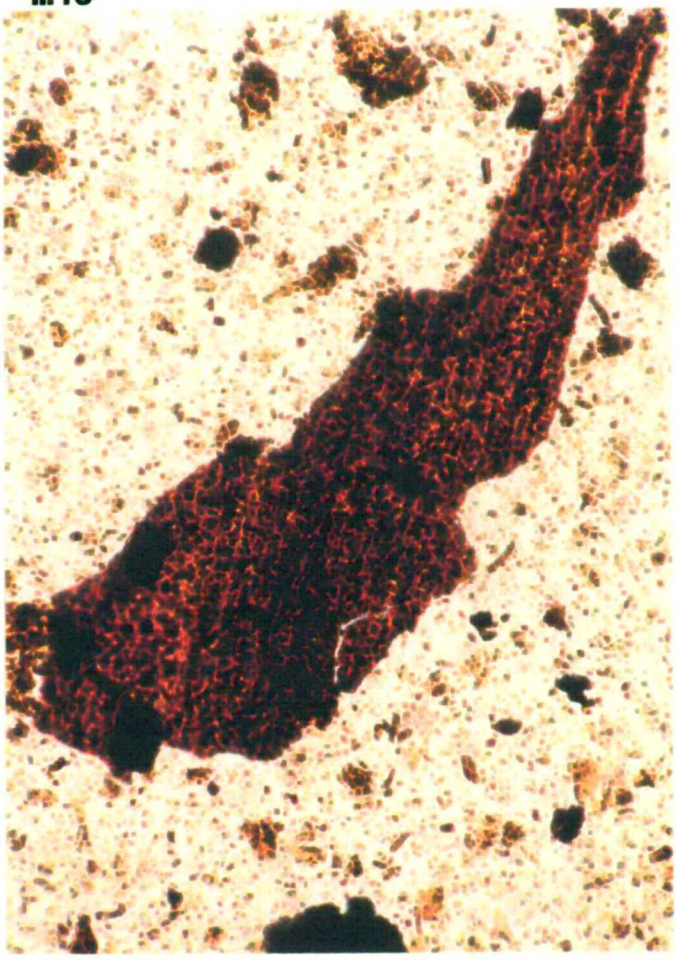
II.17



II.18



II.16



II.19



APPENDIX III
Abstracts of Presented Work

ABSTRACT 1

Enclosed is an extended abstract to a poster presented at the European Association of Organic Geochemists 16th International Meeting on Organic Geochemistry (20-24 September, 1993) in Stavanger, Norway. It is published in : K. Oygard (Ed.) EAOG Poster sessions from the 16th International Meeting on Organic Geochemistry, Stavanger, 1993, 67-72.

1.18 Source rock evaluation and thermal maturity of middle-late miocene sequence in the Northern part of Sabah Basin, Malaysia

A. Anuar [1,2], R.R.F. Kinghorn, [2], M.J. Cocksedge [3] & A.D. Carr [3]

[1] PETRONAS Petroleum Research & Scientific Services, 542000 Kuala Lumpur, Malaysia
[2] Geology Department, Imperial College, London SW7 2BP
[3] British Gas plc, London Research Station, London SW6 2AD

INTRODUCTION

The 350km by 140km Tertiary Sabah Basin (figure 1) contains about 10km of sediments in its deepest part and is bounded on the east by an accretionary prism formed during the opening of the South China Sea between Middle Oligocene and Early Miocene (Taylor & Hayes, 1980). Rapid subsidence accompanied by high sediment influx during the Middle-Late Miocene led to the accumulation of a thick sedimentary sequence. The basin's stratigraphic framework is defined by four chronostratigraphic units called Stages I to IV (Bol & van Hoorn, 1980). The prospective Stage IV is further divided into 7 sub-Stages and Stage III is currently considered as the economic basement. Results from this study show that deltaic-lower coastal plain sediments are responsible for the hydrocarbons in the proximal part of the basin while deep-marine sediments containing terrigenous organic matter are the likely sources for the hydrocarbons encountered in the distal part of the basin. Maturity level determination by several parameters revealed an odd behaviour pattern of the oleanane parameter, triterpane and sterane biomarker ratios (figure 2) commonly employed to assess the maturity levels of sedimentary sequences.

ORGANIC GEOCHEMICAL TECHNIQUES

The analyses include TOC determination and pyrolysis for crushed whole rock sample; density separation, elemental analysis, visual study and VRo measurement for kerogen concentrates; and GC and GC-MS for sediment extracts and oils.

RESULTS

Type III kerogen is dominant even in marine sequences and almost all the samples have low Hydrogen Index (HI) and Genetic Potentials (GP), less than considered necessary for the accumulation of hydrocarbons (Table 1). Examination of strewn slides revealed the presence of cuticular fragments, palynomorphs, resinous material and both brown and black woody particles. The abundance and type of organic matter vary with their environment of deposition, the most significant being the apparent enrichment of exinitic particles further offshore (figure 3). All maturity indicators confirm the immaturity of the sediments analysed; however, the biomarker

maturity parameters decrease with depth, inconsistent with normal diagenetic evolution (MacKenzie & Maxwell, 1981).

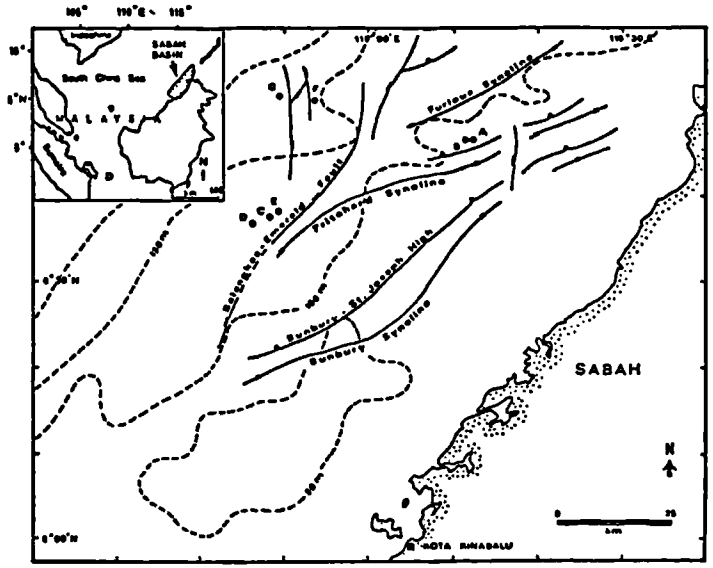


Fig. 1. Location and generalised structural map of the northern Sabah Basin. The study area is marked by the black box and the wells included in this study are labelled A to G.

DISCUSSION OF RESULTS

None of the analysed sediments is the effective source rock for the basin's hydrocarbons, Stage IV, however, does contain several horizons of potential source rocks and there are three hydrocarbon kitchens in which these horizons have already reached the hydrocarbon-generating window; the Pritchard and Furious Synclines, and the graben between Wells F and G. The results indicate that the source rocks are not restricted to any particular sub-Stage but are controlled by sedimentary facies, and by preferential enrichment of H-rich particles. The low HI may reflect intermixing of good and poor quality kerogen. The success of the marginal source rocks is attributed to their great thickness (2000m) aided by effective migration and drainage provided by the numerous interbedded sandstones, and possible early hydrocarbon generation due to rapid burial. The anomalous behaviour of the biomarker maturity parameters suggests that factors other than thermal maturation may play a role. Selective biodegradation of the 20R isomer at shallower depths can result in the inversion of the ratio. Facies changes in the Sabah Basin, rapid subsidence and high burial rates may also have influenced the chemical reactions of the biomarkers.

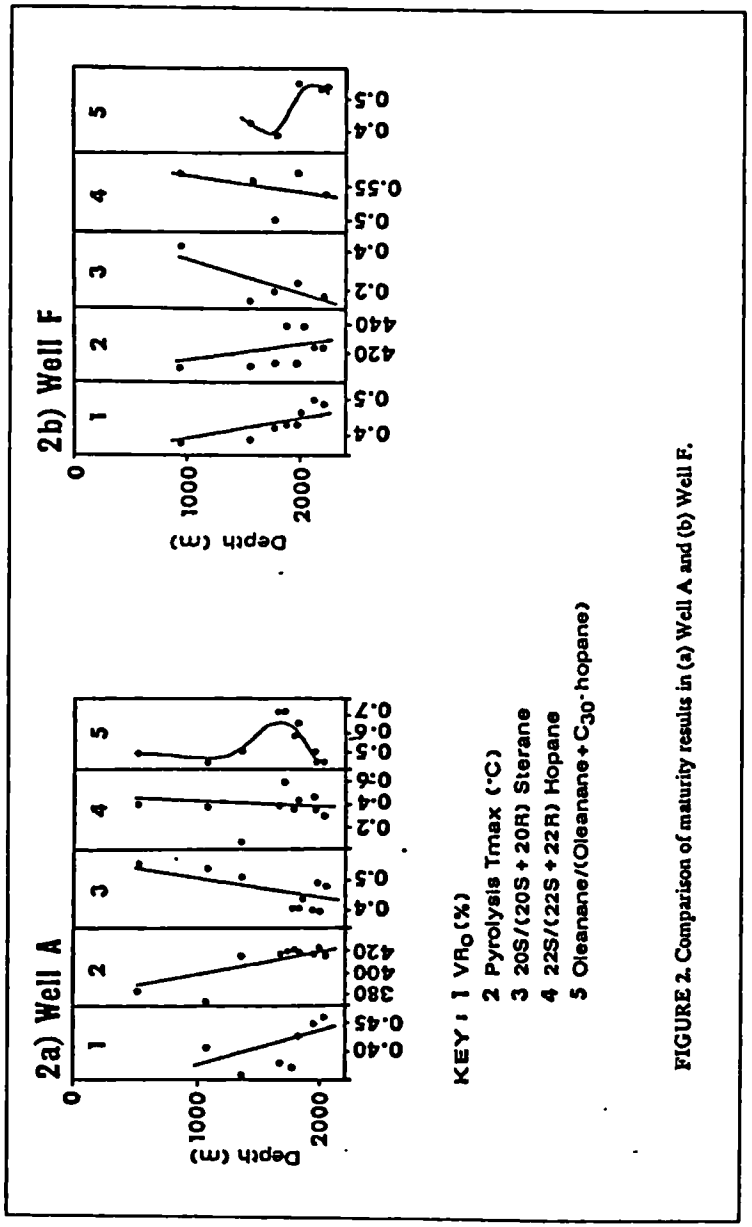


FIGURE 2. Comparison of maturity results in (a) Well A and (b) Well F.

Appendix III

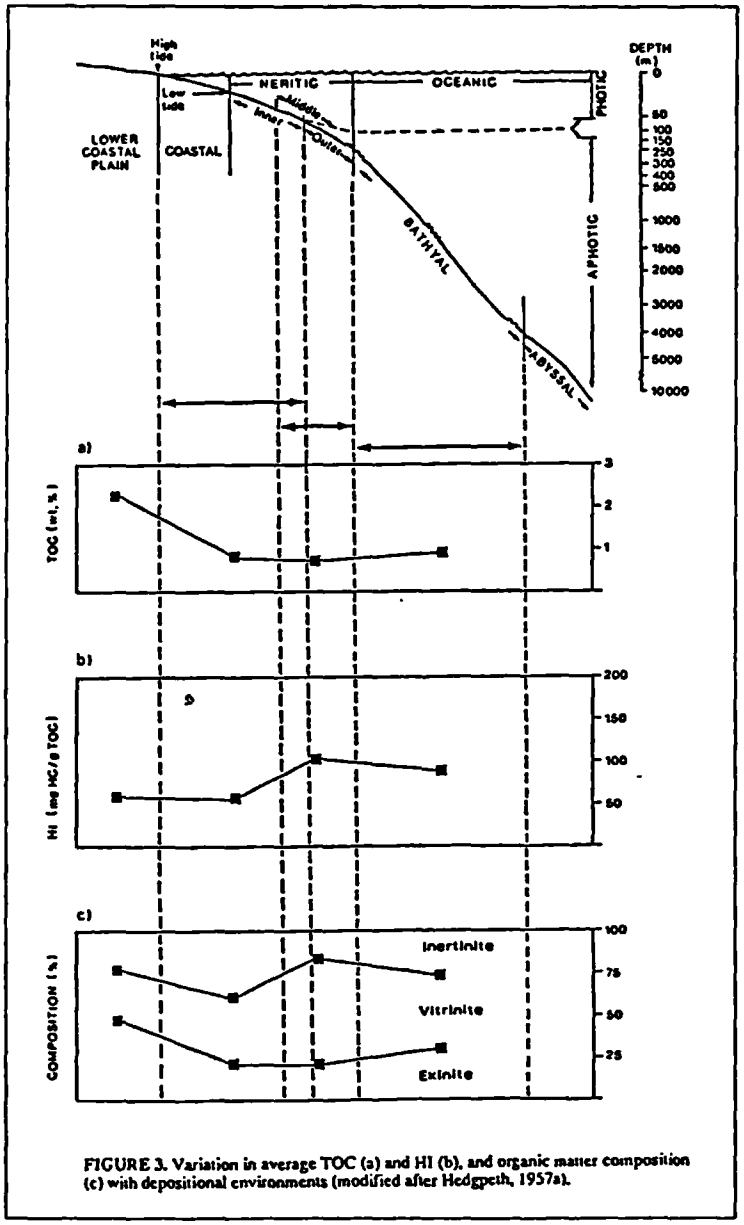


FIGURE 3. Variation in average TOC (a) and HI (b), and organic matter composition (c) with depositional environments (modified after Hedgpeth, 1957a).

WELL	STAGE	TOC (wt%)	GP (mg/g)	HI (mg/gTOC)	Tmax (°C)
C	IVD	1.05	0.69	68	427
D		0.75	0.95	80	409
E		0.52	0.30	48	419
F		0.87	2.34	169	426
G		0.82	0.41	47	425
C	IVC	0.78	0.81	80	436
D		1.00	1.94	138	417
E		0.72	0.58	62	428
F		1.00	1.97	152	422
G		0.84	0.50	85	440
F	IVB	0.84	1.60	142	425
A	IVA	1.44	1.08	59	414
B		3.07	2.52	62	422
F		0.83	1.47	154	425
A	III	2.24	1.70	68	417
B		1.60	1.60	87	425

Table 1. Average screening results.

CONCLUSIONS

1. The Sabah Basin hydrocarbons are sourced by Type III kerogen present in deltaic-lower coastal plain sediments nearer inshore and in deep-marine sediments further offshore. Selective transportation caused the enrichment of H-rich terrigenous particles in the marine sediments. The marginal source quality is offset by large sediment volume and good drainage.

2. Biomarker maturity indicators may not be useful here, seeming to be influenced by factors other than thermal maturation.

Acknowledgements: This project is funded by and presented with permission from PETRONAS PRSS. Thanks to Dr. K. Ngah for his support, Mr.

A.J. Muhamad and Mrs. M.L. Anwar for aiding data acquisition, and Mr. N. Azim-Ibrahim of Cambridge University for discussions and constructive suggestions.

REFERENCES

Bol, A.J. & van Hoorn, B. (1980). Geological Society of Malaysia Bulletin, 12, 1-16.
Hedgpeth, J.W. (1957a). Memoir Geological Society America, 67(1), 17-28.
MacKenzie, A.S. & Maxwell, J.E. (1981). *In*, J. Brooks (Ed.), Organic Maturation Studies and Fossil Fuel Exploration, 239-254.
Taylor, B. & Hayes, D.E. (1980). *In*, D.E. Hayes (Ed.), American Geophysical Union, Geophysical Monograph, 23, 89-104.

1.19 A novel kerogen classification indicating hydrocarbon generation potential: Application to quantification and classification of the Lowmead oil shale, Australia.

Dr. M. RAHMAN, Dr. R. R. F. KINGHORN & Dr. P. J. GIBSON

Geology Department, Imperial College, RSM, Prince Consort Rd, London SW7 2BP, UK

INTRODUCTION

The biological materials deposited in sedimentary rocks, of which kerogens are the diagentic products, seldom retain their morphological identity, thus posing problems in kerogen classification. We have used physicochemical and optical parameters to classify kerogens according to their source, depositional environment and hydrocarbon potential. This is especially useful to distinguish the lipid (hydrogen) rich amorphous (oil prone) kerogens from other amorphous varities which are gas sources or with no potential.

Oil shales are very rich in immature kerogen. They yield little or no free hydrocarbons upon organic solvent extraction but destructive distillation (retorting) yields shale oil (Hunt, 1979) The organic contents of the Lowmead oil shales vary greatly depending upon: organic matter source, distance from source to depositional site and depositional environment. This classification gives a better correlation between pyrolytic yield and organic matter type for oil shales than classical chemical classifications.

Although pyrolytic yield, in terms of litres per metric tonne (l/mt), is satisfactory for commercial assessment of oil shales (threshold between 25 & 42 l/mt), the addition of the TOC gives an additional indication of oil quality (ie paraffinicity and commercial value), with oil quality being inversely related to TOC for a given pyrolytic yield.

ABSTRACT 2

The following abstract has been accepted by the American Association of Petroleum Geologists for a poster presentation at the 1994 AAPG International Conference and Exhibition (21-24 August, 1994) in Kuala Lumpur, Malaysia.

ANUAR, Azlina, PETRONAS Petroleum Research & Scientific Services, Kuala Lumpur, Malaysia, and KINGHORN, Robert, Petroleum Geology Group, Imperial College, University of London, England.

Sterane and Triterpane Biomarker Characteristics from Oils and Sediment Extracts of the Middle-Late Miocene Sequences, Northern Sabah Basin, Malaysia.

Biomarker studies using oil samples and sediment extracts from wells located in the northern part of the Sabah Basin indicate the organic matter source for the basin's hydrocarbons to be dominantly terrigenous, indicated by high triterpane/sterane ratios and the presence of compounds diagnostic of land-derived organic matter such as oleanane, and resins W, T and R. The consistently similar fragmentograms suggest that the oils and sediment extracts originated either from the same source rock, or from different source rocks with similar chemical compositions. Petrographic studies of kerogen concentrates confirm the dominance of land-plant contribution and the general absence of marine organic matter even in the marine sediments. For the oils, the biomarker maturity ratios were lower than their equilibrium values of 0.55 and 0.60 for the 20S/(20S+20R)-sterane and 22S/(22S+22R)-hopane, respectively. This supports the apparent retardation of the isomerisation process previously reported to occur in Far Eastern Tertiary oils. The majority of the extracted sediments are shown to be immature by pyrolysis Tmax, vitrinite reflectance and kerogen elemental composition, indicating that the extracted hydrocarbons have migrated into the sediments from elsewhere. Therefore, biomarker ratios from the extracts cannot be used to determine the true maturity levels of the sediments as the *in situ* biomarkers will have been mixed with those already present in the migrating hydrocarbons. The variations of biomarker maturity ratios with depth resemble those of the Production Index in all the studied wells, thus confirming the influence of the non-indigenous hydrocarbons on the biomarker maturity ratios.

BIBL LONDON UNIV